Organopolymérisations du méthacrylate de méthyle induites par les carbène N-hétérocycliques et par des paires de Lewis organiques

Winnie Nzahou Ottou

université de BORDEAUX

THÈSE PRÉSENTÉE

POUR OBTENIR LE GRADE DE

DOCTEUR DE

L'UNIVERSITÉ DE BORDEAUX

ÉCOLE DOCTORALE DES SCIENCES CHIMIQUES

SPÉCIALITÉ POLYMÈRES

Par Winnie NZAHOU OTTOU

ORGANOPOLYMÉRISATIONS DU MÉTHACRYLATE DE MÉTHYLE INDUITES PAR LES CARBÈNES *N*-HÉTÉROCYCLIQUES ET PAR DES PAIRES DE LEWIS ORGANIQUES

Sous la direction de: Pr. Daniel TATON

Soutenue le : 18 décembre 2014

Devant la commission d'examen formée de :

Mme. GUILLAUME, Sophie	Directrice de recherche, Univ. de Rennes I	Rapporteur
M. ZINCK, Philippe	Professeur, Univ. Lille 1	Rapporteur
Mme. MIQUEU, Karinne	Directrice de recherche, Univ. de Pau et des Pays de l'Adour	Examinateur
M. LANDAIS, Yannick	Professeur, Univ. de Bordeaux	Examinateur
M. VIGNOLLE, Joan	Chargé de recherche, Univ. de Bordeaux	Invité
M. TATON, Daniel	Professeur, Univ. de Bordeaux	Directeur de thèse
M. CRAMAIL, Henri	Professeur, Univ. de Bordeaux	Président du jury

Les travaux de recherche présentés dans ce manuscrit ont été réalisés au cours de ma thèse au Laboratoire de Chimie des Polymères Organiques (LCPO) dans le cadre du projet de recherche CATAPULT, financé par l'Agence Nationale de la Recherche (ANR).

Je tiens tout d'abord à remercier le directeur du LCPO, M. Henri Cramail, Professeur à l'Université de Bordeaux, pour m'avoir accueillie pendant ces trois années de thèse au sein du laboratoire dont il avait la responsabilité, pour sa gentillesse au quotidien, et aussi pour avoir accepté d'être le président de mon jury de thèse. Mes remerciements à Mme Sophie Guillaume, Directrice de recherche du CNRS à l'Université de Rennes 1 et M. Philippe Zinck, Professeur à l'Université Lille 1, pour leur rapport détaillé sur ce travail et pour les remarques constructives qu'ils m'ont adressées. Merci à Mme Karinne Miqueu, Directrice de recherche à l'Université de Pau et des Pays de l'Adour et M. Yannick Landais, Professeur à l'Université de Bordeaux qui ont accepté d'examiner ces travaux de thèse.

Je remercie chaleureusement les membres du projet CATAPULT et toutes les personnes avec qui j'ai eu l'occasion de collaborer au cours de cette thèse: Karinne Miqueu, Jean-Marc Sotiropoulos et Damien Bourichon de l'IPREM pour leur expertise et leur pédagogie en chimie théorique. Merci de m'avoir aidée à mieux cerner le lien entre la chimie de paillasse et les orbitales moléculaires. Yannick Landais et Frédéric Robert de l'ISM pour leur expertise en chimie moléculaire, ainsi que Virginie Liautard et Paul Ducos pour la synthèse de dérivés silylés. Anne-Laure Wirotius du LCPO pour son expertise en RMN. Les réunions CATAPULT ont toujours été riches en discussions, suggestions et commentaires nécessaires à l'évolution du projet. Merci à Patricia Castel du CESAMO pour ses analyses de spectrométrie de masse MALDI-ToF, Brice Kauffmann de l'IECB pour ses analyses en diffraction des rayons X et Silvia Mazzaferro du LCPO pour ses analyses en microscopie TEM.

Je remercie infiniment mon directeur de thèse, le professeur Daniel Taton, pour m'avoir accordé sa confiance pour ce projet. Je le remercie de m'avoir guidée sans jamais s'imposer et de m'avoir toujours incitée à comprendre les phénomènes observés. Merci chef pour votre savoir, votre dynamisme, vos blagues. Merci pour votre rigueur et vos petits manies (attention aux couleurs ou aux espaces dans les powerpoint !) qui nous font viser la perfection dans le fond et la forme. Merci de m'avoir initiée à la recherche il y a 6 ans et de m'avoir systématiquement poussée vers l'excellence depuis notre rencontre. Merci pour tous vos conseils tant sur un plan professionnel que personnel. Ce fût vraiment formidable bien que parfois complexe de travailler avec vous et je suis très fière d'avoir été membre de la DT team.

Merci à Joan Vignolle, mon co-encadrant de thèse en coulisse. Merci d'avoir été disponible quand il le fallait et de m'avoir appris plusieurs techniques expérimentales propres à la chimie moléculaire. Merci Joan pour tes conseils, tes commentaires et pour nos échanges au cours de cette thèse.

Je remercie évidemment les membres de mon équipe directe la « DT team » :

- Maréva pour m'avoir formée aux mille et une façons de faire du PMMA sans métaux.
- Paul alias « fraise », mon collègue de bureau, de labo, de CAES, de pauses, de séminaires…. Bref la personne avec qui j'ai partagé ma thèse au quotidien. Avec ta sympathie, tes blagues, tes taquineries et parfois tes crises de colère dans le labo, tu me faisais bien rigoler et ça mettait de l'ambiance dans notre équipe. Merci d'avoir été là pendant les périodes de crises, surtout vers la fin.
- Camille, la demi-sœur super nana du N2, toujours de bonne humeur bien que tiraillée entre 3 pays pendant sa thèse. Avec Paul et toi, nous sommes les 3 en 1 du cru DT-2014.
- Blandine, l'autre demi-sœur, qui fait de l'organocatalyse sur des corps gras. Merci à toi d'être toujours partante pour les délires de l'équipe DT même si on te partage avec « l'équipe des gras ».
- Romain alias « le prince de Dordogne », un organicien qui a atterri chez les polymé ristes. Merci pour ton extrême gentillesse et merci d'avoir rajouté de la folie pendant ma dernière année. Avec Paul et toi, j'avais une équipe de choc dans le bureau et dans le labo. C'était vraiment trop cool de vous avoir.
- Enfin Mathilde, la dernière arrivée dans l'équipe qui va devoir apprendre les joies (et les peines) d'être membre de la DT team.

Vous avez participé de près au bon déroulement de ce travail. Merci pour votre bonne humeur et votre disponibilité. DT team forever !

Un clin d'œil spécial à Nicolas alias super carotte the master of the SEC et Anne-Laure Mme RMN en chef. Merci d'avoir été présents et d'être des permanents sans vraiment l'être.

Mes remerciements s'adressent naturellement aux équipes CAES, « pause-pomme », et à l'ensemble des membres passés et présents du LCPO avec qui j'ai pu discuter et rigoler au cours de cette thèse. Je vais éviter de citer des noms en particulier pour n'en oublier aucun.

Merci aux permanents qui ont été pour la majorité mes enseignants à l'université et/ou à l'école d'ingénieurs et qui sont toujours disponibles pour échanger avec les étudiants. Merci à Catherine, Corinne, Nicole, Bernadette, Loïc, Aude, Maud et Dominique qui font de leur mieux pour le bon fonctionnement de la machine LCPO. Vous contribuez à faire régner au LCPO une atmosphère quasi familiale pleine de bonne humeur. Vive la LCPO family !

Enfin, un énorme merci à mes parents et à l'ensemble de ma famille au Gabon sans qui je ne serai pas là aujourd'hui. Merci pour leur soutien inconditionnel pendant toutes ces années d'étude et pour leurs encouragements malgré la distance. Merci à ma famille de cœur qui m'a soutenue et supportée quotidiennement pendant ces 3 années de thèse. Merci d'avoir facilité et égayé ma vie en dehors du labo afin que je puisse être plus efficace pour ma thèse. Vous avez été tous géniaux. Un grand merci à vous de tout cœur.

A ma famille
et mes amis.

TABLE OF CONTENTS

Chapter 2. Polymerization versus cyclodimerization of alkyl (meth)acrylates induced by *N*-heterocyclic carbenes

Chapter 3. Polymerization of methyl (meth)acrylate catalyzed by a *N*-heterocyclic carbene in the presence of alcohols as chain regulators

Chapter 4. Lewis pair-induced polymerization of methyl methacrylate: association of a *N*-heterocyclic carbene or a phosphine as an organic Lewis base and a silicon-based Lewis acid

Introduction générale

Dans leur grande majorité, les réactions de polymérisations ou de modifications chimiques des polymères font intervenir des espèces organométalliques comme activateurs (catalyseurs ou amorceurs), à l'exception notable des polymérisations radicalaires qui permettent tout de même de produire environ 50 % des matériaux polymères. L'utilisation d'activateurs métalliques dans les réactions de polymérisation permet non seulement d'augmenter les cinétiques de réactions, mais aussi d'induire des processus hautement sélectifs. Cependant, ces espèces métalliques demeurent le plus souvent en quantité résiduelle dans le matériau final, les méthodes de purification des polymères ainsi obtenus étant difficiles ou trop coûteuses à mettre en œuvre. Cette présence non désirée dans le matériau peut entrainer des problèmes de toxicité notamment s'il s'agit d'utiliser les polymères dérivés dans des applications médicales, cosmétiques ou alimentaires ; les métaux peuvent aussi poser des problèmes de toxicité pour l'écosystème. Enfin, la présence de métaux résiduels peut induire la dégradation non désirée du matériau, lors de sa mise en œuvre ou de son utilisation, *via* des procédés d'oxydation en général. Comme alternatives, les polymérisations induites par des catalyseurs enzymatiques (d'origine naturelle) ou bien par des activateurs purement organiques ont été proposées au cours de la décennie écoulée.

Ce travail de thèse s'inscrit dans le cadre général des réactions d'organopolymérisations avec comme cibles monomères les méthacrylates d'alkyle et comme principaux catalyseurs/activateurs organiques les carbènes *N*-hétérocycliques (en anglais *N*-heterocyclic carbenes, NHCs).

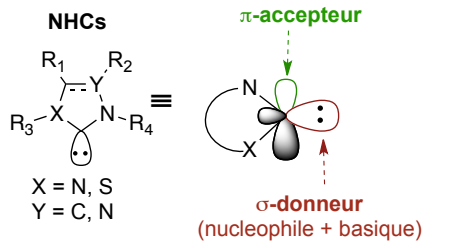

Structure et propiétés électroniques des NHCs

Du fait de leurs propriétés, à la fois π-accepteur et σ-donneur, les NHCs ont déjà révolutionné la chimie organométallique en tant que ligands de très nombreux métaux de transition.[1] Les NHCs ont aussi été employés comme véritables catalyseurs organiques pour un grand nombre de réactions en chimie moléculaire. Plus récemment, en synthèse macromoléculaire, la réactivité des NHCs a été mise à profit pour catalyser diverses réactions de polymérisation, notamment celle opérant par ouverture de monomères cycliques (*e.g.* lactide ou lactones, carbonates, oxiranes, carbosiloxanes ou anhydrides).[2-6] mais aussi pour la polymérisation en chaîne par transfert de groupe des monomères (méth)acryliques et pour des polymérisations par étapes pour la synthèse de polybenzoïne, de polyuréthanes ou de polysiloxanes.[3,6]

L'objectif principal de cette thèse a été de mettre en évidence la sélectivité des NHCs comme activateurs/catalyseurs vis-à-vis de substrats (méth)acryliques utilisés comme monomères. Deux NHCs ayant des groupements isopropyle (NHC^{iPr}) et *tert*-butyle (NHC^{tBu}) sur les atomes d'azote ont été particulièrement examinés à cet effet. Nous montrerons que des résultats très différents sont obtenus avec ces deux NHCs utilisés pour l'organopolymérisation des monomères (méth)acryliques.

Ce manuscrit est structuré en quatre chapitres distincts – tous rédigés en anglais – et est organisé comme indiqué ci-après.

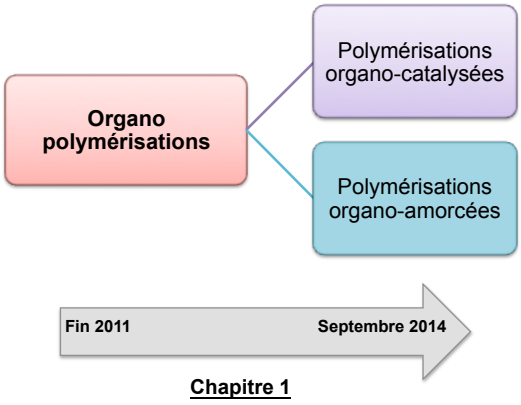

Le premier chapitre est consacré à l'état de l'art concernant les développements récents, depuis fin 2011 jusqu'à fin septembre 2014, en synthèse de polymères issus de catalyseurs/activateurs organiques. Les différentes familles de catalyseurs organiques, les différents polymères ainsi accessibles, et les mécanismes associés seront discutés en détails.

Le chapitre 2 décrit la polymérisation du méthacrylate de méthyle (MMA) amorcée directement par les deux NHCs susmentionnés, *i.e.* en l'absence de tout autre activateur. Dans ces conditions, on peut s'attendre à un mécanisme de type zwittérionique, *via* la formation d'un énolate d'imidazolium. La différence de réactivité des deux carbènes sera mise en évidence et les résultats expérimentaux seront rationalisés par des calculs théoriques par la méthode des fonctionnelles de la densité DFT (pour density functional theory, en anglais). Toute une série de monomères (meth)acryliques seront alors évalués en « polymérisation zwittérionique » induite par les NHCs.

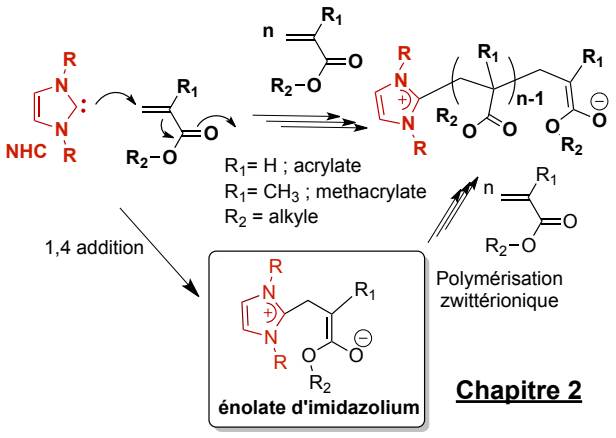

Dans le chapitre 3, un NHC particulier, celui portant les groupements *tert*-butyle sur les atomes d'azotes (NHC^{tBu}) sera étudié comme véritable catalyseur de polymérisation du MMA et de son homologue acrylique, l'acrylate de methyle (MA), en présence de différents alcools comme amorceurs.

Il sera démontré que ces polymérisations sont effectivement contrôlées par la quantité d'alcool, notamment lorsque des faibles masses molaires sont visées.

L'existence de deux mécanismes concertés de polymérisation compétitifs, impliquant l'activation du monomère ou de l'alcool, sera discutée sur la base de calculs théoriques DFT combinés aux résultats expérimentaux (cinétique de polymérisation, analyse des polymères formés, réactions modèles).

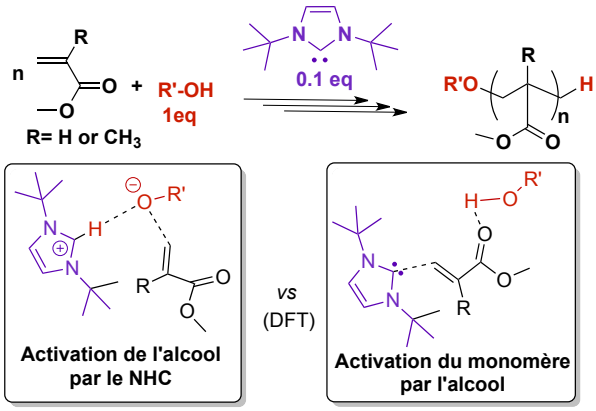

Chapitre 3

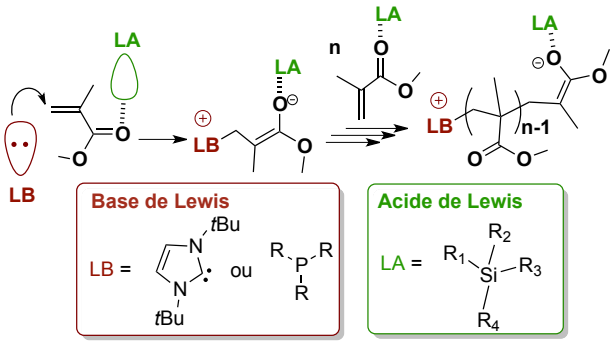

Chapitre 4

Le chapitre 4 porte sur l'utilisation de paires de Lewis (acide + base) purement organiques, comme système d'activation de polymérisation du MMA. En plus des carbènes NHCs, des phosphines commerciales seront également examinées comme bases de Lewis. Des acides de Lewis à base de silicium seront associés aux bases de Lewis. Nous montrerons que le choix des deux partenaires est primordial pour induire la polymérisation du MMA et que celle-ci peut-être relativement bien contrôlée. Ce dernier chapitre vise aussi à identifier un système d'amorçage transposable à d'autres monomères vinyliques moins polaires.

Une discussion en français des résultats majeurs obtenus au cours de ces trois années de thèse ainsi qu'un certain nombre de perspectives seront enfin présentées.

Ce travail de thèse s'inscrit dans le cadre du projet de recherche CATAPULT financé par l'Agence Nationale de la Recherche (ANR) en collaboration avec une équipe experte en chimie moléculaire (Prof. Yannick Landais et Dr. Frédéric Robert de l'Institut des Sciences Moléculaires, ISM, à Bordeaux) et une équipe de physico-chimistes (Dr. Karinne Miqueu et Dr. Jean-Marc Sotiropoulos de l'Institut Pluridisciplinaire de Recherche sur l'Environnement et les Matériaux, IPREM, à Pau) développant notamment des approches théoriques de modélisation.

Références:

(1) Hopkinson, M. N.; Richter, C.; Schedler, M.; Glorius, F. *Nature* **2014**, *510*, 485.
(2) Kamber, N. E.; Jeong, W.; Waymouth, R. M.; Pratt, R. C.; Lohmeijer, B. G. G.; Hedrick, J. L. *Chem. Rev.* **2007**, *107*, 5813.
(3) Kiesewetter, M. K.; Shin, E. J.; Hedrick, J. L.; Waymouth, R. M. *Macromolecules* **2010**, *43*, 2093.
(4) Dove, A. P. *ACS Macro Lett.* **2012**, *1*, 1409.
(5) Fèvre, M.; Vignolle, J.; Gnanou, Y.; Taton, D. In *Polymer Science: A Comprehensive Reference*; Editors-in-Chief: Krzysztof, M., Martin, M. I., Eds.; Elsevier: Amsterdam, **2012**, p 67.
(6) Fèvre, M.; Pinaud, J.; Gnanou, Y.; Vignolle, J.; Taton, D. *Chem. Soc. Rev.* **2013**, *42*, 2142.

Chapter 1.
Update and challenges in organopolymerization reactions

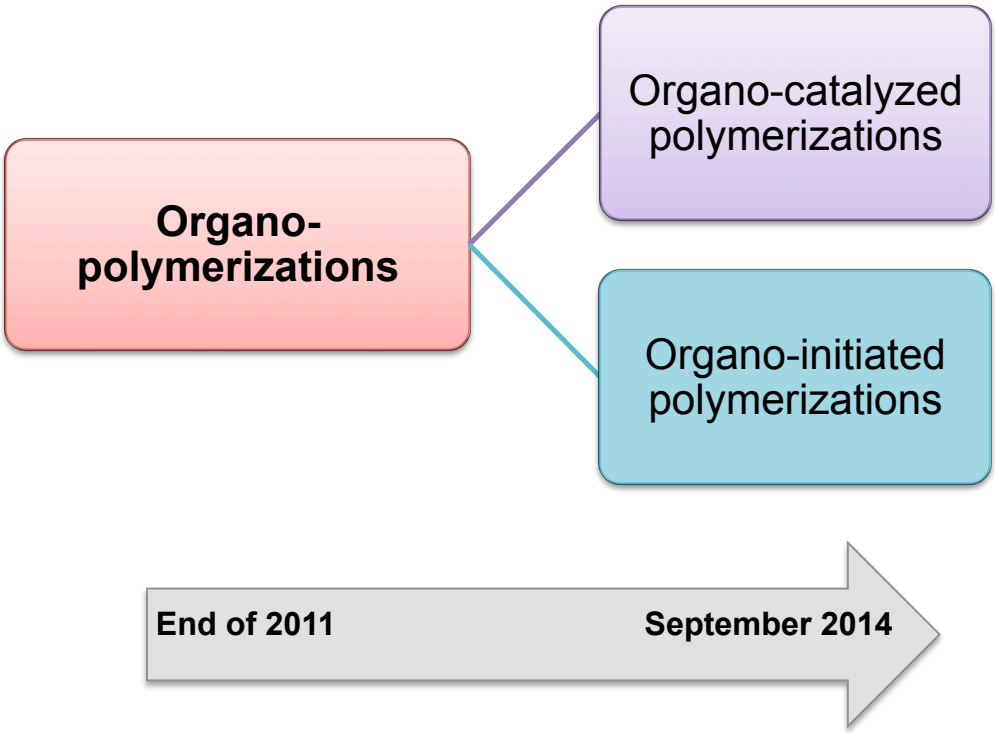

Keywords: Organic catalysts • Ring-opening polymerization • Step-growth polymerization • Group transfer polymerization • Acid catalysis • Basic catalysis • Bifunctional activation • Direct initiation •

Chapter 1.
Update and challenges in organopolymerization reactions

Table of contents

Introduction

Organocatalysis, *i.e.* the use of small organic molecules to catalyze chemical reactions, is an emerging field in enantioselective synthesis and which allows accessing a broad range of biologically active compounds.[1] For a long time, highly stereoselective transformations have been mainly achieved using enzymes and transition metal catalysts. However, organocatalysis has become the third branch of catalysis, providing various advantages over organometallic catalysis, including: (i) environmentally more friendly and inherently lower toxicity of organic small molecules; (ii) better availability of organic reagents and (iii) lower sensitivity toward oxygen and moisture.[1]

The scope of organocatalytic systems, and their roles in various elementary reactions of molecular chemistry have been discussed in detailed reviews.[2-5] They have also been introduced in macromolecular synthesis, where organic reagents can trigger polymerization reactions either as catalysts or as direct initiators, producing polymeric materials exempted of any metallic residues. Related metal-free polymers are thus expected to be employed in high-value and sensitive domains, such as biomedical and personal beauty care applications, microelectronic devices or food packaging.

Several classes of organic activators (catalysts or initiators), including Brønsted/Lewis acids or bases, and mono or bicomponent bifunctional catalytic systems have been utilized not only for step-growth and chain-growth polymerizations, but also for depolymerization reactions in a context of recycling polymeric materials.

In recent years, organic activators have aslo been applied in biorefinning processes for biomass conversion and upgrading into sustainable chemicals, materials, and biofuels as alternatives to petroleum-based compounds.[6] Metal-free polymerizations of such bio-based monomers offer a new strategy for the development of high-performance bioplastics with enhanced thermal stability and solvent resistance.

A general review on organo-catalyzed polymerizations has been published in 2010 by Hedrick, Waymouth *et al*.,[7] and articles focusing on specific topics such as, ring-opening,[8,9] group-transfer,[10] anionic,[11] zwitterionic[12] polymerizations and polymerizations induced by H-bond catalysts[13] have been published. Our group has also reviewed the general field of organo-catalyzed polymerizations at the end of 2011[14] and, more specifically, the use of *N*-heterocyclic carbenes (NHCs) as organic catalysts for metal-free polymer synthesis.[15]

From the end of 2011 to september 2014, roughly 140 papers desbribing the use of organic catalysts in polymerization reactions have appeared (Figure 1), demonstrating the ever increasing interest of organocatalysis as a new tool for macromolecular engineering.

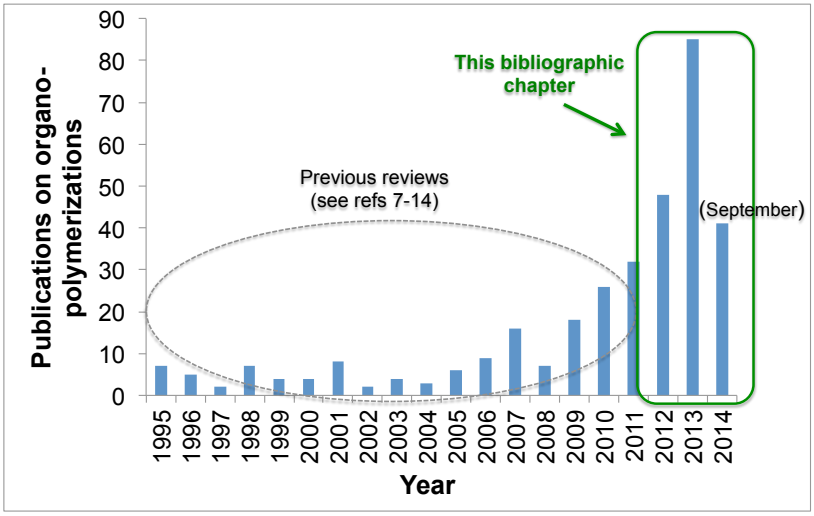

Figure 1. Evolution of publications on the topic of metal-free polymerizations since 1995. Data were obtained by a search in SciFinder and Web of science using the keywords "organo-catalyzed polymerization", "metal-free polymerization" and derivatives (September 2014).

The present bibliographic chapter focuses on these recent developments, and applications of related metal-free polymers are also highlighted. The structure of main organic activators (catalysts or initiators) employed in polymerization reactions is first presented, according to their functional group (*i.e.* acid or basic compounds, or activators featuring hydrogen-bonds with a donating or an accepting capability). Main monomer substrates and general polymerizations mechanisms are also briefly described. A focus on each category of activators is then given in the context of organo-catalyzed polymerizations although, in some cases, the catalyst is not employed in substoichiometric amounts relative to the initiator. Few examples of organo-initiated (non-catalyzed) polymerizations, utilizing specific organic initiators, *i.e.* in absence of any other co-activator are briefly discussed in the concluding remark section.

1. Scope of organic activators, monomer candidates and general polymerization mechanisms

1.1. Organic activator platform

A variety of metal-free compounds has been employed as catalysts or initiators in polymerization reactions (Figure 2), and most of them have been discussed in previous reviews.[8,14] They include Brønsted acids (*e.g.* sulfonic, phosphoric and carboxylic derivatives), Lewis acid (*e.g.* trimethylsilyltrifluoromethanesulfonimide: Me_3SiNTf_2), Brønsted or Lewis bases (*e.g.* phosphazenes, *N*-heterocyclic carbenes, amines, phosphines, amidines

or guanidines). Combination of antagonist catalysts, within the same molecule or not, leads to bifunctional ambiphilic systems. Generally, such a dual activation is based on hydrogen-bond interactions (*e.g*. thioureas and phenols derivatives).[13]

1.2. Scope of monomers

Figure 3 illustrates representative monomer families recently polymerized using organic activators. Cyclic esters (lactides and lactones) have been the most studied in the context of organo-catalyzed ring-opening polymerizations (ROP).[7,8,14] This is not only due to the significant importance of corresponding biodegradable, non-toxic and *in vivo* bioresorbable polyesters, but also to the relative easiness for polymerizing these polar cyclic monomers. Cyclic carbonates have received a special attention, because related polycarbonates exhibit a lower degration rate in water and allow for an easier introduction of reactive functionalities compared to other aliphatic polyesters, such as polylactides (PLA) or polylactones.[9]

Other cyclic monomers, such as cyclic ethers, cyclosiloxanes, *N*-carboxyanhydrides (NCAs), *O*-carboxyanhydrides (OCAs) and phosphoesters, have also been reported to undergo metal-free ROP.

Besides ROP, (meth)acrylic monomers have been subjected to the group transfer polymerization (GTP), in the presence of silyl ketene acetal (SKA) initiators, or undergo direct 1,4-conjugate addition polymerization using a specific nucleophile (*e.g.* NHC). A few examples of step-growth polymerizations leading to polyurethanes or polyaldols have also been reported.

1.3. Polymerization mechanisms

The mechanism involved in organo-polymerization reactions obviously depends on both the nature of the catalyst/chain starter and the monomer polymerizability. Polymerization can occur through an activated monomer mechanism (AMM), following either an electrophilic or a nucleophilic pathways. Polymerization operating by activation of a purposely added initiator (or *via* activation of the polymer chain-ends) refers to as the activated chain-end mechanism (ACEM). A cooperative dual activation of both the monomer and the initiator can also take place with specific mono- or bicomponent organic catalysts.

1.3.1. Activated Monomer Mechanisms (AMM)

Electrophilic reagents (E), such as Brønsted organic acids, alkylating or acylating agents, can activate the monomer, *e.g*. heterocycles such as lactide (LA) or ethylene oxide (EO), through coordination of the heteroatom, *e.g*. the oxygen atom of the carbonyl group (C = O) of cyclic esters and carbonates, the phosphoryl group (P = O) of phosphoesters, or the oxygen atom of epoxides.

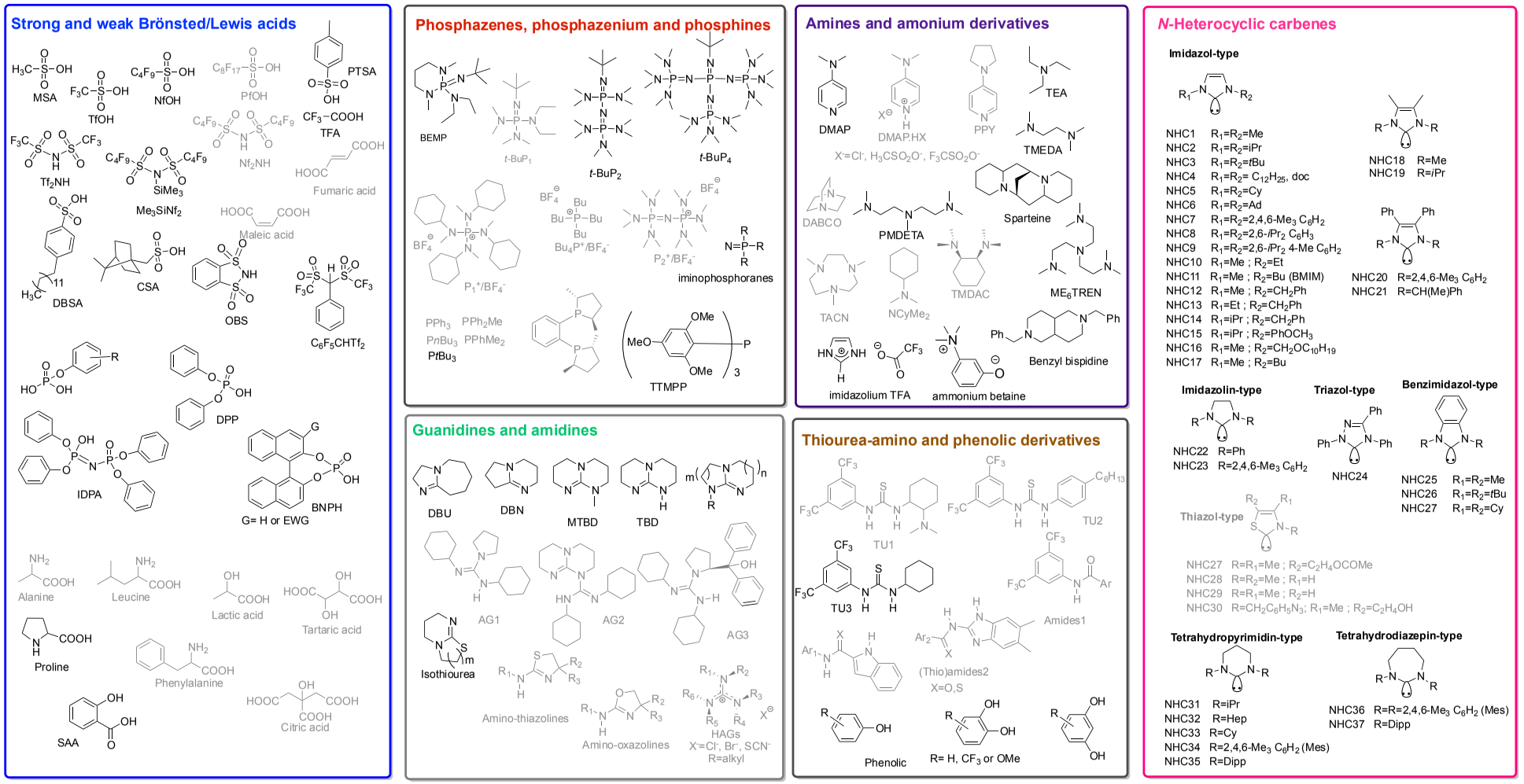

Figure 2. Representative families of organic molecules used as catalysts or initiators for organopolymerization (inspired from ref 14).

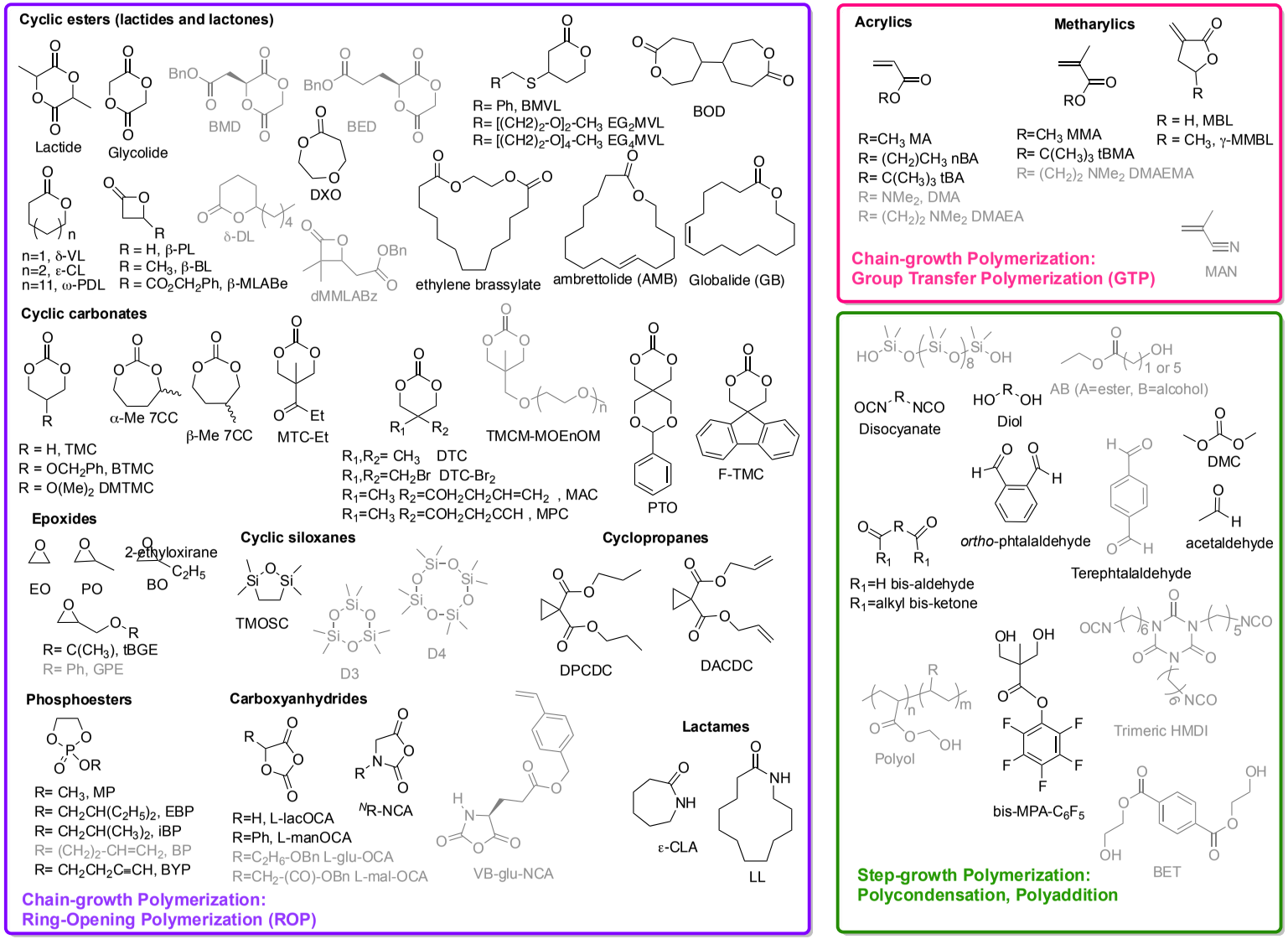

Figure 3. Representative monomers that were subjected to an organopolymerization pathway (inspired from ref 14**).**

The as-formed activated monomer **1** or **3** (Scheme 1a-b) being more electrophilic, it can easily undergo a nucleophilic addition by the initator/propagating chain-end (**2** or **4** in Scheme 1a-b), resulting in the ring-opening of the monomer and the regeneration of the catalyst.

In a Lewis-acid-catalyzed polymerization of alkyl (meth)acrylates (*e.g.* methyl methacrylate MMA), a Lewis acid E* (*e.g.* trimethylsilyltrifluoromethanesulfonimide Me_3SiNTf_2) activates the monomer by coordination onto the carbonyl group, forming the intermediate **5** (Scheme 1c). Subsequent 1,4-nucleophlic addition of the initiator (*e.g.* a trialkylsilyl ketene acetal SKA) onto **5** leads to a propagating trialkylsilyl enolate **6** (Scheme 1c).

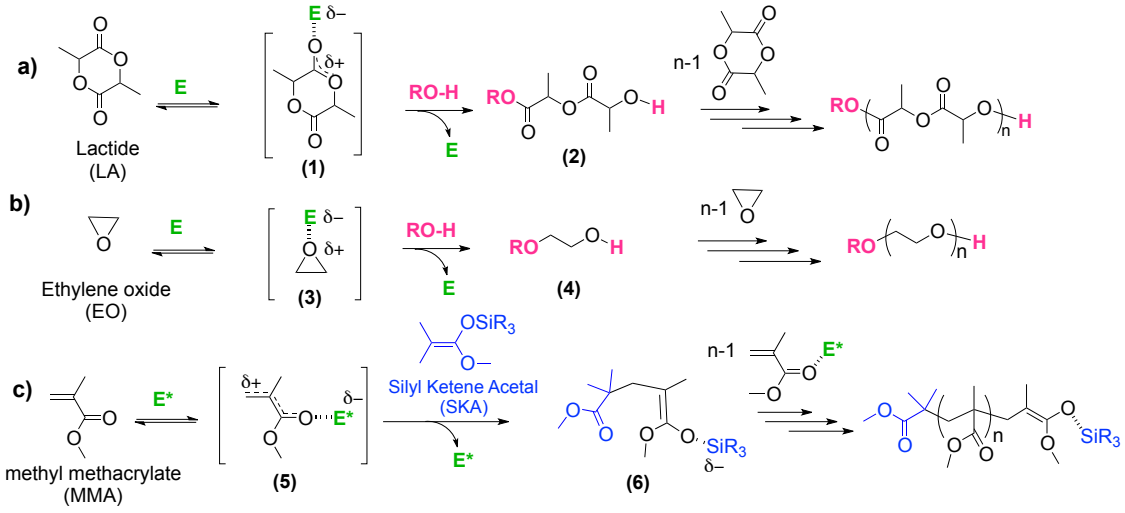

Scheme 1. Electrophile AMM mechanism *via* acid (E or E*) a) for the ROP of cyclic esters (*e.g.* LA); b) ROP of cyclic ethers (*e.g.* EO); and c) for the GTP of (meth)acrylates (*e.g.* MMA);

Nucleophiles, such as amines, phosphines or NHCs can directly ring-open some heterocyclic monomers (*e.g.* LA or EO). This yields a zwitterionic alkoxide intermediate (**7**, Scheme 3a), the protonation of which by an alcohol initiator ROH **8**, followed by displacement of Nu in α-position, leads to a dormant mono-adduct alcohol **2** and regeneration of the catalyst.

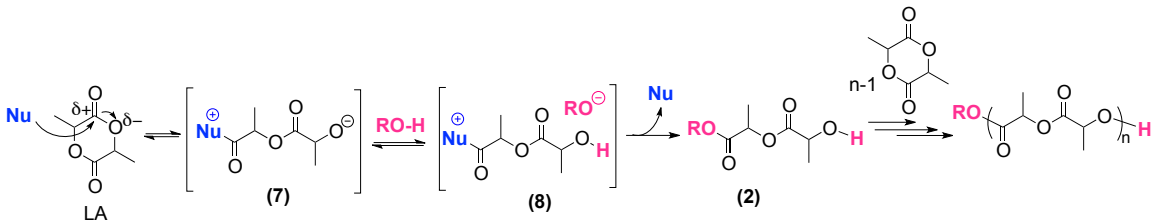

Scheme 2. Nucleophilic AMM mechanism for the ROP of cyclic monomers (*e.g.* LA) in presence of ROH as initiators.

In the absence of an alcohol initiator, after formation of the zwitterionic alkoxide **9**, the nucleophile can remain bound to the polymer chain (*e.g.* in the case of β-butyrolactone β-BL), leading to a non-catalytic process (Scheme 3b).

(Meth)acrylate monomers can also be directly activated through a 1,4-conjugate addition (Michael addition) by a Lewis base (*e.g.* NHC), forming a zwitterionic enolate intermediate **10** that can further propagate (Scheme 3c). It should be pointed out that the latter process is also not catalytic.

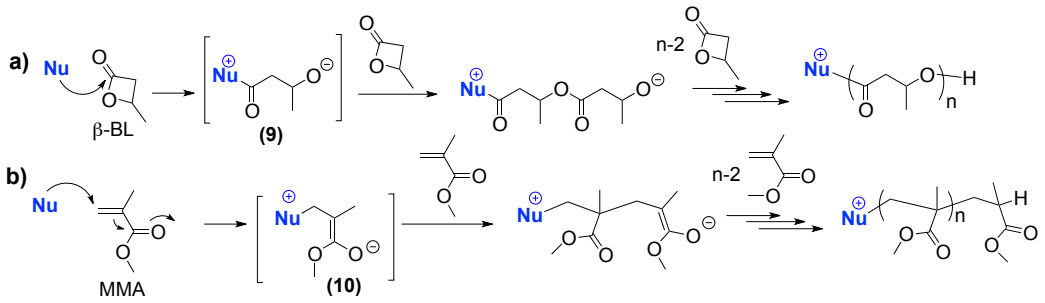

Scheme 3. Nucleophilic and non-catalytic AMM mechanism. a) in zwitterionic ROP (ZROP) of cyclic monomers (*e.g.* β-BL) and b) in zwitterionic polymerization (ZP) of (meth)acrylates (*e.g.* MMA).

1.3.2. Initiator/chain-end activated mechanism (ACEM)

Initiating alcohol (or polymer chain-ends) can be activated *via* H-bonding or deprotonated by strong Brønsted bases, generating a reactive alkoxide **12** featuring the conjugated acid of the base as countercation (in general, this is a bulky and soft organic cation; Scheme 4a). Chain-growth can then occur by repeated nucleophilic addition reations onto incoming monomers. Activation of the alcohol initiator/chain-ends actually depends on the pKa difference between the alcohol and the organic base used.

In the context of the GTP of (meth)acrylics, organic catalysts such as NHCs or phosphazenes can activate the silyl ketene acetal (SKA) initiator/ester enolate chain end (**13**, Scheme 4b) by coordination to the silicon atom. The resulting hypervalent SKA is more nucleophilic enabling the 1,4-conjugate addition to proceed. According to the nature of the Lewis base used, GTP may proceed either by an associative mechanism (*via* formation of pentacoordinate siliconates species, **14a**) or through a dissociative mechanism (*via* formation of true enolates anions, **14b**).[10]

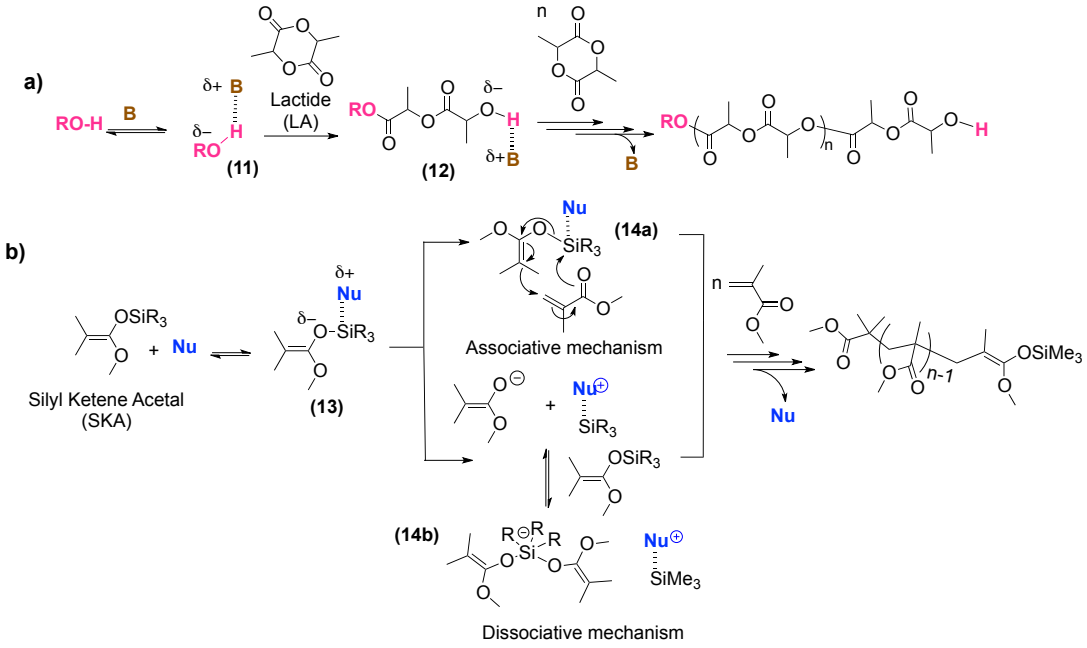

Scheme 4. Basic actived initiator/chain-end mechanism (ACEM). a) in ROP of cyclic monomers and b) in GTP of acrylates and meth)acrylates.

1.3.3. Bifunctional activation

Cooperative dual activation of both the monomer and the initiator/chain-end can be achieved with specific organic catalysts. For instance, a combination of a weak Brønsted acid (E) such as diphenyl phosphate (DPP) and a Bronsted base (B) such as dimethylaminopyridine (DMAP), can be employed in a bicomponent catalytic system to activate a cyclic monomer (Scheme 5a). Such a bifunctional activation is generally triggered using molecules capable of hydrogen-bonding (*e.g.*, DMAP, thiourea-amino derivatives or guanidine 1,5,7-triazabicyclo[4.4.0]dec-5-ene TBD).[7,14] In the case of (meth)acrylic derivatives, only examples using metallic or semi-metallic E reagents (*e.g* $B(C_6F_5)_3$) has been described to activate MMA (**5,** Scheme 5b), in combination with phosphines. A synergy between the two components is expected, providing that the pKa difference between E and B is not too high.

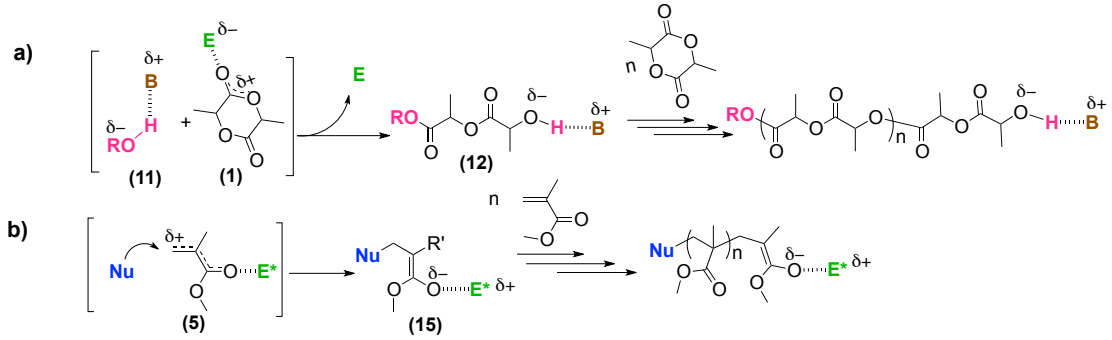

Scheme 5. Bifunctional activation mechanism AM/ACEM a) in ROP of cyclic monomers and b) in polymerization of (meth)acrylates (*e.g.* MMA).

The following sections outline the use of each family of organic catalysts for polymerization reactions, in the presence of an external molecule playing the role of the initiator (= organo-catalyzed polymerizations).

2. Polymerization catalyzed by Brønsted and Lewis acids

As mentioned above, acid-promoted polymerizations mainly proceed through an electrophilic monomer activation, *i.e.* by a pseudo-cationic mechanism, using protic compounds (typically alcohols) as initiators. The ring-opening polymerization (ROP) of cyclic monomers, including esters, carbonates, siloxanes and oxiranes, has been the most investigated. A wide range of sulfonic and sulfonimide acids have been employed to this end. However, phosphoric acid derivatives have also emerged as efficient promoters in this context. In contrast to ROP, only few examples of acid-catalyzed group tranfer polymerization (GTP) of (meth)acrylates and step-growth polymerizations have been reported. In the following lines, acid organocatalysts will be considered according to their chemical nature (*i.e.* sulfur-, phosphorus-, carboxylic-derivatives, etc), that governs their relative acidity.

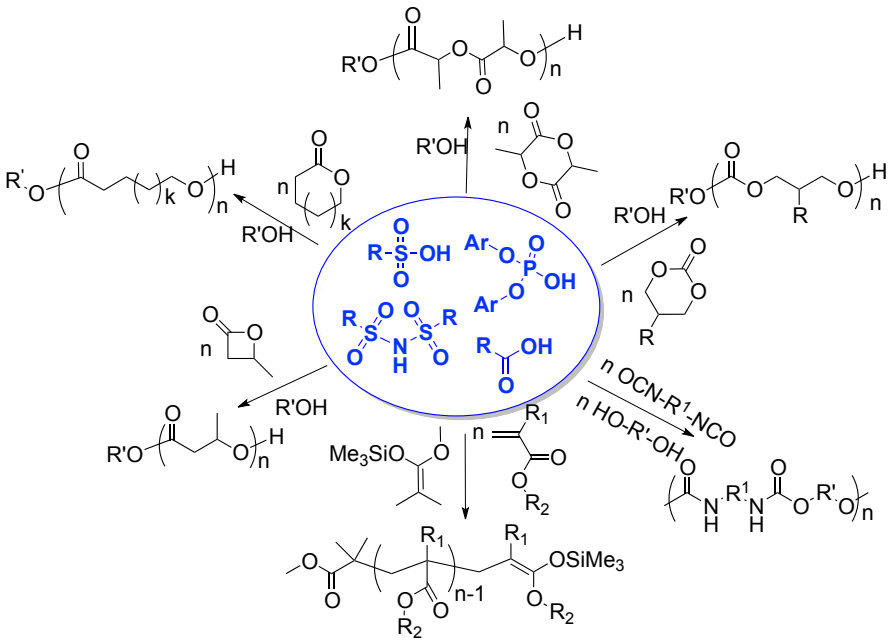

Figure 4. Overview of polymers synthesized by an acid catalysis.

2.1. Sulfonic and sulfonimide acids

Strong and “super strong” sulfonic acids have been widely investigated to trigger the ROP of not only cyclic esters (*e.g.* lactide, ε-caprolactone (ε-CL) and δ-valerolactone (δ-VL)), but also that of cyclic carbonates (*e.g.* trimethylene carbonate TMC). An overview of main acidic catalysts and related monomers that have been polymerized in this way is shown in Figure 5.

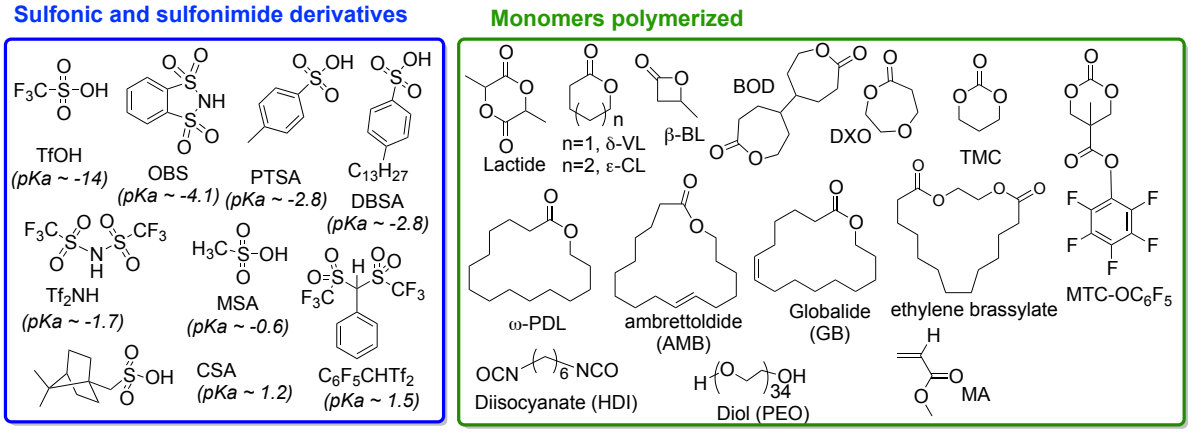

Figure 5. Representative examples of sulfonic and sulfonimide acids derivatives, as well as monomers investigated; pKa in H_2O determided by the Hammett Ho acidity function.[16]

Methanesulfonic acid (MSA; pKa ~ - 0.6 in H_2O)[16] was demonstrated to catalyze the ROP of both ε-CL and [4,4′-bioxepane]-7,7′-dione (BOD) in a one pot-fashion, with benzyl alcohol (BnOH) or propargyl alcohol (PgOH) as initiators, in dichloromethane, at r.t (Scheme 6).[17] Alternatively, the ROP of BOD could also be induced by a pre-synthesized hydroxylated poly(ε-CL) (PCL-OH) as macroinitiator.

PCL-based core cross-linked stars (CCS) with number average molar masses (M_n) ranging from 9,900 to 36,200 g.mol^{-1} and relatively low dispersity ($Đ \leq 1.3$) were successfully obtained in near quantitative yields, from an initial ratio $[BnOH]_0/[ε\text{-}CL]_0/[BOD]_0/[MSA]_0$ = 1:100:30:3. Although, the polymerization mechanism was not discussed, it was previously proposed by Bourissou, Martín-Vaca and co-workers[18] that the ROP of ε-CL likely proceeded by an AMM, in presence of ROH and MSA, while with the stronger triflic acid (TfOH; pKa ~ -14 in H_2O)[16] deactivation of the initiating/propagating alcohol competed with the activation of the monomer. However, it was suggested that the activity of these acids catalysts did not simply correlate to their relative acidity.[18]

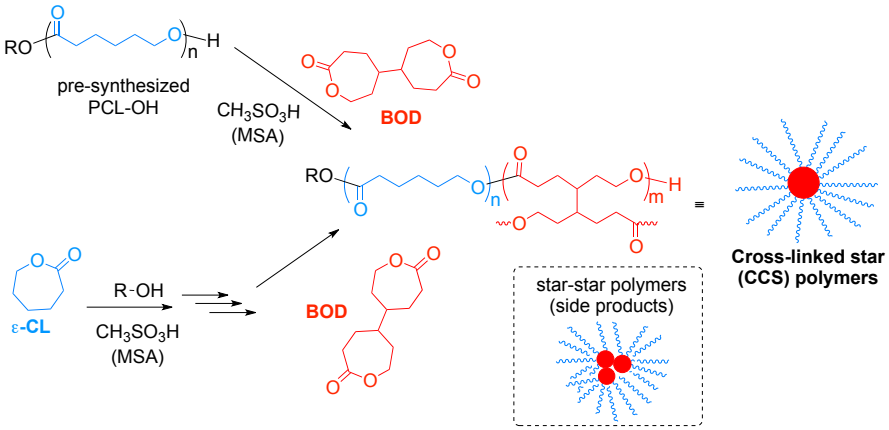

Scheme 6. Synthesis of PCL CCS Polymers *via* ROP and the " arm-first" approach.[17]

Zinck *et al*. investigated the catalytic efficiency of MSA, *p*-toluenesulfonic acid (PTSA, pKa ~ -2.8 in water) and (1*R*)-(2)-10-camphorsulfonic (CSA) as organocatalysts (1 mol%) for the ROP of ε-CL in water.[19] The reaction was found to be quantitative at 100 °C, leading to PCL's of M_n up to 5,000 g.mol^{-1} ($Đ$ = 1.7-1.9). The same reaction conducted at lower temperatures (25 or 50 °C) using polysaccharides such as dextran or methylcellulose as macroinitiators and PTSA as catalyst at 25 °C or 50 °C, afforded PCL-*graft*-water-soluble polysaccharides copolymers of M_n = 6,200 - 8,700 g.mol^{-1}. The authors proposed that the polymerization was initiated by 6-hydroxyhexanoic acid formed upon hydrolysis of the lactone, leading to either a ROP of ε-CL or a polycondensation mechanism (Scheme 7).

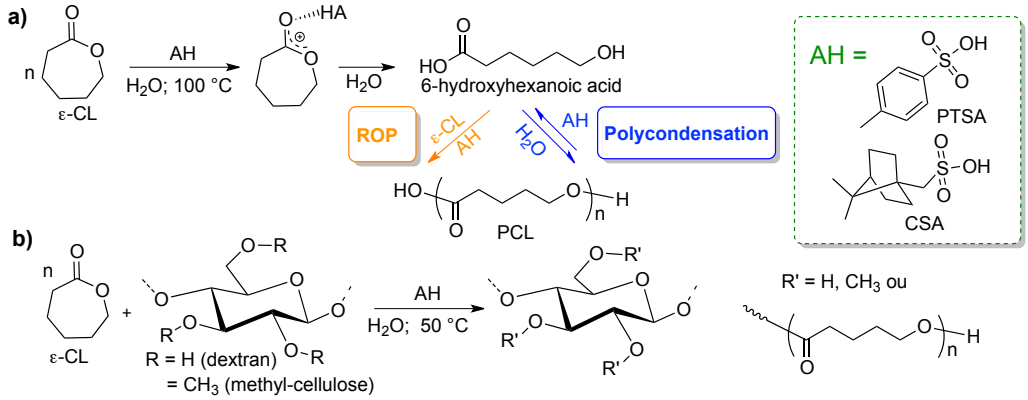

Scheme 7. Acid-catalyzed polymerization of ε-CL in water.[19]

ROP of β-butyrolactone (β-BL) initated by isopropanol (iPrOH) was catalyzed by TfOH (20-40 mol% relative to iPrOH), in dichloromethane at r.t.[20] The polymerization was controlled for a degree of polymerization (DP) lower than 30, producing poly(β-butyrolactone)s (PBL's) of M_n equal to 2,400 g.mol^{-1} ($Đ$ = 1.3). The observed deviation from linearity at higher ratios was attributed to the formation of cyclic oligomers by backbiting sidereactions. The same catalytic system was further used for the direct copolymerization of β-BL with L-lactide (LLA) present in the same batch, leading to block copolymers of molar masses M_n = 1,400 - 3,500 g.mol^{-1} ($Đ$ = 1.3-1.7) due to the different reactivity of the two monomers. The polymerization indeed proceeded in a sequential manner, PBL being formed at the first stage.

The catalytic activities of MSA and TfOH were compared for the ROP of β-BL in presence of *n*-pentanol (*n*PenOH) as initiator, in benzene at 30 °C.[21] With a ratio of acid/ROH = 3/1, TfOH proved signicantly more active than MSA, in relation with its higher acidity (pKa^{TfOH} ~ -14 *vs* pKa^{MSA} ~ -0.6). Indeed, 20 eq. of β-BL were converted in only 15 min with HOTf, whereas 60 min were required with MSA, leading to PBL of controlled molar masses M_n up to 8,200 g.mol^{-1} and narrow dispersity ($Đ$ < 1.25). A variety of well-defined block copolymers (di-, tri- and penta-block) were also prepared using dihydroxylated initiators (*i.e*. 1,4-butanediol) or macroinitiators (*i.e*. dihydroxylated poly(ethylene oxide) HO-PEO-OH or α,ω-dihydroxylated poly(butadiene) HO-PB-OH), upon successive addition of β-BL and ε-CL.

The ROP of ε-CL, 1,5-dioxepan-2-one (DXO) and racemic lactide (rac-LA) was also

successfully achieved in dichloromethane at r.t., using 3-phenyl-1-propanol (PPA) as initiator and bis(trifluoromethane)sulfonimide (Tf_2NH, pKa ~ -1.7 in H_2O[22]) as catalyst (0.1-3 eq.)[23] This afforded PCL of M_n = 11,300 g.mol^{-1} (*Đ* = 1.40), poly(1,5-dioxepan-2-one) (PDXO) of M_n = 11,400 g.mol^{-1} (*Đ* = 1.16), and poly(lactide) (PLA) of M_n = 6,190 g.mol^{-1} (*Đ* = 1.17).

In contrast to MSA, TfOH and Tf_2NH, *o*-benzenedisulfonimide (OBS; pKa ~ -4.1 in H_2O)[24] was presented as a non-toxic, non-volatile and non-corrosive (strong) acid. Its catalytic performance in the ROP of δ-VL and ε-CL was studied, using BnOH as the initiator and toluene as solvent at 30 °C.[25] The polymerization proceeded in a controlled fashion, affording PVL and PCL homopolymers, as well as PVL-*b*-PCL diblock copolymers with M_n = 3,000-6,000 g.mol^{-1} and *Đ* values in the range of 1.09-1.20. The catalytic efficiency of OBS was found equivalent to that of Tf_2NH, making OBS a more sustainable alternative to the other strong acids.

While the acid-catalyzed ROP of small- and medium-ring sized lactones has been widely studied, there are only few examples regarding the ROP of macrolactones. Three of such macrolactones, namely ω-pentadecalactone (ω-PDL), globalide (GB) and ambrettolide (AMB), were polymerized using dodecylbenzenesulfonic acid (DBSA, pKa ~ -2,8 in water) and TfOH as catalysts (0.5-10 mol% relative to monomer), under bulk and miniemulsion conditions, at 80 °C (Scheme 8) as reported by Mecerreyes *et al.*[26] In bulk, both catalysts induced relatively fast polymerizations (> 98% of conversion after 24 h), resulting in polyesters with M_n around 10,000 g.mol^{-1}, TfOH being the most efficient. The high dispersity (*Đ* = 2-3), however, suggested the occurrence of significant transesterification side reactions. On the other hand, in miniemulsion conditions, only DBSA was active, producing oligoesters of M_n = 800 - 1,660 g.mol^{-1}. Based on ^{1}H NMR analyses, a condensation mechanism, involving the hydroxyl-carboxylic ring-opened macrolactone was actually proposed. The inactivity of TfOH in water miniemulsion was attributed to the redistribution of the protic charge on the sulphonic group over two or more water molecules, making this proton less available for monomer activation.

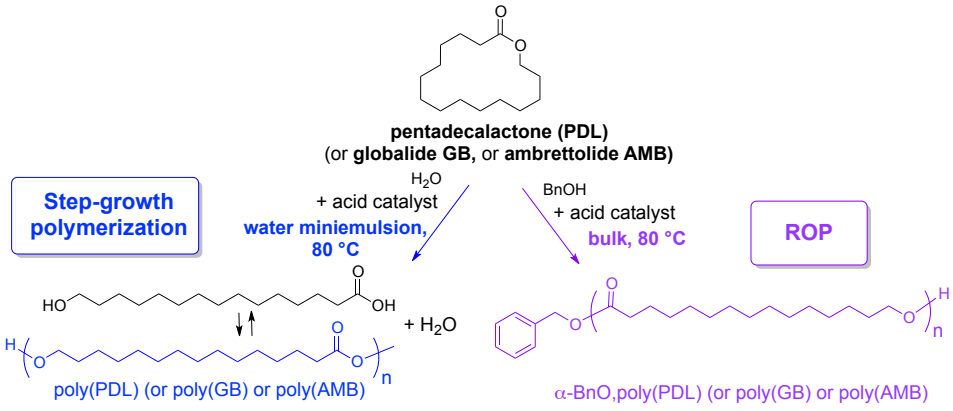

Scheme 8. Acid-catalyzed polymerization of macrolactones in bulk and miniemulsion (in the latter case, a polycondensation mechanism takes place). [26]

Later on, the same group reported the acid-catalyzed ROP of the renewable macrolactone ethylene brassylate (see Figure 3 for related structure), in bulk and in toluene, at 80 °C, using BnOH (1 eq.) as initiator.[27] Poly(ethylene brassylate)s of molar masses M_n = 5,900 g.mol^{-1} ($Đ$ = 1.9) and M_n = 2,000 g.mol^{-1} ($Đ$ = 2.7) were obtained when using DBSA and PTSA as catalyst (1 eq.), respectively. The use of a solvent avoided viscosity limitations but polymerizations were slower than that performed under bulk conditions (for a DP = 100, 58 % of monomer conversion after 96 h in toluene *vs.* 73 % after 44 h in bulk).

In this case again, although chain-ends analyses by MALDI-ToF mass spectrometry indicated an initiation by BnOH, the presence of species generated from inter- and intra-molecular transesterifications were also detected, hence a broad dispersity was observed.

Besides cyclic esters, cyclic carbonates have also been subjected to ROP by an acid catalysis. In 2010, Bourissou *et al.* first demonstrated the ability of TfOH and MSA to efficiently catalyze the ROP of trimethylene carbonate (TMC), in presence of *n*PenOH as initiator.[28] MSA was found to be a better catalyst than TfOH, avoiding side decarboxylation reactions, presumably due to its lower acidity. However, two distinct polymer populations (denoted as **A** and **B** in Scheme 9) were observed by size exclusion chromatography (SEC) with MSA. This was attributed to the competition between two mechanisms consisting in either a nucleophilic attack of the ROH onto the acid-activated monomer (Scheme 9a for population **A**), or in a nucleophilic attack of a non-activated monomer onto the acid-activated monomer (Scheme 9b for population **B**).

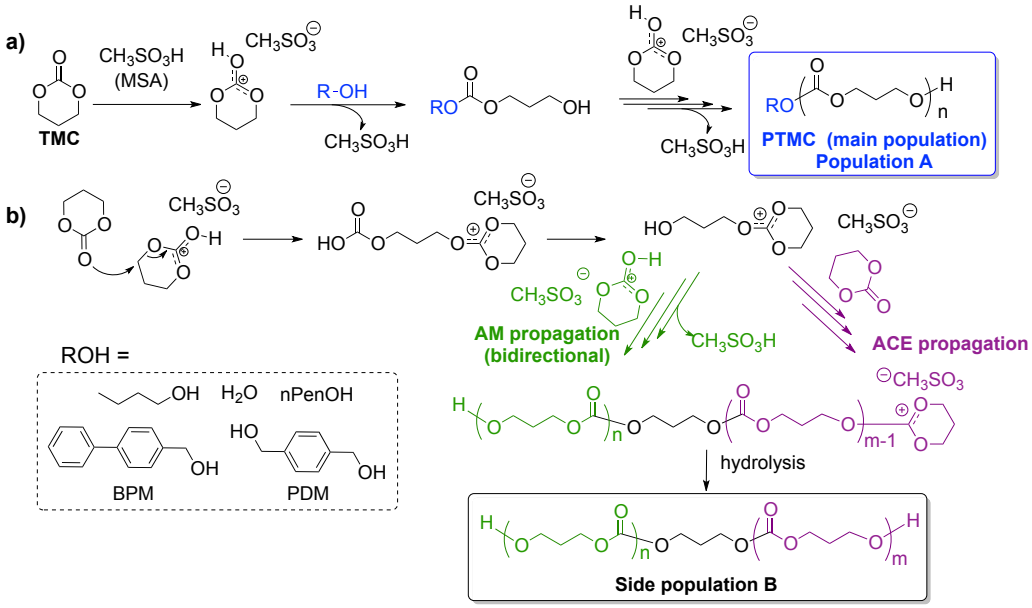

Scheme 9. ROP of trimethylene carbonate catalyzed by methanesulfonic acid a) AMM with mono-alcohol and b). AMM/ACEM combined biredictional mechanism.[28,29]

The MSA-catalyzed ROP of TMC was next investigated by Ribeiro, Peruch and co-workers, using a mono-alcohol (biphenyl-4-methanol, BPM) and a diol (1,4-phenylene-

dimethanol, PDM) as initiators, in toluene at 30 °C.[29] With BPM, PTMC with molar masses ranging from 3,000 to 15,000 g.mol^{-1} (*Đ* = 1.15-1.25) were obtained. The authors confirmed the occurrence of both the AMM and the ACEM as initially proposed by Bourissou *et al.*[28] Additionnally, they demonstrated that the use of PDM as diol initiating system (a situation where all chain propagations are bidirectional) enabled the preparation of PTMC exhibiting unimodal and narrow dispersity (*Đ* = 1.07-1.10) with M_n up to 16,800 g.mol^{-1}.

The MSA-catalyzed sequential copolymerization of ε-CL and TMC was then successfully achieved, producing PCL-*b*-PTMC diblock copolymers of M_n = 5,926-10,600 g.mol^{-1} (*Đ* <1.2) and PCL-*b*-PTMC-*b*-PCL (ROP of TMC first using H_2O as initiator) triblock copolymers of M_n = 9,080-29,370 g.mol^{-1} (*Đ* <1.2).[30,31] Simultaneous polymerization of the two monomers gave rise PCL-*gradient*-PTMC copolymers, with indeed a preferential insertion of ε-CL.

To gain a better mechanistic insight into the acid catalyzed ROP of TMC, computational calculations by density functional theory (DFT) in continuum dielectric representation of dichloromethane, with MSA or PTSA as catalysts, and 1,4-pyrenebutanol (PyBuOH) as initiator, were realized by Coady, Hedrick and co-workers.[32] DFT calculations revealed that only the AMM was operative instead of two distinct and competitive mechanisms (activation barrier ~ 17 kcal.mol^{-1} for AMM *vs.* 45 kcal.mol^{-1} for ACEM), as previously reported by Bourissou *et al.*[28] and Peruch *et al.*[29] on the basis of experimental investigations. The presence of adventitious water was most likely the cause of the two populations observed in these previous studies. Interestingly, DFT calculations also demonstrated that, instead of inducing a classical AMM, sulfonic acids actually favored a bifunctional activation of both the monomer carbonyl and the propagating hydroxyl group through H-bonding (Scheme 10). A similar mechanism was previously reported by Bourissou *et al.* regarding the ROH-initiated ROP of ε-CL catalyzed by MSA and TfOH [18,33] and, more recently, by Mecerreyes *et al.* for PTSA-catalyzed ROP of the macrolactone ethylene brassylate.[27]

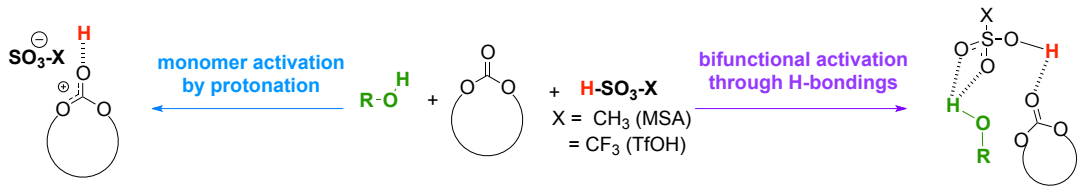

Scheme 10. Acid-catalyzed mechanism for the ROP of cyclic carbonates. Activation by protonation *vs.* bifunctional activation through H-bondings proposed by Coady, Hedrick and co-workers[32] and Bourissou *et al.*[33]

The acid-catalyzed ROP of TMC was also extended to functional carbonates. For instance, the ROP of a pentafluorophenyl activated carbonate, denoted as MTC-OC_6F_5, using *p*-toluenesulfonic acid (PTSA, pKa ~ -2.8 in water) and TfOH as catalysts (10 eq.) was reported.[34] Alcohol initiators such BnOH, PyBuOH, as well as a methoxy-terminated

poly(ethylene oxide) (MeOPEO-OH) were employed to this end (Scheme 11). Successful ROP of MTC-OC_6F_5 was achieved in dichloromethane at r.t., leading to poly(MTC-OC_6F_5) with M_n ranging from 5,000 to 37,200 g.mol^{-1} ($Đ$ <1.3). Interestingly, no reaction between ROH and the activated ester was observed under these conditions. When using PTSA, resulting polymers exhibited significantly lower M_n values than those expected, indicating a loss of control of the polymerization. These results contrasted with those previously reported for the ROP of TMC, where the weak MSA allowed a better control over the polymerization than the strong acid TfOH[28]. Although the authors did not comment the loss of control when using PTSA for the ROP of MTC-OC_6F_5, one can argue the steric hindrance of PTSA compared to TfOH. Poly(MTC-OC_6F_5) was subsequently post-functionalized, under mild reaction conditions, with a variety of primary and secondary amines including, as well as macromolecular amines such as NH_2PEO, providing rapid access to a wide range of functional polycarbonates.

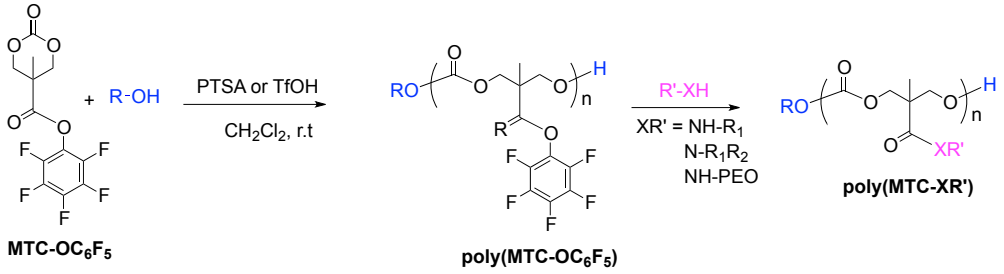

Scheme 11. ROP of MTC-OC_6F_5 catalyzed by *p*-toluenesulfonic acid (PTSA) or triflic acid (TfOH) in presence of alcohol initiator and further post-chemical modification.[34]

Besides ROP, organic acid-catalyzed step-growth polymerization reactions were also implemented. For instance, Hedrick *et al.* in collaboration with Mecerreyes *et al*. performed the polyaddition between PEO and hexamethylene diisocyanate (HDI) in dichloromethane at 20 °C, using MSA and TfOH as catalysts (Scheme 12).[35] These sulfonic acids were highly effective, yielding (98 % of monomer conversion) polyurethanes of molar masses (M_w) in the range of 18,300- 28,200 g.mol^{-1} and $Đ$ = 1.3-1.7.

DFT calculations suggested the occurrence of a dual hydrogen-bonding mechanism. This including protonation of the isocyanate nitrogen atom (*N*-activation) or the isocyanate oxygen atom (*O*-activation), with simultaneous nucleophilic activation of the alcohol by the conjugate base XSO_3^- (see insert in Scheme 12). While for the reaction catalyzed by TfOH, an unexpected preference for *N*-activation over *O*-activation was found, in the case of MSA, both pathways (*N*-activation and *O*-activation) occurred simultaneously due to the moderate acidity of MSA.

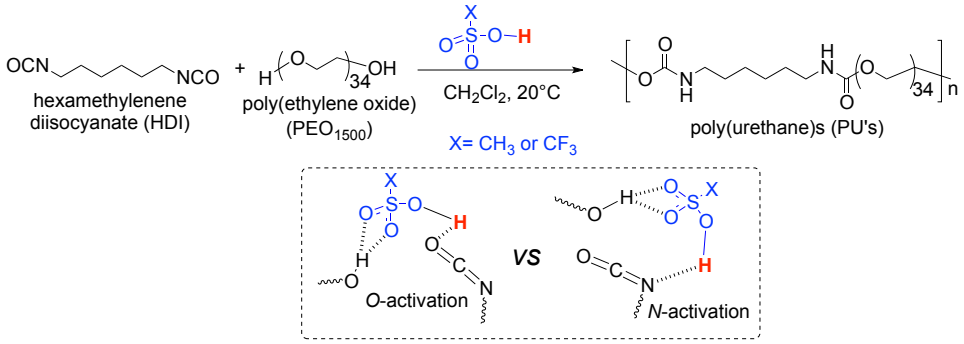

Scheme 12. Organic acid-catalyzed synthesis of PUs from diisocyanate and diol.[35]

As depicted in Scheme 13, the same team reported the post-polymerization modification of polyurethanes derived from such an acid-catalyzed polymerization.[36] Using 5 mol% of TfOH, the polyaddition between a pentafluorophenyl ester-containing diol, namely bis-MPA-C_6F_5, derived from 2,2-bis(hydroxymethyl)propanoic acid (bis-MPA), and hexamethylene diisocyanate (HDI) produced polyurethanes of M_n of 25,000-37,000 g.mol^{-1} ($Đ$ = 1.3-1.6). As previously reported,[34] these poly(bis-MPA-C_6F_5-HDI) urethanes were also post-functionalized on the side chains using various amines to give more complex functional polyurethanes.

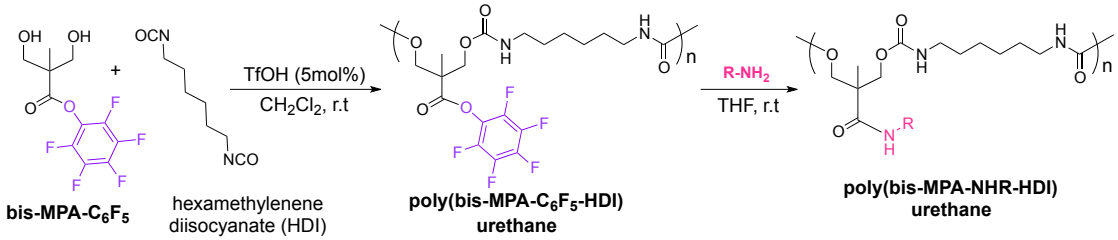

Scheme 13. Synthesis of polyurethanes (PUs) from bis-MPA-C_6F_5) and hexamethylene diisocyanate (HDI) using TfOH as catalyst.[36]

An acid-catalysis was also applied to the group transfer polymerizations (GTP) of methyl acrylate (MA) using trialkylsilyl ketene acetal (SKA) as initiators, namely, 1-trimethylsiloxy-, 1-triethylsiloxy-, and 1-triisopropylsiloxy-1-methoxy-2-methyl-1-propene (MTS^{Me}, $MTS^{Et,}$ and MTS^{iPr}, respectively). Pentafluorophenylbis(triflyl)-methane ($C_6F_5CHTf_2$, pKa ~ 1.5 in AcOH)[37] was used as a catalyst (2 mol% relative to initiator), in toluene at r.t.[38] Among these initiators, the bulkiest triisopropylsilyl ketene acetal (MTS^{iPr}) was the most suitable, minimizing back-biting reactions observed with other initiators tested. Poly(methyl acrylate)s (PMA's) of M_n = 2,900-108,000 g.mol^{-1} and narrow distributions ($Đ$ = 1.03-1.07) were thus obtained. Using the same strategy, *n*-butyl acrylate (*n*BuA) was copolymerized with MA, producing poly(methyl acrylate-*b*-*n*-butyl acrylate) (PMA-*b*-P*n*BuA) diblock copolymers of M_n = 11,500-14,200 g.mol^{-1} ($Đ$ < 1.05). According to the authors, the key intermediate species was the silicon Lewis acid, $C_6F_5C(SiR_3)Tf_2$, generated from the reaction between the SKA initiator and $C_6F_5CHTf_2$. The supposedly Lewis acid-activated monomer mechanism (see insert in Scheme

14) was thus different from either the associative or the dissociative mechanism generally proposed for the GTP of (meth)acrylates (Scheme 4b).[10]

Based on the previous results, the same group reported the use of *N*-(trimethylsilyl)bis-(trifluoroethanesulfonyl)imide (Me_3SiNTf_2) as catalyst for the GTP of *n*BuA in toluene at r.t., using MTS^{iPr} derivatives as functional initiators.[39] α-Functionalized (hydroxyl, ethynyl, vinyl, and norbornenyl) poly(nbutyl acrylate)s (PnBuA's) of M_n = 4,000-142,700 g.mol^{-1} (*Đ* =1.03-1.10) were thus synthesized. The use of 2-phenyl acrylate derivatives as terminating agents allowed synthesizing ω-functionalized (ethynyl, vinyl, hydroxyl, and bromo), as well as α,ω-functionalized polyacrylates of M_n = 4,000-4,800 g.mol^{-1} (*Đ* =1.06-1.08).

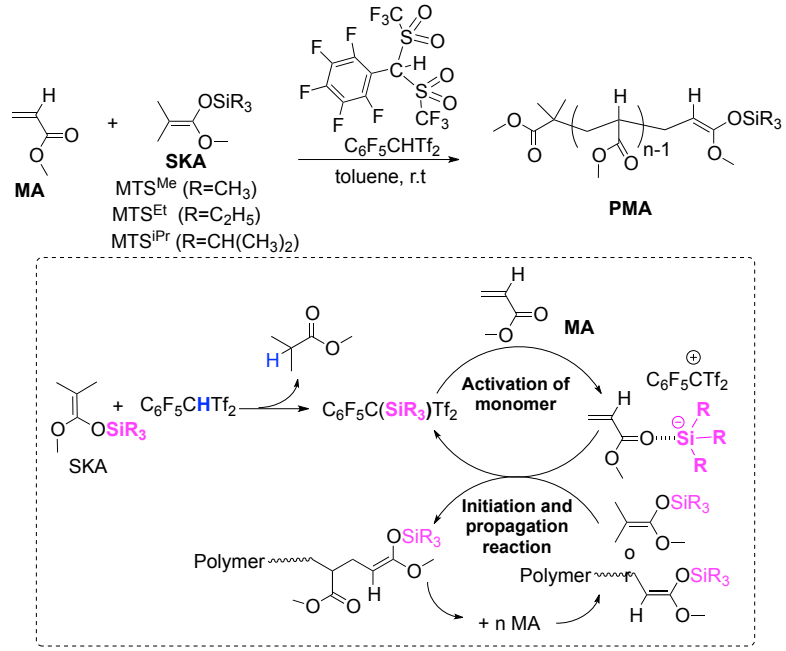

Scheme 14. C_5F_5-$CHTf_2$-promoted GTP of MA using trialkylsilyl ketene acetals initiators.[38]

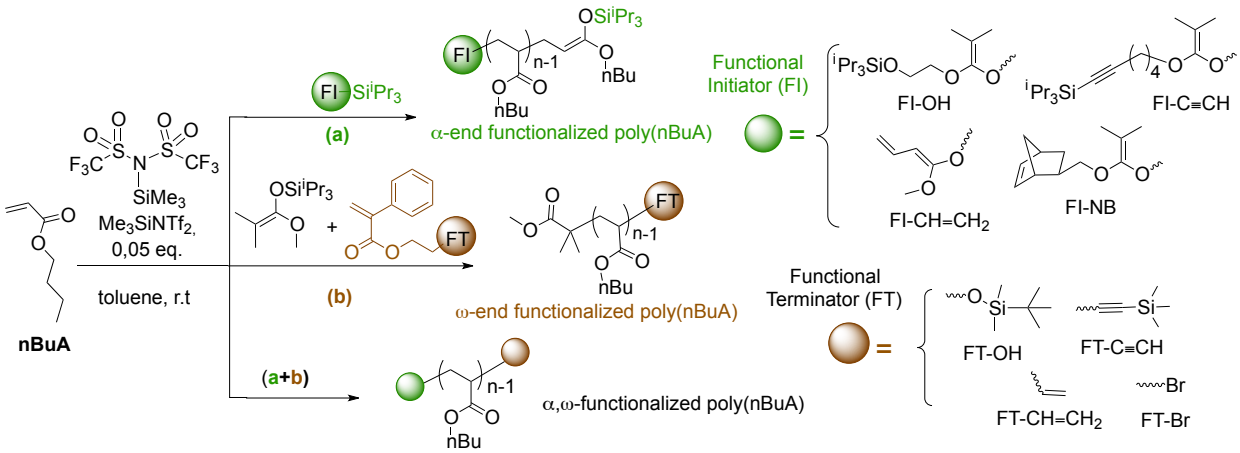

Scheme 15. Synthesis of α,ω-functionalized poly(nBuA) by Me_3SiNTf_2-catalyzed GTP using functional initiator and terminator.[39]

2.2. Carboxylic acid compounds

In comparison with sulfonic and sulfonimide acids (pka ≤ 1.5 in H_2O), carboxylic acids and amino-acids are weak acids (pka~ 3-5 in H_2O) that have been sparingly investigated as catalysts in polymerization reactions. Related studies have focused on cyclic esters and carbonates as monomer substrates (Figure 6).

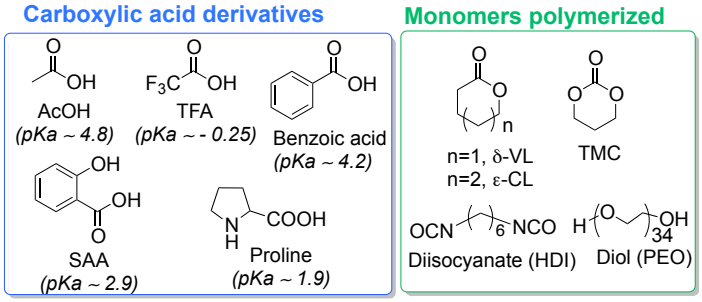

Figure 6. Represensative examples of carboxylic acids and monomers employed in organo-catalyzed polymerizations investigated (pKa in H_2O according to Evans pKa table).

For instance, the catalytic activity of salicylic acid (SAA; pKa ~ 2.9 in H_2O) was recently investigated for the ROP of ε-CL and δ-VL, with BnOH as the initiator (Scheme 16).[40] The polymerization successfully proceeded in bulk at 80 °C, leading to narrowly distributed polyesters with molar masses, M_n, in the range of 1,300-41,000 g.mol^{-1} ($Đ$ = 1.03-1.16) and M_n = 3,200-12,100 g.mol^{-1} ($Đ$ = 1.05-1.12) for PCL and PVL, respectively. Well-defined PCL-*b*-PVL diblock copolymers were also synthesized by sequential addition of ε-CL and δ-VL. In addition, end-functionalized PCLs with vinyl, propargyl and azido groups, as well as PEO-*b*-PCL copolymers could be prepared, using functionalized initiators, such as propargyl alcohol (PgOH), 6-azido-1 hexanol (AHA), 2-hydroxyethyl methacrylate (HEMA), and methoxy poly(ethylene oxide) (MeOPEO) macroinitiator. Based on interaction between SAA and ε-CL as determined by NMR, the polymerization was proposed to proceed by the AMM (see Scheme 1a) although a bifunctional activation can not be completely ruled out.

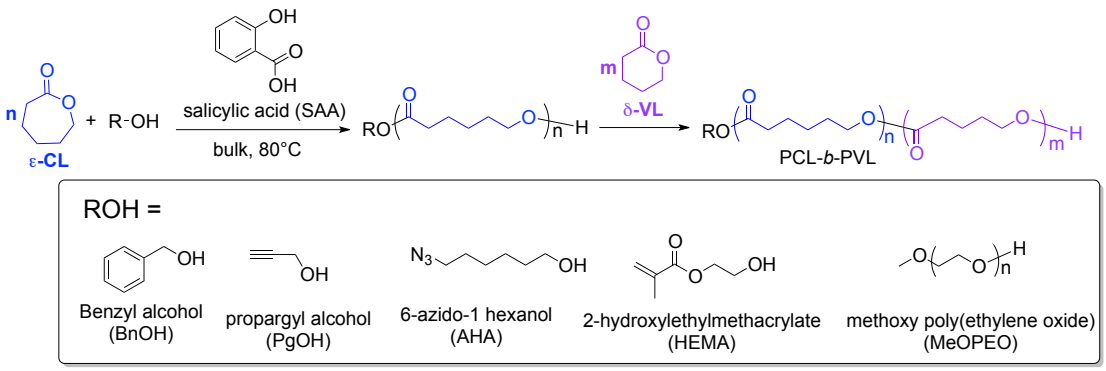

Scheme 16. Salicylic acid (SAA)-promoted ROP of ε-CL and δ-VL using alcohols as initiators.[40]

Trifluoroacetic acid (TFA, pKa~ -0.25 in H_2O), benzoic acid, and acetic acid (AcOH, pKa~ 4.2 in H_2O) were studied, both experimentally and computationally, for the ROP of TMC in dichloromethane at r.t., using PyBuOH as initiator.[32] Experimentally, no catalytic activity was found with these acids although in the case of TFA calculations showed similar energetic profiles than with the stronger acid MSA. In the latter case, instead of the pK_a argument, a bifunctional activation mechanism was put forward, with the acid bound to both monomer carbonyl and propagating hydroxyl group (see Scheme 10 above).

Regarding step growth polymerization reactions, the polyaddition between poly(ethylene oxide) and hexamethylene diisocyanate was conducted in dichloromethane, at 20 °C, using TFA and AcOH as catalysts.[35] In comparison with sulfonic acids (see Scheme 12 above), carboxylic acids were ineffective, and monomer conversions less than 3 % were reached after 6 h of reaction, as a consequence of their lower acidity.

2.3. Phosphoric acid and their derivatives

Compared to strong acids such as sulfonic and sulfonimide, phosphoric acids (pKa ~ 2-4)[41] have attracted a renewed interest as relatively mild Brønsted acids in organocatalysis in general, and in polymerization reactions in particular.[8,42] As highlighted in Figure 7, phosphoric acids exhibit a dual activation behavior by hydrogen-bonding *via* both their acidic proton and basic P = O moiety.[42] However, these catalysts are discussed here and not in the section devoted to bifunctional catalytic systems because we wish to compare them with other acid catalysts.

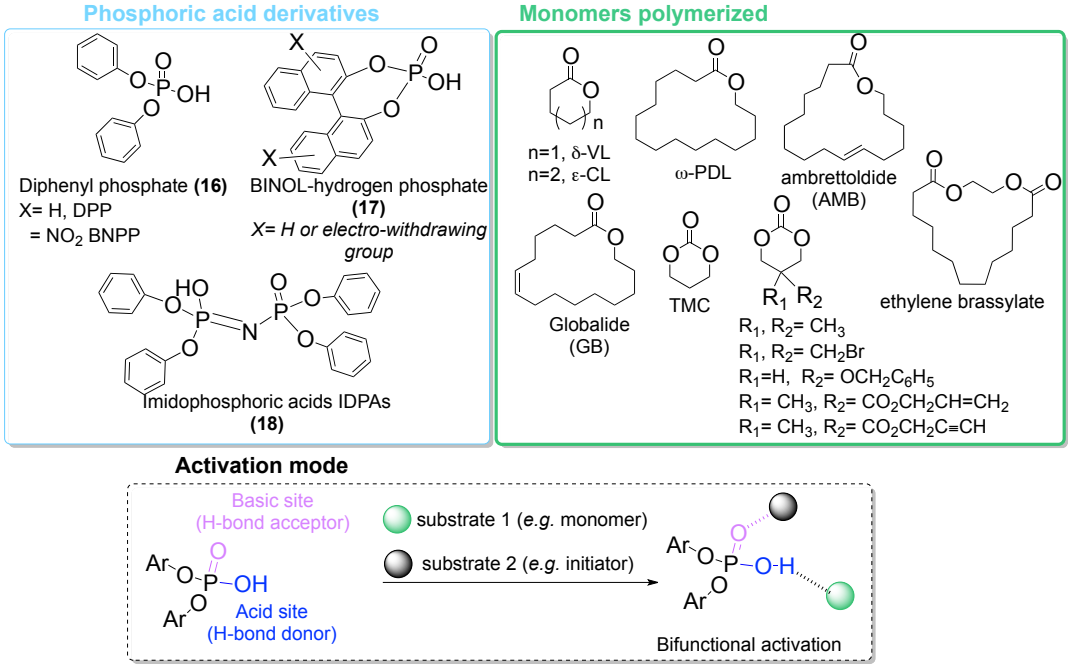

Figure 7. Representative phosphoric acids and monomers polymerized by them, as well as plausible bifunctional activation of monomer and initiator with Bronsted acid/base pair.[32,43]

In 2011, Kakuchi *et al.* described the synthesis of well-controlled PVL and PCL by ROP of δ-VL and ε-CL in toluene at r.t., using diphenyl phosphate (DPP) as organocatalyst and 3-phenyl-1-propanol (PPA) as initiator (Scheme 17a).[44] At [δ-VL or ε-CL]$_0$/[PPA]$_0$ /[DPP] ratio of 50/1/1, both polymerizations reached full conversion after a few hours, leading to polyesters of molar masses (M_n) of 5,920 g.mol^{-1} and narrow dispersity $Đ$ < 1.09 in both cases. PVL-*b*-PCL block copolymers were also synthesized by sequential ROP, regardless of the monomer addition sequence. Under the same conditions, bis(4-nitrophenyl) phosphate (BNPP; **16** in Figure 7 with X = NO_2), was shown to be an efficient organocatalyst for ROP of β-BL .[45] While DPP was insufficient, the introduction of nitro group into DPP enhanced the acidity of BNPP, resulting to the formation of PBL's of M_n = 2,240-10,650 g.mol^{-1} ($Đ$ = 1.20-1.39) in a controlled fashion.

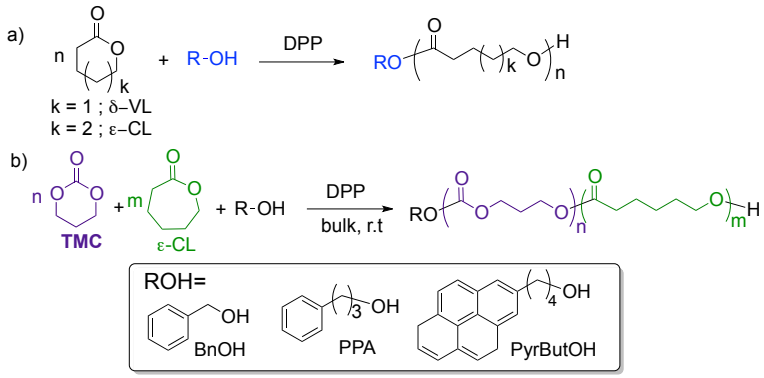

Scheme 17. ROP of δ-VL and ε-CL using phosphoric catalysts and alcohol (ROH) as the initiators.[44]

The DPP/ROH catalytic system was also applied by Mecerreyes *et al.* for the ROP of macrolactones ω-PDL, AMB, GB and ethylene brassylate in bulk and in aqueous miniemulsion at 80 °C, with BnOH as initiator (see Scheme 8).[26,27] For a DPP concentration of 0.5-10 mol% relative to BnOH, aliphatic polyesters of M_n = 5,600-21,000 g.mol^{-1} but rather high dispersity $Đ$ = 1.65-2.53 were obtained. The polymerization was slower than in the case of stronger acids, such as TfOH, DBSA, or PTSA, in agreement with the lower acidity of DPP. An activated monomer mechanism through protonation has been accounted for the DPP-catalyzed ROP of these macrolactones

DPP was also shown to catalyze the ROP of TMC in bulk or in dichloromethane at r.t., using PyBuOH, or PPA as initiators.[32,43] Polymerizations reached full conversion after 22h, producing PTMC of controlled molar masses (M_n up to 11,000 g.mol^{-1}; $Đ$ = 1.06), in accordance with the initial monomer-to-initiator ratio.

In the same way, Kakuchi *et al.* reported the ROP of cyclic carbonates possessing functional groups in the side-chain and chain-end such as, 5,5-dimethyl-1,3-dioxan-2-one, 5,5-dibromomethyl-1,3-dioxan-2-one, 5-benzyloxy-1,3-dioxan-2-one, 5-methyl-5-allyloxycarbonyl-

1,3- dioxan-2-one, and 5-methyl-5-propargyloxycarbonyl-1,3-dioxan-2-one (Figure 7), with PPA as initiator and DPP as catalyst.[43] Diblock copolymers consisting of a PTMC segment and a second PCL or PVL block were obtained in bulk at r.t., with molar masses increasing from 4,920 ($Đ$ = 1.11) to 10,500 g.mol^{-1} ($Đ$ = 1.12) for the TMC/ε-CL system, and from 4,990 ($Đ$ = 1.09) to 9,760 g.mol^{-1} ($Đ$ = 1.14) for the TMC/δ-VL one (Scheme 17b).

Curiously, ROP of MTC-OC_6F_5 using alcohols as initiators and DPP as catalyst did not proceed after 48 h, whereas TfOH allowed polymerizing this monomer under the same conditions (*vide supra)*.[34] This inactivity of DPP towards MTC-OC_6F_5 compared to TMC was ascribed to the occurrence of side reactions between the functional ester moiety and DPP.

Binaphthol (BINOL)-derived monophosphoric acids (**17**, Figure 7) represent a special class of chiral Brønsted acid catalysts widely used for enantioselective organic transformations, and have been recently applied to polymer synthesis.[46,47] In particular, the BINOL-derived phosphoric acid, namely binaphthyl-diyl hydrogen phosphate (BNPH, **17** in Figure 7 with X = H), proved to efficiently catalyze the ROP of ε-CL and δ-VL, with BnOH as initiator in bulk at 40-60 °C.[48] Polymers with M_n = 4,500-12,000 g.mol^{-1} ($Đ$ = 1.08-1.17) were produced in this way. Interestingly, the use of selectively protected monosaccharides (mono- and polyols D-glucose derivatives) as initiators led to functionalized-carbohydrate polyesters.[49]

Besides phosphoric acid catalyst, imidodiphosphoric acid (IDPA, **18** in Figure 7) have been employed for the ROP of δ-VL and ε-CL in toluene at r.t., with BnOH as initiator.[50] Well-defined PVL and PCL of M_n values in the range of 4,340-20,150 g.mol^{-1} ($Đ$ = 1.14-1.24) were thus obtained. IDPA was also studied for the BnOH-initiated ROP of TMC in toluene at r.t and 50 °C.[51] No side decarboxylation was noted at 50 °C, giving rise to well-defined PTMC's, with M_n = 1,800-18,000 g.mol^{-1} and $Đ$ = 1.12-1.19. Additionally, telechelic and star-shaped PTMC's were synthesized using various initiators. Well-defined diblock copolymers, PTMC-*b*-PVL and PTMC-*b*-PCL, could also be obtained by sequential polymerization of TMC with δ-VL and ε-CL, using IDPA as catalytic system.

In summary, organic acids, from weak to strong acids, have (re)emerged as a novel class of organic catalysts for polymerization reactions. It has been demonstrated that, in some cases, the catalyst efficiency did not simply correlate with its acidity, suggesting a different mechanism such as a dual activation of both the monomer and the initiator. Thus, the use of such acid organocatalysis proved efficient not only for the ROP of cyclic esters and carbonates, but also for polyurethane synthesis and for a few other examples of step-growth polymerizations.

3. Polymerization catalyzed by phosphorous-containing Brønsted and Lewis bases: phosphazenes and phosphines

Phosphazenes and phosphines are Brønsted and Lewis bases, respectively (Figure 7), which have been investigated as catalysts mainly for the ROP of cyclic monomers, but also for the GTP polymerizations of (meth)acrylic substrates (Figure 8).

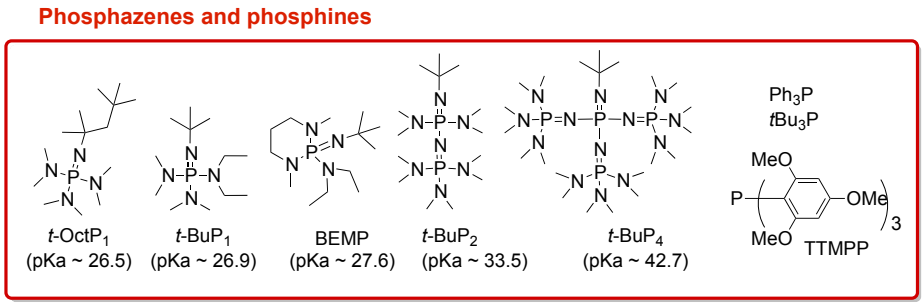

Figure 8. Represensative examples of the phosphazenes bases (pKa values in acetonitrile[52]) and phosphines.

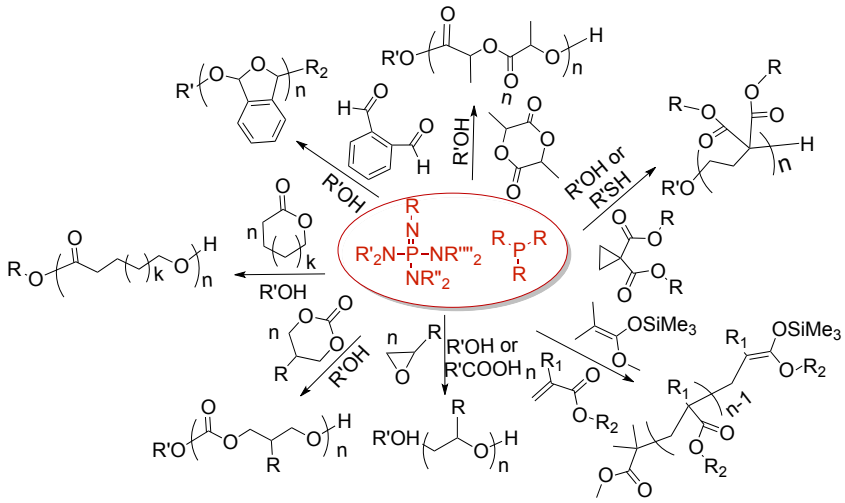

Figure 9. Overview of polymerization reactions catalyzed by phosphazenes (mainly) and phosphines

3.1. Phosphazenes

Initially developed by Schwesinger,[53] phosphazenes are strong neutral bases (pKa = 26-47 in MeCN)[52] and weak nucleophiles, which have been used to catalyze the ROP of cyclic (*e.g.* cyclopropanes) and heterocyclic (*e.g.* esters, ethers or carbonates) monomers, but also for the anionic polymerization of vinyl monomers (*e.g.* alkyl (meth)acrylates). In the presence of protic initiators, phosphazenes operate *via* an ACEM (see Scheme 4), in agreement with

their high basicity and low nucleophilicity. The deprotonation of a protic initiator, such as ROH results in the formation of a soft and bulky phosphazenium cation that allows controlling the polymerization reactions.[54] Other initiating systems containing thiols-, amide-, or even CH-containing precursor can also be used to induce a controlled/living polymerization pathway. Most of phosphazenes used in ROP and monomers investigated are shown in Figures 8 and 9.

The ROP of cyclic ethers with phosphazenes as catalysts have been (re)investigated by Hadjichristidis *et al*. For instance, the 1-*tert*-butyl-4,4,4-tris(dimethylamino)-2,2-bis[tris-(dimethylamino)phosphoranylidenamino]-2λ^5,4λ^5-catenadi(phosphazene), denoted as *t*-BuP$_4$ (see Figure 8) was employed (1.15 eq) to trigger the ROP of several epoxides in THF at 45 °C, including ethylene oxide (EO), propylene oxide (PO), 1,2-butylene oxide (BO) and *tert*-butyl glycidyl ether (*t*BGE), using poly(*N*,*N*-dimethylacrylamide-*co*-acrylamide) (CoAm) as macroinitiator (Scheme 18).[55] In contrast to EO and PO, BO and *t*BGE could not undergo direct anionic ring-opening graft polymerization (AROGP) from the CoAm precursor, most probably to due their steric hindrance. These polymerizations yielded macromolecular combs with various side chains, including single- or double graft homopolymers, block and statistical copolymers (M_n in the range of 640-1,712 kg.mol^{-1},; *Đ* = 1.17-1.31). Initiation was proposed to occur through deprotonation of primary amides by *t*-BuP$_4$.

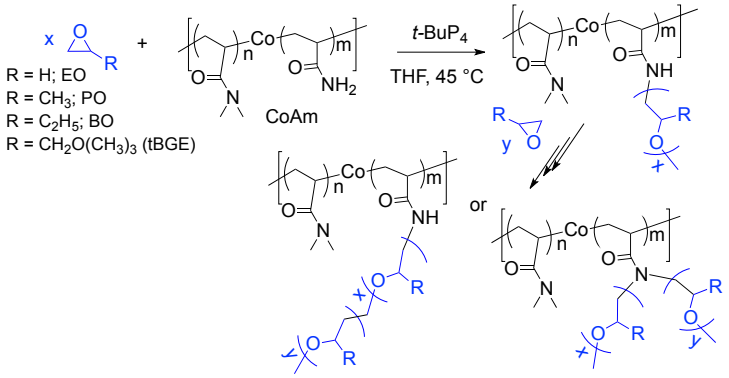

Scheme 18. *t*-BuP$_4$ promoted anionic graft polymerization of epoxides from acrylamide-based backbone.[55]

The polymerization of EO in THF at 45 °C initiated by carboxylic compounds *i.e.* 1-pyrenebutyric acid (PyBA) and palmitic acid (PmA), in presence of *t*-BuP$_4$ as catalyst (10-50 mol% relative to the initiator) was then investigated (Scheme 19).[56] PEO's thus obtained exhibited molar masses M_n = 1,740-2,270 g mol^{-1} and dispersity values in the range 1.04-1.13. Kinetic studies revealed an induction period that was explained by the rather slow ring-opening of EO by carboxylate phosphazenium (Scheme 20a), followed by slow chain-growth, with simultaneous fast end-group transesterification and proton transfer (Scheme 20b).

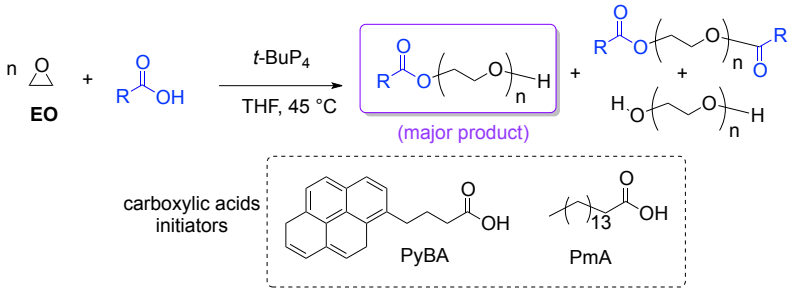

Scheme 19. *t*-BuP_4 promoted-ROP of ethylene oxide (EO) initiated by carboxylic acids.[56]

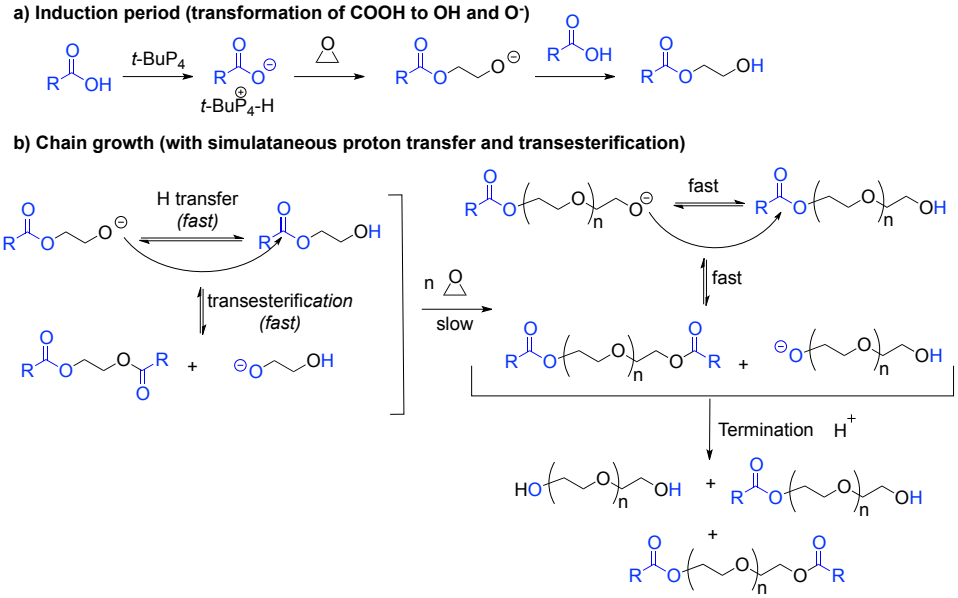

Scheme 20. Proposed mechanism for the *t*-BuP_4 promoted-ROP of ethylene oxide (EO) initiated by carboxylic acids.[56]

Sequential metal-free ROP of epoxides (EO and/or BO) and cyclic ester (ε-CL or δ-VL)/carbonate (TMC) monomers was then reported by Hadjichristidis *et al.* To this end, the authors switched the polymerization catalyst, from the *t*-BuP_4 base (for epoxides), to DPP acid (for cyclic esters/ carbonate).[57,58] EO and BO were thus first polymerized in THF at 40 °C, using PPA as initiator and *t*-BuP_4 as catalyst (0.2 eq), giving polyethers of M_n = 1,300-3,800 g.mol^{-1} and $Đ$ = 1.04-1.05. An excess of DPP (1.2 eq) was then introduced, followed by addition of ε-CL, δ-VL or TMC. Resulting polyether-polyester/polycarbonate block copolymers, with molar masses M_n = 6,200-3,800 g.mol^{-1} and $Đ$ = 1.04-1.72 were synthesized in this way.

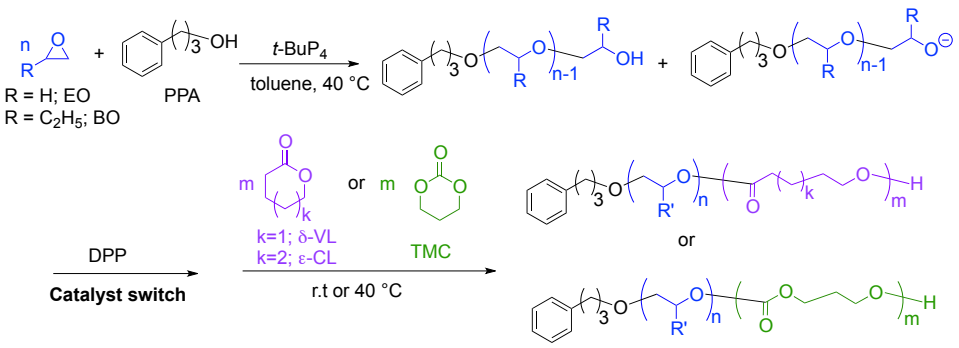

Scheme 21. Sequential ROP of EO,BO and ε-CL/δ-VL/TMC using the "catalyst switch" strategy from *t*-BuP$_4$ to DPP.[57]

Later on, the same group studied the catalytic activity of a less-hindered phosphazene base, 1-*tert*-butyl-2,2,4,4,4-pentakis(dimethylamino)-2λ^5,4λ^5-catenadi (phosphazene), denoted as *t*-BuP$_2$ (see Figure 8) for the ROP of EO, ε-CL and LLA in THF at 50 °C, using PPA or even water as initiators.[59] Complete EO conversion was achieved after 3 days, leading to PEO's with predictable molar mass (M_n = 4,600 g mol^{-1}; *Đ* = 1.03). Well-defined PEO-*b*-PCL diblock and PCL-*b*-PEO-*b*-PCL triblock copolymers of M_n = 10,900 (*Đ* = 1.09) and 13,300 g.mol^{-1} (*Đ* = 1.11), respectively, were next generated by addition of ε-CL to the PEO living chains. Triblock and even pentablock copolymers, PEO-*b*-PCL-PLLA (M_n = 16,100 g.mol^{-1}; *Đ* = 1.11), were synthesized by introduction of LLA (nearby complete conversion of LLA within 10 min). It was essential to follow EO-εCL-LLA addition order of to avoid any inter- or intra-macromolecular side reactions, which could occur extensively during the ROP of EO with PCL or PLLA block macroinitiators. The same group investigated the influence of solvents over such *t*-BuP$_2$-catalyzed ROP of εCL and LLA at r.t., using primary alcohols as initiators.[60] While a higher polymerization rate was noted in more polar solvents (comparison DCM *vs.* toluene), slower polymerization reactions were observed in cyclic ether solvents (comparison THF, 1,4-dioxane *vs.* toluene). Due to their slight basicity, these cyclic ether solvents migh interact with the initating species thus, slowing down the ROP.

Phosphazene catalysts have been also applied to the ROP of cyclic carbonates. For instance, Guillaume, Carpentier and co-workers reported the one-pot, two-step sequential copolymerization of TMC and L-LA in toluene at 100 °C, using the phosphazene 2-*tert*-butylimino-2-diethylamino-1,3-dimethylperhydro-1,3,2-diazaphosphorine (BEMP) combined with BnOH as initiator.[61] TMC was first polymerized prior to the addition of L-LA, yielding PTMC-*b*-PLLA diblock copolymers of molar masses M_n of 36,150 g.mol^{-1} (*Đ* = 1.32). While PLLA is a tough and brittle material, PTMC-*b*-PLLA copolymers demonstrated better thermo-mechanical properties, evidencing the advantage of the presence of a rubbery PTMC moiety.

In the same way, *tert*-octylimino-tris(dimethylamino)phosphorane (*t*-OctP$_1$) *t*-BuP$_2$, and *t*-BuP$_4$-catalyzed ROP of TMC, in the presence of native starch granules as inexepensive

naturally occurring macroinitiators, proceeded in bulk at 150 °C (Scheme 22).[62] This strategy allowed synthesizing polycarbonate/starch composite materials with enhanced physical properties and biodegradability over the native starch. The phosphazene catalysts showed an excellent catalytic activity (98 % of monomer conversion after only 2 min of reaction), even at very low concentration (*e.g.* with 0,01 mol% of *t*-BuP_4). PTMC's with moderate molar masses (M_n = 3,800-5,160 g.mol^{-1}; $Đ$ = 1.24-1.34) and surface modified starch-graft-PTMC having a DP = 2–12 (depending on the measurement technique) were thus obtained, demonstrating the robustness of phosphazenes toward the presence of starch and water. The successful homopolymerization of TMC was in fact explained by the presence of 1,3-propanediol formed by TMC hydrolysis and playing the role of a co-initiator. It can be hypothesized that this hydrolysis might reduce the amount of water in the system, explaining the remained activity of phosphazenes even at low concentrations.

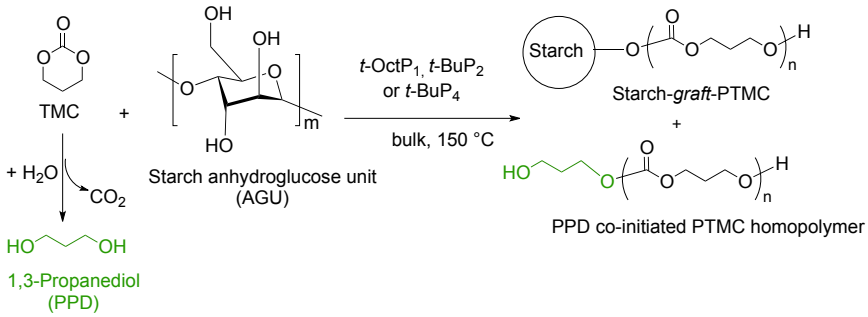

Scheme 22. Sequential ROP of TMC in the presence of native starch granules (anhydroglucose unit) using phosphazenes as catalysts.[62]

Penelle, Barbier, Boileau and co-workers developed the organo-catalyzed ROP of specific cyclopropane monomers, namely, dialkyl cyclopropane-1,1-dicarboxylates. For instance, the polymerization of di-n-allyl cyclopropane-1,1-dicarboxylate monomer (DACDC) was triggered by *t*-BuP_4 as catalyst (1eq.) in THF at r.t., in presence of thiophenol as initiator (Scheme 23a).[63] Quantitative conversions were obtained after 2 days, and final polymers exhibited experimental molar masses close to the theoretical ones (M_n = 3,900-12,500 g.mol^{-1}; $Đ$ = 1.1-1.2). Poly(DACDC)'s displayed geminated allyl groups along polymers chains, as expected. The density of allyl groups along the polymer backbone could be further modulated through copolymerization experiments with di-n-propyl cyclopropane-1,1-dicarboxylate (DPCDC; Scheme 23b). Statistical and block copolymers were obtained and post-polymerization modification of these allyl-substituted polymers could be readily achieved by thiol-ene chemistry.

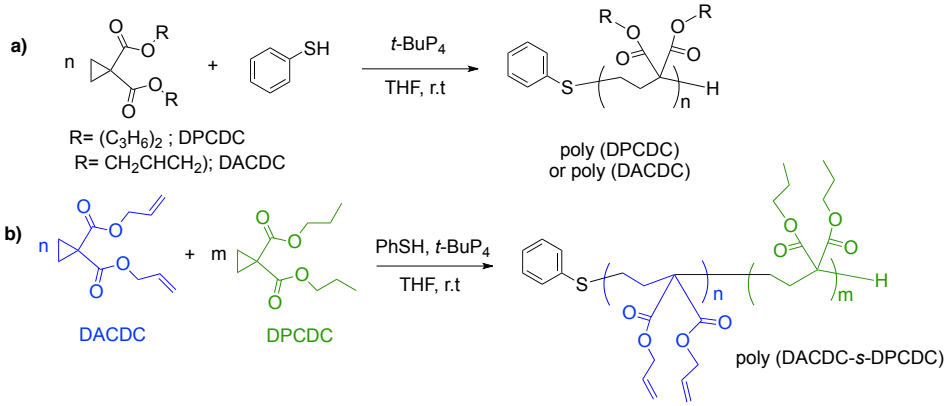

Scheme 23. ROP of cyclopropane carboxylates (DPCPC and DACPC) in the presence of PhSH as initiator and *t*-BuP$_4$ as catalyst. a) homopolymerization and b) statistical copolymerization.[63]

Phosphazenes also enabled directly polymerizing methacrylic monomers. Zhang *et al.* thus reported that *t*-BuP$_4$ could induce the copolymerization of ε-CL with methyl methacrylate (MMA), *tert*-butyl methacrylate (*t*BuMA) or glycidyl methacrylate (GMA) in toluene at r.t., in presence of various initiators, *i.*e., MeOH, ethylene glycol (EG) or ethyl acetate (EA) (Scheme 24). [64-66] According to NMR analyses and thermal characterizations, random copolymers, PCL-*co*-PMMA or PCL-*co*-P*t*BuMA, were obtained with molar masses (M_n) in the range 1,800-50,000 g.mol^{-1} and $Đ$ = 1.2-3. Hydrolysis of *tert*-butyl groups of PCL-*co*-P*t*BuMA yielded poly(ε-CL-*co*-methacrylic acid) poly(CL-*co*-MAA), *i.e.* a degradable statistical copolyelectrolyte. The authors suggested that copolymerization occured *via* a hybrid mechanism, involving a combination of vinyl polymerization and ROP through alcohol activation by *t*-BuP$_4$. The activated alcohol could attack the monomer (ε-CL or MMA, with ε-CL being the most reactive), producing two kinds of active centers **19** and **20** (Scheme 24). Then, these active centers were able to react with either MMA or CL, forming new propagating centers. The reaction mechanism was not fully elucidated, however, and some side reactions such as homopolymerization or transesterification reactions migh have occurred.

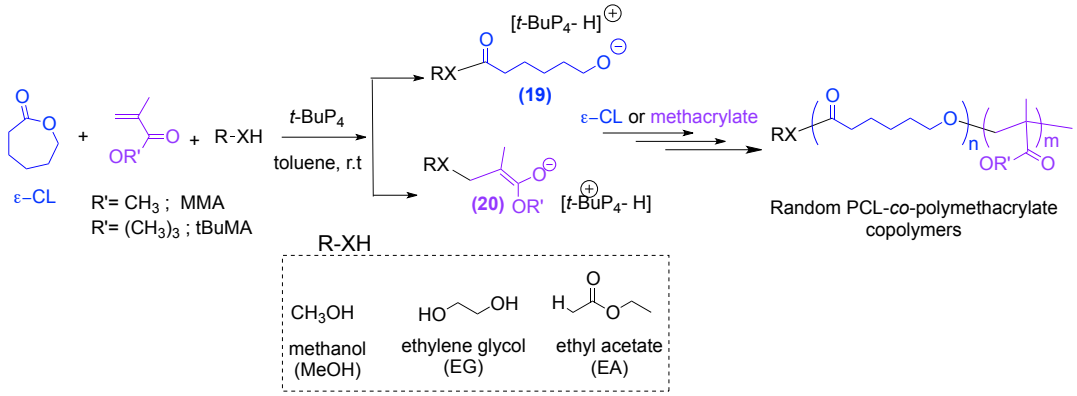

Scheme 24. Hybrid copolymerization of cyclic esters ε-CL (ROP) with methacylic monomers MMA and *t*BuMA (1,4-conjugate addition polymerization).[64 65]

Recently, Coulembier *et al.* investigated the use of *t*-BuP$_1$ as catalyst in the cyclopolymerization of ortho-phthalaldehyde (PA) initiated by either 9-anthracenemethanol or MeOPEO-OH in dichloromethane at -85 °C (Scheme 25).[67] Poly(ortho-phthalaldehyde)'s and poly(ethylene oxide)-*b*-poly(ortho-phthalaldehyde) diblock copolymers of molar masses M_n = 3,150-200,000 g mol^{-1} ($Đ$ = 1.15-1.27) were synthesized with end-group fidelity.

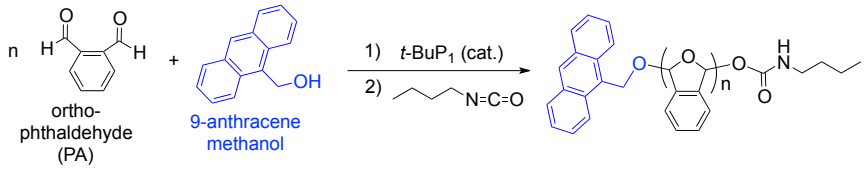

Scheme 25. *t*Bu-P1-catalyzed cyclopolymerization of ortho-phthalaldehyde.[67]

3.2. Phosphines

Even though phosphines have been widely employed as catalysts in a variety of organic transformations,[68,69] their use in polymerizations reactions has scarcely been investigated.[70] Alkyl/aryl phosphines such as tributylphopshines (Bu_3P), dimethylphenylphosphine ($PhMe_2P$), methyldiphenylphosphine (Ph_2MeP) and triphenylphosphine (Ph_3P), and related phosphines were shown to be effective catalysts for the ROP of LA, generating narrowly dispersed polylactides with predictable molar masses (M_n = 2,800-13,000; $Đ$ = 1.11-1.40) through a nucleophilic AMM (Scheme 2a). The substitution pattern of the phosphine was a dominant feature in controlling their reactivity. Thus, alkyl-substitued phosphines, being more basic and more nucleophile, proved more active than aryl-containing counterparts.[70]

In 2012, Taton *et al.* reported that tris(2,4,6-trimethoxyphenyl)phosphine (TTMPP) could efficiently catalyze the GTP of MMA and *tert*-butyl acrylate (*t*BuA), using 1-methoxy-2-methyl-1-[(trimethylsilyl)oxy]prop-1-ene (MTS) as initiator (Scheme 26).[71] GTP experiments could be conducted in bulk or in THF at r.t. This TTMPP-catalyzed GTP provided poly[alkyl(meth)acrylate]s of M_n = 3,000-10,600 g.mol^{-1} (Đ < 1.37 in bulk and Đ < 1.45 in THF), in accordance with the initial [monomer]$_0$/ [MTS]$_0$ ratio. Through sequential polymerization, PMMA-*b*-P*t*BuA diblock copolymers of controlled molar masses (M_n = 22,600 g.mol^{-1}; $Đ$ = 1.19) were also synthesized. TTMPP-derived PMMA's exhibited a tacticity of mm/mr/rr = 0.06/0.41/0.53, *i.e.* very similar to that of PMMA grown by an anionic process, suggesting the occurrence of a dissociative mechanism (Scheme 4b), though, attempts to identify enolate-type species by NMR analysis were unsuccessfull.

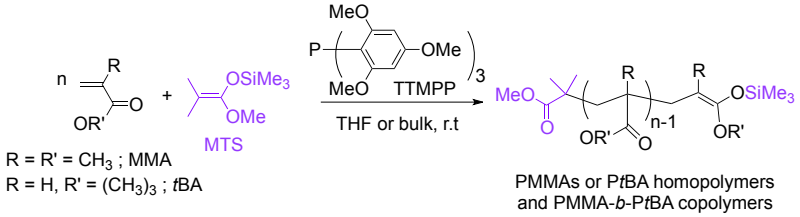

Scheme 26. Phosphine-catalyzed GTP of MMA and *t*BuA.[71]

In summary, commercially available phosphazene Brønsted “superbases” are powerful organocatalysts which have been mainly investigated for ROP of epoxides, cyclic esters, cyclic carbonates and cyclopropane-1,1-dicarboxlates, and few examples of polymerization of (meth)acrylics. Due to their strong basicity and low nucleophilicity, phosphazenes allowed for an *in situ* generation of anionic initiators by depronotantion of compounds containing OH, COOH, SH and NH functions. Polymers with a high end-group fidelity are generally produced because of the pairing of the active anionic propagating species with the bulky and soft phosphazenium cation deriving from the phosphazene catalyst.

On the other hand, despite their widespread use in molecular chemistry, phosphine Lewis bases have scarcely been investigated as catalysts in polymerization reactions. In this thesis manuscript, chapter 4 will be dedicated to the study of some trialkyl phosphines and, in particular, to the use of TTMPP in combination with a Lewis acid to induce the polymerization of MMA.

4. Polymerization catalyzed by free and latent *N*-heterocyclic carbenes (NHCs)

N-heterocyclic carbenes (NHCs) are a specific subgroup of carbenes that are neutral compounds featuring a divalent carbon atom with a six-electron valence shell; four electrons are involved in σ-bonds and two remain at the central carbon.[72-77]

While σ-donor properties of NHCs lead to either a Brønsted basic (pKa ~ 15-30 in H_2O)[78,79] or a nucleophilic-type catalysis, the combination of their σ-donor and π-acceptor properties (Figure 10), allows activating various substrates.[3,80-84] With these properties, not only can NHCs serve as powerful ligands for transition metals,[85-87] but they have also emerged as true organic catalysts in molecular chemistry (*e.g.* benzoin condensation, Stetter reaction and transesterification etc.).[88-93]

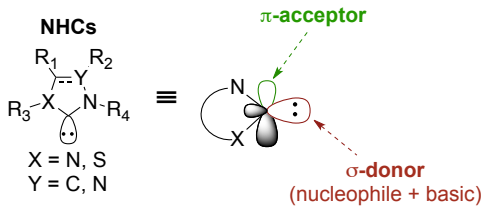

Figure 10. Electronic properties of *N*-heterocyclic carbenes (NHCs).[94]

In the context of macromolecular chemistry, NHCs have been applied for both chain-growth and step-growth polymerization reactions (Figure 11) in the past decade.[7,15,95] The field of NHC-catalyzed polymerization reactions has been reviewed in 2013 by our group.[15] Main researches have focused on the use of “free” NHCs derived from imidazol(in)ium salts, but

efforts have also been (re)directed towards the design of more air-tolerant “protected” NHCs (called “masked” NHCs). Indeed, these NHC precursors are generally easier to handle than bare NHCs, avoiding the use of controlled inert atmospheres.[96] Figure 12 illustrates the main categories of NHCs used in polymerization reactions.

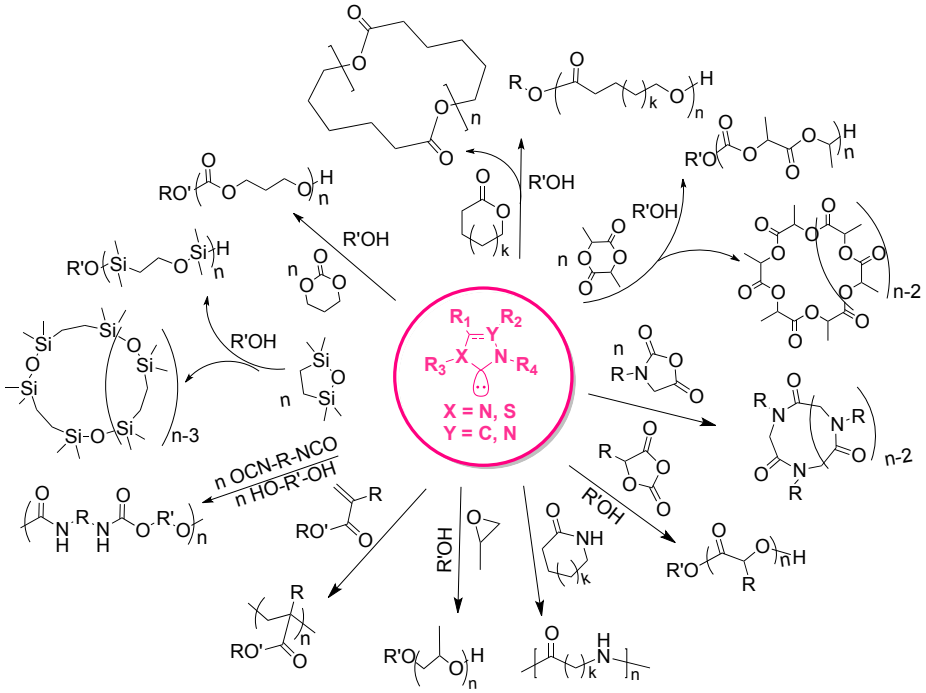

Figure 11. Scope of NHC-catalyzed polymerization reactions.

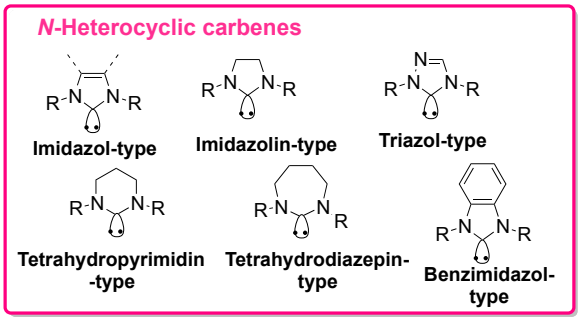

Figure 12. Represensative NHC families used in polymerization reactions.

4.1. Free NHCs

Free NHCs are generally prepared by deprotonation of corresponding imidazole(in)ium salts with a strong base (*e.g.* NaH or *t*BuOK) (Scheme 27a).[97] Other routes for NHC preparation include: b) electrochemical reduction of imidazol(in)ium salts,[98,99] c) chemical reduction of imidazol-2(3H)-thiones by a metal (typically. potassium)[100] or d) thermal activation of “masked” NHCs.[96]

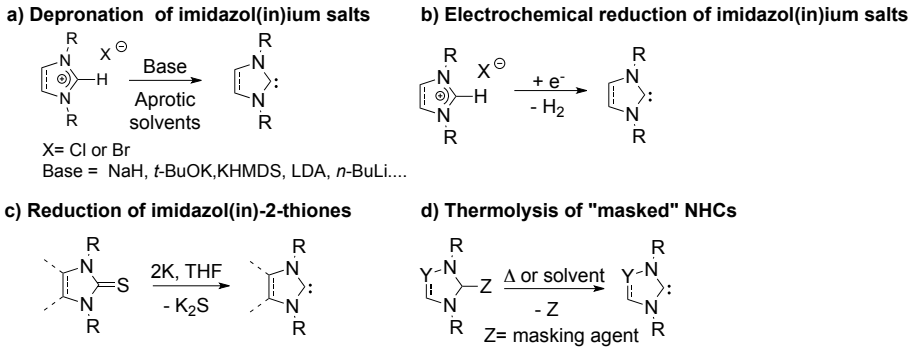

Scheme 27. Main synthetic routes for the generation of imidazol(in)-2-ylidenes. [96-100]

Hedrick, Waymouth and co-workers previously demonstrated that, in the presence of alcohol initiators, NHCs could efficiently catalyze the ROP of cyclic esters (lactide and lactones) with a turn over frequency (TOF) of 18 s^{-1}, while exhibiting many features of a controlled polymerization.[7] In agreement with experimental observations, DFT calculations suggested that the polymerization operated by a combination of both a nucleophilic AMM (Scheme 3a) and a H-bonding ACEM (Scheme 4a). Competiton between both mechanisms might occur, particularly at very low alcohol concentration (high monomer/initiator ratios), for which experimental molar masses deviated from those predicted.

The ROP of cyclic esters have been extensively described, with a variety of NHCs. For instance, a series of 1,3-non symetrically substituted imidazol-2-ylidenes (NHC12-15; Scheme 28) have been re-investigated as catalysts for the ROP of L-LA[101], ε-CL and 2,2-dimethyltrimethylene carbonate (DTC)[102], in the presence of BnOH as initiator (Scheme 28). Homopolymers (M_n up 26,800 $g.mol^{-1}$; $Đ$ = 1.3-1.5) were obtained in quantitative yield, as well as PCL-*b*-PDTC diblock copolymers (M_n up 28,500 $g.mol^{-1}$; $Đ$ = 1.4-1.5). The catalytic activities of these NHCs significantly increased with the electron-donating ability of the substituents. For instance, NHC14 (see Scheme 26 for related structure) was found more efficient than NHC12 and NHC13 to control the ROP of ε-CL and DTC.[102]

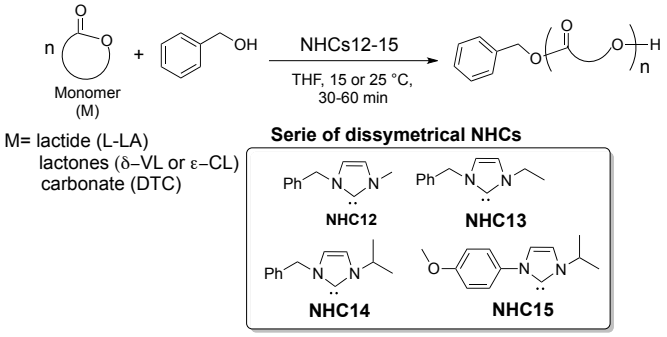

Scheme 28. ROP of cyclic esters and carbonates catalyzed by dissymmetrical NHCs in presence of BnOH as initiator.[101,102]

Symetrical imidazol-2-ylidenes (NHC1, NHC7-8; see Figure 2 for related structures) and

imidazolin-2-ylidenes (NHC18-19) were screened for the ROP of the *O*-carboxyanhydride (OCA) of L-lactic acid (L-lacOCA), using BnOH as initiator (Scheme 29).[103] All NHCs allowed polymerizing L-lacOCA in THF at r.t., yielding poly(L-lacOCA) of controlled molar masses (M_n = 1,080-12,670 g.mol^{-1}; $Đ$ = 1.10-1.41). No significant differences between imidazol- (unsaturated) and imidazolin-type (saturated) carbenes were noted. Within a same family, kinetics and polymerization control increased with the steric hindrance of the carbene (NHC7 > NHC8 >> NHC1). This difference was attributed to the lower stability of the less hindered carbenes, and their tendency to dimerize, especially for NHC1.[104]

Additionally, polylol-type macroinitiators were used to derive *α,ω*-dihydroxy telechelic, star-shaped polymers and diblock poly(*α*-hydroxy acid) (PAHA) by NHC-catalyzed ROP of L-lacOCA and L-manOCA (OCA of L-mandelic acid; Scheme 29).

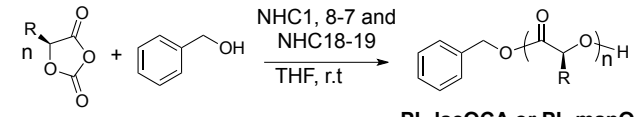

Scheme 29. BnOH-initiated ROP of L-lacOCA and L-manOCA catalyzed by NHCs.[103]

Besides chain-growth polymerizations, free NHCs were successfully used to catalyze the step-growth polymerisation of diols and aliphatic diisocyanates, yielding polyurethanes (PUs), as reported by Destarac *et al*.[105] For instance, the NHC$^{t\text{Bu}}$-catalyzed polymerization (NHC3) between 1,4-butanediol and isophorone diisocyanate (IPDI) in THF at 30-50 °C, gave soluble linear PUs with complete monomers consumption within 15 min (Scheme 30).[105] A slight increase of molar masses with time, was observed from M_n = 1,935 g.mol^{-1} to 2,820 gmol^{-1} after 15 min and 2 h polymerization, respectively. Although NHCs are capable to catalyze the di- and/or the trimerization reaction of monoisocyanate,[106] only traces of uretdione (cyclic dimer) and isocyanurate (cyclic trimer) products (Scheme 31), were detected whith alkyl isocyanates, while with phenyl isocyanate a mixture of cyclodimer (70 %) and cyclotrimer (30 %) was obtained. Thus, it was postulated that the NHC catalyst activated the alcohol through H-bonding, followed by a nucleophilic addition of the activated alcohol onto the isocyanate moiety (see insert in Scheme 30).

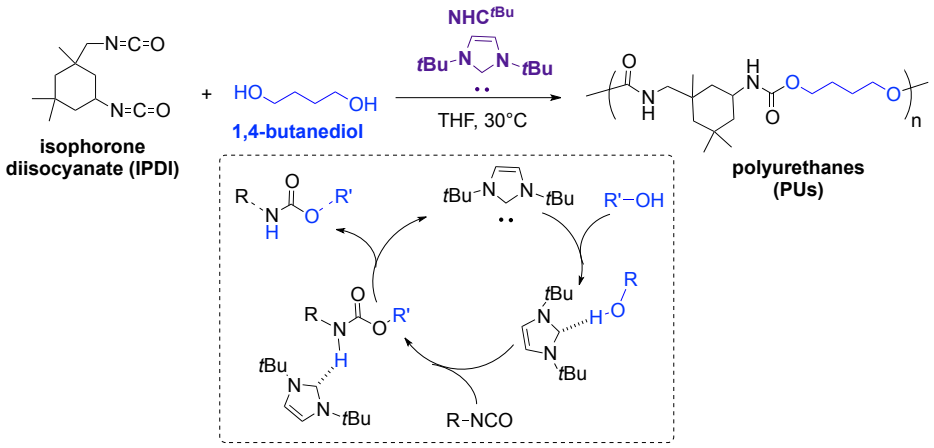

Scheme 30. NHC-catalyzed step-growth polymerization of diisocyanates with diols.[105]

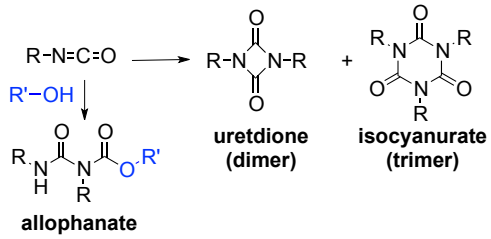

Scheme 31. Potential side reactions during polyurethanes formation.

Despite the efficiency of free NHCs as catalysts for polymerization reactions, their air- and moisture-sensitivity have limited their widespread adoption. Thus, recent studies have focused on the development of protected-NHCs, as air-tolerant precursors of NHCs.

In the present PhD work, NHCs have been the main organic activators investigated as catalyts or as direct initiators for polymerization of alkyl (meth)acrylates (chapters 2 and 3 and part of chapter 4). The NHCs that were used were mainly obtained by deprotonation of imidazolium salts and reduction of imidazol-2(3H)-thiones.

4.2. Protected-NHCs

In 2014, Buchmeiser and Naumann have published a mini-review describing the advantages and disavantages of several classes of protected-NHCs used in metal-free polymerization reactions.[96] Protected- or masked-NHCs are adducts or complexes that can release the free NHC upon application of an external stimulus, such as temperature or solvent effect.[96] Examples of these protected NHCs include imidazol(in)ium carboxylates (NHC-CO_2), NHC-alcohol-adducts, NHC-metal complexes and azolium hydrogen carbonates ([NHC(H).HCO_3]) (Figure 13).

In this context, various protected-NHCs adducts have been designed for an use as latent catalysts in polymerization reactions.

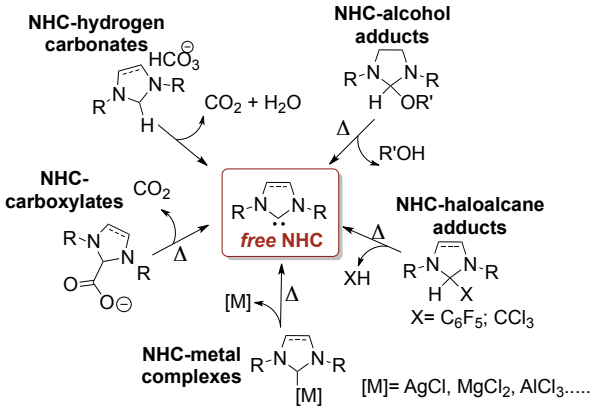

Figure 13. Thermal generation of free NHC from NHC-adducts.[96]

For instance, NHC-carboxylate pre-catalysts (NHC-CO_2 adducts) have been studied for the ROP of cyclic esters, such as lactide and lactones. Plasseraud *et al.* thus reported the solvent-free ROP of *rac*-LA, using 1-*n*-butyl-3-methylimidazolium-2-carboxylate (BMIM-CO_2; NHC11; 1 mol%) initiated by alcohol initiators, such as BnOH, ethylene glycol (EG), glycerol and pentaerythritol, in vacuo at 75 °C.[107] Conversions in the range of 50-70 % were achieved, leading to PLA's oligomers (M_n = 524-973 g.mol^{-1}; $Đ$ = 1.16-1.62). The incomplete conversion observed was attributed to the increase of the viscosity during PLA formation, thus limiting the polymerization process.

In contrast, the solvent-free ROP of D,L lactide (D,L-LA) using imidazolium-2-carboxylates compounds, namely 1,3-bis(isopropyl)imidazolium carboxylate (NHC^{iPr}-CO_2; NHC2), 1,3-bis(dodecyl)imidazolium carboxylate (NHC^{Doc}-CO_2; NHC4) and 1,3-bis(mesityl)imidazolium carboxylate (NHC^{Mes}-CO_2; NHC7) were succesfully achieved by Taton *et al.* at r.t and at 80 °C, in presence of BnOH (1 eq.).[108] With 0.03-1.5 eq. of NHC-CO_2 adduct, PLA with molar masses M_n of 5,000 g.mol^{-1} ($Đ$ = 1.13) were obtained. No induction period was noted while catalyzing the ROP of LA with such NHC-CO_2 adducts, evidencing that the NHC could readily be generated at r.t. Hence, under these experimental conditions, these precursors did not exhibit a latent behavior.

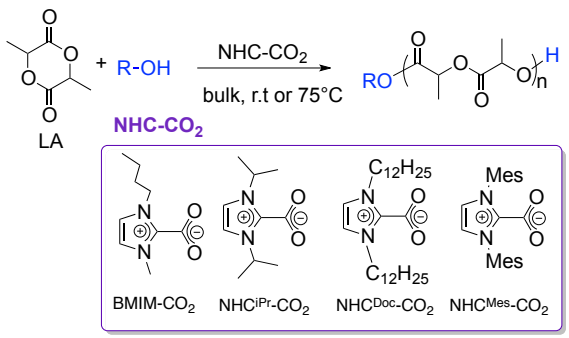

Scheme 32. ROP of LA using NHC-CO_2 pre-catalysts and ROH as initiators.[107,108]

A poor efficiency of NHC^{iPr}-CO_2, NHC^{Doc}-CO_2, NHC^{Mes}-CO_2 for the ROP of ε-CL was

noted at r.t., presumably due to the limited solubility of these pre-catalysts in the monomer.[108] In contrast, at 75 °C, full conversion of ε-CL was observed using BMIM-CO_2, leading to linear and star-branched PCL oligomers (M_n = 2,300-11,700 g.mol^{-1}; $Đ$ = 1.2-2.2).[107] Other NHC-CO_2 adducts, including imidazolium- (NHC2-3; 5-8), imidazolinium- (NHC23), tetrahydropyrimidinium-(NHC32-36) and tetrahydrodiazepinium-carboxylates (NHC37-38), bearing alkyl- and aryl-substituents (see Figure 2 for related structures), were screened by Buchmeiser *et al*. for the ROP of ε-CL, in presence of BnOH as initiator at 70 °C.[109]

In contrast to oligomers obtained previously with BMIM-CO_2 by Plasseraud *et al*,[107] PCL of M_n = 5,000-17,000 g.mol-1 ($Đ$ = 1.20-1.70) were obtained with this series of NHC-CO_2 adducts.[109] Less hindered imidazolium- (NHC2-3) and imidazolinium (NHC23) carboxylates were the most active for the ROP of ε-CL upon decarboxylation. Importantly, these protected NHCs were completely inactive at r.t., while a fast and quantitative consumption of the monomer was observed at 70 °C, evidencing the thermally latent behavior of these pre-catalysts. A nucleophilic AMM (Scheme 2) was postulated, but the occurence of an ACEM (Scheme 4a) could not totally be ruled out. The latter mechanism was likely even more favored with NHCs derived from tetrahydropyrimidinium carboxylates, due to the higher basicity of the related free NHCs compared to than that of imidazol-2-ylidenes (pKa^{DMSO} = 27.8-28.2 *vs.* pKa^{DMSO} = 20-25)[78]. 7-Membered ring tetrahydrodiazepinium-carboxylates were ineffective pre-catalysts in these conditions.

The ROP of PO catalyzed by imidazolium NHC^{Me}-CO_2, NHC^{iPr}-CO_2, NHC^{tBu}-CO_2 NHC^{Mes}-CO_2, imidazolinium (NHC23) or benzimidazolium (NHC25) carboxylates was also reported.[110] Diethylene glycol (DEG) was employed as initiator, in bulk at 120 °C. In most cases, diol-functionalized PPO's oligomers were obtained after 4 h (40-74 % of conversion), with M_n = 315-1,200 g.mol^{-1} and $Đ$ = 1.08-1.23. Catalytic activity of NHC^{iPr}-CO_2 was close to that observed, in a previous work by Taton *et al*., with the corresponding free NHC.[111] Imidazolium pre-catalysts were by far the most active (the least-bulky substituents affording the best activity, NHC^{Me}-CO_2 > NHC^{iPr}-CO_2 > NHC^{tBu}-CO_2 > NHC^{Mes}-CO_2), compared to the benzimidazol-type (NHC25), that proved ineffective. The same system was also efficient for the sequential ROP of PO and ε-CL and L-LA, leading to poly(ether)-*b*-poly(ester) copolymers of low M_n (750-3,700 g.mol^{-1} and $Đ$ = 1.38-1.77).

Based on DFT calculations and *in situ* IR spectroscopy, it was proposed that decarboxylation was a slow process, which allowed a continuous delivery of the free carbene catalyst, thus providing a better control over the ROP. ROP of PO would occur *via* a monomer activation by NHC, forming a zwitterionic imidazolium alkoxide **21** (Scheme 33). The latter species would be subsequently displaced by the ROH, generating an α-alkoxide monoadduct **23**, whereas an imidazolium would be released, the polymerization proceeding through an anionic mechanism (route $\mathbf{A_1}$). Such a mechanism contrasted with that proposed by Taton *et*

al. who proposed that NHCs could serve either as catalysts (route **A_2**) or as direct initiator (route B).[111] Further inverstigations would be needed, however, to clarify this point.

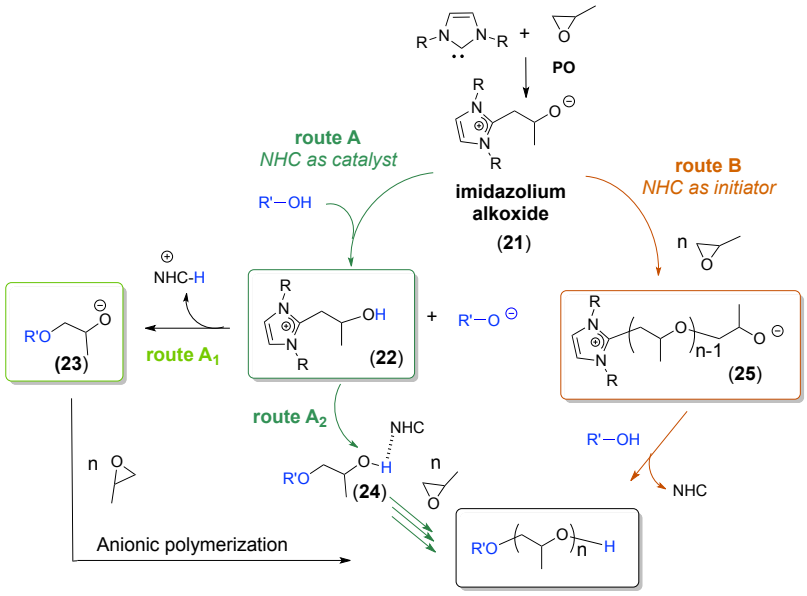

Scheme 33. Possible mechanisms for the NHC-catalyzed ROP of PO in the presence of alcohol as initiator.

NHC-CO_2 adducts were also used to trigger the ROP of cyclic carbonates. For instance, NHC^{iPr}-CO_2 (0,1 mol%) was found particularly active for the ROP of TMC in THF at r.t., using BnOH as initiator.[108] The polymerization reached 91 % of TMC conversion after 1 h, leading to PTMC of M_n = 3,500 g.mol^{-1} (*Đ* = 1.07), confirming that the free NHC was generated under such conditions. TMC was also polymerized in bulk and in THF or toluene solution at 60, 80 and 100 °C, in the presence of NHC^{Mes}-CO_2 as pre-catalyst and BnOH as initiator.[112] While at 60 °C and 80 °C, solvent-free polymerizations were quite similar, giving PTMC of M_n = 11,000 g.mol^{-1} (*Đ* = 1.4), slightly higher molar masses (M_n = 13,400 g.mol^{-1}) and a broader dispersity (*Đ* = 1.7) were obtained at 100 °C. Polymerization in solution at 60 °C were less controlled, yielding PTMC of lower molar masses (M_n = 2,000-3,000 g.mol^{-1}), but higher dispersities (*Đ* = 1.3-3.0). These observations evidenced the temperature-dependence of this NHC-catalyzed ROP of TMC, with decarboxylation of TMC occurring preferentially at high temperatures.

NHC^{iPr}-CO_2 was reported to be an efficient pre-catalyst also for the GTP of MMA, using MTS as initiator at r.t., both in bulk and THF.[108] With 3 mol% of NHC^{iPr}-CO_2 (relative to MTS), PMMA's of molar masses M_n of 6,300 g.mol^{-1} and *Đ* = 1.12-1.37, with a good control over the polymerization, were obtained.

Taton *et al.* reported the ROP of D,L-LA using imidazolium hydrogen carbonates, denoted as [NHC(H)][HCO_3], as pre-catalysts and BnOH as initiator.[113] The saturated [NHC^{Mes}

(H)][HCO_3] (NHC23 in Figure 2) precursor was found to be the most efficient precursor, high monomer conversions of lactide being achieved in THF at r.t., resulting in PLA of molar masses (M_n = 4,000-7,800 g.mol^{-1}; $Đ$ < 1.07).

The catalytic efficiencies of [NHC(H)][HCO_3] were found to be approximately three times lower for the ROP of D,L-lactide than in the case of NHC-CO_2 counter-parts and obviously lower than free (naked) NHC homologues ([NHC(H)][HCO_3] < NHC–CO_2 adducts < free NHCs).

Comparatively to NHC-CO_2 adducts, [NHC(H)][HCO_3] were not effective for the solvent-free GTP of MMA using MTS as initiator at r.t., owing to a loss of control over the polymerization, because of the poor solubility of the salt precursor in the monomer substrate.[108]

The first example of a NHC exhibiting phtotoswitchable activity in response to light irradiation, was reported by Bielwaski *et al.* Such a latent photocatalytic system was employed for the ROP of ε-CL and δ-VL initiated by BnOH in THF at r.t (Scheme 34).[114] Polymerizations proceeded efficiently in natural light, producing PCL and PVL of controlled molar masses (M_n up to 15,900 g.mol^{-1}; $Đ$ = 1.15), after 30 min of reaction. Upon UV irradiation, the polymerization rate was attenuated, due to the formation of the photocyclized NHC–alcohol adduct (NHC-C, Scheme 34), that was catalytically inactive, due to the decreased electron density at the carbenoid center. Subsequent visible light exposure reversed the photocyclization, regenerating the active imidazolium species (NHC-O) and re-engaged the catalytic cycle.

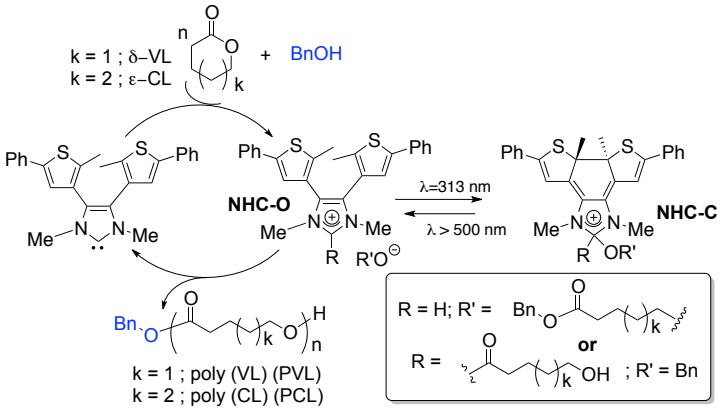

Scheme 34. Catalytic cycle for the photoswichtable NHC-catalyzed ROP of ε-CL and δ-VL in presence of BnOH initiator.[114]

In conclusion, NHCs have been successfully used as organic catalysts for chain-growth polymerization, including ROP of cyclic esters, carboxyanydrides, as well as for the synthesis of polyurethanes *via* step-growth polymerization. Protected NHCs provide a genuine source of NHCs for metal-free polymerizations. However, their catalytic efficiencies often remain lower than the corresponding free NHCs, probably due to the slow or incomplete generation of the

active species under the polymerization conditions. Further developments towards air-stable protected NHCs, that can be efficiently activated by an external stimulus, could expand the scope of NHC-catalyzed polymerization reactions.

5. Polymerization catalyzed by nitrogen-containing Brønsted and Lewis bases: alkyl amines, amidines and guanidines

5.1. Alkyl (aryl) amines

In comparison to NHCs, pyridine derivatives, such as dimethyaminopyridine (DMAP) and alkyl(aryl) amines, are relatively moderate Brønsted bases but can behave as nucleophiles.[115] These nitrogen-containing organocatalysts have been used for the ROP of various heterocycles, including lactide, lactones, carbonates and *O*-carboxyanhydrides. An overview of recent polymerization reactions catalyzed by amines is illustrated in Figure 14.

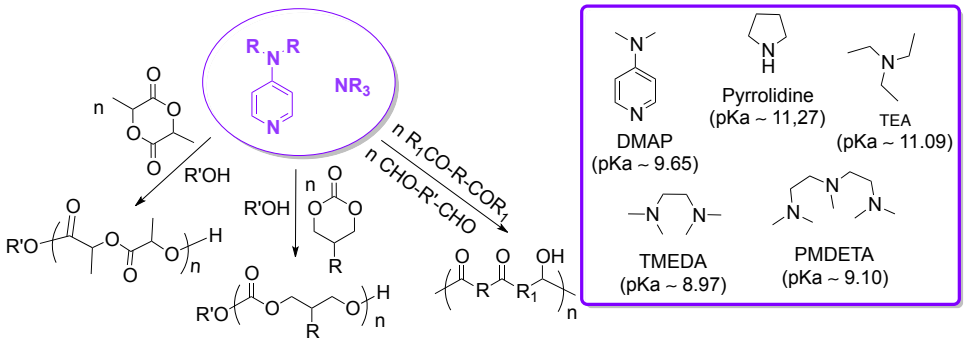

Figure 14. Scope of amine-catalyzed polymerization reactions and represensative catalysts (pKa values are given in water).

DMAP (pKa~ 9.65 in H_2O) was used as catalyst by Zinck *et* al. for the ROP of D,L-lactide using carbohydrate-based initiators such as glucose and cyclodextrin derivatives (DMAP/ROH) = 2.[116] According to the solubility of the initial carbohydrate, the polymerizations were conducted in solution (dichloromethane or chloroform) at 35 °C or in bulk at 120 °C. Carbohydrate-functionalized polylactides of number-average DP ranging from 2 – 210 ($Đ$ = 1.07 - 1.48), considering the growth of one polymeric chain per initiating hydroxyl group with a quantitative functionalization efficiency, were thus obtained.[116]

In the same manner, DMAP served as catalyst for the copolymerization of L-LA and TMC in toluene at 130 °C, using BnOH as initiator.[61] The ROP of L-LA, using a pre-synthesized BnO-PTMC-OH prepolymer or through direct sequential copolymerization of the two monomers, afforded PTMC-*b*-PLLA diblock copolymers of molar masses, M_n, of 26,200 g.mol^{-1} ($Đ$ = 1.32). DMAP was thought to operate *via* an ACEM (Scheme 4a), but

under the same conditions, the phosphazene BEMP was more effective than DMAP, presumably due to its higher basicity.

Aliphatic tertiary amines, including triethylamine (TEA; pKa ~ 11.09 in H_2O), *N*,*N*,*N*″,*N*′-tetramethylethylenediamine (TMEDA; pKa ~ 8.97 in H_2O) and *N*,*N*,-*N*′,*N*″,*N*″-pentamethyl diethylenetriamine (PMDETA; pKa ~ 9.10 in water), were used to catalyze the BnOH initiated-ROP of TMC in THF at 55 °C (Scheme 35).[117] Under those conditions, PMDETA and TMEDA were the most efficient catalysts, yielding PTMC of M_n = 1,615-10,400 g.mol^{-1} and *Đ* = 1.17-1.55, at full TMC conversion. The catalytic activity correlated with the properties of tertiary amines to activate ROH by H-bonding, but also with the number of nitrogen atoms in the catalyst (see insert in Scheme 35). The active conformations were calculated to have nitrogen atoms spaced approximately of 3.07 and 3.18 Å, respectively for TMEDA and PMDETA, apart with an orientation angle of 60 and 58 °C.[118] Such spatial conditions and nitrogen lone pair orientations explained the catalytic activity of these amines. According to NMR characterizations, this amine-catalyzed ROP of TMC presumably proceeded through the ACEM (Scheme 4a). Using a PEO_{99}-PPO_{65}-PEO_{99} macroinitiator, poly(ether-carbonate) copolymers with a well-defined structure could be easily prepared using this amine-catalytic pathway.

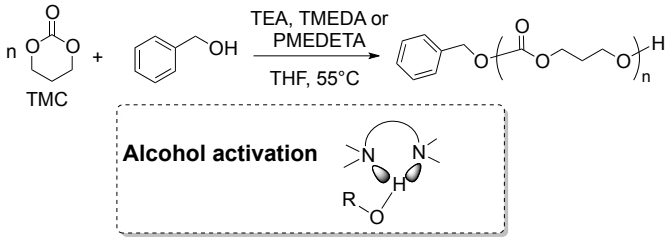

Scheme 35. ROP of TMC catalyzed by tertiary amines (TMEDA or PDMTA) and initiated by BnOH.[117]

5.2. Amidines and guanidines

Compared to trialkyl or aryl amines, amidines and guanidines are strong organic bases (pKa ~ 23-26 in MeCN)[119], due to the stability of their corresponding conjugated acid (the positive charge is delocalized over two nitrogen atoms).[52] Amidines and guanidines are slightly less basic (by approximately 2-3 pKa units) than phosphazenes such as 2-*tert*-butylimino-2-diethylamino-1,3-dimethylperhydro-1,3,2-diazaphosphorine (BEMP in Figure 8; pKa ~ 27.6). As phosphazenes, amidines and guanidines have been mainly used as deprotonationg agents of acidic OH-, SH- or CH-containing initiators (see section 3.1), but a particular guanidine, namely 1,5,7-triazabicyclo[4.4.0]dec-5-ene (TBD) (pKA^{MeCN} = 26.0)[119] can also serve as dual activator in some molecular or macromolecular reactions.[7,8,14] Represensative examples of guanidines and amidines employed in metal-free polymerizations are shown in Figure 15.

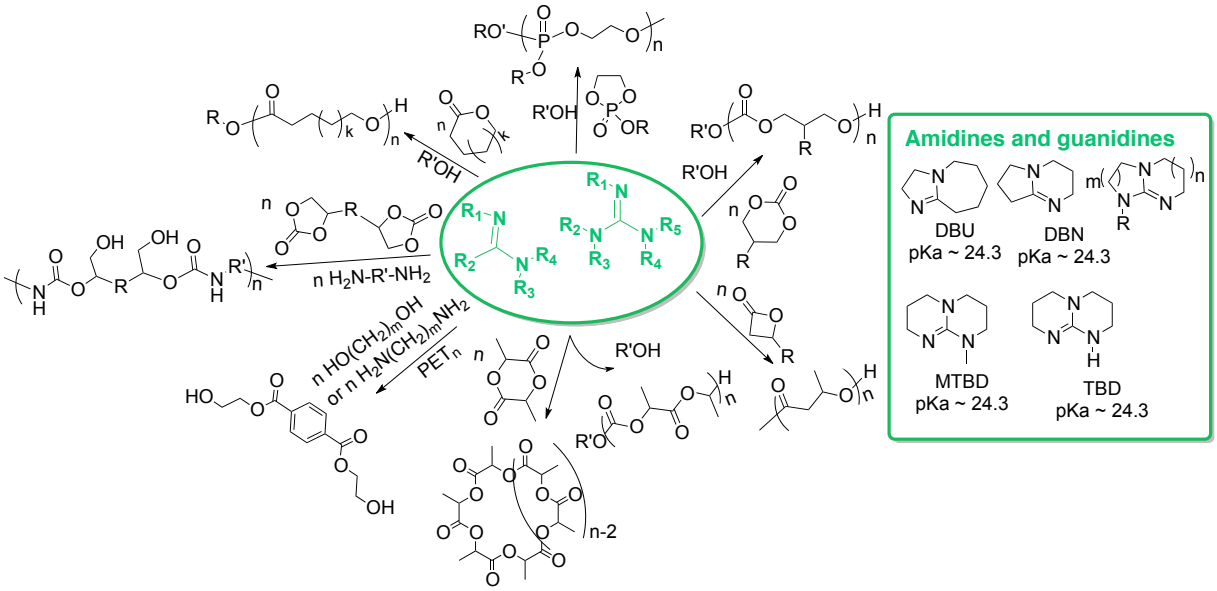

Figure 15. Scope of polymerization reactions catalyzed by amidines and guanidines.

5.2.1. Amidines

The amidine 1,8-diazabicyclo[5.4.0]undec-7-ene (DBU) (pKA = 24.3 in MeCN)[119] was found to be an excellent Brønsted basic catalyst for the ROP of lactide in presence of alcohol initiators.[7,8,14] However, the polymerization of lactones required a thiourea cocatalyst for the reaction to proceed, because transesterification was more noticeable than in lactide polymerization.[120]

Based on previous results obtained for DBU-catalyzed ROP of LA,[7] Coulembier *et al.* explored the bulk polymerization of the eutectic L-LA/TMC (50/50) melt, using BnOH as initiator, at 23 °C (Scheme 36).[121] Pure PLLA homopolymers of molar masses M_n = 15,500 g.mol^{-1} ($Đ$ = 1.33) were obtained from this particular mixture of monomers. This homopolymerization was attributed to the limiting diffusion of TMC during the very fast ring-opening process of LA (conversion of 95 % in 30 s), resulting from PLLA crystallization out of the eutectic melt. Nevertheless, ROP of TMC was observed when the medium was quickly solubilized in dichloromethane after PLLA formation, affording poly(LLA-*g*-TMC) gradient copolymers of M_n = 22,000 g.mol^{-1} and $Đ$ = 1.64 after 16 h (63 % of TMC conversion)

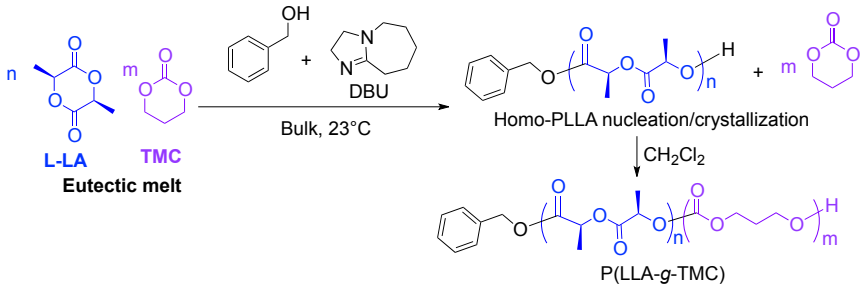

Scheme 36. DBU-catalyzed ROP of eutectic melt of L-LA and TMC monomers initated by BnOH.[121]

ROP of a particular cyclic carbonate, namely spiro[fluorene-9,5'-[1,3]-dioxan]-2'-one (F-TMC) was also reported by Hedrick *et al.*, using BnOH as initiator and DBU as catalyst (1eq) (Scheme 37).[122] Polymerizations proceeded at r.t in dichloromethane, leading poly (F-TMC) of predictable molar masses (M_n of to 4,500 g.mol^{-1}; $Đ$ = 1.3). When employing MeOPEO-OH of different molar masses (M_n = 1,600-10,000 g.mol^{-1}; $Đ$ < 1.2) as macroinitiators, the polymerization was almost completed in 15 min (monomer conversion > 95 %), leading to well-defined amphiphilic diblock copolymers of M_n of poly(F-TMC) = 5,000 g.mol^{-1}, as determined by NMR. Depending on the molar masses of the PEO block, spheres, elongated rod-like micelles or lamellar phases such as tapes could be generated from an aqueous self-assembly of these copolymers.

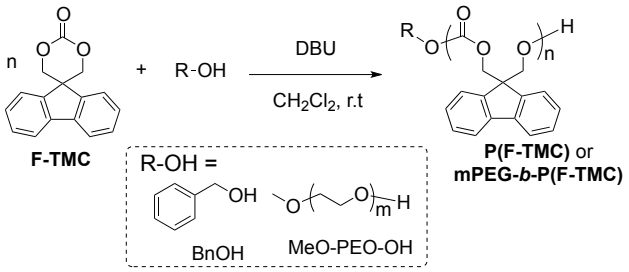

Scheme 37. DBU-catalyzed ROP of fluorene-fonctionalized aliphatic cyclic carbonate monomer.[122]

Besides polyesters and polycarbonates, polyphosphoesters are attractive materials for bioapplications because they also exhibit biocompatible and biodegradable properties.[123] In this context, Iwasaki *et al.* reported in 2010 the first solvent-free ROP of cyclic phospholanes such as 2-isopropoxy-2-oxo-1,3,2-dioxaphospholane (IPP) and 2-methacryloyloxyethyl-phosphoryl choline (PIPP) using DBU as catalyst, in presence of alcohols as initiators.[124] Polyphosesters of M_n = 2,400-7,700 g.mol^{-1} ($Đ$ = 1.03-1.09) were produced and the polymerization was thought to occur by a basic ACEM, on the basis of NMR analysis.

In the same way, Wooley *et al.* described the DBU-catalyzed ROP of butynyl phospholane (BYP) in dichloromethane at r.t., using BnOH as initiator (Scheme 38a).[125] Using 1.5 eq. of DBU relative to BnOH, poly(BYP)'s of molar masses M_n of 20,000 g.mol^{-1} ($Đ$ = 1.14-1.19) containing a pendent alkyne function were obtained after only 6 min (conversion of 95 %). Post-functionalization of the obtained polyphosphoesters was accomplished *via* azide-alkyne Huisgen cycloaddition and thiol-yne reactions.

The ROP of 2-isobutoxy-2-oxo-1,3,2 dioxaphospholane (iBP) was initiated BY BnOH (1eq.) in presence of DBU as catalyst (5 eq.), in toluene at 0 °C (Scheme 38a).[126] Although M_n of the obtained poly(iBP)'s (M_n = 6,900-15,800 g.mol^{-1}; $Đ$ = 1.19-1.32) evolved with the monomer conversion, this polymerization was very slow (24 h to achieve 80 % for DP = 50) and a multimodal molar mass distribution was observed, especially for high monomer conversion and long polymerization time. This was explained by the occurrence of side

reactions, such as intra- and/or intermolecular transeterifications. Sequential copolymerization of BYP and L-LA (BYP was first polymerized) produced poly(butynyl phospholane)-*b*-poly(lactide) (PBYP-*b*-PLLA) diblock copolymer of M_n = 21,900 g.mol^{-1} and $Đ$ = 1.17.[127] After suitable modifications, as-obtained amphiphilic copolymers were manipulated to self-assemble into spherical nanoparticles, with distinct negative and positive surface charges, and uniform size distributions.

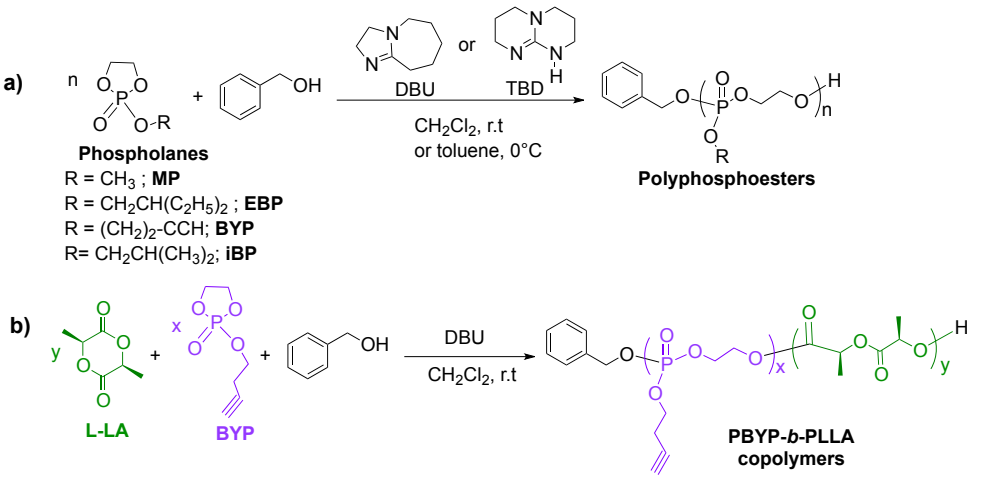

Scheme 38. DBU (or TBD)-catalyzed ROP of phospholanes and copolymerization with L-LA using alcohol initiators.[125-127]

5.2.2. Guanidines

Among guanidines, the bicyclic guanidine 1,5,7-triazabicyclo[4.4.0]dec-5-ene (TBD) (pKA = 26.0 in MeCN)[119] has been the most studied and has proven a powerful catalyst for various polymerization reactions, mainly ROP of cyclic esters and cyclic carbonates.

In presence of alcohol initiators, TBD was reported to specifically operate as a bifunctional activator (Scheme 39) activating the alcohol by H-bonding while creating concomitantly an incipient guanidinium ion that activate the carbonyl group of the monomer in a cooperative fashion (see also section 6 for other examples of organic catalyst providing a dual activation).[7,14] TBD is discussed here for the purpose of comparison with other guanidines or amidines.

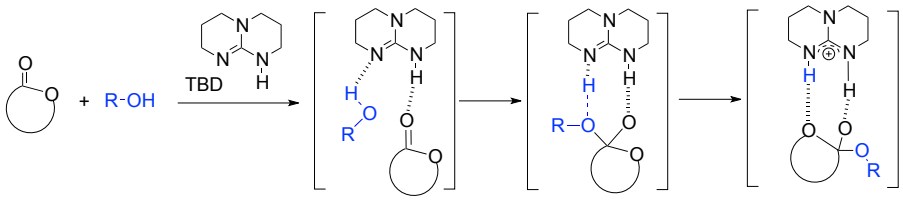

Scheme 39. Activation mode of TBD catalyst during the ROP of cyclic esters.[14]

Hillmyer *et al.* reported the solvent-free ROP of the renewable δ-decalactone (δ-DL), using 1,4-phenylenedimethanol (PDM) diol as initiator and TBD as catalyst (0.3 eq).[128]

At 100 °C, full monomer conversion was reached, leading to high molar masses PDL (M_n of 83,000 g.mol^{-1}; Đ < 1.25). Sequential addition of L-LA, and δ-DL produced PLLA-*b*-PDL-*b*-PLLA triblock copolymers (M_n = 100,000 g.mol^{-1}; *Đ* = 1.4), that exhibited two distinct glass transition temperatures, at -51 and 54 °C for PDL and PLLA domains, respectively, consistent with a microphase segregation.

Similarly, starting from either 1-pyrenemethanol or PEO as (macro)initiator, the TBD-catalyzed ROP of LA and ε-CL was investigated in bulk at 90 °C.[129] This allowed synthesizing PCL's and PLA's homopolymers, as well as PEO-*b*-PCL(or PLA) diblock and PEO-*b*-P(CL-*co*-LA) triblock amphiphilic copolymers of molar masses M_n in the range of 3,500-23,700 g.mol^{-1} (*Đ* = 1.4-2.0). These amphiphilic copolymers were shown to self-organize into micelles hydrodynamic radius R_h between 27 and 35 nm.

The ROP of δ-VL catalyzed by TBD (0.17 eq), using BnOH as initiator (1 eq.) was reported in toluene at r.t. (Scheme 40).[130] The corresponding PVL of M_n = 3,000 g.mol^{-1} (*Đ* = 1.06) was obtained within 15 min of reaction for an initial DP = 30. Addition of a crosslinking agent, such as 5,5'-bis(oxepanyl-2-one) (BOP) to this PVL macroinitiator, led to a polyester nanogel star of M_n = 333 kg.mol^{-1} (*Đ* = 1.21). Alternatively, and more practically, such branched polyesters could also be obtained by mixing all reagents at the early stage of the reaction.

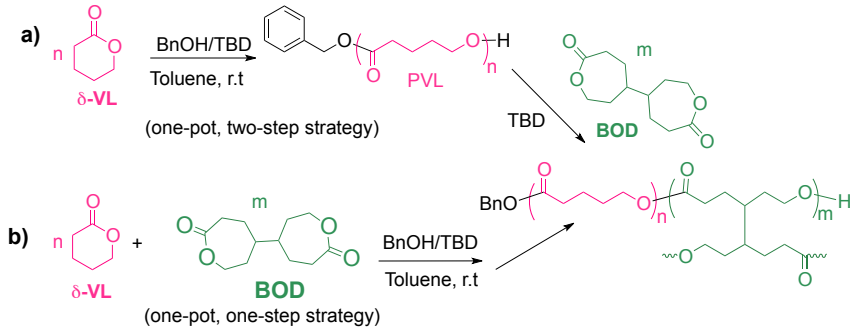

Scheme 40. Synthesis of a polyester-based nanogel star polymer by TBD-catalyzed ROP of δ-VL and BOD initiated by BnOH: a) one-pot/two-step strategy and b) one-pot/one step strategy.[130]

The TBD-catalyzed ROP of functionalized lactones, namely 3-benzyl mercaptanvalerolactone (BMVL), 2-(2-methoxyethoxy) ethanethiolvalerolactone (EG_2MVL) and 1-mercapto-3,6,9,12-tetraoxotridecanevalerolactone(EG_4MVL) (Scheme 41a), were also described.[131] 1,4-Pyrenebutanol (PyBuOH) was used as initiator (1-5 mol% of TBD relative to alcohol) and reactions were carried out in bulk or in toluene at r.t.[131] Well-defined functionalized polyesters (M_n = 500–8,900 g.mol^{-1}; *Đ* = 1.32-1.45) featuring benzyl mercaptans or oligoethylene glycol pendant groups, could thus be obtained. In addition, aliphatic functionalized polyesters (M_n = 5,800–6,900 g.mol^{-1}; *Đ* = 1.21-1.47) were successfully prepared by the copolymerization of 3-mercaptovalerolactones with ε-CL (Scheme 41b).

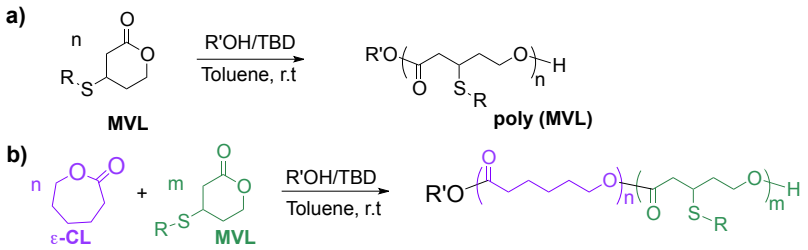

Scheme 41. TBD-catalyzed: a) ROP of substituted valerolactones (MVL); b) random copolymerization of MVL and ε-CL.[131]

In the same manner, various functionalized lactones, including α-allyl-δ-valerolactone (AVL), α-propargyl-δ-valerolactone (PgVL), TMS-protected PgVL (TMS-PgVL), and α-propargyl-δ-caprolactone (PgCL), could be polymerized at r.t in toluene, using BnOH and TBD (2 mol% of relative to monomer) as initator and catalyst, respectively.[132] Functionalized aliphatic homopolymers, as well as copolymers of molar masses M_n = 8,800-22,000 g.mol^{-1} and $Đ$ = 1.01-1.23, incorporating pendent alkene and alkyne groups were prepared. Post-polymerization modification of these polyesters by "click-type" chemistries, allowed hydrophilic solubilizing groups and fluorescent moieties to be incorporated for delivery and controlled release applications.

As an example of base-mediated polymerization of macrolactones, ROP of ω-pentadecalactone (ω-PDL) and its copolymerization with ε-CL was investigated by Duchateau *el al*.[133] The combination of TBD/BnOH (1/1) proved catalytically active, in bulk or toluene at 100 °C, producing PCL, PDL homopolymers (M_n = 2,500-27,000 g.mol^{-1}; $Đ$ = 1.3-2.1), as well as random poly(PDL-*co*-CL) copolymers (M_n = 9,500 and 11,500 g.mol^{-1}; $Đ$ = 1.5). At high monomer conversion, a broadering of the molar masses distribution was observed, suggesting the occurrence of transesterification reactions. Accordingly, a general ACEM was ruled out due to the inactivity of the methylated guanidine homologue, *N*-methyl-1,5,7-triazabicyclododecene (MTBD) under such conditions. Although experimental evidences were lacking, a dual activation of monomer and growing polymer chain by TBD was the most likely mechanism for such macrolactones polymerization. The TBD-catalyzed ROP of ethylene brassylate was also investigated by Mecerreyes *et al*., leading to polyester of M_n = 7,000-13,900 g.mol^{-1} ($Đ$ = 1.6-1.9).[27] Compared to the acid catalysis by sulfonic acids, the TBD/BnOH combination proved to be the fastest system for this reaction and side reactions were limited. DFT calculations revealed that both TBD and PTSA acted as dual activator *via* H-bonding, but the polymerization was kinetically more favored when TBD was used.

In contrast to the numerous examples of ROP of lactones, there are only few recent reports regarding the polymerization of lactide. For instance, the ROP of PEO-grafted lactide (PEO-LLA) has been described, using BnOH/TBD (1/0.5), in dichloromethane at r.t (Scheme

42).[134] Well-defined PEO-functionalized poly(lactic acid) were thus obtained with molar masses M_n = 11,000-14,000 g.mol^{-1} and $Đ$ = 1.4-2.1

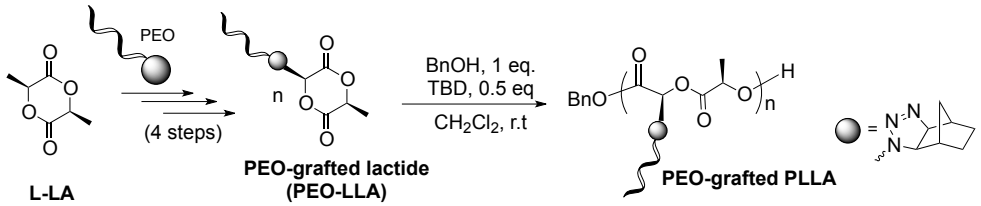

Scheme 42. Synthesis of PEO-grafted PLLA from L-lactide.[134]

Similarly to DBU, TBD could also catalyze the ROP of some phospholane monomers. In particular, ROP of 2-isobutoxy-2-oxo-1,3,2 dioxaphospholane (iBP) was carried out in toluene at 0 °C, using BnOH as initiator (Scheme 38a).[126] In comparison with DBU, TBD provided faster reaction kinetics, complete conversion being obtained within 2 min (DP = 100, 78 % conversion after 11 h with DBU). However, these TBD-derived polyphosphoesters poly(iBP)'s exhibited a bimodal molar masses distribution, presumably originating from chains coupling by intermolecular transesterification.

The sequential copolymerization of 2-ethylbutyl phospholane (EBP) and butynyl phospholane (BYP) (EBP being polymerized first) was performed in dichloromethane at 0 °C by Wooley *et al.* (Scheme 38a).[135] In this way, $PEBP_{50}$-*b*-$PBYP_{50}$ diblock copolymers (M_n = 7,100-17,200 g.mol^{-1}; $Đ$ < 1.17) could be prepared successfully. In contrast, DBU was reported to be only active towards the polymerization of BYP, potentially because of the bulkier ethylbutyl group in EBP. Post-functionalization of the above copolymers by thiol-yne reactions, with various thiols, resulted in nonionic, anionic, cationic and zwitterionic amphilic block copolymers that were shown to self-assemble into micelle-like nanostructures.

The TBD-catalyzed ROP of cyclic carbonates proved to be a practical synthetic strategy to polycarbonates with enhanced thermo-mechanical properties. For instance, Guillaume, Carpentier and co-workers reported the ROP of the binary system L-LA-TMC in toluene at 110 °C, using a combination based on TBD/BnOH (1/5).[136] Under these conditions, random P(LLA-TMC) copolymers were obtained with molar masses in the range M_n = 6,500-11,050 g.mol^{-1} ($Đ$ = 1.4-2.1). Although this copolymerization proceeded without decarboxylation, extensive transesterification side-reactions were observed upon prolonged reaction time.

The same group achieved the ROP of racemic trans-cyclohexene carbonate (*rac*-CHC) using TBD in combination with BnOH as co-initiator, in toluene at 60 °C t (Scheme 43a).[137] The reaction proceeded with a good efficiency (75-85 % conversion in 1-4 h), affording well-defined isotactic PCHC's with M_n up to 18,100 g.mol^{-1} ($Đ$ = 1.16 -1.54).

Glucose-derived polycarbonates (M_n = 4,140-13,000 g.mol^{-1}; $Đ$ = 1.11-1.15) were also successfully produced, through the TBD-catalyzed ROP of a glucose-based cyclic carbonate

initiated by 4-methylbenzyl alcohol, in dicloromethane at r.t (Scheme 43b).[138] DSC analysis of these polycarbonates revealed glass transition temperatures significantly higher than those of PTMC (106 °C for glucose-polycarbonate *vs.* -18 °C for PTMC).

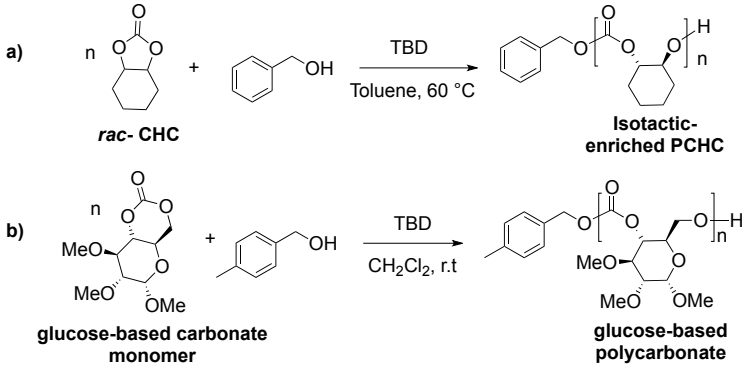

Scheme 43. TBD-catalyzed ROP of glucose-based monomer initiated by 4-methylbenzyl alcohol.[137 138]

Similarly, starch-*graft*-PTMC copolymers were also synthesized by TBD-catalyzed ROP of TMC in bulk at 150 °C, in the presence of native starch granules as macroinitiators (Scheme 22).[62] However, PTMC homopolymers (M_n = 4,670 g.mol^{-1}; $Đ$ = 1.24) were also detected by NMR spectroscopy, suggesting initiation by propan-1,3-diol generated from hydrolysis of TMC.

Recently, Coulembier *et al.* reported a CO_2-based switchtable "on/off" ROP of ε-CL using a mixture of TBD/DBU (10/1) as catalytic system and BnOH as initiator (Scheme 44).[139] The ROP of ε-CL was performed in toluene at r.t., yielding PCL of molar masses M_n = 1,400-37,000 g.mol^{-1} ($Đ$ = 1.1-1.8). While TBD alone was active toward the ROP of ε-CL, DBU was inactive, but the association of both TBD and DBU resulted in the formation of a hydrogen-bond based-complex (see insert in Scheme 44) that allowed polymerizing this monomer by tempering the reactivity of the TBD catalyst. The switchable "on/off" behavior between active and dormant propagating species was demonstrated by repetitive cycles of CO_2/N_2 additions and eliminations, where the addition of CO_2 resulted in a dormant "off" state. In the same manner, the TBD-catalyzed ROP of TMC could also be activated and deactivated on demand by the reversible fixation of CO_2.

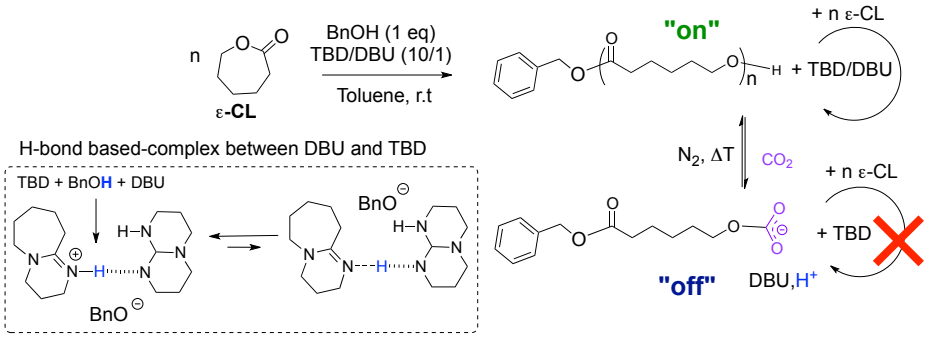

Scheme 44. CO_2-based switchable ROP of CL using TBD/DBU (10/1) catalytic mixture with BnOH as initiator.[139]

There is also an example of step-growth polymerization reactions utilizing guanidines as organocatalysts. For instance, a series of cyclic guanidines was shown to trigger the polyaddition of PEO diols and isophorone diisocyanate (IPDI), in bulk at 60 °C (Scheme 45), affording polyurethanes with M_n = 21,700-39,800 g.mol^{-1} ($Đ$ = 1.33-1.89).[140] In contrast to the NHC catalysis,[105] where traces of uretdione (dimer) and isocyanurate (trimer) were detected (see Scheme 31), the guanidine catalysis proceeded without any detectable side reactions, demonstrating the high selectivity of these catalysts.

The mechanism of this polyaddition was not clearly established, however, and the authors suggested two possible pathways (Scheme 45). In the nucleophilic mechanism, the addition of the guanidine onto the C = O of the isocyanate (AMM) is followed by the reaction of the activated zwitterionic acyl intermediate with the alcohol partner, providing the urethane linkage. However, activation of the alcohol by the base (ACEM) is also plausible.

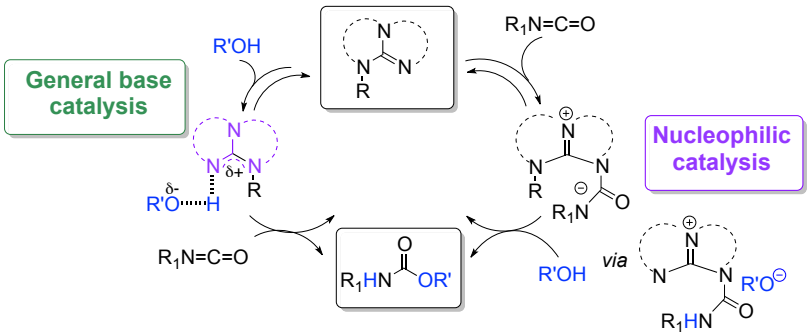

Scheme 45. Guanidine catalyzed-synthesis of polyurethanes (PUs) from IPDI and PEO.[140]

In the context of a sustainable synthesis of PUs starting from non-isocyanate-based monomers,[141] the organo-catalyzed aminolysis of cyclic carbonates, forming (poly)hydroxyurethanes (PHU's) is an interesting alternative to isocyanate-based chemistry.[142] PHU's of molar masses M_n = 12,400-.53,400 g.mol^{-1} and $Đ$ = 1.18-1.38 were thus obtained by step-growth polymerization in DMSO at r.t., between difunctional cyclic carbonate (4-(phenoxymethyl)-l,3-dioxolan-2-one derivative (B5CC) and diamines, using TBD as catalyst (Scheme 46).[143] Consequently, this organo-catalyzed polymerization appeared as an interesting strategy to avoid the use of toxic isocyanate precursors.

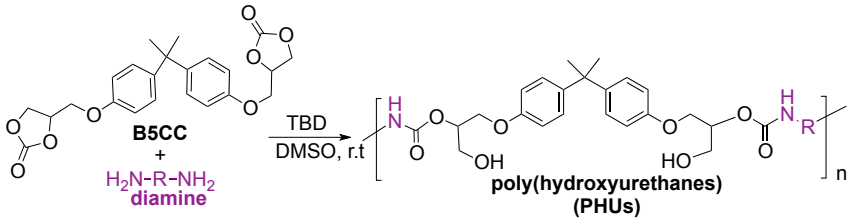

Scheme 46. TBD-catalyzed step-growth polymerization between difunctional cyclic carbonate and diamines.[143]

DBU and 1,5-diazabicyclo[4.3.0]non-5-ène (DBN) amidines, as well as the TBD guanidine were reported by Hedrick *et al.* to selectively degrade poly(ethylene therephtalate) (PET), providing an interesting metal-free strategy for depolymerization of this important aromatic polyester.[144-146] Chemical degradation occurred at 150 °C, in the presence of either ethylene glycol (EG) forming bis(2-hydroxyethyl)terephthalester (BHET), or ethylene diamine (EDA) generating bis(2-aminoethyl)terephtalamide (BAETA) by-product. DBU proved more efficient than TBD for the glycolysis with EG, whereas the opposite trend was noted for amidation with EDA.

DFT calculations performed with methylbenzoate (MB) as monomer model predicted that the nucleophilic addition of the activated alcohol (or amine) onto the carbonyl group of the ester was the rate-determining step. Even though both TBD and DBU activated alcohols better than amines, theoretical studies suggested that transesterification and amidation reactions were kinetically comparable. Thermodynamically, however, the transesterification was reversible while the amidification was exergonic, hence, it was likely to revert to the starting materials.

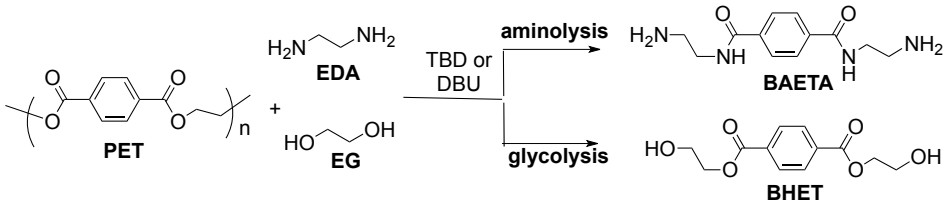

Scheme 47. Depolymerization of PET using TBD or DBU catalysis. [145,146]

Among nitrogen-containing bases, amidines and guanidines efficiently catalyzed the ROP of cylic esters, cyclic carbonates and phospholanes, as well as the depolymerization of PET. While DBU amidine was found to only activate the alcohol, TBD guanidine played the role of a bifunctional activator for both the monomer and the alcool. In contrast, only a few examples of amine-catalyzed ROPs (*i.e.* lactide and cyclic carbonates) and step-growth polymerizations (*i.e.* bis-aldehyde with bis-ketone) have been reported, presumably due to their lower basicity compared to amidines and guanidines. The variety and commecial availability of these nitrogen-containg catalysts, combined with their ability to promote control over the polymerization reactions under mild conditions, are key advantages that make them attractive catalytic options for polymer synthesis.

6. Mono- or bicomponent dual catalytic systems

One of the simplest strategy to provide simultaneous activation of both the monomer and the initiator/chain end is to combine (in a bicomponent catalytic system) a weak Brønsted acid (A) with a weak Brønsted base (B). These ambiphilic properties can also be found in a single molecule (monocomponent), providing a more pratical reaction set-up. Generally, such

dual activation is based on the formation of two different H-bonded complexes: a Brønsted acid-monomer and a Brønsted base-initiator or growing chain H-bond complexes (Figure 15). For this purpose, some of the organocatalysts previously described (*e.g.* amidines, amines and phosphoric acids) can be employed.

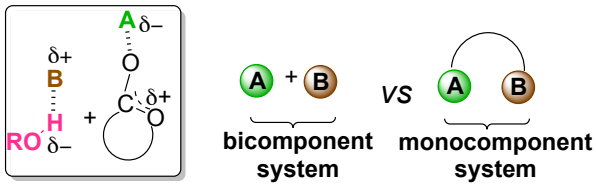

Figure 16. Unimolecular or bimolecular dual activation based on H-bonding interactions

In a recent review, Bibal and Thomas highlighted the scope of H-bondings organocatalyts for ROP, and discussed the structure-catalytic activity relationships.[13] Here we briefly describe recent ROP examples, based on such a dual activation.

Urea and thiourea (TU) derivatives are well known to activate carbonyl-containing substrates through hydrogen-bonding.[147] Such catalysts have also been largely applied to induce the ROP of cyclic esters and carbonates, mainly in association with amines and amidines (Figure 18).[7,14]

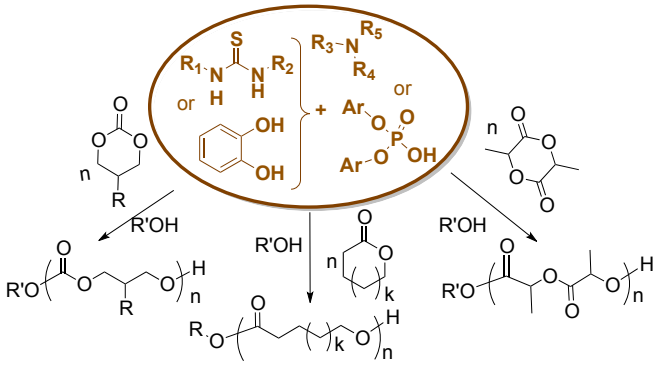

Figure 17. Overview of ROP induced by a dual-activation.

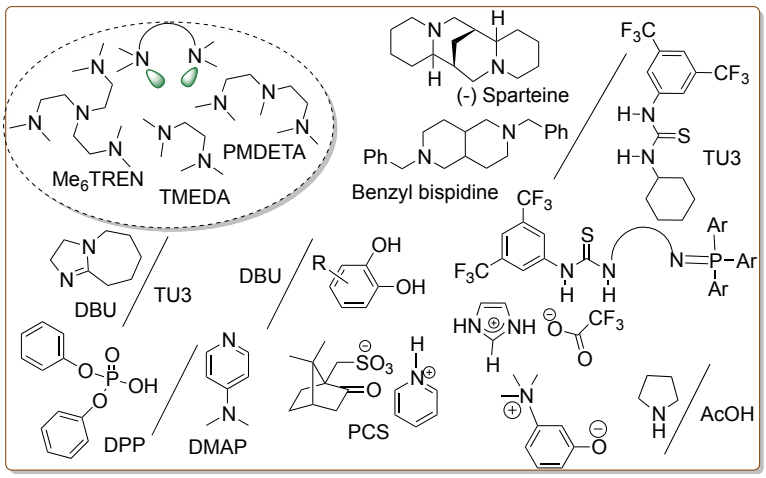

Figure 18. Representative organic activators used to induce dual activation.

A series of commercially available amines, namely TMEDA, PMDETA and tris[2-(dimethylamino)ethyl]amine (Me_6TREN) (see Figure 18 for related structures) combined with (*N*'-(3,5-bis(trifluoromethyl)phenyl)-*N*-cyclohexyl-thiourea (TU3; 5eq), was screened as catalytic system for the ROP of L-LA in dichloromethane at r.t., using PyBuOH as initiator (Scheme 48).[118] Among the various amines investigated, Me_6TREN was found the most efficient catalyst, yielding PLLA's of molar masses M_n = 23,000 g.mol^{-1} and *Đ* = 1.06.

This high efficiency of Me_6TREN, which was comparable to that of (-)sparteine, was proposed to arise from the presence of multiple basic sites and the locked spatial geometry allowing for a better alcohol activation through chelative effect (see insert in Scheme 48).

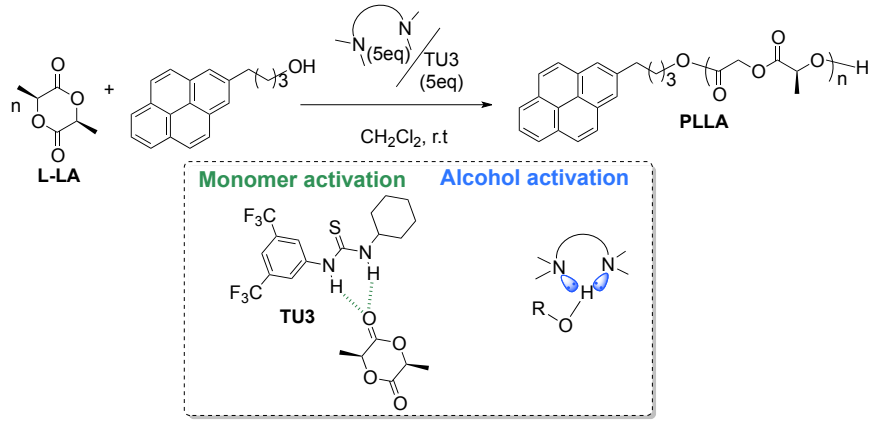

Scheme 48. ROP of L-LA using TU/amine catalytic system in the presence of pyrenbutanol.[118]

The ability of (-)sparteine/TU or DBU/TU catalytic systems for the ROP of functionalized cyclic carbonates, using alcohol initiators has been investigated in details by Dove *et al.* and by Hedrick *et al.*

The ROP of 5-methyl-5-allyloxycarbonyl-1,3-dioxan-2-one (MAC) was succeesfully achieved in chloroform at r.t., in presence of BnOH as initiator and (-)sparteine/TU3 as organocatalyst, leading to PMAC's of molar masses M_n = 4,600-10,470 g.mol^{-1} and *Đ* = 1.12-1.49 (Scheme 49a).[148] Block copolymers of PMAC with PLA (M_n = 4,260-7,130 g.mol^{-1}; *Đ* = 1.17-1.28) were synthesized either by ROP of LA from a PMAC prepolymer in a one-pot process, or by ROP of MAC using PLA as macroinitiator. Copolymerization of MAC with 5-methyl-5-ethyloxycarbonyl-1,3-dioxane-2-one (MTC-Et) was also reported under the same condtions, producing allyl-functionalized PMAC-*b*-PMTC-Et copolymers of M_n = 5,000 g.mol^{-1} (*Đ* = 1.25-1.56).[149] Under the same conditions, dibenzyl-functional bispidine in combination with TU3 co-catalyst achieved rates almost identical to those observed using (-)sparteine for the ROP of TMC and MAC.[150] The polymerization was well-controlled, leading to polycarbonates of molar masses Mn = 6,100-9,100 g.mol-1 and *Đ* = 1.03-1.31, demonstrating that benzyl bispidine is an excellent replacement for (-)sparteine that becomes difficult to obtain commercially.

The (-)sparteine/TU3-catalyzed ROP of acrylamide-functionalized cyclic carbonates in

dichloromethane at r.t gave well-defined *tert*-butylacrylamide-functionalized homo- and copolycarbonates of M_n = 4,600-5,100 g.mol^{-1} and $Đ$ = 1.12-1.32 (Scheme 49b).[151] With the same catalytic system, the ROP of 5-methyl-5-propargyloxycarbonyl-1,3-dioxan-2-one (MPC) in chloroform at r.t. afforded PMPC's of molar masses M_n = 6,750 g.mol^{-1} ($Đ$ = 1.18).[152] However, the polymerization of this monomer could be improved by switching to a DBU/TU3 catalysis. In the latter case, a PMPC of M_n = 16,540 g.mol^{-1} ($Đ$ = 1.11) was obtained. The synthesis of telechelic PMPC's, poly(ether)-*b*-poly(carbonate)s and poly(ester)-*b*-poly(carbonate)s copolymers was also reported by using various hydroxyl-functional initiators, including disulfides, diols and MeOPEO-OH, as well as by copolymerization with L-LA.[152] Post-polymerization modification of these polymers by 'thiol-yne click-chemistry" allowed accessing a range of functional poly(carbonate)s.

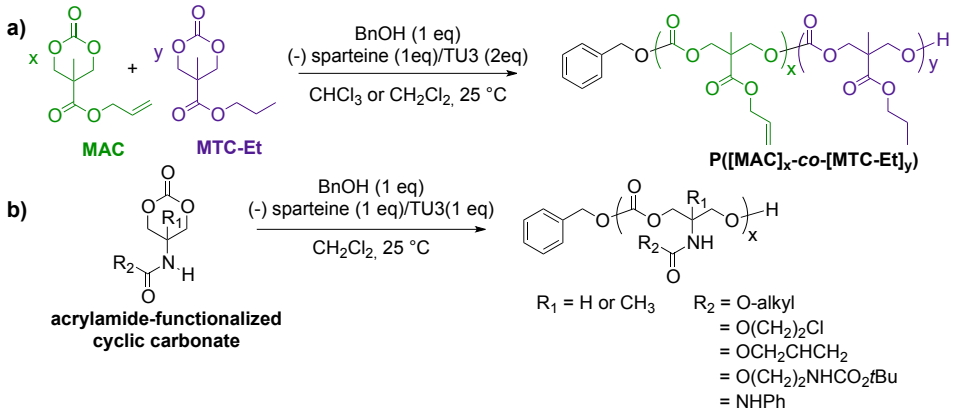

Scheme 49. Synthesis of functional polycarbonates using (-)sparteine/TU3 as catalyst and BnOH as initiator.[148,149,151]

In the same manner, the DBU/TU3-catalyzed, BnOH-initiated ROP of benzyl-MTC (MTC-Bn), quinine-MTC (MTC-Q) and Boc-MTC (MTC-bocG) was carried out in dichloromethane at r.t., yielding homopolycarbonates of molar masses M_n (M_n = 2,400-7,300 g.mol^{-1}; $Đ$ < 1.3) in agreement with values predicted from the initial monomer-to-initiator ratio.[153] Copolymerization of MTC-Q with MTC-bocG afforded, after deprotection, water-soluble cationic poly[(MTC-Q)-*b*-(MTC-G)] copolymers (M_n = 3,900 g.mol^{-1}; $Đ$ = 1.5), functionalized with both quinine and pendant guanidinium groups (Scheme 50).

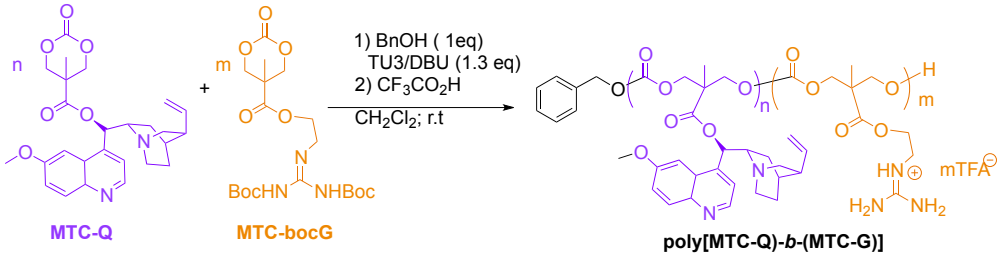

Scheme 50. DBU/TU-catalyzed synthesis of (co) polymers bearing both quinine and guanidinium groups.[153]

The benzyl-protected dihydroxylated bicyclic carbonate, namely 9-phenyl-2,4,8,10 tetraoxaspiro[5,5]undecan-3-one (PTO), was readily polymerized in dichloromethane at r.t., using 1,4-butanediol, MeOPEO-OH or HO-PCL-OH as (macro)initiator and DBU/TU3 as catalytic system (Scheme 51).[154,155] Poly(PTO)'s of controlled molar masses M_n = 6,250 g.mol^{-1} and $Đ$ = 1.06 were obtained in this way. Sequential copolymerization with D,L lactide provided an amphiphilic functional PEO-*b*-polyester-polycarbonate (M_n = 12,000 g.mol^{-1}; $Đ$ = 1.07). Optimized post-modification allowed tuning the physicochemical properties of these copolymers, enabling for a potential use as biodegradable materials.

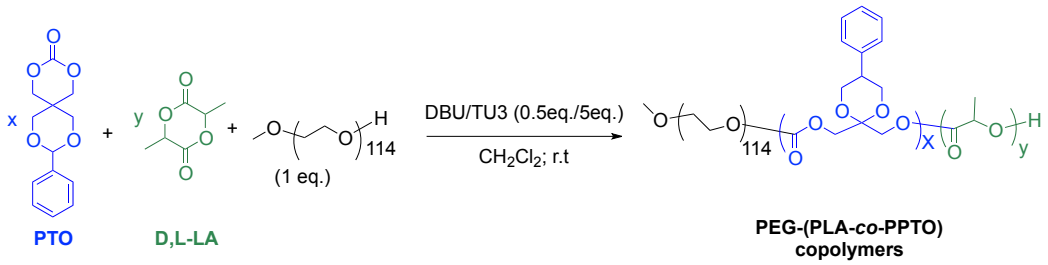

Scheme 51. Synthesis of amphiphilic PEO-poly(ester carbonate) using TU3/DBU catalysis.[154]

Phenol derivatives represent another class of small molecules with H-bond donor capabilities and that can be involved in polymerization reactions, by analogy with the activation of monomer by thiourea derivatives.

DBU/phenol combination readily catalyzed the ROP of δ-VL and ε-CL, with 4-biphenylmethanol (BPM) as initiator (Scheme 52).[156] Reactions were performed in dichloromethane at r.t., under bench conditions (no pre-dyring of reactants, 4 Å molecular sieves). Quantitative conversion of δ-VL was obtained after 24 h, leading to PVL's of controlled molar masses M_n = 1,230-6,890 g.mol^{-1}, and narrow dispersities $Đ$ = 1.08-1.12. In contrast the DBU/phenol-catalyzed ROP of ε-CL required longer reaction times (48 h and 120 h), and reached only 57-79 % of conversion. This lower reactivity of ε-CL compared to δ-VL, in presence of H-bonding catalysts, was already reported and attributed to the occurrence of transesterification in the case of ε-CL.[120] Using this strategy, block copolyesters PVL-*b*-PLA and PCL-*b*-PLA were successfully prepared. A supramolecular mechanism involving formation of H-bond phenol:monomer and DBU:initiator (or chain-end) complexes was proposed (see insert in Scheme 52) . Compared to DBU/TU catalytic systems, DBU/phenol have the practical advantage that phenol derivatives are commercially available, operating at r.t under mild experimental conditions.

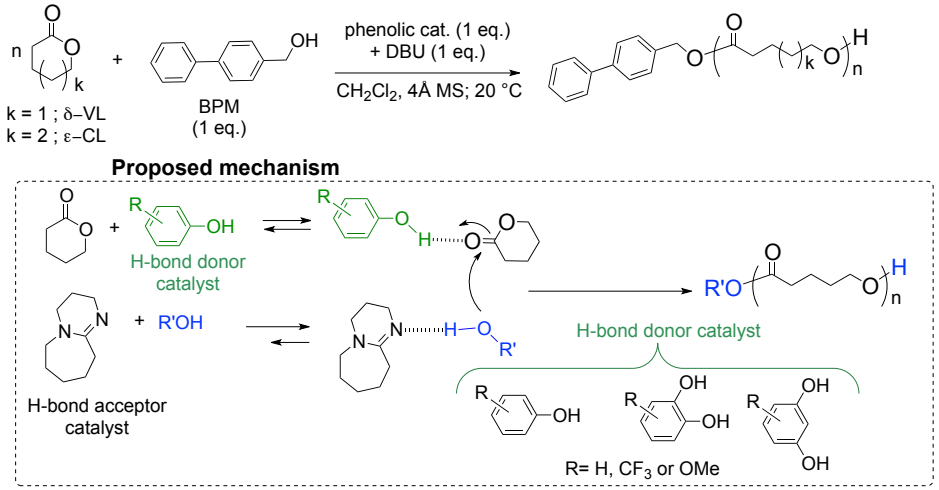

Scheme 52. DBU/phenol-catalyzed ROP of δ-VL and ε-CL in presence of an alcohol initiator.[156]

Kakuchi *et al.* combined DMAP (6 eq. relative to initiator) and diphenyl phosphate (DPP; 3 eq.) to induce the ROP of ε-CL and L-LA in dichloromethane at r.t., in presence of 3-phenyl-1-propanol (PPA) as initiator (Scheme 53).[157] DMAP was added as co-catalyst because DPP alone was inactive, leading to a dual activation system. This led to a well-defined PLLA of M_n = 19,200 g.mol^{-1} and $Đ$ = 1.10. Furthermore, this combination allowed synthesizing various copolyesters, including, PVL-*b*-PLLA (M_n = 11,600 g.mol^{-1}; $Đ$ = 1.16), PCL-*b*-PLLA (M_n = 12,100 g.mol^{-1}; $Đ$ = 1.12), PDXO-*b*-PLLA (M_n = 12,100 g.mol^{-1}; $Đ$ = 1.08) and PTMC-*b*-PLLA (M_n = 11,000 g.mol^{-1}; $Đ$ = 1.1) diblock copolymers.

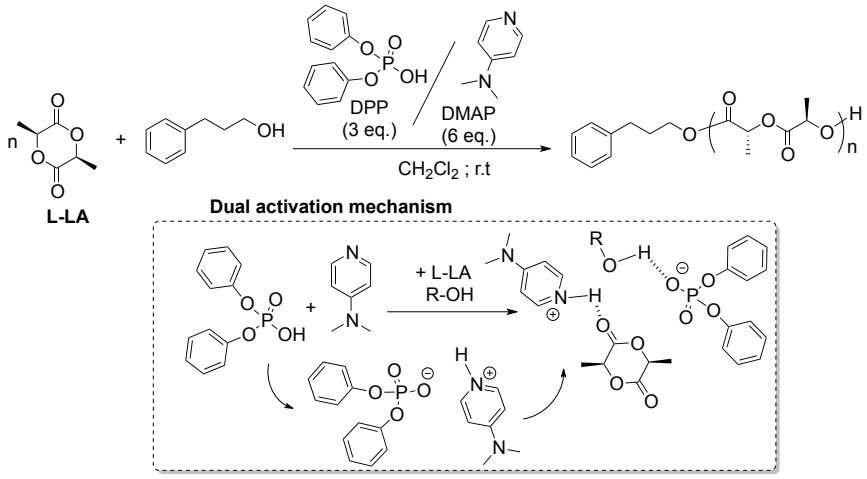

Scheme 53. Polymerization of L-LA using DPP/DMAP catalyst in presence of alcohol initiatior.[157]

In the same manner, Zinck *et al.* triggered the ROP of *rac*-LA using DMAP combined with acid-base salts such as (*R*)-(1)-binaphathyl-diyl hydrogen phosphate (BNPH)/DBU and (1*R*)-(-)-10-camphorsulfonic acid (CSA)/DMAP as catalytic systems and BnOH as initiator in dichloromethane at 35 °C.[158] Well-defined PLA's of M_n = 2,700 – 10,900 g.mol^{-1} ($Đ$ = 1.07-1.09) were obtained, although the polymerization proceeded slowly (70 % of monomer conversion after two weeks).

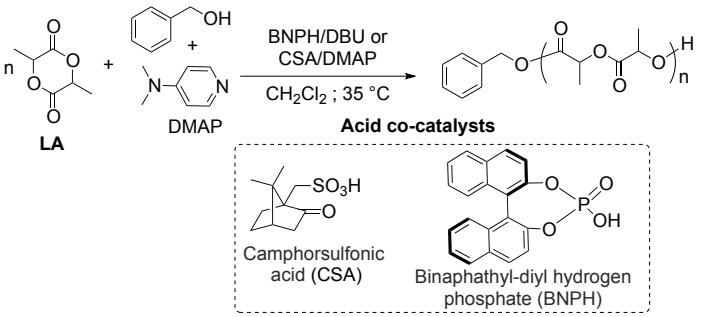

Scheme 54. ROP of LA using acid-base salts as catalytic systems in presence of DMAP/BnOH as initiatic system.[158]

Recently, Cramail, Taton *et al.* have reported the step-growth polymerization of bis(aldehyde)s and bis(ketone)s with pyrrolidine as catalyst in THF at r.t. (Scheme 55).[159] After 72 h of reaction, poly(aldol)'s of M_n = 6,700 g.mol^{-1} and M_w = 12,900 g.mol^{-1} ($Đ$ = 1.9) could be prepared. Addition of acetic acid (AcOH, 150 mol% relative to monomers) allowed increasing the molar masses, while broadering the molar mass distribution (M_n = 11,100 g.mol^{-1} and M_w = 55,000 g.mol^{-1}; $Đ$ = 2.6-4.9). Analysis of these poly(aldol)s by NMR spectroscopy confirmed the formation of β-keto alcohol units, but also evidenced the presence of 20-30 % of conjugated ketones, as a result of the dehydratation of β-keto alcohol units (see Scheme 55).

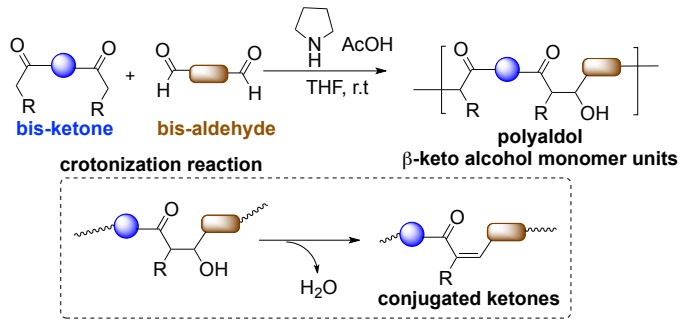

Scheme 55. Polymerization between bis(ketone)s and bis(aldehydes)s forming poly(aldol)s.[159]

The direct bulk aldol polymerization of acetaldehyde at r.t., catalyzed by Brønsted acids, including acetic acid and proline-derived catalysts, was also described (Scheme 56).[160] Only polyene-type oligomers **I** (M_n = 200 g.mol^{-}1) and polyol-type oligomer **II** (M_n = 200-300 g.mol^{-1} and M_w = 800-1,100 g.mol^{-1}) were obtained. Poly(vinyl alcohol-*co*-ethylene)-type oligomers were subsequently prepared, under hydrogenation and deacetalization conditions.

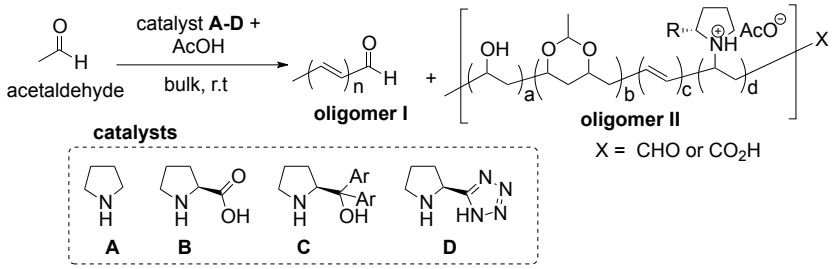

Scheme 56. Direct aldol polymerization of acetaldehyde using acid catalysts. [160]

Cramail, Taton *et al.* have also reported the synthesis of hyperbranched polyacetals (HBPA's) with a degree of branching (DB) equal to unit, by an acid-catalyzed step-growth polymerization of a simple AB_2 type monomer.[161] Indeed, the direct polycondensation of *p*-hydroxymethylbenzaldehyde dimethylacetal (**24**, Scheme 57) and its nonprotected homologue, namely, *p*-hydroxymethylbenzaldehyde **25**, was catalyzed by pyridinium camphorsulfonic acids (PCS) in toluene or in THF at r.t.[161] While HBPA's with a DB around 0.5 were produced through polytransacetalization of monomer **24**, monomer **25** led to HBPA's with DB = 1 by polyacetalization. This major difference was attributed to the reactivity of the intermediates formed during the first condensation reaction for each monomer. Upon condensation of monomer **24**, a stable acetal was formed in contrast to the unstable hemiacetal intermediate arising from monomer **25**, and that readily evolved to a stable dendritic acetal unit after reaction with another alcohol function. Previous works by Ramakrishnan *et al.* had shown shown that hyperbranched polyacetals with DB ≈ 0.5 could be achieved using various AB_2-type hydroxymethylbenzaldehyde dialkyl acetal (**26**).[162,163]

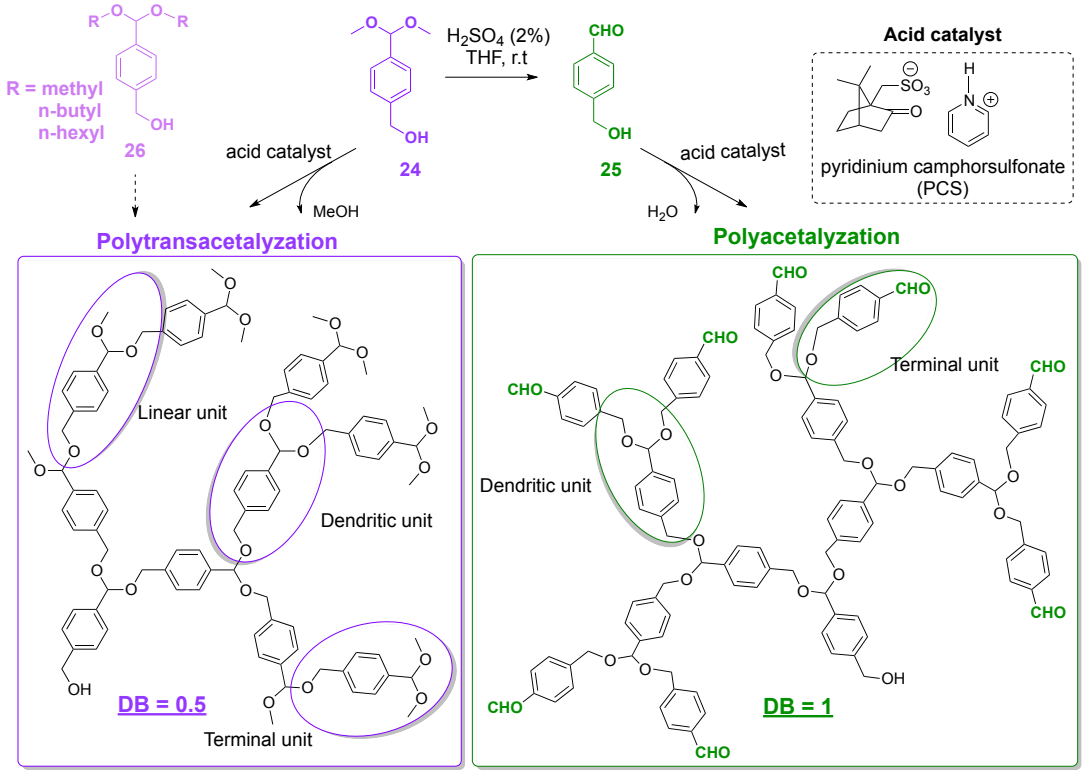

Scheme 57. Synthesis of hyperbranched polyactelas (HBPAs) via polytransacetalyzation of monomer 1 (DB≈0.5) and polyacetalyzation of monomer 2 (DB = 1) using acid catalysts. [161]

As mentioned above, instead of using two molecules promoting a dual activation, bifunctionality can be provided from one single molecule. Thus, triaryl iminophosphoranes featuring a thiourea moiety, were reported to efficiently catalyze the ROP of L-LA, δ-VL and ε-CL in dichloromethane at r.t., using PyBuOH as initiator (Scheme 58).[164] Quantitative conversion was obtained within 10 min, affording polyesters of molar masses M_n = 4,860

(*Đ* = 1.23), 32,922 g.mol^{-1} (*Đ* = 1.04) and 37,400 g.mol^{-1} (*Đ* = 1.08) for PCL, PLLA and PVL, respectively. PVL-*b*-PLA and PCL-*b*-PLA diblock copolymers were also obtained by sequential addition of the monomers. Importantly, mono-functional iminophosphorane, that is without the thiourea moiety, did not induce any polymerization, demonstrating the crucial role of the thiourea co-catalyst for monomer activation (Scheme 58).

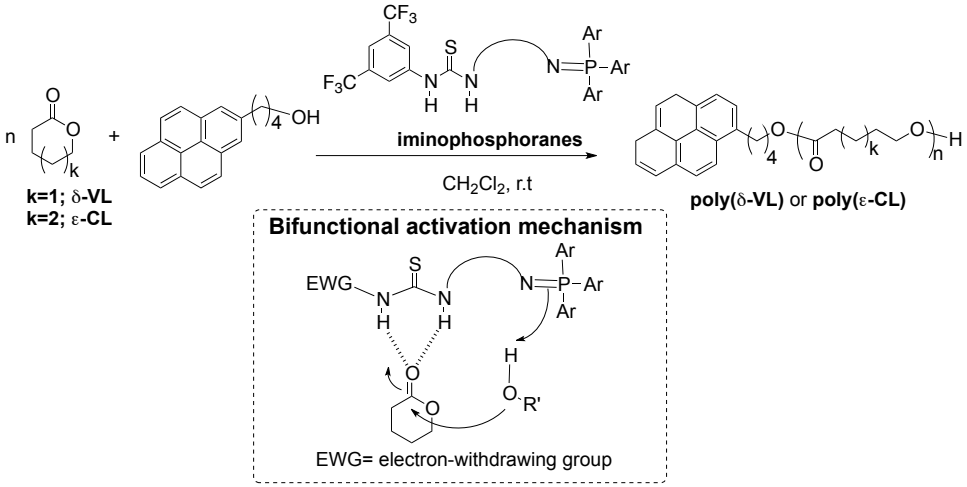

Scheme 58. ROP of cyclic esters catalyzed by iminophosphoranes in presence of alcohol.[164]

Ionic catalyst where the cation and the anion could activate both monomer and ROH, has been described by Coulembier *et al.*[165,166] More specifically, imidazolium trifluoroacetate salt allowed controlling the ROP of L-LA in bulk at 140 °C, using BnOH as initiator (Scheme 59). [159] PLLA of molar mass M_n = 8,700 g.mol^{-1} (*Đ* = 1.28) were rapidly obtained after 3.7 h of reaction (84 % of monomer conversion). It was proposed that polymerization proceeded by a bifunctional mechanism ressembling that operating with lipase B (produced by the yeast *Candida antartica*), where the imidazolium activates the carbonyl moiety through H-bonding, while the trifluorocarboxylate interacts with the initiating/propagating alcohol (see insert in Scheme 59). In the same manner *meta*-(trimethylammonio)phenolate betaine proved efficient catalyst for the ROP of L-LA, ε-CL and TMC in chloroform at 21 °C using 1-pyrenemethanol as the initiator, leading to polymers of M_n = 12,300-48,000 g.mol^{-1} (*Đ* = 1.04-1.47).[166] In this case, the ammonium betaine was proposed to activate the initiating and propagating alcohol site, allowing for a very rapid and controlled polymerization.

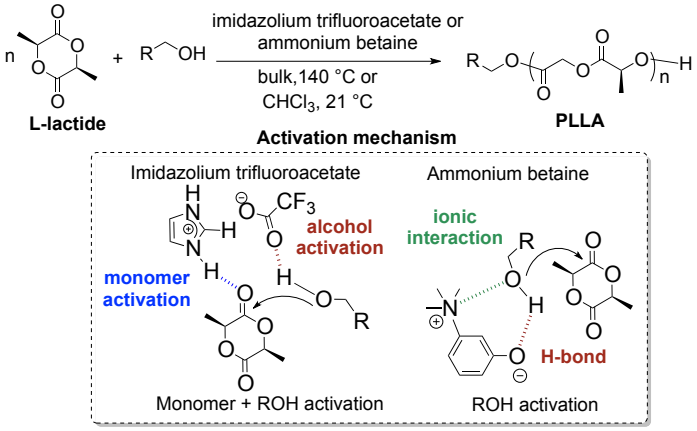

Scheme 59. ROP of L-LA using imidazolium-salt or ammonium betaine as catalyst in the presence of ROH. [165,166]

In summary, the capability of thioureas (TU) or phenol derivatives to activate carbonyl substrates combined with the use of a base to deprotonate alcohol initiator, has been applied through both mono- and bicomponent catalytic systems to the ROP of cyclic esters and cyclic carbonates. Such an activation, inspired from the H-bonding motifs found in enzyme active sites, provides high chemoselectivity with very few side reactions (*e.g.* transesterification reactions) during the polymerization.

Concluding remarks

This bibliographical chapter has reviewed the contributions of the post 3 years regarding organo-catalyzed reactions. The diverse reactivity and selectivity of small organic molecules have been efficiently transfered in recent years, from organocatalysis in molecular chemistry to precise macromolecular syntheses. Organic catalysts are most often easily available and can improve polymerization kinetics, controlling the polymerization process by favouring selective propagation step over side reactions. In some cases, they exhibit performances that compare or even exceed those of commonly used organometallic compounds, making them powerful alternatives to produce polymers free of any metallic residues.

Due to space limitations, polymerization reactions mediated by organic small molecules as direct initiators *i.e.* in absence of any other co-activator, and not as catalysts, were not discussed in the present chapter. In such “organo-initiated” polymerizations, Lewis bases including NHCs,[167-172], amidines[173], isothioureas,[174] phosphazenes[175-178] and even (+)sparteine[179] were employed to trigger chain-growth polymerization reactions, either through ring-opening (for cyclic monomers; Scheme 60a)[12] or through 1,4 conjugate addition (for (meth)acrylates derivatives; Scheme 60b). Only one example of an acid initiator (*i.e.*

(di)hydrogenphosphates) was reported.[180] Although these direct polymerizations were not well controlled, the reactant structures (initiator and monomer) drastically influenced the topology of the final polymer, with either cyclic or/and linear structures being obtained. A complete review, covering both organo-catalyzed and organo-initiated polymerization reactions is under preparation in our group.

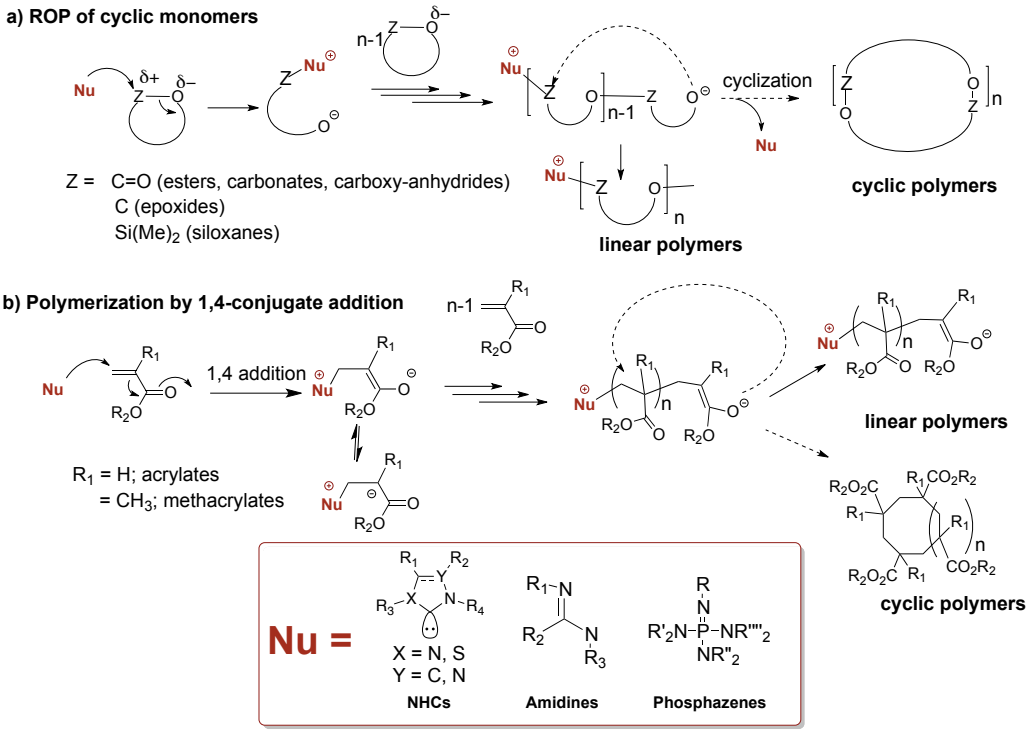

Scheme 60. Nucleophilic-induced: a) ROP; b) vinyl polymerization in the absence of a co-initiator.

The architecture of organo-synthesized polymers can be easily tuned to impart interesting properties, by polymerizing pre-functionalized monomers or through post-polymerization functionalization. Thereby, various homo- or copolymers – though mainly poly(esters) and poly(carbonates)- have been synthesized by ROP and some of them have been then post-functionalized.

Some of these metal-free polymeric materials demonstrated valuable physico-chemical properties as well as *in vivo* biocompatibility, making them promising materials for applications in tissue engineering, drug delivery and regenerative medicine. For instance, cationic polycarbonates were found to form dynamic micelles that allowed increasing bacterial cell interactions and demonstrated to be strong antimicrobial films against drug-resistant bacteria.[181-183] Copolymers PEO-polycarbonates or PEO-polyphosphoesters were demonstrated to self-assembly into micelles with high loading capacity of the hydrophobic anticancer drug paclitaxel (PTX). These PTX-loaded micelles were preferentially accumulated in tumor tissue with limited distribution to healthy organs.[184-186] These few examples of metal-

free synthesized polymers in bio-applications illustrated the expansion of organo-polymerization, from precise and controlled chemistry to specific and targeted applications.

The absence of metal traces is therefore sought after in several applications, ranging from medicine to electronics, where metallic residues could interfere with the polymer end use. Moreover and most importantly, these residues could drastically shorten the polymer lifespan due to an increase in degradation during either polymer processing or weathering.[187] However, although toxicity issues are often neglected concerning organic activators, health and environmental risks of these compounds in the final material are so far almost unknown and need to be clarified.[188]

As also emphasized in this chapter, most of organo-catalyzed and organo-initiated polymerization reactions are widely based on the ring-opening of carbonyl-containing monomers such as, cyclic esters and cyclic carbonates. However, few organic compounds, such as *N*-heterocyclic carbenes (NHCs) were proved efficient for the ROP of non-containing C = O cyclic monomers such as ethers and siloxanes, the GTP of alkyl (meth)acrylates, as well as for some step-growth polymerizations. So far, and to the best of our knowledge, the field of organo-polymerization of non-polar monomers, *e.g.* conjugated dienes or styrenics is still unexplored.

The main objective of the present PhD work is to investigate the reactivity of NHCs towards alkyl (meth)acrylates, as vinyl model substrates, in order to expand the scope of NHC-mediated polymerizations. It will be demonstrated that the outcomes of NHC-mediated polymerization dramatically depend on the NHC structure/reactivity.

In the next chapters of this manuscript, the influence of the NHC structure/reactivity for the direct NHC-initiated polymerization of alkyl (meth)acrylates monomers is investigated (chapter 2). In chapter 3, NHC-catalyzed polymerization in presence of alcohols as chain regulators is described. Chapter 4 discusses the use of NHCs associated to silicon-based Lewis acids to induce Lewis-pair polymerization (LPP) *via* a true organic bicomponent activators system using cooperative/dual activation.

References

(1) MacMillan, D. W. *Nature* **2008**, *455*, 304.
(2) Wende, R. C.; Schreiner, P. R. *Green Chem.* **2012**, *14*, 1821.
(3) Bugaut, X.; Glorius, F. *Chem. Soc. Rev.* **2012**, *41*, 3511.
(4) Volla, C. M. R.; Atodiresei, I.; Rueping, M. *Chem. Rev.* **2013**, *114*, 2390.
(5) Dalko, P. I. *Comprehensive Enantioselective Organocatalysis: Catalysts, Reactions, and Applications, 3 Volume Set*; John Wiley & Sons, 2013.
(6) Liu, D.; Chen, E. Y. X. *Greem Chemistry* **2014**, *16*, 964.
(7) Kiesewetter, M. K.; Shin, E. J.; Hedrick, J. L.; Waymouth, R. M. *Macromolecules* **2010**, *43*, 2093.
(8) Dove, A. P. *ACS Macro Lett.* **2012**, *1*, 1409.
(9) Mespouille, L.; Coulembier, O.; Kawalec, M.; Dove, A. P.; Dubois, P. *Prog. Polym. Sci.* **2014**.
(10) Fuchise, K.; Chen, Y. G.; Satoh, T.; Kakuchi, T. *Polym. Chem.* **2013**, *4*, 4278.
(11) Hirao, A.; Goseki, R.; Ishizone, T. *Macromolecules* **2014**, *47*, 1883.
(12) Brown, H. A.; Waymouth, R. M. *Acc. Chem. Res.* **2013**, *46*, 2585.
(13) Thomas, C.; Bibal, B. *Green Chem.* **2014**.
(14) Fèvre, M.; Vignolle, J.; Gnanou, Y.; Taton, D. In *Polymer Science: A Comprehensive Reference*; Editors-in-Chief: Krzysztof, M., Martin, M. I., Eds.; Elsevier: Amsterdam, 2012, p 67.
(15) Fèvre, M.; Pinaud, J.; Gnanou, Y.; Vignolle, J.; Taton, D. *Chem. Soc. Rev.* **2013**, *42*, 2142.
(16) Bordwell, F. G. *Acc. Chem. Res.* **1988**, *21*, 456.
(17) Ren, J. M.; Fu, Q.; Blencowe, A.; Qiao, G. G. *ACS Macro Lett.* **2012**, *1*, 681.
(18) Gazeau-Bureau, S.; Delcroix, D.; Martín-Vaca, B.; Bourissou, D.; Navarro, C.; Magnet, S. *Macromolecules* **2008**, *41*, 3782.
(19) Stanley, N.; Bucataru, G.; Miao, Y.; Favrelle, A.; Bria, M.; Stoffelbach, F.; Woisel, P.; Zinck, P. *J. Polym. Sci., Part A: Polym. Chem.* **2014**, *52*, 2139.
(20) Basko, M.; Duda, A.; Kazmierski, S.; Kubisa, P. *J. Polym. Sci., Part A: Polym. Chem.* **2013**, *51*, 4873.
(21) Couffin, A.; Martin-Vaca, B.; Bourissou, D.; Navarro, C. *Polym. Chem.* **2014**, *5*, 161.
(22) Foropoulos, J.; DesMarteau, D. D. *Inorg. Chem.* **1984**, *23*, 3720.
(23) Makiguchi, K.; Kikuchi, S.; Satoh, T.; Kakuchi, T. *J. Polym. Sci., Part A: Polym. Chem.* **2013**, *51*, 2455.
(24) King, J. F. In *Sulphonic Acids, Esters and their Derivatives (1991)*; John Wiley & Sons, Ltd: 2006, p 249.
(25) Jin, Y.; Ji, Y.; He, X.; Kan, S.; Xia, H.; Liang, B.; Chen, J.; Wu, H.; Guo, K.; Li, Z. *Polym. Chem.* **2014**.
(26) Pascual, A.; Leiza, J. R.; Mecerreyes, D. *Eur. Polym. J.* **2013**, *49*, 1601.
(27) Pascual, A.; Sardon, H.; Veloso, A.; Ruipérez, F.; Mecerreyes, D. *ACS Macro Lett.* **2014**, *3*, 849.
(28) Delcroix, D.; Martin-Vaca, B.; Bourissou, D.; Navarro, C. *Macromolecules* **2010**, *43*, 8828.
(29) Campos, J. M.; Ribeiro, M. R.; Ribeiro, M. F.; Deffieux, A.; Peruch, F. *Macromol. Chem. Phys.* **2013**, *214*, 85.
(30) Campos, J. M.; Ribeiro, M. R.; Ribeiro, M. F.; Deffieux, A.; Peruch, F. *Eur. Polym. J.* **2013**.
(31) Couffin, A.; Delcroix, D.; Martin-Vaca, B.; Bourissou, D.; Navarro, C. *Macromolecules* **2013**, *46*, 4354.
(32) Coady, D. J.; Horn, H. W.; Jones, G. O.; Sardon, H.; Engler, A. C.; Waymouth, R. M.; Rice, J. E.; Yang, Y. Y.; Hedrick, J. L. *ACS Macro Lett.* **2013**, *2*, 306.
(33) Susperregui, N.; Delcroix, D.; Martin-Vaca, B.; Bourissou, D.; Maron, L. *J. Org. Chem.* **2010**, *75*, 6581.
(34) Engler, A. C.; Chan, J. M. W.; Coady, D. J.; O'Brien, J. M.; Sardon, H.; Nelson, A.; Sanders, D. P.; Yang, Y. Y.; Hedrick, J. L. *Macromolecules* **2013**, *46*, 1283.

(35) Sardon, H.; Engler, A. C.; Chan, J. M. W.; Garcia, J. M.; Coady, D. J.; Pascual, A.; Mecerreyes, D.; Jones, G. O.; Rice, J. E.; Horn, H. W.; Hedrick, J. L. *J. Am. Chem. Soc.* **2013**, *135*, 16235.
(36) Sardon, H.; Chan, J.; Ono, R.; Mecerreyes, D.; Hedrick, J. *Polym. Chem.* **2014**, *5*, 3547.
(37) Ishihara, K.; Hasegawa, A.; Yamamoto, H. *Angew. Chem. Int. Ed.* **2001**, *40*, 4077.
(38) Takada, K.; Fuchise, K.; Chen, Y.; Satoh, T.; Kakuchi, T. *J. Polym. Sci., Part A: Polym. Chem.* **2012**, *50*, 3560.
(39) Takada, K.; Fuchise, K.; Kubota, N.; Ito, T.; Chen, Y.; Satoh, T.; Kakuchi, T. *Macromolecules* **2014**, *47*, 5514.
(40) Xu, J.; Song, J.; Pispas, S.; Zhang, G. *J. Polym. Sci., Part A: Polym. Chem.* **2014**, *52*, 1185.
(41) Christ, P.; Lindsay, A. G.; Vormittag, S. S.; Neudörfl, J.-M.; Berkessel, A.; O'Donoghue, A. C. *Chem. Eur. J.* **2011**, *17*, 8524.
(42) Akiyama, T. *Chem. Rev.* **2007**, *107*, 5744.
(43) Makiguchi, K.; Ogasawara, Y.; Kikuchi, S.; Satoh, T.; Kakuchi, T. *Macromolecules* **2013**, *46*, 1772.
(44) Makiguchi, K.; Satoh, T.; Kakuchi, T. *Macromolecules* **2011**, *44*, 1999.
(45) Makiguchi, K.; Saito, T.; Satoh, T.; Kakuchi, T. *J. Polym. Sci., Part A: Polym. Chem.* **2014**, *52*, 2032.
(46) Werner, T. *Adv. Synth. Catal.* **2009**, *351*, 1469.
(47) Terada, M.; Momiyama, N. In *Science of Synthesis, Asymmetric Organocatalysis 2, Brønsted Base and Acid Catalysts, and Additional Topics*; Maruoka, K., Ed.; Georg Thieme Verlag KG: New York, 2012, p 219.
(48) Miao, Y.; Phuphuak, Y.; Rousseau, C.; Bousquet, T.; Mortreux, A.; Chirachanchai, S.; Zinck, P. *J. Polym. Sci., Part A: Polym. Chem.* **2013**, *51*, 2279.
(49) Miao, Y.; Mortreux, A.; Zinck, P. In *Carbohydrate Chemistry: Volume 40*; The Royal Society of Chemistry: 2014; Vol. 40, p 298.
(50) Kan, S.; Jin, Y.; He, X.; Chen, J.; Wu, H.; Ouyang, P.; Guo, K.; Li, Z. *Polym. Chem.* **2013**, *4*, 5432.
(51) He, X.; Ji, Y.; Jin, Y.; Kan, S.; Xia, H.; Chen, J.; Liang, B.; Wu, H.; Guo, K.; Li, Z. *J. Polym. Sci., Part A: Polym. Chem.* **2014**, *52*, 1009.
(52) Ishikawa, T. *Superbases for organic synthesis: guanidines, amidines and phosphazenes and related organocatalysts*; Wiley Online Library, 2009.
(53) Schwesinger, R.; Schlemper, H. *Angew. Chem. Int. Ed.* **1987**, *26*, 1167.
(54) Boileau, S.; Illy, N. *Prog. Polym. Sci.* **2011**, *36*, 1132.
(55) Zhao, J. P.; Alamri, H.; Hadjichristidis, N. *Chem. Commun.* **2013**, *49*, 7079.
(56) Zhao, J.; Pahovnik, D.; Gnanou, Y.; Hadjichristidis, N. *Macromolecules* **2014**, *47*, 1693.
(57) Zhao, J.; Pahovnik, D.; Gnanou, Y.; Hadjichristidis, N. *Macromolecules* **2014**, *47*, 3814.
(58) Zhao, J.; Pahovnik, D.; Gnanou, Y.; Hadjichristidis, N. *J. Polym. Sci., Part A: Polym. Chem.* **2014**, DOI: 10.1002/pola.27332.
(59) Hadjichristidis, N.; Zhao, J.; Pahovnik, D.; Gnanou, Y. *Polym. Chem.* **2014**, *5*, 3750.
(60) Alamri, H.; Zhao, J.; Pahovnik, D.; Hadjichristidis, N. *Polym. Chem.* **2014**, *5*, 5471.
(61) Guerin, W.; Helou, M.; Carpentier, J.-F.; Slawinski, M.; Brusson, J.-M.; Guillaume, S. M. *Polym. Chem.* **2013**, *4*, 1095.
(62) Samuel, C.; Chalamet, Y.; Boisson, F.; Majeste, J.-C.; Becquart, F.; Fleury, E. *J. Polym. Sci., Part A: Polym. Chem.* **2014**, *52*, 493.
(63) Illy, N.; Boileau, S.; Winnik, M. A.; Penelle, J.; Barbier, V. *Polymer* **2012**, *53*, 903.
(64) Yang, H. J.; Xu, J. B.; Pispas, S.; Zhang, G. Z. *Macromolecules* **2012**, *45*, 3312.
(65) Xu, J. B.; Yang, H. J.; Zhang, G. Z. *Macromol. Chem. Phys.* **2013**, *214*, 378.
(66) Yang, H.; Xu, J.; Pispas, S.; Zhang, G. *RSC Advances* **2013**, *3*, 6853.
(67) De Winter, J.; Dove, A. P.; Knoll, A.; Gerbaux, P.; Dubois, P.; Coulembier, O. *Polym. Chem.* **2014**, *5*, 706.
(68) Methot, J. L.; Roush, W. R. *Adv. Synth. Catal.* **2004**, *346*, 1035.
(69) Marinetti, A.; Voituriez, A. *Synlett* **2010**, 174.

(70) Myers, M.; Connor, E. F.; Glauser, T.; Mock, A.; Nyce, G.; Hedrick, J. L. *J. Polym. Sci., Part A: Polym. Chem.* **2002**, *40*, 844.
(71) Fèvre, M.; Vignolle, J.; Heroguez, V.; Taton, D. *Macromolecules* **2012**, *45*, 7711.
(72) Arduengo, A. J.; Harlow, R. L.; Kline, M. *J. Am. Chem. Soc.* **1991**, *113*, 361.
(73) Bourissou, D.; Guerret, O.; Gabbai, F. P.; Bertrand, G. *Chem. Rev.* **2000**, *100*, 39.
(74) Nair, V.; Bindu, S.; Sreekumar, V. *Angew. Chem. Int. Ed.* **2004**, *43*, 5130.
(75) Hahn, F. E.; Jahnke, M. C. *Angew. Chem. Int. Ed.* **2008**, *47*, 3122.
(76) Dröge, T.; Glorius, F. *Angew. Chem. Int. Ed.* **2010**, *49*, 6940.
(77) Hopkinson, M. N.; Richter, C.; Schedler, M.; Glorius, F. *Nature* **2014**, *510*, 485.
(78) Magill, A. M.; Cavell, K. J.; Yates, B. F. *J. Am. Chem. Soc.* **2004**, *126*, 8717.
(79) Higgins, E. M.; Sherwood, J. A.; Lindsay, A. G.; Armstrong, J.; Massey, R. S.; Alder, R. W.; O'Donoghue, A. C. *Chem. Commun.* **2011**, *47*, 1559.
(80) Fischer, C.; Smith, S. W.; Powell, D. A.; Fu, G. C. *J. Am. Chem. Soc.* **2006**, *128*, 1472.
(81) Biju, A. T.; Padmanaban, M.; Wurz, N. E.; Glorius, F. *Angew. Chem. Int. Ed.* **2011**, *50*, 8412.
(82) Ryan, S. J.; Candish, L.; Lupton, D. W. *Chem. Soc. Rev.* **2013**, *42*, 4906.
(83) Mahatthananchai, J.; Bode, J. W. *Acc. Chem. Res.* **2014**, *47*, 696.
(84) Chauhan, P.; Enders, D. *Angew. Chem. Int. Ed.* **2014**, *53*, 1485.
(85) Diez-Gonzalez, S.; Marion, N.; Nolan, S. P. *Chem. Rev.* **2009**, *109*, 3612.
(86) Nelson, D. J.; Nolan, S. P. *Chem. Soc. Rev.* **2013**, *42*, 6723.
(87) Herrmann, W. A. *Angew. Chem. Int. Ed.* **2002**, *41*, 1290.
(88) Breslow, R. *J. Am. Chem. Soc.* **1958**, *80*, 3719.
(89) Grossmann, A.; Enders, D. *Angew. Chem. Int. Ed.* **2012**, *51*, 314.
(90) Moore, J. L.; Rovis, T. *Top. Curr. Chem.* **2010**, *291*, 77.
(91) Marion, N.; Diez-Gonzalez, S.; Nolan, S. P. *Angew. Chem. Int. Ed.* **2007**, *46*, 2988.
(92) Enders, D.; Niemeier, O.; Henseler, A. *Chem. Rev.* **2007**, *107*, 5606.
(93) Nair, V.; Vellalath, S.; Babu, B. P. *Chem. Soc. Rev.* **2008**, *37*, 2691.
(94) Grossmann, A.; Enders, D. *Angew. Chem., Int. Ed.* **2012**, *51*, 314.
(95) Kamber, N. E.; Jeong, W.; Waymouth, R. M.; Pratt, R. C.; Lohmeijer, B. G. G.; Hedrick, J. L. *Chem. Rev.* **2007**, *107*, 5813.
(96) Naumann, S.; Buchmeiser, M. *Catal. Sci. Technol.* **2014**.
(97) Arduengo, A. J.; Dias, H. V. R.; Harlow, R. L.; Kline, M. *J. Am. Chem. Soc.* **1992**, *114*, 5530.
(98) Orsini, M.; Chiarotto, I.; Sotgiu, G.; Inesi, A. *Electrochim. Acta* **2010**, *55*, 3511.
(99) Orsini, M.; Chiarotto, I.; Feeney, M. M. M.; Feroci, M.; Sotgiu, G.; Inesi, A. *Electrochem. Commun.* **2011**, *13*, 738.
(100) Kuhn, N.; Kratz, T. *Synthesis* **1993**, 561.
(101) Wang, Y.; Zhang, L.; Guo, X.; Zhang, R.; Li, J. *Journal of Polymer Research* **2013**, *20*.
(102) Zhang, R.; Zhang, L.; Wang, J.; Guo, X. *Polym. Bull.* **2013**, *70*, 1289.
(103) Xia, H.; Kan, S.; Li, Z.; Chen, J.; Cui, S.; Wu, W.; Ouyang, P.; Guo, K. *J. Polym. Sci., Part A: Polym. Chem.* **2014**, *52*, 2306.
(104) Wanzlick, H. W. *Angew. Chem. Int. Ed.* **1962**, *1*, 75.
(105) Coutelier, O.; El Ezzi, M.; Destarac, M.; Bonnette, F.; Kato, T.; Baceiredo, A.; Sivasankarapillai, G.; Gnanou, Y.; Taton, D. *Polym. Chem.* **2012**, *3*, 605.
(106) Duong, H. A.; Cross, M. J.; Louie, J. *Org. Lett.* **2004**, *6*, 4679.
(107) Hoppe, A.; Sadaka, F.; Brachais, C. H.; Boni, G.; Couvercelle, J. P.; Plasseraud, L. *Beilstein J. Org. Chem* **2013**, *9*, 647.
(108) Fèvre, M.; Vignolle, J.; Taton, D. *Polym. Chem.* **2013**, *4*, 1995.
(109) Naumann, S.; Schmidt, F. G.; Frey, W.; Buchmeiser, M. R. *Polym. Chem.* **2013**, *4*, 4172.
(110) Lindner, R.; Lejkowski, M. L.; Lavy, S.; Deglmann, P.; Wiss, K. T.; Zarbakhsh, S.; Meyer, L.; Limbach, M. *ChemCatChem* **2014**, *6*, 618.
(111) Raynaud, J.; Nzahou Ottou, W.; Gnanou, Y.; Taton, D. *Chem. Commun.* **2010**, *46*, 3203.
(112) Reitz, A.; Wilhelm, R.; Kuckling, D. *Macromol. Symp.* **2013**, *334*, 92.

(113) Fèvre, M.; Pinaud, J.; Leteneur, A.; Gnanou, Y.; Vignolle, J.; Taton, D.; Miqueu, K.; Sotiropoulos, J. M. *J. Am. Chem. Soc.* **2012**, *134*, 6776.
(114) Neilson, B. M.; Bielawski, C. W. *Chem. Commun.* **2013**, *49*, 5453.
(115) Murugan, R.; Scriven, E. F. V. *Aldrichim. Acta* **2003**, *36*, 21.
(116) Miao, Y.; Rousseau, C.; Mortreux, A.; Martin, P.; Zinck, P. *Polymer* **2011**, *52*, 5018.
(117) Mingfa, Y.; Tao, W.; Na, Q.; Yongkai, H.; Daping, Q. *Polym. Int.* **2012**, *61*, 1525.
(118) Coady, D. J.; Engler, A. C.; Horn, H. W.; Bajjuri, K. M.; Fukushima, K.; Jones, G. O.; Nelson, A.; Rice, J. E.; Hedrick, J. L. *ACS Macro Lett.* **2012**, *1*, 19.
(119) Kaljurand, I.; Kutt, A.; Soovali, L.; Rodima, T.; Maemets, V.; Leito, I.; Koppel, I. A. *J. Org. Chem.* **2005**, *70*, 1019.
(120) Lohmeijer, B. G. G.; Pratt, R. C.; Leibfarth, F.; Logan, J. W.; Long, D. A.; Dove, A. P.; Nederberg, F.; Choi, J.; Wade, C.; Waymouth, R. M.; Hedrick, J. L. *Macromolecules* **2006**, *39*, 8574.
(121) Coulembier, O.; Lemaur, V.; Josse, T.; Minoia, A.; Cornil, J.; Dubois, P. *Chem. Sci.* **2012**, *3*, 723.
(122) Venkataraman, S.; Hedrick, J. L.; Yang, Y. Y. *Polym. Chem.* **2014**, *5*, 2035.
(123) Zhao, Z.; Wang, J.; Mao, H.-Q.; Leong, K. W. *Adv. Drug Delivery Rev.* **2003**, *55*, 483.
(124) Iwasaki, Y.; Yamaguchi, E. *Macromolecules* **2010**, *43*, 2664.
(125) Zhang, S.; Li, A.; Zou, J.; Lin, L. Y.; Wooley, K. L. *ACS Macro Lett.* **2012**, *1*, 328.
(126) Clément, B.; Grignard, B.; Koole, L.; Jérôme, C.; Lecomte, P. *Macromolecules* **2012**, *45*, 4476.
(127) Lim, Y. H.; Heo, G. S.; Cho, S.; Wooley, K. L. *ACS Macro Lett.* **2013**, *2*, 785.
(128) Martello, M. T.; Burns, A.; Hillmyer, M. *ACS Macro Lett.* **2012**, *1*, 131.
(129) Guillerm, B.; Lemaur, V.; Ernould, B.; Cornil, J.; Lazzaroni, R.; Gohy, J.-F.; Dubois, P.; Coulembier, O. *RSC Advances* **2014**, *4*, 10028.
(130) Appel, E. A.; Lee, V. Y.; Nguyen, T. T.; McNeil, M.; Nederberg, F.; Hedrick, J. L.; Swope, W. C.; Rice, J. E.; Miller, R. D.; Sly, J. *Chem. Commun.* **2012**, *48*, 6163.
(131) Kim, H.; Olsson, J. V.; Hedrick, J. L.; Waymouth, R. M. *ACS Macro Lett.* **2012**, *1*, 845.
(132) Silvers, A. L.; Chang, C. C.; Emrick, T. *J. Polym. Sci., Part A: Polym. Chem.* **2012**, *50*, 3517.
(133) Bouyahyi, M.; Pepels, M. P. F.; Heise, A.; Duchateau, R. *Macromolecules* **2012**, *45*, 3356.
(134) Castillo, J. A.; Borchmann, D. E.; Cheng, A. Y.; Wang, Y.; Hu, C.; Garcia, A. J.; Weck, M. *Macromolecules* **2012**, *45*, 62.
(135) Zhang, S.; Zou, J.; Zhang, F.; Elsabahy, M.; Felder, S. E.; Zhu, J.; Pochan, D. J.; Wooley, K. L. *J. Am. Chem. Soc.* **2012**, *134*, 18467.
(136) Guerin, W.; Helou, M.; Slawinski, M.; Brusson, J. M.; Guillaume, S. M.; Carpentier, J. F. *Polym. Chem.* **2013**, *4*, 3686.
(137) Guerin, W.; Diallo, A. K.; Kirilov, E.; Helou, M.; Slawinski, M.; Brusson, J.-M.; Carpentier, J.-F. o.; Guillaume, S. M. *Macromolecules* **2014**, *47*, 4230.
(138) Mikami, K.; Lonnecker, A. T.; Gustafson, T. P.; Zinnel, N. F.; Pai, P. J.; Russell, D. H.; Wooley, K. L. *J. Am. Chem. Soc.* **2013**, *135*, 6826.
(139) Coulembier, O.; Moins, S. b.; Todd, R.; Dubois, P. *Macromolecules* **2014**, *47*, 486.
(140) Alsarraf, J.; Ammar, Y. A.; Robert, F.; Cloutet, E.; Cramail, H.; Landais, Y. *Macromolecules* **2012**, *45*, 2249.
(141) Maisonneuve, L.; Lebarbe, T.; Grau, E.; Cramail, H. *Polym. Chem.* **2013**, *4*, 5472.
(142) Blain, M.; Jean-Gerard, L.; Auvergne, R.; Benazet, D.; Caillol, S.; Andrioletti, B. *Green Chem.* **2014**, *16*, 4286.
(143) Lambeth, R. H.; Henderson, T. J. *Polymer (United Kingdom)* **2013**, *54*, 5568.
(144) Fukushima, K.; Coady, D. J.; Jones, G. O.; Almegren, H. A.; Alabdulrahman, A. M.; Alsewailem, F. D.; Horn, H. W.; Rice, J. E.; Hedrick, J. L. *J. Polym. Sci., Part A: Polym. Chem.* **2013**, *51*, 1606.
(145) Horn, H. W.; Jones, G. O.; Wei, D. S.; Fukushima, K.; Lecuyer, J. M.; Coady, D. J.; Hedrick, J. L.; Rice, J. E. *J. Phys. Chem. A* **2012**, *116*, 12389.
(146) Fukushima, K.; Lecuyer, J. M.; Wei, D. S.; Horn, H. W.; Jones, G. O.; Al-Megren, H. A.; Alabdulrahman, A. M.; Alsewailem, F. D.; McNeil, M. A.; Rice, J. E.; Hedrick, J. L. *Polym. Chem.* **2013**, *4*, 1610.

(147) Zhang, Z.; Schreiner, P. R. *Chem. Soc. Rev.* **2009**, *38*, 1187.
(148) Tempelaar, S.; Mespouille, L.; Dubois, P.; Dove, A. P. *Macromolecules* **2011**, *44*, 2084.
(149) Stevens, D. M.; Tempelaar, S.; Dove, A. P.; Harth, E. *ACS Macro Lett.* **2012**, *1*, 915.
(150) Todd, R.; Rubio, G.; Hall, D. J.; Tempelaar, S.; Dove, A. P. *Chem. Sci.* **2013**, *4*, 1092.
(151) Venkataraman, S.; Veronica, N.; Voo, Z. X.; Hedrick, J. L.; Yang, Y. Y. *Polym. Chem.* **2013**, *4*, 2945.
(152) Tempelaar, S.; Barker, I. A.; Truong, V. X.; Hall, D. J.; Mespouille, L.; Dubois, P.; Dove, A. P. *Polym. Chem.* **2013**, *4*, 174.
(153) Edward, J. A.; Kiesewetter, M. K.; Kim, H.; Flanagan, J. C. A.; Hedrick, J. L.; Waymouth, R. M. *Biomacromolecules* **2012**, *13*, 2483.
(154) Aguirre-Chagala, Y. E.; Santos, J. L.; Herrera-Najera, R.; Herrera-Alonso, M. *Macromolecules* **2013**, *46*, 5871.
(155) Brannigan, R. P.; Walder, A.; Dove, A. P. *J. Polym. Sci., Part A: Polym. Chem.* **2014**, *52*, 2279.
(156) Thomas, C.; Peruch, F.; Bibal, B. *RSC Advances* **2012**, *2*, 12851.
(157) Makiguchi, K.; Kikuchi, S.; Yanai, K.; Ogasawara, Y.; Sato, S.-i.; Satoh, T.; Kakuchi, T. *J. Polym. Sci., Part A: Polym. Chem.* **2014**, *52*, 1047.
(158) Miao, Y.; Stanley, N.; Favrelle, A.; Bousquet, T.; Bria, M.; Mortreux, A.; Zinck, P. *J. Polym. Sci., Part A: Polym. Chem.* **2014**, DOI: 10.1002/pola.27488.
(159) Liu, N.; Martin, A.; Robert, F.; Vincent, J.-M.; Landais, Y.; Vignolle, J.; Cramail, H.; Taton, D. *Macromolecules* **2014**, *47*, 525.
(160) Kusumoto, S.; Ito, S.; Nozaki, K. *Asian J. Org. Chem.* **2013**, *2*, 977.
(161) Liu, N.; Vignolle, J.; Vincent, J.-M.; Robert, F.; Landais, Y.; Cramail, H.; Taton, D. *Macromolecules* **2014**, *47*, 1532.
(162) Chatterjee, S.; Ramakrishnan, S. *Macromolecules* **2011**, *44*, 4658.
(163) Chatterjee, S.; Ramakrishnan, S. *ACS Macro Lett.* **2012**, *1*, 593.
(164) Goldys, A. M.; Dixon, D. J. *Macromolecules* **2014**.
(165) Coulembier, O.; Josse, T.; Guillerm, B.; Gerbaux, P.; Dubois, P. *Chem. Commun.* **2012**, *48*, 11695.
(166) Guillerm, B.; Lemaur, V.; Cornil, J.; Lazzaroni, R.; Dubois, P.; Coulembier, O. *Chem. Commun.* **2014**, *50*, 10098.
(167) Brown, H. A.; Xiong, S.; Medvedev, G. A.; Chang, Y. A.; Abu-Omar, M. M.; Caruthers, J. M.; Waymouth, R. M. *Macromolecules* **2014**.
(168) Acharya, A. K.; Chang, Y. A.; Jones, G. O.; Rice, J. E.; Hedrick, J. L.; Horn, H. W.; Waymouth, R. M. *J. Phys. Chem. B* **2014**, *118*, 6553.
(169) Brown, H. A.; Chang, Y. A.; Waymouth, R. M. *J. Am. Chem. Soc.* **2013**, *135*, 18738.
(170) Zhang, Y.; Chen, E. Y. X. *Angew. Chem. Int. Ed.* **2012**, *51*, 2465.
(171) Zhang, Y.; Schmitt, M.; Falivene, L.; Caporaso, L.; Cavallo, L.; Chen, E. Y. X. *J. Am. Chem. Soc.* **2013**, *135*, 17925.
(172) Naumann, S.; Schmidt, F. G.; Schowner, R.; Frey, W.; Buchmeiser, M. R. *Polym. Chem.* **2013**, *4*, 2731.
(173) Brown, H. A.; De Crisci, A. G.; Hedrick, J. L.; Waymouth, R. M. *ACS Macro Lett.* **2012**, *1*, 1113.
(174) Zhang, X.; Waymouth, R. M. *ACS Macro Lett.* **2014**, 1024.
(175) Jaffredo, C. G.; Carpentier, J. F.; Guillaume, S. M. *Macromol. Rapid Commun.* **2012**, *33*, 1938.
(176) Jaffredo, C. G.; Carpentier, J. F.; Guillaume, S. M. *Polym. Chem.* **2013**, *4*, 3837.
(177) Schmitt, M.; Falivene, L.; Caporaso, L.; Cavallo, L.; Chen, E. Y. X. *Polym. Chem.* **2014**.
(178) Jaffredo, C. G.; Carpentier, J. F.; Guillaume, S. M. *Macromolecules* **2013**, *46*, 6765.
(179) Coulembier, O.; De Winter, J.; Josse, T.; Mespouille, L.; Gerbaux, P.; Dubois, P. *Polym. Chem.* **2013**.
(180) Malik, P.; Chakraborty, D. *Inorg. Chim. Acta* **2013**, *400*, 32.
(181) Qiao, Y.; Yang, C.; Coady, D. J.; Ong, Z. Y.; Hedrick, J. L.; Yang, Y.-Y. *Biomaterials* **2012**, *33*, 1146.

(182) Ding, X.; Yang, C.; Lim, T. P.; Hsu, L. Y.; Engler, A. C.; Hedrick, J. L.; Yang, Y.-Y. *Biomaterials* **2012**, *33*, 6593.
(183) Chan, J. M. W.; Ke, X.; Sardon, H.; Engler, A. C.; Yang, Y. Y.; Hedrick, J. L. *Chem. Sci.* **2014**, *5*, 3294.
(184) Lee, A. L. Z.; Venkataraman, S.; Sirat, S. B. M.; Gao, S.; Hedrick, J. L.; Yang, Y. Y. *Biomaterials* **2012**, *33*, 1921.
(185) Zou, J.; Zhang, F.; Zhang, S.; Pollack, S. F.; Elsabahy, M.; Fan, J.; Wooley, K. L. *Adv Healthc Mater* **2013**.
(186) Zhang, S.; Zou, J.; Elsabahy, M.; Karwa, A.; Li, A.; Moore, D. A.; Dorshow, R. B.; Wooley, K. L. *Chem. Sci.* **2013**, *4*, 2122.
(187) White, J. R.; Turnbull, A. *J. Mater. Sci.* **1994**, *29*, 584.
(188) Nachtergael, A.; Coulembier, O.; Dubois, P.; Helvenstein, M.; Duez, P.; Blankert, B.; Mespouille, L. *Biomacromolecules* **2014**, DOI: 10.1021/bm5015443.

Chapter 2.

Polymerization *versus* cyclodimerization of alkyl (meth)acrylates induced by *N*-heterocyclic carbenes

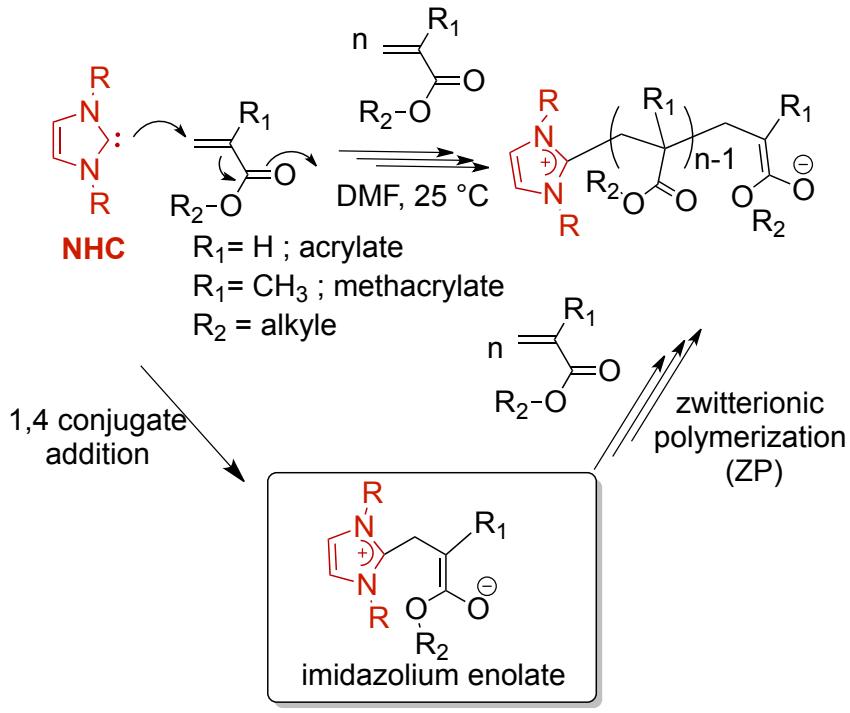

Keywords: *N*-Heterocyclic Carbenes • Alkyl (meth)acrylates • Zwitterionic polymerization • Cyclodimerization • DFT calculations.

Chapter 2.
Polymerization versus cyclodimerization of alkyl (meth)acrylates induced by *N*-heterocyclic carbenes

Table of contents

Introduction

As emphasized in the previous chapter, organocatalysis has been highlighted as a powerful route to complete challenges in macromolecular syntheses, in the past decade.[1-3] Among organocatalysts, *N*-heterocyclic carbenes (NHCs) have been successfully employed both in metal-free chain- and step-growth polymerization reactions.[4]

While the NHC-mediated ring-opening polymerization (ROP) of cyclic esters and other heterocyclics has been extensively investigated, polymerization of vinyl monomers such as alkyl (meth)acrylates by NHCs has been less considered.

In the context of the "group transfer polymerization" (GTP) of alkyl (meth)acrylates, NHCs can activate silyl ketene acetal (SKA) groups carried by the initiator and the polymer chain ends, the polymerization occurring through repetitive Mukaiyama-Michael reactions.[5] While Hedrick Waymouth *et al.* have postulated a dissociative mechanism, forming truly enolate-type species, using 1,3–bis(isopropyl)-4,5-(dimethyl)imidazol-2-ylidene (NHC^{iPrMe}; Figure 1) as NHC catalyst, [6] our group has proposed that GTP could occur by an associative mechanism, when catalyzed by either 1,3-bis(isopropyl)imidazol-2-ylidene (NHC^{iPr}) or 1,3-bis(*tert*-butyl)imidazol-2-ylidene (NHC^{tBu}).[7] No significant difference has been noted, however, between the latter NHCs, though NHC^{iPr} proved slightly more efficient than NHC^{tBu} in the GTP of methyl methacrylate (MMA).

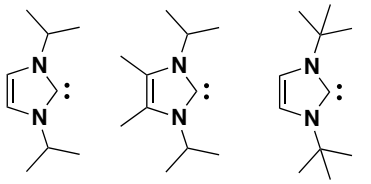

Figure 1. NHCs as organocatalysts for the GTP of alkyl (meth)acrylates.

Lately, Chen *et al.* have reported that the use of certain NHCs in conjunction with an alane, such as $Al(C_6F_5)_3$, could induce the direct polymerization of monomers such as methacrylates, acrylamides and methylene butyrolactone, in absence of any SKA initiator.[8,9] Computational studies have suggested that polymerization occured *via* a bimetallic zwitterionic dual mechanism, involving the formation of an Al-activated monomer (**1**), followed by the formation of an imidazolium enolaluminate active species (**2**), upon reaction with NHC. Propagation then took place *via* addition of **2** onto an incoming activated monomer (Scheme 1).

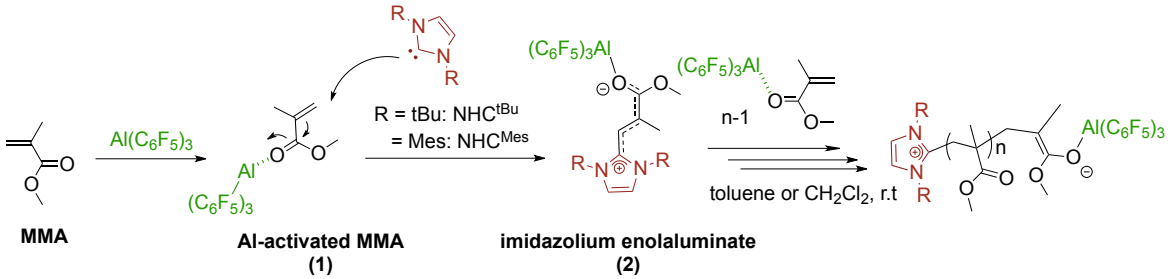

Scheme 1. Zwitterionic polymerization (ZP) of MMA induced by NHC/Al(C_6F_5) as Lewis pair.[8,9]

The potential of NHCs alone, as direct initiators for the ZP of (meth)acrylics, has also been reported. Hedrick, Waymouth *et al.* have first noted that NHC^{iPrMe} (see Figure 1) could directly initiate the ZP of *tert*-butyl acrylate (^{t}BuA) in THF at r.t, in absence of any other reagent.[6]

During the course of this PhD work, the ZP of MMA in DMF at r.t. induced by NHC^{tBu} has also been reported by Chen *et al.* (path A, Figure 3).[10,11] Very recently, Buchmeiser *et al.* have highlighted the ability of carbon dioxide-protected NHCs (NHC-CO_2 adducts) to behave as thermally latent initiators for the direct polymerization of MMA.[12] For instance, 1,3-bis(*tert*-butylimidazolium-2-carboxylate) (NHC^{tBu}-CO_2) initiates MMA polymerization at 85 °C, both in polar and non-polar solvents, as well as in bulk, whereas the isopropyl equivalent (NHC^{iPr}-CO_2) is totally inactive under the same conditions.

More generally, direct reaction of NHCs with carbonyl-containing substrates has been investigated, exploiting the σ donor and/or π acceptor properties of NHCs (see Figure 10 in chapter 1, p42).[13-18] Interestingly, the combination of these peculiar properties allows the polarity of substrates to be inverted, which is referred to as the Umpolung reaction.[13,14,18] Indeed, NHCs can readily react with aldehydes, through 1,2-addition onto the C=O bond, yielding the so-called Breslow intermediate (**3** ; Scheme 2) after proton transfer. The latter intermediate can further react in a 1,2- or 1,4- fashion with an aldehyde (= benzoin condensation; **4**) or with an α,β-unsaturated Michael acceptor (= Stetter reaction; **5**), respectively. These two important NHC-catalyzed reactions are illustrated in Scheme 2.

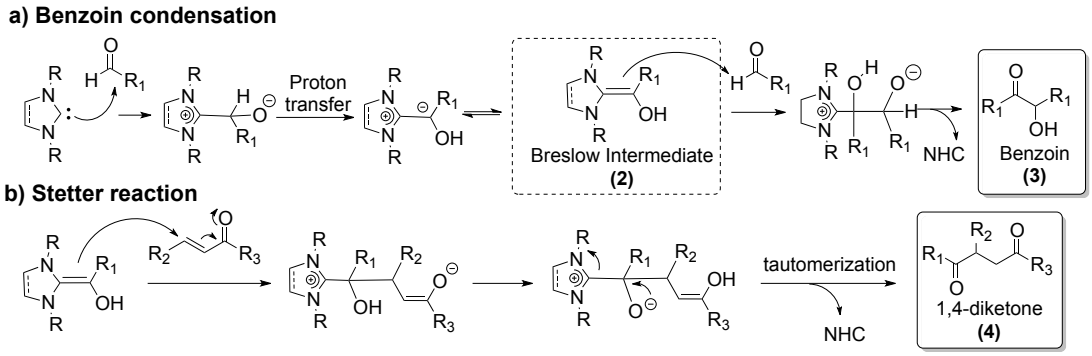

Scheme 2. Reactions mechanism involving a) a NHC and an aldehyde in the benzoin condensation; b) a NHC and an α,β-unsaturated Michael acceptor in the Stetter reaction.

Because NHCs are strong Lewis bases, miscellaneous adducts involving the reaction between NHCs and small electrophilic molecules such as CO_2,[19] CS_2,[19,20] N_2O,[21] aldehydes,[14,22-24] esters[14], ketenes[25,26] or C_{60}[27] have been recently characterized in solution or in the solid state (Figure 2).

The combination of umpolung and basic/nucleophilic catalysis by NHCs allowed synthesizing complex products such as azolium enolate[25] or diamino dienol.[24] The isolation and characterizations of these compounds have provided a better understanding of the intermediates involved in those transformations.

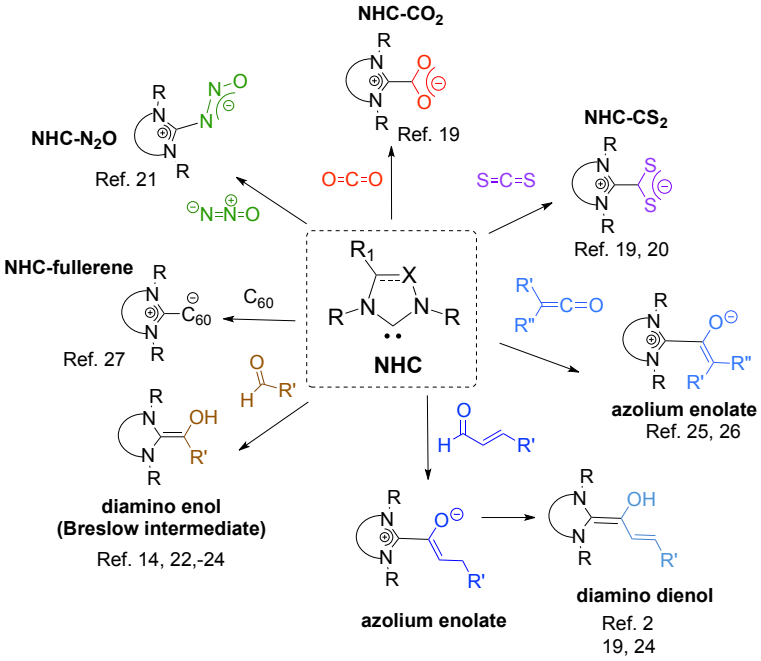

Figure 2. General structures of NHC adducts formed with electrophilic small molecules.[14,16,28-31]

Remarkably, while the reactivity of NHCs towards small organic molecules is not sensitive to the nature of NHCs, their reactivity towards Michael (meth)acrylate acceptors, such as MMA, is noticeably influenced by the steric and electronic properties of the

carbene.[10,11,13,32-35] The imidazolium enolate intermediate (**6** Figure 3) resulting from the initial 1,4-addition of the carbene to the (meth)acrylate substrate can further react *via* a [1,2-H] shift or by a 1,4-addition onto a second molecule of the substrate. Different 1:1 or 1:2 carbene: MMA adducts have thus been isolated.

For instance, 1,3-bis(mesityl)imidazol-2-ylidene (NHC^{Mes}) forms a single-addition 1:1 product, so-called deoxy-Breslow intermediate (**8**; path B, Figure 3),[10,11] while 1,3,4-triphenyl-4,5-dihydro-1H-1,2,4-triazol-5-ylidene (TPT) can catalyze the tail-to-tail dimerization of MMA (**9;** path C).[10,11,13,32,33] In contrast, and as mentioned above, multiple 1,4-additions of MMA can be initiated by NHC^{tBu}, ultimately leading to poly(methyl methacrylate) (PMMA; **7**; path A)[10,12] All these examples evidence the remarkable influence of the nature of the NHC over the reaction outcome.

Some selectivity has also been observed in the case of methyl acrylate (MA). More specifically, NHC^{Mes} was recently found to catalyze the cyclotetramerization of methyl acrylate (MA), giving rise to a trisubstituted cyclopentenone (**10**; path D).[34] Surprisingly, TPT was inactive under similar conditions.[34]

In this chapter, we aim at providing further evidence of the unique behavior of some NHCs in the reaction with (meth)acrylic monomer substrates. For this purpose, the direct polymerization, *i.e.* in absence of any other reagent, of miscellaneous acrylate- and methacrylate-type substrates by different NHCs has been investigated. Depending on the carbene/(meth)acrylate combination, significant differences in the reaction outcomes have been observed. Reaction mechanisms are postulated in some cases to account for the product formation.

The next part presents a detailed investigation into the reaction between either NHC^{iPr} or NHC^{tBu} and MA or MMA as model substrates. Unexpected differences have been observed between these two carbenes, despite their apparent similarity. In order to rationalize our experimental results, computational studies by density functional theory (DFT) have been performed on model reactions involving the carbene and the (meth)acrylate.

These calculations have been conducted by Damien Bourichon, completing his PhD under the supervision of Dr. Karinne Miqueu and Dr. Jean-Marc Sotiropoulos, at the Institut Pluridisciplinaire de Recherche sur l'Environnement et les matériaux (IPREM) at the Université de Pau & des Pays de l'Adour (UPPA).

The potential of both NHC^{iPr} or NHC^{tBu} as nucleophiles has been then evaluated for the direct polymerization of different (meth)acrylic monomers, with a view at establishing the scope of reactivity of NHCs towards these monomers.

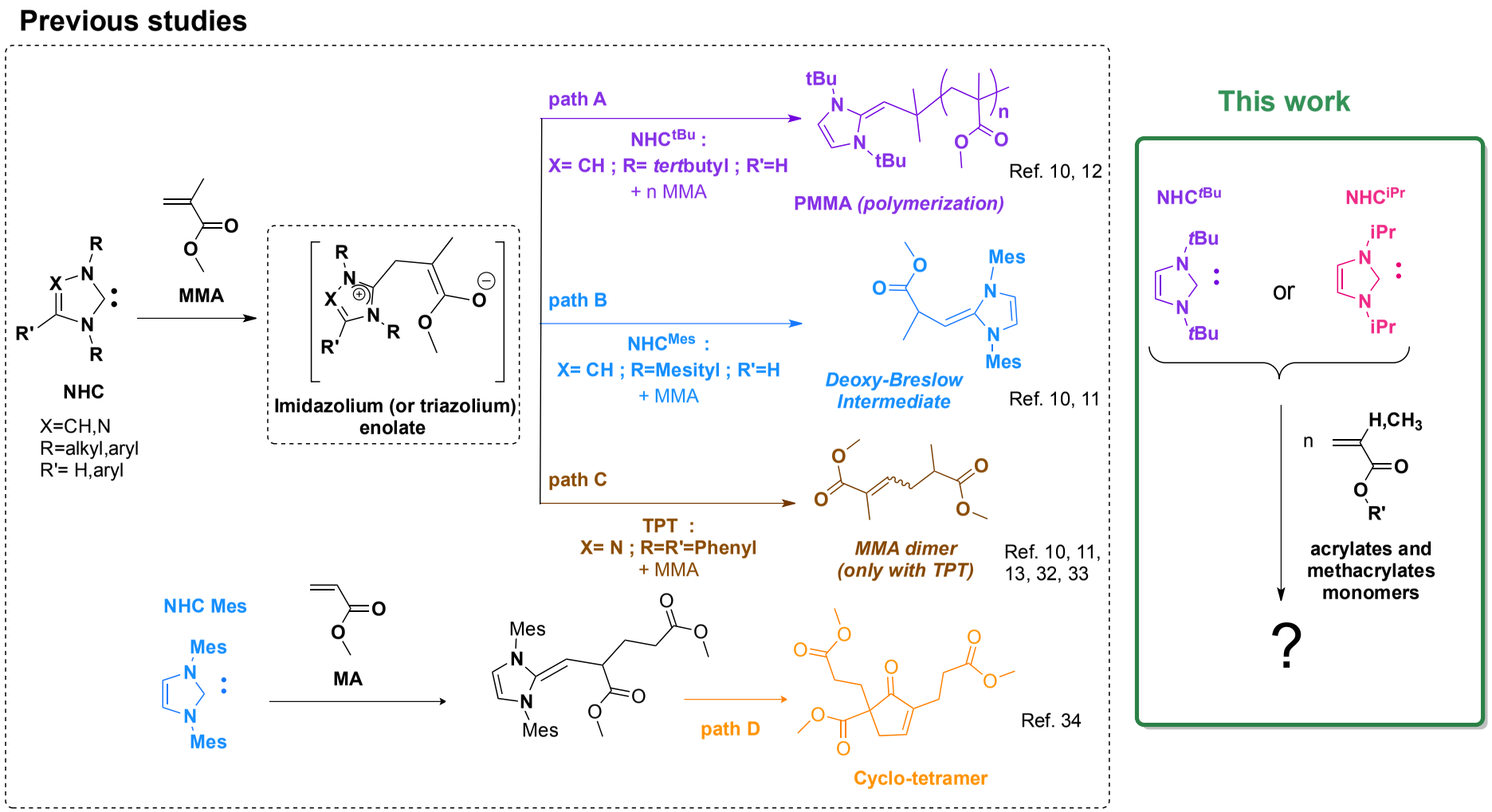

Figure 3. Scope of NHCs reactivity towards methyl acrylate (MA) and methyl methacrylate (MMA).[10-13,32-34]

1. Polymerization of methyl acrylate (MA) and methyl methacrylate (MMA)

1.1. Case of methyl acrylate (MA)

1.1.1. Polymerization reactions

As mentioned above, Hedrick, Waymouth *et.al.* noted that direct NHC-initiated ZP of *tert*-butyl acrylate (^{t}BuA) was a slow and a noncontrolled process, in THF at r.t.[6] More recently, Chen *et al.* reported that the rapid ZP of acrylic monomers initiated by NHCs occurred in DMF at r.t.[10,11] DMF was then selected as solvent for the polymerization of methyl acrylate (MA) at 25 °C, in the presence of NHC^{iPr} or NHC^{tBu} as direct initiator, *i.e.* in absence of any other co-activator or initiator.

For each NHC, the initial concentration was kept constant, $[NHC]_0$ = 10 mM, and [MA] was progressively varied to observe the influence of the monomer concentration on the molar masses. Table 1 summarizes the results of these polymerizations. In the case of a controlled polymerization, a linear evolution of molar masses with the initial $[MA]_0/[NHC]_0$ ratio, as well as concordance between experimental and theoretical molar masses based on this ratio, should be observed.

Table 1. NHC-induced polymerizations of MA in DMF at 25 °C.

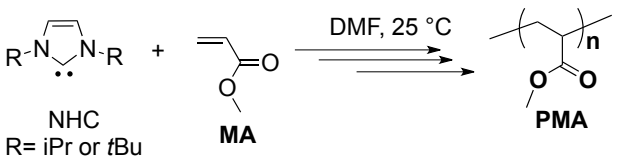

entry	NHC	$[MA]_0/[NHC]_0$	Time (h)	Conv.[a] (%)	$\overline{M_n}^{theo}$ [b] (g.mol^{-1})	$\overline{M_n}$ [c] (g.mol^{-1})	M_p [c] (g.mol^{-1})	$\overline{M_w}$ [c] (g.mol^{-1})	$Đ$ [c]
1	NHC^{iPr}	25	1	100	2,000	1,600	2,200	2,400	1.5
2	NHC^{iPr}	50	1	100	4,000	2,000	3,200	4,900	2.4
3	NHC^{iPr}	100	1	100	8,000	3,075	5,000	6,300	2.1
4	NHC^{iPr}	200	1	92	16,000	4,000	11,200	8,900	2.3
5	NHC^{tBu}	30	1	100	2,600	3,400	4,500	4,900	1.4
6	NHC^{tBu}	50	1	100	4,300	2,800	8,700	6,300	2.3
7	NHC^{tBu}	80	1	100	6,800	3,800	10,700	8,000	2.1
8	NHC^{tBu}	120	1	100	10,000	4,300	14,000	13,300	3.1

a. Conv.= % monomer conversion determined by ^{1}H NMR spectroscopy; b. Theoretical molar mass $\overline{M}_n^{theo} = M_{MA} \times \frac{[MA]}{[NHC]} \times conv.$; c. Characterization of PMA's by SEC in THF using polystyrene standards for calibration.

For both NHC^{iPr} and NHC^{tBu}, molar masses ($\overline{M_n}$, $\overline{M_p}$ and $\overline{M_w}$), as delivered by size exclusion chromatography (SEC), of the obtained poly(methyl acrylate)s (PMA's) were found to increase as the initial $[MA]_0/[NHC]_0$ ratio increased (Figure 4). However, deviation of these experimental molar masses from linearity, observations of rather large dispersities and, in some cases, shouldered trace, seemed to indicate the occurrence of side reactions. Nevertheless, the influence of SEC calibration utilizing polystyrene (PS) standards cannot be totally ruled out, since PS and PMA have a different hydrodynamic volume.[36]

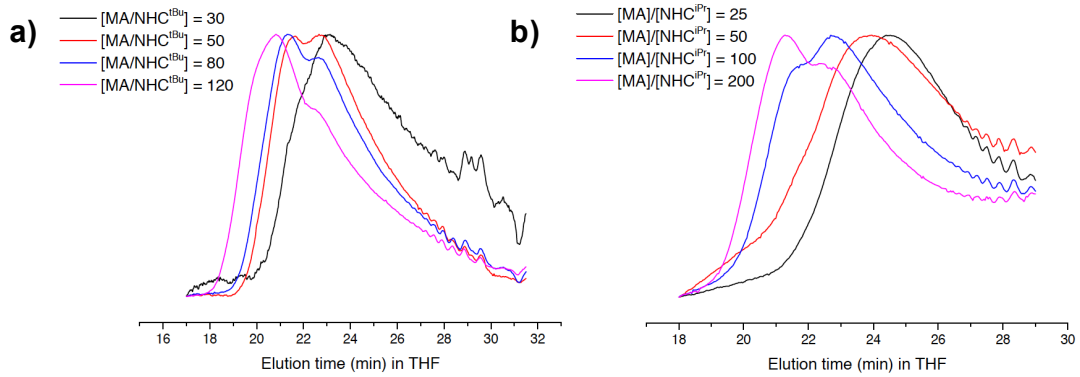

Figure 4. SEC-RI traces of PMA' obtained with a) NHC^{iPr} and b) NHC^{tBu} in DMF at 25 °C.

In such conditions, initiation supposedly occurs by a conjugate 1,4-addition of the NHC onto the monomer substrate, forming a zwitterionic imidazolium enolate intermediate **11** (Scheme 3). The propagation step should then proceed through the attack of the latter zwitterion onto incoming monomers, by a zwitterionic polymerization (ZP) mechanism, as highlighted in Scheme 3. In the context of such a direct initiation, NHC-induced zwitterionic ring-opening polymerization (ZROP) has already been reported for lactides,[37] lactones,[38-40] *N*-carboxyanhydrides,[41] and carbosiloxanes.[42] (see section 8 in Chapter 1).

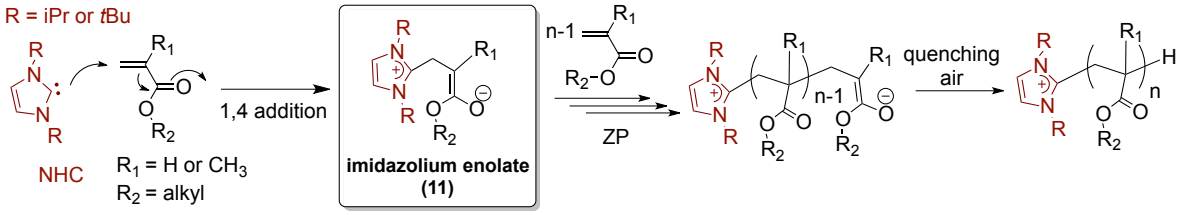

Scheme 3. Zwitterionic polymerization (ZP) of alkyl (meth)acrylates directly induced by NHCs.

In the specific case of the ZP of (meth)acrylate monomers, propagating species are in the form of imidazolium enolates (Scheme 4). Such active species must be distinguished from those involved in the GTP of methacrylic monomers, where polymeric silyl ketene acetal allows controlling the polymerization (Scheme 4).

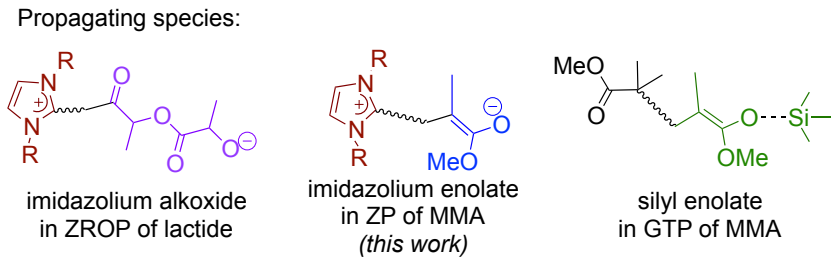

Scheme 4. Propagating species involved in the ZROP of lactide, the ZP and the GTP of MMA.

One can however expect that free enolates can give rise to different side reactions like, for instance, those observed in "conventional" anionic polymerization of acrylates and methacrylates.[43-45] PMA's obtained in this work thus gave rise to SEC traces with a UV absorption at λ = 260 nm, which was indicative of the formation of cyclic β-keto ester by intra-molecular polymer termination (back-biting reaction Scheme 5), hence leading to a loss of control over the molar masses. This back-biting reaction is the most frequent side reaction occurring during anionic polymerization of (meth)acrylics.[44,45]

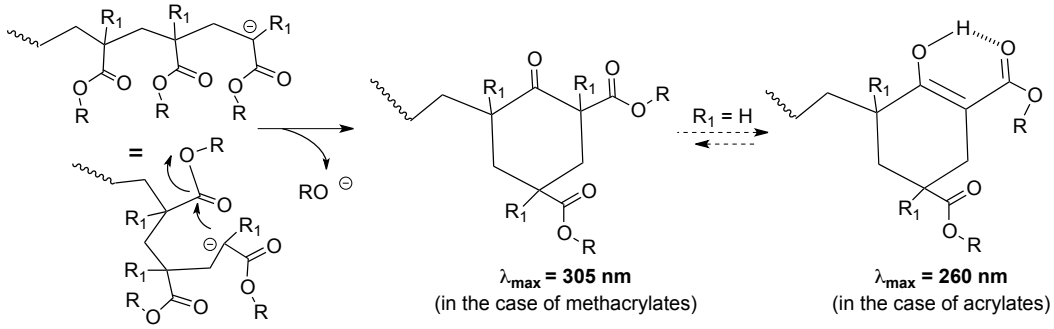

Scheme 5. Back-biting reaction in anionic polymerization of alkyl (meth)acrylate (the counteraction has been purposely omitted for clarity).[44,45]

Attempts to implement chain extension by adding a new load of monomer, after complete conversion, were also ineffective, confirming the premature deactivation of the propagating species (Table 2 and Figure 5).

Table 2. SEC results of PMA's obtained upon sequential addition of MA using NHC$^{t\mathrm{Bu}}$ in DMF at 25 °C.

Entry	$[MA]_0/[NHC]_0$	Time (h)	Conv.[a] (%)	$\overline{M_n}^{theo}$ [b] (g.mol^{-1})	$\overline{M_n}$ [c] (g.mol^{-1})	M_p [c] (g.mol^{-1})	$\overline{M_w}$ [c] (g.mol^{-1})	$Đ$ [c]
1	35 (run 1)	1	100	3,000	2,700	4,500	4,300	1.6
2	run 1 + 35 eq. MA	+ 24	n.d.	6,000	1,800	3,500	3,800	2.1

a. Conv.= % monomer conversion determined by ^{1}H NMR spectroscopy; b. Theoretical molar mass $\overline{M}_n^{theo} = M_{MA} \times \frac{[MA]}{[NHC]} \times conv.$; c. Characterization of PMA's by SEC in THF using PS standards for calibration.

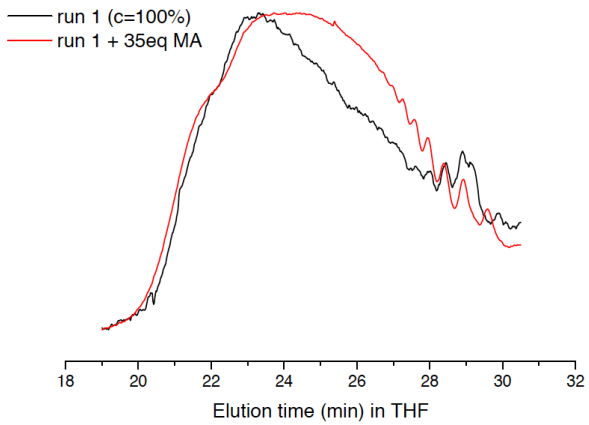

Figure 5. SEC-RI traces of PMA's obtained by sequential addition of MA using NHC^{tBu}.

Model reactions, utilizing equimolar amounts of the NHC and MA were next implemented, as a mean to identify the putative imidazolium enolate zwitterion **11** (Scheme 3), resulting from conjugate addition of NHC onto MA (= initiation step).

1.1.2. Stoichiometric reactions between MA and NHC^{iPr}

The equimolar reaction between MA and NHC^{iPr} was performed in a J-Young NMR tube in dried DMF-d_7, and the homogeneous solution was monitored by ^{1}H NMR spectroscopy.

After 24 h of reaction, no more signals of MA was noted, suggesting its rapid consumption by NHC^{iPr} (Figure 6). In the meantime, signals of the imidazole moiety were observed at δ_{CH3} = 1.52 ppm, δ_{CH} = 4.56 ppm and δ_{vinyl} = 5.30 ppm. All these signals are downfield shifted (by ~ 0.1 ppm compared to the free NHC), suggesting a charged imidazolium structure. After, evaporation of the solvent, a visquous oil was obtained. Unfortunately, attempts to purify this oil failed, making impossible the identification of the reaction product.

In conclusion, both NHC^{iPr} and NHC^{tBu} can trigger the polymerization of methyl acrylate (MA), though in a non-controlled fashion. Attempts to isolate the imidazolium enolate intermediate were not conclusive, but one can postulate that an initial 1,4-conjugate addition of the NHC^{iPr} onto MA takes place.

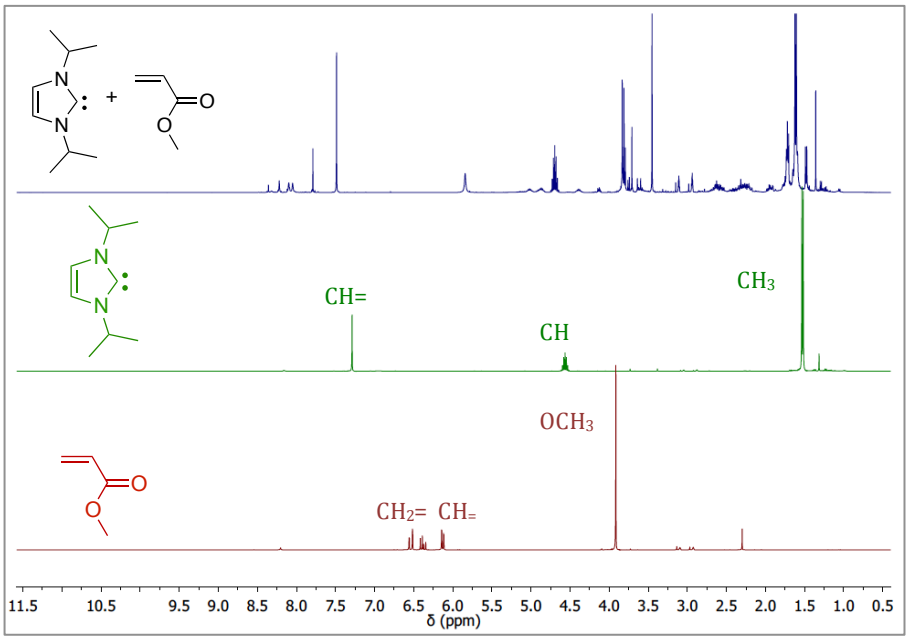

Figure 6. ^{1}H NMR spectra in DMF-d_7 of, from bottom to top: MA, NHC^{iPr} and MA+NHC^{iPr} (1:1).

1.2. Case of methyl methacrylate (MMA)

1.2.1. Polymerization reactions

The reaction between MMA and NHC^{iPr} or NHC^{tBu} was also carried out in DMF at 25 °C, and the results are summarized in Table 3 and illustrated in Figure 7.

In the case of NHC^{iPr}, no poly(methyl methacrylate) (PMMA) was formed, even at 50 °C. In sharp contrast, and as already reported by Chen *et al.*,[10] NHC^{tBu} could readily trigger the polymerization of MMA under similar conditions, leading to 35 % monomer conversion, in 5 h (for $[MMA]_0/ [NHC^{tBu}]_0$ = 100, Table 3, entry 5). This preliminary screening thus evidenced that despite their structural similarities, NHC^{iPr} and NHC^{tBu} exhibited a distinct reactivity towards MMA. Curiously, both in toluene or in THF at 25 °C, NHC^{tBu} did not produce any PMMA, while a non-controlled polymerization was observed in these solvents at 50 °C (entries 7-8).

Buchmeiser *et al.* have reported, in the course of this PhD work, that the equivalent carbene precursor, NHC^{tBu}-CO_2, could directly induce the polymerization of MMA in DMF and DMSO as well, at 85 °C (entry 9).[12] All these observations demonstrated the crucial role of the solvent in the polymerization, the propagating (zwitterionic) species being seemingly more reactive in polar solvents such as DMF and DMSO.

Table 3. NHC-induced polymerizations of MMA in DMF at 25 °C.

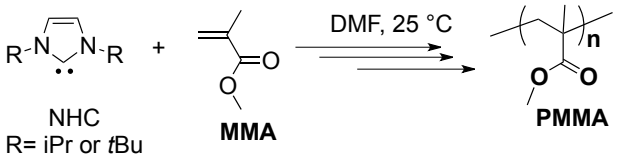

entry	NHC	$[MMA]_0/[NHC]_0$	Solvent	Time (h)	Conv.[a] (%)	$\overline{M_n}^{theo}$ [b] (g.mol^{-1})	$\overline{M_n}$ [c] (g.mol^{-1})	M_p [c] (g.mol^{-1})	$\overline{M_w}$ [c] (g.mol^{-1})	$Đ$ [c]
1	NHC^{iPr}	100	DMF	72	0	-	-	-	-	-
2	NHC^{tBu}	10	DMF	5	26	260	2,800	3,700	3,800	1.3
3	NHC^{tBu}	25	DMF	5	29	730	3,100	4,400	4,700	1.5
4	NHC^{tBu}	50	DMF	5	36	1,800	5,200	9,900	8,300	1.6
5	NHC^{tBu}	100	DMF	5	35	3,500	5,600	10,900	9,650	1.7
6	NHC^{tBu}	250	DMF	5	26	6,400	12,200	20,200	21,700	1.9
7[d]	NHC^{tBu}	200	THF	48	75	15,000	255,000	375,000	370,500	1.5
8[d]	NHC^{tBu}	200	Toluene	48	80	16,000	239,400	477,300	458,300	1.9
9[e]	NHC^{tBu}-CO_2	200	DMSO	68	44	12,320	14,000	-	-	1.7

a. Conv.= % monomer conversion determined by ^{1}H NMR spectroscopy; b. Theoretical molar mass $\overline{M}_n^{theo} = M_{MMA} \times \frac{[MMA]}{[NHC]} \times conv.$; c Characterization of PMMA's by SEC in THF using PS standards for calibration. d. Polymerization performed at 50 °C; e. Polymerization performed at 85 °C reported by Buchmeiser *et al.* [12]

As expected, NHC^{tBu}-induced polymerization of MMA was slower (for $[MMA]_0/[NHC^{tBu}]_0$ = 25, 29 % of conversion after 5 h; entry 3) than polymerization of MA with the same carbene (100 % of conversion after 1 h), owing to the less polymerizability of MMA, resulting from both the donor inductive effect (+I) and the steric effect of the methyl group. Molar masses of the as-obtained PMMA's also increased by varying the initial monomer concentration (with $[NHC]_0$ = 10 mM kept constant; Figure 7), though $\overline{M_n}$ values were higher than the theoretical ones based on the initial monomer-to-carbene ratio, while dispersities were in the range $Đ$ = 1.3-1.9. It has to be mentioned that the true molar masses M_n and M_w could be calculated by multiplying equivalent polystyrene molar masses (obtained by SEC analysis) by the correction factor B = 1.10 (Benoit factor for PMMA in THF).[36]

Even at low $[MMA]_0/[NHC^{tBu}]_0$ ratios, PMMA's of higher molar masses were achieved (*e.g.* $\overline{M_n}^{exp}$ = 3,100 g.mol^{-1} *vs.* $\overline{M_n}^{theo}$ = 730 g.mol^{-1} for a targeted degree of polymerization, DP, of 25; entry 3). In addition, dispersities were found to increase when targeting higher DP's.

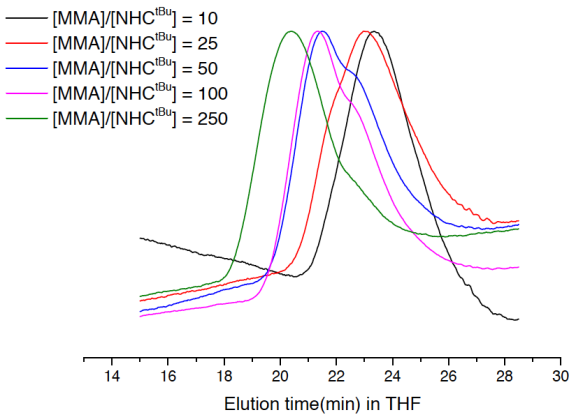

Figure 7. SEC-RI traces of PMMA's obtained with NHC^{tBu} as direct initiator in DMF at 25 °C.

Three hypotheses can be put forward to explain these observations.

(1) It might happen that the carbene did not fully react with the monomer (some NHC remained in solution), resulting in a partial formation of the active zwitterionic species. Thus, initiation would be a slow process relative to the propagation step;

(2) The carbene might have been partly deactivated, either by traces of impurities or by side reaction, involving the carbonyl group of the monomer. Nucleophilic addition of the NHC onto the ester moiety, for instance, could lead to a nonreactive acyl imidazolium alkoxide (**12**; Scheme 6). The NHC would thus be trapped, hence polymers of higher molar masses than expected would be provided;

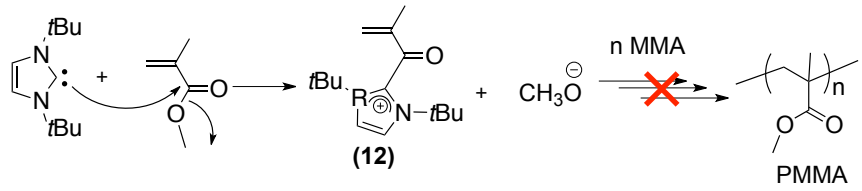

Scheme 6. Carbene deactivation *via* reaction with carbonyl group of the monomer.

(3) Reaction of the propagating enolate anion with a carbonyl group of another polymer chain could occur, leading to a chain coupling (branching; Scheme 7). Such a reaction has been already reported during anionic polymerization of alkyl (meth)acrylates.[43,44]

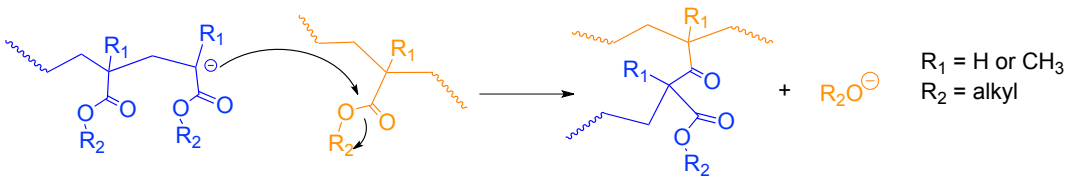

Scheme 7. Inter-molecular termination reaction in anionic polymerization of alkyl methacrylate (the countercation has been purposely omitted for clarity).[44,45]

The presence of free NHC^{tBu} in solution can eventually be verified, by adding a small excess of carbon disulfide (CS_2) onto the reaction mixture. Indeed, CS_2 is known to form a colored zwitterionic adduct when reacting with carbenes (Figure 8). By doing so, the initial pale yellow solution (Figure 9a) indeed instantaneously turned red (Figure 9b), a color characteristic of the 1,3-bis(*tert*-butyl)imidazolium dithiocarboxylate (NHC^{tBu}-CS_2 adduct). This experience thus indirectly evidenced the presence of some free carbene in the solution.

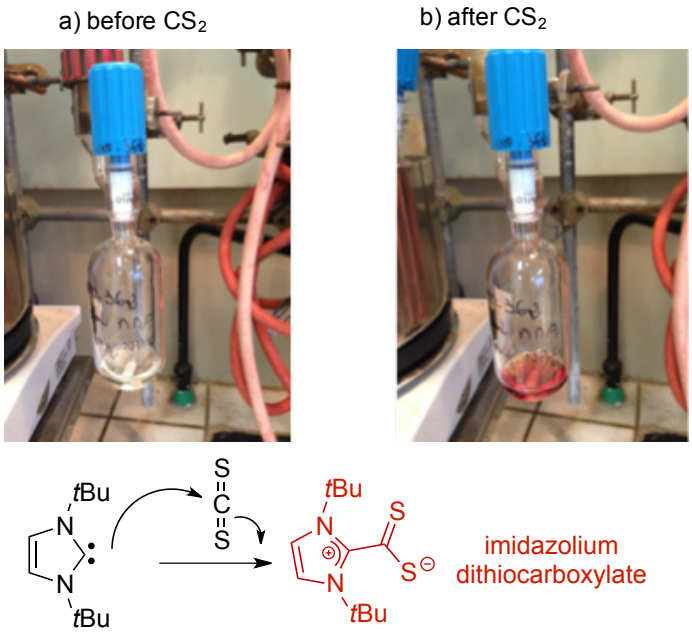

Figure 8. Color change due to the addition of CS_2 (20 eq.) into the reaction mixture containing MMA (10 eq.) and NHC^{tBu} (1 eq.) at the completion of the polymerization in DMF at 25 °C.

However, this result did not necessary mean that a slow initiation (first hypothesis) occurred. Indeed, the carbene might have been released by intra-molecular cyclization reaction (Scheme 8), leading to cyclic PMMA's. Such events have been evidenced by a few groups in the case of the ZROP of lactide,[37] lactones,[38-40] *N*-carboxyanhydrides,[41] and carbosiloxanes.[42]

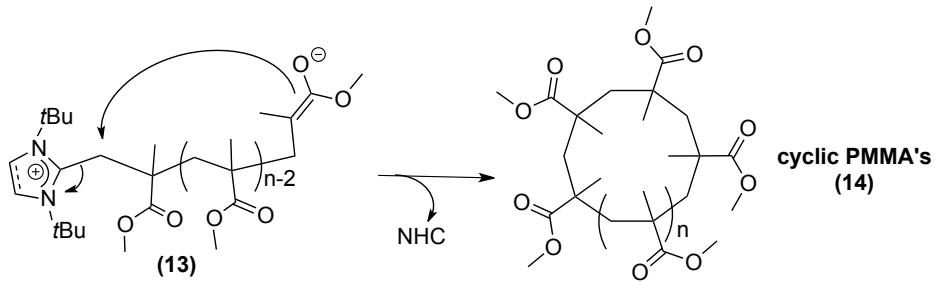

Scheme 8. Intra-molecular cyclization in ZP, leading to cyclic polymers.

Chain extension experiments, by sequential addition of monomer, were thus implemented to examine the potential "living" character of this NHC^{tBu}-induced polymerization of MMA. Results are summarized in Table 4 and illustrated in Figure 9.

First, MMA was polymerized in DMF with an initial ratio $[MMA]_0/[NHC^{tBu}]_0$ = 100. After reaching 74 % of conversion (Table 4, entry 1), another load of MMA (50 eq.) was added to a total monomer equivalent of 150 (entry 2). After additional 24 h of reaction, SEC analysis revealed that chain extension did not occur at all, thus suggesting that chain cleavage did take place during the first polymerization step.

Table 4. Sequential addition of MMA in the presence of NHC^{tBu} in DMF at 25 °C.

entry	$[MMA]_0/[NHC^{tBu}]_0$	Time (h)	Conv.[a] (%)	$\overline{M_n}^{theo\ b}$ (g.mol^{-1})	$\overline{M_n}^{c}$ (g.mol^{-1})	M_p [c] (g.mol^{-1})	$\overline{M_w}^{c}$ (g.mol^{-1})	$Đ$ [c]
1	100 (run 1)	18	74	7,400	12,000	19,300	19,400	1.6
2	run1+ 50 eq MMA	+ 24	n.d.	n.d.	11,000	18,600	18,800	1.7

a. Conv.= % monomer conversion determined by ^{1}H NMR spectroscopy; b. Theoretical molar mass $\overline{M}_n^{theo} = M_{MMA} \times \frac{[MMA]}{[NHC]} \times conv.$; c Characterization of PMMA's by SEC in THF using PS standards for calibration

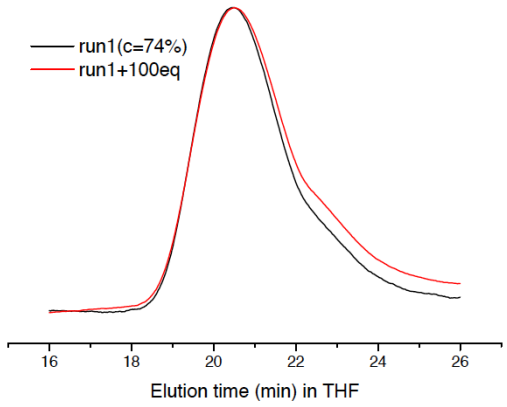

Figure 9. SEC traces of PMMA's obtained by sequential addition of MMA using NHC^{tBu}.

It is again worth mentioning that, in the course of this work, Chen *et al.* reported a detailed study of the polymerization of MMA mediated by NHC^{tBu} in DMF.[11] On a basis of both experimental and theoretical investigations, the authors suggested that the polymerization was a non-catalytic process (no NHC release), explaining the production of experimental molar masses much higher than those calculated from the $[MMA]_0/[NHC^{tBu}]_0$ ratio.

In particular, the authors suggested that a chain termination reaction occurred by a proton transfer from the $-CH_2-$ group (bound to the NHC^{tBu}) to the enolate C atom of the growing chain, generating a diamino ethylene (enamine) chain end (**13**, Scheme 9). This was

evidenced by matrix assited laser desorption/ionization time-of-flight (MALDI-ToF) mass spectrometry and by ^{1}H NMR analysis. According to DFT calculations, this mechanism proved to be both kinetically ($\Delta G^{\neq}$ = 8 kcal.mol^{-1}) and thermodynamically (ΔG = -13 kcal.mol^{-1}) favoured.

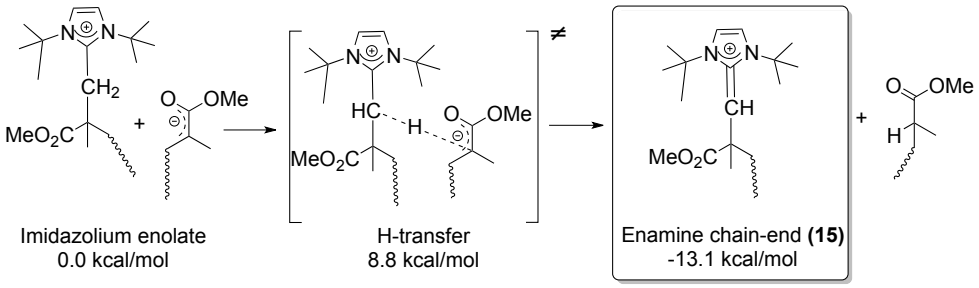

Scheme 9. Energetics for formation of the enamine chain-end during the polymerization of MMA directly induced by NHC$^{t\text{Bu}}$ in DMF, as proposed by Chen *et al.*[11]

In sharp contrast, in our hands, only linear α-methoxide PMMA's **16** were detected by MALDI-ToF (Figure 10). Accordingly, a series of peaks was observed at m/z = 32.04 + 100.05 n + 23, where 32.04 is the molar mass of the methoxide and H-end-groups, 100.05 the mass of one MMA unit, and 23 the molar mass of sodium ion used for ionization. In particular, the expected α-1,3-bis(*tert*-butyl)imidazolium PMMA's **13** or the enamine-ended PMMA's **15** were not observed, as depicted in the simulations of isotopic profiles of these structures (Figure 10). Origins of the differences observed between experimental observations by Chen *et al.* and in our case are still under question.

The population featuring α-methoxide chain-end could be explained by the occurrence of a side reaction resulting from 1,2-addition of the NHC onto the carbonyl group of the monomer (Scheme 10a). The acyl imidazolium methoxide **12** thus generated could either (1) initiate the polymerization of MMA by 1,4-conjugate addition of methoxide onto MMA (Scheme 10b) or (2) displace the imidazolium moiety by nucleophilic addition (with NHC release) onto an α-imidazolium PMMA chain (Scheme 10c). The first hypothesis involves the addition of a hard nucleophile to a soft carbon and it is probably high in energy. The second hypothesis is somewhat related to our previous work regarding the post-functionalization of α-imidazolium poly(ethylene oxide) (PEO) or α-imidazolium poly(propylene oxide) (PPO) chains by alcohol derivatives,[46,4758] it is thus more likely to occur.

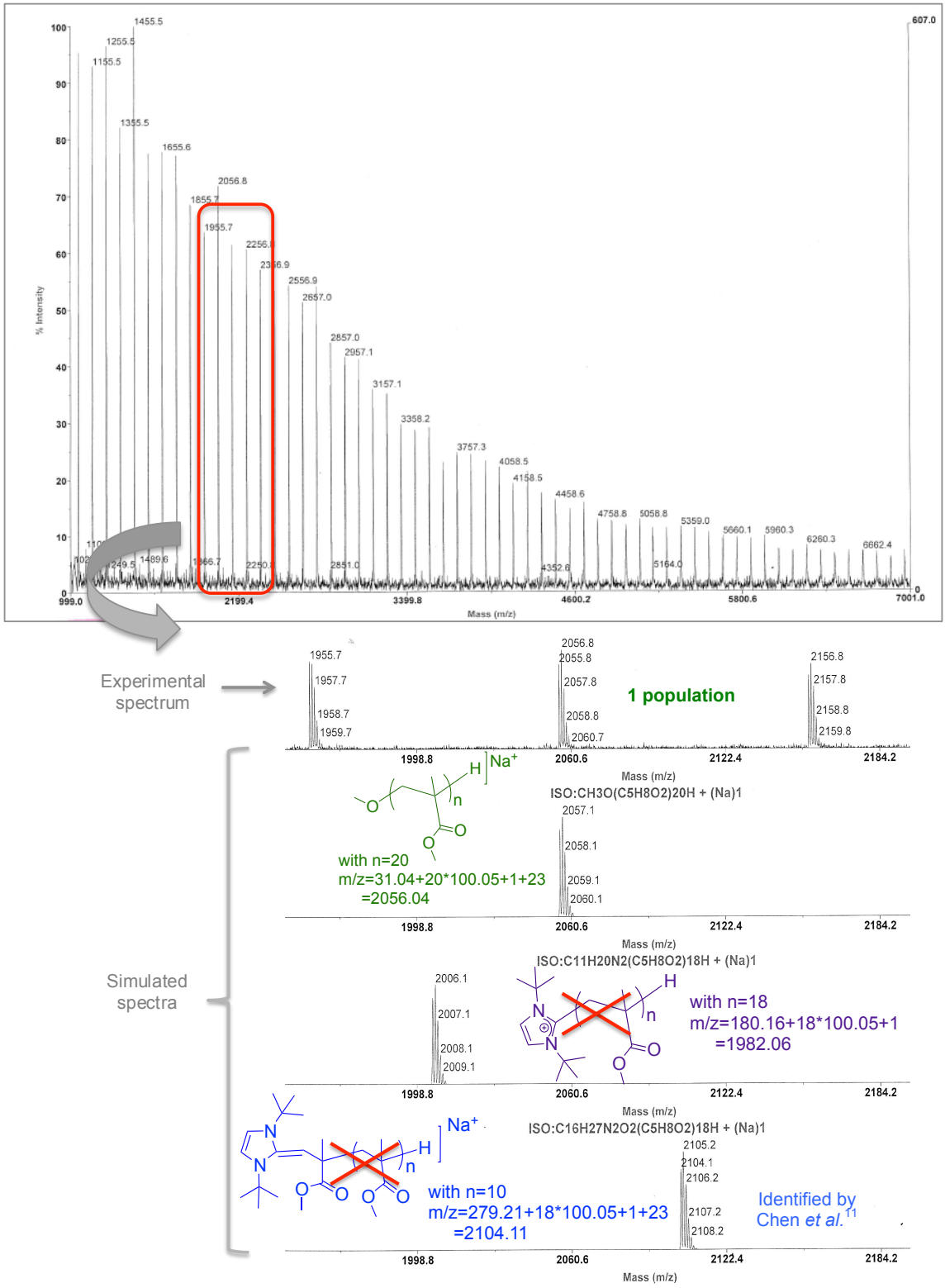

Figure 10. MALDI-ToF MS spectrum of PMMA's ($[MMA]_0/[NHC]_0$ = 10; Table 3, entry 2).

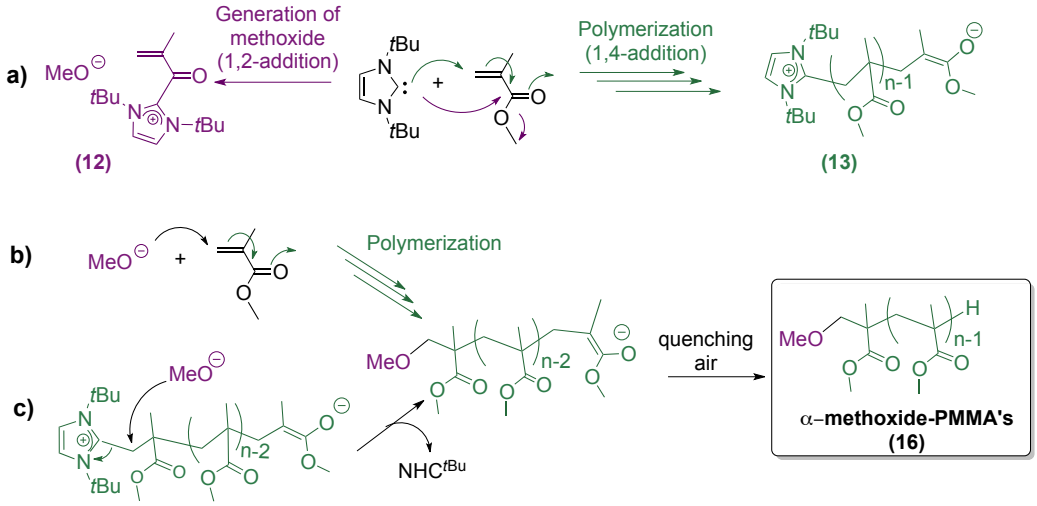

Scheme 10. Side reaction generating an α-methoxide-PMMA's.

Chain coupling reaction between the enolate form of a growing chain and a carbonyl group of another chain might also take place, leading to α-methoxide-PMMA's (Scheme 11). As already mentioned, this could explain the somewhat higher molar masses observed.

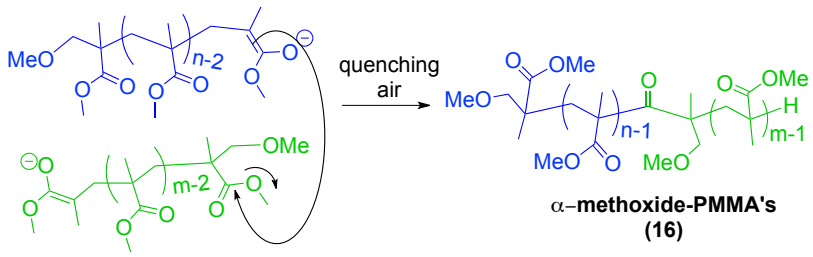

Scheme 11. Chain coupling forming α-methoxide-PMMA's.[44,45]

SEC traces of PMMA's obtained by direct initiation with NHC^{tBu} showed a UV absorption at λ = 305 nm, the characteristic maximum of absorbance of β-keto-ester chain-ends generated by backbiting (see Scheme 5). However, such a population was not detected by MALDI-ToF, probably because of its lower molar mass than the MALDI-ToF cut-off (m/z = 1,000 g.mol^{-1}).

Further analysis by ^{1}H NMR allowed us to determine the tacticity of these polymers based on integration of CH_3 groups signal (Figure 11).[48] The results were as follows: syndiotacticity (% of triad rr) = 51 %, heterotacticity (% of triad mr) = 40 % and isotacticity (% of triad mm) = 9 %. These values are typical tacticity of a PMMA grown by anionic polymerization in THF at r.t (in % rr/mr/mm = 56/39/5).[45,49,50] This similarity is presumably due the presence of "free" enolates during the NHC^{tBu}-initiated polymerization of MMA.

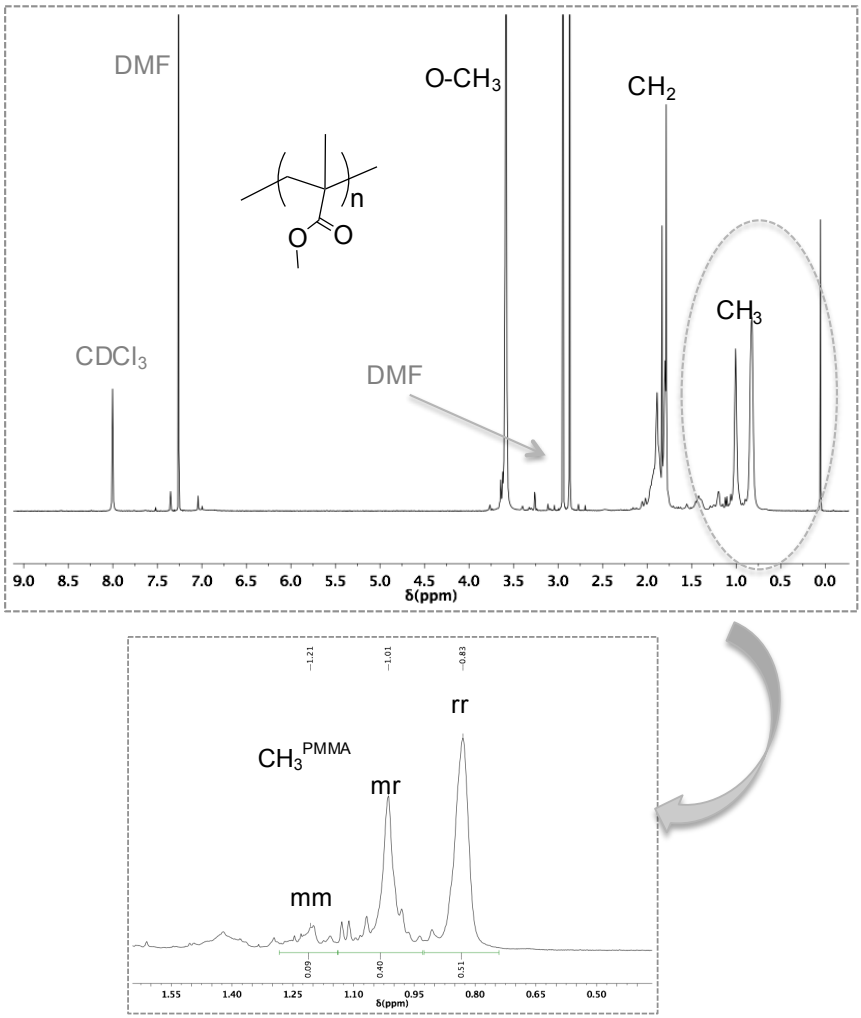

Figure 11. ^{1}H NMR spectrum (in $CDCl_3$) of NHC^{tBu}-obtained PMMA's.($[MMA]_0/[NHC]_0$ = 10 ; Table 3, entry 2).

All together, these results thus establish the ability of NHC^{tBu} to directly trigger the polymerization of MMA, in DMF at 25 °C, but with a rather low carbene efficiency. The use of DMF as solvent is crucial for these polymerizations to occur, likely owing to the favorable formation of the zwitterionic imidazolium enolates. However, these active species might favor the occurrence of side reactions, as those described in the more classic anionic polymerization (initiator deactivation, transfer to monomer and/or branching).[45,50]

As for the NHC^{iPr}, no polymerization of MMA took place. Instead, another reaction pathway has to be taken into account, as discussed in the following lines.

We attempted to isolate the intermediate species that could explain the different reactivities observed with the two carbenes (NHC^{iPr} and NHC^{tBu}) towards MMA.

1.2.2. Stoichiometric reactions between MMA and NHC^{iPr} or NHC^{tBu}

To gain insight into the mechanism of polymerization observed with NHC^{tBu} and the absence of polymerization with NHC^{iPr}, stoichiometric reactions between these NHCs and MMA were performed.

First, an equimolar reaction between NHC^{tBu} and MMA (1:1) was performed in a J-Young NMR tube, in dried DMF-d_7. Unfortunately, the imidazolium enolate species, resulting from the 1,4 conjugate addition of the NHC^{tBu} onto MMA was not observed by ^{1}H NMR. Instead, PMMA was generated, confirming our previous hypothesis that only a few amount of carbene reacts with MMA to form the putative imidazolium enolate, leading to molar masses higher than those expected.

The same reaction was performed in a less polar solvent such as THF-d_8, with the aim at decreasing the reactivity of the imidazolium enolate. However, no reaction occured between the two reagents at r.t. This is illustrated in the ^{1}H NMR (Figure S5 in supporting information, SI), showing that protons of NHC^{tBu} (δ_{CH3} = 1.53 ppm and δ_{vinyl} = 7.28 ppm) and those of MMA (δ_{CH3} = 1.89 ppm, δ_{OCH3} = 3.70 ppm and δ_{vinyl} = 5.68 and 6.07 ppm) were detected separately. Polymerization was observed after a few days at 50 °C in THF. Hence, direct addition of NHC^{tBu} onto MMA would only take place at r.t in a high polar solvent such as DMF, as already discussed above.

As already mentioned also, NHC^{iPr} did not trigger the polymerization of MMA in DMF, in sharp contrast to NHC^{tBu}. In order to investigate whether or not NHC^{iPr} does react with MMA, a model reaction utilizing stoichiometric amounts of MMA and NHC^{iPr} was implemented. In toluene, this 1:1 reaction gave a pale yellow precipitate in a very low yield, after a few minutes only. According to NMR and SEC analyses, this precipitate did not correspond to PMMA. No further reaction seemed to occur, even after adding more MMA onto the latter solid.

Recrystallization of this solid from dichloromethane-diethyl ether (*via* solvent diffusion) afforded single crystals that could be analyzed by X-ray diffraction. Unexpectedly, the product proved to be a zwitterionic imidazolium enolate cyclodimer adduct (**23** in Figure 12 and Scheme 31), formally resulting from the reaction between one molecule of NHC^{iPr} and two MMA molecules (= 1:2 adduct).

The crystal structure of **23** and selected bond lengths are provided in Figure 12.[51] Compound **23** was found to co-crystallize in the P^{-1} space group as a 64:36 mixture of *cis* and *trans* diastereoisomers (based on the relative orientation of C_2-Me and C'_2-Me groups), as can be seen from the two positions of the stereogenic C'_2H(Me) carbon in Figure 12. (see SI, for details). X-ray data show that the imidazolium backbone and the cyclopentenolate moieties are orthogonal (torsion angle N_1−C−C_1−C'_3 of 88.8°), thus leading to a formal zwitterionic structure where the negative charge is localized on the enolate moiety and the

positive charge on the cationic imidazolium part. Accordingly, the C_1-C'_3 bond is rather long (1.45 Å), in agreement with the absence of electronic delocalization between the two charged sites.

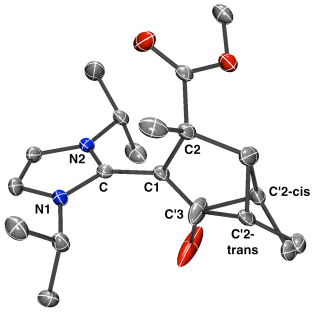

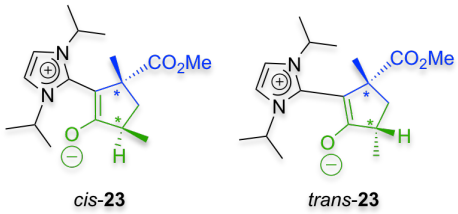

imidazolium enolate **23** (1 :2)

Figure 12. Solid-state structure of **23** with thermal ellipsoid plot at the 50% levels of probability. C'2-*cis* and C'2-*trans* represent the two diastereomeric positions of C'2 in **23**. Hydrogen atoms are omitted for clarity. The water molecule hydrogen-bound to the enolate is omitted for clarity. Selected bond lengths (Å) and angles (°): C−N1, 1.352(3); C−N2, 1.354(4); C−C1, 1.454(4); C1−C'3, 1.350(4); C−C1−C'3, 123.5(6); C'3−C1−C2, 113.0(7); C2−C1−C, 123.3(3); N1−C−C1−C'3, 88.7(5).

Moreover, both nitrogen atoms are planarized (Σ = 359.3° and 359.7°) and both C–N bond are short (1.35 Å in both cases). The C1 atom is in a planar environment (Σ = 360.0°) and the C1-C'3 bond (1.35 Å) is short, in agreement with the zwiterrionic imidazolium enolate structure of **23**.

Given that the stoichiometry of this cyclodimer is NHC^{iPr}:MMA (1:2), the reaction of 1 eq. of NHC^{iPr} with 2 eq. of MMA was next performed with in toluene. This afforded **23** (162 mg ; 51 %) as pale yellow crystals, after recrystallization. Combination of ^{1}H, ^{13}C and 2D NMR (HSQC and HMBC; Figure 13; see also SI for 2D experiments), analyses allowed us to further confirm the chemical structure of the cyclodimer adduct **23**. A 75:25 mixture of *cis* and *trans* diastereoisomers, denoted as **A** and **B** was determined. For simplicity, only protons of the major isomer (**A**) are next described.

Signals corresponding to the imidazolium moiety could be identified at 1.41 ppm (CH_3^{iPr}), 4.61 ppm (CH^{iPr}) and 7.79 ppm (CH=CH). Observation of two methyl signals at 1.07 ppm (doublet, $^{3}J_{HH}$ = 4.0 Hz) and 1.39 ppm (singlet overlapping with CH_3^{iPr}), corresponding to the CH_3^{MMA}, corroborated with the presence of two incorporated MMA monomer units. The CH_2 of **23** appeared as diastereotopic protons at 1.98 (doublets dd, $^{3}J_{HH}$ = 8.0 Hz, $^{3}J_{HH}$ = 4.0 Hz) and 2.15 ppm (dd, $^{3}J_{HH}$ = 8.0 Hz, $^{3}J_{HH}$ = 4.0 Hz), while the methine signal was detected at 2.32 ppm (multiplet). Only one methoxy group was observed at 3.56 ppm, suggesting that one equivalent of MeOH was lost during the reaction.

In the ^{13}C NMR spectrum, the two quaternary carbons at 73.6 and 186.0 ppm could be attributed to the enolate moiety and the one at 149.5 ppm to the imidazolium carbon (Figure 14).

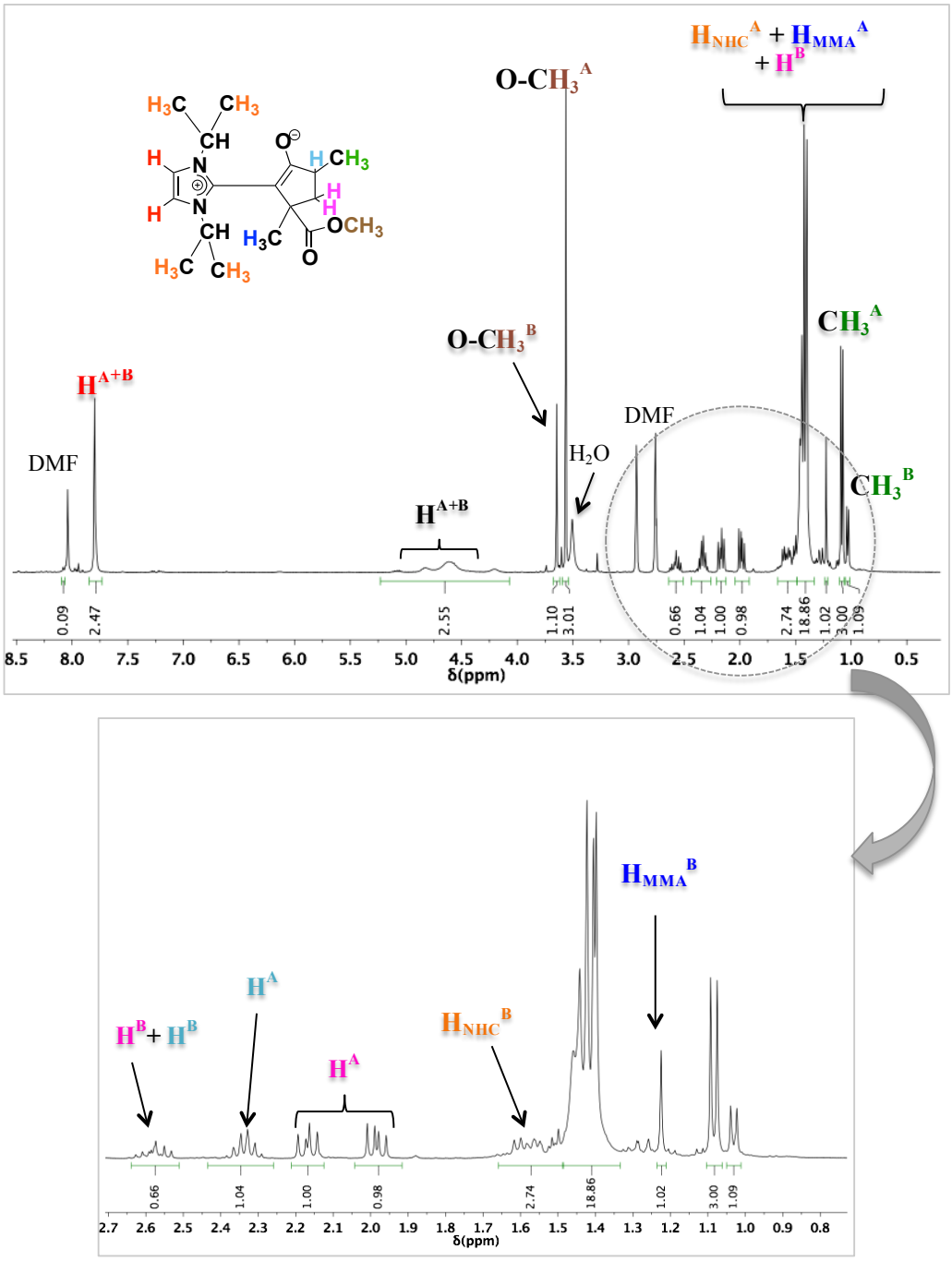

Figure 13. ^{1}H NMR spectrum of the mixture of *cis* and *trans* diasteroisomers of the cyclodimer adduct **23** (forms **A** and **B**) in DMF-d_7.

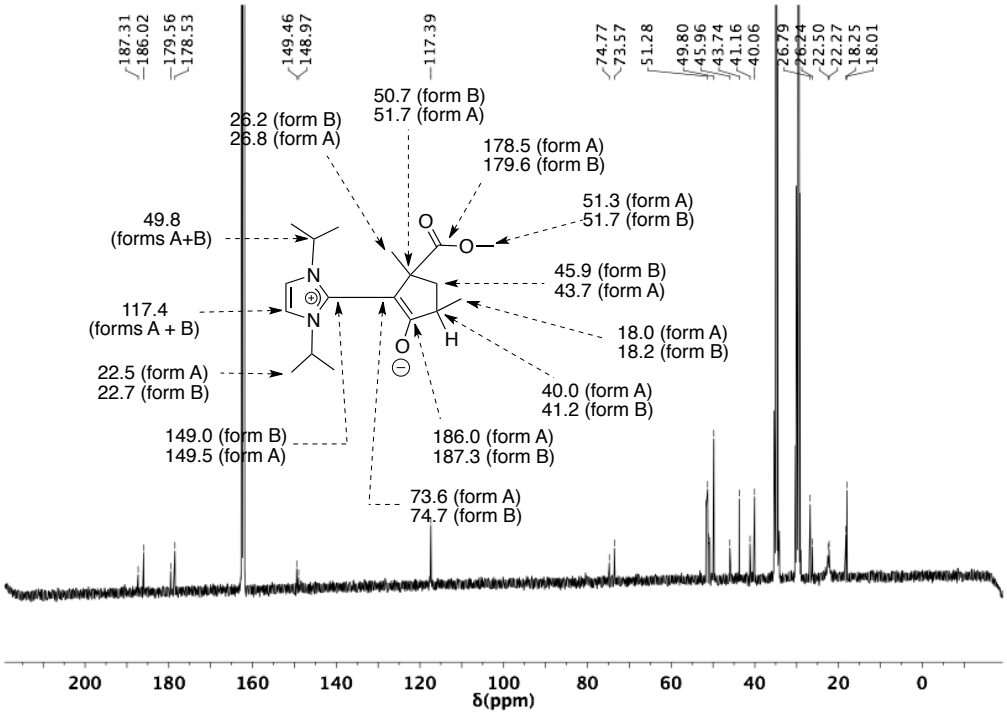

Figure 14. ^{13}C NMR spectrum of the mixture of *cis* and *trans* diasteroisomers of the cyclodimer adduct **23** (forms **A** and **B**) in DMF-d_7.

Inter-conversion between the *cis* and the *trans* diastereoisomer was noted, probably due to the epimerization of the C'$_2$(H)Me stereogenic center 5 , in α- position of the C=O (Scheme 12). Indeed, the imidazolium-enolate **23** is in equilibrium with the diamino ethylene keto form **X** and the diamino ethylene enolate **Y**. At this point, the sterogenic center C_5 is transformed to a Csp^2 prochiral center. Because reprotonation of **Y** can either occur from the top or bottom face, epimerization of C_5 is observed. Unfortunately, the relative configurations of the major **A** and minor **B** compounds observed by ^1H NMR could not be attributed (Figure 13) to either the *cis* or to the trans diastereoisomer.

A proposition of a reaction mechanism leading to **23**, and involving one NHC^{iPr} and two MMA molecules is depicted in Scheme 13. The presence of the imidazolium backbone suggests an initial 1,4-nucleophilic (conjugate) addition of NHC^{iPr} onto MMA, generating the zwitterionic enolate **18**. The presence of two MMA molecules, as attested by ^1H NMR, is in accordance with a second nucleophilic attack of zwitterion **18** onto a second MMA molecule, forming a novel zwitterionic intermediate **18** (Scheme 13). Upon H transfer, **20** would undergo a ring closure to afford **21**. Finally, the release of one equivalent of methanol would yield to the imidazolium cyclopentenolate **23**, that was experimentally isolated.

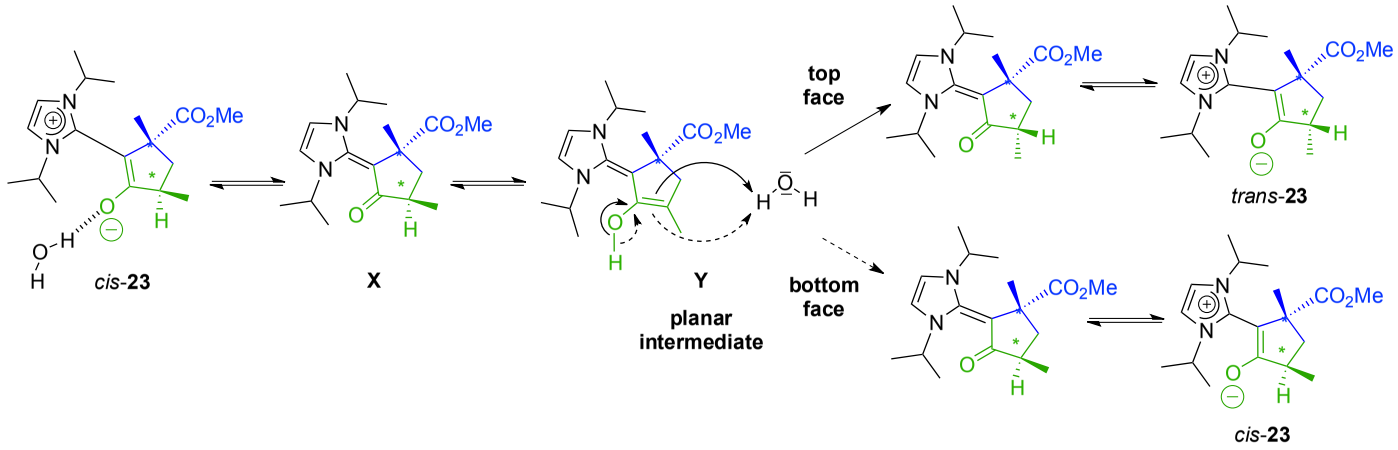

Scheme 12. *cis*-**23**/*trans* **23** interconversion (epimerization) mechanism of imidazolium-enolate **23**.

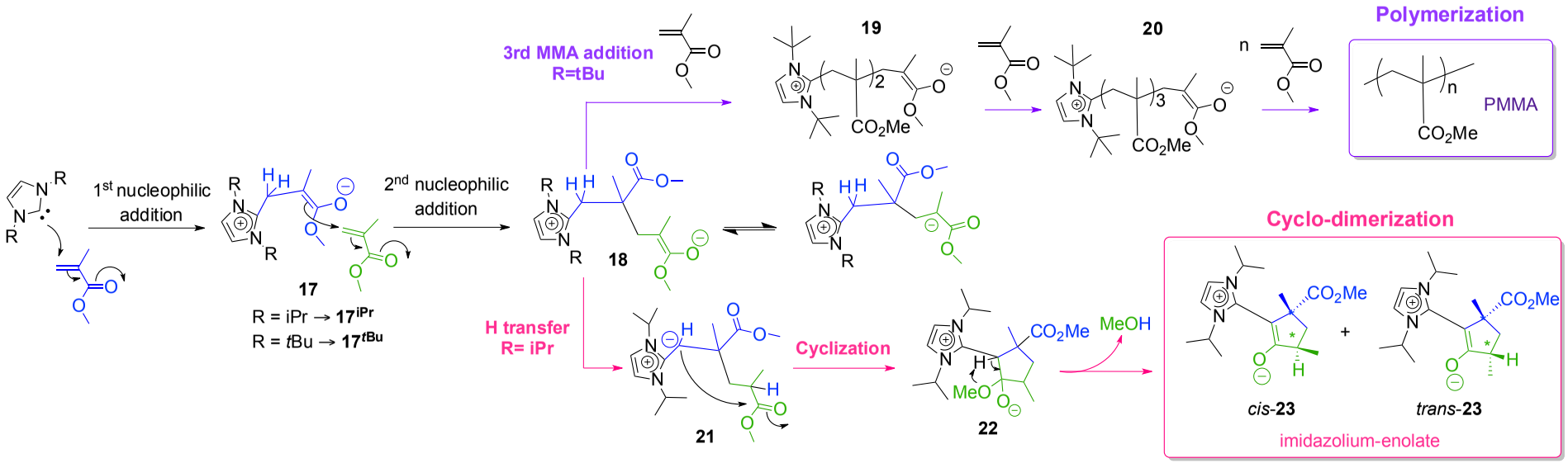

Scheme 13. Proposed mechanism for the cyclodimerization and the polymerization reaction employing NHC^{iPr} or NHC^{tBu} and MMA.

These experimental results prompted us to perform computational studies to gain a better insight, not only for the cyclodimerization of MMA triggered by NHC^{iPr}, but also for the ability of NHC^{tBu} to induce the polymerization of MMA. It is worth emphasizing that such bicyclic cyclodimer was neither observed in the case of $NHC^{tBu,}$, nor with any other NHC such as NHC^{Mes} and TPT, (paths B and C in Figure 3, respectively). Hence the subtle changes in the structure of the carbene dramatically impacts the reaction outcomes with MMA as substrate.

2. Reactivity of NHC with MMA: density functional theory (DFT) calculations

These calculations were performed at the Institut Pluridisciplinaire de Recherche sur l'Environnement et les Matériaux (IPREM), at the Université de Pau & des Pays de l'Adour (UPPA) by Damien Bourichon, completing his PhD under the supervision of Dr. Karinne Miqueu and Dr. Jean-Marc Sotiropoulos.

DFT calculations were performed at the M06-2X/6-31G** level of theory (see SI for computational details) on the **23RS** enantiomer (where R and S are the configuration at C2 and C'2 respectively). Moreover, for sake of comparison, the absolute configurations of these two stereocenters were kept the same along both the cyclodimerization and polymerization pathways. For each NHC, both polymerization and cyclodimerization reactions were investigated computationally. For clarity and space limitation, details about transition states (TS) geometries have been provided in the supporting information (SI).

As already mentioned, both reactions likely proceed by the initial 1,4-addition of the NHC on a first molecule of MMA (initiation step), leading to the zwitterionic imidazolium enolate **17** (Scheme 13). Then, **17** reacts with a second molecule of MMA, yielding the new imidazolium enolate **18** (propagation step).

At this point, the polymerization proceeds by addition of a third molecule of MMA forming the zwitterion **19**, and addition of n monomers leads to PMMA. For sake of simplicity, only the addition of three molecules of MMA is considered here, in order to understand the effect of the NHC on the polymerization (compound $\mathbf{19^R}$) *versus* the cyclodimerization (compound $\mathbf{23^R}$) pathways (*vide infra*). From an energetic point of view, the imidazolium enolate **19** is thus considered as a model of the polymer growing chain. On the other hand, imidazolium enolate **18** may undergo a proton transfer, followed by ring closure and loss of MeOH, affording the cyclized imidazolium enolate **23** (Scheme 13).

The initiation and propagation steps are first described in the following sections, since they are common to both polymerization and cyclodimerization mechanisms.

2.1. First addition of MMA (initiation step)

As illustrated in Figure 15, this reaction was predicted to be more favourable for NHC^{iPr}, not only thermodynamically (0.7 *vs*. 14.5 kcal.mol^{-1} for **17^{iPr}** and **17^{tBu}** respectively), but also kinetically (activation barrier 17.3 and 25.6 kcal.mol^{-1} for NHC^{iPr} and NHC^{tBu}, respectively), in agreement with a greater steric hindrance for NHC^{tBu}. In addition, the geometry of both TS revealed a concerted but strongly asynchronous initiation step for both NHCs. Here again, for clarity and space limitation, details about TS geometries have been provided in the supporting information (see Figures S7 and S9).

2.2. Second addition of MMA (propagation step)

Calculations show that, in both cases, the second addition of MMA is kinetically more favorable by 11 to 17 kcal.mol^{-1} for both NHC^{iPr} and NHC^{tBu} than the first addition. Corresponding barriers are close in energy: 6.7 and 8.3 kcal.mol^{-1} for the transformation **17^{iPr}→18^{iPr}** and **17^{tBu}→18^{tBu}**, respectively (Figure 15). This is due to a decrease of the steric hindrance in the corresponding TS**17-18**, as compared to TS**NHC-17** in the initiation step. Moreover, this second addition reaction leads to a greater stabilization of zwitterions **18^{iPr}** and **18^{tBu}** (-3.2 and -0.2 kcal.mol^{-1}, respectively) than those of generated in the initiation step. It also proceeds by a concerted but asynchronous mechanism (see Figures S10 and S12).

At this point, polymerization of MMA may proceed by addition of a third molecule of MMA, while the cyclodimerization pathway is initiated by a $H_{1\rightarrow 2'}$ proton transfer from C_1 to C_2'.

2.3. Third addition of MMA

Addition of a third MMA molecule onto zwitterions **18^{iPr}** and **18^{tBu}** was next investigated. In order to compare accurately the effect of the substituents (iPr *vs.* *t*Bu), similar structures have been used for both compounds. Both reactions **18→19** were predicted to be endergonic (ΔG = 19.5 and 18.6 kcal.mol^{-1} for **19^{iPr}** and **19^{tBu}**, respectively), and activation barriers proved close to those determined for the initiation step (20.4 and 19.5 kcal.mol^{-1} from **18^{iPr}** and **18^{tBu}**, respectively). This indicates that addition of a third molecule of MMA is strongly disfavoured thermodynamically for both **18^{iPr}** and **18^{tBu}** (see Figure 15). Compared to the initiation step, the increase of the activation barrier and the destabilization of the final compound **19** can be explained by an important steric hindrance between the two CO_2Me moieties and CH_3.

However, from a kinetic point of view, the reactions **18→19** were comparable to the first step of the polymerization (**NHC→17)** and related activation barriers (~ 21 kcal.mol^{-1}) do not appear to be influenced by substituents on the NHC (iPr *vs*. *t*Bu).

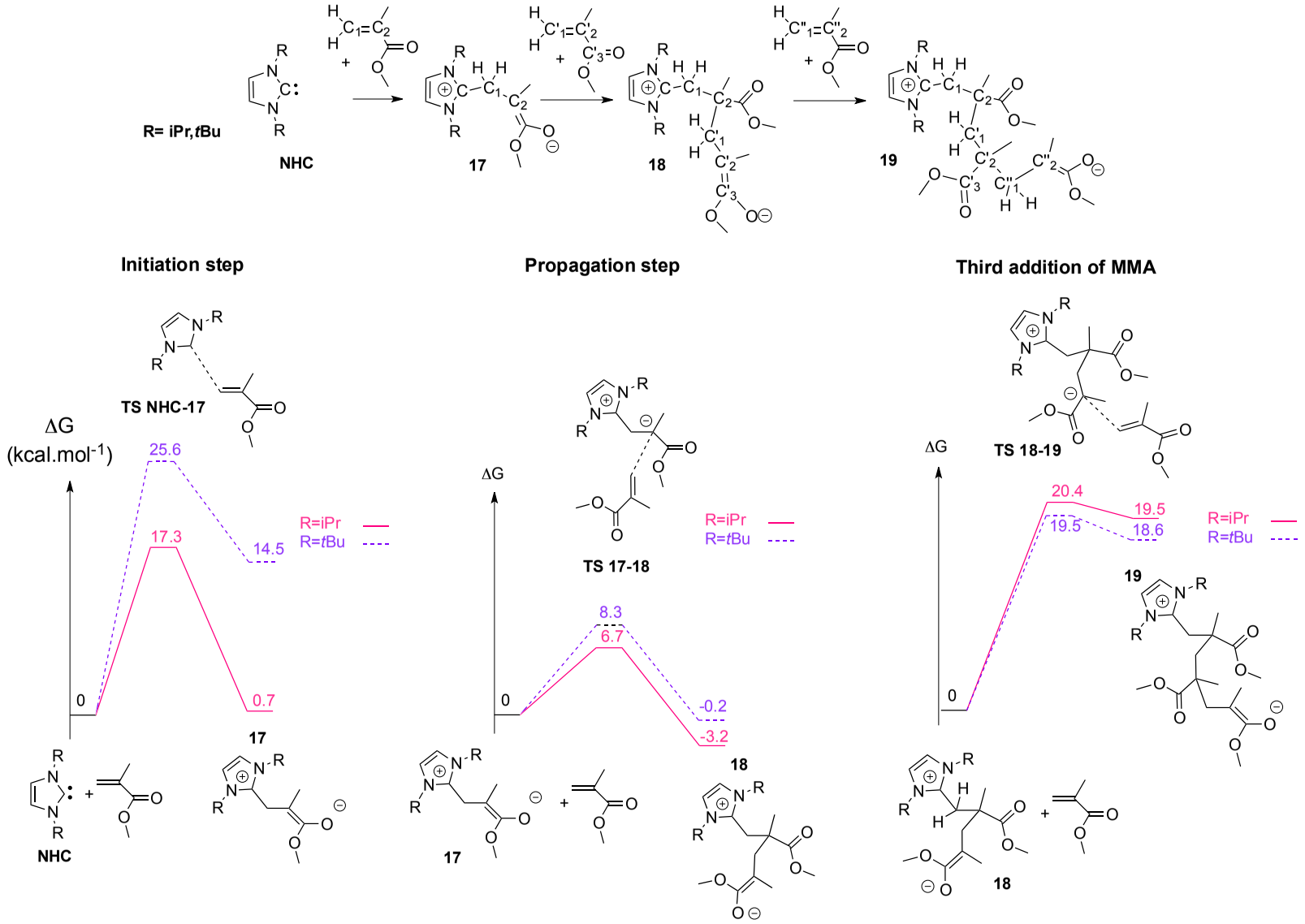

Figure 15. Energy profile (ΔG in kcal.mol^{-1}) computed at the M06-2X/ 6-31G** level of theory in gas phase for the reactions **1**+MMA → [NHC-MMA]**2**, **2** + MMA → [NHC-(MMA)$_2$] **3** and **3** + MMA → [NHC-(MMA)$_3$] **4**.

This is in agreement with the similar energy of the highest occupied molecular orbital HOMO ($\pi_{C'2=C'3}$; strong weight on C'_2 atom) in **18^{iPr}** and **18^{tBu}** (-4.3 eV and -4.2 eV, respectively), that are involved in the nucleophilic addition of the NHC onto MMA, the lowest unoccupied molecular orbital LUMO being the $\pi^*_{C''1=C''2}$ orbital (see Figure S15).

Analysis of the geometry of the TS revealed that the third addition of MMA was also a concerted but asynchronous process, as observed for the first and second addition of MMA. Details about TS geometries are provided in the SI (see Figures S7 and S9).

Overal, these calculations evidenced that the three additions of MMA are kinetically compatible with a low temperature process, but formation of the zwitterion enolate **19** is not thermodynamically favoured. Further calculations regarding subsequent additions of MMA and/or on the energetic profiles of the different diastereoisomers formed during the polymerization pathway might help to identify discriminating steps for this mechanism.

Nevertheless, the fourth addition of MMA **19→20** (Figure S14) was predicted to be much less endergonic than in the case of the third addition (1.7 and 8.0 kcal.mol^{-1} for NHC^{iPr} and NHC^{tBu}), while activation barriers remained low (8.1 and 13.3 kcal.mol^{-1}for NHC^{iPr} and NHC^{tBu}, respectively). This might suggest that addition of n molecules of MMA (= polymerization pathway) would be thermodynamically favoured.

2.4. Cyclodimerization reaction

2.4.1. Cyclodimerization: proton transfer

After addition of two molecules of MMA, the imidazolium enolate **18** might undergo a $H_{1\rightarrow 2'}$ proton transfer, generating the neutral compound **21**. Both reactions **18^{iPr}→21^{iPr}** and **18^{tBu}→21^{tBu}** were predicted to be exergonic (by 6.3 and 13.6 kcal.mol^{-1}, respectively) with rather low energetic barriers (11.5 and 12.9 kcal.mol^{-1} for NHC^{iPr} and NHC^{tBu}, respectively). Analysis of the geometry of TS^{iPr}**18-21** and TS^{tBu}**18-21** suggests a concerted and quasi-synchronous mechanism for the $H_{1\rightarrow 2'}$ proton transfer (see Figures S11 and S13).

2.4.2. Cyclodimerization: cyclization

As depicted in Figure 16, the cyclization pathway involves the intramolecular addition of the nucleophilic C_1 atom of diaminoalkene **21** onto the methyl ester moiety. This intramolecular cyclization was predicted to be endergonic with both NHCs, by 5 and 19.6 kcal.mol^{-1}for **21^{iPr}→22^{iPr}** and **21^{tBu}→22^{tBu}**. A 14.4 kcal.mol^{-1} difference was computed between the energetic barriers of these two reactions (6.8 and 20.8 kcal.mol^{-1} for **21^{iPr} →22^{iPr}** and **21^{tBu}→22^{tBu}**, respectively), indicating that the cyclization process is strongly disfavoured for **21^{tBu}**. The higher energetic barrier $\Delta G^{\#}_{\mathbf{21\rightarrow 22}}$ observed for **21^{tBu}** may be correlated to the greater steric hindrance resulting from the larger *t*Bu groups (relative to *i*Pr) and the shorter

C_1-C'_3 bond length observed in TS^{tBu}**21-22** ($dC_1C'_3$ = 1.922 Å *vs.* 2.005 Å in TS^{iPr}**21-22**). It might also be correlated to the energies of the molecular orbitals (MO) involved in the cyclization process, where a higher HOMO-LUMO (or HOMO-LUMO+1 in the *t*Bu derivative) gap in **21**^{tBu} (7.5 eV) than that in **21**^{iPr} (7.1 eV) was observed. The HOMO presents a strong $\pi_{C=C1}$ character, with a strong weight at C1 and the LUMO (or LUMO+1) presents a strong $\pi*_{C=O}$ character with a strong weight at C (see Figure S15).

These data indicate that, depending on both the steric hindrance and electronic effects of the substituents on the nitrogen atoms of the NHC, the cyclization process is the discriminating step for the cyclodimerization mechanism. Analysis of the geometry of TS^{iPr}**21-22** and TS^{tBu}**21-22** suggests a concerted and asynchronous mechanism for the cyclization (see Figures S11 and S13).

2.4.3. Cyclodimerization: loss of MeOH

The loss of MeOH from the zwitterionic imidazolium hemi-acetal **22** giving rise to the experimentally observed cyclodimer **23** was next investigated. As shown in Figure 16, both reactions **22**^{iPr}→**23**^{iPr} and **22**^{tBu}→**23**^{tBu} were calculated to be highly exergonic (by 18-19 kcal.mol^{-1} for both reactions). A TS could be located in both cases on the potential energy surface. TS^{iPr}**22-23** and TS^{tBu}**22-23** lie at 20.1 and 14.3 kcal.mol^{-1} above **22**^{iPr} and **22**^{tBu}, respectively, and 25.1 and 33.9 kcal.mol^{-1} above the most stable intermediates **5**^{iPr} and **5**^{tBu}, respectively, representing the highest energetic barriers calculated for the overall cyclization process. In other words, the loss of MeOH proved to be the kinetically limiting step, regardless of the nature of the substituent on the NHC. However, this step is more disfavored for NHC^{tBu} (8.8 kcal.mol^{-1} higher than for NHC^{iPr}). This difference mainly arises from the electronic stabilization of **21**^{tBu} *vs.* **21**^{iPr}. The geometries of TS**22-23** indicate that the loss of MeOH is a concerted but strongly asynchronous mechanism, where a methanolate equivalent formally deprotonates the acidic C_1-H bond (see Figures S11 and S13).

Calculations also corroborate structural data about the structure of the cyclodimer **23** that was isolated experimentally. In particular, imidazolium and cyclopentanenolate moieties appear to be twisted by 89.5° from planarity in **23**^{iPr}, in agreement with RX data (88.8°, see Figure 12). Moreover, the C−C_1 (1.45 Å) and C_1−C'_3 (1.35 Å) bond distances measured experimentally are well reproduced by the calculations (1.44 and 1.40 Å for the C−C_1 and C_1−C'_3 bonds respectively), which theoretically supports the zwitterionic structure of **23**^{iPr}.

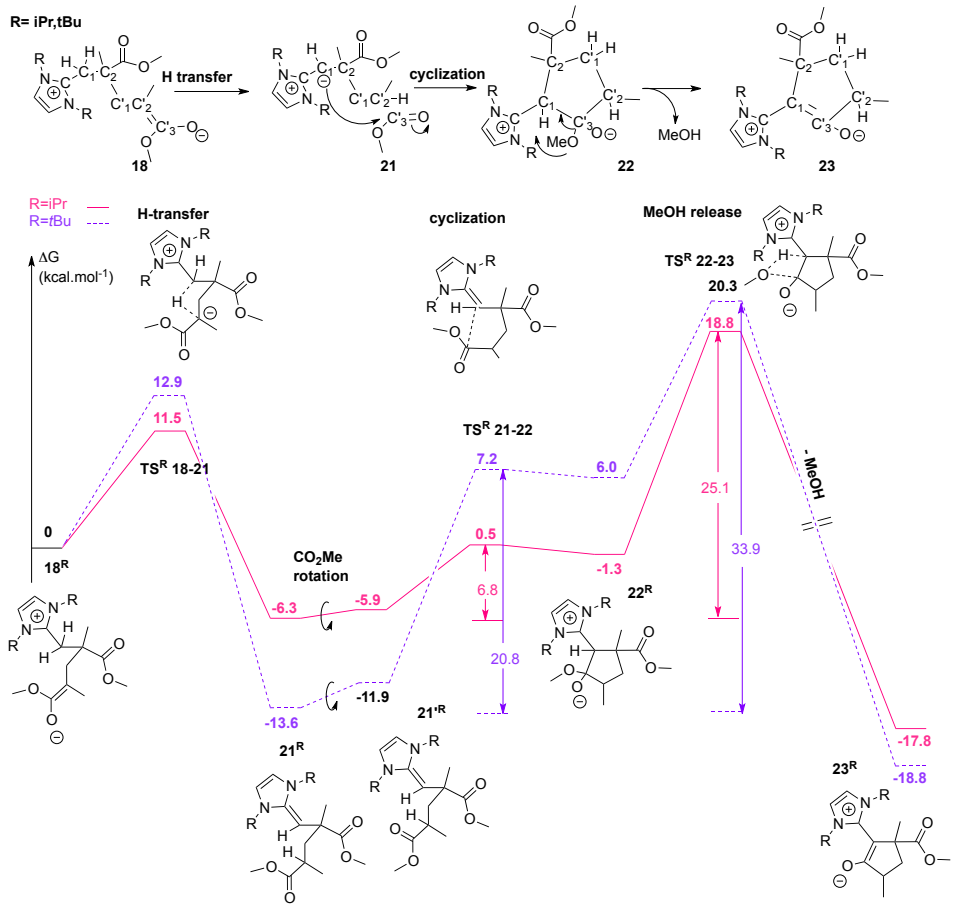

Figure 16. Energy profile (ΔG in kcal.mol^{-1}) computed at the M06-2X / 6-31G** level of theory in gas phase for the mechanism of cyclodimerization induced by NHC^{iPr} and NHC^{tBu}.

Overall, the cyclodimerization pathway was predicted to be exergonic for both NHC^{iPr} and NHC^{tBu}. However, the higher energetic barriers calculated in the case of NHC^{tBu}, both for the cyclization ($\Delta\Delta G^{\#}_{21\text{-}22}$ = 14.4 kcal.mol^{-1}) and the loss of MeOH ($\Delta\Delta G^{\#}_{22\text{-}23}$ = .8 kcal.mol^{-1}), explain that cyclodimerization is kinetically prevented, in agreement with experimental findings.

All DFT calculations discussed above helped us to understand the mechanism of both cyclodimerization and polymerization pathways occurring with NHC^{iPr} and NHC^{tBu}, respectively. However, these calculations did not explain the reason why, from a structural viewpoint, such a difference between two carbenes of very similar structure in reactivity occurred in the course of the reaction process. Interactions between the carbonic center and the enolate moiety could exist in NHC-MMA_2 adduct (**18,** Scheme 13), prior to further reaction, either by the cyclodimerization or the polymerization pathway. Such interactions were investigated by molecular dynamics simulation (MD).

In the case of NHC^{iPr}, the possible interaction between the proton –CH- of the iPr group and the oxygen atom of the enolate could result in a folded conformation, thus favoring the

cyclization pathway leading to **23**. In contrast, as for NHC^{tBu}, there might have no specific interaction involving the enolate and the *t*Bu groups. Thus, the corresponding zwitterion NHC^{tBu}-MMA$_2$ **18^{tBu}** might adopt a more stretched conformation, preventing cyclization, and the preference for the polymerization pathway with this particular carbene.

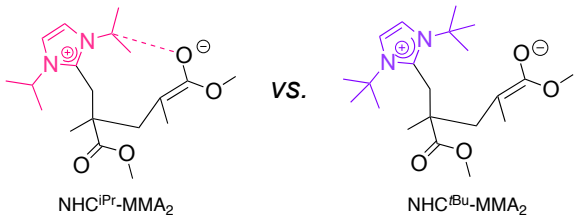

Scheme 14. Interactions between the imidazolium and the enolate moieties in the zwitterion NHC-MMA$_2$ determined by molecular dynamics simulation (MD).

In conclusion, and as summarized in Scheme 15, the direct reaction of NHC^{iPr} or NHC^{tBu} with MA or MMA as model substrates showed major differences. Both NHCs could initiate the polymerization of MA in DMF at 25 °C, giving rise to PMA's whose molar masses increased with the $[MA]_0/[NHC]_0$ ratio. Reaction with MMA showed a very selective behavior: while NHC^{tBu} directly polymerized MMA, NHC^{iPr} led to an unprecedented stable zwitterionic cyclodimer. Experimental results were supported by density functional theory (DFT) calculations and molecular dynamics simulations (MD), evidencing a remarkable selectivity of NHCs towards MMA. Both experimental and theoretical results thus allowed us to propose a reaction mechanism for the cyclodimer formation.

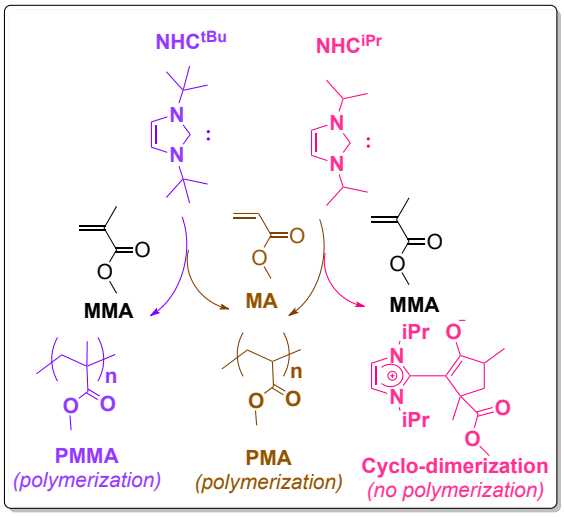

Scheme 15. Reactivities of NHC^{iPr} and NHC^{tBu} towards MA and MMA in DMF at 25 °C.

The next section describes new experimental investigations regarding the reaction of some to other acrylic and methacrylic derivatives with the same NHCs (NHC^{iPr} or NHC^{tBu}). This is expected to provide a general view about the polymerization activity of NHC^{iPr} and NHC^{tBu} towards various acrylates and methacrylates.

3. Direct polymerization of miscellaneous alkyl (meth)acrylates induced by NHCs

Let us first remind that both NHC^{iPr} and NHC^{tBu} have been succesfully employed as organocatalysts, in presence of methoxy-trimethylsilyloxy-dimethylketene acetal (MTS) as initiator for the group transfer polymerization (GTP) of various (meth)acrylates.[7,52-54] In light of the differences observed between NHC^{iPr} and NHC^{tBu} as direct initiators for the zwitterionic polymerization (ZP) of MA and MMA (Scheme 15), we investigated the activity of these two NHCs towards miscellaneous monomers, including not only acrylic monomers, namely, *tert*-butyl acrylate (^{t}BuA) and *N*,*N*-(dimethylamino)ethyl acrylate (DMAEA), but also methacrylics such as *tert*-butyl methacrylate (^{t}BuMA), *N*,*N*-(dimethylamino)ethyl methacrylate (DMAEMA) and benzyl methacrylate (BnMA). We indeed reasoned that direct addition of the NHC onto (meth)acrylic monomers might be dramatically influenced by both the polarity and the steric hindrance of the substrate. Scheme 16 displays the selected monomers.

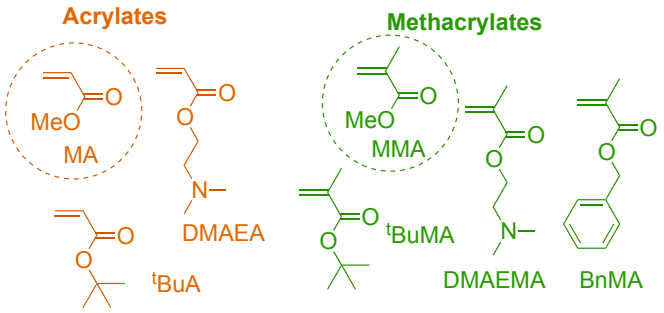

Scheme 16. Others monomers investigated in this study in addition to MA and MMA.

3.1. Case of *tert*-butyl acrylate (^{t}BuA) and *tert*-butyl methacrylate (^{t}BuMA)

Polymerizations of these two monomers were performed in DMF at 25 °C, using either NHC^{iPr} or NHC^{tBu} as initiators, under the same conditions previously described for MA and MMA. In particular, experiments were carried out using various monomer concentrations, with $[NHC]_0$ = 10 mM for all reactions. Table 5 summarizes the different experiments and the molecular characteristics of the as-obtained polymers.

Table 5. NHC-induced polymerizations of ^{t}BuA and ^{t}BuMA in DMF at 25 °C.

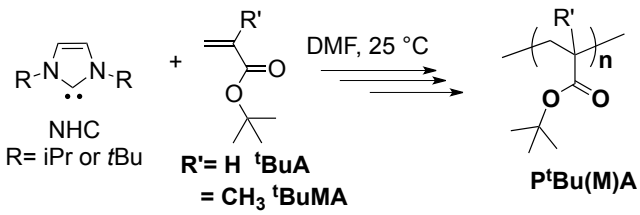

entry	NHC	M	$[M]_0/[NHC]_0$	Time (h)	Conv.[a] (%)	$\overline{M_n}^{theo}$ [b] (g.mol^{-1})	$\overline{M_n}$ [c] (g.mol^{-1})	M_p [c] (g.mol^{-1})	$\overline{M_w}$ [c] (g.mol^{-1})	$Đ$ [c]
1	NHC^{iPr}	^{t}BuA	25	3	100	3,200	2,400	3,300	3,300	1.4
2	NHC^{iPr}	^{t}BuA	50	3	99	6,300	3,600	4,500	5,100	1.4
3	NHC^{iPr}	^{t}BuA	100	3	97	12,400	4,600	5,400	6,400	1.4
4	NHC^{iPr}	^{t}BuA	200	3	95	24,300	12,500	17,200	22,500	1.8
5	NHC^{tBu}	^{t}BuA	25	3	77	2,500	1,800	2,700	2,500	1.3
6	NHC^{tBu}	^{t}BuA	50	5	71	4,500	3,400	4,600	4,500	1.3
7	NHC^{tBu}	^{t}BuA	100	3	90	11,700	12,000	17,700	16,200	1.3
8	NHC^{iPr}	^{t}BuMA	100	72	0	-	-	-	-	-
9	NHC^{tBu}	^{t}BuMA	100	12 (72)	20	2,850	300,000	473,300	358,000	1.5

a. Conv.= % monomer conversion determined by ^{1}H NMR spectroscopy; b. Theoretical molar mass $\overline{M}_n^{theo} = M_M \times \frac{[M]}{[NHC]} \times conv.$; c. Characterization of polymers by SEC in THF using PS for calibration.

Use of NHC^{iPr} as a chain starter allowed producing poly(*tert* butyl acrylate)s (P^{t}BuA's) with apparent molar masses, $\overline{M_n}$, in the range 2,400-12,500 g.mol-1 and a dispersity $Đ$ in the range 1.4-1.8 (Table 5, entries 1-4). In the same manner, NHC^{tBu}-initiated polymerizations of ^{t}BuA ledto P^{t}BuA's of $\overline{M_n}$, ranging from 1,800 to 12,000 g.mol^{-1}, with a dispersity of $Đ$ = 1.4-1.8 (entries 5-7). Hence, both NHCs were found to initiate the polymerization of this monomer, with molar masses increasing with the initial $[^t BuA]_0/[NHC]_0$ ratio as illustrated in Figure 18.

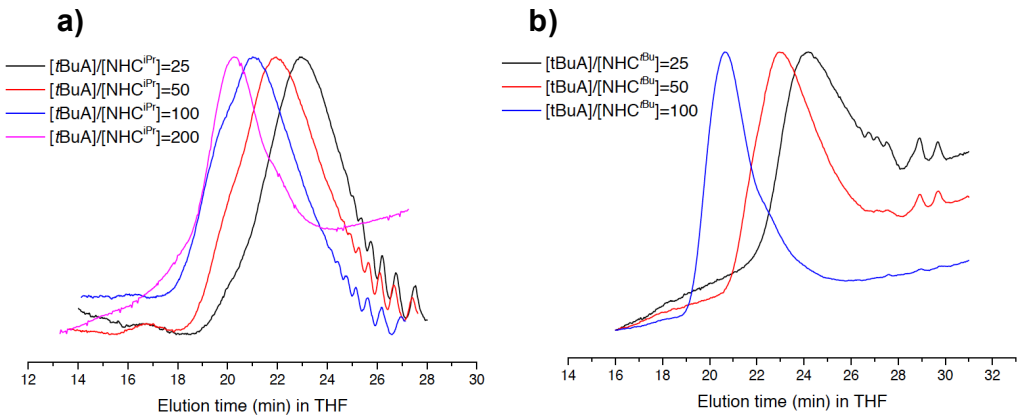

Figure 17. SEC-RI traces of P^{t}BuA's obtained with: a) NHC^{iPr}; b) NHC^{tBu} in DMF at 25 °C (Table 5, entries 1-7).

Reactions with NHC^{tBu} were slower than those with NHC^{iPr} (*e.g.* after 5 h of reaction for a degree of polymerization DP = 25, quantitative conversion for NHC^{iPr} *vs.* 77 % for NHC^{tBu}, entries 1 and 5), but provided molar masses closer to theoretical values compared to those obtained from NHC^{iPr}. These differences might be attributed to the steric hindrance of NHC^{tBu}, that reduces its nucleophilicity compared to that of NHC^{iPr}. Both NHCs, nonetheless,

led to P^{t}BuA's whose SEC traces exhibited a UV absorption at λ = 260 nm, suggesting the occurrence of back-biting reactions.

Like for MMA, NHC^{iPr} was not able to induce the polymerization of ^{t}BuMA, even after 72 h of reaction (Table 5, entry 8). With this other methacrylic monomer, one can hypothesize that formation of a similar cyclodimer imidazolium enolate adduct, NHC^{iPr}-^{t}BuMA$_2$, to that identified with MMA and this carbene. Nevertheless, detailed characterizations by NMR or mass spectrometry are needed to confirm this hypothesis.

In contrast, the polymerization of ^{t}BuMA by NHC^{tBu} reached only 20 % of monomer conversion after 72h of reaction (entry 9). This lower polymerization activity, compared to that of MMA with the same carbene, might be due to the inductive effect (+I) of *t*-butyl group that decreased the reactivity of the double bond of the monomer. Additionally, the steric hindrance of *t*-butyl group might also decrease the reactivity of propagating enolates. Such observations were already reported for the more classical anionic polymerization of ^{t}BuMA that proceeded in a controlled way.[55] In our case, NHC^{tBu} might not be nucleophilic enough to efficiently induce the direct polymerization of ^{t}BuMA.

3.2. Case of benzyl methacrylate (BnMA)

The same trends were observed with benzyl methacrylate (BnMA) in the sense that only NHC^{tBu} initiated the polymerization of this monomer in DMF at 25 °C, while NHC^{iPr} likely induced the same cyclodimerization reaction described above. Again the latter point would need further experimental evidences. The results obtained with this monomer are summarized in Table 6.

Table 6. NHC-induced polymerizations of BnMA in DMF at 25 °C.

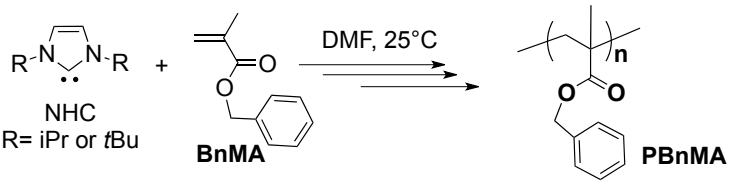

entry	NHC	$[M]_0/[NHC]_0$	Time (h)	Conv.[a] (%)	$\bar{M}_n^{theo}$ [b] (g.mol^{-1})	$\bar{M}_n$ [c] (g.mol^{-1})	M_p [c] (g.mol^{-1})	$\bar{M}_w$ [c] (g.mol^{-1})	$Đ$ [c]
1	NHC^{iPr}	100	72	0	-	-		-	-
2	NHC^{tBu}	50	15	100	8,800	12,600	27,000	25,200	2.0
3	NHC^{tBu}	100	15	100	17,600	15,700	51,200	46,200	2.9

a. Conv.= % monomer conversion determined by ^{1}H NMR spectroscopy; b. Theoretical molar mass $\bar{M}_n^{theo} = M_{BnMA} \times \frac{[BnMA]}{[NHC]} \times conv.$; c. Characterization of PBnMA's by SEC in THF using PS standards for calibration.

Molar masses of poly(benzyl methacrylate)s (PBnMA's) obtained from NHC^{tBu} were found to vary with the initial monomer concentration $[BnMA]_0$, keeping $[NHC^{tBu}]_0$ = 10 mM, as illustrated in the SEC traces shown if Figure 18. Complete monomer conversion was reached after 15 h, leading to PBnMA's of much higher molar masses ($\overline{M_w}$ up to 46,200 g.mol^{-1}) than those expected and rather large dispersity $Đ \geq 2.0$ (Table 6, entries 2-3). These molecular characteristics witnessed a rather poor degree of control during the polymerization. However, the influence of SEC calibration based on PS standards should be taken in account, since PS and PBnMA have a different hydrodynamic volume.[36]

The polymerization rate of BnMA was also higher than that of MMA: 100% of BnMA conversion after 15 h of reaction (Table 6, entry 3) *vs.* 74 % for MMA (Table 4, entry 1). This difference could be explained by the aromaticity of phenyl group in BnMA that might increase the reactivity of the enolate moiety.

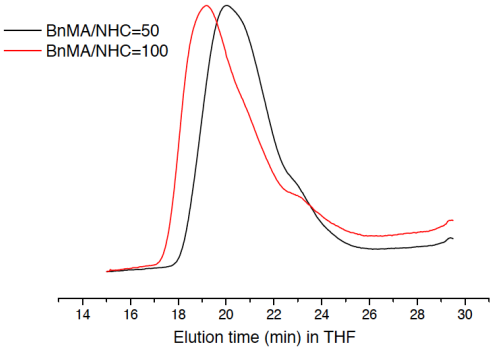

Figure 18. SEC-RI traces of NHC^{tBu}-induced polymerization of BnMA in DMF at 25 °C (Table 6, entries 2-3).

Analysis of NHC^{tBu}- derived PBnMA's chain-ends by MALDI-ToF showed three distinct populations (A, B and C) with peak-to-peak mass increment of 176 mass units (= mass of one BnMA unit) in all cases. (Figure 19). However, populations A and B could not be identified, even considering various combination of polymer chain-ends. In contrast, population C was found to correspond to α-benzyloxy-PBnMA's. As already proposed in the case of MMA, the carbene probably reacted with the carbonyl of the monomer, releasing a benzyloxide anion that further displaced the imidazolium in the α-position, (see Scheme 10c).

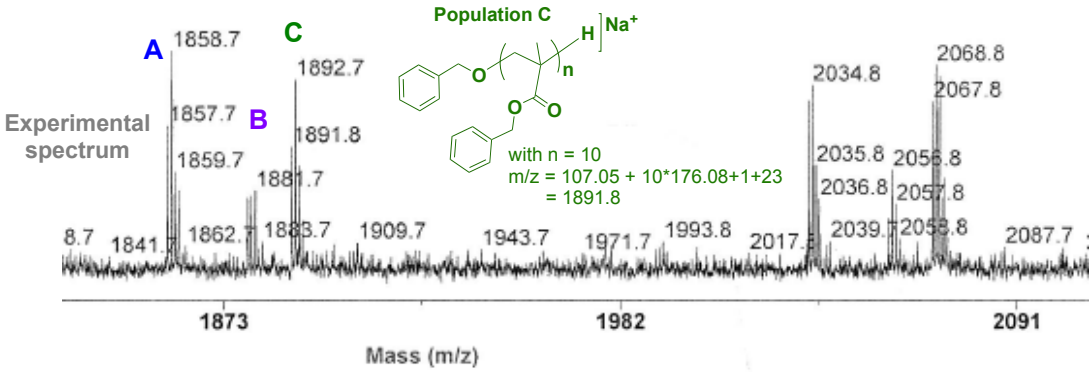

Figure 19. MALDI-ToF MS spectrum of PBnMA ($[BnMA]_0/[NHC^{tBu}]_0$ = 100 (Table 6, entry 2).

3.3. Case of *N*,*N*-(dimethylamino)ethyl acrylate (DMAEA) and *N*,*N*-(dimethyl amino)ethyl methacrylate (DMAEMA)

Polymerizations by NHCs of *N*,*N*-(dimethylamino)ethyl acrylate (DMAEA) and its methacrylic equivalent, *N*,*N*-(dimethylamino)ethyl methacrylate (DMAEMA) were also studied. Corresponding polymers, PDMAEA and PDAEMA, are weak polybases that are water-soluble and thermo-responsive. [56-59]

Polymerizations of both DMAEA and DMAEMA were performed under the same conditions described above, *i.e.* in DMF at 25 °C using either NHC^{iPr} or NHC^{tBu} as initiators. To avoid possible interactions of PDMAE(M)A's with the SEC columns with THF as solvent, the analysis by SEC was carried out using DMF at 80 °C in the presence of 0.1% LiBr. Table 7 summarizes these experiments and the molecular characteristics of the obtained compounds.

Table 7. NHC-induced polymerizations of DMAEA and DMAEMA in DMF at 25 °C.

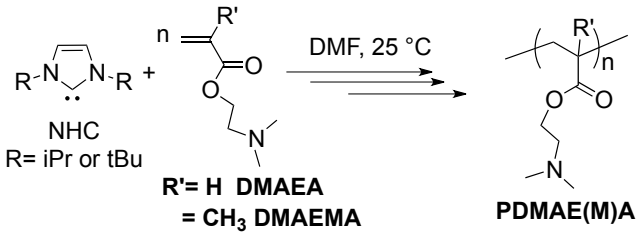

entry	NHC	M	$[M]_0$/ $[NHC]_0$	Time (h)	Conv.[a] (%)	$\overline{M_n}^{theo}$ [b] (g.mol^{-1})	$\overline{M_n}$ [c] (g.mol^{-1})	M_p [c] (g.mol^{-1})	$\overline{M_w}$ [c] (g.mol^{-1})	$Đ$ [c]
1	NHC^{iPr}	DMAEA	25	5	96	3,500	4,400	4,400	4,750	1.1
2	NHC^{iPr}	DMAEA	50	5	83	6,800	6,000	8,900	9,600	1.4
3	NHC^{iPr}	DMAEA	100	5	81	11,600	9,000	12,600	13,800	1.5
4	NHC^{iPr}	DMAEA	200	5	64	18,400	10,600	17,900	18,500	1.8
5	NHC^{iPr}	DMAEA	500	5	46	33,000	15,000	24,100	24,000	1.6
6	NHC^{tBu}	DMAEA	100	5	97	13,900	8,100	11,700	12,100	1.5
7	NHC^{iPr}	DMAEMA	100	72	0	-	-	-	-	-
8	NHC^{tBu}	DMAEMA	100	18	45	7,000	31,000			1.65

a Conv.= % monomer conversion determined by 1H NMR spectroscopy. b. Theoretical molar mass $\overline{M}_n^{theo} = M_M \times \frac{[M]}{[NHC]} \times conv.$; c. Characterization of polymers by SEC in DMF using PS standards for calibration.

Both NHC^{iPr} and NHC^{tBu} were capable to trigger the direct polymerization of the acrylate monomer, DMAEA, yielding poly(.*N*,*N*-(dimethylamino)ethyl acrylate (PDMAEA's) with similar polymerization rates (monomer conversion ≥ 80 % after 5 h for DP = 100). Focusing in the NHC^{iPr}-induced polymerization of DMAEA, we noted that the molar masses increased by increasing the monomer concentration (Table 7, entries 1-5), as depicted in Figure 20. Nonetheless, molar masses were found, in this case also, to deviate from linearity,

likely owing to the occurrence of the same side reactions described above for the other monomers. The UV absorption at λ = 260nm on the SEC traces of the obtained polymers attested the presence of chain-end PDMAEA's generated by back-biting.

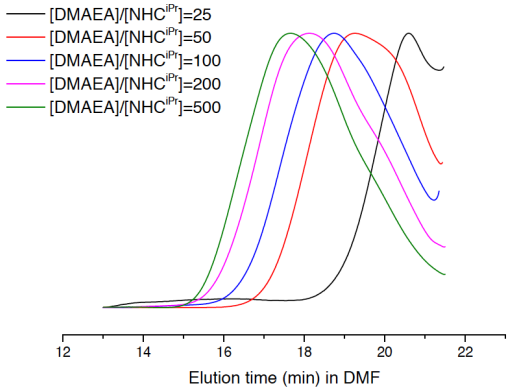

Figure 20. SEC-RI traces of NHC^{iPr}-induced polymerization of DMAEA in DMF at 25 °C (Table 7; entries 1-6).

As for the methacrylic DMAEMA, we again noted that NHC^{iPr} was not able to trigger the polymerization of this monomer (entry 7), in contrast to NHC^{tBu}. In the latter case, the reaction was found slower than that of the DMAEA acrylic monomer, reaching only 45 % of conversion after 18 h of reaction probably due to steric reasons.

In conclusion and as summarized in Figure 21, while NHC^{tBu} induced the direct polymerization of both acrylic (^{t}BuA and DMAEA) and methacrylic monomers (DMAEMA and BnMA), NHC^{iPr} was only active towards acrylates. We hypothesized that the selective cyclodimerization reaction occurring between with NHC^{iPr} and MMA also prevailed with other methacrylic substrates although experimental evidences for that statement should be provided.

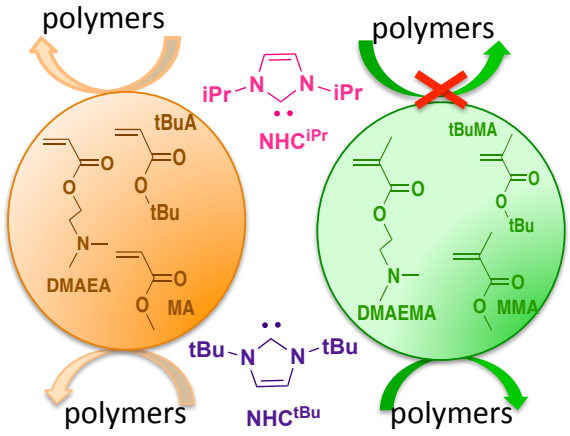

Figure 21. Overview of reactivities of NHC^{iPr} and NHC^{tBu} towards various (meth)acrylates monomers in DMF at 25 °C.

4. Post-polymerization functionalization of NHC^{tBu}-produced PMMA

The previous sections have shown that NHC^{tBu} can directly induce the polymerization of MMA in DMF 25 °C, though in a relatively slow manner (35 % of conversion after 5 h for $[MMA]_0/[NHC]_0 = 100$, Table 3; entry 5). A progressive loss of control over the polymerization is also noted, which is attributed to the low carbene efficiency and the presence of free (non-protected) imidazolium enolate propagating species, growing PMMA chains by a zwitterionic polymerization mechanism.

To gain a better insight into the fate of these supposedly free enolates and α-imidazolium chain ends, we attempted to quench the polymerization using functionalizing "killing" E- or NuE-type agents, where Nu and E are nucleophilic and electrophilic moieties of the molecule,either at the completion or in the course of the polymerization.

Two methods of quenching were thus tested, at low monomer conversion (less than 30 % of conversion), assuming that side reactions would not prevail under these conditions.

(1) The first method consisted in quenching with electrophiles (E) such as aldehydes, ketones or alkyl halides that could terminate the propagating enolates by a *C*-alkylation or a *O*-alkylation, depending on the nature of E, expectedly leading to α-imidazolium,ω-E end-capped PMMA's (Scheme 17).

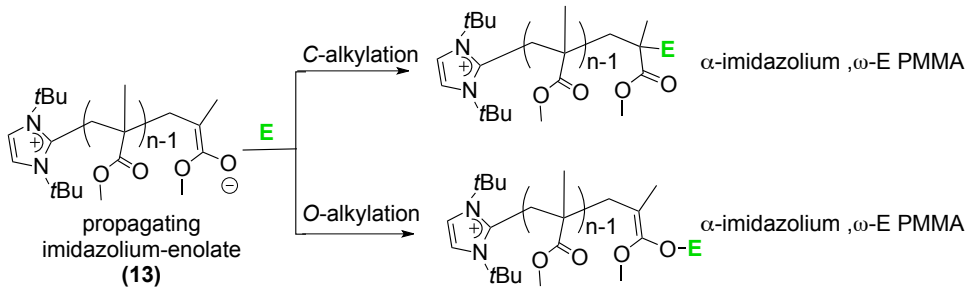

Scheme 17. Quenching with E agents leading to α-imidazolium,ω-E PMMA chains

(2) The second method employed NuE-type terminators, such as alcohols or silyl ethers (Nu = RO and E = H or $SiMe_3$) that were expected to displace the imidazolium moiety with the Nu group and, in the same time, quench the propagating enolate with the E moiety. This strategy would provide α-Nu PMMA's as shown in Scheme 18. This "α-strategy" using NuE-type quenchers have been successfully achieved by our group for the ring-opening polymerization of both ethylene and propylene oxides, using a NHC as direct initiator (chain starter).[46,47,60]

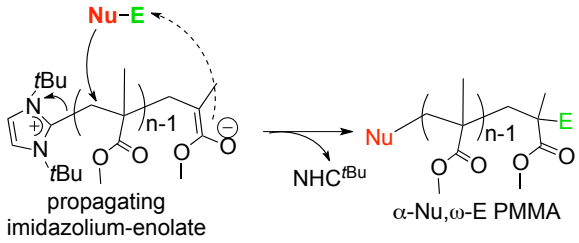

Scheme 18. Quenching with NuE agents leading to α-Nu,ω-E PMMA chains

4.1. Functionalization in ω-position of PMMA chains: method (1)

Use of benzyl bromide ($PhCH_2Br$) or benzaldehyde (PhCHO) following method (1) was expected to introduce an aromatic group in ω-position of PMMA chains, and that could be easily detected by a UV detector connected to the SEC device, and by NMR as well.

The polymerization of MMA was thus performed using NHC^{tBu} as initiator, under the conditions described above. At low conversion (≤ 30-35 %), that was, when a significant fraction of oligomers were formed, the polymerization was quenched with 3 eq. of $PhCH_2Br$ or PhCHO (relative to NHC^{tBu}), and the reaction was allowed to stir for additional 16 h. Table 8 summarizes the results obtained with $PhCH_2Br$ and PhCHO.

Table 8. Quenching of the NHC^{tBu}-polymerization of MMA using $PhCH_2Br$ or PhCHO.

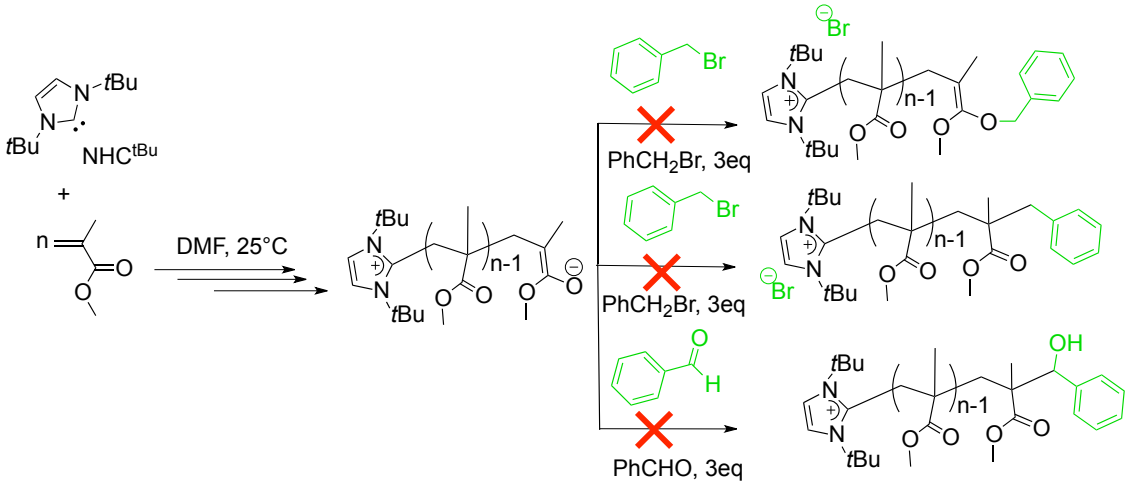

entry	E	$[NHC]_0/[MMA]_0/[E]_0$	Time (h)	Conv.[a] (%)	$\overline{M_n}^{theo}$ [b] (g.mol^{-1})	$\overline{M_n}$ [c] (g.mol^{-1})	M_p [c] (g.mol^{-1})	$Đ$ [c]
1a	-	1/100/-	2	29	2,900	9,600	15,700	1.7
1b	$PhCH_2$ Br	1/100/3	16	30	3,000	11,900 669,100	15,700 650,000	1.1 1.2
2a	-	1/100/ -	2	20	2,000	3,600	4,550	1.5
2b	$PhCH_2$ Br	1/100/53	16	32	3,200	4,200 331,700	4,200 462,000	1.4 1.2

3a	-	1/100/-	2	30	3,000	4,300	8,200	1.6
3b	PhCHO	1/100/10	16	41	4,100	5,700	24,400	1.6
4a	-	1/100/-	2	23	2,300	5,700	11,000	1.8
4b	PhCHO	1/100/50	16	31	3,100	5,700	10,800	1.8

a. Conv.= % monomer conversion determined by ^{1}H NMR spectroscopy; b. Theoretical molar mass $\overline{M}_n^{theo} = M_{MMA} \times \frac{[MMA]}{[NHC]} \times$conv.; c. Characterization of PMMA's by SEC in THF using PS standards for calibration.

Before addition of the quenching agent, the obtained molar masses ($\overline{M_n}$) of PMMA oligomers were closed to the targeted values based on the initial $[MMA]_0/[NHC^{tBu}]_0$ molar ratios, with dispersities in the range $Đ$ = 1.1-1.8 (Table 8). This rather good agreement between $\overline{M}_n^{theo}$ and $\overline{M}_n^{exp}$ at low monomer conversion contrasted with our previous results (see Table 3), where $\overline{M}_n^{exp}$ were generally higher than $\overline{M}_n^{theo}$ at high monomer conversion, due to side reactions.

Unexpectedly, with $PhCH_2Br$ as functionalizing agent, the monomer conversion slightly increased, from 20 % before quenching to 32% after (Table 8,entry 1). The obtained polymer exhibited, a UV absorption (λ = 260 nm) after termination with $PhCH_2Br$ (population **A** Figure 22b). In addition, after quenching, a second population was generated, (population **B**, Figure 22b), and this new population did not shown any UV traces as observed in the SEC traces of the final polymer. We hypothesized that the second population was generated from initiation of new chains by residual free carbene in solution.

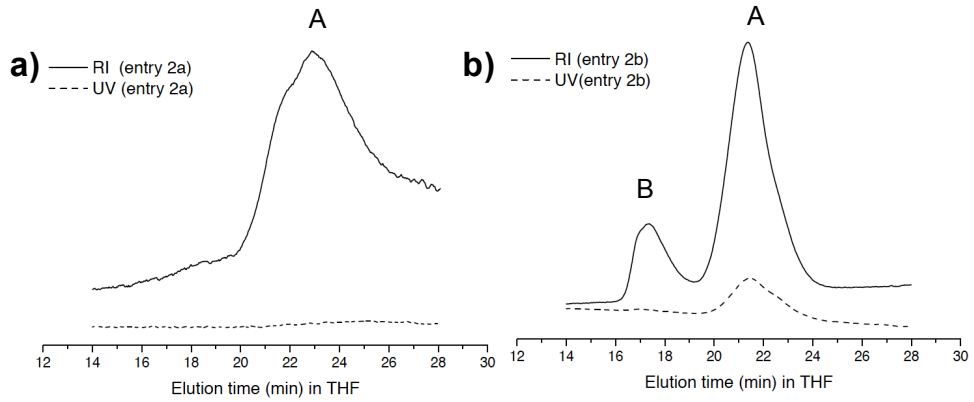

Figure 22. SEC traces of NHC^{tBu}-produced PMMA: a) before quenching ; b) after quenching with BnBr in DMF at 25 °C (Table 8, entry 2).

With benzaldehyde (PhCHO) as quenching agent, conversion again slightly increased from 30 % to 41 %, after 16 h of reaction (entry 3). Polymers thus obtained exhibited a UV absorption at λ = 260 nm, illustrating the presence of phenyl group from benzaldehyde onto polymer chains (Figure 27). No other population was detected in this case, presumably because the remaining carbene reacted with benzaldehyde, forming the

benzoin (see Scheme 2).[13-16,61] We thus assumed that there was a competition between initiation of new chains and termination through reaction with benzaldehyde.

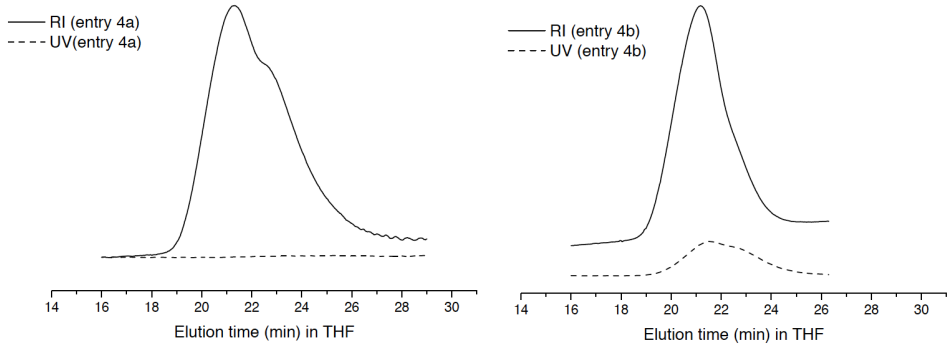

Figure 23. SEC traces of NHC$^{t\text{Bu}}$-produced PMMA a) before quenching b) after quenching with PhCHO in DMF at 25 °C (Table 8, entry 4).

Attempts to further characterize PMMA chain-ends (α-imidazolium and ω-(hydroxyl) benzyl) of final polymers by ^{1}H NMR and MALDI-ToF analyses were unsuccessful, however, presumably due to the presence of high molar masses chains, masking the functionalized oligomers.

4.2. Functionalization in α-position of PMMA chains: method (2)

The polymerization of MMA was quenched at monomer conversion around 30-40 %, using Nu-E-type agents such as benzyl trimethylsilyl ether ($BnOSiMe_3$), benzyl alcohol (BnOH) or trimethylsilyl azide (N_3SiMe_3). Polymerizations quenched by H_2O served as reference to compare the efficiency of the NuE agents employed. The results obtained in these cases are summarized in Table 9.

Table 9. Quenching of the NHC$^{t\text{Bu}}$-polymerization of MMA using H_2O, N_3SiMe_3, $BnOSiMe_3$ and BnOH

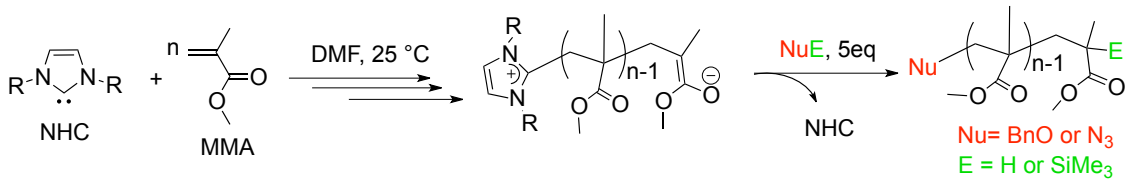

entry	NuE	$[NHC]_0/[MMA]_0/[NuE]_0$	Time (h)	Conv.[a] (%)	$\overline{M_n}^{theo}$ [b] (g.mol^{-1})	$\overline{M_n}$ [c] (g.mol^{-1})	M_p [c] (g.mol^{-1})	$Đ$ [c]
1a	H_2O	1/100/-	5	33	3,300	3,400	4,700	1,6
1b	H_2O	1/100/5	16	34	3,400	3,500	4,800	1.5
2a	N_3SiMe_3	1/100/-	5	36	3,600	3,100	3,300	1.5
2b	N_3SiMe_3	1/100/5	16	44	4,400	3,600	4,300	1.5

3a	$BnOSiMe_3$	1/100/-	5	34	3,400	3,550	5,100	1.6
3b	$BnOSiMe_3$	1/100/5	16	45	4,500	5,200	10,000	1,7
4a	BnOH	1/100/-	2	18	1,800	1,800	1,770	1.2
4b	BnOH	1/100/5	24	100	10,000	3,700	4,700	1.7

a. Conv.= % monomer conversion determined by ^{1}H NMR spectroscopy; b. Theoretical molar mass $\overline{M}_n^{theo} = M_{MMA} \times \frac{[MMA]}{[NHC]} \times conv.$; c.Characterization of PMMA's by SEC in THF using PS standards for calibration.

Upon quenching with 5 eq. (relative to NHC) of N_3SiMe_3 or $BnOSiMe_3$, the monomer conversion slightly increased (from rather 36 % to 45 %), maybe because of a slow dissociation of NuE or a chain re-initiation by some remaining carbene. The UV SEC traces of the obtained polymers ($\overline{M_n}$ = 3,600 g.mol^{-1}; *Đ* = 1.5) showed only a slight absorption at λ = 260 nm, no matter the terminating agent used (Figure 24). We concluded that, in such conditions, the nucleophilic part (Nu = N_3 or BnO) could not displace the imidazolium moiety and remained bond to the trimethylsilyl group.

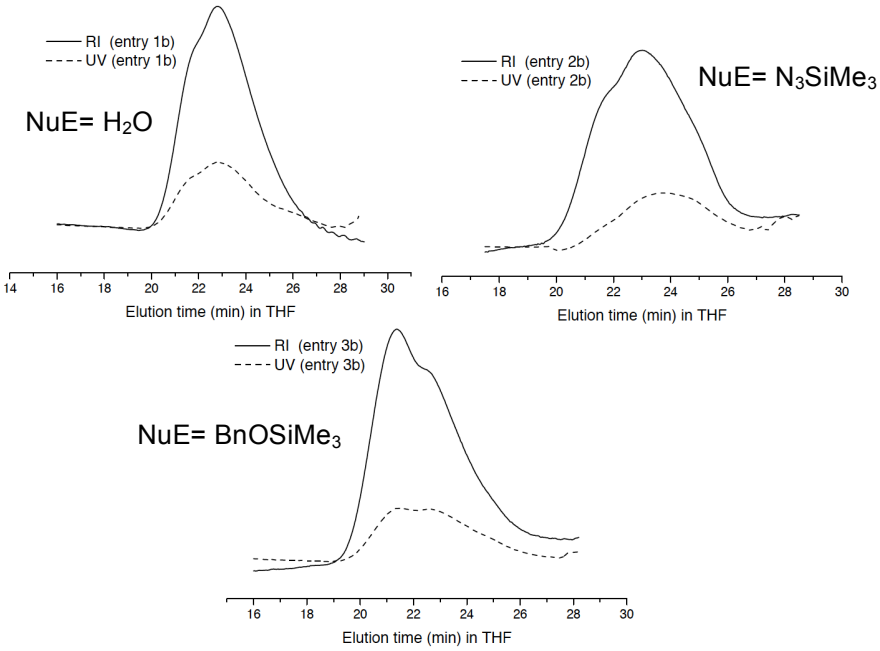

Figure 24. SEC traces of NHC^{tBu}-produced PMMA after quenching H_2O , N_3SiMe_3 and $BnOSiMe_3$ in DMF at 25 °C (Table 9, entry 1-3).

When using 5 eq. (relative to NHC) of BnOH, a complete conversion was reached, after 18 h of reaction, leading to PMMA's of molar masses $\overline{M_n}$ = 3,700 g.mol^{-1} and a dispersity *Đ* = 1.7 (Table 9, entry 4b). In addition, the final polymer, precipitated several times in pentane, exhibited a UV absorption at λ = 260 nm, illustrating the presence of the aromatic group from benzyl alcohol onto polymer chain. (Figure 25).

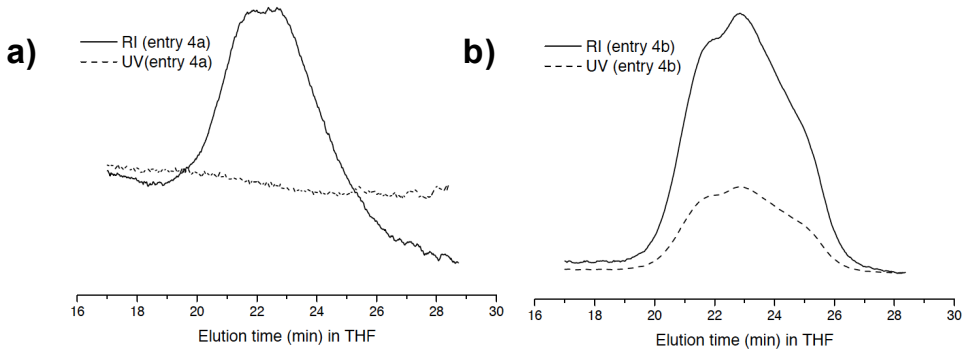

Figure 25. SEC traces of NHC^{tBu}-produced PMMA: a) before quenching; b) after quenching with BnOH in DMF at 25 °C (Table 9, entry 4).

The unexpected increasing of conversion in presence of alcohol prompted us to investigate the chain-ends of this polymer by ^{1}H NMR and MALDI-ToF. The ^{1}H NMR spectrum (Figure 26) confirmed the presence of benzyl group in α-position, this PMMA having a molar mass $\overline{M_n}^{NMR}$ = 3,600 g.mol^{-1}, in close agreement with the value obtained by SEC ($\overline{M_n}$ = 3,700 g.mol^{-1}).

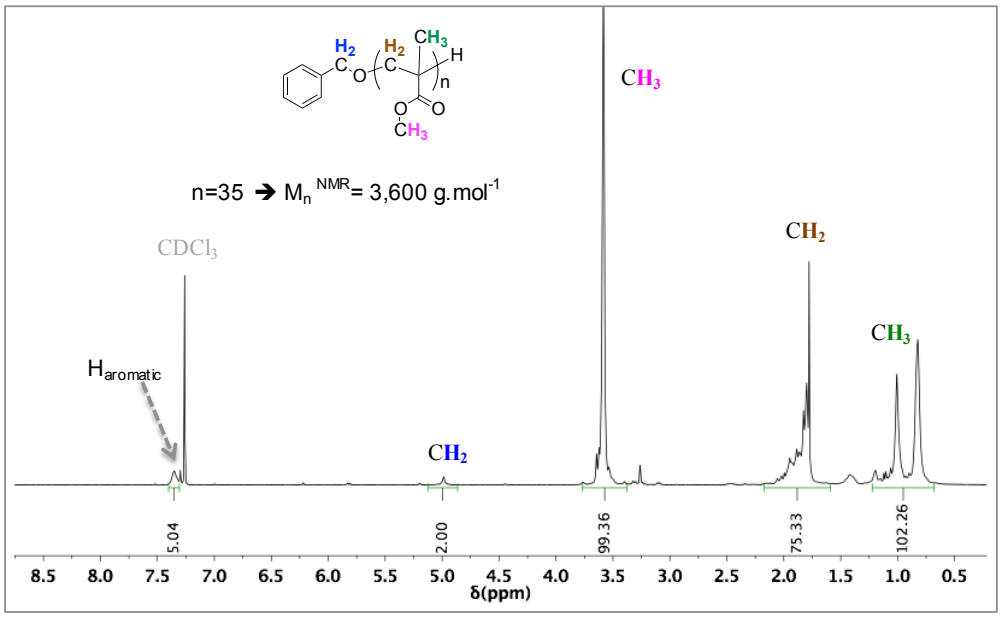

Figure 26. ^{1}H NMR spectrum (in $CDCl_3$) of NHC^{tBu}-produced PMMA after quenching with BnOH in DMF at 25 °C (Table 9, entry 4b).

In addition, MALDI-ToF analysis of the same oligomeric PMMA revealed four different populations (A, B_1, B_2 and C), with individual peaks being separated by m/z = 100 mass units, corresponding to the molar mass of one MMA unit (Figure 27 and Scheme 19). Population A was ascribed to α-1,3-bis(*tert*-butyl)imidazolium PMMA's that could be

generated from the direct conjugate-addition of NHC^{tBu} onto MMA. Population C was attributed to α-methoxide PMMA chains, as already observed for the NHC^{tBu}-initiated polymerization of MMA (**16** see Scheme 10). As for population B_1, it could correspond to the α-benzyloxide PMMA chain populations formed after displacement of the imidazolium by benzyloxide (see Scheme 18), while population B_2 was likely due to a rearrangement of B_1 after a loss of NaH during the ionization process, forming a cationized oxygen.

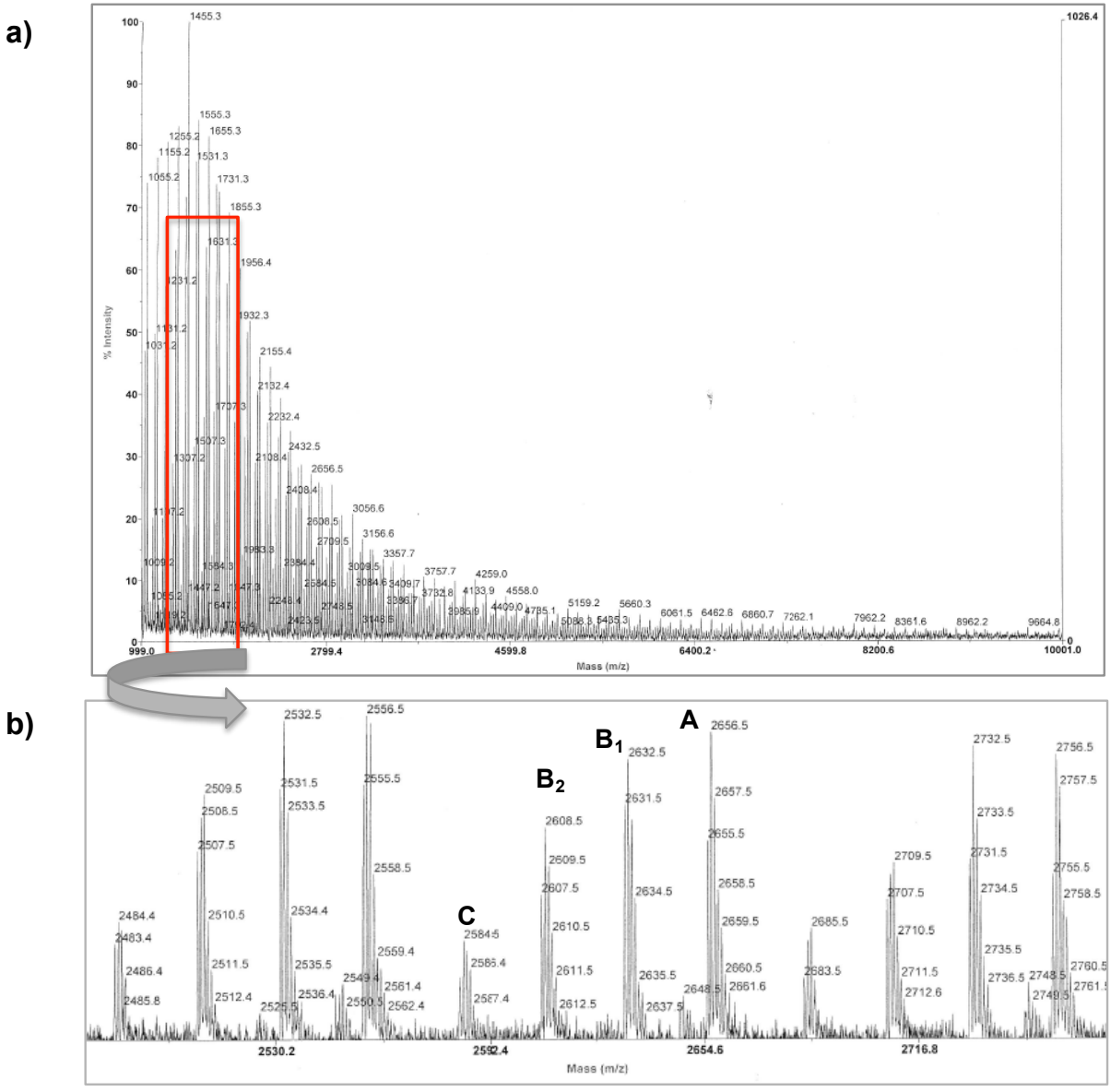

Figure 27. a) MALDI-TOF mass spectrum in reflector mode of NHC^{tBu}-produced PMMA after quenching with BnOH in DMF at 25 °C (Table 9; entry 4b); b) zoom.

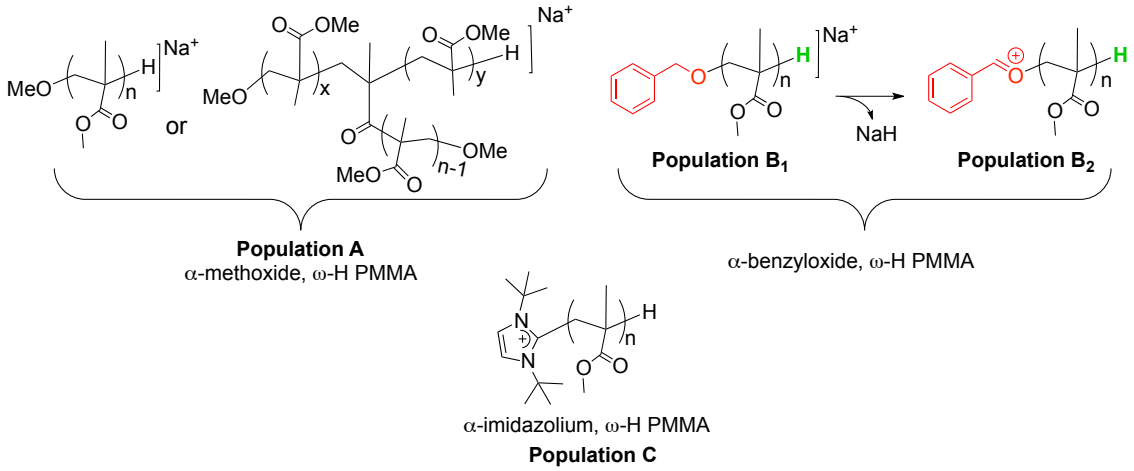

Scheme 19. Different populations observed in the MALDI-ToF spectrum.

To summarize, and as illustrated in Figure 28, post-polymerization functionalization of NHC^{tBu}-produced PMMA remains challenging, presumably owing to the occurrence of side reactions during the polymerization. The chain ends of polymers ended by electrophiles E compounds (method (1)) were not clearly identified due to the presence of high molar masses polymers. In contrast, the functionalization with benzyl alcohol as NuE-type terminating agent (method (2)) was partial, but additional side populations were also detected.

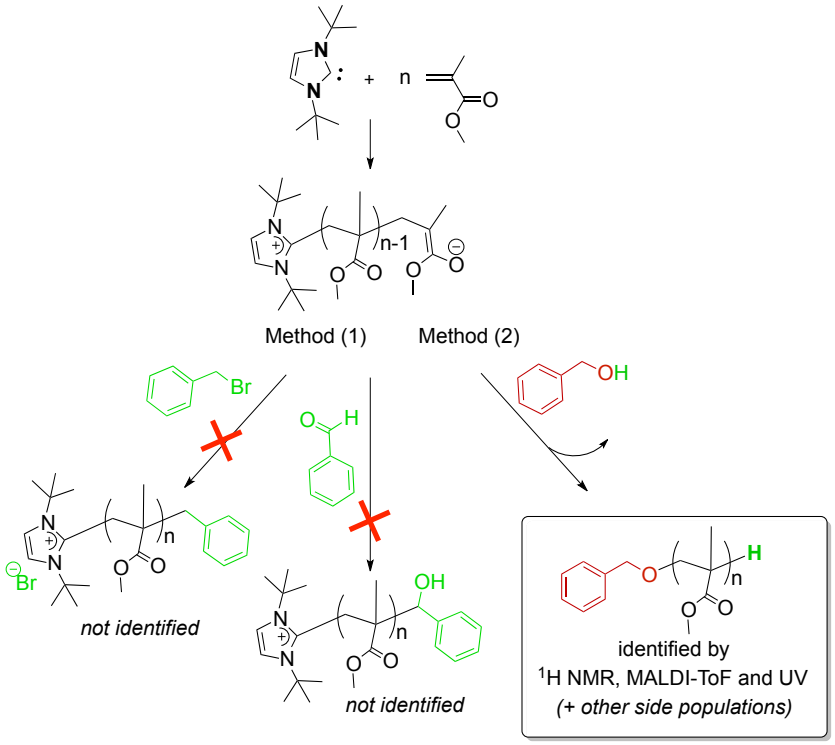

Figure 28. Post-polymerization functionalinalization of NHC^{tBu}-produced PMMA using method (**1**) or method (2).

Conclusions and perspectives

The direct polymerization of both acrylic and methacrylic monomers induced by two distinct NHCs, namely NHC^{iPr} and NHC^{tBu}, in absence of any other reagents has been investigated in this chapter. While NHC^{iPr} allows the polymerization of MA, an unexpected and singular behavior of NHC^{iPr} in reaction with MMA has been experimentally evidenced. This particular carbene indeed reacts with two equivalents of MMA, affording an unprecedented imidazolium enolate cyclodimer (NHC^{iPr}:MMA = 1:2), as evidenced by X-Ray diffraction, NMR and mass spectrometry analyses.

DFT calculations have allowed rationalizing experimental results, evidencing significant differences between NHC^{iPr} and NHC^{tBu}. Experimental results and theoretical calculations support a cyclodimer formation mechanism involving the reaction of NHC^{iPr} with two molecules of MMA, followed by proton transfer, intramolecular cyclization and methanol release. In sharp contrast, NHC^{tBu} can selectively promote the direct polymerization of MA and MMA.

Calculations have shown that the nature of the NHC does not seem to affect the polymerization process, excepted in the first step (initiation step), where steric hindrance of the NHC influences the approach of MMA. In contrast, both the discriminating cyclization step and the limiting step of MeOH release are strongly influenced by the steric hindrance of the NHC substituents, as well as by their electronic nature. This gives rise to higher energetic barriers in the case of NHC^{tBu} (kinetic control of the reaction).

Investigation into the polymerization of miscealleneous (meth)acrylic monomers has shown that the reaction outcome (polymerization or cyclodimerization) is dramatically influenced by the structure of the carbene: NHC^{iPr} is only active for acrylate polymerization, while NHC^{tBu} initiated the polymerization of both acrylate and methacrylate monomers.

Overall, the direct zwitterionic polymerization (ZP) of (meth)acrylic monomers induced by NHC^{tBu} as chain starters seems to be characterized by a slow initiation and side reactions, precluding the possibility for true “controlled/living” polymerization process. However, the use of this particular NHC as true catalyst, *i.e.* in the presence of a chain regulator could be a strategy to gain in control.

This part of the work has thus established that NHCs are appropriate nucleophilic candidates for the direct 1,4-conjugate addition of activated Michael acceptors, and further expands the scope of reactivity and selectivity of NHCs towards (meth)acrylic substrates. The generalization with other substrates of such reactivity would be of interest for the synthesis of specific NHC-adducts. In the context of stereoselective transformations, the design of chiral carbene precursors and their reactivity towards small molecules are currently underway in our group.

Experimental and supporting information

General instrumentation. NMR spectra were recorded on a Bruker AC-400 spectrometer (^{1}H, ^{13}C, 400.2 MHz and 100.6MHz respectively) in appropriate deuterated solvents. Molar masses of PMAs, PMMAs, P^{t}BuAs, P^{t}BuMAs and PBnMAs were determined by size exclusion chromatography (SEC) at 25 °C, in THF as the eluent (1 mL/min) and with trichlorobenzene as a flow marker, using both refractometric (RI) and UV detectors (Varian). Analyses were performed using a three-column set of TSK gel TOSOH (G4000, G3000, G2000 with pore sizes of 20, 75 and 200Å respectively, connected in series) calibrated with polystyrene standards. SEC in DMF was used for the characterization of PDMAEAs and PDMAEMAs using a 3-column set of TSK gel TOSOH (G4000, G3000, G2000 with pore sizes of 20, 75 and 200Å, respectively, connected in series) calibrated with polystyrene (PS) standards with DMF as eluent (0.8 mL.min^{-1}) and toluene as a flow marker at 80°C, in the presence of LiBr (1 g.L^{-1}) using both refractometric and UV detectors (Varian).

MALDI-MS and Electrospray (ESI) Mass spectra were performed by the CESAMO (Bordeaux, France). ESI was performed on a QStar Elite mass spectrometer (Applied Biosystems). The instrument is equipped with an ESI source and spectra were recorded in the positive mode. The electrospray needle was maintained at 4500 V and operated at room temperature. Samples were introduced by injection through a 20 mL sample loop into a 400 mL/min flow of methanol from the LC pump. MALDI-Tof MS spectrum were performed on a Voyager mass spectrometer (Applied Biosystems). The instrument is equipped with a pulsed N2 laser (337 nm) and a time-delayed extracted ion source. Spectra were recorded in the positive-ion mode using the reflectron and with an accelerating voltage of 20 kV. Samples were dissolved in THF at 10 mg/ml. The IAA matrix (trans-3-Indoleacrylic acid) solution was prepared by dissolving 10 mg in 1 ml of THF. A MeOH solution of cationisation agent (NaI, 10 mg/ml) was also prepared. The solutions were combined in a 10:1:1 volume ratio of matrix to sample to cationisation agent. One to two microliters of the obtained solution was deposited onto the sample target and vacuum-dried.

Materials. Toluene was refluxed over CaH_2 and cryo-distilled from polystyryllithium (PS-Li) prior to use. Dimethylformamide (DMF; technical grade) was first cryo-distilled over CaH_2 and stored over molecular sieves, and freshly cryo-distilled prior to use. DMF-d_7 was purchased from Cambridge Isotope Laboratories, Inc stored in ampoules and was used as received. THF-d_8 was purchased from Euriso-top and distilled over Na prior to use. Methyl acrylate (MA), methyl methacrylate (MMA), *tert*-butyl acrylate (^{t}BuA), *tert*-butyl methacrylate (^{t}BuMA), *N,N*-dimethylaminoethyl acrylate (DMAEA), *N,N*-dimethylaminoethyl methacrylate (DMAEMA) and *N,N*-dimethylacrylamide (DMA) were purchased from Sigma-Aldrich or Alfa

Aesar (purity : 97-99%) degased, dried over CaH_2, cryo-distilled into a burette and stored at -20°C. 1,3-Bis-(*tert*-butyl) imidazol-2-ylidene (NHC^{tBu}) was purchased from Strem Chemical as used as received. 1,3-Bis-(isopropyl)imidazol-2-ylidene(NHC^{iPr}) was prepared according to the procedure already reported [7]. All NHCs were kept under an argon glovebox in a freezer at 4 °C.

General polymerization procedure.

In a typical procedure, 8.5 mg (47 µmol) of NHC^{tBu} were added in a flame-dried Schlenk flask in the glovebox. After removal of the Schlenk from the glovebox, 5 mL of DMF were introduced under vacuum. After 5 min homogenization, 0.5 mL MMA (4.7mmol) was added dropwise *via* a syringe under a flux of argon and vigorous stirring. After 5 h at 25 °C, an aliquot of the polymerization mixture was taken to determine the conversion by ^{1}H NMR analysis in $CDCl_3$. The reaction was then quenched with 1mL of degased MeOH and stirred for 1h. All the volatiles were removed under vacuum. The crude product was re-dissolved in THF and precipitated in pentane. PMMA was recovered as a white solid after drying under vacuum.

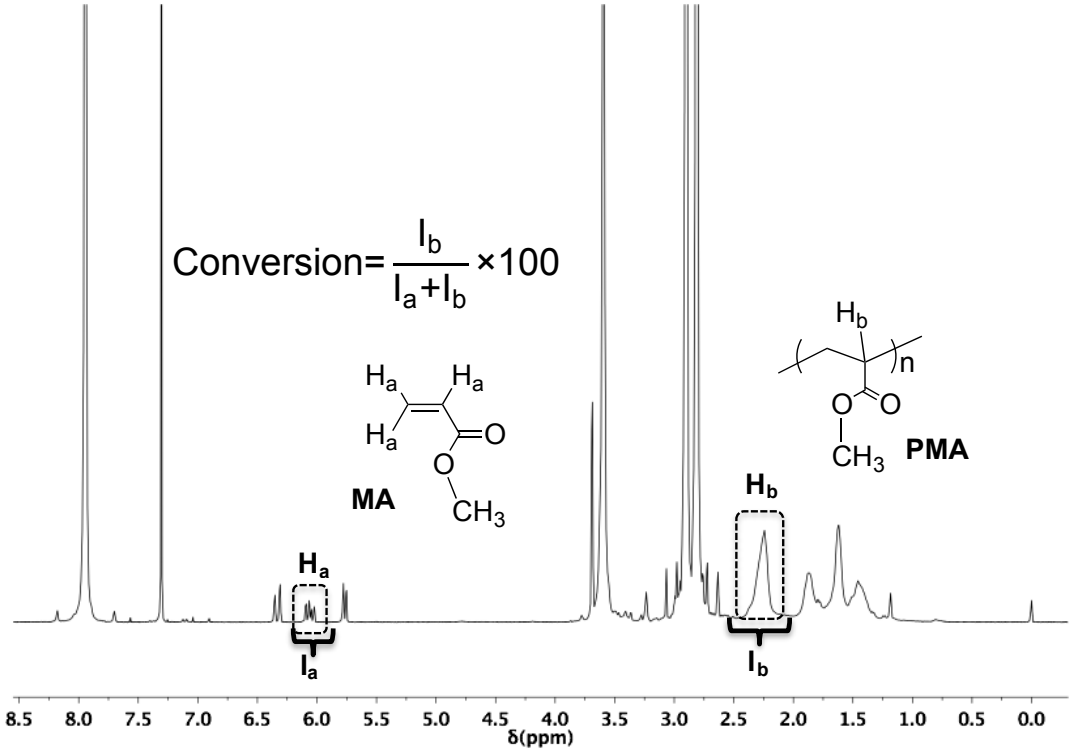

Figure S1. ^{1}H NMR spectra in $CDCl_3$ of PMA solution to determine the monomer conversion during the polymerization of MA by NHC^{iPr} or NHC^{tBu} in DMF at 25 °C. Idem in the case of ^{t}BuA

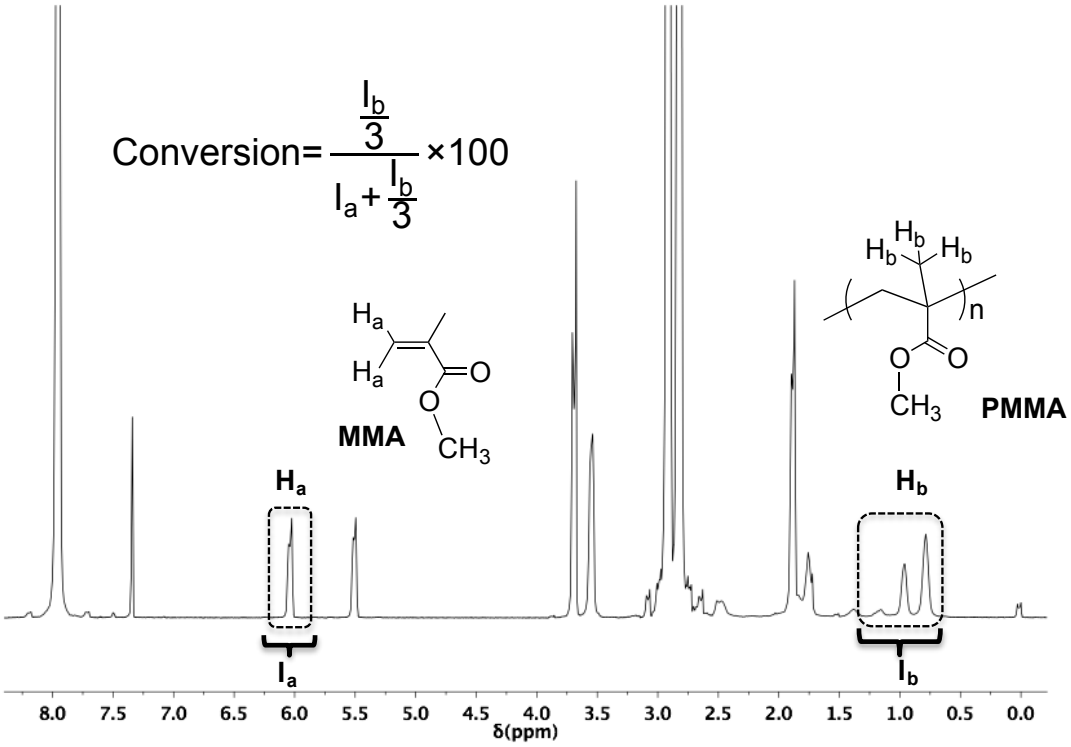

Figure S2. ^{1}H NMR spectra in $CDCl_3$ of PMMA solution to determine the monomer conversion during the polymerization of MMA by NHC^{tBu} in DMF at 25 °C. Idem in the case of BnMA and DMAEMA

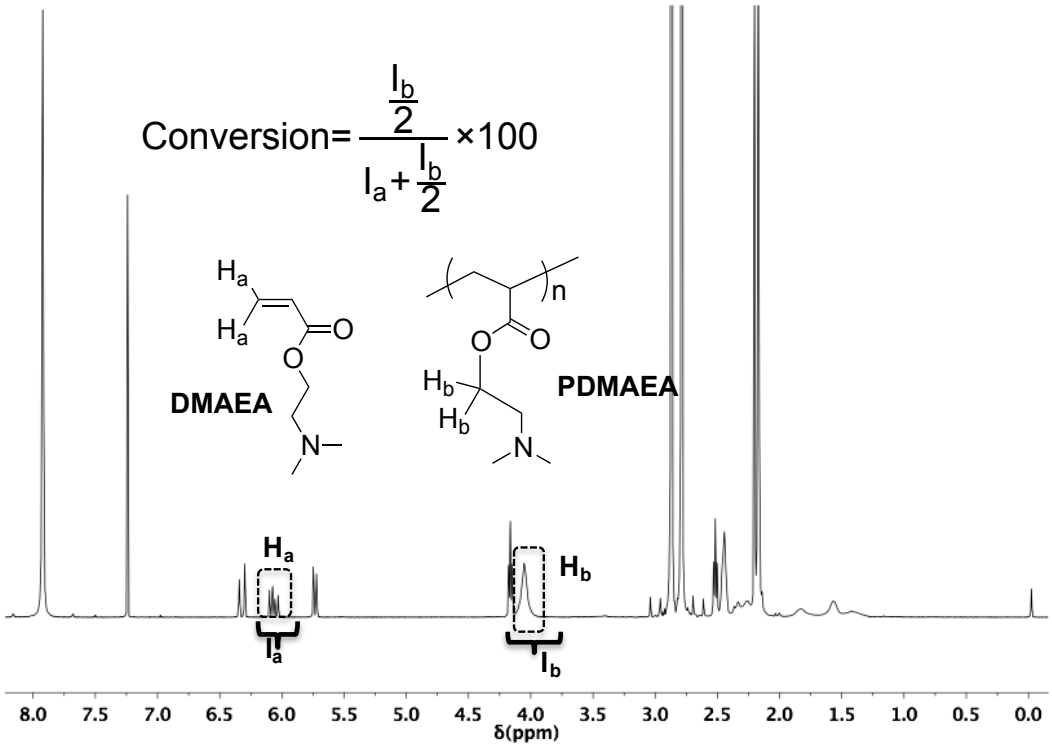

Figure S3. ^{1}H NMR spectra in $CDCl_3$ of PDMAEA solution to determine the monomer conversion during the polymerization of DMAEA by NHC^{iPr} or NHC^{tBu} in DMF at 25 °C.

Reaction of NHC^{iPr} with MMA.

A flamed Schlenk was charged with a solution of NHC^{iPr} (150mg, 0.98 mmol , 2mL of toluene). A solution of MMA (210 µL, 1.96 mmol, 3mL of toluene) was added to this Schlenk via a syringe at room temperature. A precipitate was formed instantaneously and the orange mixture was allowed to react for 24 h. The precipitate was recovered using a cannula system, and dried under vacuum ((215.7 mg, 67%). The white powder obtained was recrystallized from dichloromethane-diethyl ether to afford single crystals suitable for X-ray diffraction. (161.6 mg, 51%). ^{1}H NMR (400.2 MHz, DMF-d_7, 25°C, TMS) δ=1.07 ppm (d, ^{3}J(H,H)=4.0 Hz, 3H; CH_3,), 1.41 ppm (m, 15H; 4×CH_3^{NHC} + CH_3^{MMA}), 1.98 (dd, ^{3}J(H,H)=8.0 Hz ^{3}J(H,H)=4.0 Hz 1H; CH), 2.15 (dd, ^{3}J(H,H)=8.0 Hz ^{3}J(H,H)=4.0 Hz 1H; CH), 2.32 (m, 1H; CH), 3.56 (s, 3H; CH_3), 4.61 (s, 1H; CH), .7.79 (s, 2H; CH,); ^{13}C NMR (100.6 MHz, DMF-d_7, 25°C,TMS) δ 18.0 (CH_3^{MMA}-CH), 22.5 (CH_3^{NHC}), 26.8 (CH_3^{MMA}), 40.0 ($CH(CH_3)CH_2$), 43.7 (CH_2-$C^{MMA}(CH_3)$), 49.8 (CH^{NHC}), 51.3 (O-CH_3), 51.7 ($C^{MMA}(CH_3)$C=O), 74.7 (C=C-O), 117.4 (N-CHC), 149.5 (N-C-N), 178.5 (C=O), 186.0 (C=C-O). ESI-MS calcd for $C_{18}H_{29}N_2O_3$ [M^+]: 320,2; found [M-H^+]: 321,2; [M-Na^+]: 343,2; [M_2-H^+]: 641.5 and [M_2-Na^+]: 663.5

Electrospray Ionization Mass spectrometry (ESI-MS)

Electrospray ionization (ESI) Mass spectra were performed on a QStar Elite mass spectrometer (Applied Biosystems). The instrument is equipped with an ESI source and spectra were recorded in the positive mode. The electrospray needle was maintained at 4500 V and operated at room temperature. Samples were introduced by injection through a 20 mL sample loop into a 400 mL/min flow of methanol from the LC pump.

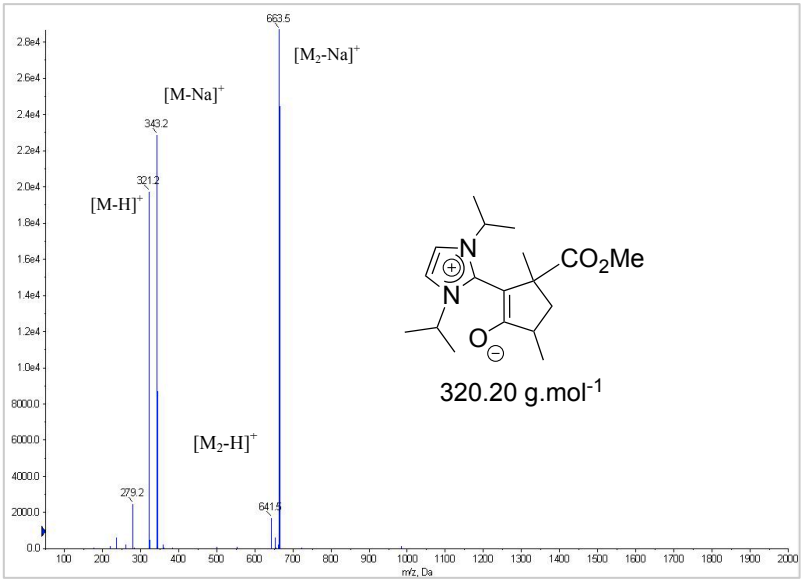

Figure S4. ESI-MS spectrum of imidazolium enolate cylodimer adduct **23**.

NMR analyses of equimolar reactions

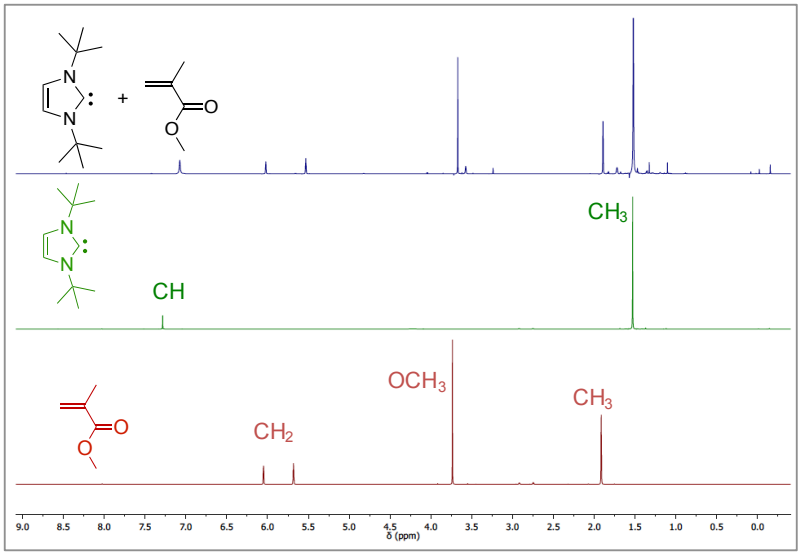

Figure S5. ^{1}H NMR spectra in THF- d_8 of (from bottom to top): MMA, NHC^{tBu} and mixture.

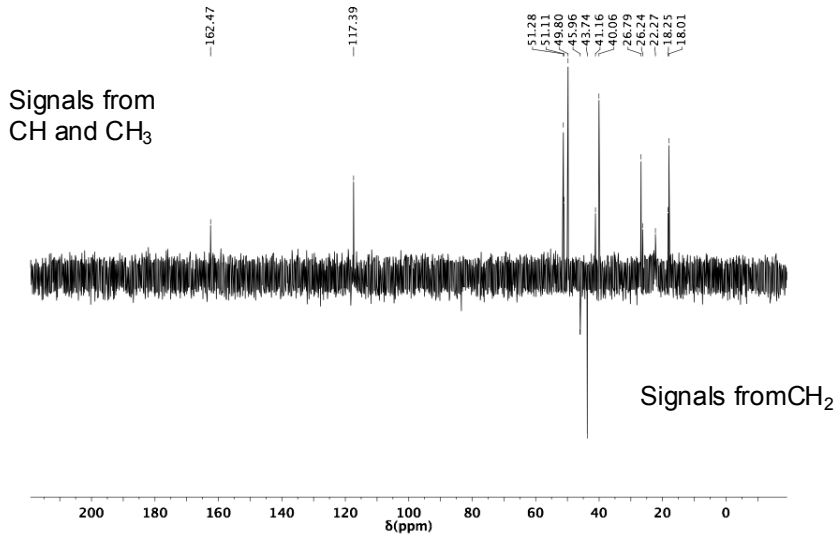

Figure S6. ^{13}C (DEPT 135) NMR spectrum of imidazolium enolate cylodimer adduct **23** in DMF-d_7

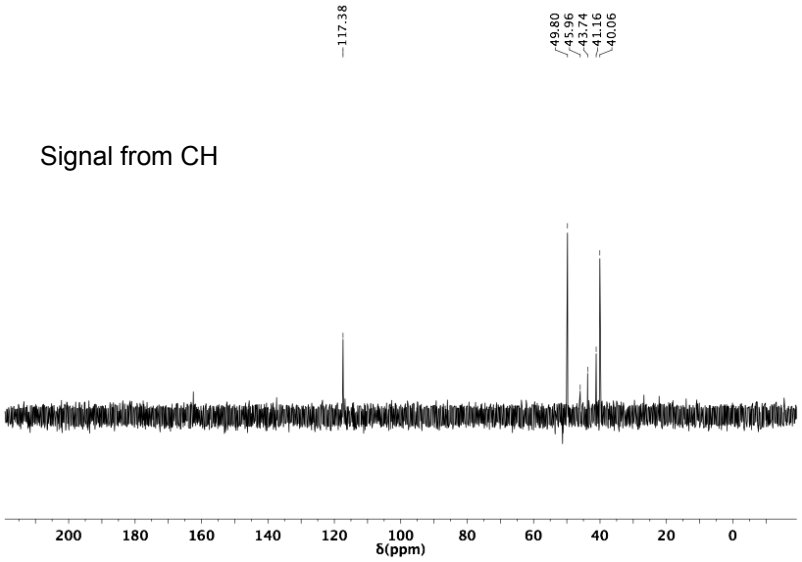

Figure S7. ^{13}C (DEPT 90) NMR spectrum of imidazolium enolate cylodimer adduct **23** in DMF-d_7

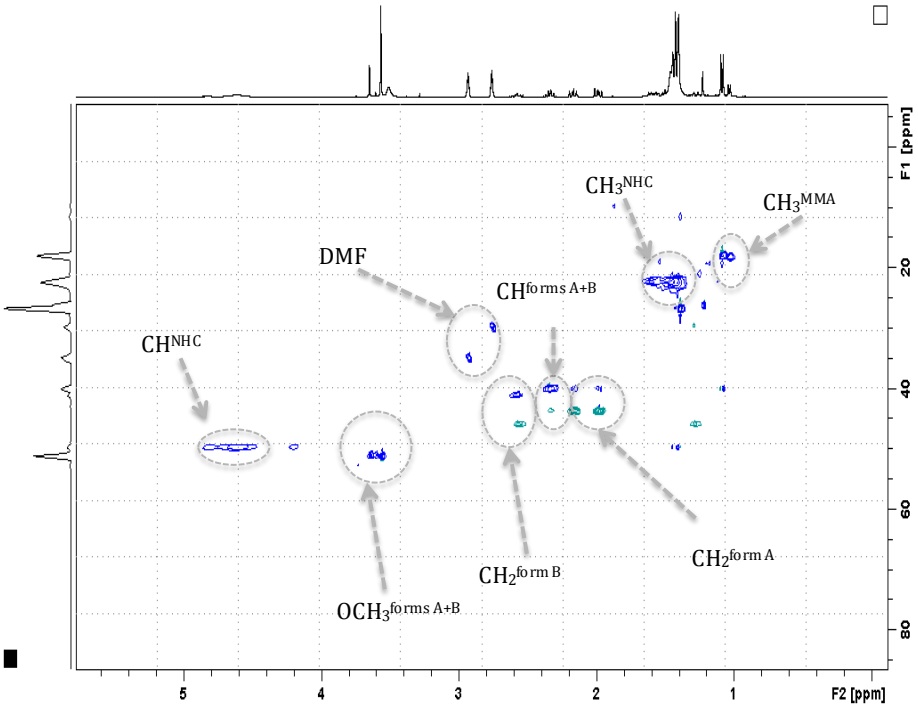

Figure S8. ^{1}H-^{13}C coupling NMR spectrum (HSQC) of of imidazolium enolate cylodimer adduct **23** in DMF-d_7

X-Ray Crystallographic data for NHC^{iPr}-MMA_2 adduct

Most of the crystals of NHC^{iPr}-MMA_2 adduct were twinned. Prior to data collection crystals had to be cut in small needles. Only few of them were diffracting nicely enough to be indexed and collected. The data for the crystal structure of compound X was collected on a Bruker microstar X8 PROTEUM with a classical kappa geometry and Platinum135 CCD camera. All the statistics are compiled in table SX. The structure was solved by the ab-initio method implemented in SHELXD and refined with SHELXL (Sheldrick, G.M. Acta Cryst. A64, 2008, 112-122). Full-matrix least-squares refinement was performed on F^2 for all unique reflections, minimizing $w(Fo^2- Fc^2)^2$, with anisotropic displacement parameters for non-hydrogen atoms. The positions of the H atoms were deduced from coordinates of the non-H atoms. The non-H atoms were refined with anisotropic temperature parameters. H atoms were included for structure factor calculations but not refined except for the two hydrogen atoms from the water molecule involved in the crystal packing.

CCDC code	
Formula	$C_9 H_{15}NO_2$
M	169.22
Crystal system	triclinic
Space group	P-1
a/Å	9.1921(16)
b/Å	9.6142(17)
c/Å	12.370(2)
α/o	82.514(5)
β/o	79.403(5)
γ/o	62.267(5)
V/Å^3	949.9(3)
T /K	293(2)
Z	4
ρ/g cm^{-1}	1.183
size (mm)	0.1x 0.02x 0.01
λ/ Å	1.54178
μ/mm^{-1}	0.674

Independent reflections	2094
measured reflections	14823
parameters/restraints	220/5
*R*1, *wR*2	0.0745/ 0.1909
goodness of fit	1.127

Computational studies

Calculations were carried out with the Gaussian 09 program[1] at the DFT level of theory using the M06-2X functional.[2] All the different atoms (C, N, H, O) have been described with a 6-31G(d,p) double-ζ basis set.[3] Geometry optimizations were carried out without any symmetry restrictions, the nature of the *extrema* (*minima* or transition state) was verified with analytical frequency calculations. All total energies and Gibbs free energies have been zero-point energy (ZPE) and temperature corrected using unscaled density functional frequencies. The connection between the transition states and the corresponding minima was confirmed by IRC calculations.[4]

Molecular Orbitals were plotted by using the molecular graphic package Molekel.[5]

The electron density of **21^{R}** was subjected to an Atoms-In-Molecules analysis (QTAIM analysis)[6] using AIMAll software[7] in order to identify hydrogen bonds.

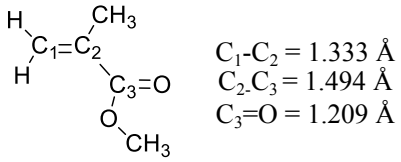

Figure S9. Selected bond lengths (in Å) for the MMA at the M06-2X/6-31G** level of theory.

[1] *Gaussian 09. Revision C.01* M. J. Frisch. G. W. Trucks. H. B. Schlegel. G. E. Scuseria. M. A. Robb. J. R. Cheeseman. G. Scalmani. V. Barone. B. Mennucci. G. A. Petersson. H. Nakatsuji. M. Caricato. X. Li. H. P. Hratchian. A. F. Izmaylov. J. Bloino. G. Zheng. J. L. Sonnenberg. M. Hada. M. Ehara. K. Toyota. R. Fukuda. J. Hasegawa. M. Ishida. T. Nakajima. Y. Honda. O. Kitao. H. Nakai. T. Vreven. J. A. Montgomery. Jr.. J. E. Peralta. F. Ogliaro. M. Bearpark. J. J. Heyd. E. Brothers. K. N. Kudin. V. N. Staroverov. R. Kobayashi. J. Normand. K. Raghavachari. A. Rendell. J. C. Burant. S. S. Iyengar. J. Tomasi. M. Cossi. N. Rega. J. M. Millam. M. Klene. J. E. Knox. J. B. Cross. V. Bakken. C. Adamo. J. Jaramillo. R. Gomperts. R. E. Stratmann. O. Yazyev. A. J. Austin. R. Cammi. C. Pomelli. J. W. Ochterski. R. L. Martin. K. Morokuma. V. G. Zakrzewski. G. A. Voth. P. Salvador. J. J. Dannenberg. S. Dapprich. A. D. Daniels. Ö. Farkas. J. B. Foresman. J. V. Ortiz. J. Cioslowski. and D. J. Fox. Gaussian. Inc. Wallingford CT. **2009**.

[2] Y. Zhao, D. G. Truhlar, *Theor. Chem. Acc.*, **2008**, 120, 215-241.

[3] P. C. Hariharan, J. A. Pople, *Theor. Chim. Acta* **1973**, *28*, 213-222.

[4] a) C. Gonzalez, H. B. Schlegel. *J. Chem. Phys.* **1989**, *90*, 2154-2161; b) C. Gonzalez, H. B. Schlegel. *J. Phys. Chem.* **1990**, *94*, 5523-5527.

[5] *Varetto, U. MOLEKEL 5.4; Swiss National Supercomputing Centre: Lugano (Switzerland)*

[6] a) R. F. W. Bader, *Atoms in Molecules: A Quantum Theory*; Oxford University Press: New-York Ed., **1990**; b) R. F. W. Bader, *Chem. Rev.* **1991**, *91*, 893-928.

[7] AIMAll (Version 10.10.11), Todd A. Keith, **2010** (aim.tkgristmill.com).

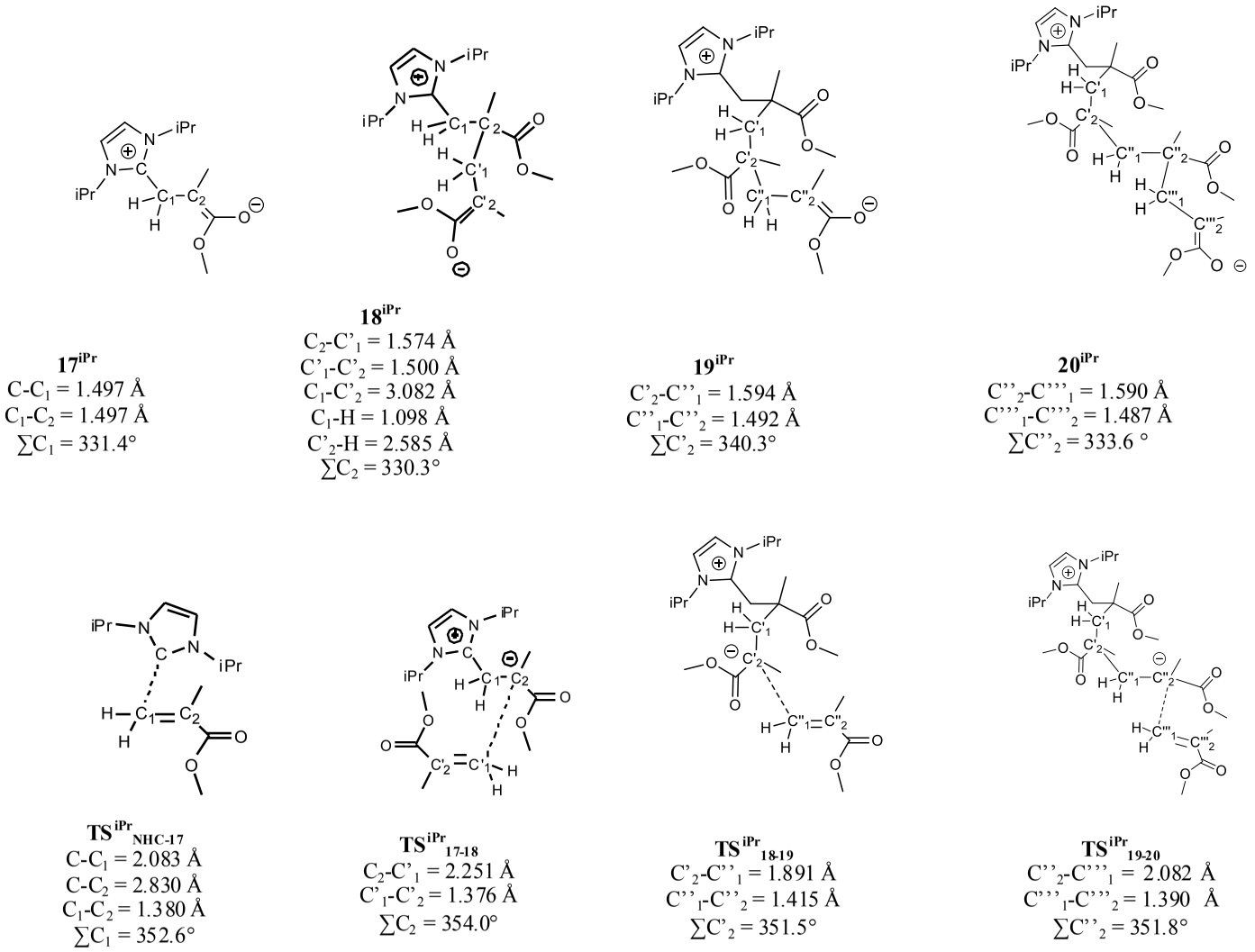

Figure S10. Selected bond lengths and bond angles (in Å and °, respectively) for the different minima and TS involved in the polymerization and cyclization process as optimized at the M06-2X/6-31G** level of theory for the NHC^{iPr}

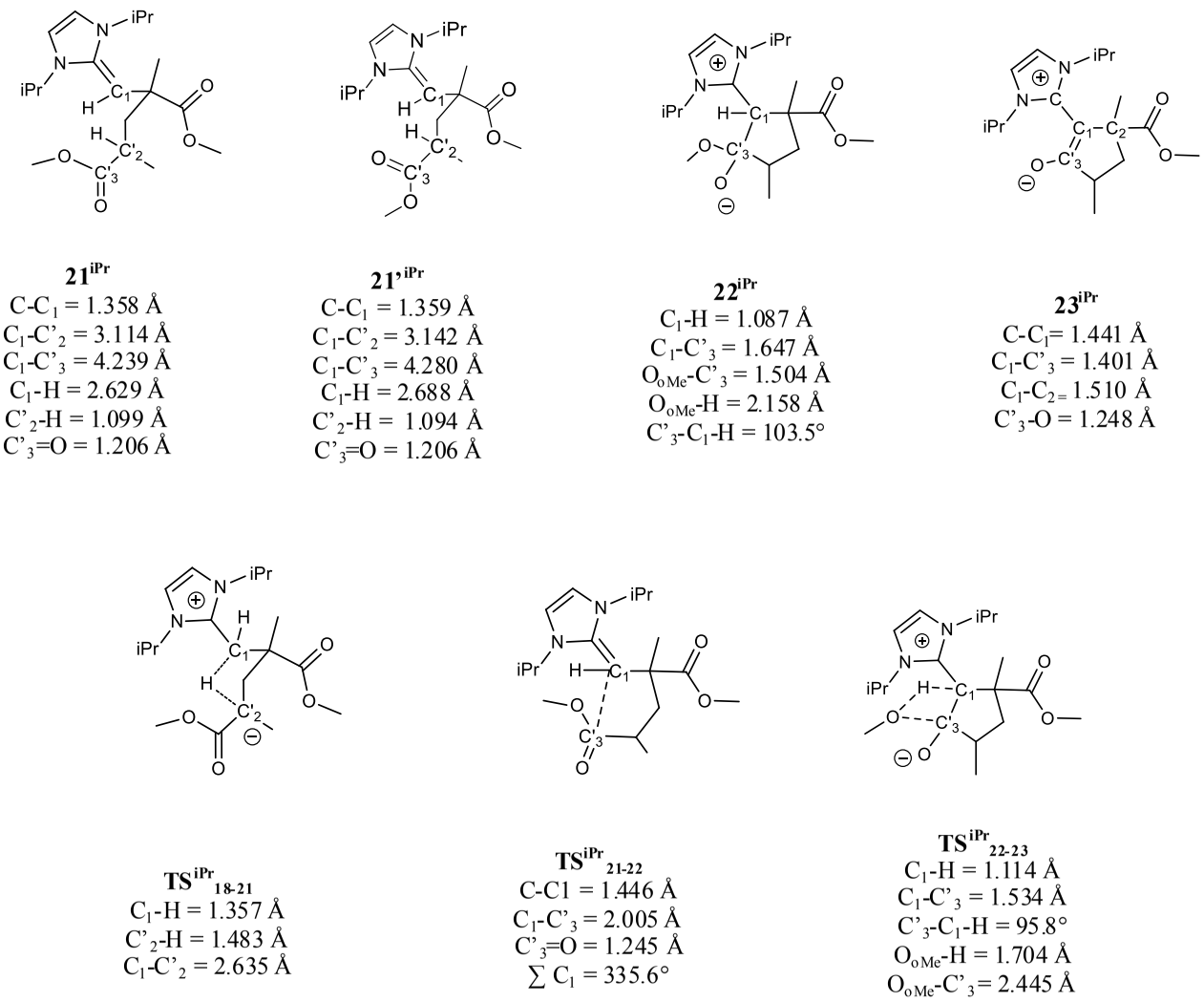

Figure S11. Selected bond lengths and bond angles (in Å and °, respectively) for the different minima and TS involved in the cyclization process as optimized at the M06-2X/6-31G** level of theory for the NHC^{iPr}

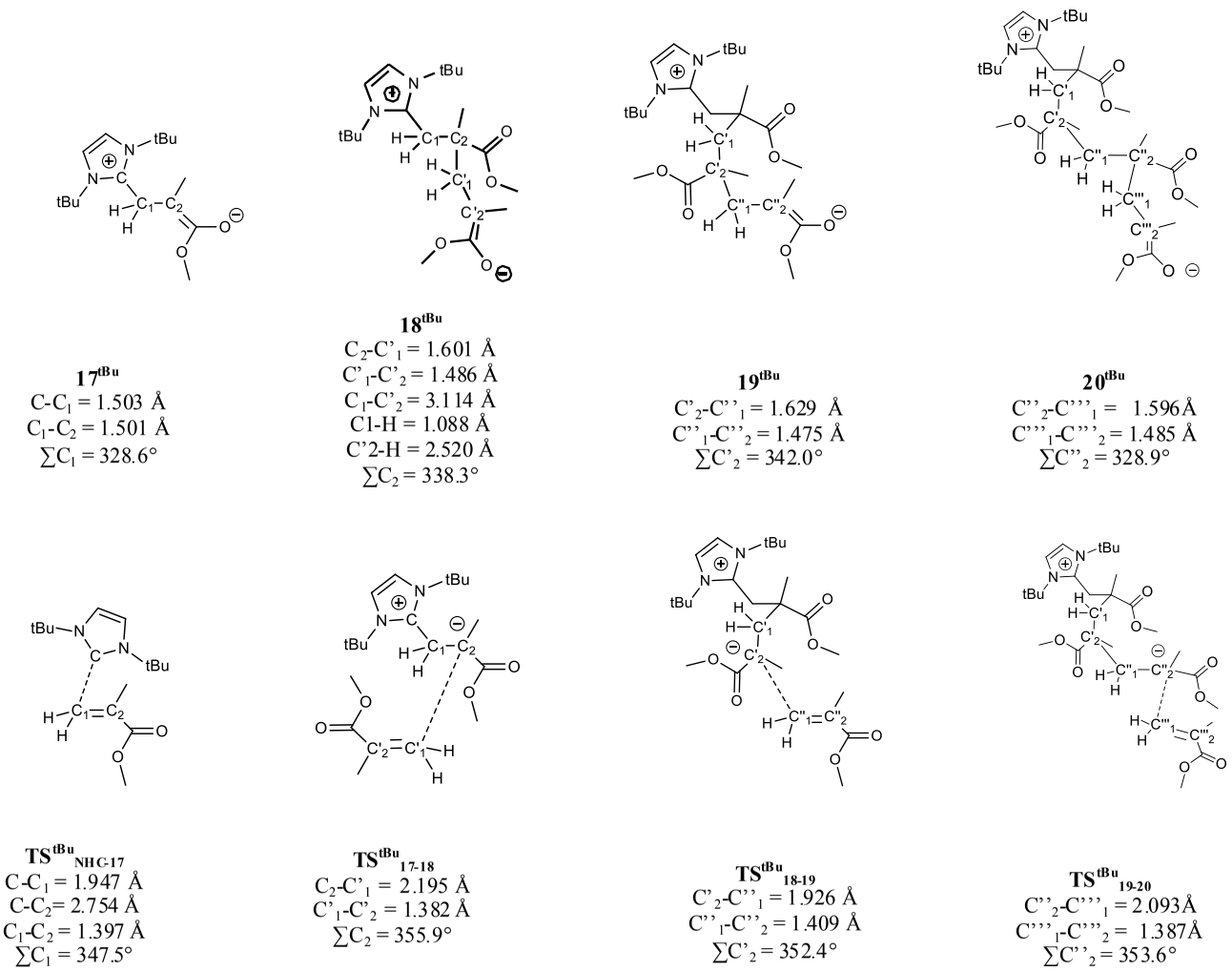

Figure S12. Selected bond lengths and bond angles (in Å and °, respectively) for the different minima and TS involved in the polymerization process as optimized at the M06-2X/6-31G**) level of theory for the NHC^{tBu}

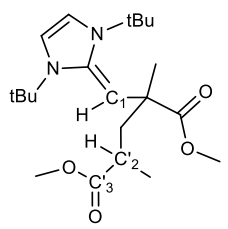

21^{tBu}
C-C_1 = 1.358 Å
C_1-H = 3.287 Å
C'_2-H = 1.095 Å
C_1-C'_2 = 3.067 Å
C'_3=O = 1.209 Å
C_1-C'_3 = 2.927Å

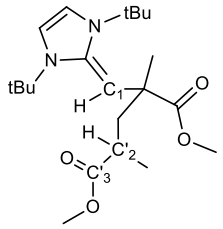

21'^{tBu}
C-C1 = 1.360 Å
C_1-H = 3.411 Å
C'_2-H = 1.094 Å
C_1-C'_2 = 3.138 Å
C'_3=O = 1.208 Å
C_1-C'_3 = 3.044 Å

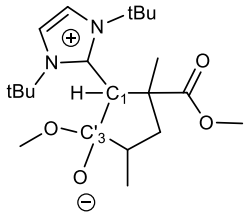

22^{tBu}
C_1-H = 1.083 Å
C_1-C'_3 = 1.640 Å
O_{oMe}-C'_3 = 1.517 Å
O_{oMe}-H = 2.095 Å
C'_3-C_1-H = 100.4°

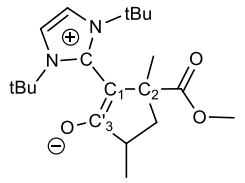

23^{tBu}
C-C_1= 1.449Å
C_1-C'_3 = 1.398Å
C_1-C_2 = 1.529Å
C'_3-O_{oMe} = 1.249 Å

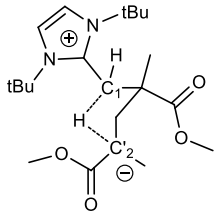

TS$^{tBu}_{18\text{-}21}$
C_1-H = 1.354 Å
C'_2-H = 1.495Å
C_1-C'_2 = 2.653 Å

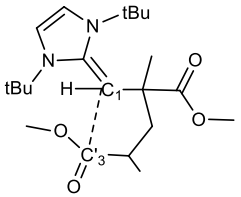

TS$^{tBu}_{21\text{-}22}$
C-C_1 = 1.458 Å
C_1-C'_3 = 1.922 Å
C'_3=O = 1.252 Å
∑ C_1 = 326.6°

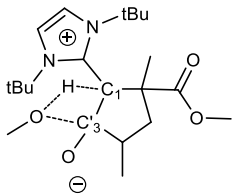

TS$^{tBu}_{22\text{-}23}$
C_1-H = 1.094Å
C_1-C'_3 = 1.543Å
C'_3-C_1-H = 96.8°
O_{oMe}-H = 1.793Å
O_{oMe}-C'_3 = 2.405Å

Figure S13. Selected bond lengths and bond angles (in Å and °, respectively) for the different minima and TS involved in the cyclization process as optimized at the M06-2X/6-31G**) level of theory for the NHC^{tBu}.

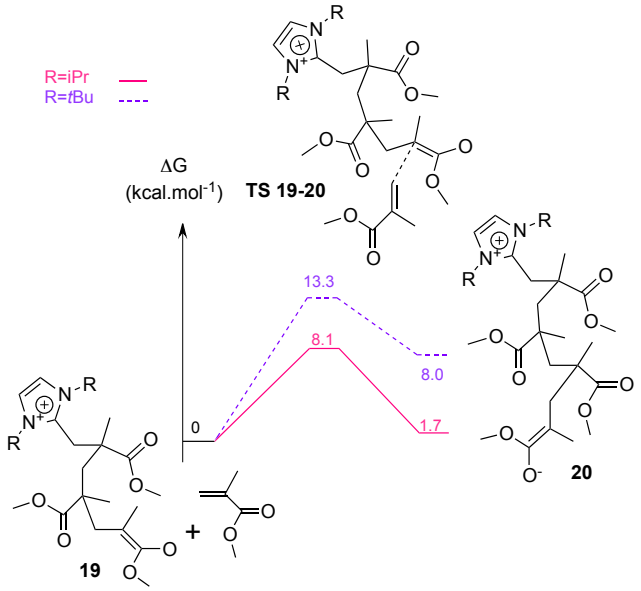

Figure S14. Energy profile (ΔG in kcal.mol^{-1}) for the addition of the fourth molecule of MMA in the polymerization process as optimized at the M06-2X/6-31G** level of theory for the NHC^{R} carbene (R : iPr, *t*Bu).

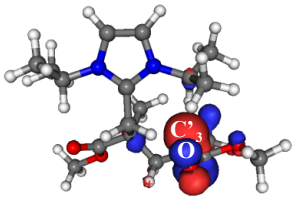

18^{iPr}
HOMO = -4.29eV

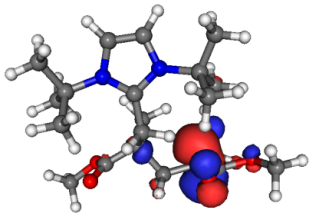

18^{tBu}
HOMO = -4.16eV

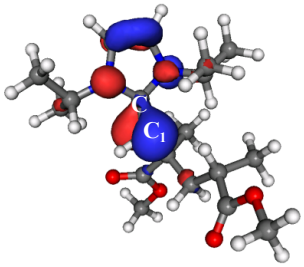

21^{iPr}
HOMO = -5.25eV

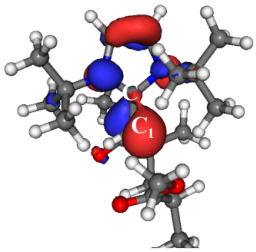

21^{tBu}
HOMO = -5.57eV

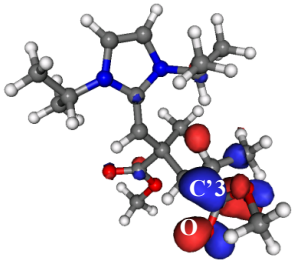

21^{iPr}
LUMO = 1.83eV

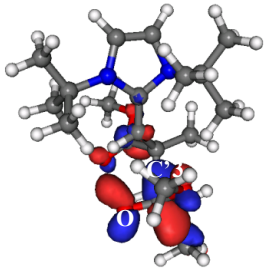

21^{tBu}
LUMO +1 = 1.90eV

Figure S15. Molecular plot (cutoff : 0.04) of the HOMO for compounds 3^{R} and of the two MO involved in the cyclization for 5^{R} [HOMO and LUMO (iPr) or LUMO+1 (tBu)], with R : iPr or ^{t}Bu.

References

(1) Kiesewetter, M. K.; Shin, E. J.; Hedrick, J. L.; Waymouth, R. M. *Macromolecules* **2010**, *43*, 2093.
(2) Fèvre, M.; Vignolle, J.; Gnanou, Y.; Taton, D. In *Polymer Science: A Comprehensive Reference*; Editors-in-Chief: Krzysztof, M., Martin, M. I., Eds.; Elsevier: Amsterdam, 2012, p 67.
(3) Dove, A. P. *ACS Macro Lett.* **2012**, 1409.
(4) Fèvre, M.; Pinaud, J.; Gnanou, Y.; Vignolle, J.; Taton, D. *Chem. Soc. Rev.* **2013**, *42*, 2142.
(5) Fuchise, K.; Chen, Y.; Satoh, T.; Kakuchi, T. *Polym. Chem.* **2013**.
(6) Scholten, M. D.; Hedrick, J. L.; Waymouth, R. M. *Macromolecules* **2008**, *41*, 7399.
(7) Raynaud, J.; Gnanou, Y.; Taton, D. *Macromolecules* **2009**, *42*, 5996.
(8) Zhang, Y.; Miyake, G. M.; Chen, E. Y. X. *Angew. Chem. Int. Ed.* **2010**, *49*, 10158.
(9) Zhang, Y.; Miyake, G. M.; John, M. G.; Falivene, L.; Caporaso, L.; Cavallo, L.; Chen, E. Y. X. *Dalton Trans.* **2012**, *41*, 9119.
(10) Zhang, Y.; Chen, E. Y. X. *Angew. Chem. Int. Ed.* **2012**, *51*, 2465.
(11) Zhang, Y.; Schmitt, M.; Falivene, L.; Caporaso, L.; Cavallo, L.; Chen, E. Y. X. *J. Am. Chem. Soc.* **2013**, *135*, 17925.
(12) Naumann, S.; Schmidt, F. G.; Schowner, R.; Frey, W.; Buchmeiser, M. R. *Polym. Chem.* **2013**, *4*, 2731.
(13) Biju, A. T.; Padmanaban, M.; Wurz, N. E.; Glorius, F. *Angew. Chem. Int. Ed.* **2011**, *50*, 8412.
(14) Bugaut, X.; Glorius, F. *Chem. Soc. Rev.* **2012**, *41*, 3511.
(15) Ryan, S. J.; Candish, L.; Lupton, D. W. *Chem. Soc. Rev.* **2013**, *42*, 4906.
(16) Chauhan, P.; Enders, D. *Angew. Chem. Int. Ed.* **2014**, *53*, 1485.
(17) Martin, D.; Canac, Y.; Lavallo, V.; Bertrand, G. *J. Am. Chem. Soc.* **2014**, *136*, 5023.
(18) Hopkinson, M. N.; Richter, C.; Schedler, M.; Glorius, F. *Nature* **2014**, *510*, 485.
(19) Delaude, L. *Eur. J. Inorg. Chem.* **2009**, *2009*, 1681.
(20) Delaude, L.; Demonceau, A.; Wouters, J. *Eur. J. Inorg. Chem.* **2009**, *2009*, 1882.
(21) Tskhovrebov, A. G.; Vuichoud, B.; Solari, E.; Scopelliti, R.; Severin, K. *J. Am. Chem. Soc.* **2013**, *135*, 9486.
(22) Berkessel, A.; Elfert, S.; Etzenbach-Effers, K.; Teles, J. H. *Angew. Chem. Int. Ed.* **2010**, *49*, 7120.
(23) Berkessel, A.; Elfert, S.; Yatham, V. R.; Neudörfl, J.-M.; Schlörer, N. E.; Teles, J. H. *Angew. Chem. Int. Ed.* **2012**, *51*, 12370.
(24) Berkessel, A.; Yatham, V. R.; Elfert, S.; Neudörfl, J.-M. *Angew. Chem. Int. Ed.* **2013**, *52*, 11158.
(25) Maji, B.; Mayr, H. *Angew. Chem. Int. Ed.* **2013**, *52*, 11163.
(26) Hans, M.; Wouters, J.; Demonceau, A.; Delaude, L. *Chem. Eur. J.* **2013**, *19*, 9668.
(27) Li, H.; Risko, C.; Seo, J. H.; Campbell, C.; Wu, G.; Brédas, J.-L.; Bazan, G. C. *J. Am. Chem. Soc.* **2011**, *133*, 12410.
(28) Biju, A. T.; Kuhl, N.; Glorius, F. *Acc. Chem. Res.* **2011**, *44*, 1182.
(29) Grossmann, A.; Enders, D. *Angew. Chem., Int. Ed.* **2012**, *51*, 314.
(30) Izquierdo, J.; Hutson, G. E.; Cohen, D. T.; Scheidt, K. A. *Angew. Chem. Int. Ed.* **2012**, *51*, 11686.
(31) Sarkar, S. D.; Biswas, A.; Samanta, R. C.; Studer, A. *Chem. Eur. J.* **2013**, *19*, 4664.
(32) Matsuoka, S.-I.; Ota, Y.; Washio, A.; Katada, A.; Ichioka, K.; Takagi, K.; Suzuki, M. *Org. Lett.* **2011**, *13*, 3722.
(33) Kato, T.; Ota, Y.; Matsuoka, S.-I.; Takagi, K.; Suzuki, M. *J. Org. Chem.* **2013**, *78*, 8739.
(34) Matsuoka, S.-I.; Namera, S.; Washio, A.; Takagi, K.; Suzuki, M. *Org. Lett.* **2013**, *15*, 5916.
(35) Kato, T.; Matsuoka, S.-I.; Suzuki, M. *J. Org. Chem.* **2014**, *79*, 4484.
(36) Busnel, J. P. *Polymer* **1982**, *23*, 137.
(37) Culkin, D. A.; Jeong, W.; Csihony, S.; Gomez, E. D.; Balsara, N. P.; Hedrick, J. L.; Waymouth, R. M. *Angew Chem Int Ed* **2007**, *46*, 2627.

(38) Shin, E. J.; Brown, H. A.; Gonzalez, S.; Jeong, W.; Hedrick, J. L.; Waymouth, R. M. *Angew. Chem. Int. Ed.* **2011**, *50*, 6388.
(39) Shin, E. J.; Jeong, W.; Brown, H. A.; Koo, B. J.; Hedrick, J. L.; Waymouth, R. M. *Macromolecules* **2011**, *44*, 2773.
(40) Brown, H. A.; Xiong, S.; Medvedev, G. A.; Chang, Y. A.; Abu-Omar, M. M.; Caruthers, J. M.; Waymouth, R. M. *Macromolecules* **2014**.
(41) Guo, L.; Zhang, D. *J. Am. Chem. Soc.* **2009**, *131*, 18072.
(42) Brown, H. A.; Chang, Y. A.; Waymouth, R. M. *J. Am. Chem. Soc.* **2013**, *135*, 18738.
(43) Gerner, F. J.; Höcker, H.; Müller, A. H. E.; Schulz, G. V. *Eur. Polym. J.* **1984**, *20*, 349.
(44) Baskaran, D. *Prog. Polym. Sci.* **2003**, *28*, 521.
(45) Baskaran, D.; Müller, A. H. E. *Prog. Polym. Sci.* **2007**, *32*, 173.
(46) Raynaud, J.; Absalon, C.; Gnanou, Y.; Taton, D. *Macromolecules* **2010**, *43*, 2814.
(47) Raynaud, J.; Nzahou Ottou, W.; Gnanou, Y.; Taton, D. *Chem. Commun.* **2010**, *46*, 3203.
(48) Hatada, K.; Kitayama, T. In *NMR Spectroscopy of Polymers*; Springer Berlin Heidelberg: **2004**, p 73.
(49) Sogah, D. Y.; Hertler, W. R.; Webster, O. W.; Cohen, G. M. *Macromolecules* **1987**, *20*, 1473.
(50) Baskaran, D.; Müller, A. H. E. Anionic Vinyl Polymerization,In *Controlled and Living Polymerizations*; Wiley-VCH Verlag GmbH & Co. KGaA: 2010, p 1.
(51) CCDC-242948 contains the supplementary crystallographic data for this paper. These data can be obtained free of charge via http://www.ccdc.cam.ac.uk/conts/retrieving.html (or from the Cambridge Crystallographic Data Centre,deposit@ccdc.cam.uk).
(52) Raynaud, J.; Ciolino, A.; Baceiredo, A.; Destarac, M.; Bonnette, F.; Kato, T.; Gnanou, Y.; Taton, D. *Angew. Chem., Int. Ed.* **2008**, *47*, 5390.
(53) Raynaud, J.; Liu, N.; Gnanou, Y.; Taton, D. *Macromolecules* **2010**, *43*, 8853.
(54) Raynaud, J.; Liu, N.; Fevre, M.; Gnanou, Y.; Taton, D. *Polym. Chem.* **2011**, *2*, 1706.
(55) Müller, A. H. E. *Die Makromolekulare Chemie* **1981**, *182*, 2863.
(56) Bütün, V.; Armes, S. P.; Billingham, N. C. *Polymer* **2001**, *42*, 5993.
(57) Rungsardthong, U.; Ehtezazi, T.; Bailey, L.; Armes, S. P.; Garnett, M. C.; Stolnik, S. *Biomacromolecules* **2003**, *4*, 683.
(58) Plamper, F. A.; Ruppel, M.; Schmalz, A.; Borisov, O.; Ballauff, M.; Müller, A. H. E. *Macromolecules* **2007**, *40*, 8361.
(59) Agut, W.; Taton, D.; Brûlet, A.; Sandre, O.; Lecommandoux, S. *Soft Matter* **2011**, *7*, 9744.
(60) Raynaud, J.; Absalon, C.; Gnanou, Y.; Taton, D. *J. Am. Chem. Soc.* **2009**, *131*, 3201.
(61) Fischer, C.; Smith, S. W.; Powell, D. A.; Fu, G. C. *J. Am. Chem. Soc.* **2006**, *128*, 1472.

Chapter 3.

Polymerization of methyl (meth)acrylate catalyzed by a *N*-heterocyclic carbene in the presence of alcohols as chain regulators

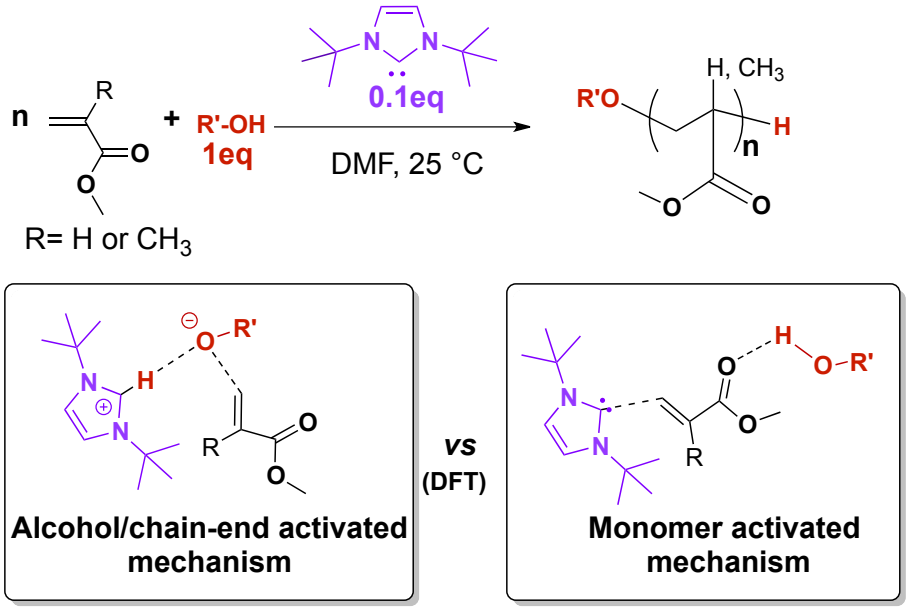

Keywords: Organocatalysis • *N*-Heterocyclic Carbenes • Alcohols• Polymerization • methyl (meth)acrylate • DFT calculations • Concerted mechanisms •

Chapter 3.
Polymerization of methyl (meth)acrylate catalyzed by a *N*-heterocyclic carbene in the presence of alcohols as chain regulators

Table of contents

Introduction

As highlighted in the previous chapters, *N*-heterocyclic carbenes (NHCs) are powerful nucleophiles that can react with Michael (meth)acrylate acceptors in various ways.[1-8] Indeed, it has been demonstrated that the azolium (imidazolium or triazolium) enolate resulting from the initial 1,4-addition of the carbene to methyl methacrylate (MMA) can further react *via* a [1,2-H] shift or by a 1,4-addition onto a second molecule of MMA (Figure 1).

Different 1:1 or 1:2 carbene/MMA adducts have thus been isolated (Figure 1; paths A_1 and A_2).[1-3,6,7] In contrast, multiple 1,4-additions of MMA can be initiated by 1,3-bis(*tert*-butyl)imidazol-2-ylidene (NHC^{tBu}), ultimately leading to poly(methyl methacrylate) (PMMA; path C)[6,9,10]

In chapter 2, we have demonstrated that 1,3-bis(isopropyl)imidazol-2-ylidene (NHC^{iPr}) unexpectedly led to an imidazolium ester enolate cyclodimer (NHC^{iPr}:MMA = 1:2), further evidencing the remarkable selectivity of NHCs towards MMA (path B).[6,7,9-11] Differences also appeared when screening miscellaneous acrylates and their methacrylic analogues. Indeed, NHC^{tBu} induced the polymerization of both acrylate and methacrylate monomers, while NHC^{iPr} was only active towards acrylates. Although experimental evidences are lacking, one can hypothesize the formation of such cyclodimer adduct between NHC^{iPr} and other methacrylate substrates, which would explain the absence of polymers in these cases. It is worth pointing out that, in such direct conjugate-addition polymerizations, NHC plays the role of an initiator and not that of a catalyst.

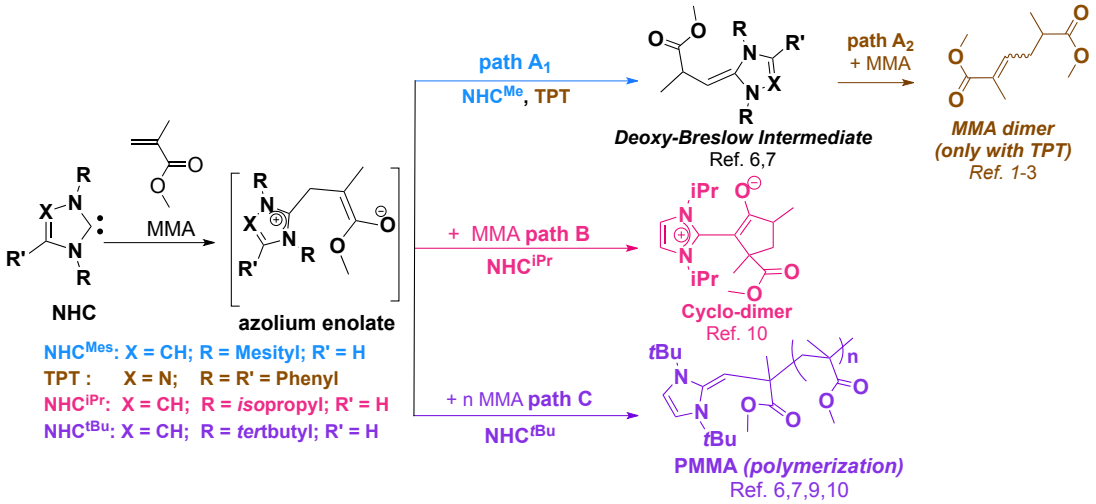

Figure 1. Scope of NHCs reactivity towards methyl methacrylate (MMA).

The NHC-catalyzed group transfer polymerization (GTP) of alkyl (meth)acrylates using silyl ketene acetals (SKA's) as initiators has been reported, both by Hedrick, Waymouth *et al.* and our group.[12-16] These SKA's are also rather expensive and unstable compounds.

Therefore, there would be a great need to employ widespread reagents for organo-catalyzed polymerization of alkyl (meth)acrylic monomers.

In the presence of protic initiators (mainly alcohols), NHCs were found to efficiently catalyze the ring-opening polymerizations (ROP) of cyclic monomers, such as cyclic esters (lactides and lactones), cyclic ethers (ethylene and propylene oxides) and cyclic carbonates (see section 4 of chapter 1).[17,18] These polymerizations were proposed to proceed either through a nucleophilic activated-monomer mechanism (AMM, see Scheme 2 in chapter 1) or by a hydrogen-bonding activated-alcohol mechanism (ACEM, see Scheme 4a in chapter 1), depending on the alcohol concentration. In such polymerizations, the alkoxide chain growing species may interact with the alcohol, during the polymerization, as illustrated in Scheme 1a.

Based on these successful ROP's using NHC/alcohol association, and following our investigations discussed in chapter 2, we were interested in the polymerization of alkyl (meth)acrylics using the peculiar NHC$^{t\mathrm{Bu}}$ as catalyst, in the presence of alcohols as chain regulators. Our first intuition was that alcohols would irreversibly deactivate the propagating enolate species, through C-H bond formation, after protonation of the enolate (Scheme 1b). In contrary, our preliminary results (see sections 4.2 in chapter 2) demonstrated that the polymerization continued to proceed even with alcohol in the medium, providing an excellent control over molar masses and dispersities.

a) rapid exchange in ROP of cyclic esters (ethers) in presence of ROH

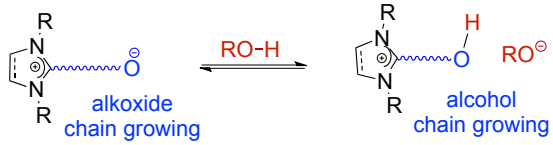

b) expected chain termination in ZP of (meth)acrylics in presence of ROH

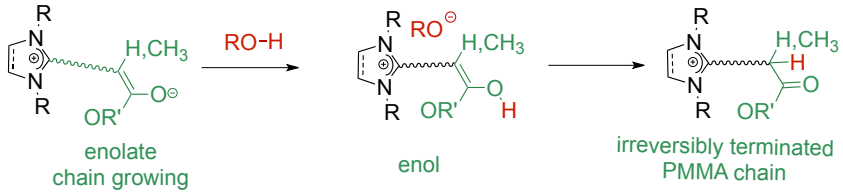

Scheme 1. Interaction between active chain-end and ROH: a) in the ROP of cyclic esters (ethers); b) in ZP of (meth)acrylics.

In the present chapter, we aim at investigating the use of simple alcohols (ROH) as initiators for the NHC-catalyzed polymerization of both methyl acrylate (MA) and methyl methacrylate (MMA) (Figure 2). A reactivity screening of various NHCs and alcohols is presented first. Parameters influencing the polymerization (*e.g.* concentration, order of addition of the reagents), as well as the control and "living" behavior of these polymerizations

were also studied in details. Experimental and computational investigations on the polymerization mechanism are thus discussed. Preliminary results regarding block copolymerization experiments of MMA and MA are finally presented.

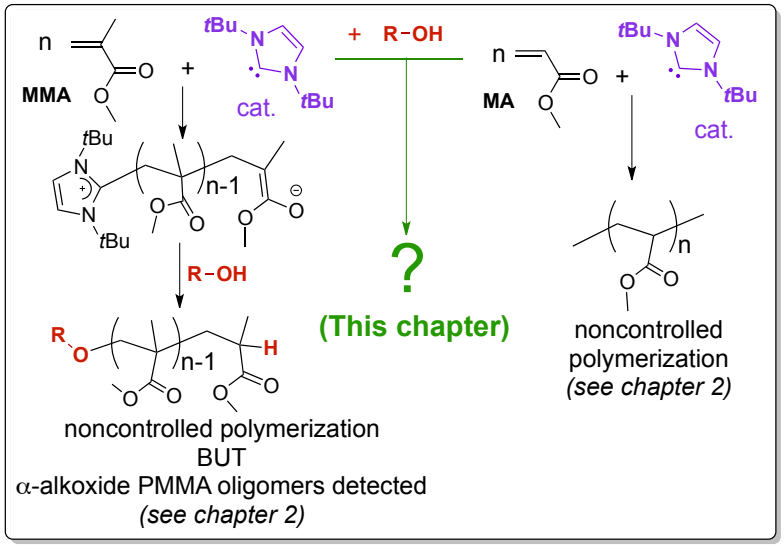

Figure 2. Scope of NHC^{tBu}-mediated polymerization of MA and MMA in DMF at 25 °C.

1. Polymerization of methyl methacrylate (MMA) by NHCs and ROH: reactivity screening

1.1. NHC effect

As emphasized above, the alkyl or aryl substituents of the NHC have a dramatic influence on the carbene reactivity towards a given substrate such as MMA. Among the imidazole-ylidenes, 1,3-bis(mesityl)imidazol-2-ylidene (NHC^{Mes} in Figure 3, pKa^{DMSO} = 17.0)[19] and 1,3-bis(isopropyl)imidazol-2-ylidene (NHC^{iPr}, pKa^{DMSO} = 22.3)[19] were reported to form the so-called deoxy-Breslow intermediate and cyclodimer adduct, respectively, when reacting with MMA (see Figure 1).[6,7,10] In contrast, 1,3-bis(*tert*-butyl)imidazol-2-ylidene (NHC^{tBu}, pKa^{DMSO} = 22.8)[19] was found to initiate the polymerization of MMA, but with a low carbene efficiency, and the occurrence of chain termination reactions.[6,7]

Here, the catalytic activity of these three NHCs, in presence of alcohols as initiators was investigated for the polymerization of MMA. For a sake of comparison, we also studied 1,3–bis(isopropyl)-4,5-(dimethyl)imidazol-2-ylidene (NHC^{iPrMe}, pKa^{DMSO} = 24.7)[19], which was reported to induce the direct polymerization of *tert*-butyl acrylate.[12]

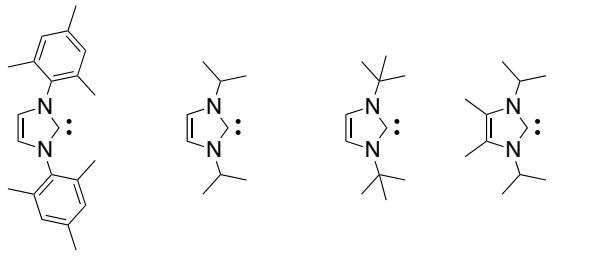

Figure 3. Structures of NHCs studied in this work (pKa values are those reported in ref.19, in DMSO).

For this preliminary screening, benzyl alcohol (BnOH) was selected, as initiator because its presence in α-position of polymer chains was expected to be easily revealed, both by NMR and UV spectroscopies. Polymerizations of MMA ($[MMA]_0$ = 9.4 mM) were thus carried out in the presence of each NHC as catalyst ($[NHC]_0$ = 47 µM) and BnOH as initiator ($[BnOH]_0$ = 0.94 mM), in DMF at 25 °C. The results obtained are summarized in Table 1.

Table 1. NHC^{tBu}-catalyzed polymerization of MMA in presence of BnOH in DMF at 25 °C.

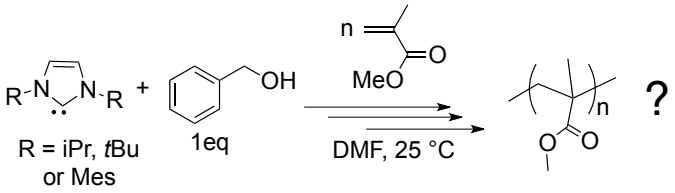

entry	NHC	$[NHC]_0/[BnOH]_0/[MMA]_0$	Time (h)	Conv.[a] (%)	$\overline{M_n}^{theo}$ [b] (g.mol^{-1})	$\overline{M_n}$ [c] (g.mol^{-1})	$Đ$ [c]
1	NHC^{Mes}	0.05/1/10	36	0	-	-	-
2	NHC^{iPr}	0.05/1/10	36	0	-	-	-
4	NHC^{iPrMe}	0.05/1/10	24 (72)	20	n.d.	n.d.	n.d.
3	NHC^{tBu}	0.05/1/10	5	96	960	725	1.2

a. Conv.= % monomer conversion determined by ^{1}H NMR spectroscopy; b. Theoretical molar mass $\overline{M}_n^{theo} = M_{ROH} + M_{MMA} \times \frac{[MMA]}{[ROH]} \times conv.$; c Characterization of PMMA's by SEC in THF using polystyrene standards for calibration.

Intriguingly, no polymer was formed when attempting to polymerize MMA with NHC catalysts others than NHC^{tBu}, in the presence of BnOH (Table 1, entries 1-3). Furthermore, NHC^{iPr} gave rise to the same cyclodimer product observed in absence of alcohol and that has been described in details in chapter 2.[10] This is illustrated in the ^{1}H NMR spectrum of the reaction product (Figure 4).

Hence, the presence of BnOH did not play any key role in this reaction pathway, and could not prevent the formation of the cyclodimer from occurring. Note that the stoichiometric

reaction of NHC^{iPr} with BnOH (Figure 4b) led to a downfield shift of the hydroxyl proton from (5.15 to 7.82 ppm), in accordance to the formation of a [NHC…H…OBn] complex.

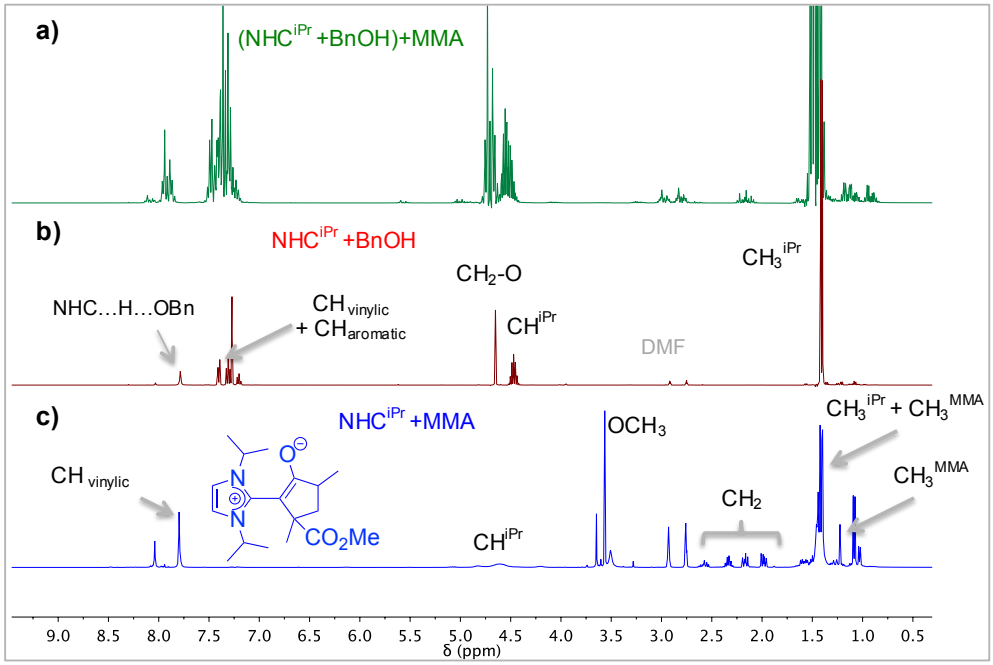

Figure 4. ^{1}H NMR spectra in DMF-d$_7$ of: a) NHC^{iPr}/BnOH/MMA (1/1/1); b) NHC^{iPr}/BnOH (1/1); c) NHC^{iPr}/MMA (1/1) (see also chapter 2 for a complete distribution and discussion about the cyclodimer formation).

Although NHC^{iPrMe} was the most basic and nucleophilic carbene of this series, it gave almost no polymer at all, neither in presence (20 % of conversion after 36 h or 72 h; entry 4) nor in absence of the alcohol (17 % of MMA conversion after 36 h or 72 h). This observation demonstrated that the deprotonation of the alcohol by the carbene was not a key step of the polymerization involving of NHC^{tBu}, in contrast to the classical oxy-anionic polymerization of MMA where the alkoxide formation was essential.[20-22]

This reactivity screening of NHCs again evidenced the selectivity of NHC^{tBu} as appropriate organocatalyst to trigger MMA polymerization. This carbene was thus selected to catalyze the polymerization of MMA in presence of various alcohols.

1.2. Alcohol effect

To demonstrate the versatility of this NHC^{tBu}-catalyzed polymerization, mono- and dihydroxylated compounds were tested as initiators/chain regulators. The structure of these precursors with their name and abbreviation is shown in Figure 5.

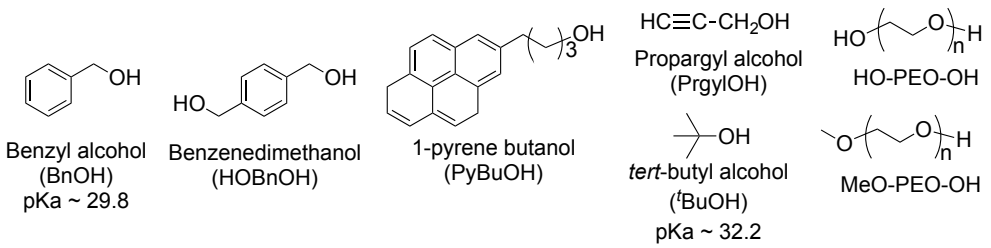

Figure 5. Structures of chain regulators studied in this work. (pKa values are those reported in ref. 23 in DMSO).

1.2.1. Polymerization with molecular ROH

MMA polymerization was again performed at 25 °C, in the presence of NHC^{tBu} as catalyst and the alcohol as initiator in DMF (Table 2). Poly(methy methacrylate)s (PMMA's) of low molar masses, *i.e.* $\overline{M_n}$ ≈ 1,000-2,000 g.mol^{-1} were purposely targeted to facilitate the characterization of polymer chain-ends.

Table 2. NHC^{tBu}-catalyzed polymerizations in presence of various ROH in DMF at 25 °C.

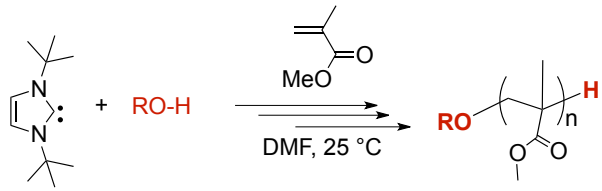

entry	ROH	[NHC^{tBu}]$_0$/ [ROH]$_0$/ [MMA]$_0$	Time (h)	Conv.^{a} (%)	$\overline{M_n}^{theo\ b}$ (g.mol^{-1})	$\overline{M_n}^{NMR\ c}$ (g.mol^{-1})	$\overline{M_n}^{SEC\ d}$ (g.mol^{-1})	$M_p^{SEC\ d}$ (g.mol^{-1})	$Đ^d$
1	BnOH	0.1/1/10	24	100	1,100	1,100	1,400	1,830	1.3
2	PyBuOH	0.1/1/10	24	100	1,300	1,400	1,300	1,800	1.4
3	PrgylOH	0.1/1/10	24	10	100	n.d.	n.d.	n.d.	n.d.
4	HOBnOH	0.1/0.5/10	7	100	2,140	1,500 2,900	2,900	3,600	1.8
5	^{t}BuOH	0.1/1/10	24 (96)	72 (100)	1,000	n.d	7,700	8,100	1.3

a. Conv.= % monomer conversion determined by ^{1}H NMR spectroscopy; b. Theoretical molar mass $\overline{M_n}^{theo} = M_{ROH} + M_{MMA} \times \frac{[MMA]}{[ROH]} \times conv.$; c. $\overline{M_n}$ determined by ^{1}H NMR based on chain-end protons integration.
d. Characterization of PMMA's by SEC in THF using PS standards for calibration.

As illustrated in Figure 6, PMMA's generated from primary mono-alcohols, such as BnOH and pyrene-butanol (PyBuOH), showed monomodal distribution of molar masses $\overline{M_n}$, with $\overline{M_n}$ values in close agreement with the expected values based on the initial monomer-to alcohol [MMA]$_0$/[R-CH$_2$OH]$_0$ ratio (Table 2, entries 1-2). It has to be mentioned that the true molar masses M_n and M_w of these PMMA's could be calculated by multiplying equivalent polystyrene molar masses (obtained by SEC analysis) by the correction factor B = 1.10 (Benoit factor for PMMA).[24]

The absorbance detected in the UV SEC traces at λ = 260 nm and 305 nm demonstrated the presence of the benzyl and the pyrene end groups, respectively (Figure 6).

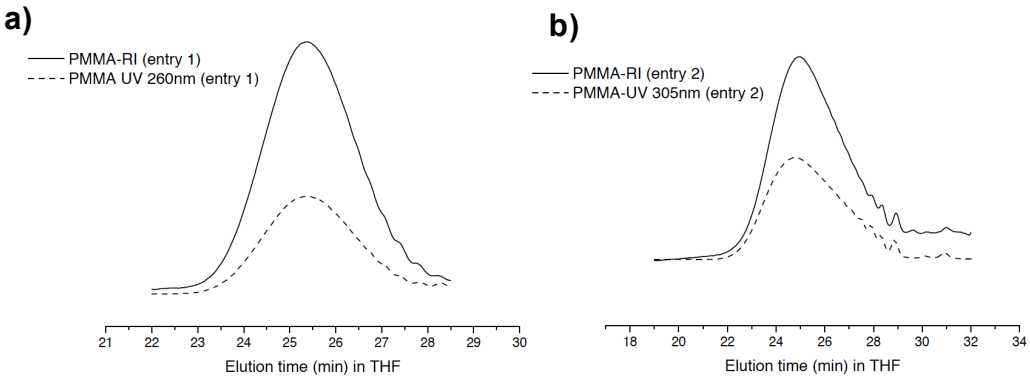

Figure 6. SEC traces of PMMA's obtained with: a) NHC^{tBu}/ BnOH (Table 2 entry 1); b) NHC^{tBu}/ PyBuOH (entry 2) in in DMF at 25 °C.

In both cases, the ^{1}H NMR spectrum (Figure 7 and 8) of corresponding PMMA's –that were precipitated twice in cold methanol– revealed the presence of the benzyl and the pyrene groups in α-position (δ_{CH2} = 4-5 ppm and $\delta_{aromatic}$ = 7-8 ppm, respectively), the calculated molar mass being in accordance with the theoretical value ($\overline{M_n}^{NMR} \approx \overline{M_n}^{theo}$ = 1,200 g.mol^{-1}). Furthermore, the tacticity of these polymers (based on the integration of CH_3 groups signal)[25] was as follows: syndiotacticity (% of triad rr) = 51 %, heterotacticity (% of triad mr) = 41 % and isotacticity (% of triad mm) = 8 %. Such tacticity is similar to that generally observed for PMMA produced by anionic polymerization in THF at r.t (% rr/mr/mm = 56/39/5).[26,27]

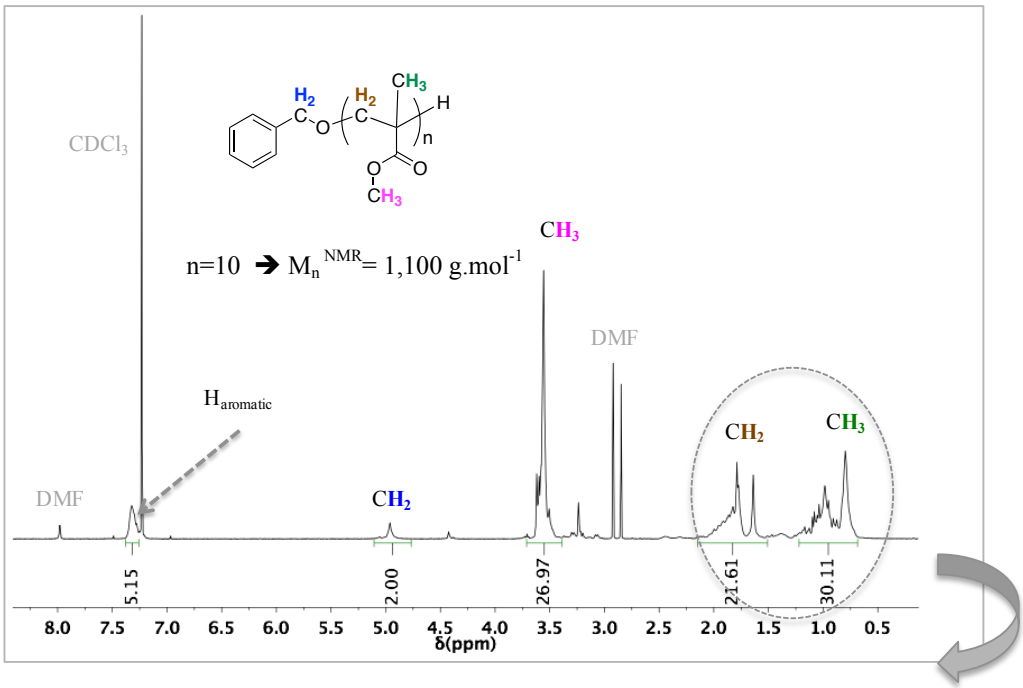

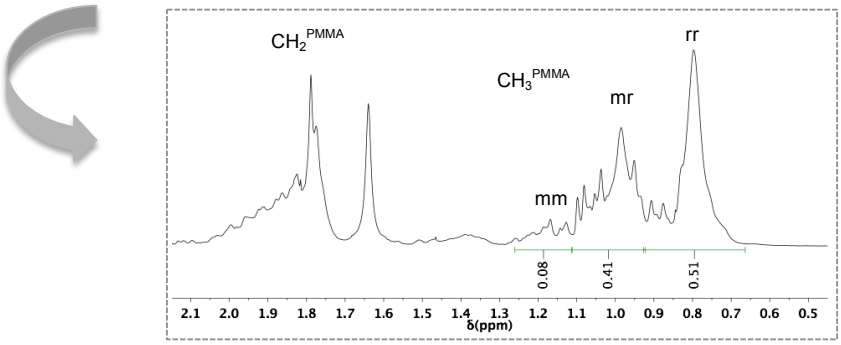

Figure 7. ^{1}H NMR (in $CDCl_3$) spectrum of α-benzyloxy,ω-H PMMA ($[MMA]_0/[BnOH]_0$ = 10 Table 2, entry 1).

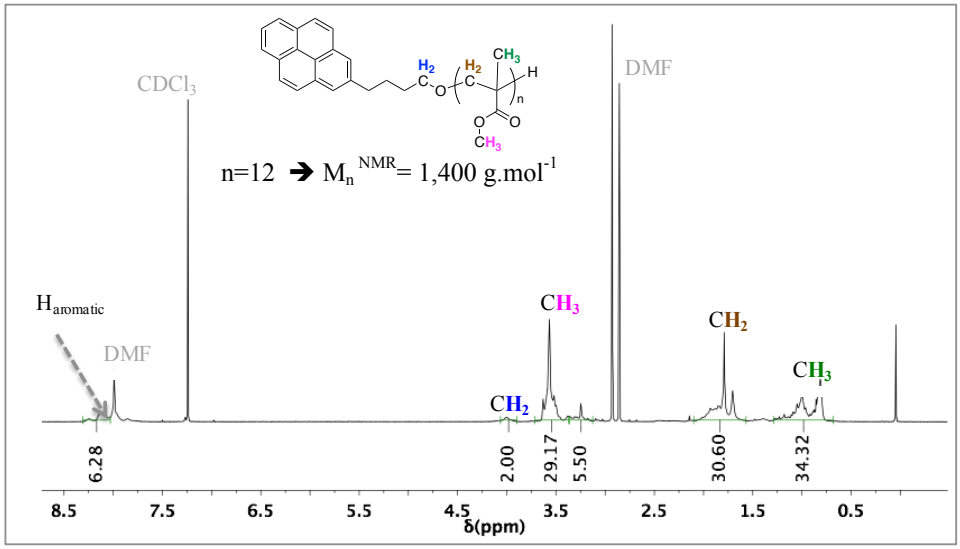

Figure 8. ^{1}H NMR (in $CDCl_3$) spectrum of α-pyrenebutanoxy,ω-H PMMA ($[MMA]_0/[PyBuOH]_0$ = 10 Table 2, entry 2).

The MALDI-ToF spectrum of both samples (Figure 9 and 10) showed the presence of four distinct populations (A, B, C and D), with peak-to-peak mass increment of 100 mass units (= mass of one MMA unit) in all cases.

Population A was in agreement with the formation of α-benzyloxy (or α-pyrenebutanoxy) PMMA chains (initiation by BnOH or PyBuOH in Scheme 2). Population B likely resulted from a chemical modification of population A by release of NaH during ionization (Scheme 2). Population C was ascribed to α-1,3 bis(*tert*-butyl)imidazolium PMMA's generated by the direct initiation of MMA polymerization by NHC^{tBu} *via* the formation of a zwitterionic enolate **1** (Scheme 2).

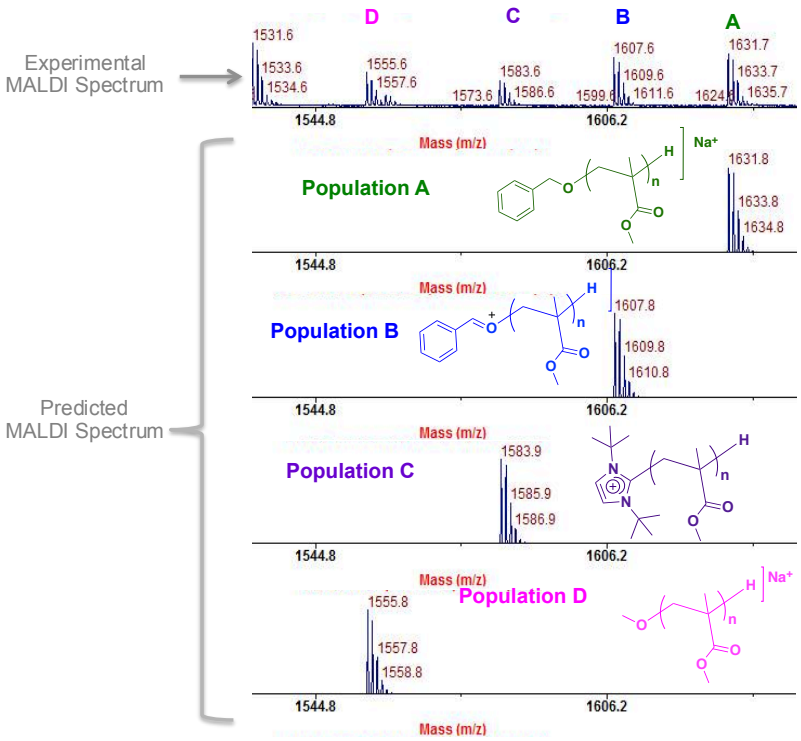

Figure 9. MALDI-ToF spectrum of α-benzyloxy,ω-H PMMA (Table 2, entry 1).

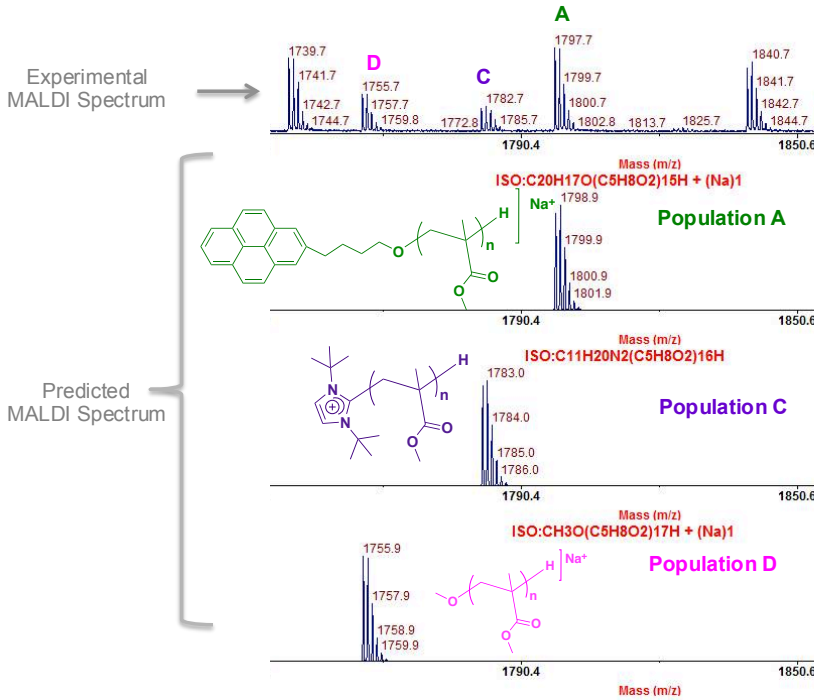

Figure 10. MALDI-ToF spectrum of α-pyrenebutanoxy,ω-H PMMA (Table 2, entry 2).

Finally, population D could correspond to α-methoxy PMMA chains arising from methoxide generated after the attack of NHC^{tBu} onto the carbonyl group of MMA, forming the acyl imidazolium methoxide **3** (Scheme 2). The latter species could then (1) either displace the carbene moiety of an α-imidazolium PMMA growing chain **2**, or (2) initiate new PMMA chains. As already discussed in chapter 2, we assumed that the first hypothesis was more likely, based on similar observations during the NHC-catalyzed ROP of ethylene and propylene oxides in presence of alcohol derivatives.[28-30]

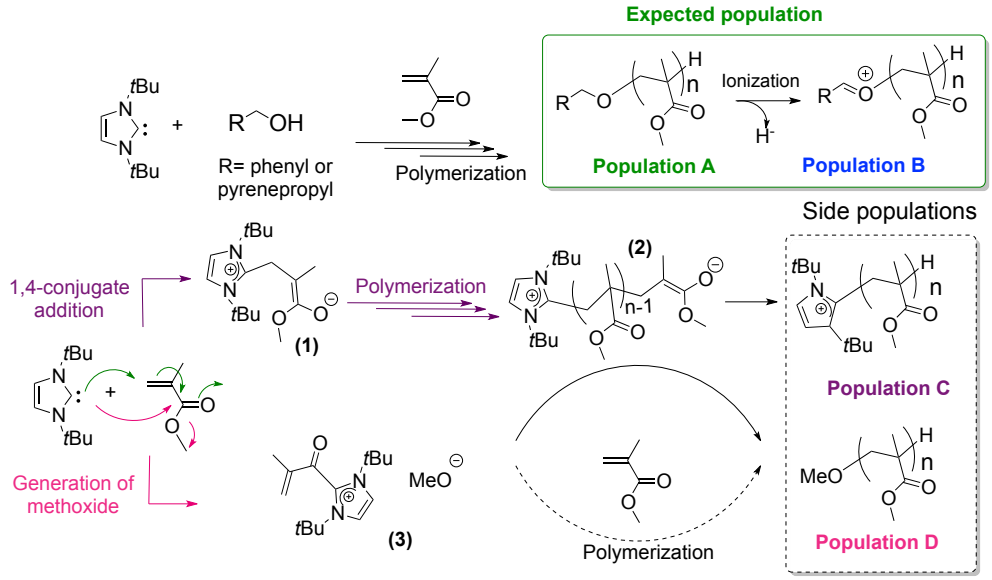

Scheme 2. Different reactions of NHC^{tBu} towards MMA producing populations observed in MALDI-ToF spectrum.

Since experimental molar masses as determined both by SEC and NMR were in good agreement with theoretical values at a low $[MMA]_0/[ROH]_0$ ratios, the relative proportion of the different populations in MALDI-ToF spectrum did not seem to reflect the sample composition. Hence, we assumed that both populations C and D were not representative of the sample composition.

With propargyl alcohol (PrgylOH) as initiator (entry 3), almost no polymerization was noted. This could presumably be due to the presence the relatively acidic proton of the propargyl group (pKa^{DMSO} = 20-21) that might have deactivated the carbene NHC^{tBu} (pKa^{DMSO} = 22.8)[19] and formed an imidazolium propargyl anion **4** (Scheme 3).

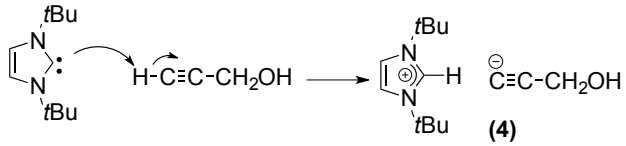

Scheme 3. Quenching of the NHC upon reaction with propargyl alcohol.

In the case of the di-hydroxylated chain regulator, namely, 1,4-benzenedimethanol (OHBnOH), the polymerization was less controlled (entry 4) than with BnOH. Indeed, a shoulder was clearly visible in the SEC traces in the high molar mass region (Figure 11) and a higher dispersity $Đ$ = 1.8 was obtained.

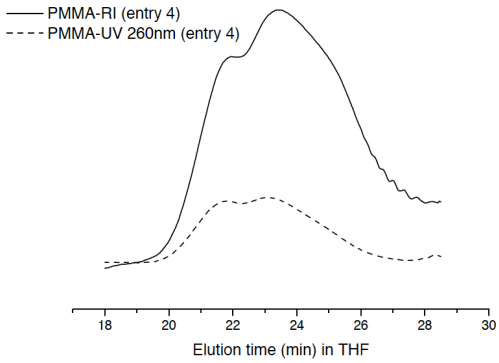

Figure 11. SEC traces of PMMA obtained with NHC^{tBu}-1,4-benzenedimethanol (Table 2,entry 4).

This broadening of the molar mass distribution might result from the presence of different species arising from the two hydroxyl groups. Polymerization could be induced by one hydroxyl, forming species **6** (Scheme 4a). The latter species can then serve as macroinitiator and lead to population **7**. Chain coupling reaction could also occur forming species **8** (Scheme 4b).

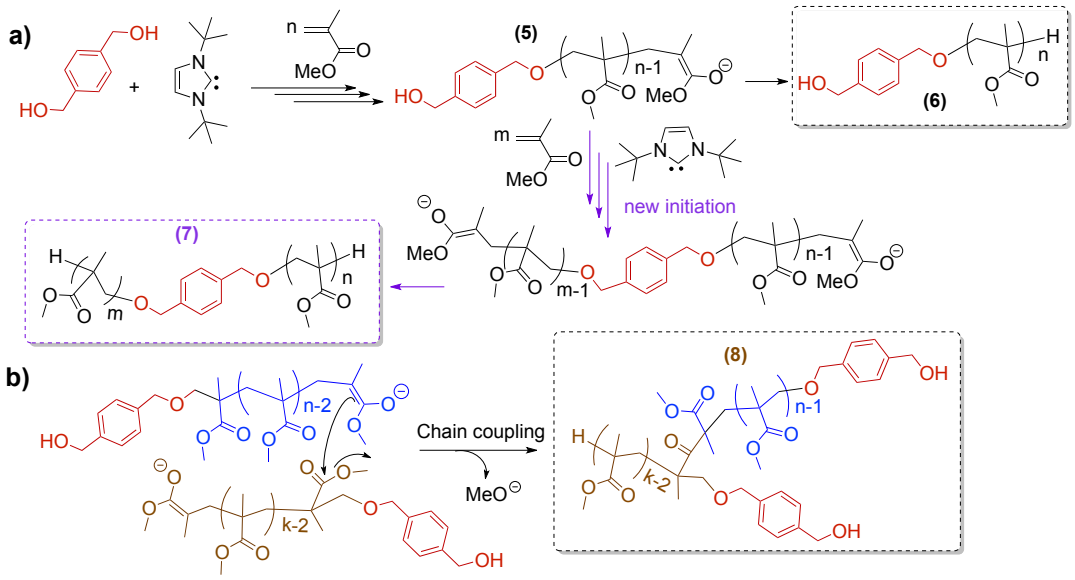

Scheme 4. NHC^{tBu}-catalyzed polymerization of MMA in presence of 1,4-benzenedimethanol (OH-Bn-OH): a) initiation from one or two hydroxyl group; b) chain coupling reaction.

MMA polymerization carried out in the presence of the tertiary alcohol *tert*-butanol (^{t}BuOH) reached 72 % of MMA conversion after 24 h (entry 5), while, primary alcohols (*i.e.* BnOH and PyBuOH) reached complete conversion under the same conditions. In addition,

the molar mass of the ^{t}BuOH-derived PMMA's was much higher than the expected value ($\overline{M_n}^{exp}$ = 7,700 g.mol^{-1} for a targeted value of 1,000 g.mol^{-1}). The hydroxyl proton of ^{t}BuOH being slightly less acidic (pKa ~ 32.2 for ^{t}BuOH *vs.* 29.8 for EtOH in DMSO)[23] and more hindered than primary alcohols, it can be assumed that ^{t}BuOH led to a partial initiation, providing a less controlled polymerization. Investigations into the kinetics of these NHC^{tBu}-catalyzed polymerizations in the presence of alcohols are discussed in section 1.2.3.

1.2.2. Polymerization with ROH macroinitiators

The previous method was next applied to the synthesis of amphiphilic PEO-*b*-PMMA block copolymers, through the use of either a mono- or a dihydroxylated poly(ethylene oxide)s (PEO's) as macroinitiators. MeOPEO$_{33}$-OH and OH-PEO$_{33}$-OH were tested and corresponding results are presented in Table 3.

Examples of such PEO/PMMA-based amphiphilic copolymers have been scarcely described in the literature.

To the best of our knowledge, PEO/PMMA diblock copolymers have been previously synthesized by anionic polymerization of EO from PMMA macroinitiator (Figure 12a-b) [31,32] or MMA polymerization by PEO living chain (Figure 12c),[33] and by atom transfer radical polymerization (ATRP) of MMA using PEO-based macroinitiator (Figure 12d).[34] However, regarding the anionic polymerization using PEO living chain, the authors did not provide any information about the obtained molar masses and the polymerization did not seem to be well-controlled.

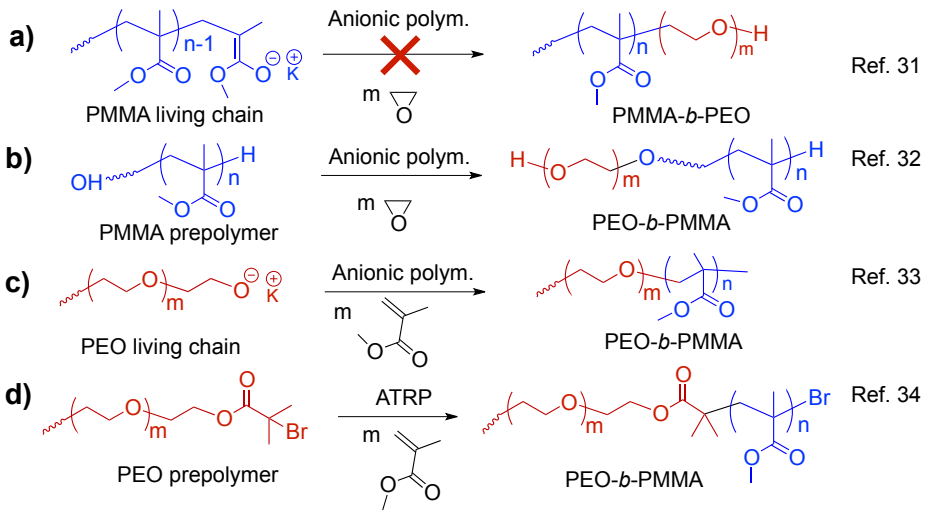

Figure 12. Synthesic route to PEO/PMMA block copolymers.[31-34]

Table 3. NHC^{tBu}-catalyzed polymerization of MMA in presence of OH-PEO$_{33}$-OH and MeO-PEO$_{33}$-OH as macroinitiator in DMF at 25 °C.

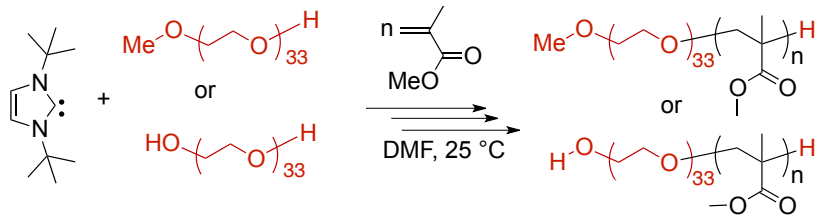

entry	ROH	[NHC^{tBu}]$_0$/ [ROH]$_0$/ [MMA]$_0$	Time (h)	Conv.^{a} (%)	$\overline{M}_n^{theo\ b}$ (g.mol^{-1})	$\overline{M}_n^{NMR\ c}$ (g.mol^{-1})	$\overline{M}_n^{SEC\ d}$ (g.mol^{-1})	$M_p^{SEC\ d}$ (g.mol^{-1})	$Đ^d$
1	HO-PEO$_{33}$-OH	0.1/0.5/10	7	100	2,200	2,900	2,900	3,600	1.8
2	MeOPEO$_{33}$-OH	1/1/50	24	100	6,100	6,800	6,200	10,130	1.3
3	MeOPEO$_{33}$-OH	1/1/100	24	100	11,100	14,400	13,200	16,300	1,3
4	MeOPEO$_{33}$-OH	1/1/200	24	100	21,100	19,300	19,300	28,500	1,6

a. Conv.= % monomer conversion determined by ^{1}H NMR spectroscopy; b. Theoretical molar mass $\overline{M}_n^{theo} = M_{ROH} + M_{MMA} \times \frac{[MMA]}{[ROH]} \times conv.$; c. $\overline{M}_n$ determined by ^{1}H NMR based on chain-end protons integration. d. Characterization of PMMA's by SEC in THF using PS standards for calibration.

In the presence of OH-PEO$_{33}$-OH or MeO-PEO$_{33}$-OH, SEC traces shifted to the higher molar masses region after MMA polymerization catalyzed by NHC^{tBu}, in comparison to the SEC traces of the macroinitiator (Table 3 entries 1-4 and Figure 13). This attested to the formation of PEO-*b*-PMMA block copolymers.

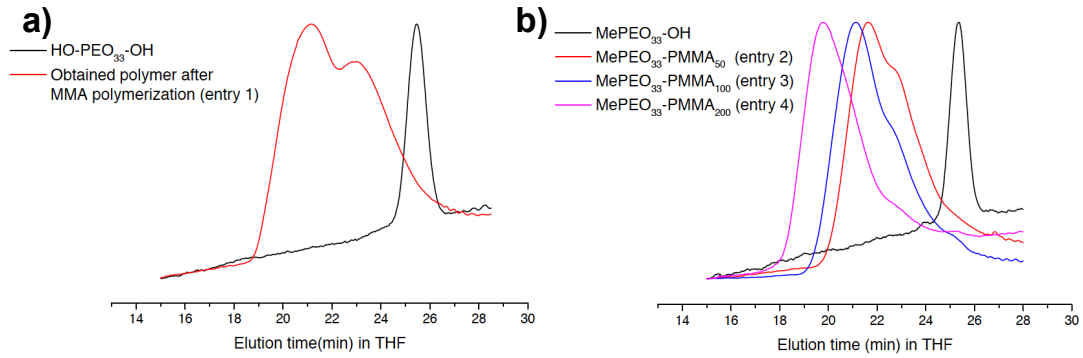

Figure 13. SEC-RI traces of PMMA's obtained with: a) OH-PEO$_{33}$-OH (Table 3; entry 1); b) MeOPEO$_{33}$-OH macroinitiators (Table 3; entries 2-4).

However, in the case of OH-PEO$_{33}$-OH used as macroinitiator, the dispersity was relatively broad and clearly exhibited a bimodality (entry 1 and Figure 13a). This could be ascribed to the co-existence of both PEO-*b*-PMMA diblock and PMMA-*b*-PEO-*b*-PMMA triblock copolymers, due to a slow or incomplete initiation from both OH groups of this precursor. This situation was already observed when using benzenedimethanol as initiator (see Figure 11 and Scheme 4).

In contrast, with the $MeOPEO_{33}$-OH macroinitiator, the formation of block copolymers was relatively controlled by the initial $[MMA]_0/[MeOPEO_{33}\text{-}OH]_0$ ratio (entries 2-4).

As illustrated in Figure 14 (see also Figures S1-S2 in supporting information,SI), the ^1H NMR spectrum of diblock copolymers showed the presence of signals corresponding to both PEO and PMMA segments. Indeed, signals observed at δ = 3.37 and 3.59 ppm are associated to the CH_2 and the CH_3O protons of the PEO macroinitiator. PMMA signals are identified at δ = 0.8-1.2; 1.7-2 and 3.6 ppm for the CH_3, CH_2 and OCH_3 groups, respectively. It is worth mentioning that before being analyzed, the final material was recovered by precipitation in pentane, followed by further precipitation in methanol to remove traces of unreacted PEO. The presence of signals from both PEO and PMMA thus seemed to confirm the formation of a PEO-*b*-PMMA block copolymer. Moreover, molar masses obtained from NMR analysis were in agreement with both the expected values and those determined by SEC (*e.g.* for $MeOPEO_{33}$-$PMMA_{50}$ $\overline{M_n}^{SEC} \approx \overline{M_n}^{NMR} \approx \overline{M_n}^{theo}$ = 6,100 $g.mol^{-1}$; Table 3, entry 2).

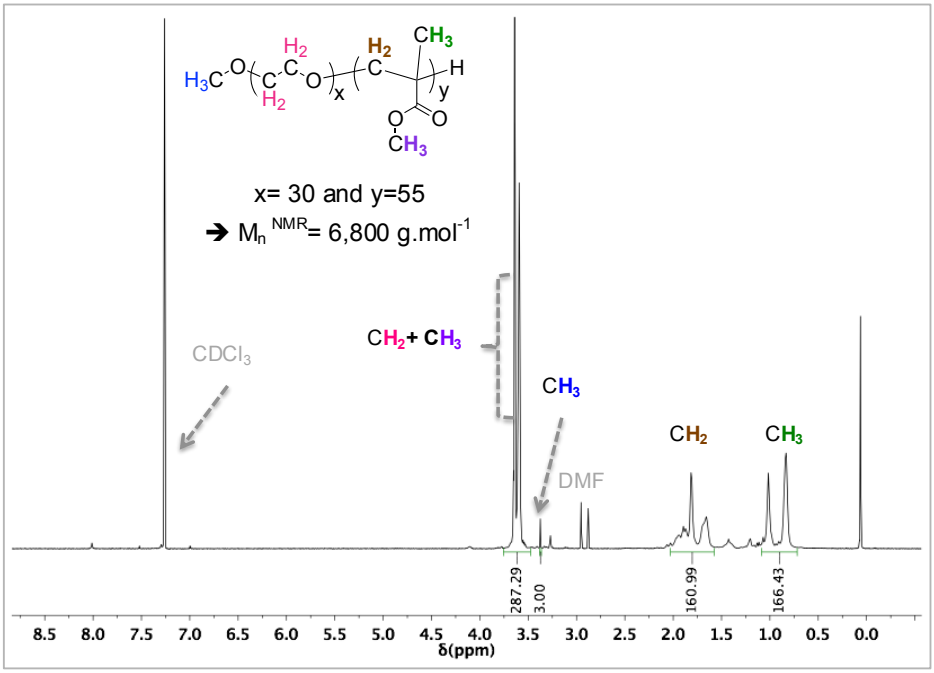

Figure 14. ^1H NMR (in $CDCl_3$) spectrum of $MeOPEO_{33}$-$PMMA_{50}$ (Table 3, entry 2).

Analysis by diffusion-ordered NMR spectroscopy (DOSY) allowed the diffusion coefficient of the copolymers to be determined, which are related to their hydrodynamic radius and molar masses.[35,36] In the DOSY NMR spectra of MeOPEO-PMMA sample (Figure 15), only one diffusion coefficient was observed, evidencing the formation of a pure copolymer with a unimodal distribution. Indeed, different diffusion coefficients would be observed with a mixture of homopolymers or with copolymers of various molar masses. As expected, values of the experimental diffusion coefficients were found to decrease as the molar mass of the copolymer increased (Figure 15), since the diffusion of similar species is related to their size, species having a lower diffusion coefficient.

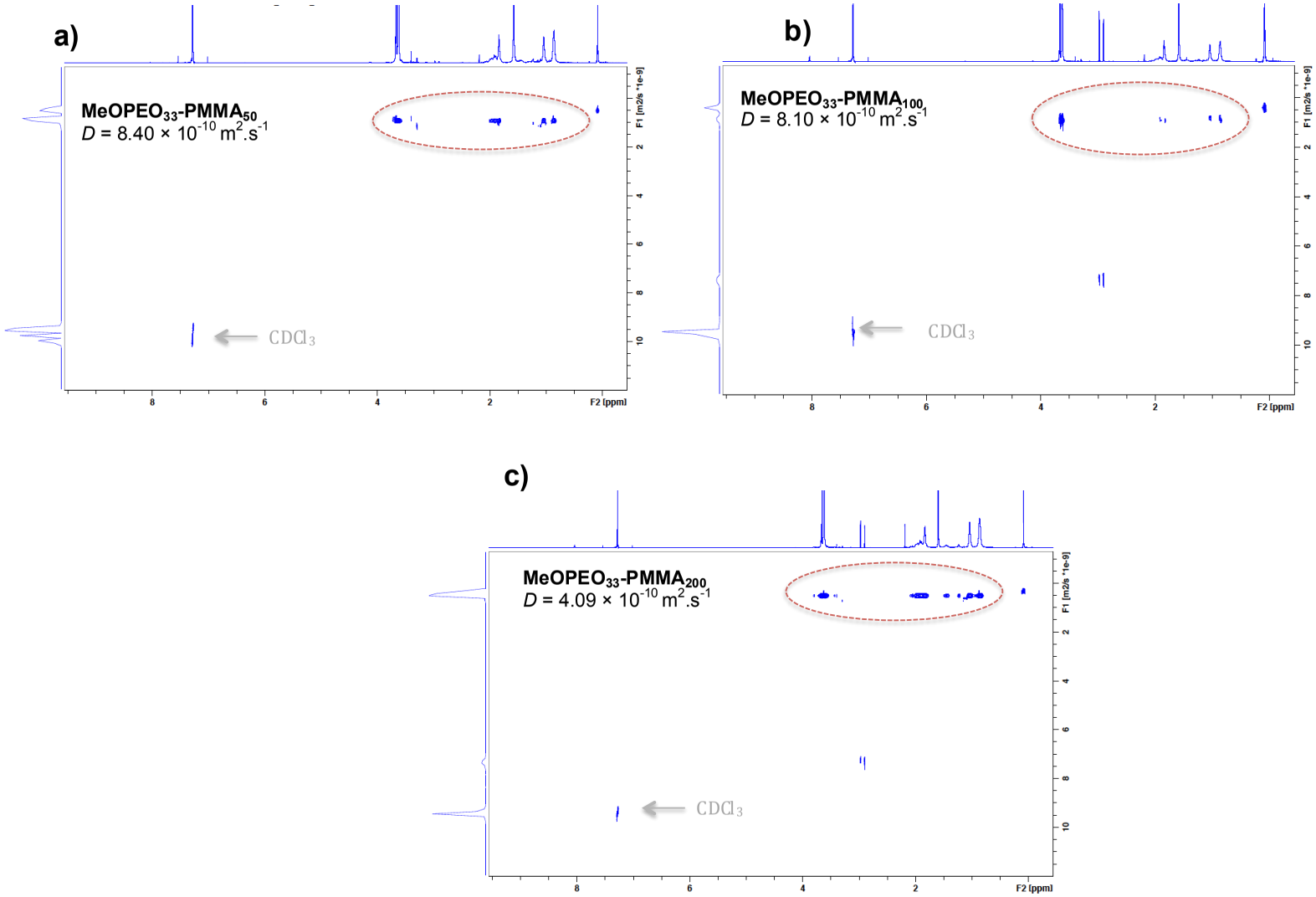

Figure 15. DOSY NMR spectrum (in $CDCl_3$) of: a) $MeOPEO_{33}$-*b*-$PMMA_{50}$ (Table 3, entry 2); b) $MeOPEO_{33}$-*b*-$PMMA_{100}$ (entry 3); c) $MeOPEO_{33}$-*b*-$PMMA_{200}$ (entry 3). X-axis demonstrates all the H resonances of the components in solution; Y-axis is the diffusion dimension.

As the PEO-*b*-PMMA diblock copolymers are expected to be amphiphilic, they should in principle self-assemble into micelles (micellization) in appropriate solvents (Figure 16).

In contrast to $MeOPEO_{33}$-$PMMA_{200}$ that was found insoluble in water, presumably because of the high content in PMMA, $MeOPEO_{33}$-$PMMA_{50}$ and $MeOPEO_{33}$-$PMMA_{100}$ samples proved to solubilize in water, forming a turbid solution. The latter observation suggests that micellization occurred. In order to characterize the corresponding structure, $MeOPEO_{33}$-$PMMA_{50}$ was first dissolved in a small amount of THF (a good solvent for both blocks), and the resulting solution was diluted with water (1 mg/mL), a selective solvent of PEO segment. Transmission electron microscopy (TEM) of $MeOPEO_{33}$-$PMMA_{50}$ aqueous solution revealed a nano-organization into spherical aggregates of a diameter in the range 28-32 nm (Figure 16), compatible with the formation of polymeric micelles as a result of the self-assembly of the amphiphilic PEO/PMMA-based copolymer.

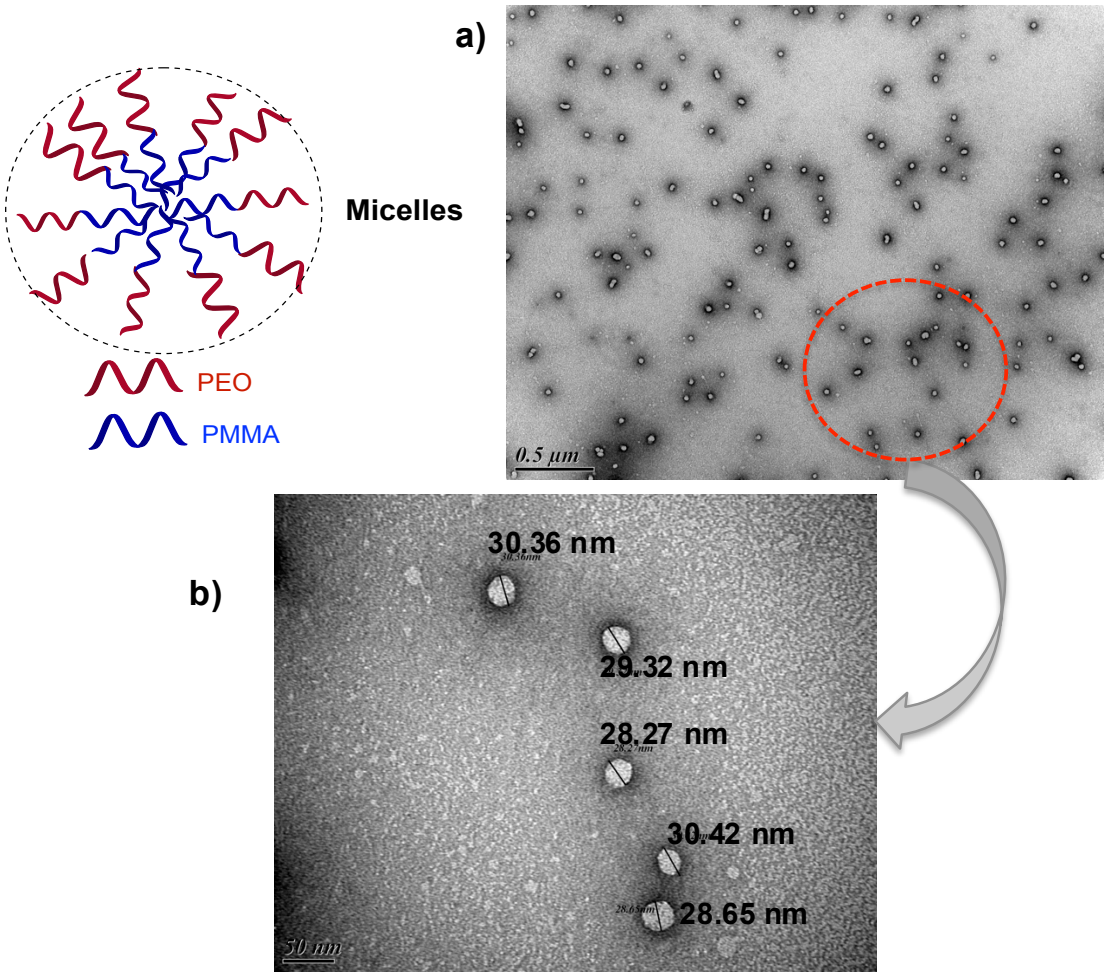

Figure 16. TEM images of a) aqueous self-assemblies of block copolymer $MeOPEO_{33}$-$PMMA_{50}$ (Table 3, entry 2); b) zoom.

The previous screening experiments have revealed that, in presence of non-functional alcohols, the NHC^{tBu}-mediated polymerization of MMA can be relatively well-controlled. To better understand the effect of the alcohol structure over the polymerization rate, kinetic investigations were performed, using both BnOH and ^{t}BuOH as alcohol representatives.

1.2.3. Preliminary kinetic investigations

Polymerizations of MMA using both BnOH and ^{t}BuOH, were thus conducted in DMF at 25 °C, with an initial ratio $[MMA]_0/[ROH]_0/[NHC^{tBu}]_0$ = 10/1/0.1. Aliquots were withdrawn at different intervals to determine both the monomer conversion and molar masses, by ^{1}H NMR and SEC, respectively. The first-order kinetic plots $\ln([MMA]_0/[MMA])$ *vs.* time are shown in Figure 17. The linear part of these variations represented the apparent rate constant, denoted as k_{app}. Results are summarized in Table 4.

Table 4. NHC^{tBu}-catalyzed polymerization of MMA using BnOH or ^{t}BuOH as initiators, in DMF at 25 °C. For sake of comparison, polymerization without any alcohol was also performed

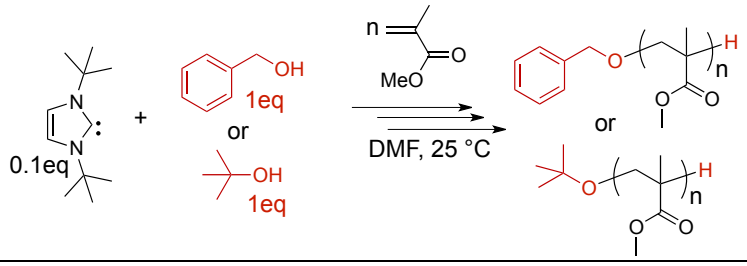

entry	ROH	$[NHC^{tBu}]_0$/ $[ROH]_0$/ $[MMA]_0$	Time (h)	Conv.[a] (%)	$\overline{M_n}^{theo}$ [b] (g.mol^{-1})	$\overline{M_n}$ [c] (g.mol^{-1})	M_p [c] (g.mol^{-1})	$Đ$ [c]
1	-	0.1/-/10	24 (48)	72 (100)	7,200	9,300	13,800	1,4
2	BnOH	0.1/1/10	9	100	1,100	1,100	1,400	1.3
3	^{t}BuOH	0.1/1/10	24 (48)	72 (100)	1,000	7,700	8,100	1.3

a. Conv.= % monomer conversion determined by ^{1}H NMR spectroscopy; b. Theoretical molar mass $\overline{M}_n^{theo} = M_{ROH} + M_{MMA} \times \frac{[MMA]}{[ROH]} \times conv.$; c. Characterization of PMMA's by SEC in THF using PS standards for calibration.

As described above, only the polymerization of MMA using NHC^{tBu}/BnOH allowed reaching molar masses close to the targeted values (Table 4, entry 2). When using NHC^{tBu}/^{t}BuOH, experimental molar masses were higher than expected (entry 3), as also observed in the absence of any alcohol (entry 1).

Interestingly, the evolution of NHC^{tBu} and NHC^{tBu}/^{t}BuOH polymerizations were similar (Figure 17), indicating that ^{t}BuOH did not significantly affect the polymerization rate, likely due to the steric hindrance of the *tert*-butyl group and its less acidic character. Observation of

a linear first order kinetic plot both with NHC^{tBu} alone and NHC^{tBu}/^{t}BuOH seemed to indicate the absence of termination reactions, at least at the earlier stage of the polymerization.

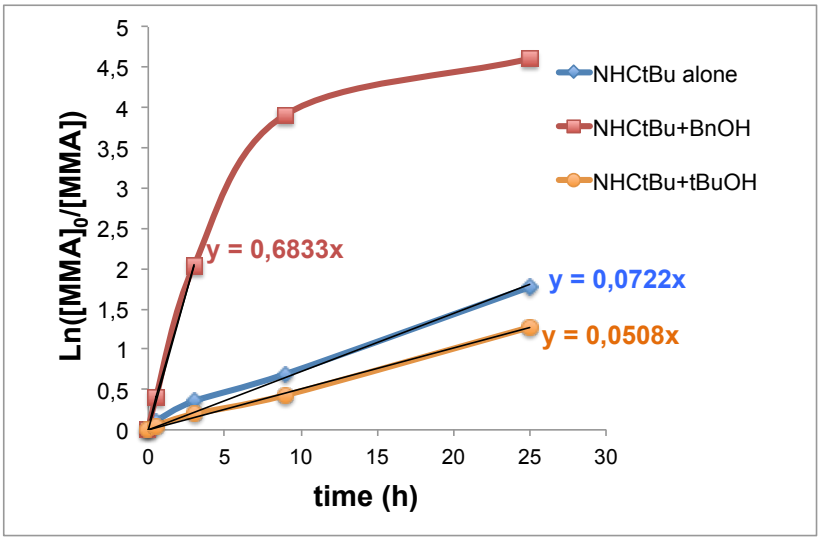

Figure 17: Comparison of rates of MMA polymerization with NHC^{tBu} alone, and in presence of BnOH and ^{t}BuOH as initiators in DMF at 25 °C.

On the other hand, the NHC^{tBu}/BnOH polymerization of MMA was significantly faster than that induced by NHC^{tBu} alone or by NHC^{tBu}/^{t}BuOH. However, deviation from linearity appeared at higher reaction times. Taking the linear part of the evolution only, the apparent rate constant k_{app} could be determined (= slope of the straight line): $k_{app}^{NHC+BnOH}$ = 0.7 h^{-1} >>> $k_{app}^{NHC+tBuOH} \approx k_{app}^{NHC} \approx$ 0.05-0.07 h^{-1}. These k_{app} values thus witness that the polymerization is influenced by:

(1) the formation of an alcohol-carbene complex **A** ($k_{app}^{NHC+ROH} > k_{app}^{NHC}$), presumably through H-bonding, as illustrated in Scheme 5.[37,38]

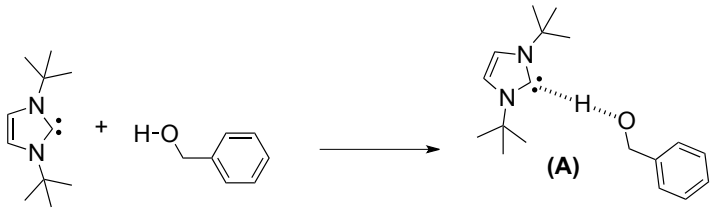

Scheme 5. Hydrogen bond interaction between NHC^{tBu} and BnOH.[37,38]

(2) the availability of the OH group that is more accessible in primary alcohol than in tertiary alcohol ($k_{app}^{NHC+BnOH} >> k_{app}^{NHC+tBuOH}$), forming the aforementioned alcohol-carbene complex.

Further investigations regarding this alcohol–carbene association will be provided in the section related to mechanistic considerations.

In summary, a preliminary screening of different NHCs and alcohol initiators allowed us to identify a combination that can provide a good control over the NHC-catalyzed polymerization of MMA. Among all NHCs tested, only NHC^{tBu} proved capable of triggering such a polymerization in the presence of alcohols at 25 °C, using DMF as solvent. The use of primary monohydroxylated compounds, such as benzyl alcohol (BnOH) and 1-pyrenebutanol (PyBuOH) was found crucial to achieve a good control of the reaction. In the next sections, investigations into the association between NHC^{tBu} and BnOH are discussed.

1.3. Influence of the concentration of NHC^{tBu}, BnOH and MMA

1.3.1. Influence of the concentration of NHC^{tBu}

To examine the influence of the NHC^{tBu} concentration over the polymerization, only the carbene quantity was varied, keeping constant both the initial concentration in alcohol $[BnOH]_0$ ($[BnOH]_0$ = 0.19 M) and the initial concentration of monomer $[MMA]_0$ ($[MMA]_0$ = 1.9 M) constant. The results obtained are summarized in Table 5 and are shown in Figure 18.

Table 5. NHC^{tBu}-catalyzed polymerizations in presence of BnOH using different $[NHC^{tBu}]_0$ concentrations, in DMF at 25 °C.

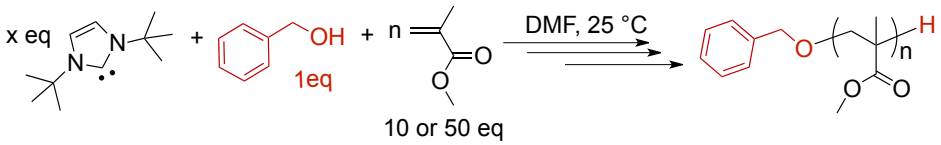

entry	$[NHC^{tBu}]_0$/ $[BnOH]_0$/ $[MMA]_0$	Time (h)	Conv.[a] (%)	$\overline{M_n}^{theo}$ [b] (g.mol^{-1})	$\overline{M_n}$ [c] (g.mol^{-1})	M_p [c] (g.mol^{-1})	$Đ$ [c]
1	0,05/1/10	8	99	990	980	1,000	1.1
2	0,2/1/10	8	100	1,100	1,100	1,200	1.1
3	0,1/1/50	30	90	4,600	8,000	16,400	1.9
4	0,5/1/50	6	96	4,800	8,900	17,400	1.9
5	1/1/50	2	100	5,000	8,300	14,150	1.6

a. Conv.= % monomer conversion determined by ^{1}H NMR spectroscopy; b. Theoretical molar mass $\overline{M}_n^{theo} = M_{ROH} + M_{MMA} \times \frac{[MMA]}{[ROH]} \times conv.$; c. Characterization of PMMA's by SEC in THF using PS standards for calibration.

As expected, the carbene concentration did not seem to affect the molecular characteristics of the obtained polymers, when targeting PMMA oligomers ($\overline{M_n}$ = 1,000 g.mol^{-1};Table 5, entries 1-2 and Figure 18a). The same was true when targeting higher degree of polymerization ($\overline{M_n}$ = 5,000 g.mol^{-1}; entries 3-5). In the latter case, the polymerization rate increased by increasing the initial carbene concentration, as expected,

but no significant differences were noted in the evolution of molar masses and dispersities (Figure 18b).

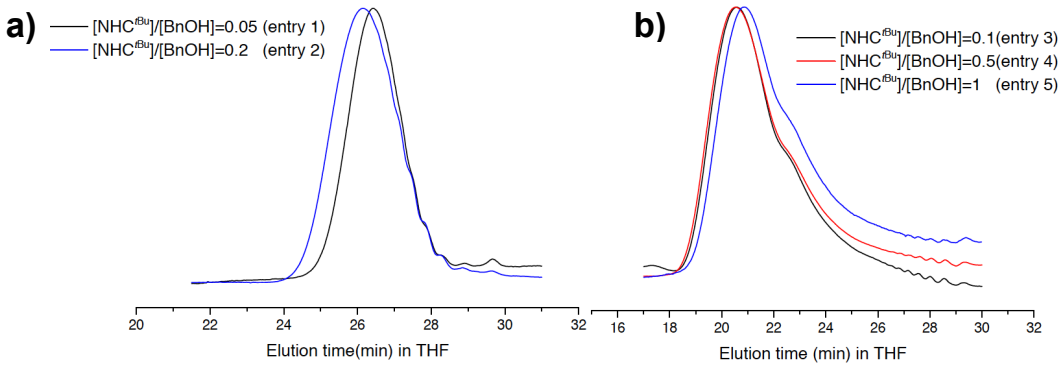

Figure 18. SEC traces of PMMA's obtained from various NHC^{tBu} concentration (Table 5): a) targeting oligomers of $\overline{M}_n$ = 1,000 g.mol^{-1}; and b) targeting a PMMA of $\overline{M}_n$ = 5,000 g.mol^{-1}.

1.3.2. Influence of the concentration of BnOH

The influence of the BnOH concentration, [BnOH], over the rate of polymerization was also studied. Hence, the alcohol concentration was varied, keeping constant both the initial concentration of carbene ([NHC^{tBu}]$_0$ = 19 mM) and that of the monomer ([MMA]$_0$ = 1.9 M). The results obtained for the final polymers (after work-up) are summarized in Table 6 and shown in Figure 19.

Table 6. NHC^{tBu}-catalyzed polymerizations using different [BnOH]$_0$ concentrations, in DMF at 25 °C .

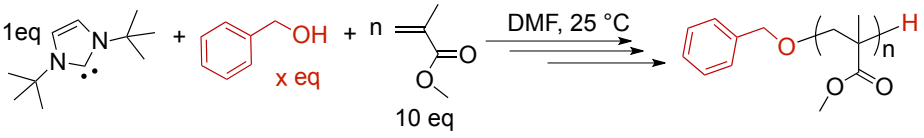

entry	[NHC^{tBu}]$_0$/ [BnOH]$_0$/ [MMA]$_0$	Time (h)	Conv.^{a} (%)	$\overline{M}_n^{theo\ b}$ (g.mol^{-1})	$\overline{M}_n^{\ c}$ (g.mol^{-1})	$M_p^{\ c}$ (g.mol^{-1})	$Đ^{\ c}$
1	1/0.5/100	8	48	9,600	4,500	5,400	1.6
2	1/1/100	8	70	7,000	5,100	9,000	1.5
3	1/5/100	8	90	1,800	2,100	2,900	1.4
4	1/10/100	8	100	1,000	1,400	1,800	1.2

a. Conv.= % monomer conversion determined by ^{1}H NMR spectroscopy; b. Theoretical molar mass $\overline{M}_n^{theo} = M_{ROH} + M_{MMA} \times \frac{[MMA]}{[ROH]} \times conv.$; c. Characterization of PMMA's by SEC in THF using PS standards for calibration.

As illustrated in Figure 19, for the NHC^{tBu}-catalyzed polymerization of MMA using BnOH as initiator, the molar masses of the final polymer depended on the initial alcohol concentration.

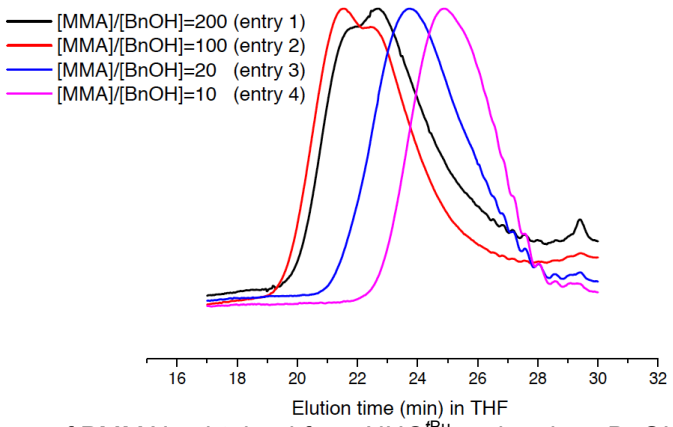

Figure 19. SEC-RI traces of PMMA's obtained from NHC^{tBu} and various BnOH concentration in DMF at 25°C (Table 6, entries 1-4).

In addition, these molar masses increased almost linearly with monomer conversion, as illustrated in Figure 20. At low alcohol concentrations (Table 6, entries 1-2), however, the obtained molar masses deviated from the predicted values by the initial $[MMA]_0/[BnOH]_0$. In contrast, at high alcohol concentration (entries 3-4), experimental molar masses were close to theoretical values and lower dispersities were achieved.

We hypothesized that, at low alcohol concentrations (entries 1-2), the carbene could hardly react with alcohol molecules, so as to form the active NHC^{tBu}-H…OBn complex (see Scheme 6). With only a few activated alcohol in the reaction medium, the polymerization was not influenced by the alcohol and rather proceeded through direct initiation of MMA by NHC^{tBu}. This might explain the deviation of molar masses from linearity observed (see Figure 20).

When using high alcohol concentration (entries 3-4), the molar masses were in accordance with theoretical values, but relatively broad dispersities of 1.2 - 1.8 were noted during the reaction (Figure 21). Such a trend in the evolution of dispersity values was already reported by Waytmouth *et al.*[39-41] in polymerizations where initiation was slow or comparable to the rate of propagation, and where there is an activation/deactivation equilibrium between species of different reactivity.[42]

In our case, both active free enolate propagating species (**P*** in Scheme 6) and dormant species **P** might be present during the polymerization process. The reactivity of the imidazolium-enolate **P*** is expected to be higher than that of the enol **P**. A slow rate of exchange between **P*** and **P** would allow both species to participate in propagation steps at two distinct rates, which could explain the bimodal distribution observed by SEC (Figure 19, entries 3-4).

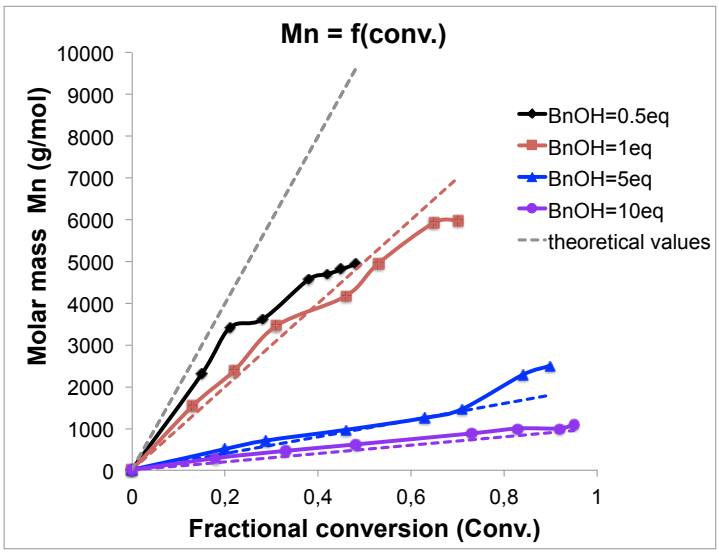

Figure 20. Evolution of molar masses ($\overline{M}_n$) *vs.* monomer conversion during the NHC^{tBu}-catalyzed polymerization of MMA using BnOH as initiator in DMF at 25 °C (Aliquots of the solutions; Table 6, entries 1-4).

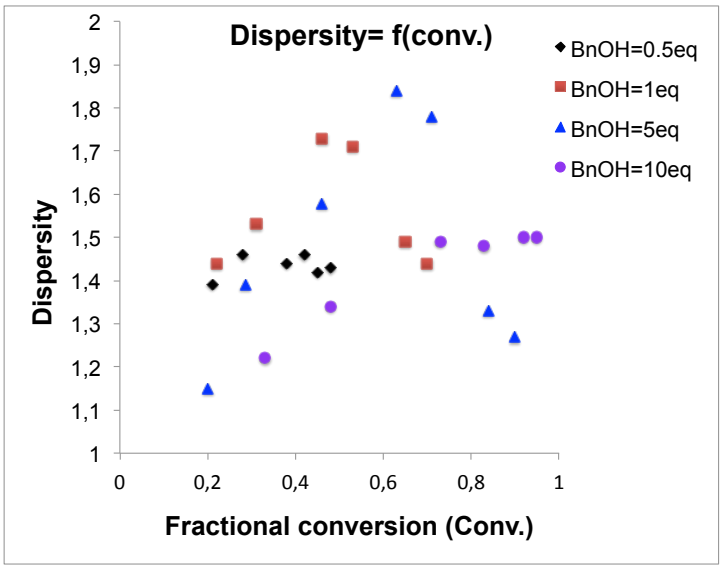

Figure 21. Evolution of dispersities *Đ vs.* monomer conversion during the NHC^{tBu}-catalyzed polymerization of MMA using BnOH as initiator (Aliquots of the solutions; Table 6, entries 1-4).

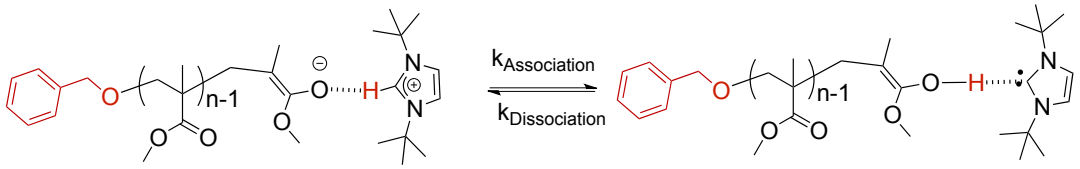

Imidazolium enolate (P*)
active growing chains

Imidazolium enol (P)
dormant growing chains

Scheme 6. Equilibrium between active species (P*) and dormant species (P).

As shown in Figure 22, the polymerization rate increased dramatically as the concentration of alcohol initiator increased. In other words, the concentration of the active species increased with the concentration of initiator.

In addition, the kinetic of MMA polymerization mediated by NHC^{tBu}/BnOH did not obey a first-order law and deviated from linearity. The linear part of these variations represented the apparent rate constant, k_{app}, that apparently remained the same (Figure 22).

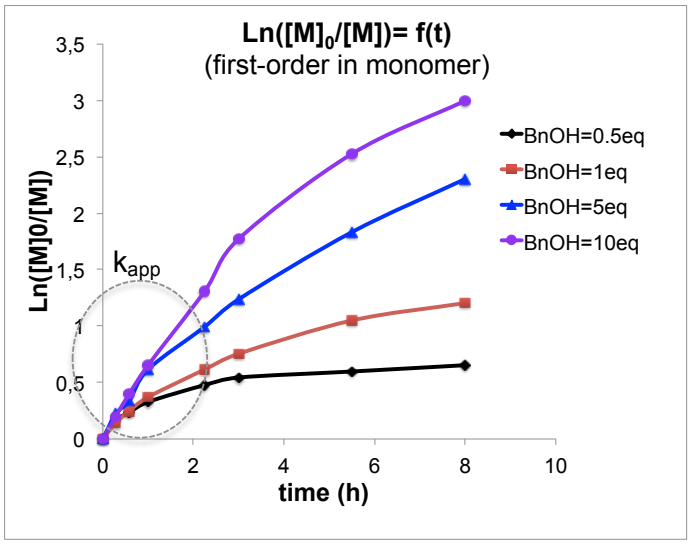

Figure 22. Evolution of ln([M]$_0$/[M]) *vs.* time during the NHC^{tBu}-catalyzed polymerization of MMA using BnOH as initiator in DMF at 25 °C (Aliquots of the solutions; Table 6, entries 1-4).

Hypotheses that can be put forward to explain these features are the following:

(1) the non-variation of k_{app} with the alcohol concentration may be ascribed to an induction period related to the formation of the active alcohol-carbene complex **A** (Scheme 6). The latter complex is required to initiate the polymerization *via* the 1,4-addition onto the monomer, as illustrated in Scheme 7.

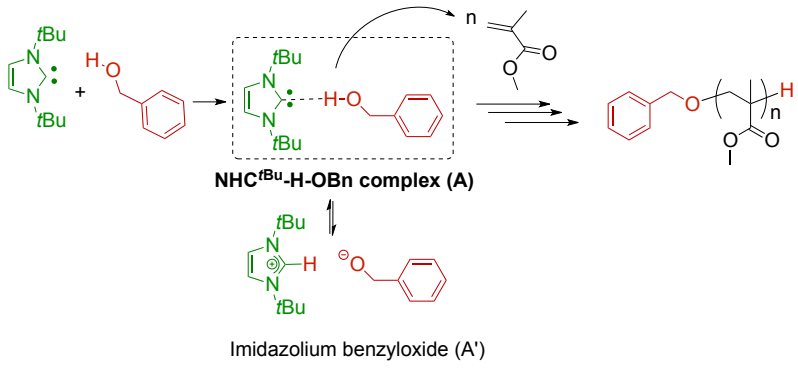

Scheme 7. Initiation and propagation steps of NHC^{tBu}-catalyzed polymerization of MMA using BnOH as initiator.

(2) when [BnOH] increases, more MMA can react *via* a 1,4-addition of the alcohol-carbene complex. This would explain the increase in polymerization rate with the alcohol concentration.

(3) a slow exchange between active and dormant chain-ends might occur, as depicted in Scheme 7 which could cause the deviation of molar masses from linearity.

(4) the carbene catalyst could be deactivated in the course of the polymerization by reaction involving the carbonyl group of the monomer, or with the pendant ester group of the propagating chain (see Scheme 8 below). In this case, there may not be enough carbene to activate the alcohol. Furthermore, this side reaction would form imidazolium methoxide type species competing with imidazolium benzyloxide, and producing α-methoxide PMMA chains. Such populations were indeed observed in the MALDI-ToF spectrum as discussed above (see Figure 9). Such reaction has been previously discussed in NHC-catalyzed transesterification reactions in the context of polymer chemistry.[43] These side reactions could also induce the deviation of the plot $\ln([M]_0/[M]$ *vs.* time from linearity observed on the kinetics, at high monomer conversion.

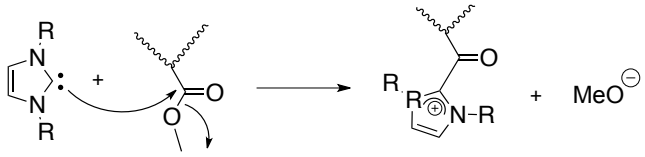

Scheme 8. Carbene deactivation through reaction with the carbonyl.

The kinetics of NHC^{tBu}-catalyzed ROH-initiated polymerization of MMA are thus more complex than expected, because of the occurrence of different mechanisms. Both initiation and propagation mechanisms will be discussed in more details in section 2, based on computational studies.

1.3.3. Influence of the concentration of MMA

The influence of the monomer concentration over the polymerization was also studied. The polymerization was again performed in DMF at 25 °C, and both the initial concentration of NHC^{tBu} ($[NHC^{tBu}]_0$ = 19 mM) and BnOH ($[BnOH]_0$ = 0.19 M) were kept constant. MMA was then progressively added, dropwise, under an inert argon atmosphere. Corresponding results are summarized in Table 7 and illustrated in Figure 23.

Table 7. NHC^{tBu}-catalyzed polymerizations in presence of BnOH using different $[MMA]_0$, in DMF at 25 °C.

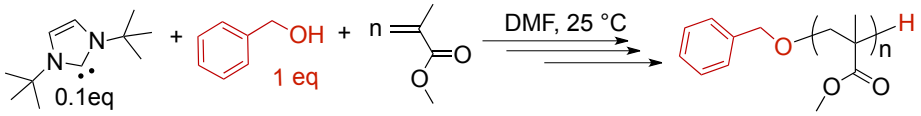

entry	$[NHC^{tBu}]_0/[BnOH]_0/[MMA]_0$	Time (h)	Conv.[a] (%)	$\overline{M_n}^{theo}$ [b] (g.mol^{-1})	$\overline{M_n}$ [c] (g.mol^{-1})	M_p [c] (g.mol^{-1})	$Đ$ [c]
1	0.1/1/5	5	100	600	900	1,000	1.1
2	0.1/1/10	5	100	1,100	1,400	1,500	1.2
3	0.1/1/25	24	100	2,600	2,600	3,600	1.4
4	0.1/1/50	24	92	4,600	8,000	10,000	1.9

a. Conv.= % monomer conversion determined by ^{1}H NMR spectroscopy; b. Theoretical molar mass $\overline{M}_n^{theo} = M_{ROH} + M_{MMA} \times \frac{[MMA]}{[ROH]} \times conv.$; c. Characterization of PMMA's by SEC in THF using PS standards for calibration.

Remarkably, these conditions yielded PMMA's with molar masses controlled by the initial $[MMA]_0/[BnOH]_0$ ratio and narrow dispersities $Đ$ (Table 7; entries 1-4). However, at higher monomer concentration, a tailing in the low molar masses region was noted in the SEC trace (Figure 23), and molar masses somewhat deviated from the expected values (entry 4). Similar observations have been reported by Hedrick, Waymouth *et al.* regarding the NHC-catalyzed polymerization of D,L-lactide in presence of alcohol initiators.[40,41,44] This was attributed to the occurrence of both competitive nucleophilic and basic mechanisms (monomer and alcohol activation by NHC, respectively; see further discussion in section 2.).

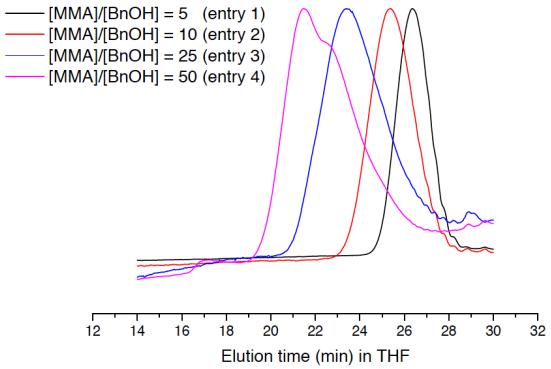

Figure 23. SEC-RI traces of PMMA's obtained from NHC^{tBu} and BnOH with various monomer concentration in DMF at 25 °C (Table 7; entries 1-4).

In our case, further attempts to achieve optimal control of the NHC^{tBu}-catalyzed polymerization of MMA using BnOH as initator, including either an increase of the carbene concentration or implementation of a very slow monomer addition process, did not allow us to achieve higher molar mass PMMA's in a controlled fashion ($\overline{M_n}$ up to 3,000 g.mol^{-1}).

Addition of new load of MMA to the putative growing chain, in the course of the polymerization, was expected to result in an increase of molar masses, as a means to evidence the living character of the polymerization. Chain extension experiments were thus performed by sequential addition of MMA (Table 8).

Table 8. Sequential monomer addition during NHC^{tBu}-catalyzed polymerization of MMA in presence of BnOH initiator, in DMF at 25 °C.

run	$[NHC^{tBu}]_0/[BnOH]_0/[MMA]_0$	Time (h)	Conv.[a] (%)	$\overline{M_n}^{theo}$ [b] (g.mol^{-1})	$\overline{M_n}^{NMR}$ [c] (g.mol^{-1})	$\overline{M_n}^{SEC}$ [d] (g.mol^{-1})	M_p^{SEC} [d] (g.mol^{-1})	$Đ$ [d]
1	0.1/1/10	4	100	1,000	n.d.	1,200	1,400	1.2
2	0.1/1/10	24	100	2,000	n.d.	1,700	4,300	2.2
3	0.1/1/10	24	100	3,000	3,200	3,300	5,000	1.7

a. Conv.= % monomer conversion determined by ^{1}H NMR spectroscopy; b. Theoretical molar mass $\overline{M}_n^{theo} = M_{ROH} + M_{MMA} \times \frac{[MMA]}{[ROH]} \times conv.$; c. $\overline{M_n}$ determined by ^{1}H NMR based on chain-end protons integration d. Characterization of PMMA's by SEC in THF using PS standards for calibration.

Polymerization of MMA was first conducted in DMF at 25 °C, in the presence of NHC^{tBu} as catalyst and BnOH as initiator, using a ratio $[MMA]_0/[BnOH]_0/[NHC^{tBu}]_0$ = 10/1/0.1. Quantitative conversion was achieved after 5 h, leading a PMMA of molar mass $\overline{M}_n$ = 1,200 g.mol^{-1} and $Đ$ = 1.2 (Table 8, run 1 and Figure 24). Adding a new load of MMA (10 eq.) to this PMMA precursor did increase the molar mass, from 1,200 to 1,700 g.mol^{-1}, after additional 24 h of reaction and complete conversion (run 2). Subsequent addition of 10 eq.of MMA (run 3) afforded a new PMMA of molar mass $\overline{M}_n$ = 3,300 g.mol^{-1}, after 24 h of reaction and purification by precipitation in pentane (Figure 24).

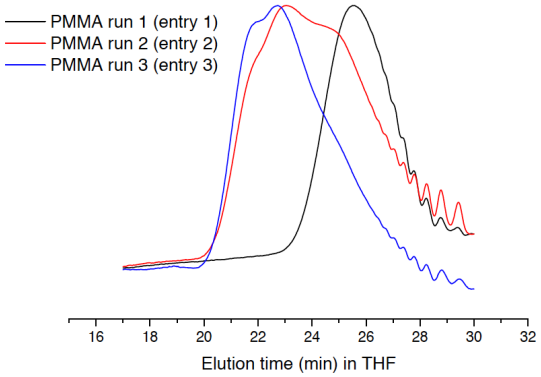

Figure 24. SEC-RI traces of PMMA's obtained upon sequential MMA addition (Table 8).

The shoulder observed in the high molar masses region of PMMA from runs 2 and 3 (Figure 24), might be ascribed either to chain coupling or to the presence of two types of propagating chains (P* and P), as already discussed (see Scheme 6). Nevertheless, the possibility of new chain initiation after adding new loads of MMA cannot be totally ruled out.

These chain extension experiments demonstrated that the NHC^{tBu}-catayzed polymerization of MMA, in presence of BnOH as initiator, afforded PMMA chains that could be reactivated. However, side reactions (likely chain re-initiation or chain coupling) seemed to occur in the course of the polymerization, thus limiting the production of high molar masses PMMA's.

1.4. Influence of the order of addition of the reagents

The order of addition of the reagents (MMA, BnOH and NHC^{tBu}) during the polymerization should provide information about the mechanism involved in this NHC^{tBu}/BnOH-mediated polymerization of MMA. For this purpose, polymerizations of MMA were performed in DMF at 25 °C, keeping constant the initial concentration of MMA, BnOH and NHC^{tBu} ([MMA]$_0$ = 1.9 M, [BnOH]$_0$ = 0.19 M and [NHC^{tBu}]$_0$ = 19 mM, respectively). Only the order of addition of each reagent was changed here and data from these polymerizations are provided in Table 9 and shown in Figure 25.

Table 9. Influence of order of addition of MMA, BnOH and NHC^{tBu} during the NHC^{tBu}-catalyzed polymerization of MMA in DMF at 25 °C.

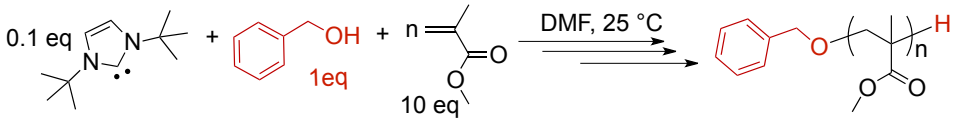

entry	order	Time (h)	Conv.[a] (%)	$\overline{M_n}^{theo\ b}$ (g.mol^{-1})	$\overline{M_n}^{c}$ (g.mol^{-1})	M_p^{c} (g.mol^{-1})	$\overline{M_w}^{c}$ (g.mol^{-1})	$Đ^{c}$
1	(MMA+NHC^{tBu}) + BnOH	2 (12)	13 (100)	1,300	16,000 1,100	20,200 1,200	22,800 1,200	1.4 1.2
2	(NHC^{tBu}+BnOH) + MMA	10	100	1,100	1,300	1,300	1,400	1.1
3	(MMA+BnOH) + NHC^{tBu}	10	100	1,100	1,500	1,900	1,900	1.2

a. Conv.= % monomer conversion determined by ^{1}H NMR spectroscopy; b. Theoretical molar mass $\overline{M}_n^{theo} = M_{ROH} + M_{MMA} \times \frac{[MMA]}{[ROH]} \times$conv.; c. Characterization of PMMA's by SEC in THF using PS standards for calibration.

As illustrated in Figure 25, the order of addition of the reagents played an important role in this polymerization. When the monomer and the carbene were first mixed together, which was followed by addition of the alcohol (order 1: [(MMA+NHC^{tBu})+BnOH]; Table 9, entry 1), the direct activation of MMA by the carbene (in absence of ROH), was supposedly favoured (this mechanism has been discussed in details in chapter 2, section 3). With this order, two populations (**W** and **X**) were observed by SEC (Figure 25). The first population **W** was attributed to the direct polymerization of MMA by NHC^{tBu}, producing PMMA's of higher molar masses (see chapter 2). The second population **X**, which appeared after the addition of the alcohol, exhibited molar mass close to the expected based on the [MMA]$_0$/[BnOH]$_0$ ratio.

The latter population **X** was similar to that observed for the polymer resulting from the addition of MMA onto the preformed NHC^{tBu}-BnOH complex (order 2 = [(NHC^{tBu} + BnOH) + MMA; entry 2). In this case, an ACEM was presumably favoured. These results thus

established that the alcohol allowed controlling the polymerization, and that the mechanism involving the direct attack of the monomer by the carbene (AMM) might not be that significant under these conditions.

Interestingly, when the monomer was mixed with the alcohol end stirred for a few hours or overnight, followed by addition of the NHC^{tBu} (order 3= [(MMA+BnOH) + NHC^{tBu}]; entry 3), the PMMA thus obtained exhibited a slightly higher molar mass and dispersity than that synthesized using the following order 2: [(NHC^{tBu}+BnOH)+MMA]. This could be explained by the formation of a MMA-BnOH complex through H-bonding as depicted in Scheme 10.2 below. In such a case, the alcohol concentration is decreased, hence a higher molar mass PMMA was generated.

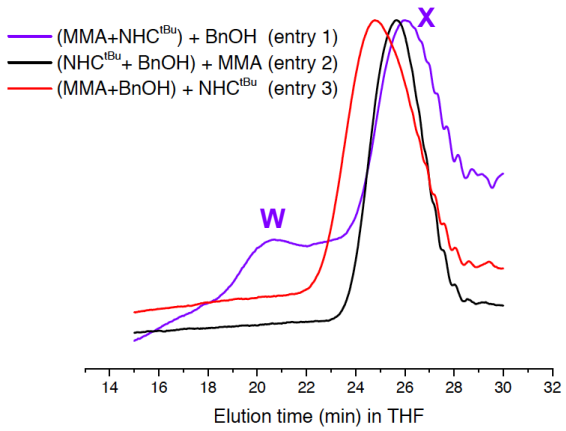

Figure 25. SEC traces (RI) of PMMA's obtained by changing the order of addition of MMA, BnOH and NHC^{tBu} (Table 9).

Based on the above results, it was preferred to add the different reagents in the following order: 1) NHC^{tBu}+BnOH, then 2) MMA to better control the polymerization.

1.5. Equimolar reactions between NHC^{tBu}, BnOH and MMA

In order to gain a better mechanistic insight into the NHC^{tBu}-catalyzed polymerization of MMA in presence of alcohol as initiator, equimolar reactions between the three reagents, MMA, BnOH and NHC^{tBu} were also implemented. These equimolar reactions were performed in a J-Young NMR tube, in dried DMF-d_7 at 25 °C, and the reactions were monitored by ^{1}H and ^{13}C NMR spectroscopies.

Interestingly, and in accordance with previous reports,[38,45] deprotonation of BnOH by NHC^{tBu} did not occur under these conditions. Instead, a NHC^{tBu}-BnOH adduct was formed, as attested by the downfield shift of the hydroxyl proton of BnOH from 5.15 to 8.25 ppm ($\Delta\delta$ = 3.1 ppm) observed in ^{1}H NMR spectrum (Figure 26). The multiplicity (singulet) of this proton did not change after the reaction with NHC^{tBu}. Moreover, in the ^{13}C NMR, the signal

corresponding to the carbone C_a of NHC^{tBu} is upfield shifted by 25 ppm (δ C_a = 196 and 220 ppm in NHC-H-OBn and free NHC, respectively; Figure S3a-b), supporting the formation of an H-bond complex. In the case of an imidazolium alkoxide-type structure, the chemical shift of C_a would have been close to the value observed in an imidazolium chloride for instance (δ $C_{a'}$ = 134 ppm; Figure S3).

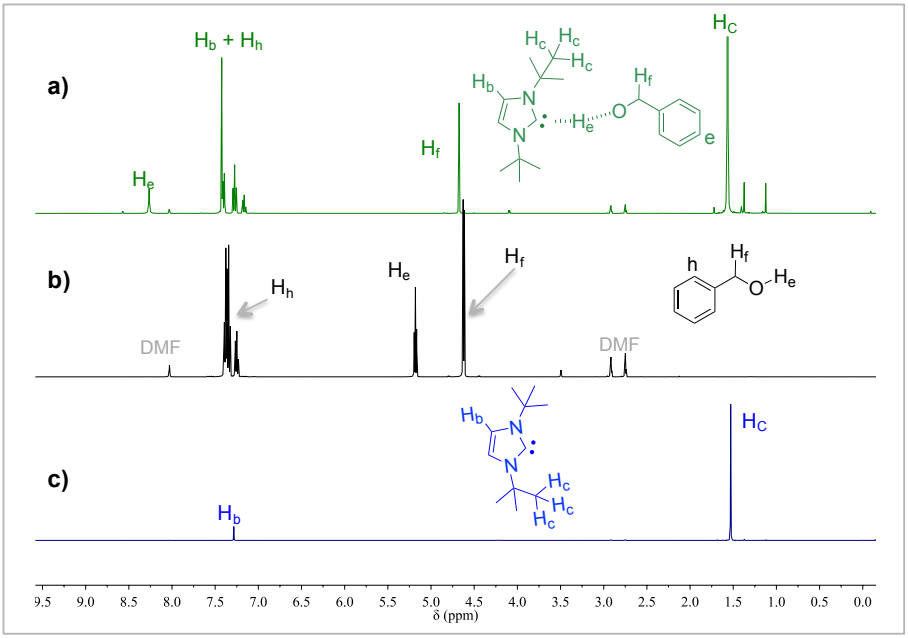

Figure 26. ^{1}H NMR spectrum in DMF-d_7 of: a) NHC^{tBu} + BnOH (1:1) mixture; b) BnOH; and c) NHC^{tBu}

An equimolar amount of MMA was added onto the NHC-alcohol (1:1) complex, in order to identify the key intermediate during the polymerization (imidazolium-enolate-benzyloxide *vs.* benzyloxide-enolate-imidazolium). As illustrated in Figure 27, the proton that was in equilibrium in the NHC-alcohol complex was upfielded, from 8.9 ppm to 8.3 ppm. Protons from MMA splitted into two different set of signals after 10 mn of reaction, and new rather broad signals appeared at δ = 1.1-1.3, 4.5 ppm and 5.2 ppm. Although complex, these changes were ascribed to the presence of multiple species, and to the equilibrium between active/dormant form as well as Z/E configurations (Scheme 9).

Due to the complexity of the spectrum obtained, ^{1}H and ^{13}C NMR (1D or 2D) analyses did not allow us to conclude whether the reaction NHC^{tBu} +BnOH +MMA (1/1/1) produced an α-benzyloxide imidazolium enolate (α or α') or an α-imidazolium enolate (β). Theoretical calculations discussed in the next section will shed new light on the polymerization mechanism.

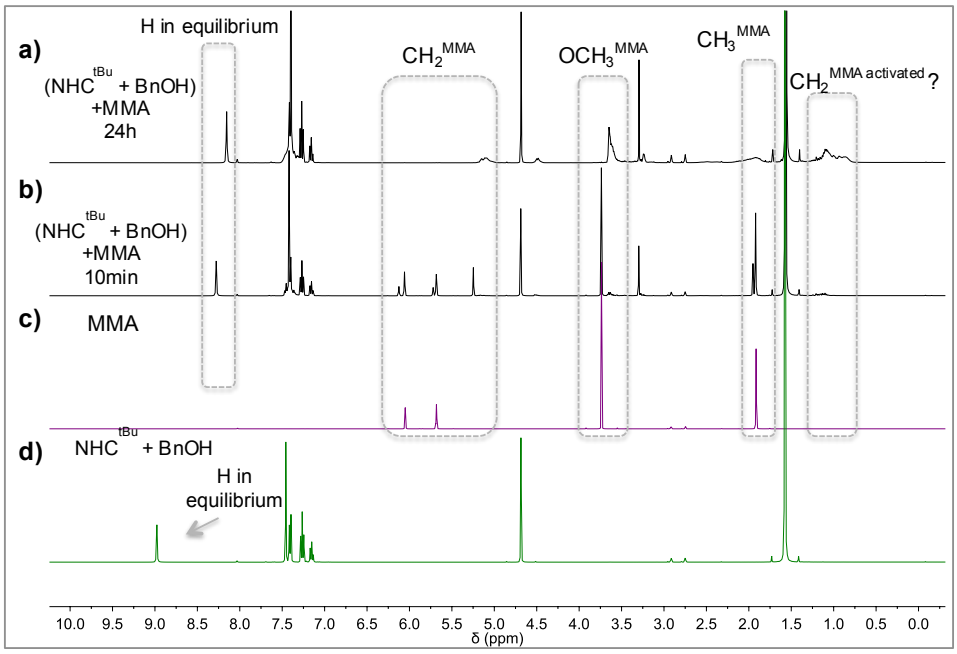

Figure 27. ^{1}H NMR spectra in DMF-d_7 of a) NHC^{tBu} + BnOH +MMA (1/1/1) mixture; b) MMA; c) NHC^{tBu}+BnOH (1/1) mixture

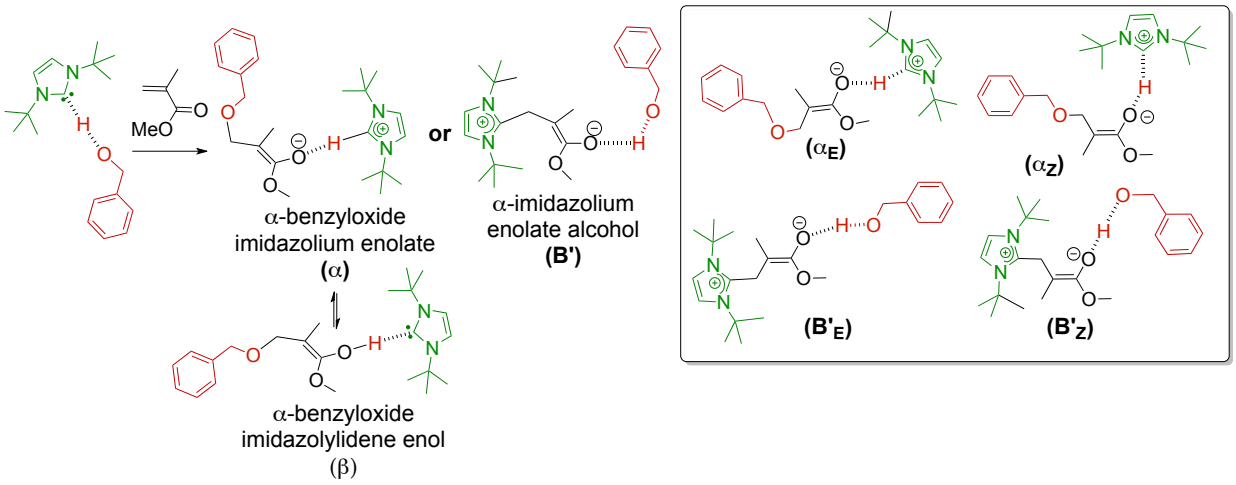

Scheme 9. Possible species formed after reaction between MMA and [NHC^{tBu}-H-OBn] complex.

2. Polymerization mechanism: density functional theory (DFT) calculations

By analogy to the NHC-catalyzed polymerization of cyclic esters in presence of alcohol initiators,[40] two distinct mechanisms can be proposed to explain the formation of α-alkoxy PMMA's observed during the NHC$^{t\text{Bu}}$-catalyzed polymerization of MMA from alcohols as initiators: 1) an initiatior/chain-end activation (ACEM) and 2) a monomer activation mechanism (AMM). In a basic ACEM (Scheme 10.1), the NHC$^{t\text{Bu}}$ might activate the alcohol initiator, forming a pseudo [NHC$^{t\text{Bu}}$..H..OBn] H-bond complex (**A**). It has to be noticed that, depending on the pKa of the NHC, an imidazolium alkoxide (**A'**), resulting from the deprotonation of the ROH, could be envisaged. Upon subsequent addition onto MMA, the 1,3-bis(*tert*-butyl)imidazolium enolate ion pair (α), featuring an benzyloxy group in α-position would be generated, and might be in equilibrium with enol-type dormant forms (β) that are hydrogen-bound to the NHC.

In a nucleophilic AMM (Scheme 10.2), the monomer, which is H-bond to BnOH (**B**), can undergo a 1,4-conjugate addition of NHC$^{t\text{Bu}}$, generating a zwitterionic 1,3-bis(*tert*-butyl)imidazolium enolate (**B'**). The latter compound is stabilized by the alcohol through H-bonding, forming an α-imidazolium enol benzyloxide.

To evaluate and compare the two mechanisms 1 and 2, both from a kinetic and thermodynamic viewpoint, density functional theory (DFT) calculations were carried out at the M06-2X/6-31G** level of theory taking into account solvents effects (DMF) by using a SMD solvatation model. The polymerization mechanism involving a direct initiation of MMA by NHC$^{t\text{Bu}}$ has been discussed in chapter 2. Therefore, only the influence of the alcohol on the polymerization will be considered in this particular case. For each mechanism, cases, the initiation step (= addition of the first MMA molecule) will be first described, followed by a discussion of the propagating step (= addition of the second MMA molecule). The geometrical description of the compounds and the transition state (TS) involved along the different pathways, can be found in the supporting information (Figures S4-S6)

These calculations were again performed at the Institut Pluridisciplinaire de Recherche sur l'Environnement et les Matériaux (IPREM, Université de Pau & des Pays de l'Adour, UPPA) by Damien Bourichon, completing his PhD under the supervision of Dr. Karinne Miqueu and Dr. Jean-Marc Sotiropoulos.

1) Activated initiator/chain-end mechanism (ACEM)

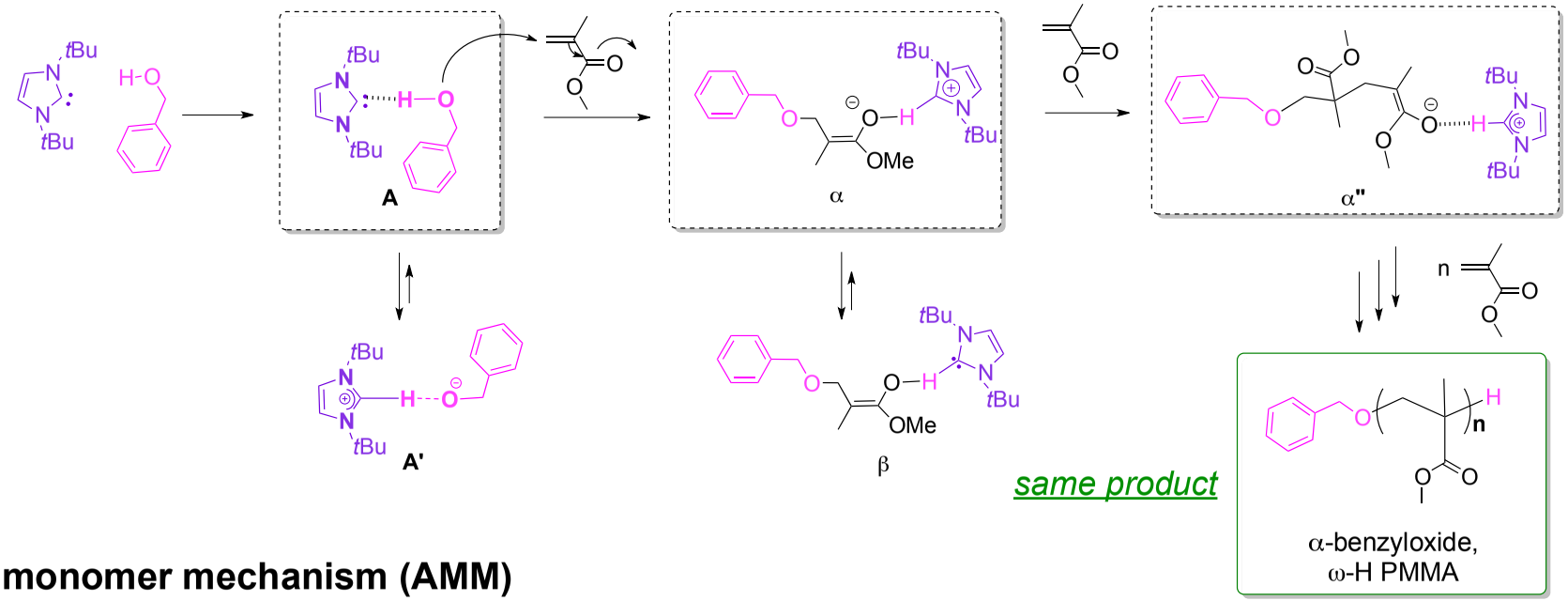

2) Activated monomer mechanism (AMM)

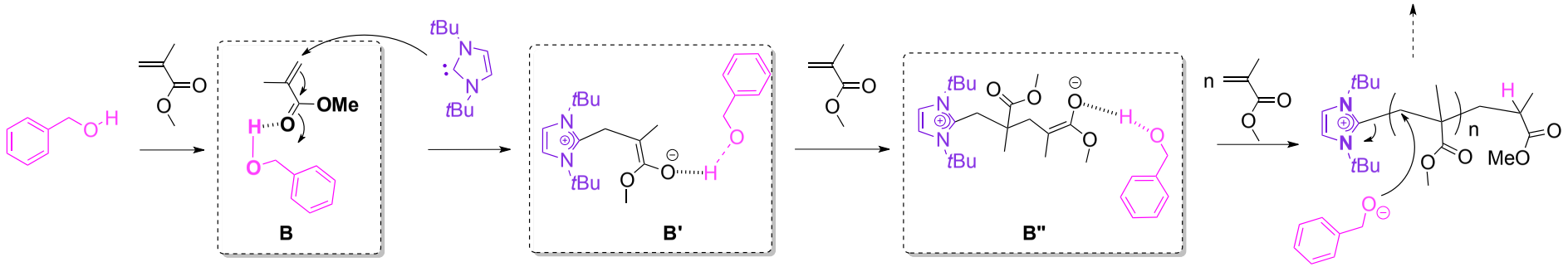

Scheme 10. Proposed mechanisms for NHC^{tBu}-catalyzed polymerization of MMA in presence of BnOH as initiator.

2.1. Activated initiator/chain-end mechanism (ACEM): mechanism 1

In the NHC$^{t\text{Bu}}$-catalyzed, BnOH-initiated polymerization, the ACEM initiation (Scheme 10.1) consists in the conjugate addition of BnOH onto MMA, assisted by NHC$^{t\text{Bu}}$. The energy profile of this mechanism is provided in Figure 28.

The carbene was indeed found to strongly interact with BnOH, leading to a BnOH-NHC$^{t\text{Bu}}$ adduct **A** (ΔH = -11.1 kcal.mol^{-1}), while an equilibrium between this adduct and the corresponding imidazolium alkoxide **A'**, in favor of **A**, was computed (**A'** is less stable than **A** by 6.9 kcal.mol^{-1}). Interestingly, and in accordance with previous reports,[38] deprotonation of BnOH by NHC$^{t\text{Bu}}$ did not occur under these conditions. Instead, a BnOH-NHC$^{t\text{Bu}}$ adduct was formed, as attested by the 3.1 ppm downfield shift of the hydroxyl proton of BnOH in ^{1}H NMR, and by the chemical shift of the C_a carbon of NHC$^{t\text{Bu}}$ at 196 ppm in ^{13}C NMR (δ = 220 and 134 ppm for C_a in the free carbene and $C_{a'}$ in the imidazolium, respectively; see NMR spectra in Figures 26 and S3).

Addition of the activated alcohol **A** onto MMA was next investigated computationally. This reaction formed the imidazolium enolate **1** (ΔH = 2.8 kcal.mol^{-1}), where the imidazolium cation was hydrogen-bound to the O atom of the BnO moiety. Transfer of the imidazolium, from the benzyloxy to the enolate moiety, was predicted as being exothermic (ΔH = -5.2 kcal.mol^{-1}) and barrier-less. Overall, both BnOH-NHC$^{t\text{Bu}}$ adduct **A** and the corresponding benzyloxyenolate featuring an imidazolium counter-cation, α, were found quasi iso-energetic (**A** being less stable than α by 2.4 kcal.mol^{-1}), and a small activation E_a of 10.8 kcal.mol^{-1} was computed from **A** to **TS1** (Figure S4). This transformation was calculated to occur *via* a concerted but strongly asynchronous transition state, corresponding to alkoxide-imidazolium structure (see **TS1**). Note that the active form α was in equilibrium with a dormant form β (equilibrium shifted in the direction of α), where the carbene is H-bound to the enol chain end.

The second addition of MMA onto α lead to the imidazolium enolate α', and was found highly exothermic (ΔH = -14.7 kcal.mol^{-1}) and the corresponding energetic barrier was calculated very low (2.9 kcal.mol^{-1}). Here again, a concerted but asynchronous TS could be located on the potential energy surface (see **TSα'** in Figure S4). The imidazolium cation, that is hydrogen-bound to the ester group of the first MMA molecule incorporated during the initiation in α', is then transferred to the enolate chain end in α" (ΔH = -4.6 kcal.mol^{-1}). As already observed in the initiation step, the active imidazolium enolate α'' is in equilibrium with a dormant form β'' (ΔH = 6.0 kcal.mol^{-1} in favor of α''). Overall, this process not only appeared thermodynamically and kinetically favored, but also proved compatible with experimental observations made at 25 °C.

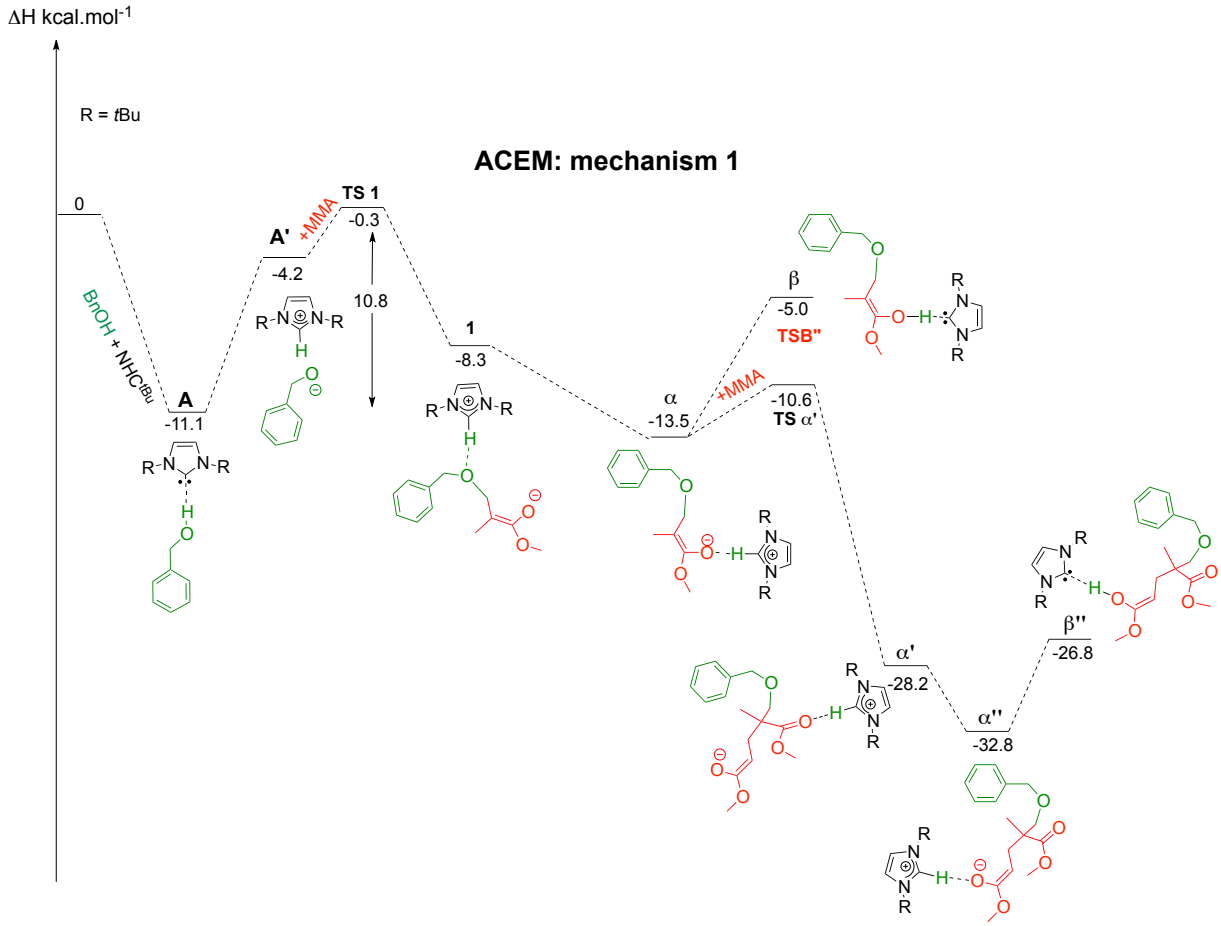

Figure 28. Energy profile computated at the B3LYP/6-31G** level of theory in DMF solvent for the ACEM (mechanism 1, Scheme 11). All enthalpies values (ΔH) are in kcal.mol^{-1}.

2.2. Activated monomer mechanism (AMM): mechanism 2

In a nucleophilic AMM initiation (Scheme 10.2), the polymerization starts by a 1,4-conjugate addition of NHC^{tBu} onto the alcohol-activated monomer. This mechanism was also investigated computationally, and the corresponding energy profile is depicted in Figure 29.

As expected, BnOH interacted with MMA through H-bonding, leading to a BnOH-MMA adduct **B** (ΔH = -5.4 kcal.mol^{-1}). The 1,4-conjugate addition of NHC^{tBu} onto **B,** forming the imidazolium enolate **B'** H-bound to BnOH, was predicted exothermic (ΔH = 8.9 kcal.mol^{-1}) and kinetically more favoured (E_a = 12.1 kcal.mol^{-1}) than the corresponding reaction in absence of BnOH forming the NHC^{tBu}-MMA zwitterion **C** (E_a of 12.1 *vs*. 15.6 kcal.mol^{-1}, with and without alcohol, respectively; see Figure 29).

The second addition of MMA onto **B'**, forming a new imidazolium enolate **B''**, was predicted to be exothermic (ΔH = -12.3 kcal.mol^{-1}) and associated with a low E_a of 4.5 kcal.mol^{-1}.

It has to be mentioned that in the absence of BnOH (direct monomer activation by NHC^{tBu}), the second addition of MMA onto a NHC^{tBu}-MMA zwitterion **C** forming the zwitterion NHC^{tBu}-MMA$_2$ **C'** (see Figure 30), was also found to be feasible both kinetically (E_a = 2.9 kcal.mol^{-1}) and thermodynamically (ΔH = -9.9 kcal.mol^{-1}), in agreement with calculations performed in chapter 2. The small differences observed for the propagation step without and in the presence of BnOH (ΔE_a = 1.6 kcal.mol^{-1} and $\Delta\Delta H$ = -2.4 kcal.mol^{-1}, the mechanism with BnOH being favoured) could explained the α-imidazolium PMMA population (population C) observed experimentally by MALDI-ToF MS analysis during the NHC^{tBu}-catalyzed polymerization of MMA initiated by BnOH (see section 1.2, Figures 9 and 10).

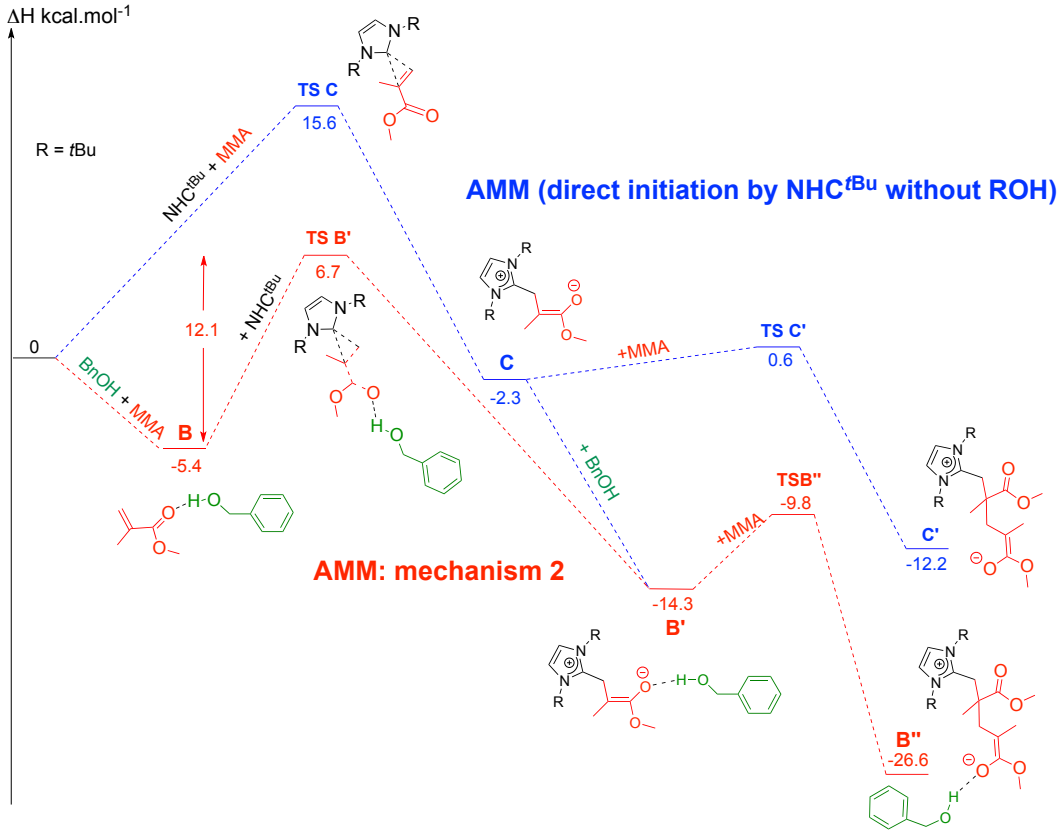

Figure 29. Energy profile computated at the B3LYP/6-31G** level of theory in DMF solvent for the AMM (mechanism 2, Scheme 11). All enthalpies values (ΔH) are in kcal.mol^{-1}.

2.3. Comparison of ACEM and AMM

As illustrated in Figure 30, the ACEM (mechanism 2) was found to be a less energy-demanding pathway for the NHC^{tBu}-catalyzed polymerization of MMA initiated by BnOH in DMF at 25 °C. As expected, NHC^{tBu} interacts more strongly with BnOH than with MMA (ΔH = -11 kcal.mol^{-1} and -5,4 kcal.mol^{-1}, respectively), in relation with their respective basicity.

However, initiation steps, *i.e.* the 1,4-addition of NHC$^{t\text{Bu}}$-BnOH onto MMA (reaction **A ⇒ α)** in the ACEM and the 1,4-addition of NHC$^{t\text{Bu}}$ onto MMA-BnOH (reaction **B ⇒ B'**) in the AMM, were similar both kinetically (E_a = 10.8 and 12.1 kcal.mol^{-1}, respectively) and thermodynamically (ΔH = 2.4 and -8.9 kcal.mol^{-11}, respectively). Moreover, for the second addition of MMA (= propagation step), both propagating species **α** and **B'** were found quasi iso-energetic (-13.5 kcal.mol^{-1} for **α** and 14.3 kcal.mol^{-1} for **B'**) and associated with low E_a (E_a = 2.9 kcal.mol^{-1} for **α⇒ α"** and 4.5 kcal.mol^{-1} for **B' ⇒ B"**), meaning that these species might kinetically compete during the polymerization. Both reactions were also found very similar thermodynamically (ΔH = -19.3 and -12.3 kcal.mol^{-11}, for **α⇒ α"** and **B' ⇒ B"**, respectively).

Consequently, the rather small differences observed computationally, in terms of energetic profile for both the initiation and the propagation steps, suggested that both concerted mechanisms, ACEM and AMM, might occur experimentally. However, considering the order of addition of the reagents, that was, 1) NHC$^{t\text{Bu}}$+BnOH and 2) addition of MMA, the ACEM might predominate especially at low $[MMA]_0/[BnOH]_0$ ratio, allowing polymer chain ends to be efficiently controlled under these conditions.

In conclusion, we have evidenced the very selective behavior of 1,3-bis(*tert*-butyl)imidazol-2-ylidene (NHC$^{t\text{Bu}}$) for the catalytic 1,4-addition polymerization of MMA, in the presence of alcohols as initiators. This simple and efficient method also allows achieving original amphiphilic block copolymers by using PEO-based macroinitiators. Combined computational and experimental investigations have revealed that both the alcohol and the monomer activation mechanisms can compete, both initiation and propagation steps proceeding by a low-energy concerted pathway. The behavior of NHC$^{t\text{Bu}}$ as a catalyst and BnOH as initiator in the polymerization of methyl acrylate (MA) was also studied as discussed in the next section.

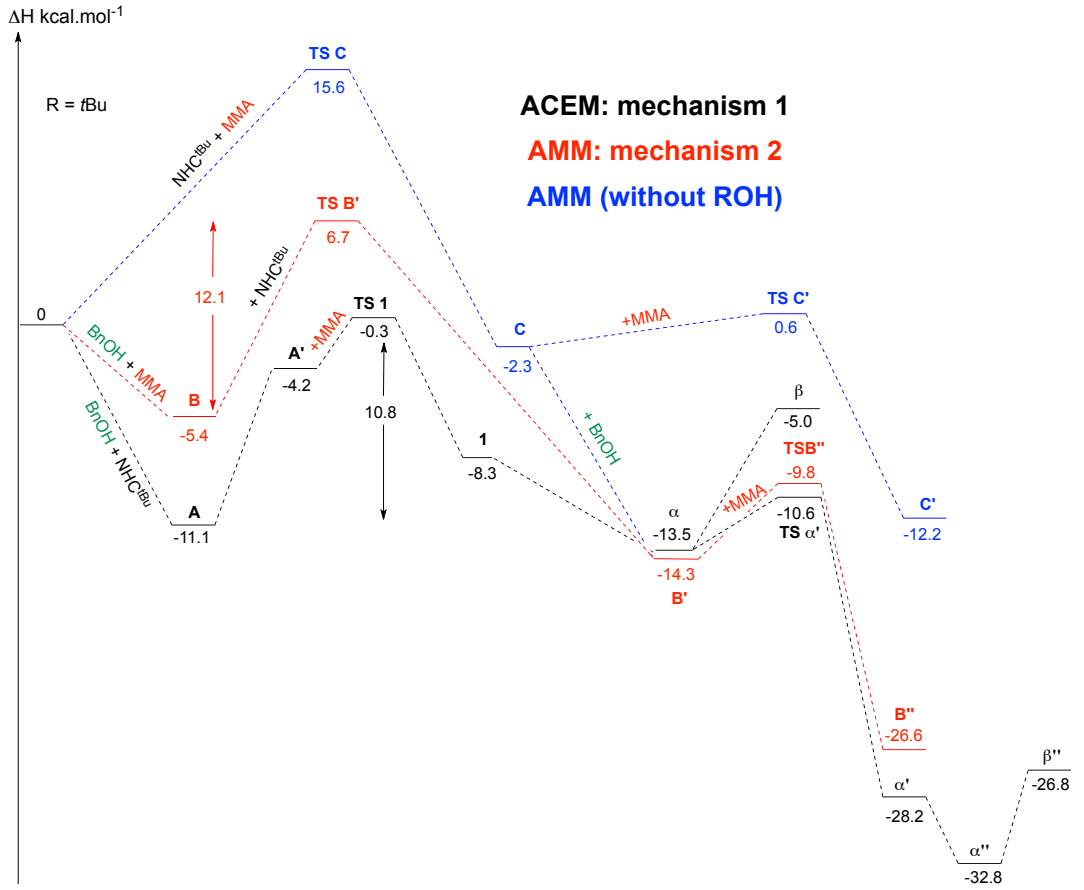

Figure 30. Energy profile computated at the B3LYP/6-31G** level of theory in DMF solvent for the ACEM (mechanism 1); AMM (mechanism 2); and direct initiation by NHC^{tBu}. All enthalpies values (ΔH) are in kcal.mol^{-1}.

3. Polymerization of methyl acrylate (MA) and copolymerization with methyl methacrylate (MMA)

3.1. Polymerization of methyl acrylate (MA)

To highlight the versatility of the NHC^{tBu}/alcohol-mediated polymerization reactions, methyl acrylate (MA) was chosen as substrate. In chapter 2, we demonstrated that NHC^{tBu} alone, was able to induce the polymerization of MA at 25 °C in DMF. Although the polymerization was fast, a rather poor control was noted.

Here, polymerization of MA was undertaken using NHC^{tBu} as true catalyst in the presence of BnOH as initiator, based on the conditions discussed above for the polymerization of MMA. The initial concentration of MA was varied, with $[NHC^{tBu}]_0$ = 19 mM and $[BnOH]_0$ = 0.19 M. Results obtained are summarized in Table 10 and are also illustrated in Figure 31.

Table 10. NHC^{tBu}-catalyzed polymerization of MA in DMF at 25 °C, in presence of BnOH as initiator.

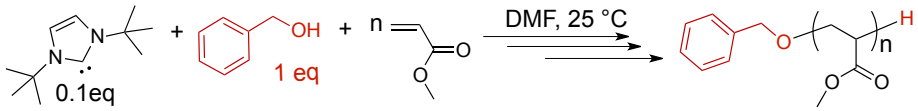

entry	[NHC^{tBu}]$_0$/[BnOH]$_0$/[MA]$_0$	Time (h)	Conv.^{a} (%)	$\overline{M}_n^{theo\ b}$ (g.mol^{-1})	$\overline{M}_n^{\ c}$ (g.mol^{-1})	$M_p^{\ c}$ (g.mol^{-1})	$Đ^c$
1	0.1/1/12	2	100	1,100	700	700	1.2
2	0.1/1/24	24	100	2,200	1,100	1,300	1.4
3	0.1/1/36	24	92	2,800	1,500	2,400	1.6
4	0.1/1/48	24	82	3,300	1,900	3,900	2.0
5a	0.1/1/12 (run1)	2	100	1,100	700	700	1.2
5b	Run 1 +12eq	24	100	2,200	1,100	1,300	1.3

a. Conv.= % monomer conversion determined by ^{1}H NMR spectroscopy; b. Theoretical molar mass $\overline{M}_n^{theo} = M_{ROH} + M_{MA} \times \frac{[MA]}{[ROH]} \times conv.$; c. Characterization of PMA's by SEC in THF using PS standards for calibration.

Under such conditions, up to 50 eq. of MA were successfully polymerized, producing poly(methy acrylate)s (PMA's) with molar masses, $\overline{M}_n$, controlled by the initial [MA]$_0$/[BnOH]$_0$ and dispersities in the range $Đ$ = 1.2-2.0 (Table 10, entries 1-4 and Figure 31).

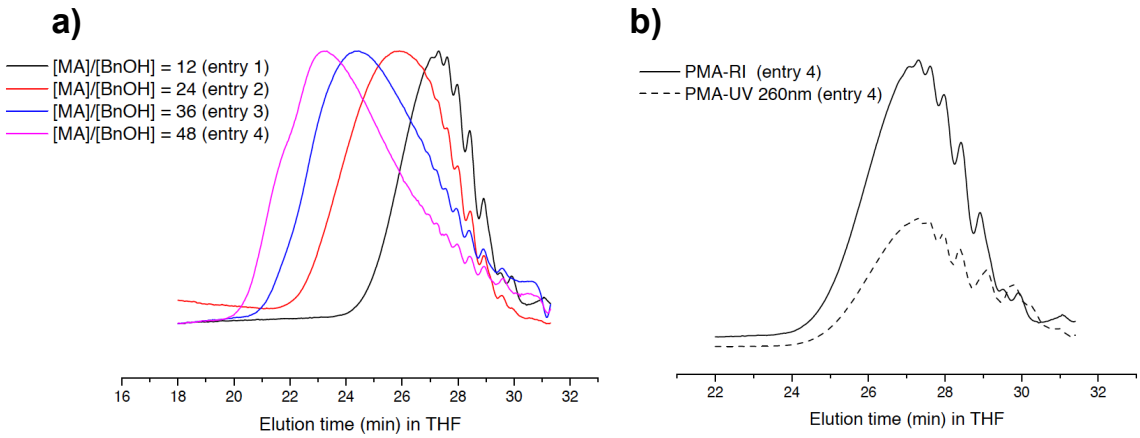

Figure 31. SEC traces of PMA's obtained with NHC^{tBu}/BnOH: a) RI traces for various [MA]$_0$; b) representative UV trace.

In addition, a chain extension experiment was successfully achieved (Figure 32). Indeed, after complete conversion, a PMA oligomer of $\overline{M}_n$ = 700 g.mol^{-1} and $Đ$ = 1.2 was obtained after 2 h of reaction (entry 5a). A new load of MA was then added (12 eq.), the molar mass of the resulting polymer increased to 1,700 g.mol^{-1} with $Đ$ = 1.3 (entry 5b) after additional 24 h of reaction.

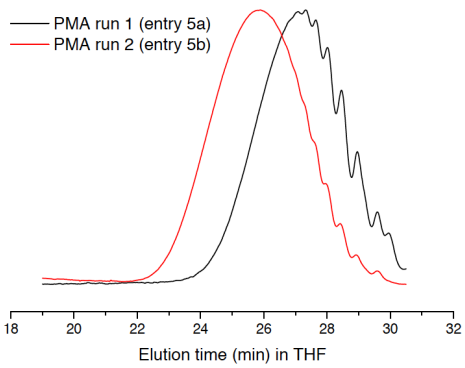

Figure 32. SEC traces of PMA's obtained upon sequential addition of monomer (Table 10, entries 5a-b).

In comparison to the NHC$^{t\text{Bu}}$-initiated polymerization of MA (chapter 2), the NHC$^{t\text{Bu}}$-catalyzed, BnOH-initiated polymerization of MA was slower: for a DP of 48, complete monomer conversion was achieved in 1 h with NHC$^{t\text{Bu}}$ alone while 24 h were required to reach 82 % of conversion with NHC$^{t\text{Bu}}$/BnOH. However, the molar masses were more controlled in the former case. The lower reactivity noted in the NHC$^{t\text{Bu}}$-catalyzed polymerization of MA could be explained by a stabilization of the propagating enolate *via* H-bond either with an imidazolium (mechanism 1, Scheme 10) or with an alcohol (mechanism 2), as discussed above. The exchange between charged active enolate and the neutral dormant form (see Scheme 6) might be slow, leading to a less controlled polymerization.

To summarize, the NHC$^{t\text{Bu}}$-catalyzed polymerization of both MMA and MA in presence of BnOH as initiator exhibited some features of a controlled polymerization. This strategy was next tested to achieve PMMA-PMA copolymers, as briefly discussed in the following section.

3.2. Copolymerization of MA with MMA

It has to be mentioned that for block copolymer synthesis by anionic polymerization, monomers must be added sequentially in the order of their increasing electron affinity, *i.e.* the first monomer should form the most nucleophilic species (*e.g.* methacrylates > acrylates).[27,46] This order of addition is crucial to avoid side reactions such as the attack of the pendant ester groups. Although this order of monomer addition was followed, the copolymerization starting from the acrylate polymerization was also tested.

The NHC$^{t\text{Bu}}$-catalyzed polymerizations of the first monomer (MMA or MA) were thus performed, in presence of BnOH as initiator, in DMF at 25 °C. After complete monomer conversion (as verified by ^{1}H NMR), the other monomer was then added. The results of these block copolymerizations are summarized in Table 11 and the corresponding SEC traces are provided in Figure 34.

Table 11. Representative NHC$^{t\text{Bu}}$-catalyzed copolymerizations of MMA with MA using BnOH as initiator, in DMF at 25 °C.

entry	M	$[NHC^{t\text{Bu}}]_0/[BnOH]_0/[M]_0$	Time (h)	Conv.[a] (%)	$\overline{M_n}^{theo}$ [b] (g.mol^{-1})	$\overline{M_n}$ [c] (g.mol^{-1})	M_p [c] (g.mol^{-1})	Đ [c]
1a	MMA	0.1/1/15	6	100	1,500	2,300	3,100	1.4
1b	MA	0.1/1/15	5	90	2,700	2,850	3,300	2.5
2a	MA	0.1/1/15	3	92	1,300	845	1,100	1.5
2b	MMA	0.1/1/15	96	0	1,300	1,100	1,241	1.3

a. Conv.= % monomer conversion determined by ^{1}H NMR spectroscopy; b. Theoretical molar mass $\overline{M}_n^{theo} = M_{ROH} + M_M \times \frac{[M]}{[BnOH]} \times conv.$; c. Characterization of polymers by SEC in THF using PS standards for calibration.

Consistently with our previous findings, MMA polymerization induced by NHC$^{t\text{Bu}}$/BnOH could be controlled for low DP_n,. Hence, the synthesis of the first block, *i.e.* PMMA, was conducted targeting a DP_n equal to 15 (Table 11, entry 1a). PMMA oligomers of $\overline{M_n}$ = 2,300 g.mol^{-1} and $Đ$ = 1.4 were thus obtained, after complete conversion, in 6 h (population **P***⇔**P** in Scheme 11). Then, 15 eq. of MA monomer were added onto this living PMMA precursor, yielding 90 % of conversion after 5 h (entry 1b). SEC traces of the final compound (Figure 33) showed a shoulder in the high molar masses region (population **Y**), but the population due to the first PMMA block (population **P***⇔**P**) was still present in large amounts.

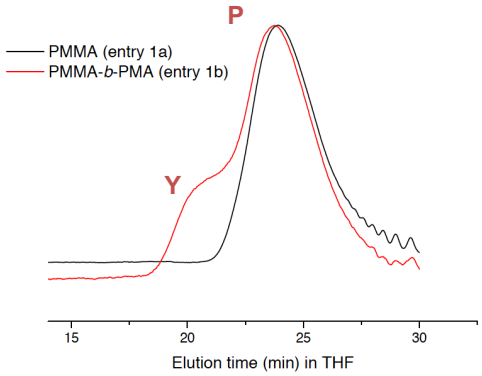

Figure 33. SEC-RI traces of copolymers PMMA-*b*-PMA obtained after sequential addition of MMA and MA using NHC$^{t\text{Bu}}$/BnOH in DMF at 25 °C (Table 11, entry 1).

A slow equilibrium between active and dormant PMMA chains could explain the features of this polymerization. The first PMMA block might remain in the dormant form **P** and the polymerization of MA is rather initiated by the NHC$^{t\text{Bu}}$-complex, leading to PMA homopolymers **Y** (see Scheme 11). Under such conditions, the concentration of both the carbene and the alcohol might be not enough to control both the homopolymerization of MA

and the stabilization of PMMA living chains, hence the population in higher molar masses region. However, the termination of PMMA chains before the addition of MA cannot be ruled out. The identification of the homopolymer or copolymer architecture of the final material required purification using a selective solvent for PMMA or for PMA, but this remains difficult to implement.

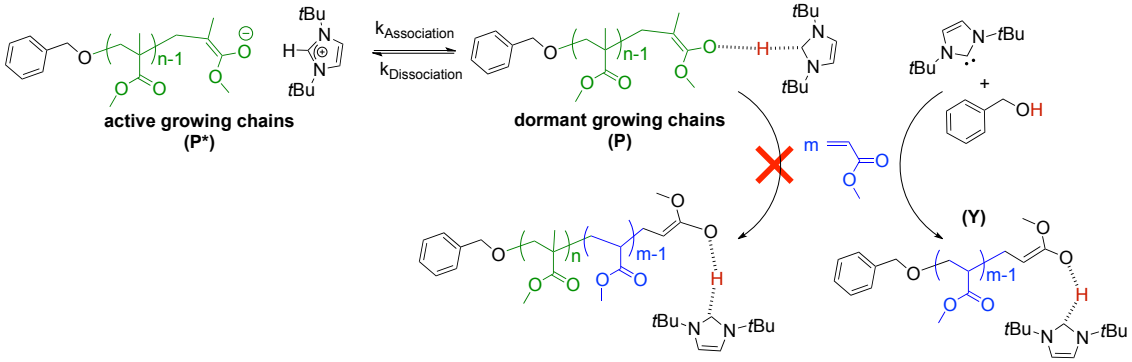

Scheme 11. Putative equilibrium between active growing chain (P*) and dormant species (P) and associated copolymerization with MA.

When the order of addition was reverse (PMA first), MMA was not polymerized at all, and only PMA homopolymer was obtained (Table 11; entry 2 and Figure 34), in accordance with the reactivity observed in anionic polymerization.[27,46]

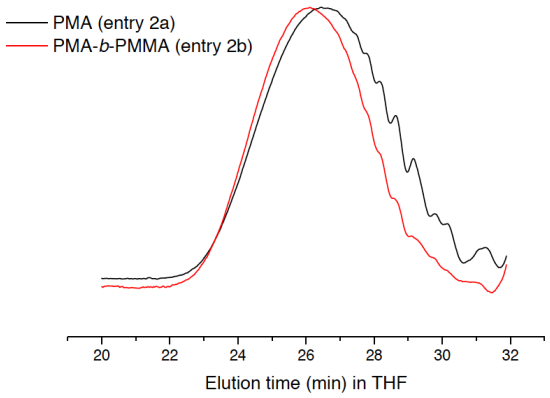

Figure 34. SEC traces (RI) of PMA-*b*-PMMA copolymers obtained after sequential addition of MA and MMA using NHC^{tBu}/BnOH in DMF at 25 °C (Table 11, entry 2).

These preliminary studies show that the copolymerization of MA and MMA, using NHC^{tBu} and BnOH as catalyst and initiator, respectively, remains challenging. As a means to optimize this copolymerization, a mixture of solvent (*e.g.* DMF/DMSO) or a decrease of the temperature of polymerization (*e.g.* from 25 °C to 0 °C) could be considered, in order to increase the ion pair dissociation.[47] A slow addition of MA, immediately after complete conversion of MMA, could also be a solution to limit chain termination of PMMA, which could have occurred before addition of MA monomer.

Conclusions and outlooks

The very specific and selective behavior of 1,3-bis(*tert*-butyl)imidazol-2-ylidene (NHC^{tBu}) for the catalytic conjugate 1,4-addition polymerization of methyl(meth)acrylate, in the presence of alcohols as initiators, was investigated in this chapter.

The polymerization was found to be controlled by the alcohol, leading to α-alkoxy-poly(methyl methacrylate)s (PMMA's) and amphiphilic block copolymers as well when using hydroxylated poly(ethylene oxide)s (PEO's) as macroinitiators. In the latter case, a nano-organization into micelles in an aqueous solution was noted. In addition, this NHC^{tBu}-catalyzed alcohol-initiated polymerization also allowed the controlled synthesis of poly(methyl acrylate)s (PMA's). However block copolymerization with MMA met with very limited success and would require further optimization, for instance, by increasing the polarity of the medium (solvent mixture) or by decreasing the temperature of the polymerization.

DFT calculations allowed us to rationalize our experimental findings by proposing two mechanisms where hydrogen-bonds are involved: an alcohol-activated mechanism through interaction with the carbene and a monomer-activated mechanism through interaction with the alcohol. Both initiation and propagation steps of these two mechanisms were found to be iso-energetic with low energy barriers, and proceeded in a concerted pathway. Both mechanisms likely compete during the polymerization reaction, though we postulated that the alcohol activation by the carbene was the preferred pathway, based on the experimental protocol used to perform the polymerization reactions (mixture of carbene and alcohol, followed by monomer addition).

This unprecedented strategy could provide poly(alkyl)(meth)acrylates suitable for post-polymerization modification, through the use of alcohols featuring functional groups, that should be compatible, however, with carbene's reactivity. Additionally, functional amphiphilic copolymers, such as PEO's grafted with (meth)acrylic groups, could thus be prepared using this simple and efficient method.

Furthermore, this NHC-catalyzed and selective conjugate 1,4 addition in presence of protic initiators, could be generalized to various Michael acceptors, in molecular chemistry. This will be a straightforward method to produce new activated compound of interest for cascades reactions, for instance.

Experimental and supporting information

General instrumentation. NMR spectra were recorded on a Bruker AC-400 spectrometer (^{1}H, ^{13}C, 400 MHz and 100MHz respectively) in appropriate deuterated solvents. Molar masses of polymers samples were determined by size exclusion chromatography (SEC) using a 3-columns set of TSK gel TOSOH (G2000, G3000, G4000 with pore sizes of 20, 75, and 200 Å respectively, connected in series) calibrated with narrow Polystyrene standards from Polymer Laboratories using both refractometric and UV detectors (Varian). THF was used as eluent (1 $mL.min^{-1}$) and trichlorobenzene as a flow marker at 40 °C. MALDI-ToF experiments were performed by the ISM-CESAMO (Bordeaux, France) on a Voyager mass spectrometer (Applied Biosystems). The instrument is equipped with a pulsed N2 laser (337 nm) and a time-delayed extracted ion source. Spectra were recorded in the positive-ion mode using the reflectron and with an accelerating voltage of 20 kV. Samples were dissolved in THF at 10 $mg.ml^{-1}$. The IAA matrix (trans-3-Indoleacrylic acid) solution was prepared by dissolving 10 mg in 1 ml of THF. A MeOH solution of cationisation agent (NaI, 10 $mg.ml^{-1}$) was also prepared. The solutions were combined in a 10:1:1 volume ratio of matrix to sample to cationisation agent. One to two microliters of the obtained solution was deposited onto the sample target and vacuum-dried. Transmission Electron Microscopy (TEM) images were recorded on a Hitachi H7650 microscope working at 80 kV. Samples were prepared by spraying a $1g.L^{-1}$ solution of the block copolymer onto a copper grid (200 mesh coated with carbon) using a homemade spray tool and negatively stained with 1.5% uranyl acetate.

Materials. Dimethylformamide (DMF; technical grade) was first cryo-distilled over CaH_2 and stored over molecular sieves, and freshly cryo-distilled prior to use. Methyl acrylate (MA) and Methyl methacrylate (MMA) were purchased from Sigma-Aldrich, degased, dried over CaH_2, cryo-distilled into a burette and stored at -20°C. Benzyl alcohol and *tert*-butyl alcohol were dried over CaH_2, purified by fractionated distillation, and stored over molecular sieves in a glovebox. 1-Pyrenebutanol was recrystallized twice from dry toluene and stored in a glovebox. 1,4-Benzenedimethanol was lyophilized from toluene solution. Propargyl alcohol was dried with molecular sieves, distilled and stored in a glovebox. Poly(ethylene oxide monomethyl ether) with an average molecular weight of ,1300 $g.mol^{-1}$ was purchased from Polymer Source, Inc. and was recrystallized from toluene 3 times, dried under vacuum and stored in a glovebox. 1,3-Bis(*tert*-butyl)imidazol-2-ylidene (NHC^{tBu}), and 1,3-bis(mesityl)imidazol-2-ylidene (NHC^{Mes}) were purchased from Strem Chemical as used as received. 1,3-bis(isopropyl)imidazol-2-ylidene (NHC^{iPr}) and 1,3–bis(isopropyl)-4,5-

(dimethyl)imidazol-2-ylidene (NHC^{iPrMe}) were prepared according to the procedure already reported [14,48]. All NHCs were kept under an argon glovebox in a freezer at 4 °C.

General polymerization procedure.

In a typical procedure, 17 mg (92 µmol) of NHC^{tBu} and 100µL of benzyl alcohol (0.92 mmol) were added in a flame-dried Schlenk flask in the glovebox. After removal of the Schlenk from the glovebox, 5 mL of DMF were introduced under vacuum. After 5 min homogenization, 1 mL MMA (9.2 mmol) was added dropwise via a syringe under a flux of argon and vigorous stirring. After 5h at 25 °C, an aliquot of the polymerization mixture was taken to determine the conversion by ^{1}H NMR analysis in $CDCl_3$ and the reaction was quenched at the air and stirred for 1h. All the volatiles were removed under vacuum. The crude product was re-dissolved in THF and precipitated in pentane twice. PMMA was recovered as a white solid.

Chain extension experiment.

In a typical experiment, 2 mL of MMA (20 equivalents) were added onto the living PMMA chain obtained after 5h (run 1,100% of conversion). After 24h, 100% of MMA conversion was reached (check by ^{1}H NMR). The work-up was the same as described above.

^{1}H NMR of MeOPEO-*b*-PMMA block copolymers

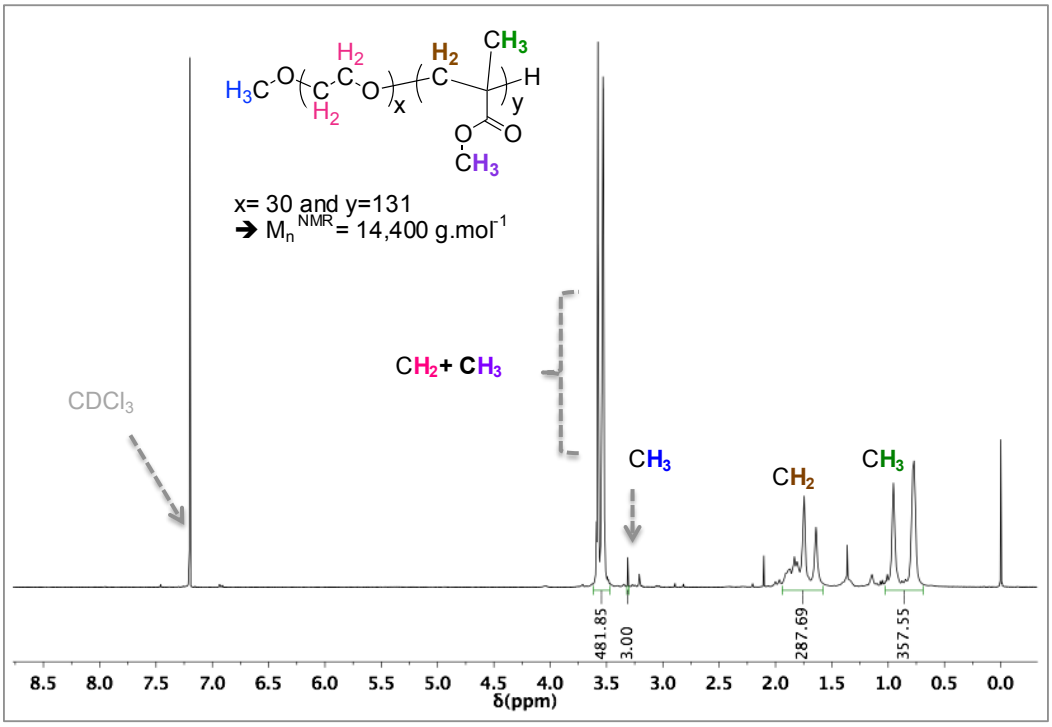

Figure S1. ^{1}H NMR (in $CDCl_3$) spectrum of $MeOPEO_{33}$-$PMMA_{100}$ (Table 3, entry 3).

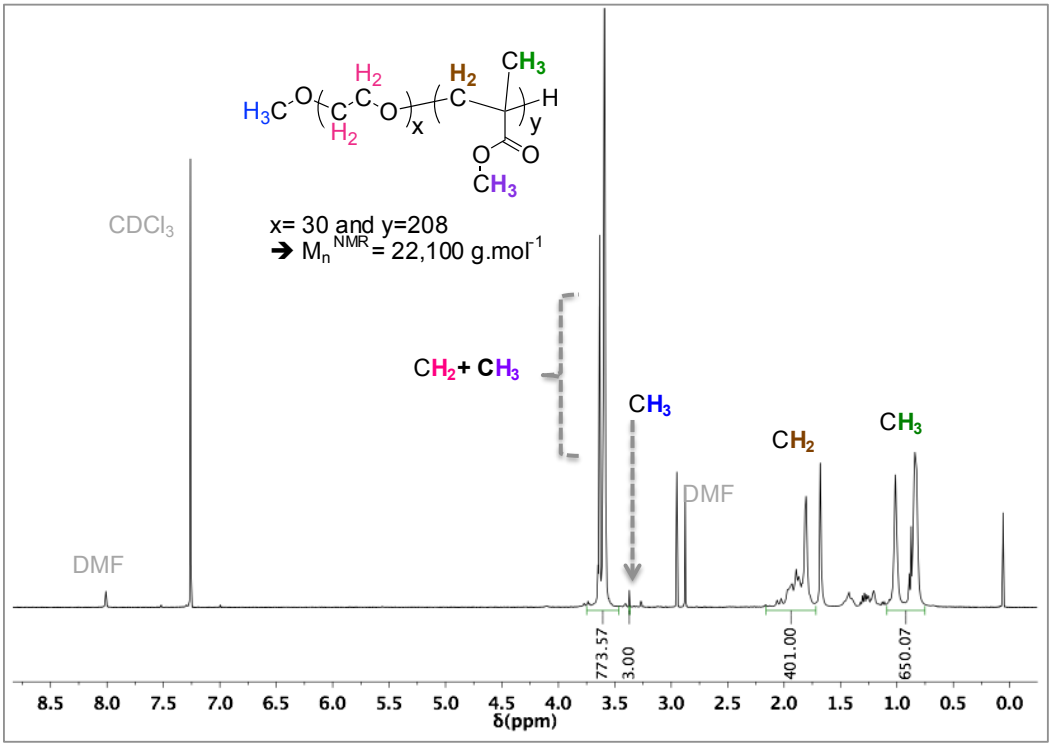

Figure S2. ^{1}H NMR (in $CDCl_3$) spectrum of $MeOPEO_{33}$-$PMMA_{200}$ (Table 3, entry 4).

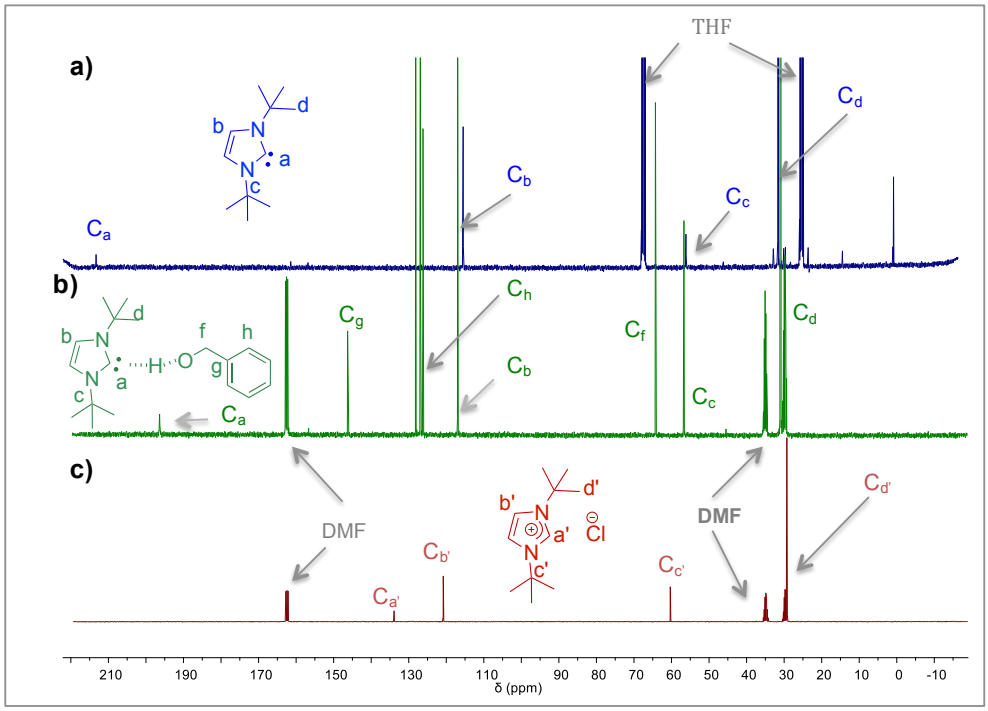

Figure S3. ^{13}C NMR spectrum in DMF-d_7 of a) NHC^{tBu} + BnOH (1:1) mixture; b) NHC^{tBu} in THF-d_8; c) NHC^{tBu}HCl.

Products of reaction and corresponding transition states

MMA

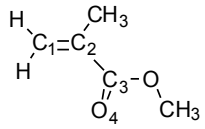

C_1-C_2 = 1.333 Å
C_2-C_3 = 1.498 Å
C_3-O_4 = 1.212 Å

BnOH

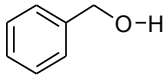

O-H = 0.965 Å

A

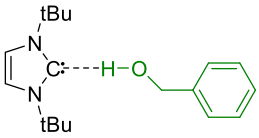

O-C : 2.871
H-O : 1.003
C-H : 1.881

A'

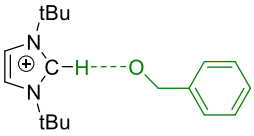

O-C : 2.651
H-O : 1.479
C-H : 1.189

TS 1

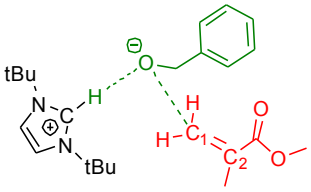

O-C1 : 2.077
O-C2 : 2.947
C1-C2 : 1.366
H-O : 1.856
C-H : 1.104

1

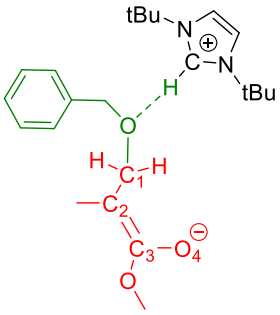

C1C2 : 1.477
C2-C3 : 1.387
C3-O4 : 1.255
O-H : 2.211
H-C : 1.085
O-C1 : 1.467
O-C2 : 2.504

α

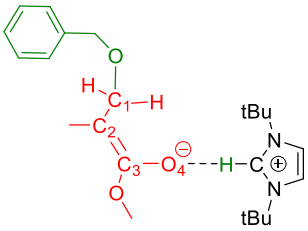

C1-C2 : 1.477
C2-C3 : 1.383
C3-O4 : 1.264
O4-H : 2.011
H-C : 1.093
O-C1 : 1.454

β

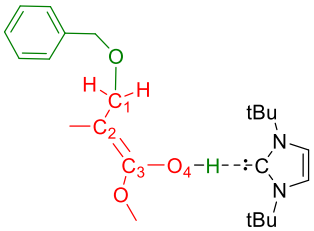

C1-C2 : 1.454
C2-C3 : 1.350
C3-O4 : 1.326
O4-H : 1.113
H-C : 1.547
O-C1 : 1.326

TS α'

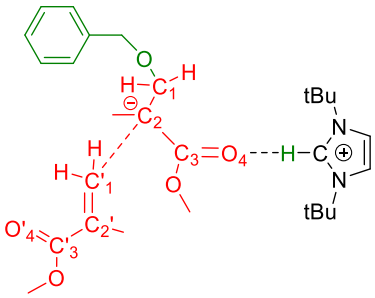

O-C1 : 1.440
C1-C2 : 1..486
C2-C3 : 1.417
C3-O4 : 1.247
C2-C'1 : 2.219
C2-C'2 : 3.065
C'1-C'2 : 1.379
C'2-C'3 : 1.444
C'3-O'4 : 1.228
O4-H : 2.080
H-C : 1.086

α'

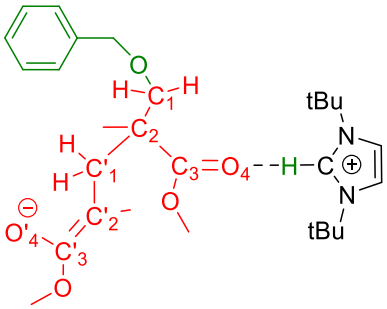

O-C1 : 1.419
C1-C2 : 1.523
C2-C3 : 1.514
C3-O4 : 1.221
C2-C'1 : 1.578
C'1-C'2 : 1.496
C'2-C'3 : 1.382
C'3-O'4 : 1.257
O4-H : 2.100
H-C : 1.083

α″

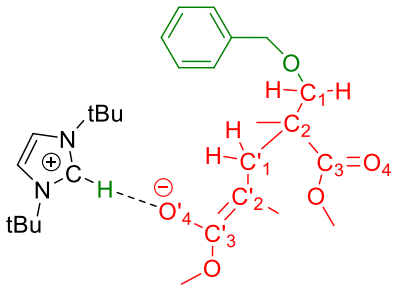

O-C1 : 1.413
C1-C2 : 1.526
C2-C3 : 1.562
C3-O4 : 1.214
C2-C'1 : 1.562
C'1-C'2 : 1.504
C'2-C'3 : 1.370
C'3-O4 : 1.277
O4-H : 1.803
H-C : 1.103

β″

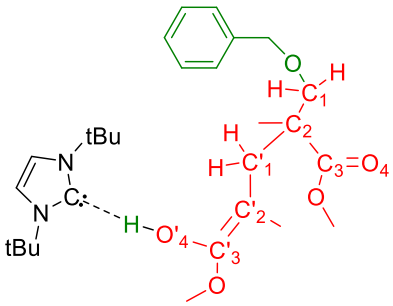

O-C1 : 1.412
C1-C2 : 1.527
C2-C3 : 1.557
C3-O4 : 1.212
C2-C'1 : 1.557
C'1-C'2 : 1.509
C'2-C'3 : 1.347
C3-O : 1.333
C'3-O'4 : 1.333
O'4-H : 1.088
H-C: 1.577

Figure S4. Selected bond lengths (in Å) and bond angles (in °) for the minima and TS involved in the activated initiator/chain-end mechanism (mechanism 1a) at the M06-2X/6-31G** level of theory.

B

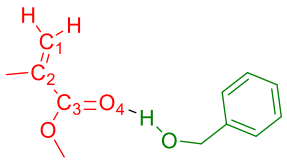

O-H : 0.972
O4-H : 1.903
C1-C2 : 1.334
C2-C3 : 1.495
C3-O4 : 1.218

TS B'

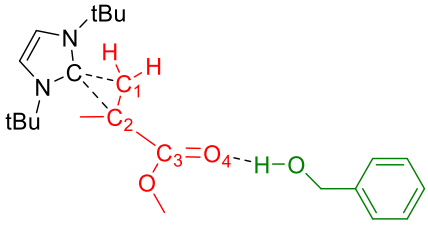

O-H : 0.976
O4-H : 1.804
C-C1 : 2.073
C-C2 : 2.855
C1-C2 : 1.389
C2-C3 : 1.434
C3-O4 : 1.239

B'

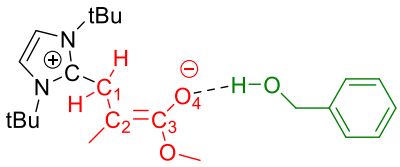

O-H : 0.993
O4-H : 1.653
C-C1 : 1.504
C-C2 : 2.508
C1-C2 : 1.512
C2-C3 : 1.375
C3-O4 : 1.273

TS B″

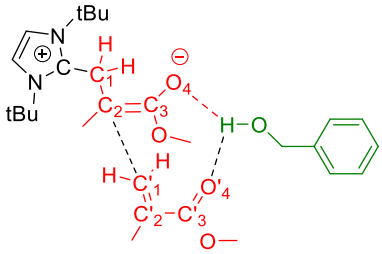

O-H : 0.975
O4-H : 2.038
O4'-H : 2.231
C-C1 : 1.509
C1-C2 : 1.515
C2-C3 : 1.414
C3-O4 : 1.248
C3-C'2 : 3.216
C2-C'1 : 2.242
C2-C'2 : 3.096
C'1-C'2 : 1.376
C'2-C'3 : 1.445
C'3-O'4 : 1.228

B″

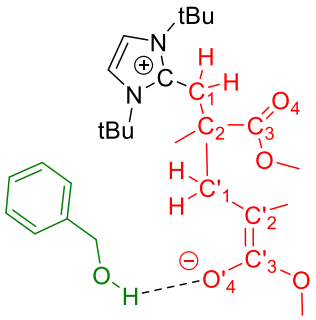

O-H : 1.004
O4'-H : 1.598
C-C1 : 1.505
C1-C2 : 1.569
C2-C3 : 1.527
C3-O4 : 1.214
C2-C'1 : 1.584
C'1-C'2 : 1.499
C'2-C'3 : 1.372
C'3-O'4 : 1.276

Figure S5. Selected bond lengths (in Å) and bond angles (in °) for the minima and TS involved in the activated monomer mechanism with BnOH (mechanism 2b) at the M06-2X/6-31G** level of theory.

TS C

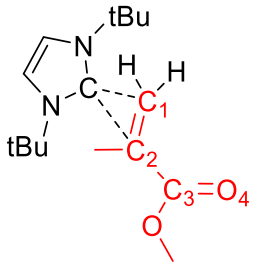

C-C1 : 2.037
C1-C2 : 1.391
C-C2 : 2.845
C2-C3 : 1.439
C3-O4 : 1.230

C

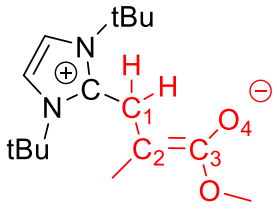

C-C1 : 1.505
C1-C2 : 1.510
C-C2 : 2.509
C2-C3 : 1.386
C3-O4 : 1.256

TS C'

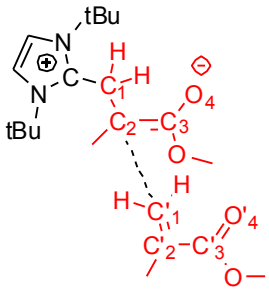

C-C1 : 1.510
C1-C2 : 1.515
C2-C3 : 1.418
C3-O4 : 1.241
C3-C'2 : 3.286
C2-C'1 : 2.259
C2-C'2 : 3.113
C'1-C'2 : 1.375
C'2-C'3 : 1.447
C'3-O'4 : 1.226

C'

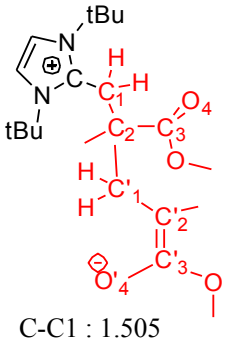

C-C1 : 1.505
C1-C2 : 1.567
C2-C3 : 1.523
C3-O4 : 1.215
C3-C'2 : 3.105
C2-C'1 : 1.592
C2-C'2 : 2.637
C'1-C'2 : 1.493
C'2-C'3 : 1.385
C'3-O'4 : 1.255

Figure S6. Selected bond lengths (in Å) and bond angles (in °) for the minima and TS involved in the activated monomer mechanism without BnOH, (mechanism 2a) at the M06-2X/6-31G** level of theory.

References

(1) Biju, A. T.; Padmanaban, M.; Wurz, N. E.; Glorius, F. *Angew. Chem. Int. Ed.* **2011**, *50*, 8412.
(2) Matsuoka, S.-I.; Ota, Y.; Washio, A.; Katada, A.; Ichioka, K.; Takagi, K.; Suzuki, M. *Org. Lett.* **2011**, *13*, 3722.
(3) Kato, T.; Ota, Y.; Matsuoka, S.-I.; Takagi, K.; Suzuki, M. *J. Org. Chem.* **2013**, *78*, 8739.
(4) Matsuoka, S.-I.; Namera, S.; Washio, A.; Takagi, K.; Suzuki, M. *Org. Lett.* **2013**, *15*, 5916.
(5) Kato, T.; Matsuoka, S.-I.; Suzuki, M. *J. Org. Chem.* **2014**, *79*, 4484.
(6) Zhang, Y.; Chen, E. Y. X. *Angew. Chem. Int. Ed.* **2012**, *51*, 2465.
(7) Zhang, Y.; Schmitt, M.; Falivene, L.; Caporaso, L.; Cavallo, L.; Chen, E. Y. X. *J. Am. Chem. Soc.* **2013**, *135*, 17925.
(8) Martin, D.; Canac, Y.; Lavallo, V.; Bertrand, G. *J. Am. Chem. Soc.* **2014**, *136*, 5023.
(9) Naumann, S.; Schmidt, F. G.; Schowner, R.; Frey, W.; Buchmeiser, M. R. *Polym. Chem.* **2013**, *4*, 2731.
(10) Nzahou Ottou, W.; Bourichon, D.; Vignolle, J.; Wirotius, A.-L.; Robert, F.; Landais, Y.; Sotiropoulos, J.-M.; Miqueu, K.; Taton, D. *Chem. Eur. J.* **2014**, *20*, 3989.
(11) Naumann, S.; Buchmeiser, M. *Catal. Sci. Technol.* **2014**.
(12) Scholten, M. D.; Hedrick, J. L.; Waymouth, R. M. *Macromolecules* **2008**, *41*, 7399.
(13) Raynaud, J.; Ciolino, A.; Baceiredo, A.; Destarac, M.; Bonnette, F.; Kato, T.; Gnanou, Y.; Taton, D. *Angew. Chem., Int. Ed.* **2008**, *47*, 5390.
(14) Raynaud, J.; Gnanou, Y.; Taton, D. *Macromolecules* **2009**, *42*, 5996.
(15) Raynaud, J.; Liu, N.; Gnanou, Y.; Taton, D. *Macromolecules* **2010**, *43*, 8853.
(16) Raynaud, J.; Liu, N.; Fevre, M.; Gnanou, Y.; Taton, D. *Polym. Chem.* **2011**, *2*, 1706.
(17) Fèvre, M.; Vignolle, J.; Gnanou, Y.; Taton, D. In *Polymer Science: A Comprehensive Reference*; Editors-in-Chief: Krzysztof, M., Martin, M. I., Eds.; Elsevier: Amsterdam, 2012, p 67.
(18) Dove, A. P. *ACS Macro Lett.* **2012**, *1*, 1409.
(19) Magill, A. M.; Cavell, K. J.; Yates, B. F. *J. Am. Chem. Soc.* **2004**, *126*, 8717.
(20) Tomoi, M.; Shibayama, Y.; Kakiuchi, H. *Polym J* **1976**, *8*, 190.
(21) Viguier, M.; Collet, A.; Schue, F. *Polym J* **1982**, *14*, 137.
(22) Suzuki, T.; Murakami, Y.; Tsuji, Y.; Takegami, Y. *J. Polym. Sci. B Polym. Lett. Ed.* **1976**, *14*, 675.
(23) Olmstead, W. N.; Margolin, Z.; Bordwell, F. G. *J. Org. Chem.* **1980**, *45*, 3295.
(24) Busnel, J. P. *Polymer* **1982**, *23*, 137.
(25) Hatada, K.; Kitayama, T. In *NMR Spectroscopy of Polymers*; Springer Berlin Heidelberg: **2004**, p 73.
(26) Sogah, D. Y.; Hertler, W. R.; Webster, O. W.; Cohen, G. M. *Macromolecules* **1987**, *20*, 1473.
(27) Baskaran, D.; Müller, A. H. E. *Prog. Polym. Sci.* **2007**, *32*, 173.
(28) Raynaud, J.; Absalon, C.; Gnanou, Y.; Taton, D. *J. Am. Chem. Soc.* **2009**, *131*, 3201.
(29) Raynaud, J.; Absalon, C.; Gnanou, Y.; Taton, D. *Macromolecules* **2010**, *43*, 2814.
(30) Raynaud, J.; Nzahou Ottou, W.; Gnanou, Y.; Taton, D. *Chem. Commun.* **2010**, *46*, 3203.
(31) Seow, P. K.; Gallot, Y.; Skoulios, A. *Makromol. Chem.* **1975**, *176*, 3153.
(32) Dhara, M. G.; Baskaran, D.; Sivaram, S. *J. Polym. Sci., Part A: Polym. Chem.* **2008**, *46*, 2132.
(33) Garg, D.; Höring, S.; Ulbricht, J. *Macromol. Rapid Commun.* **1984**, *5*, 615.
(34) Siegwart, D. J.; Wu, W.; Mandalaywala, M.; Tamir, M.; Sarbu, T.; Silverstein, M. S.; Kowalewski, T.; Hollinger, J. O.; Matyjaszewski, K. *Polymer* **2007**, *48*, 7279.
(35) Johnson Jr, C. S. *Prog. Nucl. Magn. Reson. Spectrosc.* **1999**, *34*, 203.
(36) Chen, A.; Wu, D.; Johnson, C. S. *J. Am. Chem. Soc.* **1995**, *117*, 7965.
(37) Movassaghi, M.; Schmidt, M. A. *Org. Lett.* **2005**, *7*, 2453.
(38) Schmidt, M. A.; Muller, P.; Movassaghi, M. *Tetrahedron Lett.* **2008**, *49*, 4316.

(39) Jeong, W.; Shin, E. J.; Culkin, D. A.; Hedrick, J. L.; Waymouth, R. M. *J. Am. Chem. Soc.* **2009**, *131*, 4884.
(40) Kiesewetter, M. K.; Shin, E. J.; Hedrick, J. L.; Waymouth, R. M. *Macromolecules* **2010**, *43*, 2093.
(41) Brown, H. A.; Waymouth, R. M. *Acc. Chem. Res.* **2013**, *46*, 2585.
(42) Litvinenko, G.; Müller, A. H. E. *Macromolecules* **1997**, *30*, 1253.
(43) Fèvre, M.; Pinaud, J.; Gnanou, Y.; Vignolle, J.; Taton, D. *Chem. Soc. Rev.* **2013**, *42*, 2142.
(44) Nyce, G. W.; Glauser, T.; Connor, E. F.; Mock, A.; Waymouth, R. M.; Hedrick, J. L. *J. Am. Chem. Soc.* **2003**, *125*, 3046.
(45) Phillips, E. M.; Riedrich, M.; Scheidt, K. A. *J. Am. Chem. Soc.* **2010**, *132*, 13179.
(46) Baskaran, D.; Müller, A. H. E. Anionic Vinyl Polymerization,In *Controlled and Living Polymerizations*; Wiley-VCH Verlag GmbH & Co. KGaA: **2010,** p 1.
(47) Esch, T. E. H.; Smid, J. *J. Am. Chem. Soc.* **1966**, *88*, 307.
(48) Kuhn, N.; Kratz, T. *Synthesis* **1993**, 561.

Chapter 4.

Lewis pair-induced polymerization of methyl methacrylate: association of a *N*-heterocyclic carbene or a phosphine as an organic Lewis base and a silicon-based Lewis acid

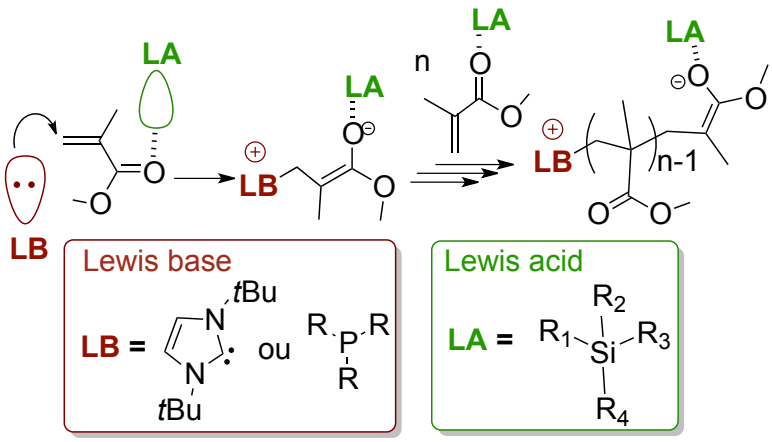

Keywords: Organopolymerization • Lewis pair • *N*-Heterocyclic Carbenes • Phosphines • Silicon • Methyl methacrylate •

Chapter 4

Lewis Pair-induced polymerization of methyl methacrylate: association of a *N*-heterocyclic carbene or a phosphine as an organic Lewis base and a silicon-based Lewis acid

Table of contents

Introduction

The previous chapters have emphasized the utilization of *N*-heterocyclic carbenes (NHCs) as viable alternatives to metal-based activators for polymerization reactions of some monomers, thus providing new strategies for precision polymer synthesis.[1,2] It is worth pointing out, however, that mainly heterocyclic monomers (*e.g.* cyclic esters, carbonates, ethers, siloxanes or *N*-carboxyanhydrides) have been investigated in NHC-mediated polymerization reactions. Polymerization of alkyl (meth)acrylates triggered by NHCs has also been addressed. The focus on these monomers is due to the relative easiness for activating polar C-heteroatom bonds of heteroatom-containing substrates. However, NHC-induced polymerization reactions of non-polar vinyl monomers (*e.g.* styrene or butadiene) still remain challenging.

The present chapter proposes to associate a NHC as a nucleophile Lewis base (LB) to an electrophilic Lewis acid (LA) as co-activators to trigger the dually activated polymerization of model vinyl monomers, such as (meth)acrylic derivatives. This type of polymerization is thus based on on a "push-pull" effect (Figure 1). In this case, the Lewis pair should play the role of a direct initiator and not that of a catalyst, and this pair is expected to enhance the reactivity of the monomer by a cooperative activation and/or to prevent side reactions from occurring,

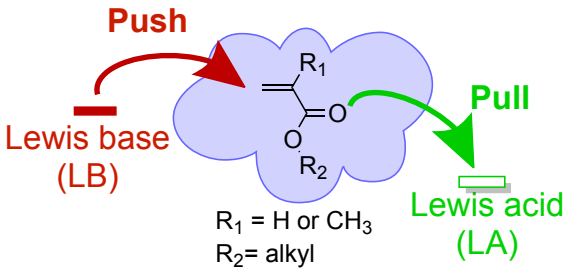

Figure 1. Monomer activation by "push-pull" effect using a LA and LB.

In order to promote this "push-pull" effect, however, the irreversible formation a "classical" 1:1 LA:LB adduct has to be prevented, so as to maintain the reactivity of both LA and LB. Such a quenching of reactivity can be avoided either (1) by adding the two reagents in a specific order, or (2) by carefully selecting the reaction partners. Indeed, based on steric hindrance, it is possible to elaborate a so-called frustrated Lewis pair (FLP, Figure 2).

The concept of FLP has been introduced by Stephan *et al.*[3,4] and Erker *et al.*[5] in 2006 and consists in a Lewis pair, where the LA and the LB are sterically precluded from forming a "classical" irreversible Lewis adduct (CLP), as illustrated in Figure 2.

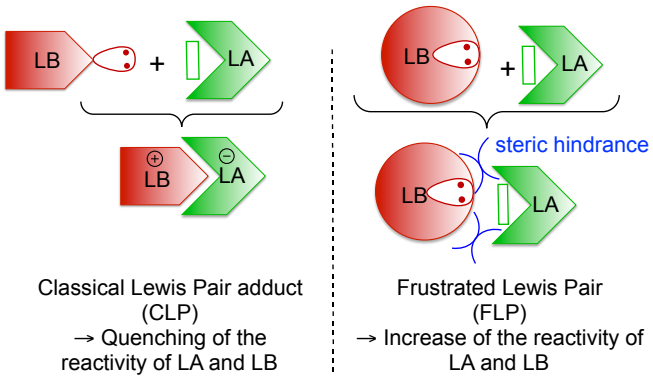

Figure 2. Formation of "classical" Lewis pair (CLP) *vs.* "frustrated" Lewis pair (FLP).

In molecular chemistry, this concept has been widely applied for the synergetic activation of a broad range of poorly reactive substrates, including H_2,[3,6] CO_2,[7,8] N_2O[9,10] alkenes,[11] alkynes,[12-14] cyclopropanes[15] or THF.[16,17] Various FLPs have been developed, including phosphines, amines and NHCs as LB's, associated with mainly boranes and alanes as LA's (Figure 3). Typical examples of intermolecular FLPs are $P^tBu_3 + B(C_6F_5)_3$; $PMes_3$, (Mes = 2,4,6-$Me_3C_6H_2$)+ $B(C_6F_5)_3$ or DTBP (= 2,6-di-*tert*-butyl pyridine)+ $Al(C_6F_5)_3$.

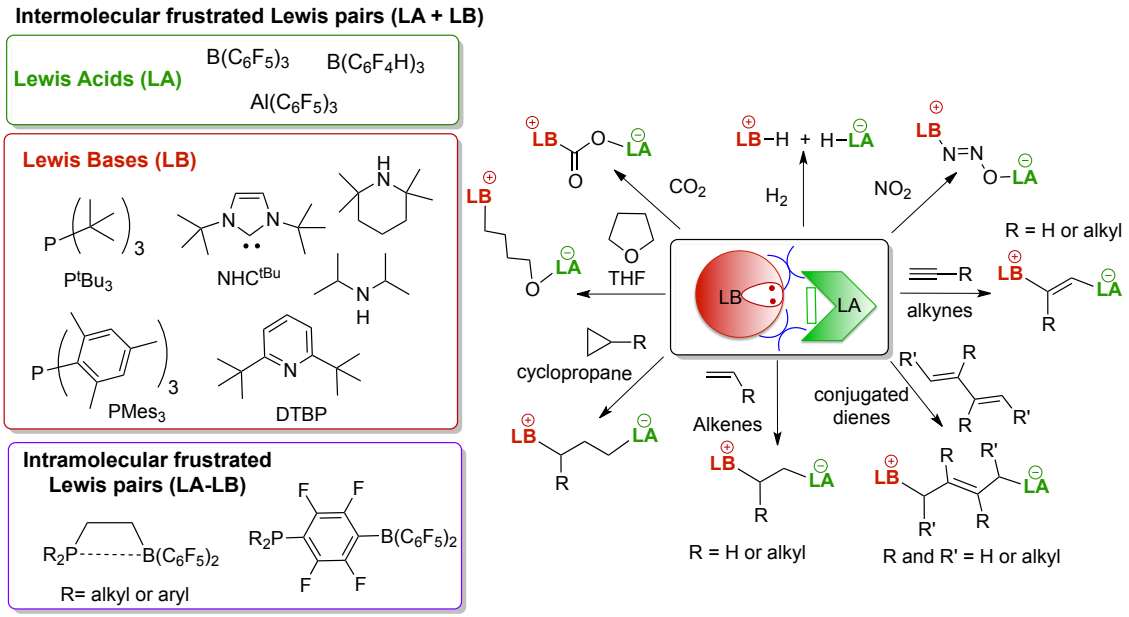

Figure 3. Representative Lewis acids (LA's) and Lewis bases (LB's) and main FLP-reactivity.

While investigations were undergoing in our group (Maréva Fèvre PhD thesis, Université de Bordeaux, 2009-2012), Chen *et al.* reported the first example of the use of Lewis pairs (either FLP's or CLP's) for the polymerization of (meth)acrylic monomers, *via* the so-called Lewis pair polymerization (LPP).[18-20] The combination of $Al(C_6F_5)_3$ with a NHC, namely 1,3-bis(mesityl)imidazol-2-ylidene (NHC^{Mes}) or 1,3-bis(*tert*-butyl)imidazol-2-ylidene (NHC^{tBu}) or a phosphine, namely tri-*tert*-butylphosphine (P^tBu_3) or tri-phenylphosphine

(PPh_3), proved to activate the monomer (**1**, Scheme 1a) in a cooperative manner and affording linear poly(meth)acrylates.

LPP typically proceeds *via* zwitterionic intermediates (**2**, Scheme 1a), but can differ from the "classic" zwitterionic polymerization (**5**, Scheme 1b), that is usually initiated by a nucleophile, since in LPP, the active propagating enolate is coordinated to the LA (**4**, Scheme 1a). According to DFT calculations, a bimetallic mechanism involving 1,4-addition of a zwitterionic enol-aluminate **2** onto an aluminium-activated MMA **1**, was favoured over the monometallic mechanism (Scheme 1a).[19]

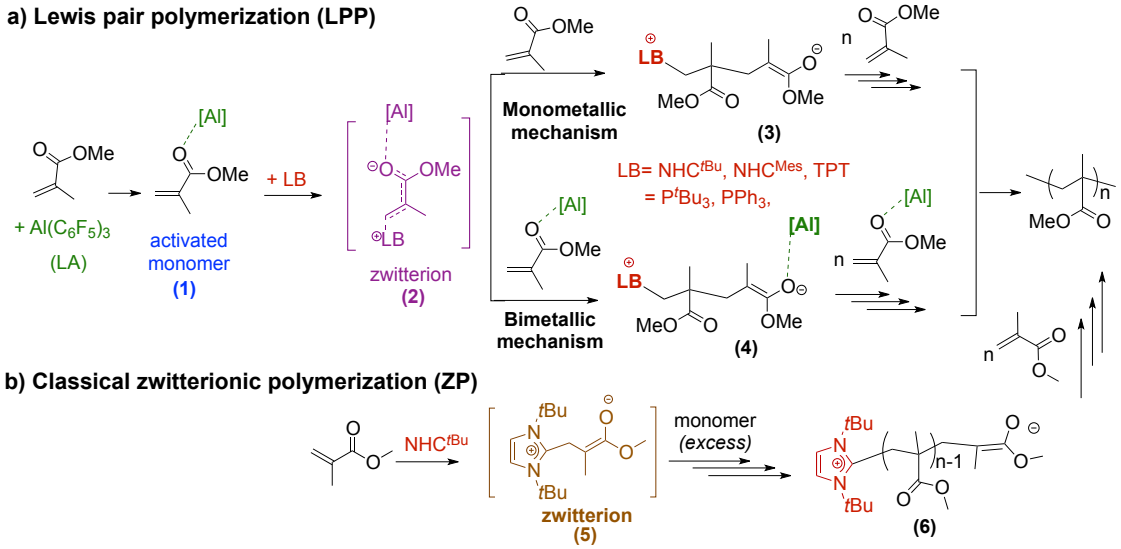

Scheme 1. a) Monometallic *vs.* bimetallic mechanisms for LPP of MMA using $Al(C_6F_5)_3$ and carbenes or phosphines.[19]; b) classical ZP of MMA using NHC^{tBu}.

When using the isoelectronic borane $B(C_6F_5)_3$ as LA in combination with the NHC^{tBu} and NHC^{Mes}, no polymerization occurred.[19] Interestingly, we observed that $B(C_6F_5)_3$ could induce the polymerization of MMA, using the 1,3–bis(isopropyl)-4,5-(dimethyl)imidazol-2-ylidene (NHC^{iPrMe}), with a certain degree of control over the polymerization (Scheme 2).[21] Accordingly, 1,3-bis(isopropyl)imidazol-2-ylidene (NHC^{iPr}) and NHC^{Mes} were found inactive for the polymerization of MMA in presence of $B(C_6F_5)_3$. These observations highlighted again that the structure of the NHC has a dramatic influence on the reaction outcome (see chapter 2).

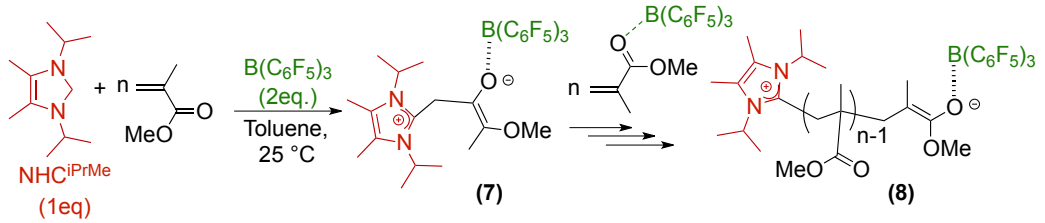

Scheme 2. LPP of MMA using $B(C_6F_5)_3$ as LA and NHC^{iPrMe} as LB in toluene at 25 °C.[21]

It has to be mentioned that LPP also differentiates from polymerization utilizing a bifunctional activation by H-bonding, as that operating in ring-opening polymerization (ROP) of cyclic monomers (*e.g.* esters and carbonates), as shown in Scheme 3. Indeed, in such H-bonding-induced ROP, a simultaneous activation of both the monomer and the initiator/chain-end occurs by a uni- or bimolecular combination of a H-donor carbonyl activator (A) and a H-acceptor Brönsted base (B) (*e.g.*, thiourea-amino derivatives, guanidines etc. ; see chapter 1, section 7). In these cases, the bifunctional system acts as a catalyst and it is used in the presence of an initiator, an alcohol in most cases.

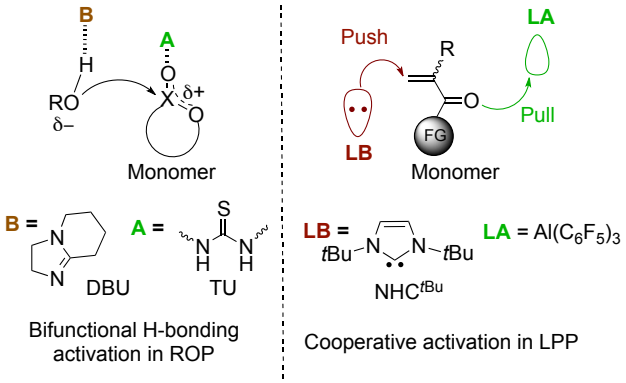

Scheme 3. Dual activation in ROP *vs* Dual activation in LPP.

In the context of ROP, Bourissou *et al.* examined the dual hybrid activating systems combining an organometallic compound, such as $Zn(C_6F_5)_3$ with an organic activator such as tertiary amine (*e.g.* 1,2,2,6,6-pentamethylpiperidine, PMP, or *N*,*N*-dimethylaminopyridine, DMAP) for the ROP of D,L-lactide and ε-caprolactone (Scheme 4). In this metallic/organic approach, PMP acted as a Bronsted base to generate a zinc enolate, while DMAP acted as a nucleophile to generate a zinc alkoxide, but both systems afforded, after work-up, high molecular weight cyclic polymers. [22]

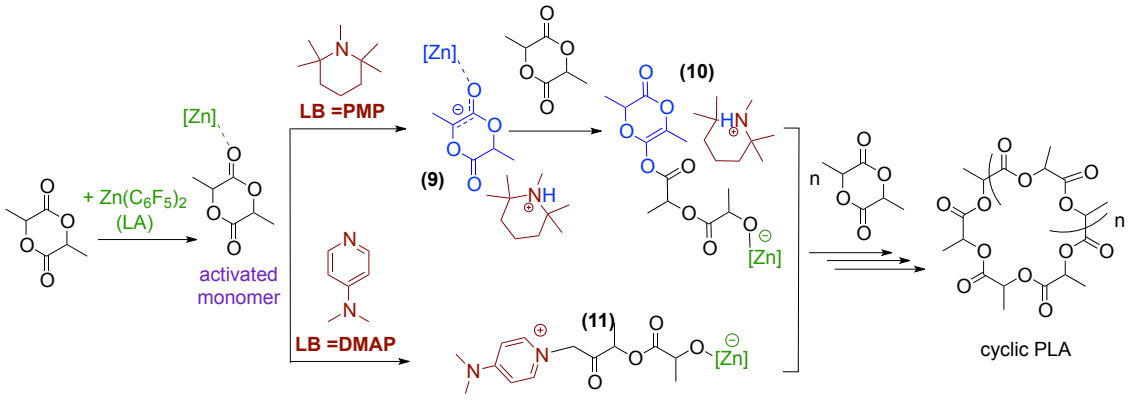

Scheme 4. LPP of D,L-lactide using a dual activating system based on $Zn(C_6F_5)_3$ and a tertiary amine (PMP or DMAP).[22]

Borane and alane derivatives, as well as one example of zinc complex featuring bulk and electro-withdrawing substituents, have been investigated as LA's in the context of LPP. In contrast, and to the best of our knowledge, silanes have not been considered despite their well-known Lewis acidic character. [23]

In the present work, we thus turned to organic silanes of general structure $R_1R_2R_3R_4Si$ and to $R_1R_2R_3Si^+$ cation as well as LA partners, in combination with NHCs or phosphines as LB's to induce the LPP of (meth)acrylic monomers (Figure 4).

The scope of LA's and LB's studied is first presented. Various combinations of LA/LB have been screened then, so as to identify a LP that could trigger the LPP of MMA as a model substrate. The LPP of MMA induced by a particular LP, consisting in trimethylsilyl triflimide ($TMSNTf_2$) as LA and tris(2,4,6-trimethoxyphenyl) phosphine (TTMPP) as LB, has then been examined in more details.

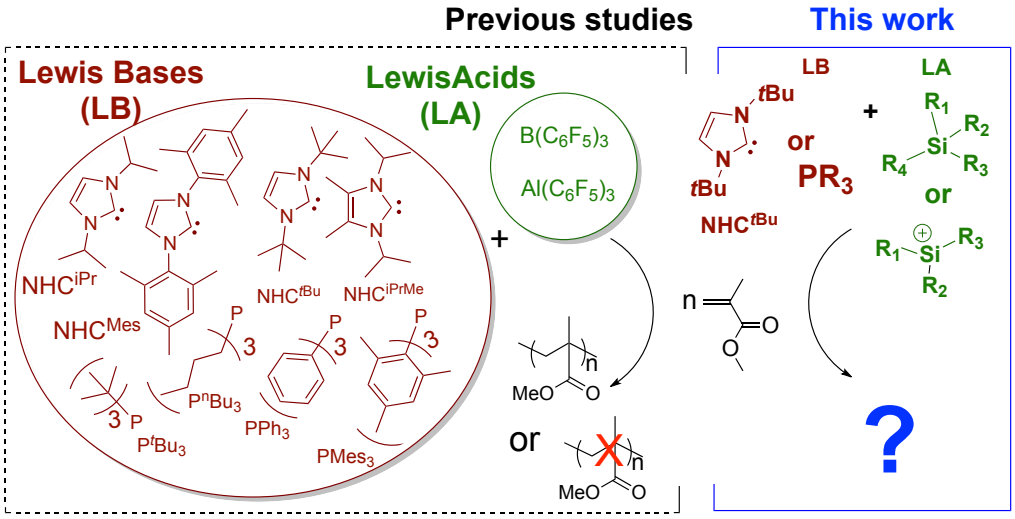

Figure 4. Overview of Lewis pair-induced polymerization of MMA.

1. Scope of Lewis acids and bases

1.1. Lewis acids

Silicon Lewis acids (SLA's), also named organosilicon compounds, have been widely employed in carbon-carbon bond formation reactions, due to the electrophilicity of the Si center when substituted with electrowithdrawing groups and its ability for hypervalency, forming five- and six-coordinated Si species.[23]

The reactivity of SLA's can be finely tuned by varying the substituents surrounding the Si atom. It is commonly admitted that, when comparing R_3SiX-type SLA's where the Si atom is bound to the same heteroatom X (from substituents), the Lewis acidity can be estimated by the chemical shift of the Si atom in ^{29}Si NMR spectroscopy.[23] Thus, tricoordinated Si

species are better SLA than tetracoordinated Si, in agreement with their very deshielded ^{29}Si NMR signal (Figure 5). However, other criteria such as the strain cycle,[24] the solvent[25] and the coordination state also account for the Lewis acidity of organosilicon derivatives.[26]

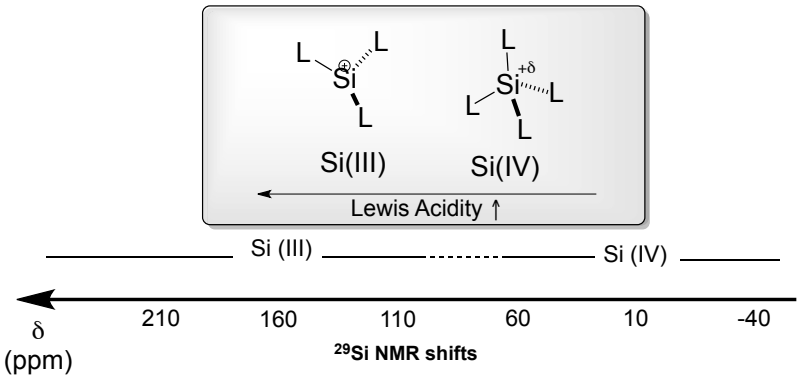

Figure 5. [29] Si NMR chemical shifts of tri- and tetracoordinated Si-based compounds.

Organosilicon candidates that we investigated in this PhD work can be divided in three distinct categories, depending on the leaving group ability of the substituents and the valency of the Si center. Note that their ^{29}Si NMR chemical shifts (Figure 5) correlate with their Lewis acidity. We thus evaluated the behavior of the following compounds:

(1) aryl or alkyl-arylsilanes featuring electron-withdrawing trifluromethane CF_3 groups (*e.g.* bis(2,5-bis(trifluoromethyl)phenyl) dimethylsilane, denoted as Si-methyl in Scheme 6). Though these compounds exhibit a relatively weak acid character, their substitution pattern can be easily modified.[27] The Lewis acidity of Martin spirosilane (denoted as Si-Martin in Scheme 6) results from the strain that is released upon formation of a pentacoordinated species.[28] In addition, the Lewis acidity of the pinacolsilane, denoted as Si-pinacol (Scheme 6) was also investigated;

(2) trialkylsilyl triflates R_3Si-OTf and trialkylsilyl triflimides R_3Si-NTf_2 are powerful alkylating agents and SLA catalysts in various reactions in molecular chemistry.[23] They have also been widely studied by Ghosez *et al.* as carbonyl activators for Diels-Alder reactions of α,β-unsaturated esters with cyclopentadiene[29,30] as well as for the reaction of α,β-insaturated amides with 2-azadienes (Scheme 5).[31,32] We thus hypothesized that these compounds could also be active for the LPP of (meth)acrylic monomers.

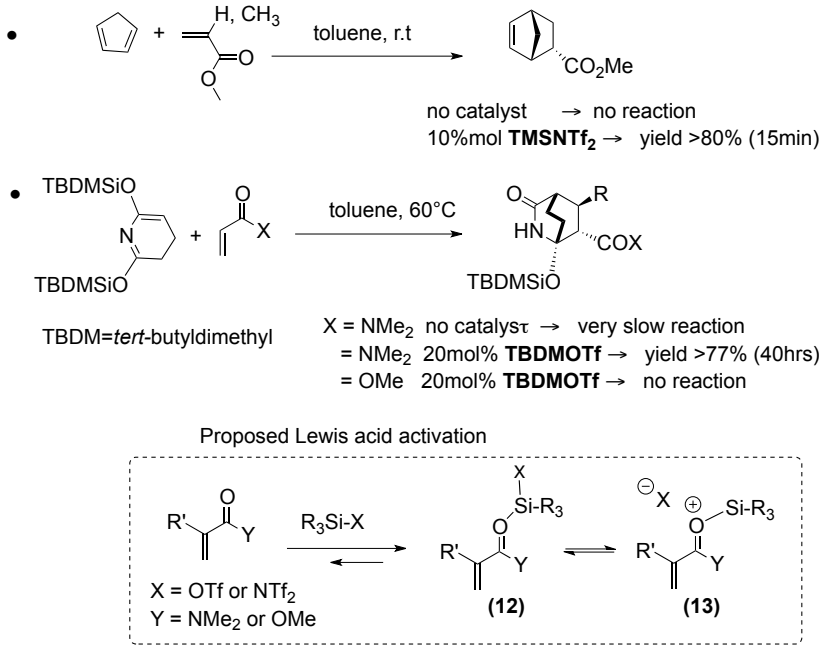

Scheme 5. Diels-Alder reactions using trialkylsilyl precursors and activation mechanism proposed by Ghosez *et al.* [29-32]

(3) tricoordinated species R_3Si^+ are true silyl cations (silylium ions) that are very powerful LA's and are expected to strongly activate the monomer substrate.[33-35] Such compounds can be generated *in situ* from the reaction of the corresponding silane RSi-H with trityl tetrakis(pentafluorophenyl)borate [$Ph_3CB(C_6F_5)_4$], for instance. However, only a few solvents are compatible with such highly reactive species.

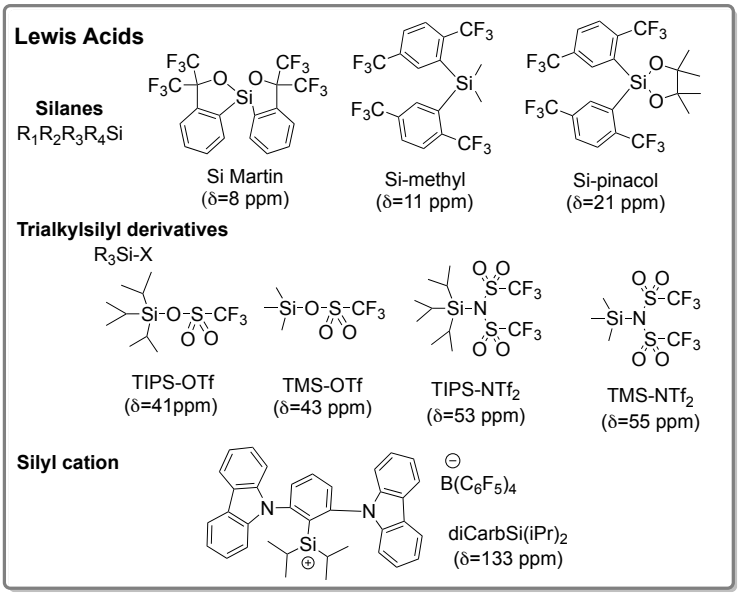

Scheme 6. Lewis acids (LA) studied in this work. ^{29}Si NMR shifts are those reported in refs 23,35,36 and also based on our experimental measurements.

Silanes (except Martin spirosilane, see experimental part for synthesis) and silylium compounds investigated in the present work were synthesized by Dr. Virginie Liautard (Post-doctoral researcher) and Paul Ducos (PhD student) in the laboratory of Prof. Yannick Landais at the Institut des Sciences Moléculaires (ISM), Université de Bordeaux. Other trialkyl silyl precursors are commercially available (except $TIPSNTf_2$; see experimental part for synthesis).

1.2. Lewis bases

As emphasized in chapter 2, among NHCs tested, only 1,3-bis(*tert*-butyl)imidazol-2-ylidene (NHC^{tBu}, Scheme 7) was able to trigger the polymerization of MMA, either in DMF at 25 °C or in toluene at 50 °C. This carbene was thus selected again as a Lewis base to induce the LPP of MMA.

Although phosphines have been widely used as organocatalysts in molecular chemistry, they have been only scarcely investigated in polymerizations reactions.[1] Two phosphines, namely, tri-*n*-butylphosphine (P^nBu_3) and tri-*tert*-butylphosphine (P^tBu_3) were here employed as other LB's (Scheme 7). These two former phosphines, indeed, proved active for the LPP of MMA in presence of $Al(C_6F_5)_3$ as LA.[19] Tris(2,4,6-trimethoxyphenyl)phosphine (TTMPP; Scheme 7), which was found to efficiently catalyze the group transfer polymerization (GTP) of both MMA and *tert*-butyl acrylate (^{t}BuA), in previous works from our group,[37] was also employed in this work.

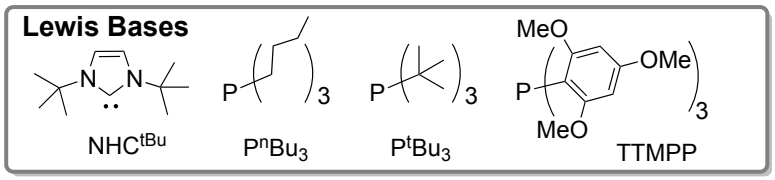

Scheme 7. Lewis bases (LB's) studied in this work.

In the following section, a screening combining the aforementioned LA's and LB's for the LPP of MMA is presented. LA's were screened according to their relative acidity, on the basis of the ^{29} Si NMR chemical shift, as discussed above.

2. Reactivity screening for the identification of an active Lewis pair

For the reactivity screening, the following parameters were taken in account.

(1) Solvent of polymerization: toluene was selected here in order to avoid any coordination of the LA entity. In this regard DMF and THF had to be avoided

(2) Temperature of polymerization: in chapter 2, it was established that NHC^{tBu} could

directly induce MMA polymerization in toluene at 50 °C ($\overline{M_n}^{exp}$ = 393,000 g.mol^{-1} and $Đ$ = 1.9 for DP_n = 250), but the process was not controlled. Here, LPP was performed at 25 °C, so as to avoid any side polymerization from the direct addition of the NHC onto the monomer.

(3) Acid concentration: 2 equivalents of LA (relative to LB) were initially employed, in agreement with a bimetallic mechanism proposed by Chen *et al.* for the LPP of MMA induced by NHCs (or phosphines) and $Al(C_6F_5)_3$.[19]

(4) Order of addition of the reagents: the monomer was first pre-mixed with the LA, followed by the addition of the LB. This order of addition was crucial in order to avoid any possible quenching between the LA and the LB (irreversible formation of LA-LB adduct Figure 2).

2.1. Reactivity screening using the combinations SiR_4/NHC^{tBu} or SiR_4/ PR_3

Firstly, the polymerization of MMA was performed under the conditions described above, *i.e.* using either NHC^{tBu} or P^{t}Bu$_3$ and TTMPP in the presence of weak LA's, namely, the Martin spirosilane (Si-Martin; δ^{Si} = 8 ppm), bis(2,5-bis(trifluoromethyl)phenyl) dimethylsilane (Si-methyl; δ^{Si} = 11 ppm), and pinacol silane (Si-pinacol; δ^{Si} = 21 ppm). The initial concentrations used were as follows: $[LA]_0$ = 20 mM, $[LB]_0$ = 10 mM and $[MMA]_0$ = 1 M, for LA, LB and MMA, respectively for reaction partner as indicated in Table 1.

Table 1. Reaction of MMA in toluene at 25 °C using silanes SiR_4 and NHC^{tBu} or phosphines.

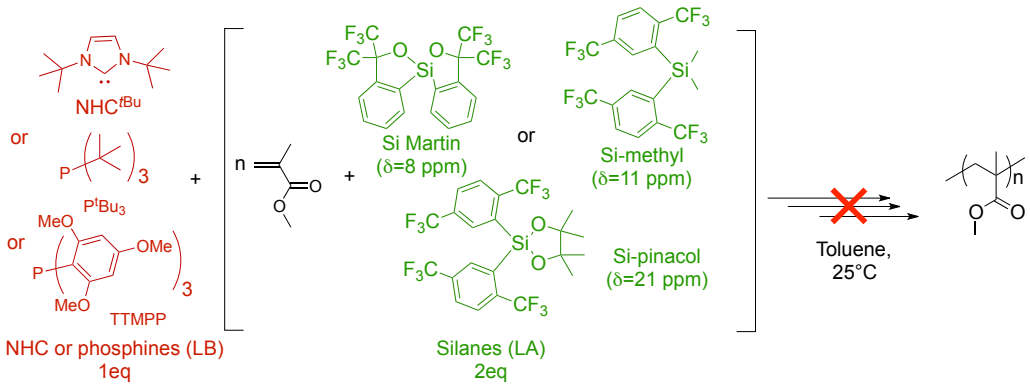

Entry	Lewis Acid (LA)	Lewis Base (LB)	[MMA]/[LA]/[LB]	Conv. (%)
1	Si Martin	NHC^{tBu}	100/2/1	0
2	Si-methyl	NHC^{tBu}	100/2/1	
3	Si-pinacol	NHC^{tBu}	100/2/1	
4	Si-pinacol	P*t*Bu$_3$	100/2/1	
5	Si-Martin	TTMPP	100/2/1	

However, no polymerization of MMA occurred at all, regardless the LP employed under these conditions. This dramatically contrasted with results obtained using NHC^{tBu} or

P^tBu_3 combined with $Al(C_6F_5)_3$, where rapid polymerization of MMA occurred in toluene at 25 °C.[19] One can thus assume that, in our case, the tested silanes were not electrophilic enough to activate MMA, hence that more Lewis acidic silylating agents were required.

2.2. Reactivity screening using the combination R_3Si^+/ PR_3

The poor activation obtained with silanes compounds prompted us to investigate more acidic compounds such as the silylium cation, namely, 9,9'-(2-(bis-isopropylsilyl)-1,3-phenylene) bis(9H-carbazole), denoted as diCarbSi(iPr)$_2$ (**15**, Scheme 8), that is associated to an almost chemically inert and non-coordinating anion, namely tetrakis[pentafluorophenyl]borate [TPFPB]. Since silyl cations are highly reactive and moisture sensitive,[34,35] the cation was prepared *in situ* from silane precursor **14**, *via* hydride transfer using trityl tetrakis[pentafluorophenyl]borate [Tr][TPFPB] (Scheme 8).[34]

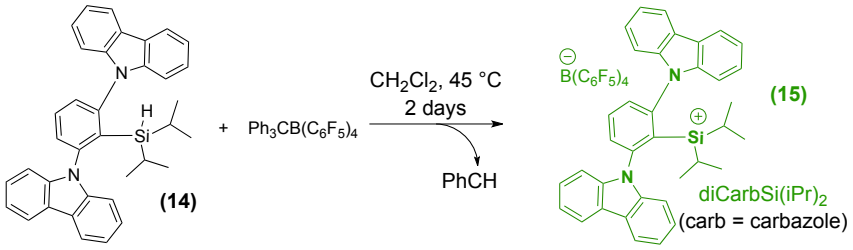

Scheme 8. Synthesis of diCarbSi(iPr$_2$) silyl cation from the silane precursor in CH_2Cl_2 at 45 °C

The salt **15** was tested afterwards as LA for LPP of MMA. It has to be mentioned that, due to the insolubility of this silyl salt in toluene, the polymerization was run in dichloromethane in this case. Because NHCs can react with dichloromethane, to form the monochoroolefin **17** and the imidazol(in)ium salt **18** (Scheme 9),[38] only phosphines could be tested as LB's in this solvent.

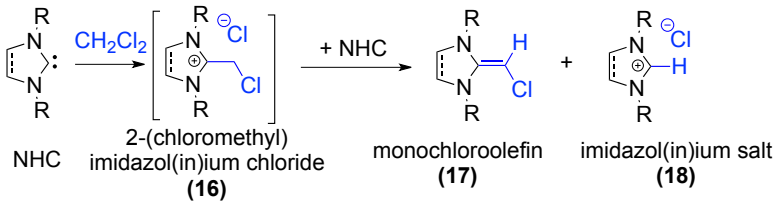

Scheme 9. Possible reaction of NHCs with CH_2Cl_2.[38]

No polymerization was noted, however, in the presence of the as *in situ* generated silyl salt diCarbSi(iPr)$_2$ in conjunction with P^tBu_3, neither at 25 °C nor at 45 °C, even after 4 days of reaction. Since $^tBu_3P$ proved efficient for the 1,4-conjugate addition polymerization of MMA in presence of $Al(C_6F_5)_3$ in CH_2Cl_2, at r.t,[19] we assumed that the absence of polymerization observed, in our case, was due to the silylium cation **15**. In particular, one can hypothesize that:

(1) the R_3Si^+ was correctly generated *in situ*, but was strongly coordinated with the carbonyl group of MMA as in compound (**19**) and (**20**) in Scheme 10, hampering any further polymerization. However, isolation and further characterizations would be needed to identify these compounds.

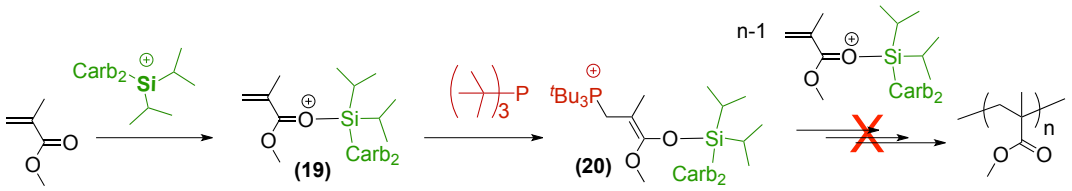

Scheme 10. Formation of O-Si bonds between MMA and R_3Si^+.

(2) the R_3Si^+ might have not been generated upon reaction between R_3Si-H (**14**) and [Tr][TPFPB]. Indeed, attempts to identify the signal from such R_3Si^+ (*e.g.* R_3Si^+ generated from $Me_3Si[B(C_6F_5)_4]$), by ^{29}Si NMR in CD_2Cl_2, were reported to be unsuccessful.[39,40] According to the authors, only signal from trimethylsilyl chloride (R_3Si-Cl) and fluoride (R_3Si-F) were detected. R_3Si-Cl would be produced by the reaction of the silyl cation with chloride ions in the system. R_3Si-F may be produced by the reaction of the silyl cation with TPFPB moiety, where the fluorines on TPFPB may serve as nucleophiles. In our case, these side reactions might explain the absence of polymerization observed, although we did not identify R_3Si-Cl and R_3Si-F side products. Thus, dichloromethane did not seem to be a good solvent for the LPP of MMA, using a silylium compound as LA.

We thus turned to other silicon derivatives of general structure R_3Si-X, where X is a counteranion such as triflate OTf^- or triflimide NTf_2^-. R_3Si-X compounds were indeed expected to be less acidic than silylium cations, but should exhibit a higher Lewis acidity than silanes, according to their ^{29} Si NMR chemical shifts (see Figure 5).

2.3. Reactivity screening using the combination R_3Si-X/NHC^{tBu}

2.3.1. Polymerization of MMA using R_3Si-X and NHC^{tBu}

The polymerization of MMA was first performed in toluene at 25 °C using NHC^{tBu} in combination with trialkylsilyl triflates, namely trimethylsilyl triflate (TMS-OTf) and triisopropyl triflate (TIPSOTf) and their triflimide analogues (TMS-NTf_2 and TIPS-NTf_2). For each polymerization, initial concentrations were as follows: $[LA]_0$ = 20 mM, $[NHC^{tBu}]_0$ = 10 mM and $[MMA]_0$ = 1 M.

It should be pointed out that traces of free acid, HX, formed upon hydrolysis of R_3-SiX can influence the outcome of the reactions (Scheme 11a). As a matter of fact, these polymerizations were carried out in the presence of 2,6-di-*tert*-butyl-4-methylpyridine (DTBMP) as a proton trap (1 eq. relative to the LA, Scheme 11b), unless otherwise mentioned. By doing so, side activation by HOTf or $HNTf_2$ traces of (Scheme 11a) can be

minimized -if not suppressed- and the NHC quenching by protonation could also be avoided (Scheme 11c). DTBMP was thus pre-mixed with the R_3Si-X solution, before adding MMA and NHC^{tBu}. Table 2 summarizes the results obtained with different trialkylsilyl precursors.

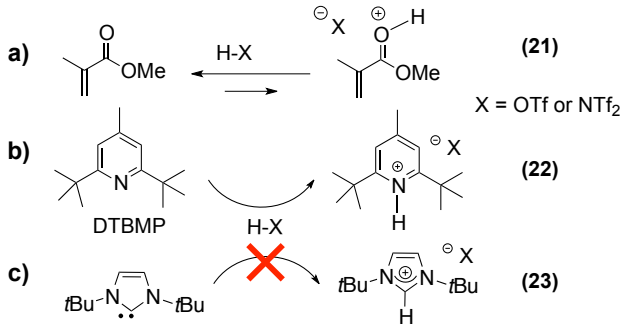

Scheme 11. a) Undesired MMA activation by Brönsted acid; b) DTBMP as proton trap and c) quenching of NHC by protonation

Table 2. LPP of MMA in toluene at 25 °C using R_3Si-X and NHC^{tBu} in presence of DTBMP as proton trap.

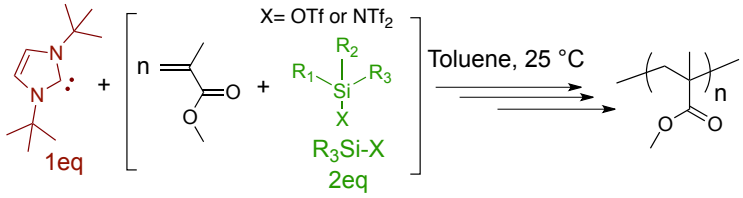

Entry	LA	$[MMA]_0/[LA]_0/[NHC^{tBu}]_0$	Time (h)	Conv.[a] (%)	$\overline{M}_n^{theo}$ [b] (g.mol^{-1})	$\overline{M}_n$ [c] (g.mol^{-1})	M_p [c] (g.mol^{-1})	$Đ$ [c]
1	TMS-OTf	100/2/1	168	0	-	-	-	-
2	TIPSOTf	100/2/1	168	0	-	-	-	-
3	$TIPSNTf_2$	100/2/1	168	0	-	-	-	-
4	$TMSNTf_2$	100/2/1	24	66	6,600	42,600 760	43,800 1,100	1.3 1.1
5	$TMSNTf_2$	100/2/-	24	12	1,200	n.d.	n.d.	n.d.
6	-	100/-/1	24	0	-	-	-	-
7[d]	$TMSNTf_2$	100/2/1	24h	5	500	n.d.	n.d.	n.d.

a. Conv. = % monomer conversion determined by ^{1}H NMR spectroscopy; b. Theoretical molar mass $\overline{M}_n^{theo} = M_{LB} + M_{MMA} \times \frac{[MMA]}{[LB]} \times conv.$; c. Characterization of PMMA's by SEC in THF using PS standards for calibration; d. Polymerization in absence of DTBMP.

None of the trialkyl triflates, TMSOTf and TIPSOTf, allowed polymerizing MMA, in the presence of NHC^{tBu} as LB and DTBMP as proton scavenger (Table 2, entries 1-2). In contrast, and under similar conditions, $TMSNTf_2$ gave a polymer, converting 66 % of MMA after 24 h of reaction (entry 4). These observations are in accordance with works by Ghosez

et al., who reported that triflimide derivatives were better carbonyl activators than triflates, for the Diels-Alder reaction of α,β-unsaturated esters with dienes, for instance.[29,30,41] This difference was proposed to result from:

(1) the higher Lewis acidity of $TMSNTf_2$ compared to that of TMSOTf based on ^{29}Si NMR chemical shifts (δ^{Si} = 55.9 and 43.5 ppm, for $TMSNTf_2$ and TMSOTf, respectively).

(2) the larger size of the triflimide anion (NTf_2^-) compared to triflate anion (OTf^-), which can favor coordination of the ester group to the Si center (Scheme 12).

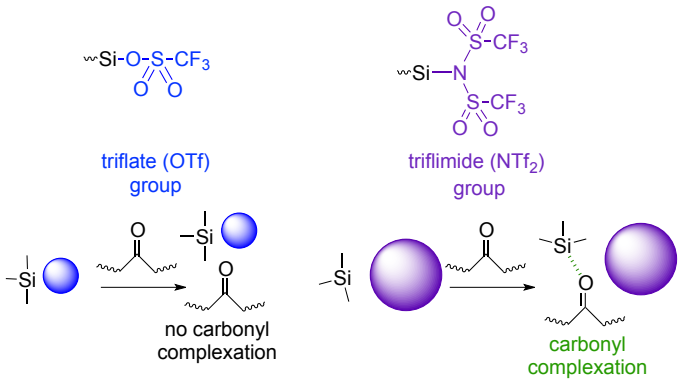

Scheme 12. Putative effect of the counteranion on MMA activation by R_3Si-X.

However, a subtle balance has to be found since $TIPSNTf_2$ that exhibits a higher sterical hindrance than $TMSNTf_2$ (Scheme 13) did not allow the polymerization of MMA (entry 3).

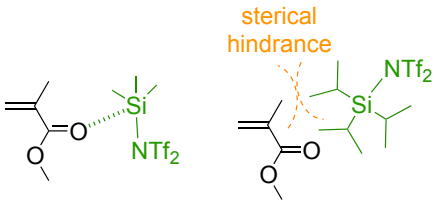

Scheme 13. Influence of alkyl groups on the MMA activation by R_3SiNTf_2.

Only $TMSNTf_2$ thus proved effective for the polymerization of MMA in the presence of NHC^{tBu} as LB and DTBMP as proton scavenger (Table 2, entry 4). A PMMA of molar mass M_n = 42,600 g.mol^{-1} ($Đ$ = 1.3), higher than expected (based on the initial monomer-to-carbene $[MMA]_0/[NHC^{tBu}]_0$ ratio) was however achieved. It has to be mentioned that the true molar masses M_n and M_w of these PMMA's could be calculated by multiplying equivalent polystyrene molar masses (obtained by SEC analysis) by the correction factor B = 1.10 (Benoit factor for PMMA in THF).[42]

As illustrated in Figure 6, two populations (**X** and **Y**) were actually observed in the SEC traces of the final polymer, likely indicating the presence of two types of propagating species.

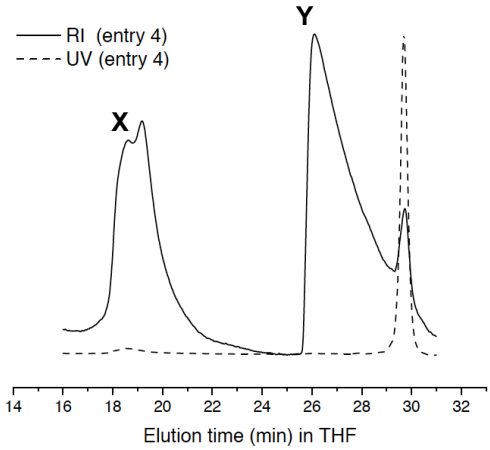

Figure 6. SEC traces (RI-UV 260 nm) of PMMA obtained with TTMPP/$TMSNTf_2$ in CH_2Cl_2 (Table 2, entry 4).

Control experiments were performed to ensure that the as-obtained PMMA did result from a dual activation by both $TMSNTf_2$ and NHC^{tBu}.

(1) When using $TMSNTf_2$ (pre-mixed with DTBMP) and NHC^{tBu} individually for MMA polymerization, no polymer formed after 24 h (Table 2, entries 5 and 6), highlighting the need of the two activators to trigger the reaction.

(2) When using NHC^{tBu}/$TMSNTf_2$ in the absence of DTBMP (entry 7), the polymerization reached only 5 % of MMA conversion in 24 h, while 66 % of conversion were reached with NHC^{tBu}/$TMSNTf_2$/DTBMP and 12% with $TMSNTf_2$/DTBMP (entries 4-5, respectively). This suggested that, as expected, DTBMP avoided the carbene quenching by trapping all the $HNTf_2$ traces, but could also initiated the polymerization of MMA. Additionally, the low conversion observed with NHC^{tBu}/$TMSNTf_2$ might resulted from a partial quenching of NHC^{tBu} by $TMSNTf_2$, forming a “classical” Lewis pair (CLP).

We thus performed equimolar model reactions to gain a better insight into the activation of MMA by $TMSNTf_2$ and to evidenced the supposed CLP formed between NHC^{tBu} and $TMSNTf_2$.

2.3.2. Equimolar reaction between MMA and $TMSNTf_2$

The equimolar reaction between MMA and $TMSNTf_2$ was performed in a J-Young NMR tube in dry toluene-d_8 at r.t. The reaction was monitored by ^{1}H,^{13}C and ^{29}Si NMR spectroscopies. Table S1 (see supporting information) summarizes chemical shifts of the different characteristic groups, and corresponding spectra are shown in Figures 7-9.

The ^{1}H NMR spectrum of the 1:1 TMSNTf$_2$-MMA mixture (Figure 7) showed a downfield shift of MMA protons ($\Delta\delta H^{MMA} \approx 0.20$ ppm; Table S1, entries 1-4). In the same manner, as illustrated in the ^{13}C NMR spectrum (Figure 9), the vinyl CH_2^{MMA} and the $C{=}O^{MMA}$ were slightly downfield shifted, from 124.9 ppm to 125.6 ppm ($\Delta\delta CH_2^{MMA} = 0.7$ ppm, Table S1; entry 9), and from 167.2 ppm to 167.8 ppm ($\Delta\delta C_{C=O}^{MMA} = 0.6$ ppm, Table S1; entry 11), respectively. These changes likely resulted from the coordination of MMA to the Si center, which affect especially the 1,2 and 1,4-positions.

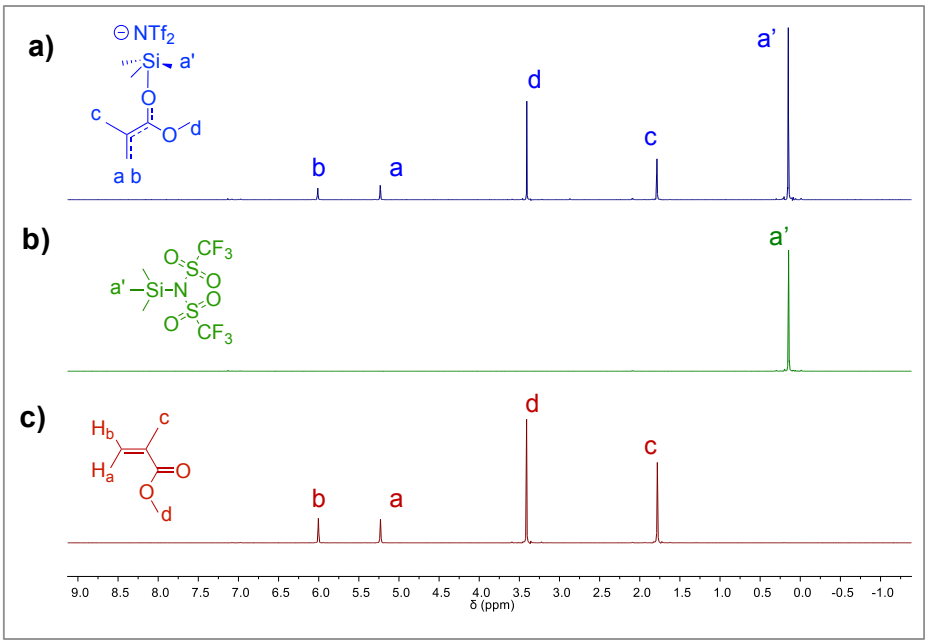

Figure 7. ^{1}H NMR spectrum in toluene-d_8 of: a) MMA+TMSNTf$_2$ (1: 1); b) TMSNTf$_2$; c) MMA.

While no significant changes was noted for both proton and carbon atoms of TMSNTf$_2$ (Figures 7 and 9), on the ^{29}Si NMR spectrum a 48 ppm shift to high field (from 54.9 to 7.06 ppm, Table S1; entry 6 and Figure 8) in TMSNTf$_2$ and in [MMA+TMSNTf$_2$] (**24**, Scheme 14), respectively. This observation is in agreement with the formation of a tetracoordinated species [MMA-TMSNT$_2$] (Scheme 14).

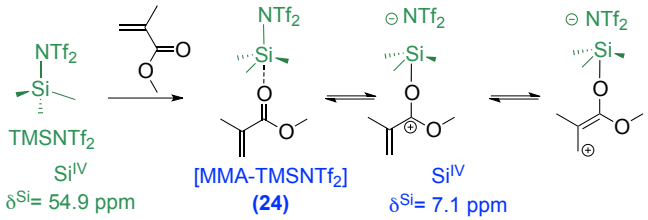

Scheme 14. Reaction of TMSNTf$_2$ with MMA.

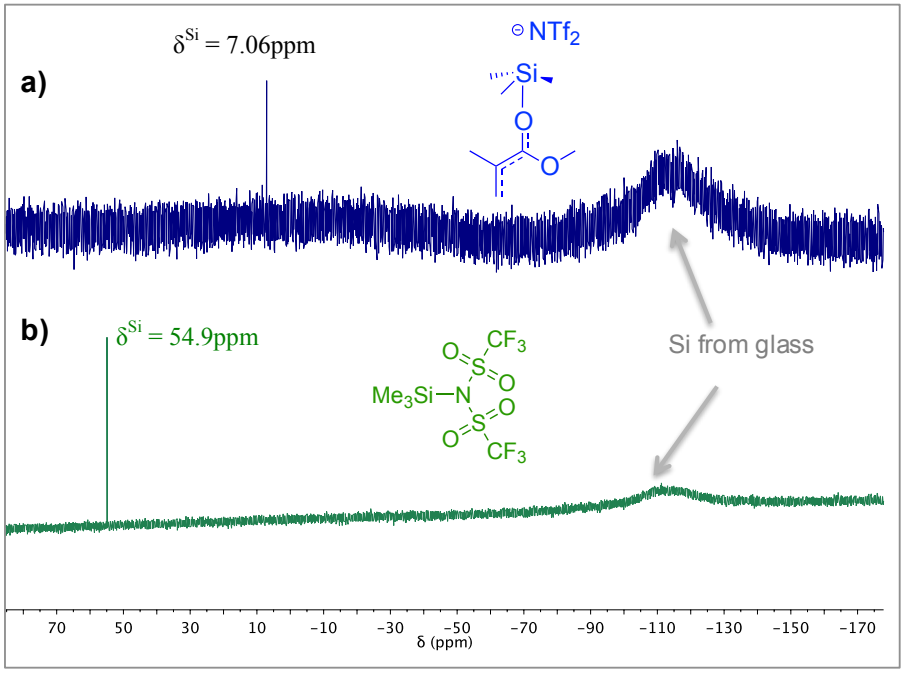

Figure 8. ^{29}Si NMR spectrum in toluene-d_8 of: a) MMA+TMSNTf$_2$ (1: 1); b) TMSNTf$_2$.

2.3.3. Equimolar reaction between NHC^{tBu} and TMSNTf$_2$

Similarly, an equimolar reaction between of NHC^{tBu} and TMS-NTf$_2$ was performed in dried toluene-d_8 in a J-Young NMR tube and monitored by ^{1}H,^{13}C and ^{29}Si NMR spectroscopies. The precipitation of a viscous oil, at the bottom of the Young tube was observed. After evaporation of toluene, the product was re-dissolved in CD_2Cl_2. Table S2 (see SI) summarizes the chemical shifts observed and, Figures 10 and 11 show the corresponding NMR spectra in CD_2Cl_2.

The ^{1}H NMR spectrum of the precipitate that was re-dissolved in CD_2Cl_2 showed the presence of characteristic protons from TMSNTf$_2$ at δ = 0.7-0.9 ppm and those of NHC^{tBu} at δ = 1.8-2.3 and 7.4-8.1 ppm (Figure 10). These downfield chemical shifts might be ascribed to the formation of an imidazolium trimethylsilyl triflimide salt [NHC^{tBu}-TMSNTf$_2$] (**25**, Scheme 15) that was not expected to be soluble in toluene. The broadening peaks of the product were presumably due to either the decomposition of the carbene moiety in CD_2Cl_2, or to the presence of both triflimide and imidazolium in the same environment.

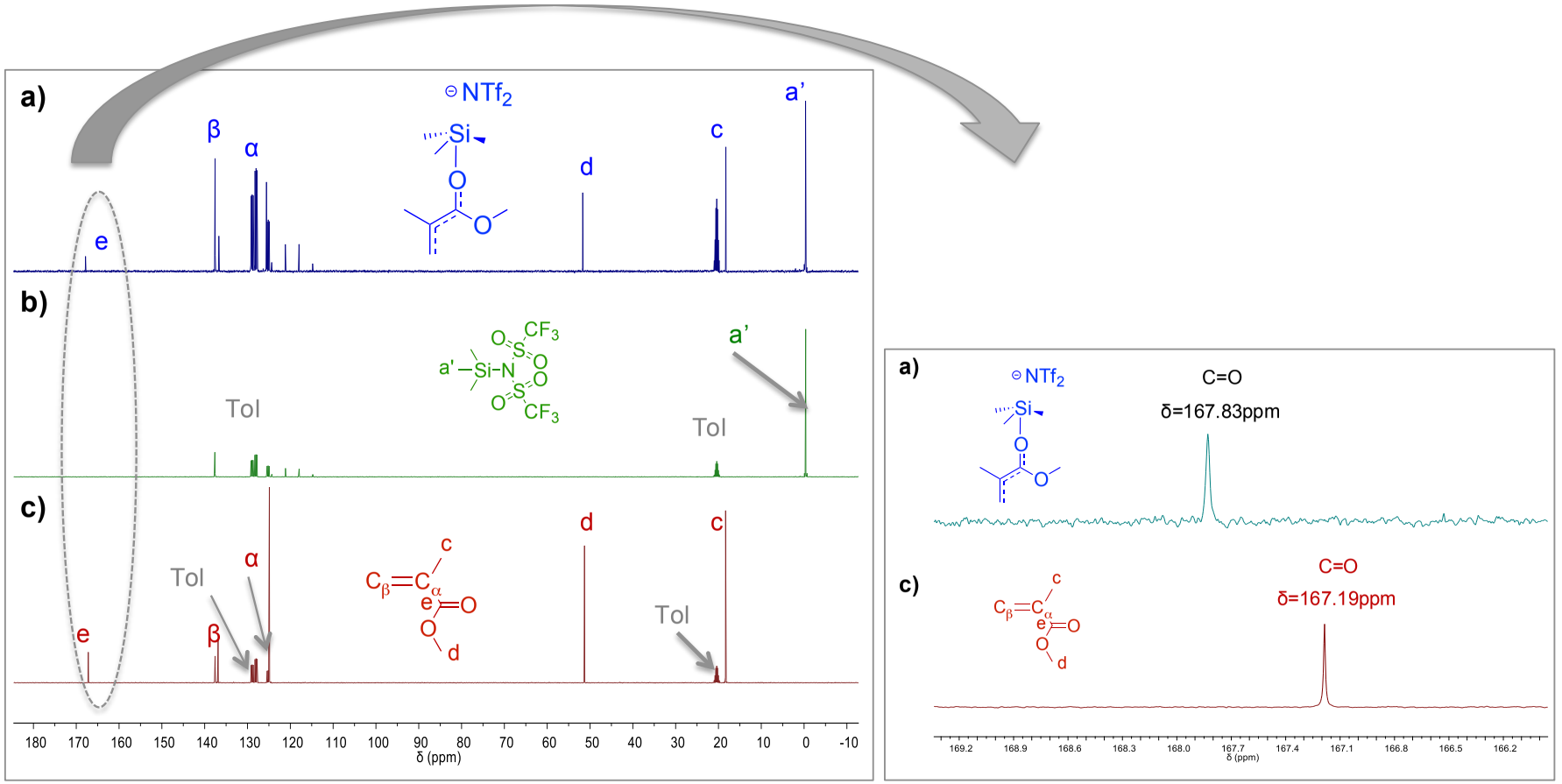

Figure 9. ^{13}C NMR spectrum in toluene-d_8 of: a) MMA+$TMSNTf_2$ (1: 1); b) MMA; c) $TMSNTf_2$.

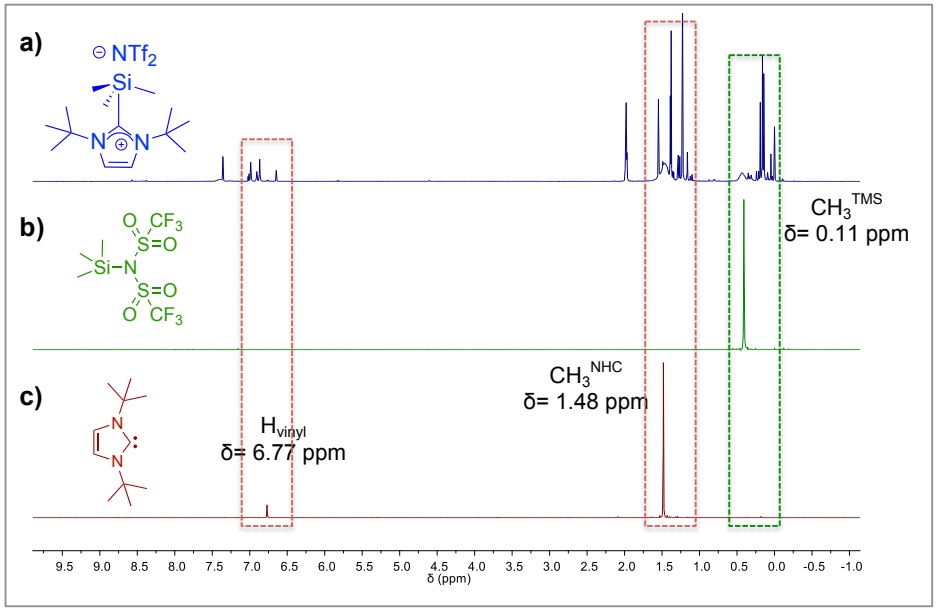

Figure 10. ^{1}H NMR in CD_2Cl_2 of: a) NHC^{tBu} +$TMSNTf_2$ (1:1); b) $TMSNTf_2$; c) NHC^{tBu} (in toluene-d_8).

As for the ^{29}Si NMR spectrum (Figure 11), a ΔδSi = - 62.26 ppm shift to high field was detected from 56.18 to - 6.07 ppm in $TMSNTf_2$ and [NHC^{tBu}+$TMSNTf_2$], respectively (Table S2; entry 4). Again, this is in agreement with the formation of a tetracoordinated species (**25**, Scheme 15). Similar compounds have already described when reacting NHCs with reactions of silicon halides.[43-46]

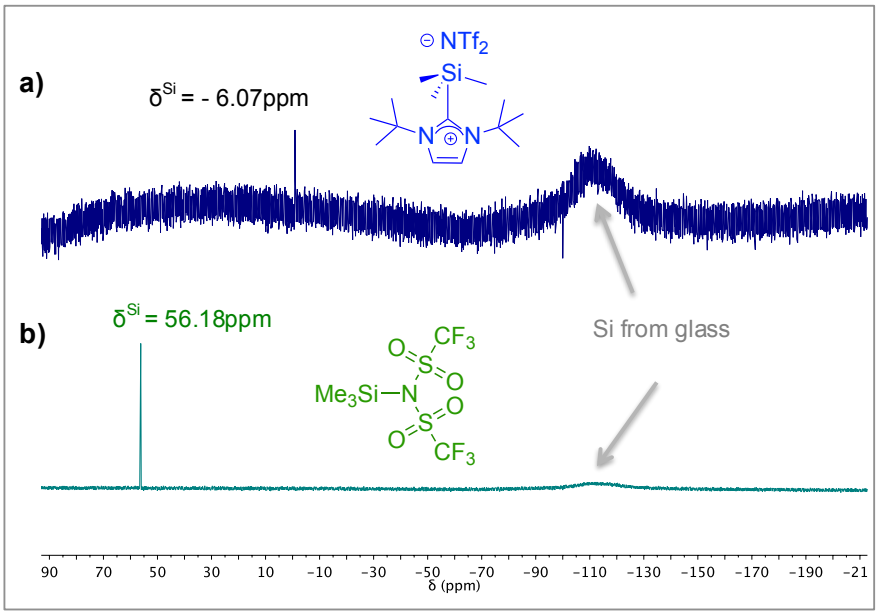

Figure 11. ^{29}Si NMR in CD_2Cl_2 of: a) NHC^{tBu} +$TMSNTf_2$ (1:1); b) $TMSNTf_2$.

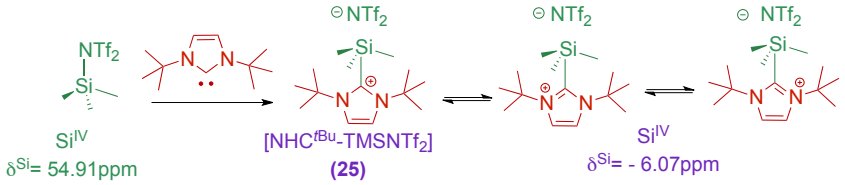

Scheme 15. Reaction of NHC^{tBu} with $TMSNTf_2$.

The two putative tetravalent species, $TMSNTf_2$-MMA (**24**) and $TMSNTf_2$-NHC^{tBu} (**25**), exhibited different ^{29}Si chemical shifts (δ^{Si} = 7.06 ppm, Scheme 14 *vs.* δ^{Si} = -6.07 ppm, Scheme 15, respectively). This difference may arise from the chemical environment of the silicon atom from one compound to another. The imidazolium being more electrophilic than the carbonyl, hence a higher upfield shift was observed in the case of $TMSNTf_2$-NHC^{tBu}.

These NMR studies revealed that $TMSNTf_2$ could effectively activate MMA through coordination with the carbonyl group. Such an activated monomer being more electrophilic, it could further be subjected to a nucleophile addition by NHC^{tBu}.

However, NHC^{tBu} and $TMSNTf_2$ were found to form a classical Lewis pair (CLP) that was inactive for the polymerization of MMA (in absence of any other base). Consequently, other Lewis pairs were tested later in our study. In particular, we employed phosphines as LB's in presence of $TMSNTf_2$ as LA for the LPP of MMA.

2.4. Reactivity screening using R_3Si-X and phosphines PR_3

2.4.1. Polymerization of MMA using R_3Si-X and phosphines PR_3

Three phosphines, namely, tri-*n*-butylphopshine (P^nBu_3), tri-*tert*-butylphosphine (P^tBu_3) and tris(2,4,6-trimethoxyphenyl)phosphine (TTMPP), were combined with $TMSNTf_2$ for the polymerization of MMA. It has to be mentioned that, in the previous section, DTBMP was found to induce slightly the non-controlled polymerization of MMA in presence of $TMSNTf_2$ (12 % of MMA conversion after 24 h). To avoid this side polymerization, DTBMP was not used when using phosphines as LB's. Reactions were performed at 25 °C in CH_2Cl_2, because of the better solubility of phosphines in this solvent compared to toluene. The following initial concentrations were used: $[TMSNTf_2]_0$ = 43.6 mM, $[R_3P]_0$ = 21.8 mM and $[MMA]_0$ = 1.8 M. Table 3 summarizes the results obtained with different trialkyl(aryl) phosphines.

Table 3. Polymerization of MMA in CH_2Cl_2 at 25 °C using $TMSNTf_2$ and PR_3 phosphines.

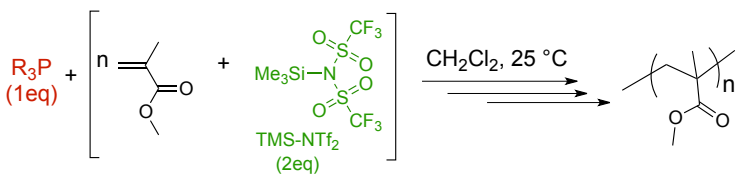

Entry	LB	$[MMA]_0/LA]_0$ $/[LB]_0$	Time (h)	Conv.[a] (%)	$\overline{M}_n^{theo\ b}$ ($g.mol^{-1}$)	$\overline{M}_n^{NMR\ c}$ ($g.mol^{-1}$)
1	-	86/2/-	48	0	-	-
2	P^tBu_3	86/2/1	2	100	8,600	8,300
3	P^tBu_3	86/-/1	48	0	-	
4	P^nBu_3	86/2/1	2	100	8,600	n.d.
5	P^nBu_3	86/-/1	48	0	-	n.d.
6	TTMPP	86/2/1	2	100	8,600	8,900
7	TTMPP	86/-/1	48	0	-	-

a. Conv.= % monomer conversion determined by ^{1}H NMR spectroscopy; b. Theoretical molar mass $\overline{M}_n^{theo} = M_{LB} + M_{MMA} \times \frac{[MMA]}{[LB]} \times conv.$; c. Molar mass $\overline{M}_n$ determined by ^{1}H NMR based on integration of protons from phosphines substituents;

To our surprise, MMA was readily polymerized when using any of the three phosphines, P^tBu_3, P^nBu_3 or TTMPP, combined with $TMSNTf_2$, achieving complete conversion after only 2 h, in CH_2Cl_2 at 25 °C (Table 3, entries 2,4 and 6). In contrast, when using $TMSNTf_2$ and phosphines (P^tBu_3, P^nBu_3 and TTMPP), independently no polymerization of MMA was noted, up to 48 h (entries 3,5 and 7). These control experiments demonstrated that both reagents, $TMSNTf_2$ (LA) and PR_3 (LB), were needed to cooperatively induce the polymerization of MMA.

However, attempts to characterize the as-obtained PMMA's by SEC in THF as eluent were all unsuccessful. We attributed this to the presence of a phosphonium cation in α-position of resulting PMMA's, arising from a direct polymerization initiated by the phosphine. Such α- phosphonium PMMA's likely interact with SEC columns during analysis. The SEC in DMF or (DMSO) being not available in our laboratory at this time, these polymers were further analyzed (after precipitation twice in methanol) by ^{31}P NMR spectroscopy. The ^{31}P NMR signal of the initial phosphines are expected at δ^P = -66,3 ppm for TTMPP in CD_3CN,[47] and δ^P = -32.3 and 62.4 P^nBu_3 and P^tBu_3 in CD_2Cl_2, respectively. Interestingly, in all the ^{31}P NMR spectra of these phosphine/$TMSNTf_2$-derived PMMA's (see Figure 12 for a representative spectrum), four different phosphorous signals, in the range of δ^P = 2-7 ppm, were detected. These chemical shifts were compatible with that of a tetracoordinated phosphorous such as phosphonium, due to an initiation by the phosphine.

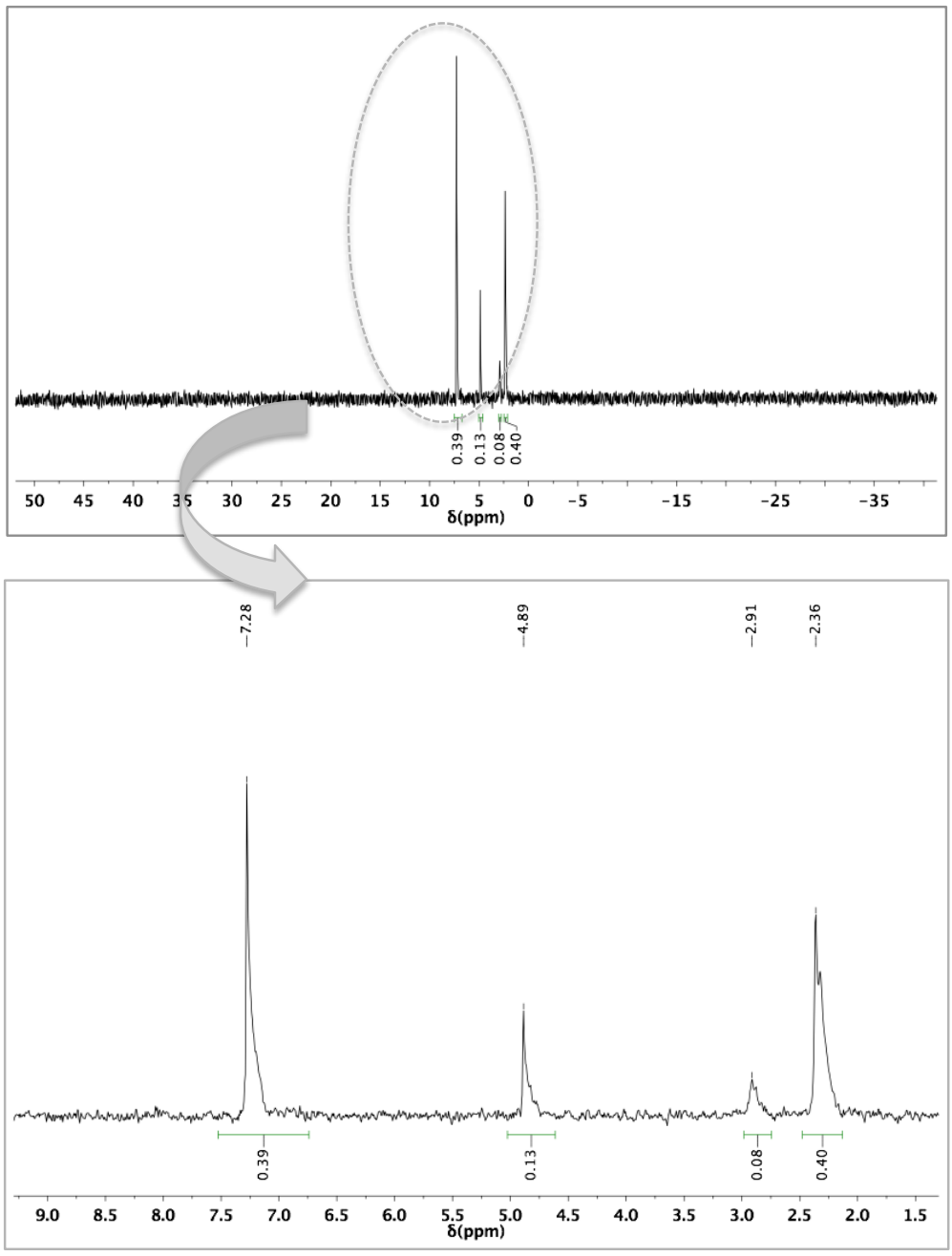

Figure 12. Representative ^{1}H decoupled-^{31}P NMR spectrum in $CDCl_3$ of PMMA obtained using TTMPP/$TMSNTf_2$ in CD_2Cl_2 (Table 3, entry 6).

Given the very similar chemical shifts and their similar solubility, all these species probably correspond to α-phosphonium PMMA's of different microstructure, counteranion or even PMMA's of different molar masses. Although we could not attributed each signal observed, one of the populations might correspond to the expected α-phosphonium PMMA chains (Population A; Scheme 16). However, the presence of species coordinated to the triflimide anion could be also considered (Populations B and C), although the equilibrium highly favors the formation of a non-coordinated phosphonium.

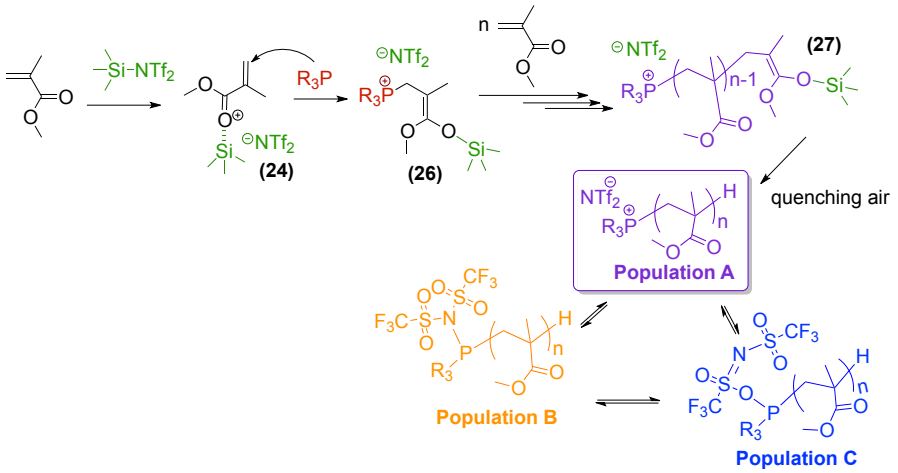

Scheme 16. $R_3P/TMSNTf_2$-initiated polymerization of MMA yielding α-R_3P^+-PMMA's

The latter α-phosphonium PMMA's (population A) can undergo an intra-molecular cyclization yielding α-phospholane cyclic PMMA's (Population D; Scheme 17).

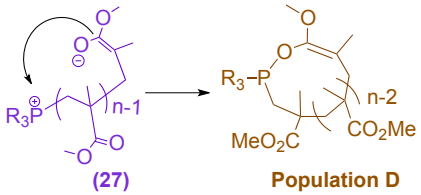

Scheme 17. Intra-molecular cyclization reaction leading to α-phosphonium cyclic PMMA's (the counteranion has been purposely omitted for clarity).

The molar mass of each sample could also be determined by ^1H NMR, based on the integration of *tert*-butyl and aromatic protons of P^tBu_3 (Figure 13) and TTMPP (Figure 15), respectively, and assuming that all chains exhibited the following structure: R_3P-PMMA-H as illustrated in each spectrum. The obtained molar masses ($\overline{M_n}^{NMR}$ = 8,300 and 8,900 g.mol^{-1}, for P^tBu_3 and TTMPP, respectively) were thus in close agreement with the expected values, based on the initial ratio $[MMA]_0/[PR_3]_0$. However, in the case of the polymer arising from P^nBu_3 initiation, the molar mass could not be determined by NMR, because the protons from the butyl groups of the phosphine were overlapping with those of the CH_3 groups of PMMA.

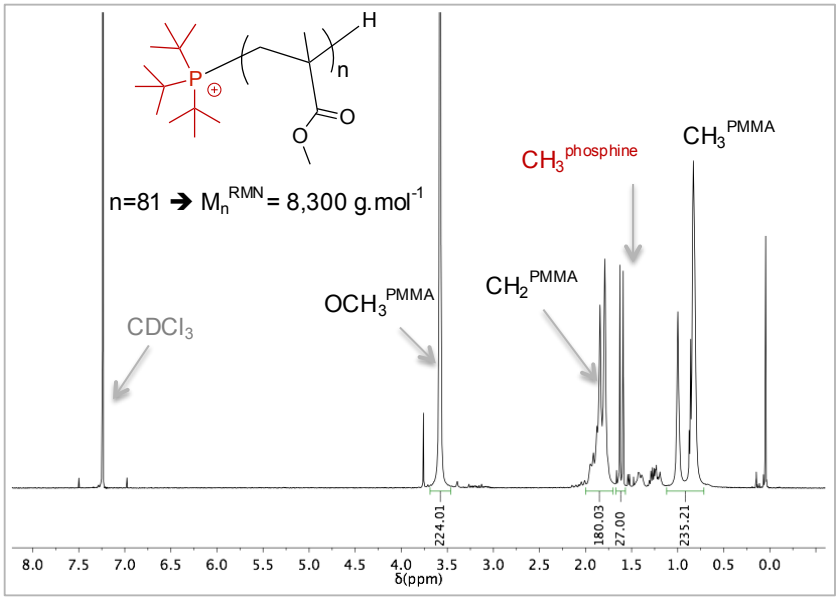

Figure 13. ^{1}H NMR spectrum in $CDCl_3$ of PMMA obtained using P^{t}Bu$_3$/TMSNTf$_2$ in CD_2Cl_2 (Table 3, entry 2).

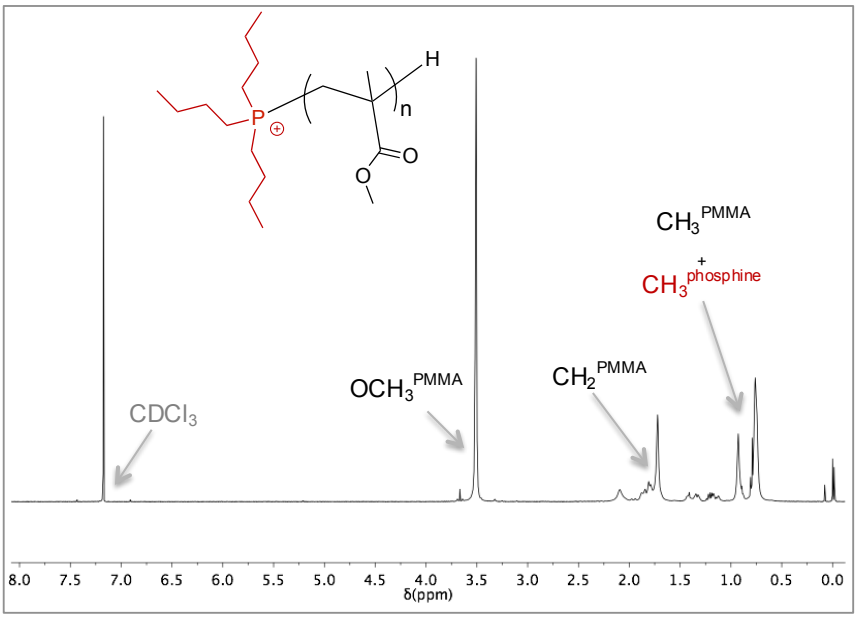

Figure 14. ^{1}H NMR spectrum in $CDCl_3$ of PMMA obtained using P^{n}Bu$_3$/TMSNTf$_2$ in CD_2Cl_2 (Table 3, entry 4).

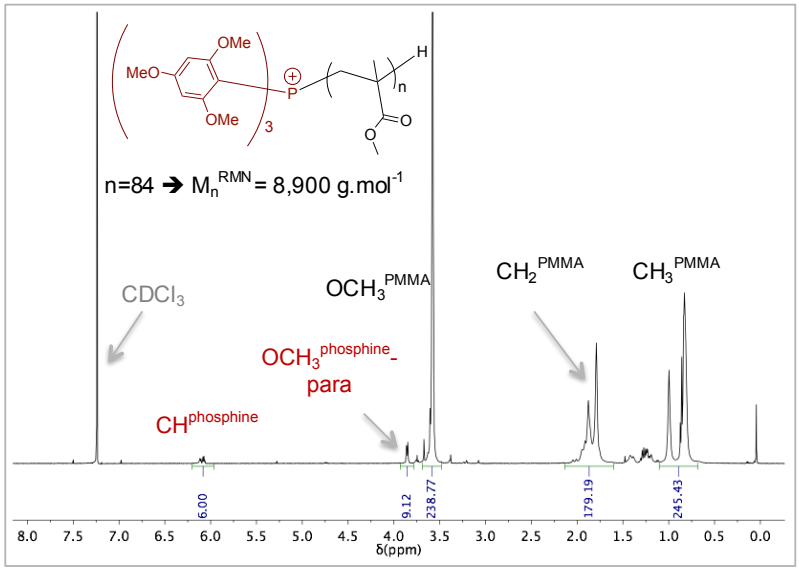

Figure 15. ^{1}H NMR spectrum in $CDCl_3$ of PMMA obtained using TTMPP/$TMSNTf_2$ in CD_2Cl_2 (Table 3, entry 6).

The above reactivity screening evidenced that combination of $^tBu_3P$, $^nBu_3P$ or TTMPP with $TMSNTf_2$ allowed triggering the LPP of MMA, in a cooperative fashion. The corresponding α-phosphonium-PMMA's were successfully characterized by ^{1}H and ^{31}P NMR spectroscopy, although further analysis would be required to clearly identify the environment surrounding the phosphorous atom. We were then interested in identifying the exact nature of the TTMPP/$TMSNTf_2$ Lewis pair (classical or frustrated?), before investigating further the scope of this TTMPP/$TMSNTf_2$-induced LPP of MMA. TTMPP was selected here as the phosphine representative because its phenyl groups could be easily revealed by NMR or UV spectroscopies.

2.4.2. Equimolar reaction between TTMPP and $TMSNTf_2$

First, the equimolar reaction between TTMPP and $TMSNTf_2$ was performed in a J-Young NMR tube, in dry CD_2Cl_2 at r.t. The evolution of the reaction mixture was monitored by ^{1}H, ^{31}P and ^{29}Si NMR spectroscopies. In the ^{31}P NMR spectrum, two signals at δ = 7ppm (96 %) and 48.11 ppm (4 %) were detected (Figure 16), and these signals appeared at different chemical shift that those expected for this phosphine (δ^P = -66.3 in CD_3CN)[47]. In addition, the presence of the corresponding phosphine oxide TTMPPO could be ruled out, because no peak was detected in the region δ = 10-15pmm (^{31}P $\delta^{TTMPP(O)}$ = 10.8 ppm in CD_3CN)[47]. The rapid decomposition of TTMPP in CH_2Cl_2 has been reported to produce the chloromethyl phosphonium salt [TTMPP-CH_2-Cl^+]Cl^- (**28**, Scheme 18).[48] We thus assumed that the major signal observed at δ = 7.00 ppm in the ^{31}P NMR spectrum arised from such a phosphonium salt. As for the other signal at δ = 48.11 ppm, we hypothesized that it could be assigned to a chlorophosphonium formed also upon reaction with dichloromethane.

Consequently, dichloromethane or other chlorinated solvents could not be used for reactions involving TTMPP.

In the ^{1}H NMR spectrum of TTMPP alone in CD_2Cl_2 (see Figure S1), the different peaks could be easily assigned: OCH_3 ortho (δ = 3.61 ppm), OCH_3 para (δ = 3.81 ppm) and CH meta (δ = 6.16-6.17 ppm). Since no additional signals were detected in ^{1}H NMR, the presence of R_3P^{+}-H phosphonium can be ruled out.

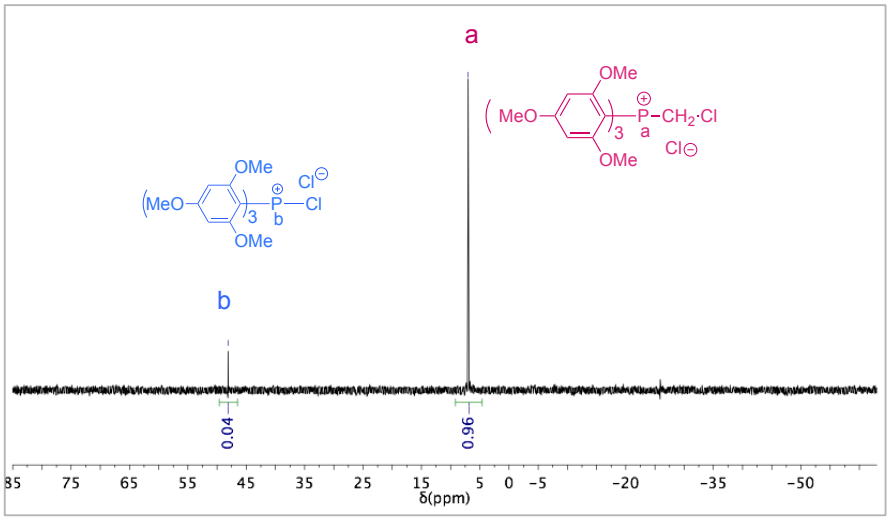

Figure 16. ^{1}H-coupled ^{31}P NMR spectrum of TTMPP alone in CD_2Cl_2.

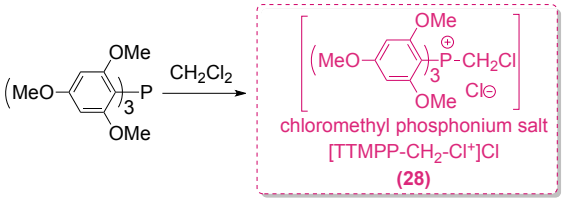

Scheme 18. Reaction of TTMPP with CH_2Cl_2.[48]

Although TTMPP was only slightly soluble in toluene, we performed the model equimolar reaction in this solvent (upon heating at 30 °C, the phosphine became completely soluble). The ^{1}H NMR (Figure S2) and ^{31}P NMR (Figure S3) chemical shifts of TTMPP were in accordance with the expected value (δ^{P} = -71.8 ppm). Upon addition of $TMSNTf_2$, a white precipitate formed in the J-Young tube. The ^{31}P NMR spectrum of the soluble fraction revealed the presence of two peaks at δ = -71.8 and -39.4 ppm, with the peak from the free TTMPP (δ = -71.81ppm) being the major one (Figure S4). However, the mixture being only partially soluble in toluene-d_8, these observations were not conclusive.

The same reaction (TTMPP + $TMSNTf_2$, 1:1) was thus carried out in the more polar bromobenzene-d_5 solvent (PhBr-d_5; ε = 5.17 and 2.38, for PhBr and toluene, respectively), and a perfectly homogenous solution was obtained. Two set of signals were detected in the ^{1}H-coupled ^{31}P NMR spectrum at δ = - 53.1 ppm (doublet, $^{1}J_{P\text{-}H}$ = 535 Hz) and δ = -34.2 ppm (singlet) in this solvent (Figure 17).

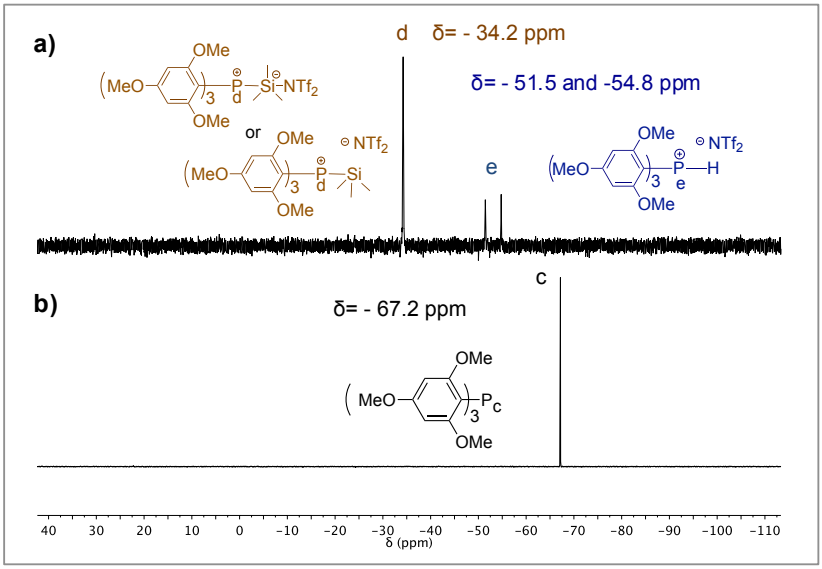

Figure 17. ^{1}H-coupled ^{31}P NMR spectrum in bromobenzene-d_5 of TTMPP+TMSNTf$_2$ (1/1).

In this case, the presence of the corresponding phosphine oxide TTMPPO could also be ruled out, no peak being detected in the region δ = 10-15pmm (^{31}P $\delta^{TTMPP(O)}$ = 10.8 ppm in CD_3CN)[47] . Similarly, no free TTMPP (δ = -67.18 ppm in d_5-PhBr) was detected either. The large characteristic coupling constant J_{PH} of 535 Hz of the signal at δ = -53.1 ppm (~26 %) could be attributed to the P-H phosphonium sulfonylimide, resulting from the protonation of the free phosphine by $HNTf_2$, presumably formed after $TMSNTf_2$ hydrolysis by water traces present in PhBr-d_5. The signal at δ = -34.2 ppm (74 %) appeared downfield shifted compared to that of the free phosphine (by 33 ppm) and strongly suggest the coordination of the phosphorus atom to the $SiNTf_2$ fragment. Unfortunately, attempts to characterize this compound by X-Ray diffraction analysis or ^{29}Si NMR spectroscopy were not successful (see Figure S5). Thus, the exact nature of this adduct is not clear at present (classical LP with a neutral tetracoordinated Si atom or a anionic pentacoordinated Si atom). However, these data seemed to indicate that TTMPP and $TMSNTf_2$ formed a reversible classical LP that remained active though to induce the polymerization of MMA. Adding 1eq. of MMA to this mixture did not allow us to isolate an intermediate of type TTMPP-MMA-$TMSNTf_2$. Peaks from each individual compound were detected, and no PMMA was obtained in this way (Figure S6).

Hence, screening of various LA's and LB's combinations enabled to identify TTMPP/$TMSNTf_2$ as an active Lewis pair for the dual-activation-induced polymerization of MMA in CH_2Cl_2. While ^{31}P NMR confirmed the presence of the phosphonium at the α-position of PMMA chains, decomposition of TTMPP in CH_2Cl_2 was also noted. However, this decomposition likely occurred at a slower rate than that of the polymerization reaction. As discussed in the next section, factors influencing the polymerization, *i.e.* LA/LB ratio, concentration of the reagents etc., were also studied.

3. TTMPP/$TMSNTf_2$-induced Lewis pair polymerization (LPP) of MMA

3.1. Polymerization in dichloromethane

3.1.1. Influence of the acid concentration

The effect of the concentration of $TMSNTf_2$ over the control of polymerization was investigated, by varying the initial $[TMSNTf_2]_0/[TTMPP]_0$ ratio. The polymerization of MMA was performed in CH_2Cl_2, at 25 °C, keeping constant $[TTMPP]_0$ = 21.8 mM and $[MMA]_0$ = 1.8 M. Polymerizations were then run with LA/LB ratio equal to 0, 0.5, 1 and 2 (Table 4)

Table 4. TTMPP/$TMSNTf_2$-induced polymerization of MMA, in CH_2Cl_2 at 25 °C, using various concentration in $TMSNTf_2$.

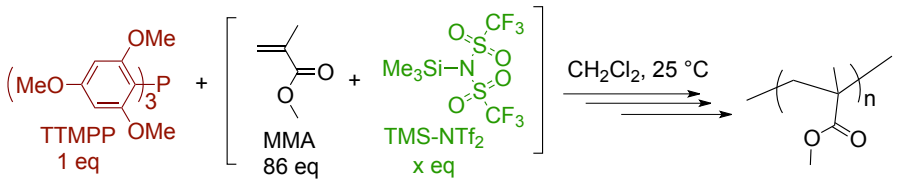

Entry	$[MMA]_0/LA]_0/[LB]_0$	Time (h)	Conv.[a] (%)	$\bar{M}_n^{theo}$ [b] (g.mol^{-1})	$\bar{M}_n^{NMR}$ [c] (g.mol^{-1})	$\bar{M}_n^{SEC}$ [d] (g.mol^{-1})	M_p^{SEC} [d] (g.mol^{-1})	$Đ$ [d]
1	86/1/-	48	0	-	-	-	-	-
2	86/-/1	48	0	-	-	-	-	-
3	86/0.5/1	24	0	-	-	-	-	-
4	86/1/1	24	0	-	-	-	-	-
5	86/2/1	3h	100	8,600	8,900	207,000	266,000	1.1

a. Conv. = % monomer conversion determined by ^{1}H NMR spectroscopy; b. Theoretical molar mass $\bar{M}_n^{theo} = M_{LB} + M_{MMA} \times \frac{[MMA]}{[LB]} \times conv.$; c. $\bar{M}_n^{NMR}$ determined by ^{1}H NMR based on integration of protons from TTMPP substituents; d. Characterization of PMMA's by SEC in DMF/DMSO (80/20) using PS standards for calibration.

Table 4 shows that TTMPP/$TMSNTf_2$-initiated polymerization of MMA only occurred when an excess of LA (2 eq. relative to LB) was used. Under such conditions, PMMA of molar mass $\bar{M}_n^{NMR}$ = 8,900 g.mol^{-1} was formed, in good agreement with the expected value (Figure 15).

In contrast to SEC run in THF, where phosphine-derived polymers were suspected to remain onto the columns, the PMMA obtained here could be analyzed by SEC run in DMF/DMSO (80/20), these elution conditions presumably minimizing the interactions between the supposed phosphonium chain-ends and SEC columns. However, it is worth mentioning that when using SEC in DMF (or DMF/DMSO), sample molar masses delivered

are generally overestimated, hence this analytic method was used to have here an information about the dispersity. As illustrated in the SEC traces (Figure 18), TTMPP-derived PMMA exhibited a UV absorption at λ = 260 nm, that was characteristic of the presence of TTMPP polymer chains. All together, these results demonstrated that polymerization of MMA (~100 eq.) by TTMPP (1 eq.) assisted by $TMSNTf_2$ (2 eq.) efficiently occurred.

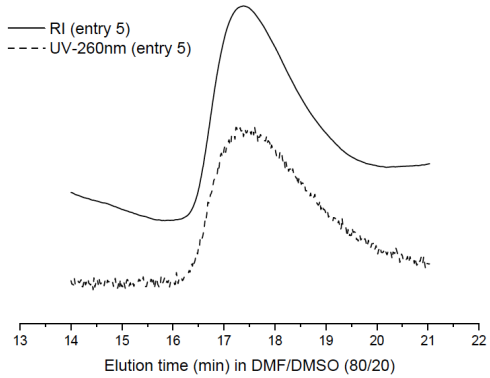

Figure 18. SEC traces (RI-UV 260 nm) of PMMA obtained with TTMPP/$TMSNTf_2$ in CH_2Cl_2 (Table 4, entry 5).

The absence of polymerization, when running experiments with LA/LB ratios equal to 0.5 and 1 (Table 4; entries 1-4), strongly suggested that the polymerization required an activation of MMA by the excess of LA (**24**; Scheme 19), consistently with a bimetallic mechanism, as reported by Chen *et al.*[19]. The activated monomer (**24**) would undergo a nucleophilic addition of TTMPP, leading to the zwitterionic intermediate species (**26**^{TTMPP}). Further 1,4 addition of activated MMA **26**^{TTMPP} yielded **27**^{TTMPP}, which was deactivated in air, forming the α-phosphonium PMMA. Since two molecules of LA seemed to be required, this ratio (LA/LB = 2) was kept in our further studies.

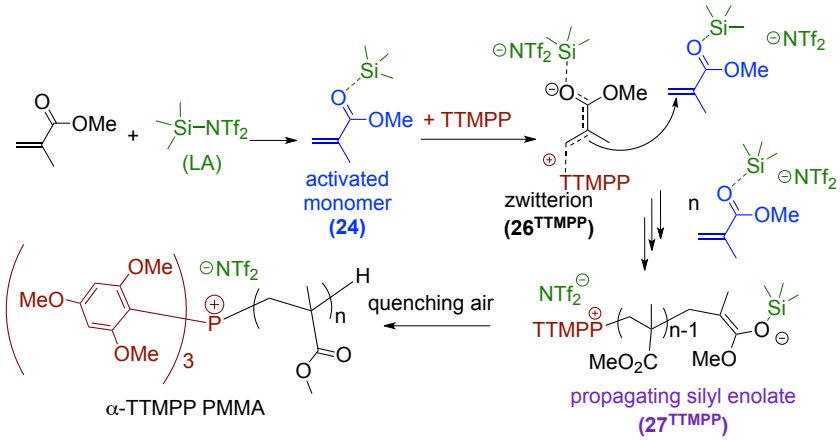

Scheme 19. Bimetallic mechanism for the LPP of MMA using the TTMPP/$TMSNTf_2$ (1/2).

3.1.2. Influence of the order of addition of reagents

We anticipated that the order of addition of each reagent was crucial in such polymerization process. As a reminder, this order of addition was always the same during the reactivity screening: (MMA + solvent + $TMSNTf_2$) + (TTMPP + solvent). Polymerizations of MMA were thus performed by varying the order of addition of TTMPP, $TMSNTf_2$ and MMA. Concentrations used where as follows: $[TTMPP]_0$ = 21.8 mM, $[TMSNTf_2]_0$ = 43,6 mM and $[MMA]_0$ = 1.8 M, Table 5 summarizes the results obtained, and Figure 19 is an overlay of the corresponding SEC traces.

Table 5. TTMPP/$TMSNTf_2$-induced polymerization of MMA, in CH_2Cl_2 at 25 °C for DP = 86.

Entry	Order	Time (h)	Conv.[a] (%)	$\overline{M}_n^{theo}$ [b] (g.mol^{-1})	$\overline{M}_n^{NMR}$ [c] (g.mol^{-1})	$\overline{M}_n^{SEC}$ [d] (g.mol^{-1})	M_p^{SEC} [d] (g.mol^{-1})	$Đ$ [d]
1	(MMA+LA)+LB	1	60	5,200	6,900	68,720	89,300	1.1
2	(MMA+LB)+LA	1	54	4,600	8,200	65,650	84,460	1.1
3	(LA+LB)+MMA	1	40	3,400	8,000	62,150	80,730	1.1

a. Conv.= % monomer conversion determined by 1H NMR spectroscopy; b. Theoretical molar mass $\overline{M}_n^{theo} = M_{LB} + M_{MMA} \times \frac{[MMA]}{[LB]} \times conv.$; c. $\overline{M}_n^{NMR}$ by ^1H NMR based on integration of protons from TTMPP substituents; d. Characterization of PMMA's by SEC in DMF using PS standards for calibration.

When pre-mixing MMA with $TMSNTf_2$ in CH_2Cl_2, followed by addition of a TTMPP CH_2Cl_2 solution onto the solution of the activated monomer, 60 % of MMA conversion were reached after 1 h (Table 5, entry 1). PMMA of molar mass $\overline{M}_n^{NMR}$ = 6,900 g.mol^{-1} were obtained in this way, in quite good agreement with the theoretical value. When the monomer was mixed first with TTMPP, which was followed by addition of $TMSNTf_2$, the polymerization rate was slightly slower (54 % of conversion after 1 h, entry 2) and the molar mass ($\overline{M}_n^{NMR}$ = 8,200 g.mol^{-1}) was higher than that expected. We assumed that, in this case, TTMPP did not interact with non-activated MMA, initiation (TTMPP + [MMA-$TMSNTf_2$]) likely competed with the formation of the classical adduct [TTMPP-$TMSNTf_2$).

As expected, adding the monomer onto the solution of TTMPP/$TMSNTf_2$ decreased the polymerization rate, reaching only 40 % of the monomer conversion after 1 h (entry 3). According to this order of addition, the as-obtained PMMA exhibited a molar mass $\overline{M}_n^{NMR}$ = 8,000 g.mol^{-1}, higher than that expected, demonstrating a loss of control over the polymerization. Again, this was ascribed to the formation of a classical Lewis adduct between TTMPP and $TMSNT_2$, as discussed above. The formation of this adduct likely reduced the concentration of the polymerization activators available, thus decreasing the number of active species, hence a higher molar mass polymer was produced.

Polymers exhibited a narrow distribution of molar masses ($Đ$ = 1.1), irrespectively of the order of addition of the reagents, and the apparent molar masses increased with the

monomer conversion (Figure 19a), as expected for a controlled polymerization process. Furthermore, a UV absorption at λ = 260 nm was detected in all cases, in accordance with direct initiation by TTMPP (Figure 19b).

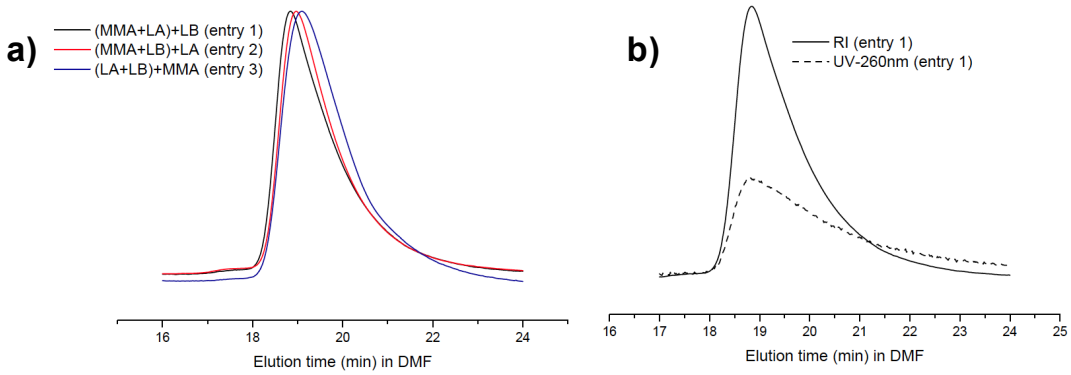

Figure 19. a) SEC-RI traces of PMMA's obtained by varying the order of addition. b) representative SEC-UV traces at λ = 260 nm (Table 5, entries 1-3).

Thus, the polymerization was better controlled and kinetically favored, when the LB was added onto a solution of the Lewis acid-activated monomer (order 1 in Table 5). This order of addition precludes premature reaction between TTMPP and $TMSNTf_2$, keeping both reagents active to initiate the polymerization in a selective, quantitative and controlled manner.

3.1.3. Influence of the monomer concentration

Here, polymerizations of MMA were carried out keeping constant the initial concentrations of TTMPP and $TMSNTf_2$ ($[TTMPP]_0$ = 27 mM and $[TMSNTf_2]_0$ = 54 mM, respectively), before MMA was progressively added. Results are summarized in Table 6 and illustrated in Figure 20.

Table 6. TTMPP/$TMSNTf_2$-induced polymerization of MMA in CH_2Cl_2 at 25 °C, using various concentration in MMA.

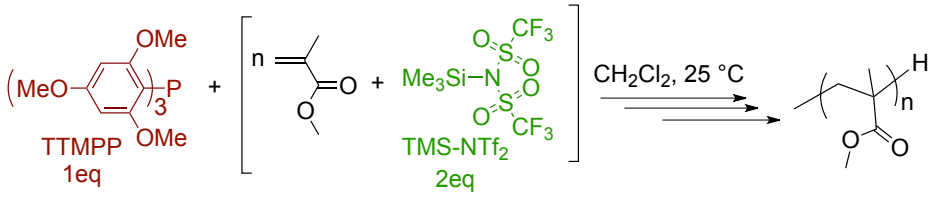

Entry	$[MMA]_0/[LA]_0/[LB]_0$	Time (h)	Conv.[a] (%)	$\overline{M}_n^{theo}$ [b] (g.mol^{-1})	$\overline{M}_n^{NMR}$ [c] (g.mol^{-1})	$\overline{M}_n^{SEC}$ [d] (g.mol^{-1})	M_p^{SEC} [d] (g.mol^{-1})	$Đ$ [d]
1	43/2/1	3	100	4,300	5,700	154,000	208,000	1.1
2	86/2/1	3	100	8,600	11,800	207,000	266,000	1.1

3	173/2/1	3	100	17,300	23,200	304,000	416,000	1.1

a. Conv.= % monomer conversion determined by 1H NMR spectroscopy; b. Theoretical molar mass $\bar{M}_n^{theo} = M_{LB} + M_{MMA} \times \frac{[MMA]}{[LB]} \times conv.$; c. $\bar{M}_n^{NMR}$ determined by ^{1}H NMR based on integration of protons from TTMPP substituents; d. Characterization of PMMA's by SEC in DMF/DMSO (80/20) using PS standards for calibration.

Quantitative conversions were reached within 3 h, and $\bar{M}_n$ values were relatively close to expected ones (*e.g.* 4,300 *vs.* 5,700 g.mol^{-1}, for a targeted DP of 43, Table 6, entry 1). As depicted in Figure 20a, $\bar{M}_n$ values increased when the monomer concentration was increased, from $\bar{M}_n^{NMR}$ = 5,700 to 23,200 g.mol^{-1} (entries 1-3). The dispersity values (*Đ*) of as-obtained PMMA's remained low (*Đ* = 1.1), even when targeting higher molar masses, and the monomodal shape of the SEC traces showed the presence of only one population. A UV absorption was also detected at λ = 260 nm, attesting to the presence of the phenyl groups deriving from TTMPP in the polymer chains (Figure 20b).

Hence, molar masses ($\bar{M}_n$) of TTMPP/TMSNTf$_2$-derived PMMA's obtained in CH_2Cl_2 were well controlled by the initial $[MMA]_0/[TTMPP]_0$ feed ratio.

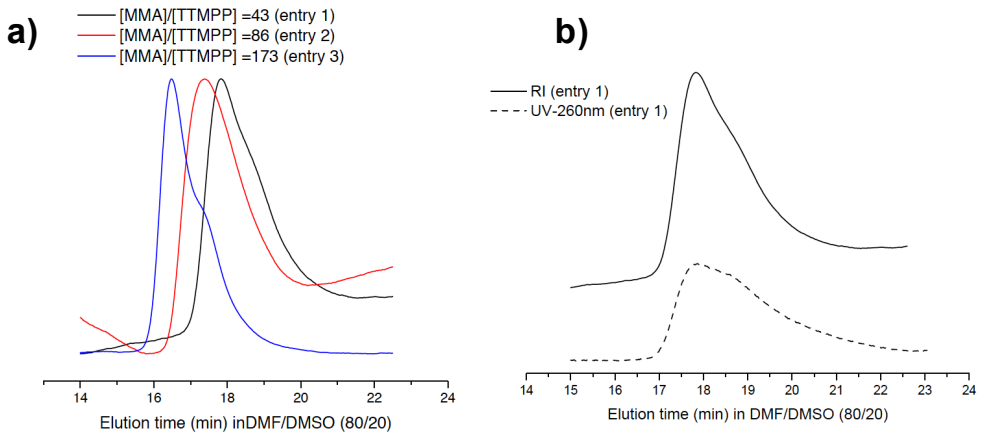

Figure 20. a) SEC-RI traces of PMMA obtained with TTMPP/TMSNTf$_2$ (1/2) in CH_2Cl_2, at 25 °C (Table 6, entries 1-3); b) representative SEC-UV traces at λ = 260 nm.

Although the experimental $\bar{M}_n$ values are higher than targeted ones, these polymerizations proceeded with a linear correlation between the apparent molar masses, as delivered by SEC and monomer conversion (Figure 21), with molar masses distributions remaining lower than 1.1 at complete conversion. These characteristics indicated that termination and transfer reactions were negligible.

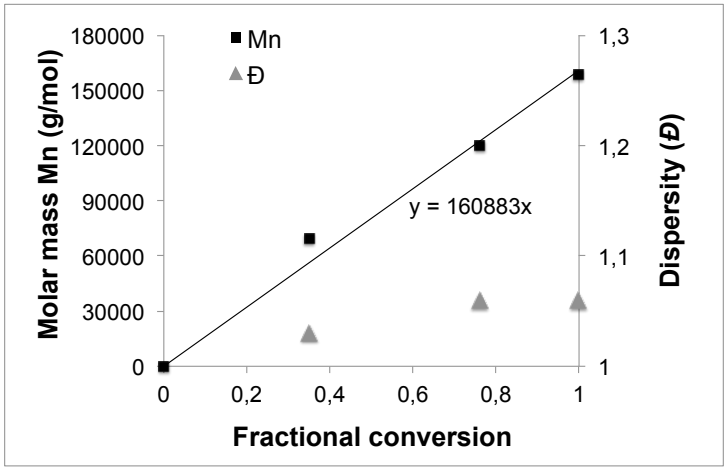

Figure 21. Evolution of molar masses ($\overline{M_n}$) and dispersity *Đ vs.* MMA conversion in CH_2Cl_2 at 25 °C: $[MMA]_0$ = 1.6 M, $[TTMPP]_0$ = 18 mM and $[TMSNTf_2]_0$ = 36 mM (DP = 86).

3.1.4. Chain-end characterization

Chain-end fidelity is another important criterion to account for a "controlled/living" polymerization process. The exact nature of polymer chain-ends also brings information about the active species propagating the polymerization. A TTMPP/$TMSNTf_2$-derived PMMA sample that was prepared in CH_2Cl_2 using the initial concentration $[TTMPP]_0$ = 36 mM, $[TMSNTf_2]_0$ = 72.4 mM, and $[MMA]_0$ = 1.6 M was thus analyzed by ^1H and ^{31}P NMR spectroscopies, as well as by MALDI-ToF spectrometry. This sample was precipitated twice in methanol and dried under vacuum for 3 h (Table 7). Figure 22 illustrates the RI and UV SEC traces of this polymer.

Table 7. TTMPP/$TMSNTf_2$-induced polymerization of MMA in CH_2Cl_2 at 25 °C.

$[MMA]_0/[LA]_0/[LB]_0$	Time (h)	Conv.[a] (%)	$\overline{M_n}^{theo}$ [b] (g.mol^{-1})	$\overline{M_n}^{NMR}$ [c] (g.mol^{-1})	$\overline{M_n}^{SEC}$ [d] (g.mol^{-1})	M_p^{SEC} [d] (g.mol^{-1})	*Đ* [d]
43/2/1	3	100	4,800	15,700	60,200	72,500	1.1

a. Conv.= % monomer conversion determined by ^1H NMR spectroscopy; b. Theoretical molar mass $\overline{M}_n^{theo} = M_{LB} + M_{MMA} \times \frac{[MMA]}{[LB]} \times conv.$; c. $\overline{M}_n^{NMR}$ determined by ^1H NMR based on integration of protons from TTMPP substituents; d. Characterization of PMMA by SEC in DMF using PS standards for calibration.

An unimodal distribution of molar masses was observed (*Đ* = 1.1) with a UV absorption at λ = 260 nm (in accordance with an initiation from TTMPP (Figure 22). However, the obtained molar mass, $\overline{M}_n$, of this sample ($\overline{M}_n^{NMR}$ = 15,700 g.mol^{-1} for $[TTMPP]_0$ = 36 mM, $[TMSNTf_2]_0$ = 72.4 mM, and $[MMA]_0$ = 1.6 M, Table 7) was higher than the one prepared for the same DP using $[TTMPP]_0$ = 27 mM, $[TMSNTf_2]_0$ = 54 mM, and $[MMA]_0$ = 1.2 M (Table 6;entry 1; M_n^{NMR} = 5,700 g.mol^{-1}). In other words, attempts to scale-up the reaction might

have caused a certain loss of control. We hypothesized that, when using higher concentrations of reagents, either the formation of a classical TTMPP-$TMSNTf_2$ adduct was favored, or higher quantity of TTMPP was deactivated by the solvent, providing a polymer of higher molar mass than that expected. Hydrolysis of $TMSNTf_2$ by traces of water might also occur.

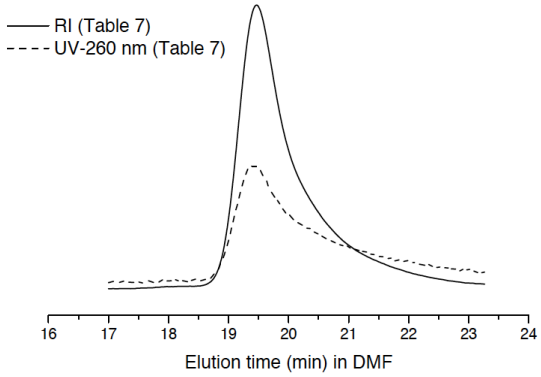

Figure 22. SEC traces (RI and UV) of PMMA obtained with TTMPP/$TMSNTf_2$ (1/2) in CH_2Cl_2, at 25 °C (Table 7).

Various species were detected in the ^{31}P NMR spectrum (Figure 23), with two major peaks at δ^P = 2.32 ppm (41 %) and 7.25 ppm (32 %), illustrating the presence of two types of phosphorus moieties. As already discussed in section 2.4, we assumed that these signals corresponded to α-phosphonium PMMA of various microstructure. However, the attribution of each signal would required further characterization

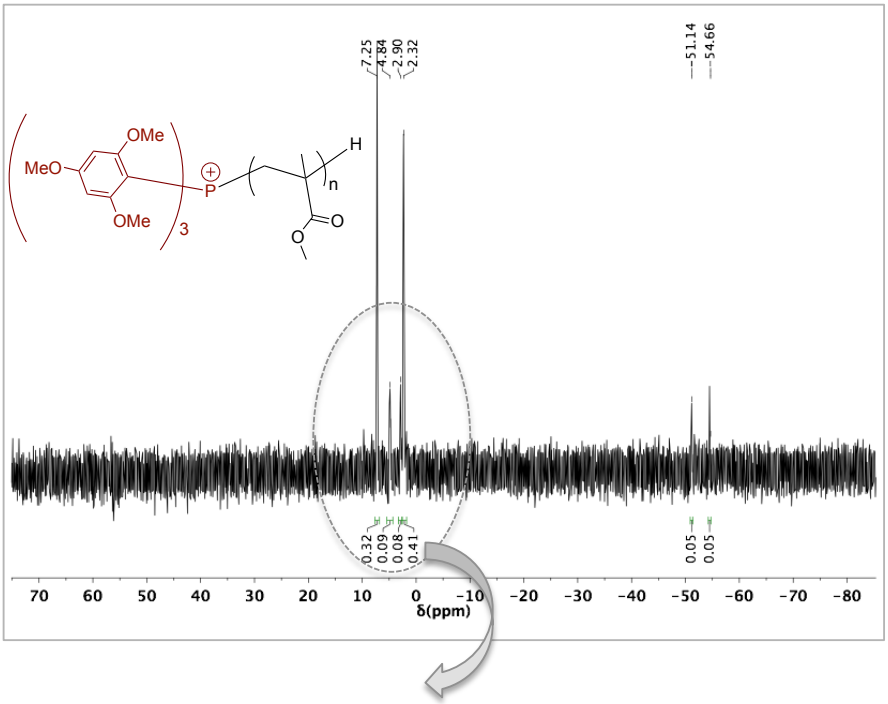

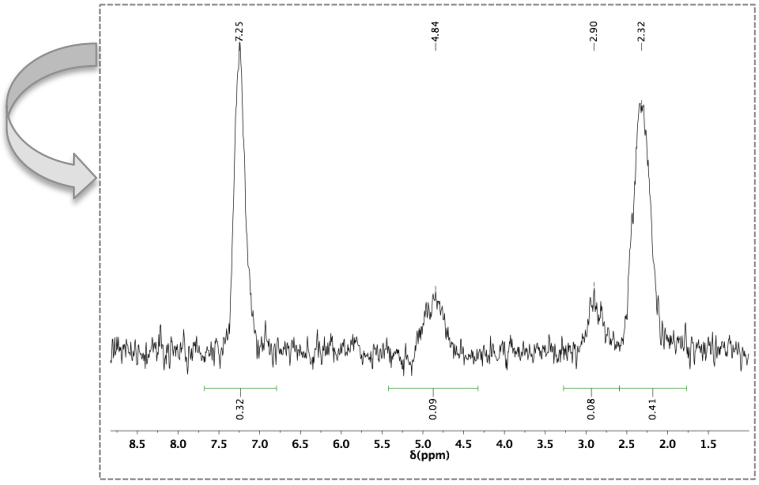

Figure 23. ^{1}H coupled-^{31}P NMR spectrum in $CDCl_3$ of PMMA obtained using TTMPP/$TMSNTf_2$ (1/2) in CH_2Cl_2 at 25 °C (Table 7).

The tacticity of this TTMPP/$TMSNTf_2$-derived PMMA was evaluated by ^{1}H NMR spectroscopy, based on the signals from CH_3 groups (Figure 24).[49] The result was as follows: syndiotacticity (% of triad rr) = 69 %, heterotacticity (% of triad mr) = 28 % and isotacticity (% of triad mm) = 3 %. The proportion of syndiotacticity was thus slightly higher than that generally observed for PMMA produced by anionic polymerization in THF (% rr/mr/mm = 56/39/5).[50] This could be explained by a preferential monomer insertion due to steric constraints, arising from the silicon coordination in both the monomer and the propagating silyl enolate (see Scheme 20).

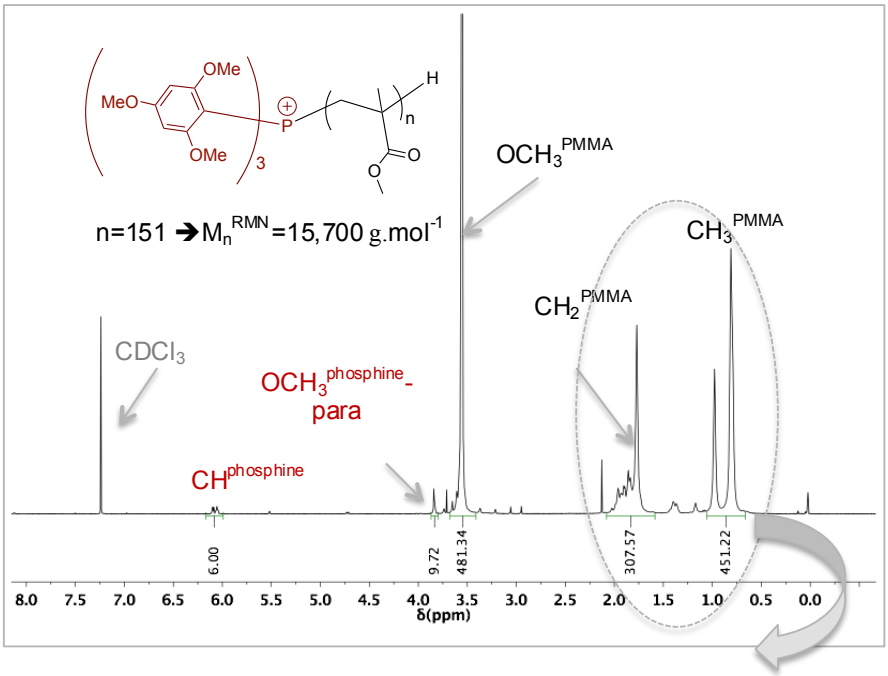

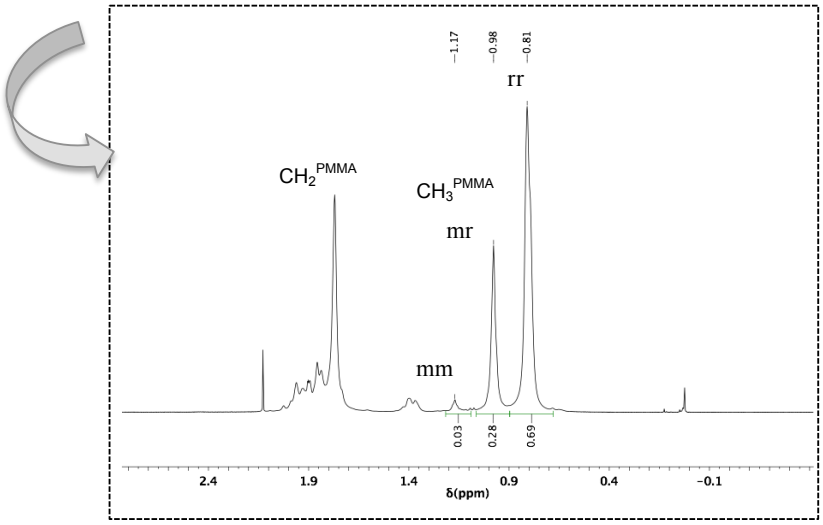

Figure 24. ^{1}H NMR spectra in $CDCl_3$ of PMMA obtained using TTMPP/$TMSNTf_2$ (1/2) in CH_2Cl_2 at 25 °C (Table 7)

The MADLI-ToF mass spectrum of the same polymer (Figure 25) revealed signals separated by 100 mass units (corresponding to the mass of one MMA unit). Two main populations were detected. The population A^{TTMPP} was ascribed to the targeted α-phosphonium,ω-H PMMA with m/z = 533.19 + 100.05 n , where 533.19 is the molar mass of the phosphonium and H-end-groups. However, two structures exhibiting the same m/z could be accounted for population A^{TTMPP}: the linear α-phosphonium,ω-H PMMA or the α-phospholane cyclic PMMA. Scheme 20 shows both proposed mechanisms for the generation of these two structures. On the NMR spectrum, these two populations might have very similar chemical shifts and could not be distinguished. Unfortunately, population E (Figure 25) could not be identified even considering structures resulting from backbiting and/or branching reactions.

Although the polymerization in CH_2Cl_2 was seemingly controlled by the initial $[MMA]_0/[TTMPP]_0$, a more detailed chain-end analysis revealed the occurrence of side reaction, probably from TTMPP decomposition in this solvent. We thus turned our attention to the use of toluene as a “more innocent “polymerization solvent.

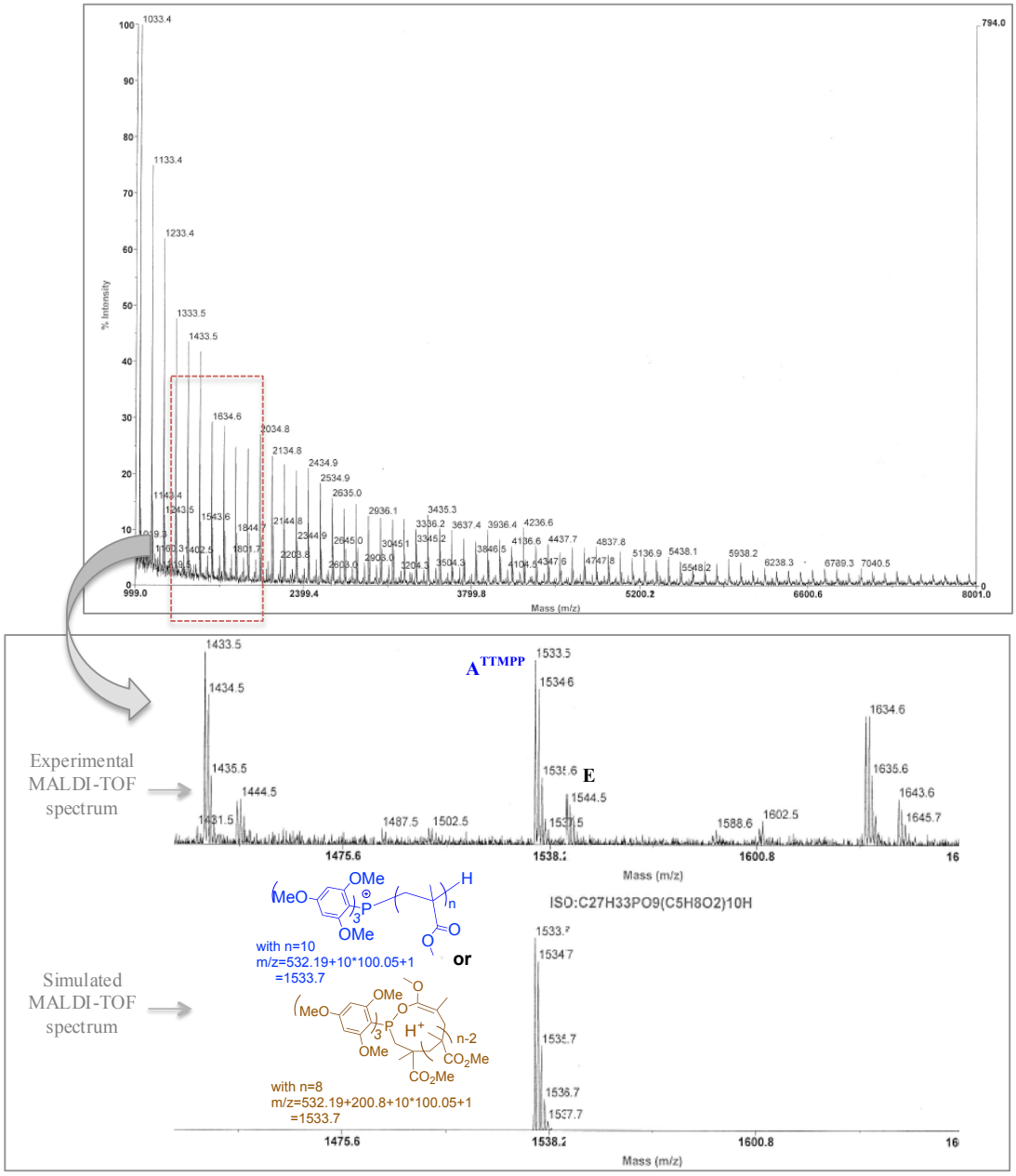

Figure 25. MALDI-ToF mass spectrum of PMMA obtained using TTMPP/$TMSNTf_2$ (1/2) in CH_2Cl_2 at 25 °C (Table 7)

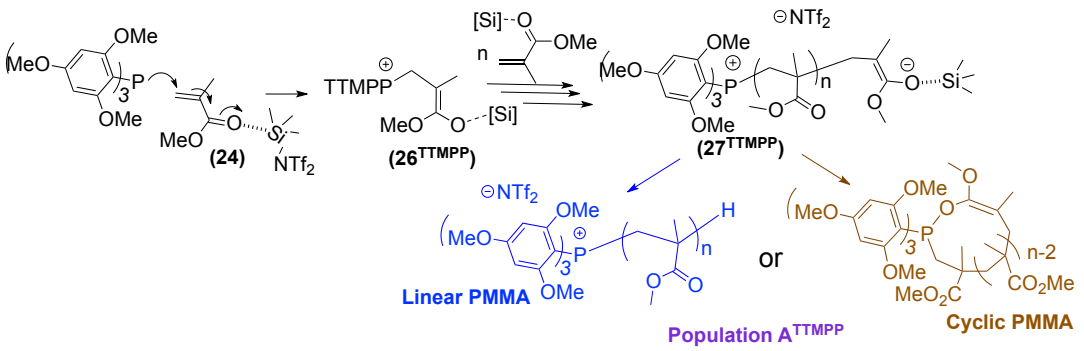

Scheme 20. Mechanisms for the generation of population observed in MALDI-ToF PMMA obtained using TTMPP/$TMSNTf_2$(1/2) in CH_2Cl_2.

3.2. Polymerization in toluene

3.2.1. Influence of the monomer concentration

In the same manner to that previously described for CH_2Cl_2, the influence of the monomer concentration was investigated in toluene. The order of reagents addition remained the same, *i.e.*, the TTMPP solution was added onto a solution of MMA activated by $TMSNTf_2$. The LA/LB ratio was kept equal to 2. The polymerization of MMA was then run using initial concentrations of $[TTMPP]_0$ = 18 mM and $TMSNTf_2]_0$ = 36 mM, and MMA was progressively added. Table 8 summarizes the result obtained under these conditions.

Table 8. TTMPP/$TMSNTf_2$-induced polymerization of MMA in toluene at 25 °C, using various concentration in MMA.

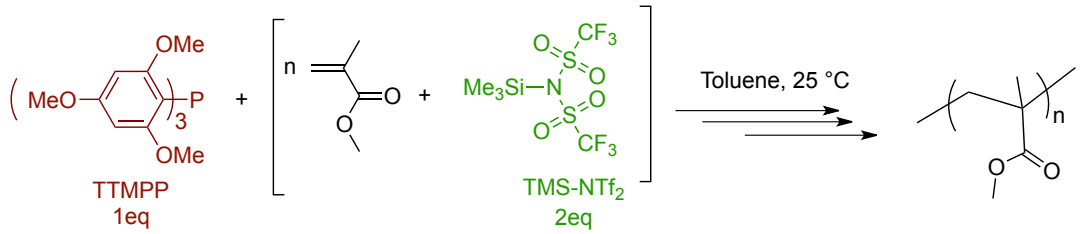

Entry	$[MMA]_0/[LA]_0/[LB]_0$	Time (h)	Conv.[a] (%)	$\overline{M}_n^{theo}$ [b] (g.mol^{-1})	$\overline{M}_n^{NMR}$ [c] (g.mol^{-1})	$\overline{M}_n^{SEC}$ [d] (g.mol^{-1})	M_p^{SEC} [d] (g.mol^{-1})	$Đ$ [d]
1	43/2/1	3	100	4,300	6,700	27,800	30,000	1.02
2	86/2/1	3	100	8,600	10,800	64,000	73,700	1.1
3	173/2/1	3	100	17,300	17,800	123,400	140,800	1.1

a. Conv.= % monomer conversion determined by 1H NMR spectroscopy; b. Theoretical molar mass $\overline{M}_n^{theo} = M_{LB} + M_{MMA} \times \frac{[MMA]}{[LB]} \times conv.$; c. $\overline{M}_n^{NMR}$ determined by 1H NMR based on integration of protons from TTMPP substituents; d. Characterization of polymers by SEC in DMF/DMSO (80/20) using polystyrene standards for calibration.

Interestingly, the polymerization of MMA using TTMPP/$TMSNTf_2$ readily proceeded in toluene at 25 °C, reaching quantitative conversion within 3 h (Table 8). The obtained molar masses ($\overline{M}_n^{NMR}$) were in good agreement with expected values, based on the initial $[MMA]_0/[TTMPP]_0$ ratio with narrow dispersities ($Đ$ = 1.1). In addition, these molar masses increased with the monomer concentration, from 6.700 to 17,800 g.mol^{-1} PMMA's in a controlled fashion (Figure 26).

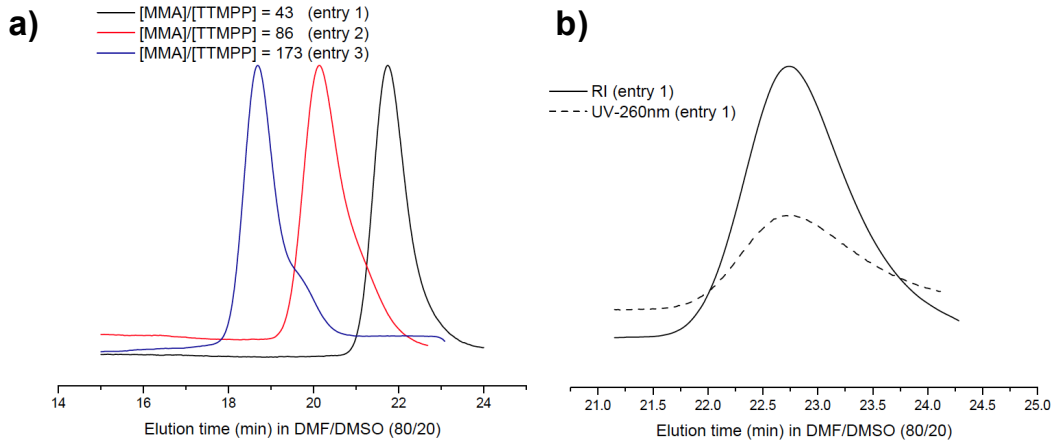

Figure 26. a) SEC-RI traces of PMMA obtained with TTMPP/$TMSNTf_2$ (1/2) in toluene, at 25 °C (Table 8); b) representative SEC-UV traces at λ = 260 nm.

Figure 27 depicts the $\overline{M}_n$ profile of PMMA *vs.* MMA conversion in a $[MMA]_0/[TTMPP]_0$ ratio equal to 86. The linear correlation is consistent with a controlled polymerization. In addition, the molar mass distribution remains low at high conversion.

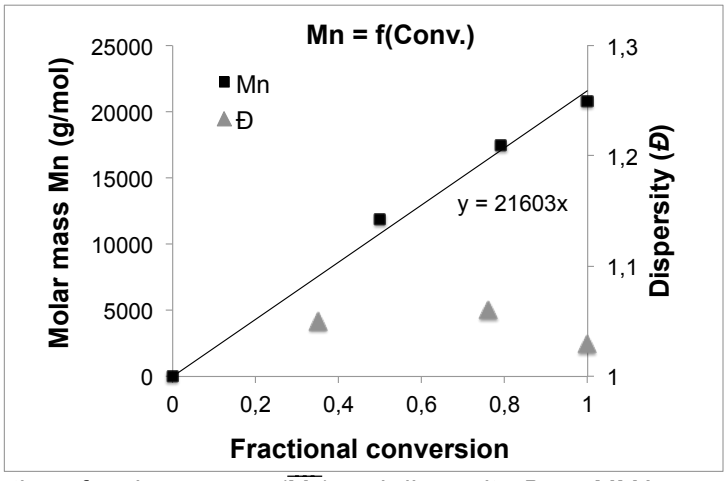

Figure 27. Evolution of molar masses ($\overline{M}_n$) and dispersity *Đ vs.* MMA conversion in toluene at 25 °C: $[MMA]_0$ = 1.6 M, $[TTMPP]_0$ = 18 mM and $[TMSNTf_2]_0$ = 36 mM (DP = 86).

Molar masses delivered by ^1H NMR, assuming all TTMPP-derived PMMA chains obtained in toluene carried a TTMPP moiety in α-position, were in the same range than those of polymers synthesized in CH_2Cl_2 (for DP = 43 $\overline{M}_n^{NMR}$ = 6,700 and 5,700 $g.mol^{-1}$, respectively). PMMA's thus produced in toluene were even better defined than those synthesized in CH_2Cl_2. Again, this could be due to the decomposition of TTMPP in CH_2Cl_2, that could have favored side reactions.

3.2.2. Chain-end characterization

As a means to identify the polymer chain-ends, the polymerization was achieved using higher amount of material. A polymerization of MMA in toluene at 25 °C was thus run, using an initial concentration $[TTMPP]_0$ = 36 mM, $[TMSNTf_2]_0$ = 72.4 mM, and $[MMA]_0$ = 1.6 mM. The corresponding sample was precipitated twice in methanol and dried under vacuum for 3 h (Table 9).

Table 9. TTMPP/$TMSNTf_2$-induced polymerization of MMA, in toluene at 25 °C

$[MMA]_0/LA]_0/[LB]_0$	Time (h)	Conv.[a] (%)	$\overline{M_n}^{theo}$ [b] (g.mol^{-1})	$\overline{M_n}^{NMR}$ [c] (g.mol^{-1})	$\overline{M_n}^{SEC}$ [d] (g.mol^{-1})	M_p^{SEC} [d] (g.mol^{-1})	$Đ$ [c]
43/2/1	3	100	4,800	9,200	22,600	23,400	1.05

a. Conv.= % monomer conversion determined by 1H NMR spectroscopy; b. Theoretical molar mass $\overline{M}_n^{theo} = M_{LB} + M_{MMA} \times \frac{[MMA]}{[LB]} \times conv.$; c. $\overline{M}_n^{NMR}$ determined by ^{1}H NMR based on integration of protons from TTMPP substituents; d. Characterization of polymers by SEC in DMF using PS standards for calibration.

This PMMA exhibited the same molecular features to that achieved in CH_2Cl_2. In toluene, indeed, a well-defined peak was observed by SEC, with a UV absorption at λ = 260 nm. The molar mass $\overline{M_n}^{NMR}$ was also higher than the expected value, as already observed in CH_2Cl_2, meaning that some loss of control over the polymerization also occurred due to the "scale-up". Since no decomposition of TTMPP could occurred in toluene, this deviation from linearity was here attributed, to the formation of a classical Lewis adduct that likely reduced the concentration of TTMPP.

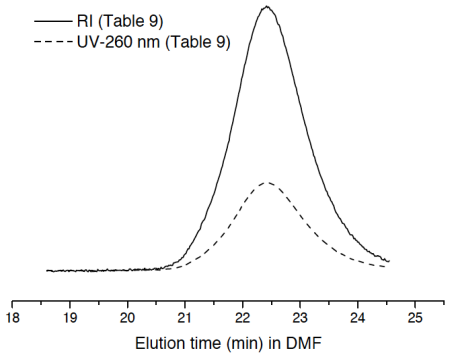

Figure 28. SEC traces (RI and UV) of PMMA obtained with TTMPP/$TMSNTf_2$ (1/2) in toluene at 25 °C (Table 9).

In the ^{31}P NMR spectrum (Figure 29), two major peaks were observed at δ^P = 2.36 ppm (73 %) and δ^P = 2.89 ppm (19 %), illustrating the presence of two phosphorus atoms of similar environment. These signals could be ascribed to the expected α-phosphonium linear PMMA's and the α-phospholane cyclic PMMA's. Further investigations are needed however to clarify this point.

The tacticity of this TTMPP/TMSNTf$_2$-derived PMMA was evaluated by ^{1}H NMR (Figure S7). The result was as follows: syndiotacticity (% of triad rr) = 62 %, heterotacticity (% of triad mr) = 34 % and isotacticity (% of triad mm) = 4%. These values were very similar to those obtained in CH_2Cl_2 (69/28/3). As already mentioned above, propoagation by sterically hindered species (see Scheme 19) can explain that predominance for syndiotacticity.

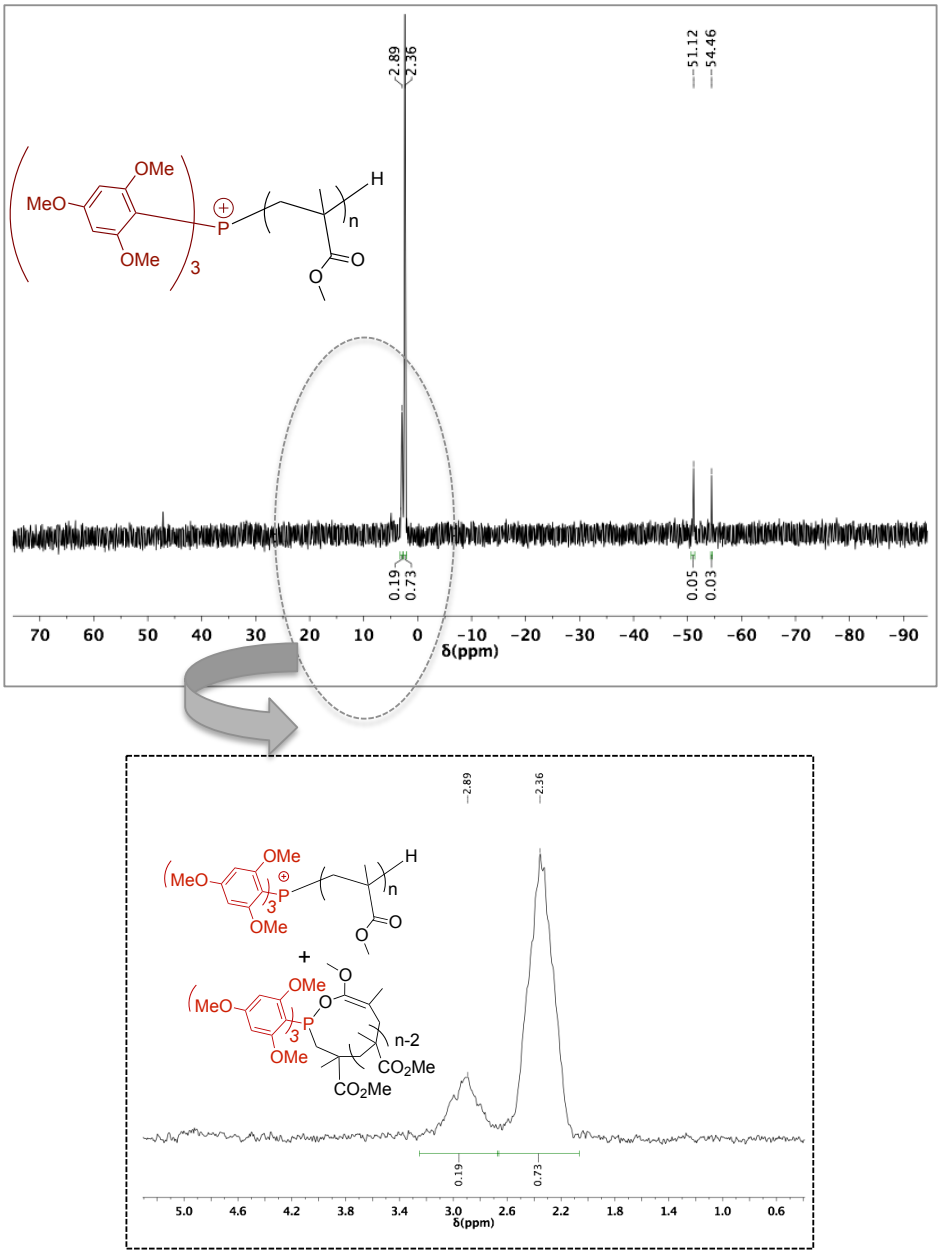

Figure 29. ^{1}H coupled-^{31}P NMR spectrum in $CDCl_3$ of PMMA obtained using TTMPP/TMSNTf$_2$ (1/2) in toluene at 25 °C (Table 9).

Analysis of this sample by MALDI-ToF revealed the presence of one main population A^{TTMPP} (Figure 30), corresponded to the targeted α-phosphonium PMMA that could exist either in a linear form or as a cyclic structure.

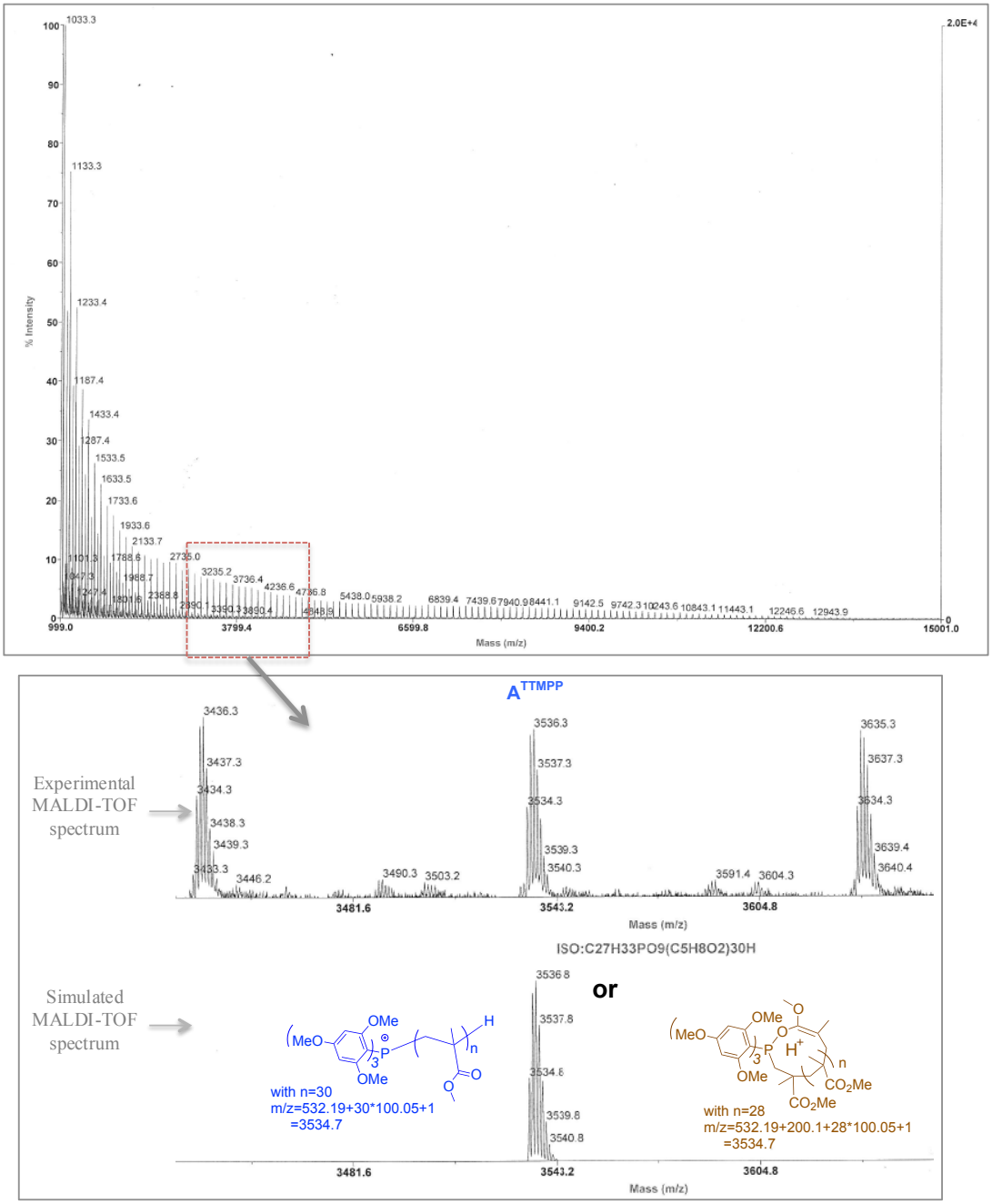

Figure 30. MALDI-ToF mass spectrum of PMMA obtained using TTMPP/TMSNTf$_2$ (1/2) in toluene at 25 °C (Table 9).

3.2.3. Chain extension experiments

Finally, the ability of the TTMPP/TMSNTf$_2$-derived PMMA chain to be reactivated was evaluated. The polymerization of MMA was run in toluene at 25 °C using initial concentrations [TTMPP]$_0$ = 11 mM, [TMSNTf$_2$]$_0$ = 22 mM and [MMA]$_0$ = 0.6 M. After complete conversion, another load of 52 eq. of MMA was added (see Table 10 and Figure 31).

For the first polymerization run (Table 10, entry 1), up to 85% of monomer conversion were reached after 3 h at 25 °C, producing PMMA of apparent molar mass

$\overline{M_n}$ = 60,200 g.mol^{-1} and narrow dispersity *Đ* = 1.02 (Figure 31). New load of 52 eq. of MMA was added onto this PMMA precursor and complete conversion was reached after 13 h, leading to PMMA of $\overline{M_n}$ = 73,900 g.mol^{-1} and *Đ* = 1.02 (run 2; entry 2). The SEC-RI traces of this second run showed a shouldered peak that may arise from the termination of few chains of the PMMA precursor from run 1 (Figure 31). After complete conversion of run 2, a new load MMA (52 eq.) was again added, increasing the polymer chains from 73,900 g.mol^{-1} to 106,000 g.mol^{-1}. The dispersity remained narrow *(Đ* = 1.0), showing the control of this polymerization.

Table 10. Sequential addition of MMA onto TTMPP/TMSNTf$_2$-derived living PMMA chains in toluene at 25 °C.

Entry	$[MMA]_0/[LA]_0/[LB]_0$	Time (h)	Conv.[a] (%)	$\overline{M_n}^{theo\ b}$ (g.mol^{-1})	$\overline{M_n}^{NMR\ c}$ (g.mol^{-1})	$\overline{M_n}^{SEC\ d}$ (g.mol^{-1})	*Đ* [c]
1	52/2/1 (run 1)	3	85	4,400	60,200	62,700	1.05
2	run 1 + 52eq (run 2)	13	100	9,600	73,900	93,900	1.1
3	run 2 + 52eq (run 3)	21	100	15,000	105,400	127,900	1.1

a. Conv.= % monomer conversion determined by 1H NMR spectroscopy; b. Theoretical molar mass $\overline{M}_n^{theo} = M_{LB} + M_{MMA} \times \frac{[MMA]}{[LB]} \times conv.$; c. $\overline{M}_n^{NMR}$ determined by ^{1}H NMR based on integration of protons from TTMPP substituents; d. Characterization of PMMA's by SEC in DMF/DMSO (80/20) using PS standards for calibration.

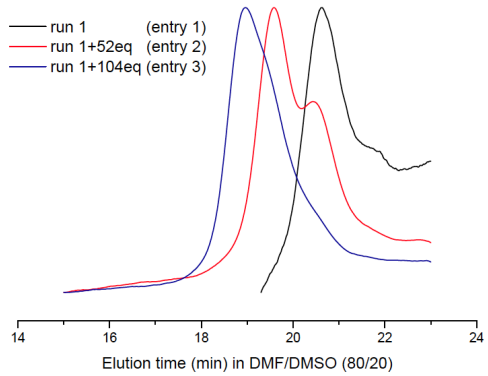

Figure 31. SEC-RI traces of PMMA obtained upon sequential addition of MMA onto TTMPP/TMSNTf$_2$-derived living PMMA chains in toluene at 25 °C (Table 10).

Based on these results, one can conclude that the polymerization of MMA induced by TTMPP and TMSNTf$_2$ exhibit a "controlled/living" character with a rather high end-group fidelity. Changing solvent polarity, from relatively polar CH_2Cl_2 (ε = 8.93) to non-polar toluene (ε = 2.38) did not significantly affect the polymerization activity, though caused a slight variation in the polymer molar masses. This was supposedly due to the suppression of some side reactions occurring in CH_2Cl_2.

Conclusions and perspectives

The Lewis pair-induced polymerization (LPP) of MMA using NHCs or phosphines as Lewis bases, and silicon-derivatives as Lewis acids, was investigated in this chapter. Among the different combinations screened, the tris(2,4,6-trimethoxyphenyl)phosphine (TTMPP)/ trimethylsilyl triflimide ($TMSNTf_2$) Lewis pair proved the best suited to efficiently initiate the polymerization of MMA in a controlled fashion. Polymerizations were typically performed in toluene at 25 °C using $[LA]_0/[LB]_0/[MMA]_0$ ratio in the range 2/1/100. Such conditions afforded α-phosphonium linear PMMA's of molar masses that could be adjusted by the initial $[MMA]_0/[TTMPP]_0$ ratio.

This is the first example of a silicon- and phosphorous-based organic Lewis pair that is active for a chain polymerization reaction. In addition, rather mild conditions can be employed (toluene, at 25 °C) and use of commercially available LB and LA. Control experiments demonstrated that both partners, LA an LB, are needed to induce the polymerization, evidencing a cooperative/dual activation polymerization process. Furthermore, the order of addition of the different reagents dramatically impact the monomer conversion and the control of the molar masses. In terms of stereoselectivity, the as-produced PMMA's exhibit a syndio-rich (60-70 % of triad rr) tacticity, presumably owing to the coordination of the silicon atom with monomer/chain growing during polymerization.

While $NHC^{tBu}/TMSNTf_2$ Lewis pair was found to form an inactive classical adduct, the $TTMPP/TMSNTf_2$ Lewis pair formed an active classical Lewis pair. This demonstrates that a pure true frustrated Lewis pair (FLP) is not required to trigger a dual Lewis pair polymerization, at least in the case of MMA as monomer substrate. Computational studies of the fundamental steps involved in this LPP (*i.e* the active species formation, chain initiation and propagations steps) are ongoing and will hopefully shed light regarding the intimate polymerization mechanism.

In terms of perspectives, post-polymerization functionalization of the α-phosphonium PMMA could be envisaged, for instance, through Wittig reactions. In the presence of a strong base (*e.g.* lithium diisopropyl amide, LDA) and functional aldehyde, the introduction of a reactive function could thus be achieved (Scheme 21), providing materials ready for further macromolecular engineering, such as copolymers synthesis for instance. Nevertheless, the base should be carefully selected in order to avoid side reactions with the esters pendant groups of the polymer.

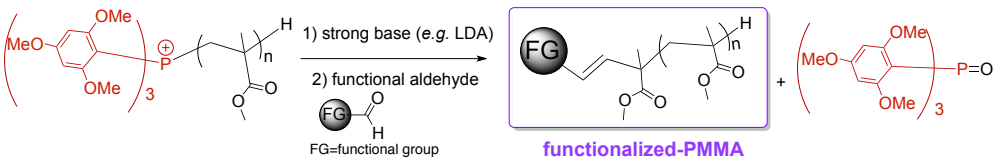

Scheme 21. Post-polymerization functionalization using Wittig reaction.

More generally speaking, true organic phosphine/silicon activating systems could be extended to other vinylic monomers, including (meth)acrylic ones or less polar monomers such as styrenics or dienes, in order to expand the utility of LPP in polymer synthesis.

Even more interestingly, such phosphine/silicon systems could also be employed as true catalytic systems,*i.e.* in presence of alcohols as initiators, for instance or other initiating species with functional groups compatible under these conditions. This new approach based on Lewis pair activation would provide a powerful strategy to synthesize polymers in a controlled manner *via* a straightforward one-pot procedure.

Experimental and supporting information

General instrumentation. NMR spectra were recorded on a Bruker AC-400 spectrometer (^{1}H, ^{13}C, ^{31}P, ^{29}Si of 400 MHz, 100MHz, 162 MHz and 79.5 MHz, respectively) in appropriate deuterated solvents. Molar masses of polymers samples were determined by size exclusion chromatography (SEC) using a 3-columns set of TSK gel TOSOH (G4000, G3000, G2000 with pore sizes of 20, 75, and 200 Å respectively, connected in series) calibrated with narrow Polystyrene standards from Polymer Laboratories using both refractometric and UV detectors (Varian). DMF or DMF/DMSO (80/20) was used as eluent (0.8 $mL.min^{-1}$) and toluene as a flow marker at 80°C, in the presence of LiBr (1 $g.L^{-1}$) using both refractometric and UV detectors (Varian). MALDI-ToF experiments were performed by the ISM-CESAMO (Bordeaux, France) on a Voyager mass spectrometer (Applied Biosystems). The instrument is equipped with a pulsed N2 laser (337 nm) and a time-delayed extracted ion source. Spectra were recorded in the positive-ion mode using the reflectron and with an accelerating voltage of 20 kV. Samples were dissolved in THF at 10 mg/ml. The IAA matrix (trans-3-Indoleacrylic acid) solution was prepared by dissolving 10 mg in 1 ml of THF. A MeOH solution of cationisation agent (NaI, 10 mg/ml) was also prepared. The solutions were combined in a 10:1:1 volume ratio of matrix to sample to cationisation agent. One to two microliters of the obtained solution was deposited onto the sample target and vacuum-dried.

Materials. Toluene was refluxed over CaH_2 and cryo-distilled from polystyryllithium (PS-Li) prior to use. Dichloromethane was cryo-distilled over CaH_2 prior to use. Methyl Methacrylate (MMA) was purchased from Sigma-Aldrich, degased, dried over CaH_2, cryo-distilled into a burette and stored at -20°C. Trimethylsilyl trifluoromethanesulfonate (TMSOTf), triisopropoylsilyltriflate (TIPSOTf) and bistrifluoromethanesulfonylimide ($HNTf_2$) were purchased from Sigma Aldrich and used as received. Trimethylsilyl-bis(trifluoromethane)sulfonimide ($TMSNTf_2$) was purchased from TCI Chemical and used as received. 2,6-di-tert-butyl-4-methylpyridine (DTBMP) and triisopropylsilane (TIPSiH) was purchased from Alfa Aesar and used as received. Tri-n-butylphosphine $P^{n}Bu_3$ was purchased from Sigma Aldrich (95 %) and cryo-distilled. Tri-*tert*-butylphosphine ($P^{t}Bu_3$) and tris(2,4,6-trimethoxyphenyl)phosphine (TTMPP) were purchased from Strem Chemical and Sigma Aldrich, respectively, and used as received. 1,3-Bis(*tert*-butyl)imidazol-2-ylidene (NHC^{tBu}) was purchased from Strem Chemical as used as received. All Lewis acids and bases were kept under an argon glovebox.

All the other experiments were performed under an inert atmosphere using standard Schlenk techniques.

Synthesis of Lewis acids. The preparation of Martin spirosilane (Si-Martin) followed published procedures.[51]

Triisopropoylsilyl triflimide ($TIPSNTf_2$) was synthesized upon reaction of triisopropylsilane with bis trifluoromethane sulfonyl imide as described in Scheme S1.

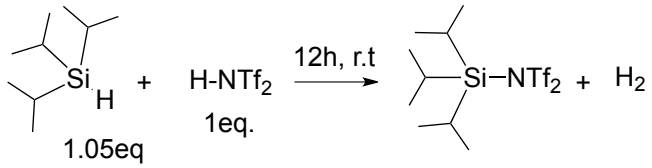

Scheme S1. $TIPSNTf_2$ synthesis

Zwitterionic polymerization of MMA inducec by TTMPP/$TMSNTf_2$. In a typical procedure, 50 µL (216 µmol) of $TMSNTf_2$ and 0.5 mL of MMA (4.7 mmol) were dissolved in 3 mL of toluene in a flame-dried Schlenck flask in the glovebox. A 3mL toluene solution of 58 mg (108 µmol) of TTMPP was added drop by drop on the solution of MMA-$TMSNTf_2$. After 2 h at 25 °C, an aliquot of the polymerization mixture was taken to determine the conversion by ^1H NMR analysis in $CDCl_3$ and the reaction was quenched at the air. All the volatiles were removed under vacuum. The crude product was re-dissolved in toluene and precipitated in methanol twice. After drying under vacuum, PMMA was recovered as a white solid.

Chain extension experiment.

0.5 mL of MMA (52 equivalents) were added onto the living PMMA chain obtained after 3 h (run 1, 85 % of conversion). After 13 h, 100 % of MMA conversion was reached (check by ^1H NMR). An addition load of 0.5 mL of MMA was again added. The work-up was the same as described above.

Equimolar reactions between MMA and $TMSNTf_2$ and betwenn NHC^{tBu} and $TMSNTf_2$

Table S1. NMR chemical shifts in toluene-d_8 of MMA, $TMSNTf_2$ and MMA+$TMSNTf_2$ (1:1).

entry	MMA	$TMSNTf_2$	MMA+$TMSNTf_2$	Δδ (ppm)	
1	CH_3: 1.58		CH_3: 1.79	0.21	^1H MMA
2	O-CH_3: 3.21		O-CH_3: 3.40	0.19	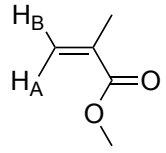
3	CH_A: 5.03		CH_A: 5.23	0.20	
4	CH_B: 5.80		CH_B: 6.01	0.21	
5		CH_3: 0,00	CH_3: 0.15	0.15	^1H CH_3SiNTf_2

6		Si: 54,91	Si: 7.06	-47.85	^{29}Si CH_3SiNTf_2
7	CH_3: 18.3		CH_3: 18.3	-0.1	^{13} C MMA
8	O-C: 51.3		O-C: 51.7	0.4	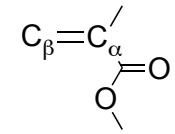
9	C_β: 124.9		C_β: 125.6	0.7	
10	C_α: 136.9		C_α: 136.7	-0.2	
11	C=O: 167.2		C=O: 167.8	0.6	
12		$CH_3 \rightarrow$ -0,4	$CH_3 \rightarrow$ -0,3	0.1	^{13}C CH_3SiNTf_2

Table S2. NMR shifts of NHC^{tBu} (in toluene-d_8), $TMSNTf_2$ and NHC^{tBu} +$TMSNTf_2$ (1:1) in CD_2Cl_2

entry	NHC^{tBu}	$TMSNTf_2$	NHC^{tBu} +$TMSNTf_2$	Δδ (ppm)	
1	CH_3: 1.48		CH_3: 1.8-2.3	n.d.	^{1}H NHC^{tBu} 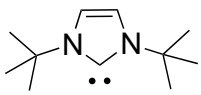
2	CH: 6.77		CH: 7.4-8.1	n.d.	
3		CH_3: 0,61	CH_3: 0.7-0.9	n.d.	^{1}H $TMSNTf_2$
4		Si: 56,19	Si:- 6.07	- 62.26	^{29}Si $TMSNTf_2$
5	C_4: 31.3		CH_3: 29-3	n.d.	^{13} C NHC^{tBu}
6	C_3: 56.4		C_3: 64.1		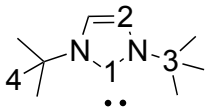
7	C_2: 116.6		C_2: 134-138	n.d.	
8	C_1: 209.5		C_1: 151.3		
9		CH_3: 0,7	CH_3: 1.5	n.d.	^{13}C $TMSNTf_2$

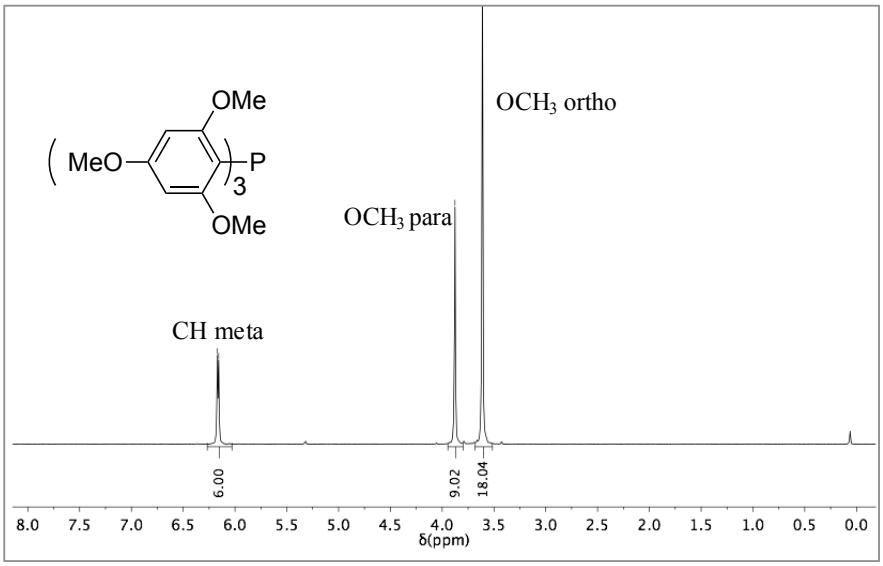

Figure S1. ^{1}H NMR spectrum in CD_2Cl_2 of TTMPP alone.

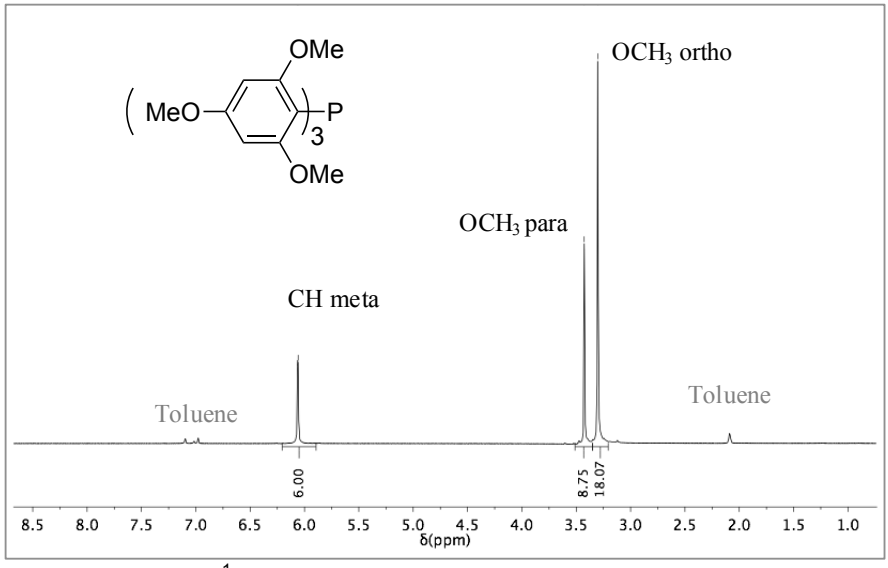

Figure S2. ^{1}H NMR spectrum in toluene-d_8 of TTMPP alone

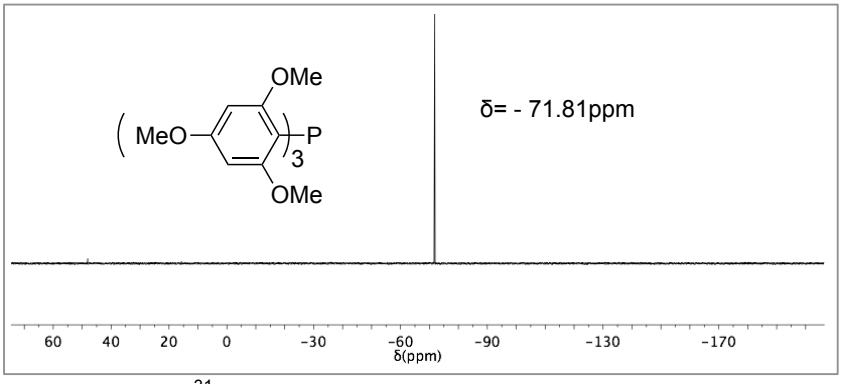

Figure S3. ^{31}P NMR spectrum in toluene-d_8 of TTMPP alone

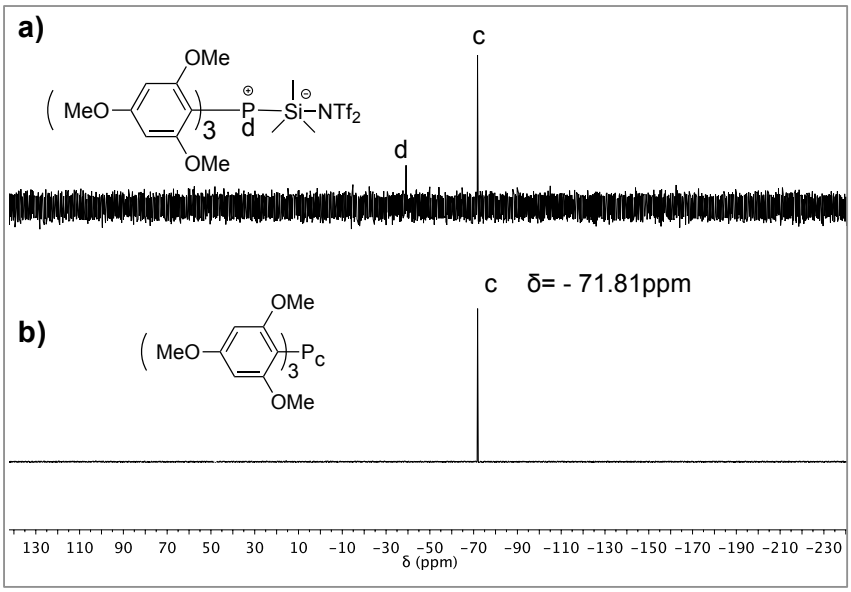

Figure S4. ^{1}H-coupled ^{31}P NMR spectrum in toluene-d_8 of: a) TTMPP+TMSNTf$_2$ (1:1); b) TTMPP alone.

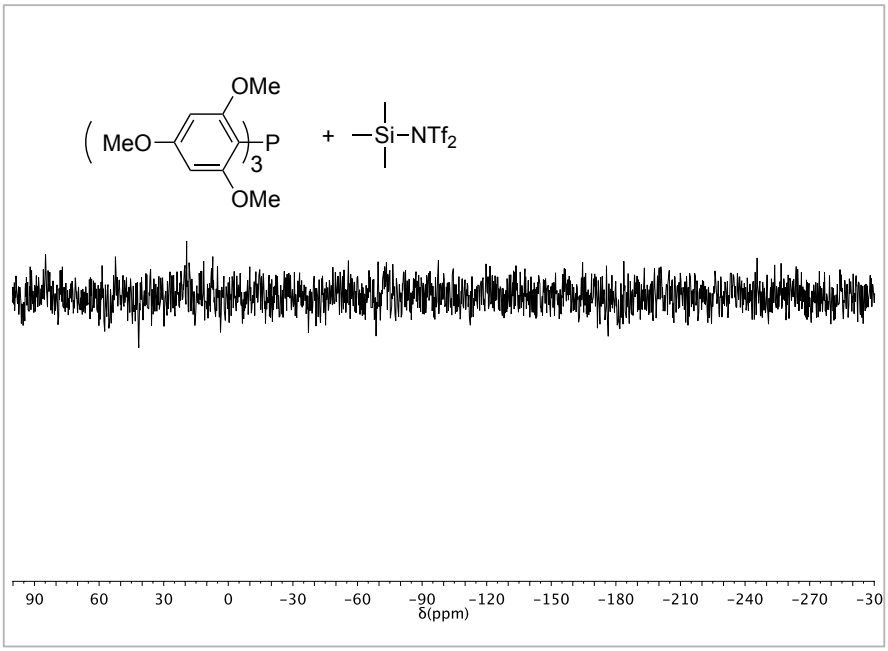

Figure S5. ^{29}Si NMR spectrum in PhBr-d_5 of TTMPP+TMSNTf$_2$ (1: 1).

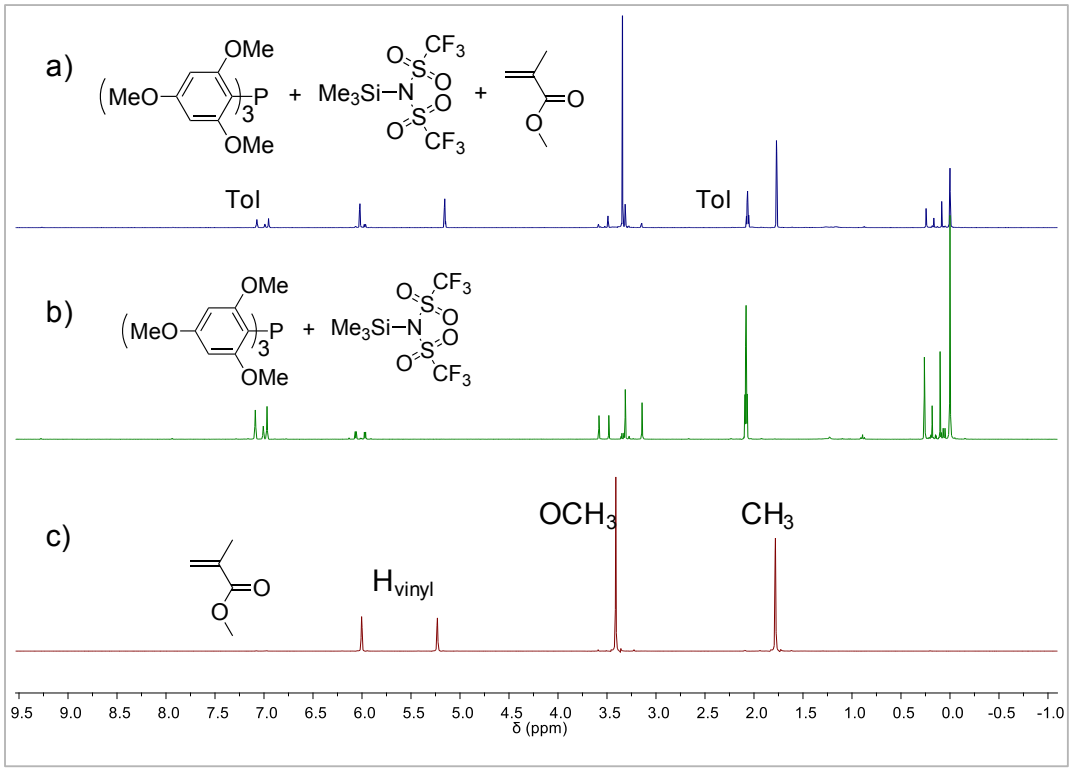

Figure S6. ^{1}H NMR spectrum in toluene-d_8. a) TTMPP+TMSNTf$_2$ +MMA (1: 1: 1), b)TTMPP+ TMSNTf$_2$ (1: 1) and c) MMA.

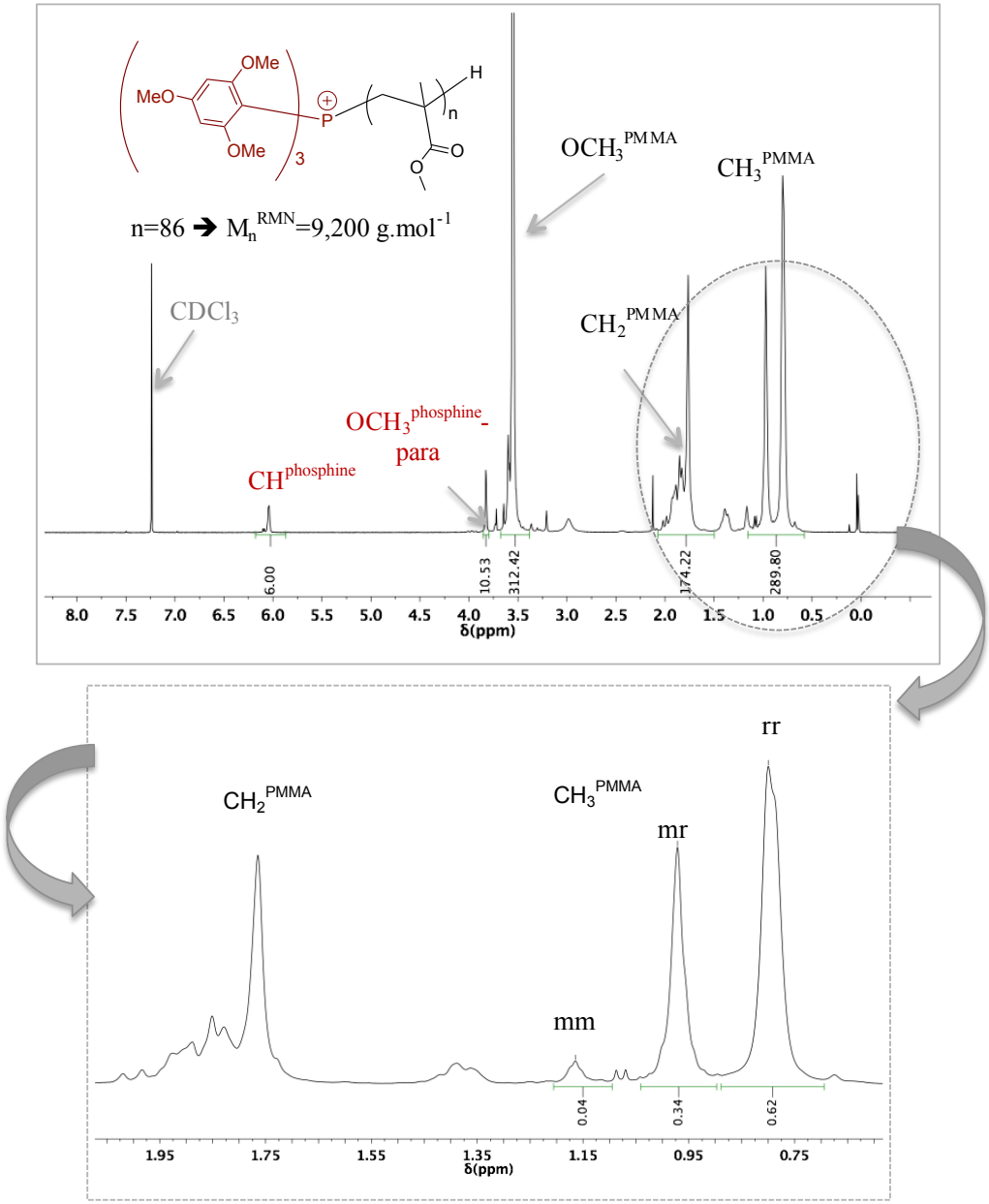

Figure S7. ^{1}H NMR spectrum in $CDCl_3$ of PMMA obtained using TTMPP/$TMSNTf_2$ (1/2) in toluene at 25 °C (Table 9).

References

(1) Kiesewetter, M. K.; Shin, E. J.; Hedrick, J. L.; Waymouth, R. M. *Macromolecules* **2010**, *43*, 2093.
(2) Fèvre, M.; Pinaud, J.; Gnanou, Y.; Vignolle, J.; Taton, D. *Chem. Soc. Rev.* **2013**, *42*, 2142.
(3) Welch, G. C.; San Juan, R. R.; Masuda, J. D.; Stephan, D. W. *Science* **2006**, *314*, 1124.
(4) Stephan, D. W. *Organic & Biomolecular Chemistry* **2008**, *6*, 1535.
(5) Stephan, D. W.; Erker, G. *Angew. Chem., Int. Ed.* **2010**, *49*, 46.
(6) Welch, G. C.; Cabrera, L.; Chase, P. A.; Hollink, E.; Masuda, J. D.; Wei, P.; Stephan, D. W. *Dalton Trans.* **2007**, 3407.
(7) Peuser, I.; Neu, R. C.; Zhao, X.; Ulrich, M.; Schirmer, B.; Tannert, J. A.; Kehr, G.; Fröhlich, R.; Grimme, S.; Erker, G.; Stephan, D. W. *Chem. Eur. J.* **2011**, *17*, 9640.
(8) Neu, R. C.; Menard, G.; Stephan, D. W. *Dalton Trans.* **2012**, *41*, 9016.
(9) Otten, E.; Neu, R. C.; Stephan, D. W. *J. Am. Chem. Soc.* **2009**, *131*, 9918.
(10) Neu, R. C.; Otten, E.; Lough, A.; Stephan, D. W. *Chem. Sci.* **2011**, *2*, 170.
(11) McCahill, J. S. J.; Welch, G. C.; Stephan, D. W. *Angew. Chem. Int. Ed.* **2007**, *46*, 4968.
(12) Dureen, M. A.; Stephan, D. W. *J. Am. Chem. Soc.* **2009**, *131*, 8396.
(13) Dureen, M. A.; Brown, C. C.; Stephan, D. W. *Organometallics* **2010**, *29*, 6594.
(14) Dureen, M. A.; Brown, C. C.; Stephan, D. W. *Organometallics* **2010**, *29*, 6422.
(15) Morton, J. G. M.; Dureen, M. A.; Stephan, D. W. *Chem. Commun.* **2010**, *46*, 8947.
(16) Breen, T. L.; Stephan, D. W. *Inorg. Chem.* **1992**, *31*, 4019.
(17) Welch, G. C.; Masuda, J. D.; Stephan, D. W. *Inorg. Chem.* **2006**, *45*, 478.
(18) Zhang, Y.; Miyake, G. M.; Chen, E. Y. X. *Angew. Chem., Int. Ed.* **2010**, *49*, 10158.
(19) Zhang, Y.; Miyake, G. M.; John, M. G.; Falivene, L.; Caporaso, L.; Cavallo, L.; Chen, E. Y. X. *Dalton Trans.* **2012**, *41*, 9119.
(20) Chen, E. X. 372,In *Frustrated Lewis Pairs II*; Erker, G., Stephan, D. W., Eds.; Springer Berlin Heidelberg: 2013; Vol. 334, p 239.
(21) Fèvre, M. PhD thesis, *unpublished results*, University of Bordeaux, **2009-2012**.
(22) Piedra-Arroni, E.; Ladavière, C.; Amgoune, A.; Bourissou, D. *J. Am. Chem. Soc.* **2013**, *135*, 13306.
(23) Dilman, A. D.; Ioffe, S. L. *Chem. Rev.* **2003**, *103*, 733.
(24) Takeuchi, Y.; Takayama, T. In *The Chemistry of Organic Silicon Compounds*; John Wiley & Sons, Ltd: **2003**, p 267.
(25) Arshadi, M.; Johnels, D.; Edlund, U.; Ottosson, C.-H.; Cremer, D. *J. Am. Chem. Soc.* **1996**, *118*, 5120.
(26) Chuit, C.; Corriu, R. J. P.; Reye, C.; Young, J. C. *Chem. Rev.* **1993**, *93*, 1371.
(27) Holmes, R. R. *Chem. Rev.* **1996**, *96*, 927.
(28) Stevenson, W. H.; Wilson, S.; Martin, J. C.; Farnham, W. B. *J. Am. Chem. Soc.* **1985**, *107*, 6340.
(29) Mathieu, B.; Ghosez, L. *Tetrahedron Lett.* **1997**, *38*, 5497.
(30) Mathieu, B.; Ghosez, L. *Tetrahedron* **2002**, *58*, 8219.
(31) Lamy-Schelkens, H. I. n.; Ghosez, L. o. *Tetrahedron Lett.* **1989**, *30*, 5891.
(32) Lamy-Schelkens, H. I. n.; Giomi, D.; Ghosez, L. o. *Tetrahedron Lett.* **1989**, *30*, 5887.
(33) Lambert, J. B.; Zhao, Y. *Angew. Chem., Int. Ed.* **1997**, *36*, 400.
(34) Lambert, J. B.; Zhao, Y.; Zhang, S. M. *J. Phys. Org. Chem.* **2001**, *14*, 370.
(35) Müller, T. 132,In *Functional Molecular Silicon Compounds I*; Scheschkewitz, D., Ed.; Springer International Publishing: 2014; Vol. 155, p 107.
(36) Stevenson, W. H.; Martin, J. C. *J. Am. Chem. Soc.* **1982**, *104*, 309.
(37) Fèvre, M.; Vignolle, J.; Heroguez, V.; Taton, D. *Macromolecules* **2012**, *45*, 7711.
(38) Arduengo, A. J.; Davidson, F.; Dias, H. V. R.; Goerlich, J. R.; Khasnis, D.; Marshall, W. J.; Prakasha, T. K. *J. Am. Chem. Soc.* **1997**, *119*, 12742.
(39) Kira, M.; Hino, T.; Sakurai, H. *J. Am. Chem. Soc.* **1992**, *114*, 6697.

(40) Arshadi, M.; Johnels, D.; Edlund, U.; Ottosson, C.-H.; Cremer, D. *J. Am. Chem. Soc.* **1996**, *118*, 5120.
(41) Mathieu, B.; de Fays, L.; Ghosez, L. *Tetrahedron Lett.* **2000**, *41*, 9561.
(42) Busnel, J. P. *Polymer* **1982**, *23*, 137.
(43) Kuhn, N.; Kratz, T.; Bläser, D.; Boese, R. *Chem. Ber.* **1995**, *128*, 245.
(44) Bottcher, T.; Bassil, B. S.; Zhechkov, L.; Heine, T.; Roschenthaler, G.-V. *Chem. Sci.* **2013**, *4*, 77.
(45) Ghadwal, R. S.; Roesky, H. W.; Merkel, S.; Henn, J.; Stalke, D. *Angew. Chem. Int. Ed.* **2009**, *48*, 5683.
(46) Filippou, A. C.; Chernov, O.; Schnakenburg, G. *Angew. Chem. Int. Ed.* **2009**, *48*, 5687.
(47) Dunbar, K. R.; Haefner, S. C. *Polyhedron* **1994**, *13*, 727.
(48) Wada, M.; Higashizaki, S. *J. Chem. Soc., Chem. Commun.* **1984**, 482.
(49) Hatada, K.; Kitayama, T. In *NMR Spectroscopy of Polymers*; Springer Berlin Heidelberg: **2004**, p 73.
(50) Sogah, D. Y.; Hertler, W. R.; Webster, O. W.; Cohen, G. M. *Macromolecules* **1987**, *20*, 1473.
(51) Perozzi, E. F.; Michalak, R. S.; Figuly, G. D.; Stevenson, W. H.; Dess, D.; Ross, M. R.; Martin, J. C. *J. Org. Chem.* **1981**, *46*, 1049.

Discussion générale – Conclusions - Perspectives

Les travaux présentés dans ce manuscrit avaient pour objectif principal d'étudier et de rationaliser l'effet de la structure de carbènes *N*-hétérocycliques (NHCs) utilisés comme catalyseurs organiques ou bien comme amorceurs directs de la polymérisation de divers monomères (méth)acryliques (Figure 1). Il s'agissait donc non seulement d'étendre le potentiel des NHCs en synthèse macromoléculaire, mais aussi de rendre compte de la possibilité d'induire des processus sélectifs, en fonction de leur structure, vis à vis d'un substrat simple comme le méthacrylate de méthyle (MMA).

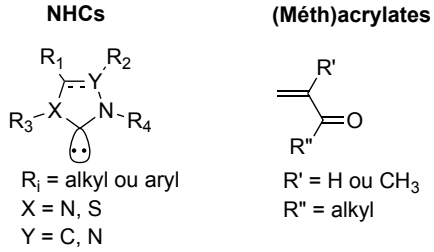

Figure 1. Structure des carbènes *N*-hétérocycliques (NHCs) et des (méth)acrylates d'alkyle.

La première partie de ce travail a ainsi illustré que deux carbènes NHCs de type imidazol-2-ylidène, différant par leurs substituants alkyle sur les atomes d'azote (isopropyle *vs. tert*-butyle), montrent un comportement très différent en réaction directe (*i.e.* en l'absence de tout autre composé) avec des substrats acryliques et méthacryliques.

En effet, le 1,3-bis(*tert*-butyl)imidazol-2-ylidene (= NHC^{tBu}) permet un amorçage direct de la polymérisation du MMA dans le DMF à 25 °C, *via*, selon toute vraisemblance, un mécanisme de type zwittérionique (Schéma 1). Dans de telles conditions, des poly(méthacrylate de méthyle)s (PMMA's) de masses molaires ($\overline{M_n}$) comprises entre 2,800 – 12,200 $g.mol^{-1}$ et de dispersité $Đ$ = 1.3 – 1.9 ont été obtenus. Ces valeurs de masses molaires sont cependant supérieures à celles prévues par le ratio initial $[MMA]_0/[NHC^{tBu}]_0$, mais elles évoluent de façon croissante quand ce ratio augmente. Une telle polymérisation zwittérionique faisant intervenir des chaines en croissance de type poly(méth)acrylate α-imidazolium,ω-énolate sont *a priori* difficiles à contrôler, du fait de l'existence probable de réactions secondaires, telles que les réactions de terminaison, intramoléculaire par rétro-scission (« back-biting »), ou intermoléculaire conduisant à des ramifications (« branchings »). Il convient aussi de souligner le rôle important du solvant, aucune réaction de polymérisation n'ayant été observée dans le THF ou le toluène à 25 °C, au contraire du DMF, plus polaire et solvant dans lequel les espèces actives supposées zwittérioniques peuvent plus facilement être générées.

En termes de stéréorégularité, les PMMA's ainsi préparés par amorçage direct par le NHC^{tBu} sont composés de 51 % de triades syndiotactiques, 40 % d'hétérotactiques et 9 % d'isotactique (Schéma 1). Cette composition est assez similaire à celle généralement observée par polymérisation anionique du MMA dans le THF à basse température (-78 °C), avec, par exemple, des organolithiens comme amorceurs. Cette similarité suggère là encore la présence de chaînes en croissance de type énolate, dans le cas de l'amorçage par le NHC^{tBu}.

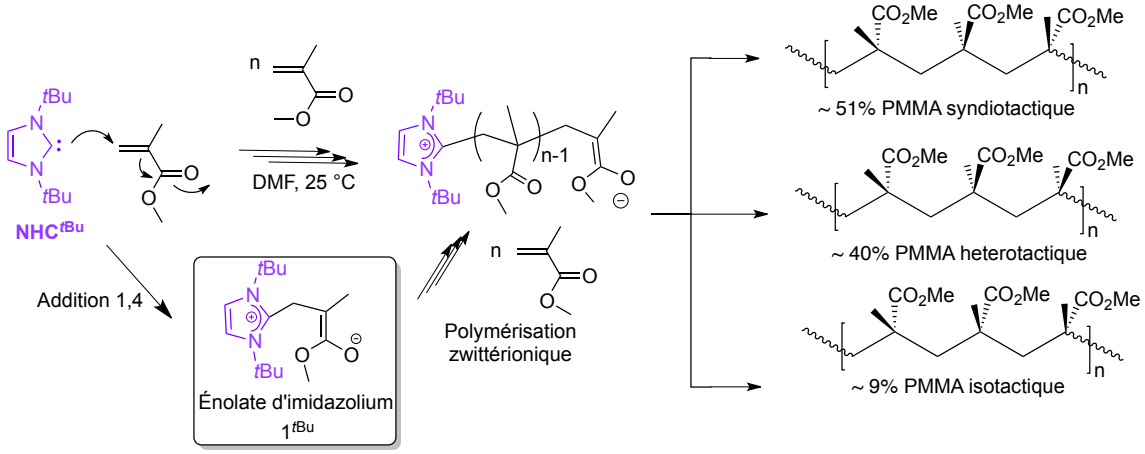

Schéma 1. Polymérisation zwittérionique du MMA induite par le NHC^{tBu} dans le DMF à 25 °C.

De manière assez inattendue, le 1,3-bis(isopropyl)imidazol-2-ylidene (= NHC^{iPr}) testé lui aussi directement comme amorceur, n'a pas permis la polymérisation du MMA, quelles que soient les conditions de réaction (THF, toluène, et même DMF à 25°C ou 50 °C). En revanche, ce carbène conduit sélectivement à la formation d'un composé zwittérionique spiro-bicyclique, résultant de la réaction entre 1 équivalent de NHC^{iPr} et de 2 équivalents de MMA (NHC^{iPr}:MMA = 1:2), ce qui n'avait jamais été décrit dans la littérature. Ce composé a pu être isolé par cristallisation et parfaitement identifié par spectroscopies RMN (^{1}H and ^{13}C), spectrométrie de masse et par rayons-X (Figure 2). Il correspond, en réalité, à un mélange de deux diastéréoisomères *cis* et *trans* qui co-cristallisent tels que montrés dans la figure ci-dessous.

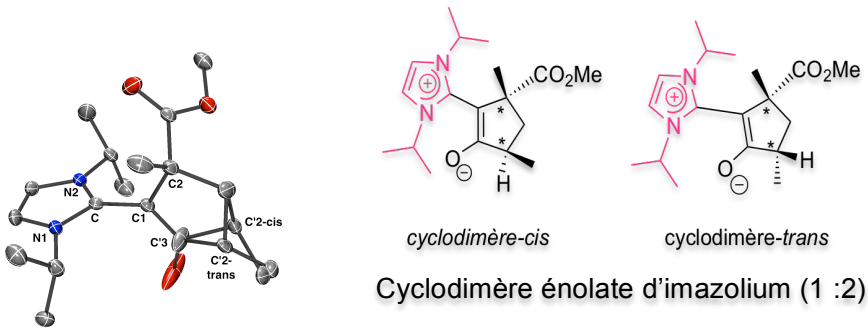

Figure 2. Structure rayons-X du cyclodimère NHC^{iPr}-MMA (1:2).

Pour expliquer ces résultats expérimentaux (polymérisation *via* le NHC^{tBu} et cyclodimérisation *via* le NHC^{iPr}), nous avons proposé un mécanisme réactionnel général illustré par le Schéma 2. Dans les deux cas, l'étape initiale correspond à l'attaque directe du NHC sur le MMA, conduisant à l'adduit zwittérionique 1 :1 (**1^{iPr}** ou **1^{tBu}**), lequel s'additionne ensuite sur un autre équivalent de MMA pour former un nouvel intermédiaire zwittérionique 1 :2 (**2^{iPr}** ou **2^{tBu}**). A ce stade, contrairement au produit dérivé du NHC^{tBu} capable d'insérer de nouvelles unités monomères MMA (chemin de polymérisation), l'adduit 1:2 zwittérionique issu du NHC^{iPr} (**2^{iPr}**), induit un transfert de proton, suivi d'une réaction de cyclisation et d' élimination d'une molécule de méthanol (chemin de cyclodimérisation ; Figure 2 et Schéma 2).

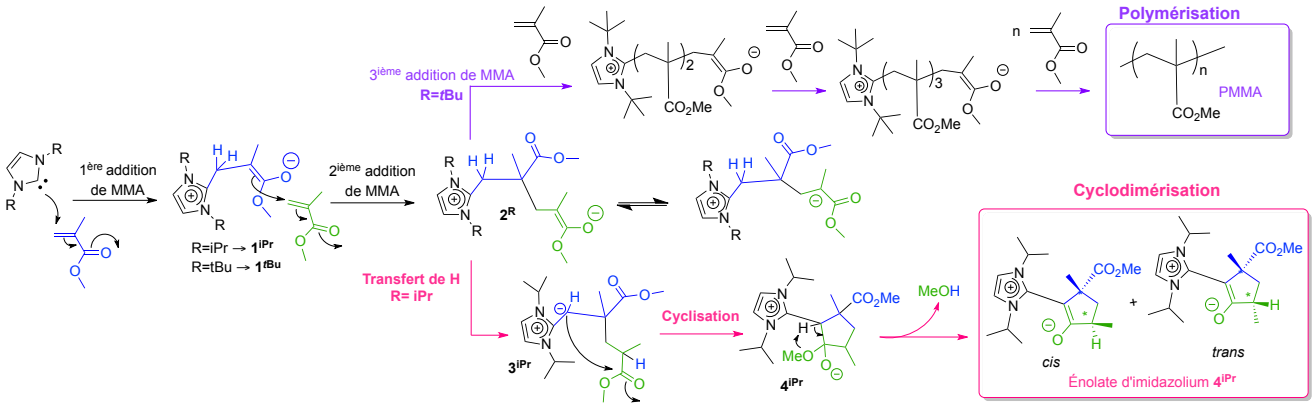

Schéma 2. Polymérisation zwittérionique *vs.* cyclodimérisation du MMA induite par NHC^{tBu} ou NHC^{iPr} dans le DMF à 25 °C.

Des calculs théoriques ont ensuite été réalisés par nos partenaires à l'IPREM (D. Bourichon/K. Miqueu/J.-M. Sotiropulos) afin de comprendre l'origine des différences entre NHC^{iPr} et NHC^{tBu}. Le profil énergétique des deux mécanismes (cyclodimérisation *vs.* polymérisation) obtenu par la méthode des fonctionnelles de la densité (DFT pour density functional theory en anglais) a ainsi permis de révéler que l'étape limitante (énergie d'activation E_a la plus élevée ≈ 25 kcal.mol^{-1}) est celle éliminant le méthanol, alors que le transfert intramoléculaire de proton correspond à l'étape discriminante (E_a ≈ 11 kcal.mol^{-1}) dans le processus de cyclodimérisation. En complément, l'étude par dynamique moléculaire en solution a mis en évidence une conformation préférentiellement étirée du zwiitérion NHC^{tBu}-MMA_2 (**2^{tBu}**, Schéma 2) par opposition à une conformation repliée dans le cas du zwittérion NHC^{iPr}-MMA_2 (**2^{iPr}**) favorisant la cyclisation.

Une telle sélectivité observée avec le MMA comme substrat ne s'applique pas cependant à l'acrylate de méthyle (MA). En effet, les deux NHCs peuvent amorcer directement la polymérisation de ce monomère dans le DMF à 25 °C. Des poly(acrylate de

méthyle)s (PMA's) de masses molaires $\overline{M_n}$ = 1,600 – 4,300 g.mol^{-1} et de dispersité $Đ$ = 1.4 – 3.1 ont ainsi été synthétisés.

Le comportement d'autres monomères acryliques et méthacryliques vis à vis de chacun des deux NHCs a ensuite été examiné afin d'obtenir une cartographie d'ensemble de la réactivité de ces deux carbènes (Figure 3). Ainsi, alors que le NHC$^{t\text{Bu}}$ induit la polymérisation de tous les monomères testés, avec les mêmes tendances que ceux observés avec le MMA (variation des masses molaires en fonction de la concentration en monomère, amorçage lent, réactions secondaires, ...), le NHC$^{i\text{Pr}}$ ne forme des polymères que dans le cas des acrylates d'alkyle. Nous avons alors supposé qu'avec les substrats méthacrylates, il se forme des cyclodimères NHC$^{i\text{Pr}}$:methacrylate = 1 :2 du même de type que celui observé avec le MMA. Des données expérimentales supplémentaires sont cependant nécessaires pour valider cette hypothèse.

Bien que qualitative, cette cartographie montre bien qu'il existe une relation structure-réactivité pour déclencher la polymérisation des monomères (méth)acryliques en présence de NHCs.

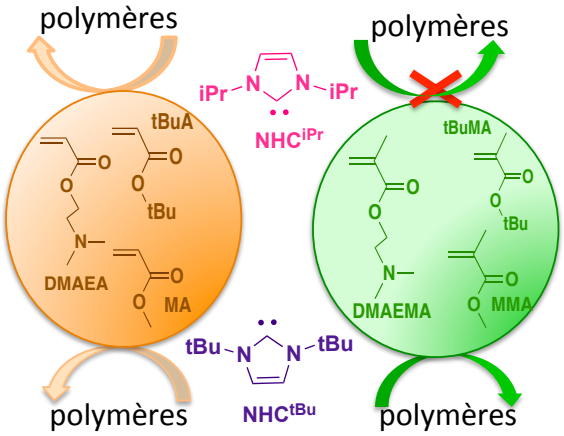

Figure 3. Réactivités des NHC$^{t\text{Bu}}$ et NHC$^{i\text{Pr}}$ sur des (meth)acrylates.

Dans la deuxième partie de ce travail, nous avons examiné le potentiel des deux mêmes NHCs non plus comme amorceurs mais comme catalyseurs organiques de la polymérisation des (méth)acrylates d'alkyle. La polymérisation du MMA dans le DMF à 25 °C a été plus particulièrement étudiée, en utilisant de simples alcools comme agents de contrôle et le NHC$^{t\text{Bu}}$ comme organocatalyseur (Schéma 3). Dans ces conditions, nous avons mis en évidence que la polymérisation peut en effet être contrôlée par le ratio $[MMA]_0/[ROH]_0$, conduisant à la formation de chaines de PMMA α-alcoxy, présentant des masses molaires $\overline{M_n}$ = 1,000 – 8,000 g.mol^{-1} ($Đ$ = 1.1– 1.9) évoluant de façon linéaire avec la conversion du MMA. Des expériences d'extension de chaines ont montré que les chaines peuvent être réactivées, en accord avec un processus ayant un certain degré de contrôle.

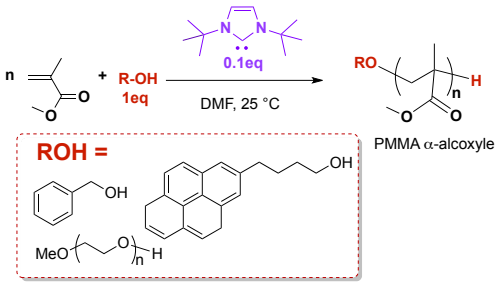

Schéma 3. Polymérisation du MMA amorcée par des ROH et catalysée par le NHC$^{t\text{Bu}}$.

En visant des degrés de polymérisation plus élevés, cependant ($[MMA]_0/[ROH]_0 \geq 50$), une perte progressive du contrôle des masses molaires a été observée. Ces résultats ont pu être rationnalisés grâce à la mise en place de réactions modèles, mais aussi grâce aux calculs théoriques par DFT réalisés à nouveau par nos partenaires à l'IPREM. L'ensemble a révélé que ces polymérisations procèdent selon deux mécanismes réactionnels compétitifs mettant en jeu des interactions de type liaisons-hydrogène de manière concertée.

Les deux mécanismes correspondent, d'une part, à l'activation de l'alcool -puis, des chaines de PMMA en croissance- par le carbène (Schéma 4a) et, d'autre part à l'activation du monomère par l'alcool et par le NHC (Schéma 4b). Le premier mécanisme induirait un contrôle de la taille des chaines par l'alcool, tandis que celle-ci serait sous le contrôle du carbène (en quantité plus faible par rapport à l'alcool) suivant le deuxième mécanisme. L'intervention d'un tel mécanisme pourrait expliquer l'augmentation des masses molaires par rapport à celles visées et prédites par le ratio $([MMA]_0/[ROH]_0$.

a) Activation de l'amorceur et des chaînes en croissance (ACEM): mécanisme anionique

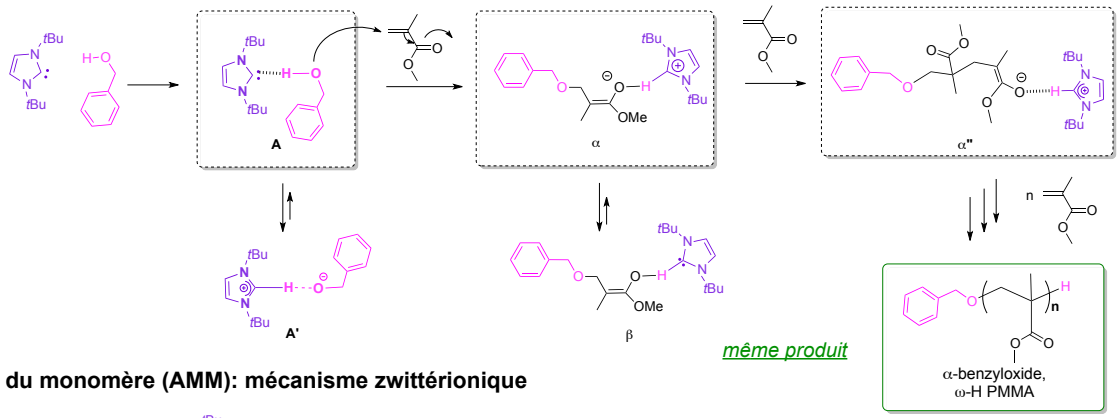

b) Activation du monomère (AMM): mécanisme zwittérionique

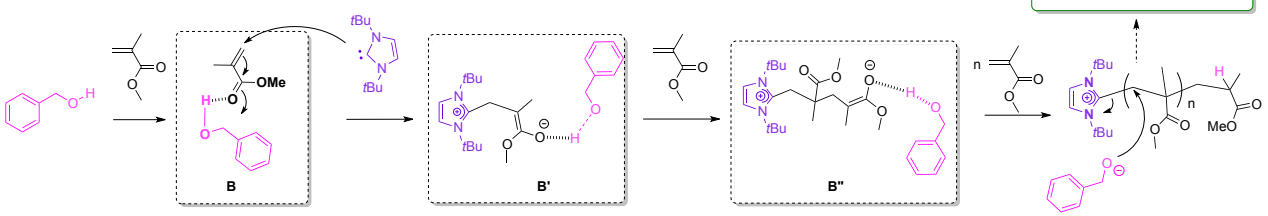

Schéma 4. Polymérisation du MMA amorcée par des alcools et catalysée par NHC$^{t\text{Bu}}$ dans le DMF à 25 °C.

Les PMMA's synthétisés par le système NHC$^{t\text{Bu}}$ comme catalyseur et l'alcool benzylique (BnOH) comme amorceur possèdent une tacticité similaire à celle observée avec le NHC$^{t\text{Bu}}$ seul : % triades syndiotactiques = 51 %, % de triades hétérotactiques = 41 % et % de triades isotactiques = 8 %. Ceci laisse supposer que la présence d'alcool n'a pas d'influence sur l'insertion du monomère et que, dans ces conditions, les chaines croissent probablement sous une forme énolate « non coordiné ».

Cette méthodologie a été ensuite appliquée en utilisant des poly(oxyde d'éthylène)s (PEO's) hydroxylés comme marco-amorceurs de la polymérisation organocatalysée du MMA. Des copolymères à blocs amphiphiles, PEO-*b*-PMMA, de masses molaires $\overline{M_n}$ = 6,800 - 19,300 g.mol^{-1} ($Đ$ = 1.3– 1.6), contrôlées par le rapport initial $[MMA]_0/[PEO]_0$ ont ainsi été synthétisés. La formation de micelles de diamètres d'environ 30 nm, résultant d'une nano-organisation de ces copolymères en solution aqueuse, a été mise en évidence par analyse microscopique.

Outre le MMA, la polymérisation de son homologue acrylate MA, amorcée par des alcools et catalysée par le NHC$^{t\text{Bu}}$, est également efficace et conduit à des PMA's α-alcoxy de masses molaires $\overline{M_n}$ = 700-1,900 g.mol^{-1} ($Đ$ = 1.2– 2.0).

En revanche, des tentatives de synthèse de copolymères à blocs PMMA-*b*-PMA par polymérisation séquentielle ont échoué et nécessitent encore une optimisation des conditions expérimentales (effet de température, addition lente du second monomère, …).

D'autres monomères (méth)acryliques pourraient être testés et permettre la synthèse de divers (co)polymères fonctionnels dépourvus de toute trace métallique.

La troisième et dernière partie de cette thèse a montré le premier exemple de double assistance par un acide et une base de Lewis purement organiques pour déclencher la polymérisation du MMA. Outre le même carbène NHC$^{t\text{Bu}}$, des trialkyle et triaryle phosphines ont servi comme bases de Lewis, en conjonction avec des acides de Lewis dérivés du silicium, notamment des silanes (R_4Si), des triflates ou triflimides de trialkyle (R_3SiOTf et R_3SiNTf_2). Le recours à ces paires de Lewis a pour double effet d'augmenter la réactivité du monomère et de moduler la réactivité des chaines en croissance sous forme d'énolates silylés.

Un criblage de différentes combinaisons a permis d'identifier une paire de Lewis particulière, en l'occurrence la tris(2,4,6-trimethoxyphenyl)phosphine (TTMPP) associée au triflimide de triméthylsilyle ($TMSNTf_2$) pour induire la polymérisation du MMA dans le toluène à 25°C. Avec un ratio initial, $[TMSNTf_2]_0/[TTMPP]_0 = 2$, des PMMA's de masses molaires $\overline{M_n}$ = 6,700 - 17.800 g.mol^{-1} ($Đ$ = 1.1) proches des valeurs prédites par le ratio $[MMA]_0/[TTMPP]_0$ ont ainsi été obtenus. L'absence totale de polymérisation lorsque chacun des partenaires est employé individuellement a démontré l'effet coopératif de la paire de

Lewis. Un mécanisme zwittérionique impliquant un équivalent d'acide activant le monomère et un autre équivalent interagissant avec la chaine en croissance a été proposé (Schéma 5). Une analyse détaillée des PMMA's par RMN et par MALDI-ToF a permis d'identifier des bouts de chaines de type α-phosphonium, de structure linéaire ou cyclique (ce dernier point n'a pu être clairement établi). De plus, les expériences d'extension de chaines ont mis en évidence le caractère « vivant/contrôlé » de cette méthode de polymérisation induite par une paire de Lewis organique.

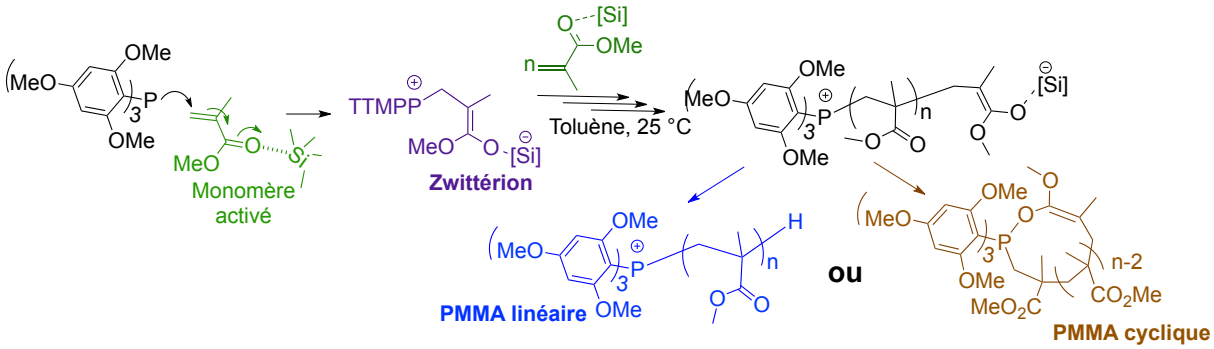

Schéma 5. Polymérisation du MMA induite par la paire de Lewis TTMPP/$TMSNTf_2$ (1/2) dans le toluène à 25 °C.

Ces résultats sont d'autant plus inattendus qu'il semblerait que la base de Lewis TTMPP et l'acide de Lewis $TMSNTf_2$ forme un adduit « classique » (paire non frustrée). L'ordre d'addition des réactifs, à savoir 1) addition du $TMSNTf_2$ et du MMA dans le toluène puis, 2) ajout de la TTMPP dans le toluène sur la solution du monomère activée, permet cependant d'éviter la formation de l'adduit. Dans les mêmes conditions, en revanche, la paire $NHC^{tBu}/TMSNTf_2$ forme aussi adduit de Lewis classique mais celui-ci est inactif en polymérisation (Schéma 6). Cette différence de réactivité entre les deux adduits TTMPP-$TMSNTf_2$ et NHC^{tBu}-$TMSNTf_2$ est probablement lié au caractère silicophile supérieur du carbène par rapport à la phosphine.

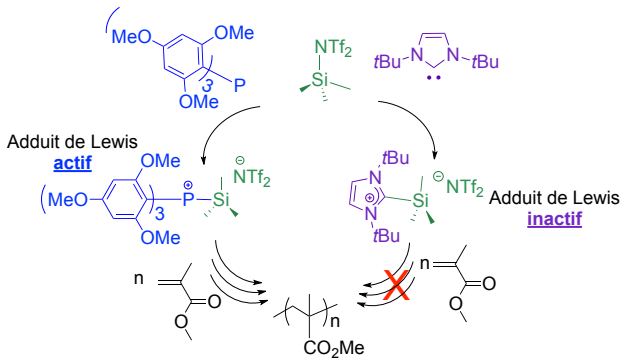

Schéma 6. Réactivité des adduit de Lewis classiques NHC^{tBu}-$TMSNTf_2$ (inactif) et TTMPP-$TMSNTf_2$ (actif).

Les PMMA's obtenus dans ces conditions montrent une légère prédominance syndiotactique (60-70% de triades rr), ce que nous avons ici attribué à une coordination de l'atome de silicum avec le monomère et avec les chaines actives, générant une gène stérique pouvant favoriser une insertion préférentielle du monomère (Figure 4).

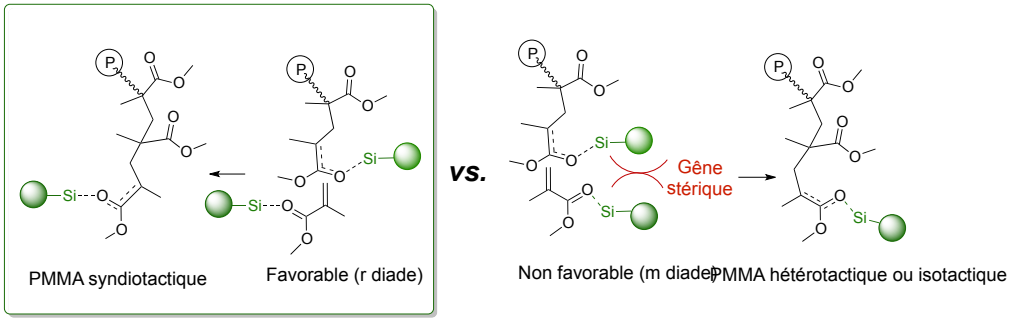

Figure 4. Stéréocontrôle supposé lors de la polymérisation du MMA induite par TTMPP/$TMSNT_2$

Une telle activation pourrait être étendue à d'autres monomères vinyliques moins polaires (e.g. diènes, styréniques, …) en adaptant la réactivité des partenaires. Là encore, des études théoriques (toujours en cours) pourront permettre de rationnaliser les résultats expérimentaux, et pourquoi pas, d'identifier d'autres paires de Lewis pour la polymérisation de tel ou tel monomère.

Au final, ce travail de thèse a établi de nouvelles voies de polymérisation sans métaux de monomères (méth)acryliques basées sur la réactivité unique des NHCs ou bien sur l'association entre une phosphine et un acide de Lewis silylé. La sélectivité des NHCs en polymérisation zwittérionique a aussi été mise clairement en évidence. Nous avons ainsi élargi la plateforme des activateurs organiques pour la synthèse macromoléculaire, dans l'optique d'étendre les possibilités d'organopolymérisation à d'autres monomères. Il serait aussi intéressant de considérer l'utilisation d'activateurs (catalyseurs/amorceurs) chiraux afin d'introduire des processus réactionnels stéréosélectifs. Par ailleurs, la possibilité de fixer des activateurs organiques sur des supports polymères pour en faciliter la manipulation, mais aussi à des fins de recyclage est un autre point d'intérêt. Ces axes de recherche sont actuellement étudiés dans d'autres travaux de thèse au sein de notre équipe.

Organopolymérisations du méthacrylate de méthyle induites par les carbènes *N*-hétérocycliques et par des paires de Lewis organiques

Résumé: Deux carbènes *N*-hétérocycliques (NHCs) de type imidazol-2-ylidène ont été étudiés en tant qu'amorceurs organiques pour la polymérisation directe de monomères vinyliques de type (méth)acrylates d'alkyle, principalement le méthacrylate de méthyle (MMA), en l'absence tout autre activateur. Une différence de réactivité a été mise en évidence en fonction des substituants du carbène et de la nature du substrat. Des études théoriques ont permis de rationaliser les résultats expérimentaux par l'influence des effets électroniques et stériques intervenant au cours des réactions mises en jeu.

Un NHC en particulier a été ensuite utilisé comme véritable catalyseur de la polymérisation du MMA en présence d'alcools comme amorceurs. En utilisant des macro-amorceurs hydroxylés de type poly(oxyde d'éthylène), des copolymères amphiphiles ont été ainsi synthétisés. Des études théoriques ont encore une fois permis d'identifier les mécanismes réactionnels de cette polymérisation.

Enfin, des paires de Lewis composées d'un acide à base de silicium et d'une base de type NHC ou phosphine trialkyle(aryle) ont été ensuite utilisées comme système d'activation de polymérisation du MMA. Ce type de polymérisation est basé sur une activation duale du monomère par effet coopératif de la base et de l'acide.

Mots clés: polymérisation organique, catalyse, méthacrylate de méthyle, carbènes *N*-hétérocycliques, paires de Lewis, phosphines, composés silylés, activation duale,

---

Organopolymerizations of methyl methacrylate directly induced by *N*-heterocyclic carbenes and by metal-free Lewis pairs

Abstract: The reactivity of imidazol-ylidene *N*-heterocyclic carbenes (NHCs) as direct initiators for the polymerization of miscellaneous (meth)acrylic monomers, mainly methyl methacrylate (MMA), has been screened in the absence of any other co-activator. Different reactivities have been observed according to the structure of the NHC and the nature of the substrate. Computational studies allowed rationalizing steric and electronic effects involved in these reactions.

The use of a peculiar NHCs as catalyst for the polymerization of MMA using alcohols as initiators has then been investigated. This simple and efficient method also allows achieving amphiphilic block copolymers by using hydroxylated poly(ethylene oxide)s as macro-initiators. Combined computational and experimental investigations have provided insights into the mechanism of polymerization.

Various Lewis pairs including a silicon-based compound as acid and NHC or a trialkyl(aryl) phosphine as base, have been investigated to trigger an efficient polymerization of MMA. In this case, the polymerization is expected to proceed *via* a cooperative/dual activation mechanism.

Keywords : metal-free polymerization, catalysis, methyl methacrylate, *N*-heterocyclic carbenes, Lewis pairs, phosphines, silicon derivatives, dual activation.

LCPO Laboratoire de Chimie des Polymères Organiques

[UMR 5629, ENSCBP 16, av. Pey Berland 33607 Pessac, France]